KIDNEY AND DISTANT ORGAN CROSSTALK IN HEALTH AND DISEASE

EDITED BY: Jonatan Barrera-Chimal, Frederic Jaisser and Natalia Lopez-Andres
PUBLISHED IN: Frontiers in Physiology and Frontiers in Medicine

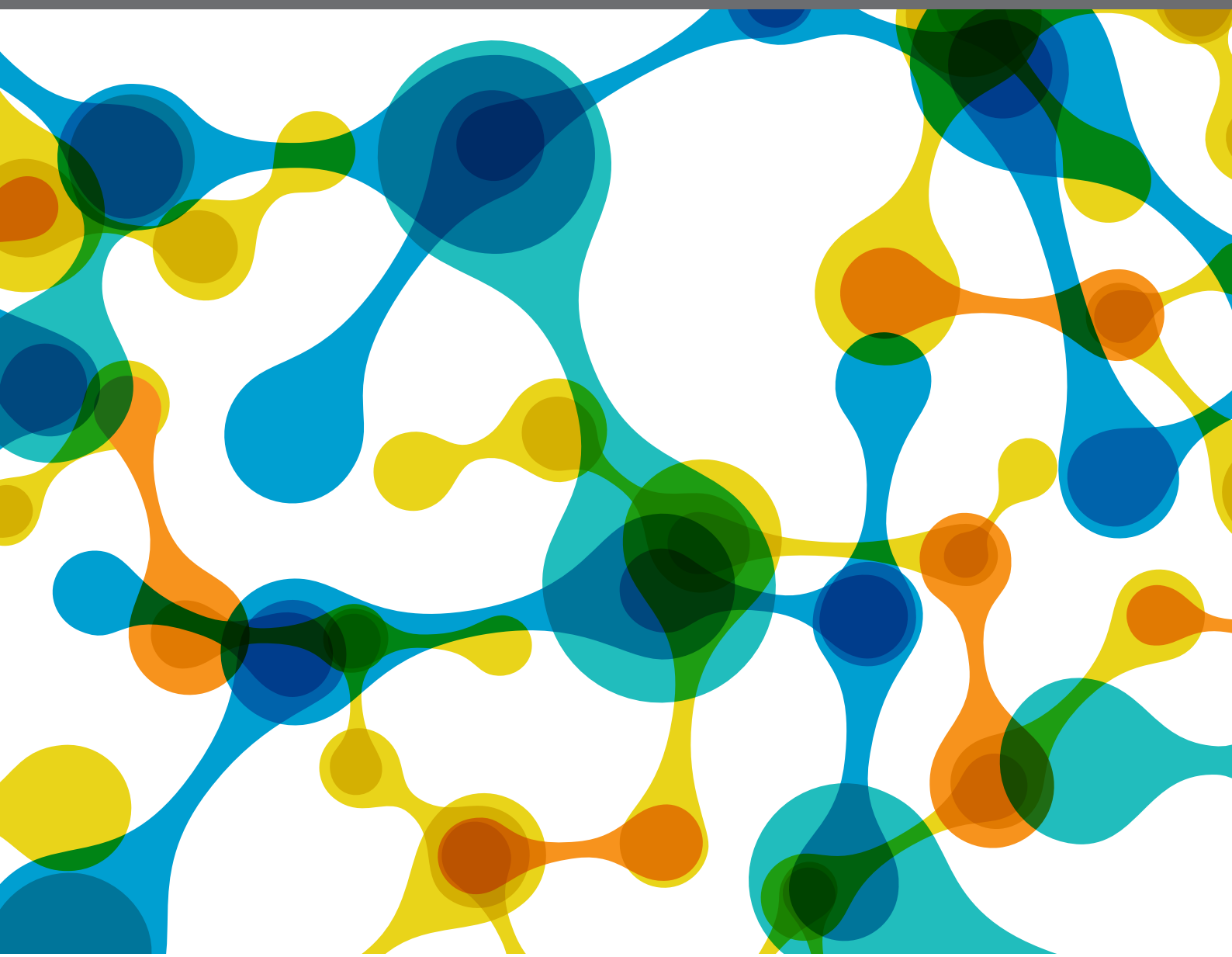

frontiers Research Topics

ISSN 1664-8714
ISBN 978-2-88971-269-4
DOI 10.3389/978-2-88971-269-4

About Frontiers

Frontiers is more than just an open-access publisher of scholarly articles: it is a pioneering approach to the world of academia, radically improving the way scholarly research is managed. The grand vision of Frontiers is a world where all people have an equal opportunity to seek, share and generate knowledge. Frontiers provides immediate and permanent online open access to all its publications, but this alone is not enough to realize our grand goals.

Frontiers Journal Series

The Frontiers Journal Series is a multi-tier and interdisciplinary set of open-access, online journals, promising a paradigm shift from the current review, selection and dissemination processes in academic publishing. All Frontiers journals are driven by researchers for researchers; therefore, they constitute a service to the scholarly community. At the same time, the Frontiers Journal Series operates on a revolutionary invention, the tiered publishing system, initially addressing specific communities of scholars, and gradually climbing up to broader public understanding, thus serving the interests of the lay society, too.

Dedication to Quality

Each Frontiers article is a landmark of the highest quality, thanks to genuinely collaborative interactions between authors and review editors, who include some of the world's best academicians. Research must be certified by peers before entering a stream of knowledge that may eventually reach the public - and shape society; therefore, Frontiers only applies the most rigorous and unbiased reviews.
Frontiers revolutionizes research publishing by freely delivering the most outstanding research, evaluated with no bias from both the academic and social point of view. By applying the most advanced information technologies, Frontiers is catapulting scholarly publishing into a new generation.

What are Frontiers Research Topics?

Frontiers Research Topics are very popular trademarks of the Frontiers Journals Series: they are collections of at least ten articles, all centered on a particular subject. With their unique mix of varied contributions from Original Research to Review Articles, Frontiers Research Topics unify the most influential researchers, the latest key findings and historical advances in a hot research area! Find out more on how to host your own Frontiers Research Topic or contribute to one as an author by contacting the Frontiers Editorial Office: frontiersin.org/about/contact

KIDNEY AND DISTANT ORGAN CROSSTALK IN HEALTH AND DISEASE

Topic Editors:
Jonatan Barrera-Chimal, Universidad Nacional Autónoma de México, Mexico
Frederic Jaisser, Institut National de la Santé et de la Recherche Médicale (INSERM), France
Natalia Lopez-Andres, NavarraBiomed, Spain

Topic Editor Dr. Frédéric Jaisser received grants from Bayer AG and AstraZeneca. All other Topic Editors declare no competing interests with regards to the Research Topic subject.

Citation: Barrera-Chimal, J., Jaisser, F., Lopez-Andres, N., eds. (2021). Kidney and Distant Organ Crosstalk in Health and Disease. Lausanne: Frontiers Media SA. doi: 10.3389/978-2-88971-269-4

Table of Contents

frontiers in Physiology

EDITORIAL
published: 01 July 2021
doi: 10.3389/fphys.2021.712535

Editorial: Kidney and Distant Organ Crosstalk in Health and Disease

Natalia López-Andrés[1]*, *Frederic Jaisser*[2,3]* and *Jonatan Barrera-Chimal*[4,5]*

[1] Cardiovascular Translational Research, Complejo Hospitalario de Navarra (CHN), Universidad Pública de Navarra (UPNA), IDISNA, Navarrabiomed (Miguel Servet Foundation), Pamplona, Spain, [2] INSERM, UMRS 1138, Centre de Recherche des Cordeliers, Sorbonne Université, Université de Paris, Paris, France, [3] Université de Lorraine, INSERM Centre d'Investigations Cliniques-Plurithématique 1433, UMR 1116, CHRU de Nancy, French-Clinical Research Infrastructure Network (F-CRIN) INI-CRCT, Nancy, France, [4] Instituto de Investigaciones Biomédicas, Universidad Nacional Autónoma de México, Ciudad Universitaria, Mexico City, Mexico, [5] Laboratorio de Fisiología Cardiovascular y Trasplante Renal, Unidad de Investigación UNAM-INC, Instituto Nacional de Cardiología Ignacio Chávez, Mexico City, Mexico

Keywords: cardiorenal, kidney disease, hemodialysis, inflammation, fibrosis

Editorial on the Research Topic

Kidney and Distant Organ Crosstalk in Health and Disease

Kidney disease is a health condition affecting a high number of patients with an estimated worldwide prevalence of 10% (Jager et al., 2019). Kidney dysfunction and the resulting accumulation of uremic toxins and chronic inflammation contribute to secondary injury in organs like the heart, vessels, lungs, gut, brain, liver, among others (Malek, 2018; Shang et al., 2020; Ambruso et al., 2021; Lai et al., 2021). On the other hand, kidney disease might be the result of co-morbidities or due to a primary insult in another organ (Ronco et al., 2018). The mechanisms by which this kidney-distant organ communication occurs remain partially understood. This Research Topic compiled original investigation and review papers that explored the connection between the kidneys and other organs/co-morbidities and result in the proposal of novel biomarkers, therapeutic strategies and bring new insights into the molecular mechanisms linking kidney disease with other organs.

THE KIDNEYS AND THE CARDIOVASCULAR SYSTEM

The close relationship between the kidneys and the cardiovascular system has long been recognized. While the main cause of death in chronic kidney disease (CKD) patients is related to major cardiovascular events, acute or chronic heart failure may also result in kidney damage (Ronco et al., 2018; Ricci et al., 2021). In this sense, a common complication in cardiac surgery patients is acute kidney injury (AKI) (O'Neal et al., 2016), however its diagnosis is limited due to the lack of sensitive and early biomarkers. To address this issue, Chen et al. explored the levels of 48 cytokines in the plasma from patients undergoing cardiac surgery. Twenty-four hours after cardiac surgery, 13 cytokines showed a remarkable increase in patients that developed AKI as compared to patients without AKI. Importantly, interferon-γ and stem cell growth factor-β plasma levels efficiently discriminated between the severity levels of AKI. Testing these biomarkers in larger cohorts will bring new insights into their usefulness to establish an early diagnosis of AKI in cardiac surgery patients. Continuing with the close connection between the cardiovascular system and kidney disease, Lim T. et al. performed a single-center retrospective cohort study in which they found that in type 2 diabetic patients, increased peripheral arterial stiffness determined by brachial-ankle pulse wave velocity tests may be risk factor for renal disease progression (HR: 8.480, $p = 0.014$).

OPEN ACCESS

Edited and reviewed by:
Ji-Bin Peng,
University of Alabama at Birmingham, United States

Correspondence:
Natalia López-Andrés
natalia.lopez.andres@navarra.es
Frederic Jaisser
frederic.jaisser@inserm.fr
Jonatan Barrera-Chimal
jbarrera@iibiomedicas.unam.mx

Specialty section:
This article was submitted to Renal and Epithelial Physiology, a section of the journal Frontiers in Physiology

Received: *20 May 2021*
Accepted: *04 June 2021*
Published: *01 July 2021*

Citation:
López-Andrés N, Jaisser F and Barrera-Chimal J (2021) Editorial: Kidney and Distant Organ Crosstalk in Health and Disease. Front. Physiol. 12:712535. doi: 10.3389/fphys.2021.712535

Three review papers addressed the mechanisms linking CKD and cardiovascular complications. Lim K. et al. focused on integrative physiology changes that occur in the CKD patient and that involve multisystemic responses resulting in perturbations of the oxygen transport system, and highlighted the possible application of cardiopulmonary exercise testing to evaluate cardiovascular functional alterations in patients with kidney disease. Junho et al. reviewed the evidence around the role that calcium/calmodulin-dependent protein kinases (CaMKs) play in the cardiorenal syndrome pathology through modulating inflammation and oxidative stress. Though more studies are required, the current evidence points out for a role of CaMKs in CKD-associated cardiac injury. Finally, Lowenstein and Nigam, present an integrative view of the multi-organ effects of uremic toxin accumulation when kidney function is compromised with special focus on the role of uremic toxins and drug transporters in inter-organ communication (intestine-liver-kidney-brain) and inter organismal communication, for example the host with the microbiome.

NOVEL THERAPEUTIC OPTIONS FOR KIDNEY DISEASE

A major complication of diabetes is diabetic kidney disease, for which the therapeutic options are limited (Barrera-Chimal and Jaisser, 2020). Xiao et al. studied the effect of the treatment with oxymatrine (OMT) in renal fibrosis induced by type 2 diabetes in mice. Following 8 weeks of treatment with OMT, diabetic mice presented decreased renal expression of fibrotic markers and increased expression of E-cadherin as an epithelial marker. This protective effect was mediated via upregulation of the inhibitor of differentiation-2 which would bind and inhibit Twist-mediated epithelial to mesenchymal transition. This mechanism was corroborated in tubular epithelial cells cultured in high glucose. Another strategy to target renal fibrosis was tested in the article by Rui-Zhi et al. who showed that the *Astragalus mongholicus* Bunge and Panax notoginseng formula and Bifidobacterium administration has functional and structural renal protective effects in a mouse model of CKD induced by 5/6th nephrectomy through the inhibition of inflammatory M1 macrophages via Mincle/NfkB pathway inhibition in the kidney. Similarly, mincle/NFkB pathway was also inhibited in the intestine, leading to the restoration of the intestinal barrier in CKD mice and a recovery of the intestinal flora similar to the one present in normal mice. Thus, by inhibiting inflammation in both, the kidney and the gut this treatment reduced renal and intestine injury induced by CKD, highlighting the role of inflammation in intestine changes observed during CKD.

Kidney injury is often associated to an imbalance of immune cell activation leading to uncontrolled and chronic inflammatory processes affecting the renal structure and function (Meng et al., 2014). Cell based therapy with T regulatory cells (Treg) as a therapy in kidney disease was studied by Lu J. et al. First, the authors showed that in RNA-seq datasets from mouse and human diseased kidneys, immune system activation related genes are upregulated with a specific enrichment of genes related to Tregs. Increased Treg abundance was confirmed in a mouse model of Adriamycin induced kidney injury. Furthermore, adoptive spleen Treg transfer from healthy to Adriamycin treated mice protected against renal structural injury. Co-culture of Treg with M2c anti-inflammatory macrophages increased Treg expression of chemotactic molecules which could facilitate its recruitment to the inflamed kidney site to resolve inflammation. This data underlines the importance of regulated inflammation in resolving kidney injury.

COMPLICATIONS ASSOCIATED TO ADVANCED CKD PATIENTS IN DIALYSIS

The understanding and characterization of the complications that develop in advanced CKD patients undergoing dialysis is important in order to adequately monitor them and provide a good care to improve survival and life quality of these patients.

Hematological alterations other than anemia are a less explored complication observed in hemodialysis (HD) patients for which the risk factors need to be known by healthcare providers to deliver an accurate management. In a single-center study, Lee et al. explored the risk factors associated to leukopenia or thrombocytopenia in HD patients. Older age (>-60) at dialysis initiation was found to be a predictor for chronic leukopenia and thrombocytopenia, while chronic liver disease and high serum ferritin levels (>800 mg/dL) were risk factors for chronic thrombocytopenia. In patients in maintenance HD, Zhang Y. et al. showed that moderate to severe tricuspid regurgitation occurs in 62.6% of the patients and that sodium, decreased fractional shortening and increased right atrium diameter were independently associated to moderate to severe tricuspid regurgitation. Zhang Q. et al. showed that increased arterial stiffness determined by pulse wave velocity together with high plasma galectin-3 levels predicted mortality and cerebral and cardiovascular events in stable HD patients. These studies are important as proof of concept that these parameters might be used to predict adverse cardiovascular events in CKD patients and further confirmation is required in larger cohorts.

Lu H. et al. present an observational retrospective single-center study to assess the prevalence of hyponatremia in hospitalized patients and its related adverse outcomes. The authors found a prevalence of hyponatremia of 32.5% and was associated with higher hospital costs and length of stay and in-hospital and 30-day mortality.

KIDNEY DISEASE AND NEUROLOGICAL DISORDERS

Kidney disease is often associated to neurological disorders. While the mechanisms remain elusive, ischemic AKI has been associated with a long-term risk of stroke and dementia (Tanaka and Okusa, 2020). In the investigation by Burek et al. the authors created an *in vitro* model to gain insights into the kidney-brain crosstalk during disease. They showed that hypoxic and glucose starved tubular cells co-cultured with brain microvascular endothelial cells (BMEC) on a transwell

system and with the addition of uremic toxins induced changes in the expression of blood brain barrier (BBB) transporters, receptors and tight junction proteins in BMEC. This changes in BBB efflux and influx transporter expression were validated in brain capillaries isolated from mice after 24 h of ischemic AKI induction.

EFFECT OF COVID-19 ON KIDNEY HEALTH

Over the past 18 months, COVID-19 pandemic has affected several millions worldwide. Numerous studies have recognized the kidney as a target for the severe acute respiratory syndrome coronavirus 2 (SARS-CoV-2) (Vijayan and Humphreys, 2020). In a timely analysis, Hong et al. presented the renal function parameters observed in a small cohort of patients diagnosed with COVID-19 at the beginning of the pandemics. Moreover, Zhou et al. performed a meta-analysis including 52 studies to evaluate the effect of COVID-19 on CKD or AKI patients. The prevalence of CKD or AKI was higher in those patients developing severe COVID-19 and in deceased cases vs. survivors. Worse prognosis of COVID-19 is observed in kidney patients, thus, focusing attention on patients with preexisting kidney disease or new kidney injury as a consequence of COVID-19 may help to prevent complications and mortality.

CONCLUSIONS

The contributions to this Research Topic illustrate the complexity of the communication between the kidneys and other organs in health and disease conditions, providing new therapeutic and diagnosis tools, and contributing to mechanistic insights into the connection of kidney disease and distant organ disorders. The review articles also highlight that further efforts are needed in order to gain complete understanding of the molecular processes involved in these pathological connections, which will help to propose novel therapeutic avenues for kidney disease and its associated distant organ injuries.

AUTHOR CONTRIBUTIONS

All authors contributed to the editorial, approved the submitted version, and performed editorial assignments for this Research Topic.

REFERENCES

Ambruso, S. L., Gil, H. W., Fox, B., Park, B., Altmann, C., Bagchi, R. A., et al. (2021). Lung metabolomics after ischemic acute kidney injury reveals increased oxidative stress, altered energy production, and ATP depletion. *Am. J. Physiol. Lung Cell Mol. Physiol.* doi: 10.1152/ajplung.00042.2020

Barrera-Chimal, J., and Jaisser, F. (2020). Pathophysiologic mechanisms in diabetic kidney disease: a focus on current and future therapeutic targets. *Diabetes Obes. Metab.* 22 (Suppl. 1), 16–31. doi: 10.1111/dom.13969

Jager, K. J., Kovesdy, C., Langham, R., Rosenberg, M., Jha, V., and Zoccali, C. (2019). A single number for advocacy and communication-worldwide more than 850 million individuals have kidney diseases. *Kidney Int.* 96, 1048–1050. doi: 10.1016/j.kint.2019.07.012

Lai, H. J., Zhan, Y. Q., Qiu, Y. X., Ling, Y. H., Zhang, X. Y., Chang, Z. N., et al. (2021). HMGB1 signaling-regulated endoplasmic reticulum stress mediates intestinal ischemia/reperfusion-induced acute renal damage. *Surgery.* 170, P239–P248. doi: 10.1016/j.surg.2021.01.042

Malek, M. (2018). Brain consequences of acute kidney injury: focusing on the hippocampus. *Kidney Res. Clin. Pract.* 37, 315–322. doi: 10.23876/j.krcp.18.0056

Meng, X. M., Nikolic-Paterson, D. J., and Lan, H. Y. (2014). Inflammatory processes in renal fibrosis. *Nat. Rev. Nephrol.* 10, 493–503. doi: 10.1038/nrneph.2014.114

O'Neal, J. B., Shaw, A. D., and Billings, F. T. T. (2016). Acute kidney injury following cardiac surgery: current understanding and future directions. *Crit. Care* 20:187. doi: 10.1186/s13054-016-1352-z

Ricci, Z., Romagnoli, S., and Ronco, C. (2021). Cardiorenal syndrome. *Crit. Care Clin.* 37, 335–347. doi: 10.1016/j.ccc.2020.11.003

Ronco, C., Bellasi, A., and Di Lullo, L. (2018). Cardiorenal syndrome: an overview. *Adv. Chronic Kidney Dis.* 25, 382–390. doi: 10.1053/j.ackd.2018.08.004

Shang, Y., Madduma Hewage, S., Wijerathne, C. U. B., Siow, Y. L., Isaak, C. K., and and, O., K. (2020). Kidney ischemia-reperfusion elicits acute liver injury and inflammatory response. *Front. Med.* 7:201. doi: 10.3389/fmed.2020.00201

Tanaka, S., and Okusa, M. D. (2020). Crosstalk between the nervous system and the kidney. *Kidney Int.* 97, 466–476. doi: 10.1016/j.kint.2019.10.032

Vijayan, A., and Humphreys, B. D. (2020). SARS-CoV-2 in the kidney: bystander or culprit? *Nat. Rev. Nephrol.* 16, 703–704. doi: 10.1038/s41581-020-00354-7

Conflict of Interest: The authors declare that the research was conducted in the absence of any commercial or financial relationships that could be construed as a potential conflict of interest.

frontiers in Physiology

ORIGINAL RESEARCH
published: 09 June 2020
doi: 10.3389/fphys.2020.00621

Regulatory T Cells as a Novel Candidate for Cell-Based Therapy in Kidney Disease

Junyu Lu[1,2†], Jianfeng Zhang[3†], Menghua Chen[2], Chun Chen[4], Zhengzhao Li[3] and Pinhu Liao[1,5*]*

[1] The First Clinical Medical College of Jinan University, Guangzhou, China, [2] Intensive Care Unit, The Second Affiliated Hospital of Guangxi Medical University, Nanning, China, [3] Department of Emergency Medicine, The Second Affiliated Hospital of Guangxi Medical University, Nanning, China, [4] Department of Cardiology and Endocrinology, The People's Hospital of Guangxi Zhuang Autonomous Region, Nanning, China, [5] Department of Emergency Medicine, The First Affiliated Hospital of Guangxi Medical University, Nanning, China

OPEN ACCESS

Edited by:
Natalia Lopez-Andres, NavarraBiomed, Spain

Reviewed by:
Bo Wang, Monash University, Australia
Hong Jiang, Zhejiang University, China

***Correspondence:**
Junyu Lu
junyulu@gxmu.edu.cn
Pinhu Liao
liaopinhu@163.com

[†] These authors have contributed equally to this work

Specialty section:
This article was submitted to Renal and Epithelial Physiology, a section of the journal Frontiers in Physiology

Received: *07 April 2020*
Accepted: *18 May 2020*
Published: *09 June 2020*

Citation:
Lu J, Zhang J, Chen M, Chen C, Li Z and Liao P (2020) Regulatory T Cells as a Novel Candidate for Cell-Based Therapy in Kidney Disease. Front. Physiol. 11:621. doi: 10.3389/fphys.2020.00621

Kidney disease is a significant health concern worldwide. Ineffective treatment can lead to disastrous consequences, such as organ failure and death. Research has turned to cell-based therapy, but has yet to produce an effective and reliable treatment for kidney disease. To address this problem, we examined four datasets of gene expression profiles from diseased and healthy kidney tissue in humans, mice, and rats. Differentially expressed genes (DEGs) were screened and subjected to enrichment analyses. Up-regulated genes in diseased kidney tissue were significantly enriched in pathways associated with regulatory T cells (Tregs). Analysis with the xCell tool showed that Tregs were generally increased in diseased kidney tissue in all species. To validate these results *in vivo*, kidneys were removed from mice with Adriamycin-induced nephropathy, and histology confirmed increase of Tregs. Furthermore, Tregs were adoptively transferred from healthy mice into mice with kidney injury, restoring normal structure to the damaged kidneys. Treg cells that were co-cultured with M2c macrophages exhibited up-regulation of chemokine receptors CCR2, CCR5, CCR7, CD62L, and CX3CR1. This may be the mechanism by which M2c cells enhance the migration of Tregs to the site of inflammation. We propose that Tregs may be an effective, novel candidate for cell-based therapy in pre-clinical kidney injury models.

Keywords: regulatory T cell, Treg, M2c macrophage, cell-based therapy, kidney injury

INTRODUCTION

Kidney disease has become a significant global public health problem, with incidence and mortality rates increasing in recent decades (Lentine et al., 2017; Fraser and Roderick, 2019). Renal failure is associated with age (Kazancioglu, 2013) and it affects both men and women (Iseki, 2005). Acute kidney injury (AKI) can increase the risk of chronic kidney disease (CKD), which can eventually

lead to end-stage renal disease (Chawla and Kimmel, 2012). The prevalence of AKI is approximately 1.9% in all hospitalized patients and more than 40% in the intensive care unit (Liangos et al., 2006) while the prevalence of CKD is estimated to be 8–16% worldwide (Jha et al., 2013). Though kidney injury is relatively common, there is no specific treatment for it, and most therapies target the underlying disease. Thus, treatment for kidney injury remains a significant challenge for clinicians (Bagshaw and Bellomo, 2007; Jha et al., 2013) and new effective therapeutic strategies are urgently need.

Cell-based regenerative therapy has been extensively evaluated as a treatment for kidney injury in animal models (Fang et al., 2012; Van Koppen et al., 2012; Zhu et al., 2013). Thus far, mesenchymal stem cells and endothelial progenitor cells have been most studied (Papazova et al., 2015). However, a clinical trial giving allogenic mesenchymal stem cells to patients with AKI did not accelerate functional recovery (Swaminathan et al., 2018). Therefore, investigating other candidate cell types is necessary. It is widely recognized that kidney injury is closely related to the immune system and immune cells (Sato and Yanagita, 2018) yet this avenue has not been thoroughly evaluated. We hypothesized that immune cells may be potential candidates for cell-based therapy against kidney injury. Indeed, we show in the present study that the proportion of regulatory T cells (Tregs) was higher in injured kidney tissue than in healthy kidney tissue. We confirmed these findings in mice with Adriamycin-induced nephropathy, suggesting that adoptive transfer of Tregs can improve injury. In addition, we observed *in vitro* that M2c macrophages up-regulate chemokine receptors in Tregs, which may recruit Tregs to sites of inflammation in injured kidney.

MATERIALS AND METHODS

Prediction of Genes Associated With AKI or CKD

We downloaded the following four gene expression datasets from the Gene Expression Omnibus (GEO) database[1]: (1) GSE12682 (Si et al., 2009) comparing human kidney tissue between 29 healthy controls and 23 CKD samples, measured by the Affymetrix Human Genome U133A 2.0 Array (Affymetrix; Thermo Fisher Scientific, Waltham, MA, United States); (2) GSE12683 (Si et al., 2009) comparing Balb/c mouse kidney tissue between 10 healthy controls and 10 samples with AKI, measured by Affymetrix Mouse Genome 430A 2.0 Array; (3) GSE102513 (Vandenbussche et al., 2018) comparing CD-1 mouse kidney tissue between four healthy controls and four samples CKD induced by Tacrolimus (1 mg/kg/day for 28 days), measured by the Agilent-028005 SurePrint G3 Mouse GE 8x60K Microarray; and (4) GSE85957 (Pavkovic et al., 2014) comparing *Rattus norvegicus* (brown rat) kidney tissue samples between 19 healthy controls and 38 rats with kidney disease induced with 1 or 3 mg/kg cisplatin. In this last dataset, tissue was collected on days 3, 5, 8, and 26, and gene expression was measured using the Rat Genome 230 2.0 Array.

[1]www.ncbi.nlm.nih.gov/geo

If one gene matched multiple probes, the average value of all probes was calculated as the expression of the corresponding gene. All sample collection and experimentation procedures were approved by the Guangxi Medical University Ethics Committee.

Screening of Differentially Expressed Genes (DEGs) and Functional Enrichment Analysis

Differentially expressed genes (DEGs) between healthy control and diseased human kidney tissue were identified using the *limma* package (Ritchie et al., 2015) in R from dataset GSE12682. Differential threshold was calculated based on two criteria: false discovery rate (FDR) P-value < 0.05 and $|\log_2(\text{fold change})| > 1$. The *ClusterProfiler* package (Yu et al., 2012) in R was used to assess enrichment in biological processes (BPs) and Kyoto Encyclopedia of Genes and Genomes (KEGG) pathways. Gene set enrichment was analyzed using the JAVA program[2] based on MSigDB immunologic signatures (*c7.all.v6.2.symbols.gmt*) (Godec et al., 2016). Gene sets with a NOM P-value < 0.05 after performing 1000 permutations were considered to be significantly enriched (Subramanian et al., 2005).

Immune Cell Enrichment Analysis

We used xCell web tool[3] (Aran et al., 2017) with Charoentong signature (Charoentong et al., 2017) to generate cell enrichment scores based on gene signature profiles. Then these data were used to quantify immune cell proportions in all four datasets. Enrichment scores were compared using Student's t-test, and $P < 0.05$ was considered to indicate a significant difference.

Mouse Model of Kidney Injury

Animal experiments were approved by the Guangxi Medical University Ethics Committee. C57BL/six mice (8 weeks old, 20 ± 2 g) were purchased from the Experimental Animal Center of Guangxi Medical University. Mice were randomly divided into a control group ($n = 27$) and a treatment group ($n = 27$). The treatment group received 10.5 mg/kg Adriamycin (Zhejiang Hisun Pharmaceutical, Taizhou, China) three times per week for 2 weeks via the tail vein (Lu et al., 2013). The control group received injections of physiological saline via the tail vein. Urine was collected for 16 h overnight on day 27 for measurement of urinary protein. Blood was obtained on day 28 for measurement of serum creatinine and creatinine clearance. All urine and blood specimens were analyzed using automated analyzers at the Experimental Animal Center of Guangxi Medical University. Animals were sacrificed using cervical dislocation on day 28, and kidneys and spleens were removed for further study.

Preparation of Cell Suspensions

Kidneys were perfused with saline before removal, cut into 1–2 mm^3 pieces and digested in Dulbecco's modified Eagle medium (DMEM) containing 1 mg/ml collagenase IV (Sigma–Aldrich) and 100 mg/ml DNase I (Roche) for 40 min at 37°C with

[2]http://www.broadinstitute.org/gsea

[3]http://xcell.ucsf.edu/

intermittent agitation. The digested cell suspension was then passed through a 40-μm cell strainer. Mononuclear cells were separated using 1.077 g/ml NycoPrep gradient (Axis-Shield, Oslo, Norway). Spleens from C57BL/6 mice were also isolated, minced, and digested for 30 min at 37°C in RPMI 1640 containing 1 mg/ml collagenase D and 100 mg/ml DNase I (both from Roche). The digested cell suspension was passed through a 40-μm cell strainer.

Flow Cytometry and Cell Sorting

Single-cell suspensions from kidney were subjected to magnetic bead separation, and CD3+ cells were purified using the CD3+ T cell kit (Miltenyi Biotec, Bergisch Gladbach, Germany). The surface of CD3+ cells was labeled with antibodies against CD25 and FOXP3 (BD Accuri C6, United States). Double-positive cells were considered Tregs and were sorted using a flow cytometer (BD Accuri C6, United States) according to the manufacturer's instructions.

Mouse Model of Adoptive Cell Transfer

Tregs were extracted from spleens of healthy C57BL/six mice, and single-cell suspensions were prepared as in Section "Preparation of Cell Suspensions." Cells were incubated *in vitro* in RPMI 1640 medium and allowed to proliferate for 7 days. Approximately 1.2×10^6 Tregs were injected via the tail vein into mice on day 5 after Adriamycin administration.

Tissue Histology and Immunofluorescence

All mice were sacrificed on day 28. Coronal sections of renal tissue were stained with rat anti-mouse CD103 antibody (M290, 1:200) and hamster anti-mouse CD11c antibody (N418, 1:100), then incubated with AF488-conjugated goat anti-rat IgG or AF546-conjugated goat anti-hamster IgG antibody (both 1:500). Tissue sections were analyzed on an inverted fluorescence microscope (BX50, Olympus). Consecutive sections from kidney cortex to kidney medulla were photographed.

In vitro Co-cultures

Bone marrow from the femurs of C57BL/6 mice was harvested and triturated with sterile syringes, and the resulting cell suspension was filtered through 40-μm nylon mesh. Approximately 2×10^6 cells were incubated in RPMI 1640 containing 50 ng/ml granulocyte-macrophage colony stimulating factor (GM-CSF) at 37°C for 10 days. The adherent marrow-derived macrophages (M0) were rinsed three times in RPMI 1640 medium and then incubated in RPMI 1640 medium containing

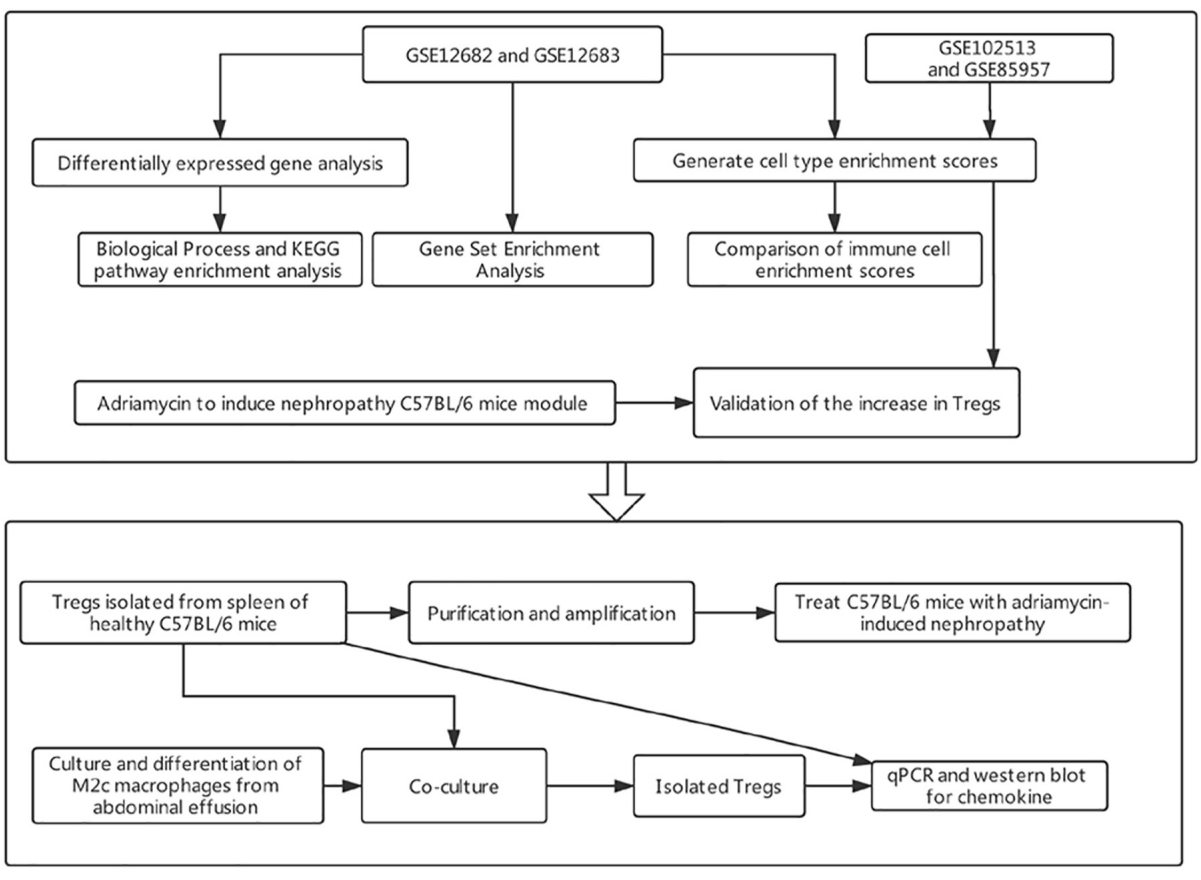

FIGURE 1 | The work flow of the present study. KEGG, Kyoto Encyclopedia of Genes and Genomes.

both IL-10 and TGF-β (10 ng/ml each) for 4 days to become M2c macrophages (Lu et al., 2013).

For co-culture experiments, M2c macrophages (1×10^6 cells/ml) were plated in six-well plates with 1.5 ml of Tregs (1×10^6 cells/ml). Co-cultures were incubated for 24 h at 37°C and 5% CO_2. Control cultures contained only Tregs. After 24 h, the floating Tregs were collected, washed in RPMI 1640, and used in subsequent experiments.

PCR Array and Quantitative PCR (qPCR)

Total RNA was extracted from control and co-cultured Tregs using the TRIzol RNeasy kit (Invitrogen, Shanghai, China), then reverse-transcribed using the Superscript IV reverse transcription Kit (Invitrogen). Quantitative PCR was performed using the SYBR qPCR (Invitrogen) master mix according to the manufacturer's instructions. The primer list is shown in **Supplementary Table S1**.

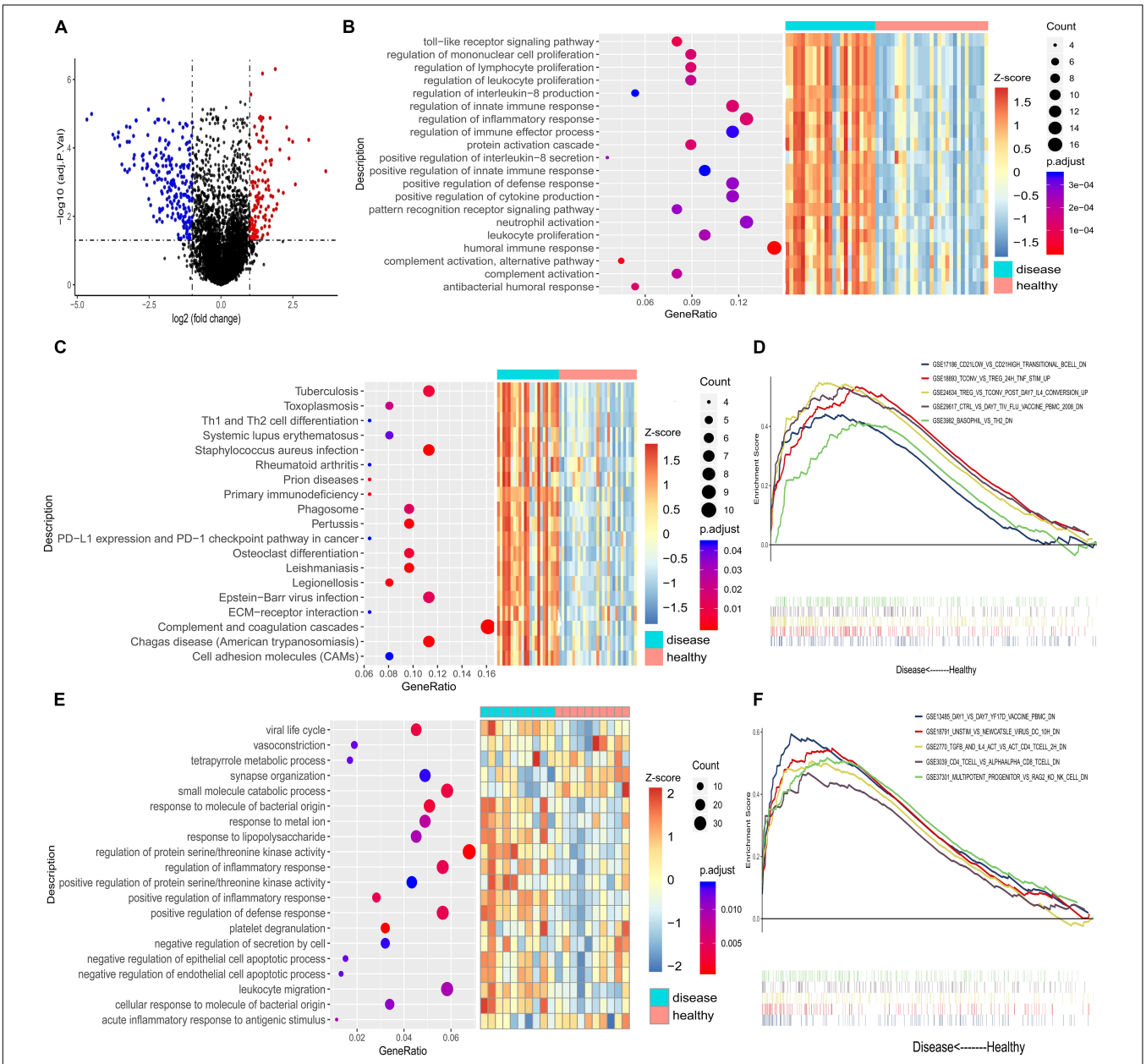

FIGURE 2 | (A) Volcano plot of the genes differentially expressed between chronic kidney disease tissue and healthy kidney tissue from humans (dataset GSE12682). Red indicates that a gene is up-regulated in chronic kidney disease, while blue indicates that it is down-regulated. **(B)** The 15 most significantly enriched biological processes from the up-regulated genes in GSE12682. **(C)** Enriched KEGG pathways for the up-regulated genes in GSE12682. **(D)** The five most significantly enriched gene sets in chronic kidney disease in GSE12682. **(E)** The 15 most significantly enriched biological processes for the up-regulated genes from Balb/c mice (dataset GSE12683). **(F)** The five most significantly enriched gene sets in Adriamycin-induced kidney injury in GSE12683.

Western Blotting

Total protein was extracted from control and co-cultured Tregs using 200 μL ice-cold RIPA lysis buffer (catalog no. R0010, Solarbio, Beijing, China) at 4°C for 2 min and centrifuged. The supernatant was collected, protein concentration was estimated using a BCA kit (Solarbio, Beijing, China), and an equal amount of total protein in each sample was mixed with 5 μl of 5× SDS buffer and 2 μl of reducing agent (Invitrogen), then boiled at 70°C for 10 min. Samples were loaded onto a sodium dodecyl sulfate-polyacrylamide gel (8–12% gradient), then transferred onto polyvinylidene fluoride membranes. Membranes were immunoblotted using antibodies (Abcam, Cambridge, United Kingdom) against the following proteins: GADPH (catalog no. ab9484), CCR2 (ab203128), CCR7 (ab32527), CCR8 (ab63772), CD62L (ab264045), and CX3CR1 (ab8021). The secondary antibody was horseradish peroxidase-conjugated goat anti-rabbit IgG H&L (ab205718). GADPH protein was used as the internal control. Bands were developed using the ECL Western Blotting Analysis System (Amersham, Sweden) and visualized with FluorChem E ProteinSimple (ProteinSimple, United States).

Statistical Analysis

Statistical tests included the unpaired, two-tailed *t*-test using Welch's correction for unequal variances and one-way ANOVA with Tukey's multiple comparisons test. Statistical analyses were performed using Prism software (version 5, GraphPad) and R software (version 3.5.3). Results were expressed as mean ± SEM. Differences associated with $P < 0.05$ were considered statistically significant.

RESULTS

The study workflow is presented in **Figure 1**.

Immune System-Related Genes Are Up-Regulated After Kidney Injury

In human kidney tissue (GSE12682), we found a total of 345 DEGs by comparing healthy control tissue with CKD tissue (**Figure 2A**), of which 123 genes were up-regulated and 222 down-regulated. The down-regulated genes were enriched in various renal system development-related BPs and KEGG pathways (**Supplementary Tables S2, S3**), whereas up-regulated genes were immune-related (**Figures 2B,C**). Although no DEGs were identified in Balb/c mice (GSE12683) using the initial threshold (FDR $P < 0.05$ and $|\log_2(\text{fold change})| > 1$), using a less stringent threshold ($P < 0.05$) identified 660. These included 330 up-regulated genes enriched in various immune-related BPs (**Figure 2E**). These results suggest that genes of the immune system are activated in injured kidney, and that identification of immune cells associated with these up-regulated genes may provide candidate therapeutic targets against kidney injury.

Tregs Enriched in Injured Kidney

Gene set enrichment analysis confirmed that among the up-regulated immune-associated gene sets, those associated with

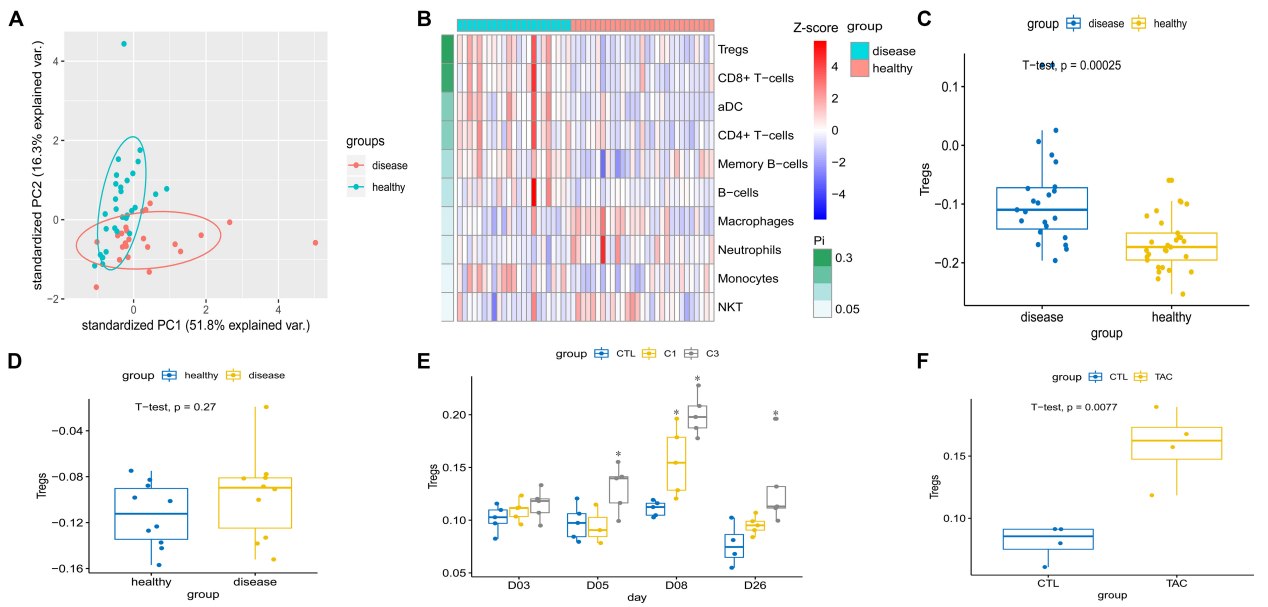

FIGURE 3 | (A) Principal component analysis showed a significant difference in the immune cell population between chronic kidney disease tissue and healthy kidney tissue in humans (dataset GSE12682). **(B)** Heatmap depicting abundance of different immune cell types between chronic kidney disease and healthy kidney in GSE12682. Enrichment analysis of Treg-related genes was calculated and numbers of cells extrapolated for **(C)** chronic kidney disease compared to healthy kidney in humans (GSE12682), **(D)** Adriamycin-induced kidney injury compared to healthy kidney in Balb/c mice (GSE12683), and **(E)** cisplatin-induced kidney injury compared to healthy kidney in rat (GSE85957). *$P < 0.05$ versus control. **(F)** Tacrolimus-induced kidney injury compared to healthy kidney in CD-1 mice (GSE102513). C1, 1 mg/kg cisplatin; C3, 3 mg/kg cisplatin; var., variance; CTL, control; TAC, tacrolimus.

Tregs were significantly enriched in both human CKD tissues (**Figure 2D**) and mouse AKI tissues (**Figure 2F**). Extraction of genetic profiles associated with different immune cells from all datasets and scoring them for enrichment (**Figure 3A** and **Supplementary Table S4**) further confirmed Tregs to be more abundant in diseased kidney tissue than in healthy control tissue from humans, mice, or rats, regardless of the cause of tissue injury (**Figures 3B–F**).

Tregs Are Increased in Kidneys From Adriamycin-Induced Injury Mouse Models

Histology confirmed Adriamycin-induced structural kidney injury in mice (**Figure 4A**), including glomerular sclerosis, tubular atrophy, and interstitial expansion. Severe functional injury was indicated by increased serum creatinine (**Figure 4B**) and proteinuria (**Figure 4C**), as well as reduced creatinine clearance (**Figure 4D**). Numbers of CD4+ CD25+ Tregs were significantly higher in Adriamycin-injured kidneys than in control kidneys (5.1 versus 0.7%) (**Figure 4E**).

Tregs Can Protect Against Induced Kidney Injury

To examine whether the influx of Tregs mitigates or aggravates pre-existing kidney damage, we used a mouse model of adoptive cell transfer. CD4+ CD25+ Tregs were isolated from spleens of healthy mice and expanded *in vitro* (**Figures 5A,B**). Treg cultures of 90% purity were injected via the tail vein into mice with Adriamycin-induced kidney injury (**Figure 5C**). Kidneys were isolated on day 28 after Adriamycin administration and histology revealed that large numbers of Tregs had been recruited to the injured kidney, such that Tregs were more abundant in injured kidney than in healthy kidney (**Figure 5D**). Fluorescence imaging (**Figure 5E**) and histological imaging (**Figure 5F**) showed that adoptive transfer of Tregs aided recovery of structural defects in the kidney injury model.

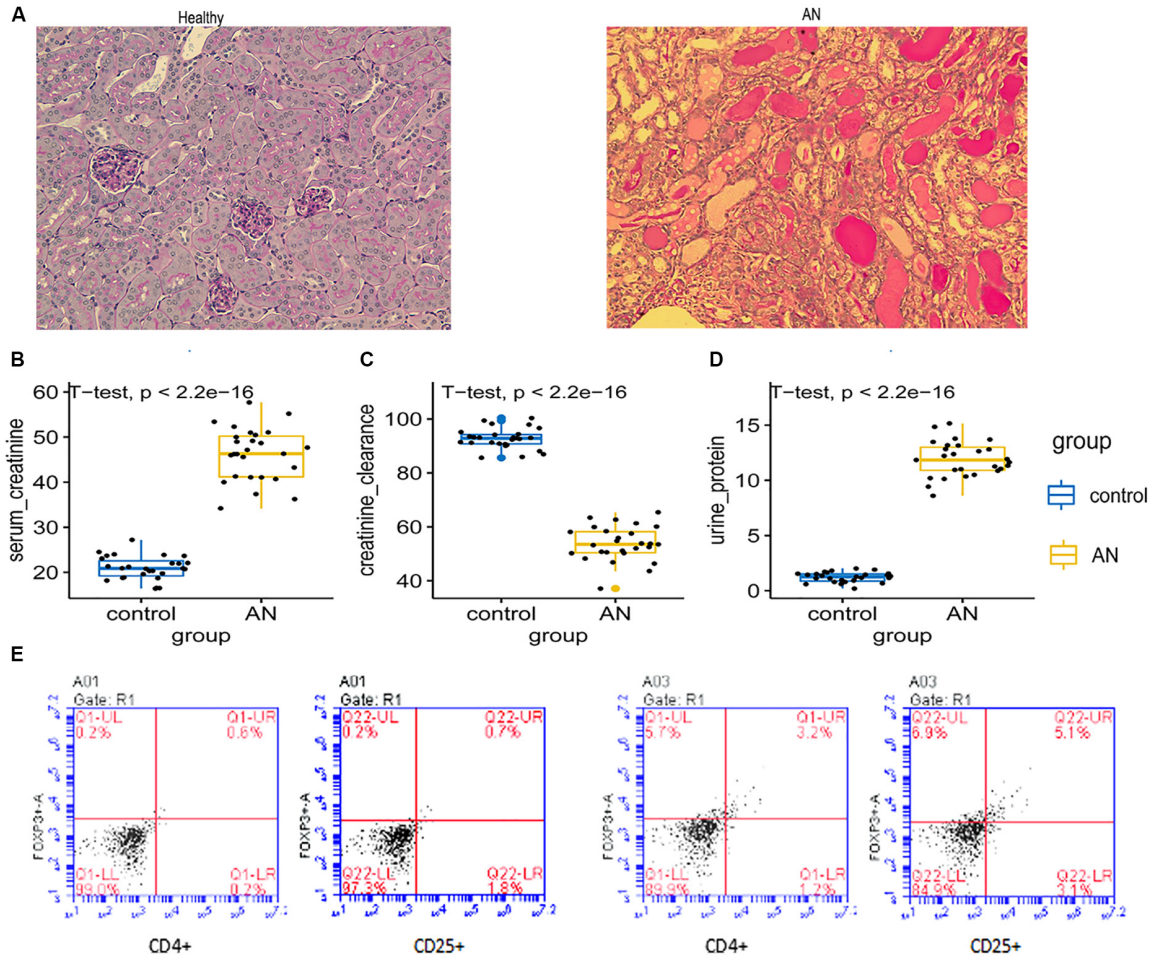

FIGURE 4 | (A) Histology of kidney with Adriamycin-induced nephropathy showed severe structural injury, in contrast to healthy control kidney. **(B–D)** Serum creatinine, urine protein, and creatinine clearance were assessed in control mice and mice with Adriamycin-induced nephropathy. **(E)** Dot plots from flow cytometry showing numbers of CD4+ CD25+ Tregs isolated from control kidney and kidney with Adriamycin-induced nephropathy. Percentages of cells are indicated within each quadrant. LL, lower left; LR, lower right; Q, quadrant; UL, upper left; UR, upper right.

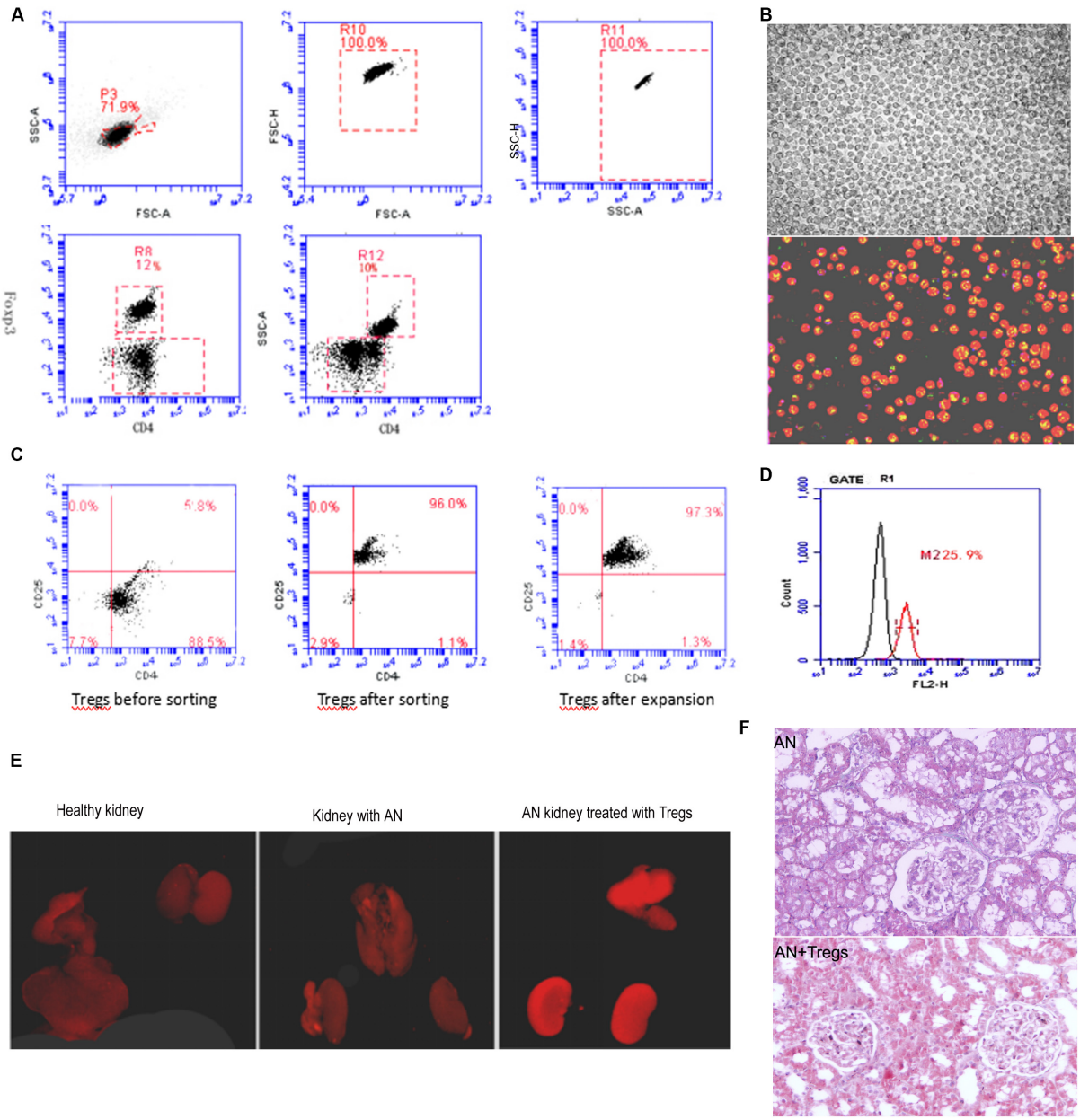

FIGURE 5 | (A) Dot plots from flow cytometry showing numbers of CD4+ CD25+ Tregs isolated from spleens of healthy mice. **(B)** Increase in Treg numbers after *in vitro* amplification. **(C)** Dot plots from flow cytometry showing purity of CD4+ CD25+ Tregs after amplification. **(D)** Flow cytometry histogram depicting Treg numbers isolated from mice with Adriamycin-induced nephropathy in which Tregs from healthy donors had been adoptively transferred. **(E)** Fluorescence images of kidneys from control mice, mice with Adriamycin-induced nephropathy, and mice with nephropathy after treatment with Tregs from healthy donors. **(F)** Histological examination suggested that kidney with AN treated with Tregs show less damage than AN. AN, Adriamycin-induced nephropathy.

M2c Macrophages May Enhance the Therapeutic Effects of Tregs

M2c macrophages may induce Tregs to prevent Adriamycin-induced injury in mice (Kinsey et al., 2012). Indeed, we found that Tregs co-cultured with M2c macrophages showed significant up-regulation of chemokines CCR2, CCR5, CCR7, CD62L, CX3CR1 at the mRNA level (**Figures 6A–C**) and protein level (**Figures 6B,C**). M2c macrophages may promote the protective effects of Tregs in kidney by increasing expression of these chemokines.

DISCUSSION

Despite the global health burden due to kidney injury, treatments are seriously lacking. In end-stage renal failure, patients require a kidney transplant. However, because of shortages in donor

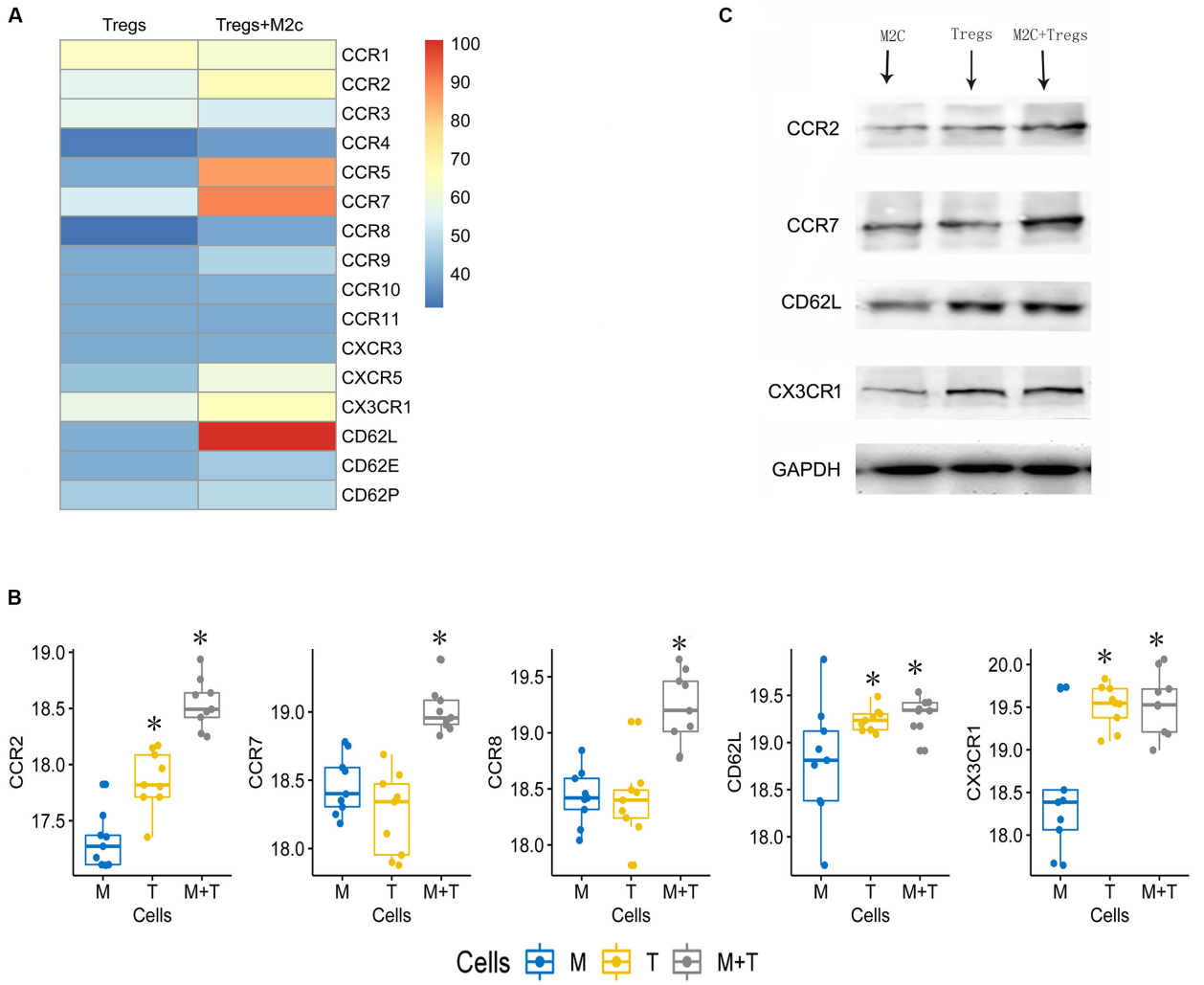

FIGURE 6 | (A) Heatmap showing expression of 16 chemokines in Tregs cultured alone or together with M2c macrophages. **(B,C)** Western blot validation of the chemokine up-regulation observed in panel. M, M2c macrophages; T, regulatory T cells. *$P < 0.05$ versus M2c macrophages.

organs, most of these patients rely on hemodialysis—but even this intervention has limited success in improving survival (Lameire et al., 2009; Ortiz et al., 2014). In recent years, cell-based therapy in various animal models has shown promise for slowing the progression of kidney disease (Togel and Westenfelder, 2012). In the present study, we found that genes up-regulated in injured kidney tissue are significantly enriched in immune-related BPs and pathways, especially those associated with Tregs. This suggests that the immune system is activated after kidney injury. Tregs were generally increased in injured kidney tissue, including CKD samples from humans (GSE12682) and mice (GSE102513), AKI samples from mice (GSE12682), and CKD samples from rat (GSE85957). We were unable to find publicly available gene expression profiles of Adriamycin-induced kidney injury. Then we validated the increase of Tregs in mice with Adriamycin-induced kidney injury, a model we selected because of its usefulness in studying the pathogenesis and progression of this condition (Lu et al., 2013; Cao et al., 2016) and because it involves inflammatory reactions that mimic those in both AKI and CKD (Chawla and Kimmel, 2012; Coca et al., 2012). We further showed that adoptive Treg transfer from healthy mice into Adriamycin-treated animals protected against kidney injury. In addition, we found evidence that M2c macrophages work synergistically with Tregs to combat kidney injury by enhancing expression of chemokines in Tregs, which likely recruits more Tregs to sites of inflammation (Zhang et al., 2009).

A previous meta-analysis study indicated that cell-based therapies improved renal function and morphology in preclinical models of CKD (Papazova et al., 2015). Unlike our study, that meta-analysis included mesenchymal stem cells, endothelial progenitor cells, hematopoietic stem cells, and bone marrow cells (Papazova et al., 2015) so the included studies involved a diversity of disease models. Mesenchymal stem cell-based therapy has been shown to improve renal function and recovery of damaged renal tissues in animal studies (Yun and Lee, 2019), but it has yet to produce strong positive results in clinical trials

(Yun and Lee, 2019). Most clinical studies using hematopoietic stem cell therapy have focused on lupus nephritis and have lacked a control group or randomization (El-Ansary et al., 2012; Alchi et al., 2013). The present study shows, through systematic analysis of different types of kidney injury in different species, that harnessing Tregs may be a strategy to treat kidney disease. We validated this hypothesis using mice with Adriamycin-induced kidney injury. Future work should identify whether other types of immune cells than Tregs also inhibit abnormal immune processes and promote kidney repair (Dong et al., 2019). If so, combining Tregs with these other cell type(s) may be an even more effective treatment.

Indeed, our own previous work showed that alternatively activated macrophages (M2 phenotype), including M2a and M2c subpopulations, exhibit anti-inflammatory functions *in vitro* and protect against renal injury *in vivo* (Wang et al., 2007). M2c macrophages appear to protect against renal injury better than M2a macrophages because of their ability to induce Tregs (Lu et al., 2013). We provide evidence here that M2c macrophages may increase CCR2, CCR5, CCR7, CD62L, and CX3CR1 expression in Tregs. This may be one of the mechanisms by which M2c cells recruit Tregs. Future work should explore whether these macrophages can promote the efficacy of Treg-based kidney therapies.

Although the current study provides data supporting a novel cell-based treatment of kidney injury, it has some limitations. First, we assessed the effects of Tregs on injured kidney purely in morphological terms, so future work should seek to explain the molecular basis of this structural recovery, such has by identifying changes in gene expression, particularly of genes involved in fibrosis. Second, we did not begin to assess the safety of adoptive Treg transfer; future work should verify and extend our adoptive transfer studies by including control animals treated with other cell types such as red blood cells. We suspect that the anti-inflammatory Tregs may induce adverse effects similar to those of immunosuppressive drugs. Those studies should also test Treg therapy in other models of kidney injury.

CONCLUSION

Tregs are a potential candidate for cell-based treatment of kidney disease. The relationship between M2c macrophages and Tregs should be explored as a potential way to increase therapeutic efficacy.

DATA AVAILABILITY STATEMENT

All datasets presented in this study are included in the article/**Supplementary Material**.

ETHICS STATEMENT

The animal study was reviewed and approved by Guangxi Medical University.

AUTHOR CONTRIBUTIONS

JL and JZ designed and coordinated the study and prepared the manuscript. MC and ZL provided assistance in the design of the study and participated in manuscript preparation. CC and PL participated in data gathering. All authors have read and approved the content of the manuscript.

FUNDING

This study was supported by the National Natural Science Foundation of China (Grant Nos. 81660132, 81760350, and 81560321), the Young Scientists Fund of the Natural Science Foundation of Guangxi (Grant No. 2017GXNSFBA198043), and the Reserve Cadre Training Program Science Foundation of The Second Affiliated Hospital of Guangxi Medical University (Grant Nos. HBRC201804 and HBRC201805).

ACKNOWLEDGMENTS

The authors would like to thank Life-Ontology Biological Technology (Nanning, China) for assisting with bioinformatics analysis.

SUPPLEMENTARY MATERIAL

The Supplementary Material for this article can be found online at: https://www.frontiersin.org/articles/10.3389/fphys.2020.00621/full#supplementary-material

REFERENCES

Alchi, B., Jayne, D., Labopin, M., Demin, A., Sergeevicheva, V., Alexander, T., et al. (2013). Autologous haematopoietic stem cell transplantation for systemic lupus erythematosus: data from the european group for blood and marrow transplantation registry. *Lupus* 22, 245–253. doi: 10.1177/0961203312470729

Aran, D., Hu, Z., and Butte, A. J. (2017). xCell: digitally portraying the tissue cellular heterogeneity landscape. *Genome Biol.* 18:220.

Bagshaw, S. M., and Bellomo, R. (2007). Early diagnosis of acute kidney injury. *Curr. Opin. Crit. Care* 13, 638–644.

Cao, Q., Lu, J., Li, Q., Wang, C., Wang, X. M., Lee, V. W., et al. (2016). CD103+ Dendritic cells elicit CD8+ T cell responses to accelerate kidney injury in adriamycin nephropathy. *J. Am. Soc. Nephrol.* 27, 1344–1360. doi: 10.1681/asn.2015030229

Charoentong, P., Finotello, F., Angelova, M., Mayer, C., Efremova, M., Rieder, D., et al. (2017). Pan-cancer immunogenomic analyses reveal genotype-immunophenotype relationships and predictors of response to checkpoint blockade. *Cell Rep.* 18, 248–262. doi: 10.1016/j.celrep.2016.12.019

Chawla, L. S., and Kimmel, P. L. (2012). Acute kidney injury and chronic kidney disease: an integrated clinical syndrome. *Kidney Int.* 82, 516–524. doi: 10.1038/ki.2012.208

Coca, S. G., Singanamala, S., and Parikh, C. R. (2012). Chronic kidney disease after acute kidney injury: a systematic review and meta-analysis. *Kidney Int.* 81, 442–448. doi: 10.1038/ki.2011.379

Dong, Q., Cai, C., Gao, F., Chen, P., Gong, W., and Shen, M. (2019). Defective Treg response in acute kidney injury was caused by a reduction in TIM-3(+) Treg cells. *Immunol. Invest.* 48, 27–38. doi: 10.1080/08820139.2018.1493497

El-Ansary, M., Saadi, G., and Abd El-Hamid, S. M. (2012). Mesenchymal stem cells are a rescue approach for recovery of deteriorating kidney function. *Nephrology* 17, 650–657. doi: 10.1111/j.1440-1797.2012.01622.x

Fang, Y., Tian, X., Bai, S., Fan, J., Hou, W., Tong, H., et al. (2012). Autologous transplantation of adipose-derived mesenchymal stem cells ameliorates streptozotocin-induced diabetic nephropathy in rats by inhibiting oxidative stress, pro-inflammatory cytokines and the p38 MAPK signaling pathway. *Int. J. Mol. Med.* 30, 85–92.

Fraser, S. D. S., and Roderick, P. J. (2019). Kidney disease in the global burden of disease study 2017. *Nat. Rev. Nephrol.* 15, 193–194. doi: 10.1038/s41581-019-0120-0

Godec, J., Tan, Y., Liberzon, A., Tamayo, P., Bhattacharya, S., Butte, A. J., et al. (2016). Compendium of immune signatures identifies conserved and species-specific biology in response to inflammation. *Immunity* 44, 194–206. doi: 10.1016/j.immuni.2015.12.006

Iseki, K. (2005). Factors influencing the development of end-stage renal disease. *Clin. Exp. Nephrol.* 9, 5–14. doi: 10.1007/s10157-005-0341-3

Jha, V., Garcia-Garcia, G., Iseki, K., Li, Z., Naicker, S., Plattner, B., et al. (2013). Chronic kidney disease: global dimension and perspectives. *Lancet* 382, 260–272.

Kazancioglu, R. (2013). Risk factors for chronic kidney disease: an update. *Kidney Int. Suppl.* 3, 368–371. doi: 10.1038/kisup.2013.79

Kinsey, G. R., Huang, L., Jaworska, K., Khutsishvili, K., Becker, D. A., Ye, H., et al. (2012). Autocrine adenosine signaling promotes regulatory T cell-mediated renal protection. *J. Am. Soc. Nephrol.* 23, 1528–1537. doi: 10.1681/asn.2012010070

Lameire, N., Van Biesen, W., and Vanholder, R. (2009). Did 20 years of technological innovations in hemodialysis contribute to better patient outcomes? *Clin. J. Am. Soc. Nephrol.* 4(Suppl. 1), S30–S40.

Lentine, K. L., Kasiske, B. L., Levey, A. S., Adams, P. L., Alberu, J., Bakr, M. A., et al. (2017). Summary of kidney disease: improving global outcomes (KDIGO) clinical practice guideline on the evaluation and care of living kidney donors. *Transplantation* 101, 1783–1792. doi: 10.1097/tp.0000000000001770

Liangos, O., Wald, R., O'bell, J. W., Price, L., Pereira, B. J., and Jaber, B. L. (2006). Epidemiology and outcomes of acute renal failure in hospitalized patients: a national survey. *Clin. J. Am. Soc. Nephrol.* 1, 43–51. doi: 10.2215/cjn.00220605

Lu, J., Cao, Q., Zheng, D., Sun, Y., Wang, C., Yu, X., et al. (2013). Discrete functions of M2a and M2c macrophage subsets determine their relative efficacy in treating chronic kidney disease. *Kidney Int.* 84, 745–755. doi: 10.1038/ki.2013.135

Ortiz, A., Covic, A., Fliser, D., Fouque, D., Goldsmith, D., Kanbay, M., et al. (2014). Epidemiology, contributors to, and clinical trials of mortality risk in chronic kidney failure. *Lancet* 383, 1831–1843. doi: 10.1016/s0140-6736(14)60384-6

Papazova, D. A., Oosterhuis, N. R., Gremmels, H., Van Koppen, A., Joles, J. A., and Verhaar, M. C. (2015). Cell-based therapies for experimental chronic kidney disease: a systematic review and meta-analysis. *Dis. Model. Mech.* 8, 281–293. doi: 10.1242/dmm.017699

Pavkovic, M., Riefke, B., Gutberlet, K., Raschke, M., and Ellinger-Ziegelbauer, H. (2014). Comparison of the mesoscale discovery and luminex multiplex platforms for measurement of urinary biomarkers in a cisplatin rat kidney injury model. *J. Pharmacol. Toxicol. Methods* 69, 196–204. doi: 10.1016/j.vascn.2013.11.003

Ritchie, M. E., Phipson, B., Wu, D., Hu, Y., Law, C. W., Shi, W., et al. (2015). limma powers differential expression analyses for RNA-sequencing and microarray studies. *Nucleic Acids Res.* 43:e47. doi: 10.1093/nar/gkv007

Sato, Y., and Yanagita, M. (2018). Immune cells and inflammation in AKI to CKD progression. *Am. J. Physiol. Renal Physiol.* 315, F1501–F1512.

Si, H., Banga, R. S., Kapitsinou, P., Ramaiah, M., Lawrence, J., Kambhampati, G., et al. (2009). Human and murine kidneys show gender- and species-specific gene expression differences in response to injury. *PLoS One* 4:e4802. doi: 10.1371/journal.pone.0004802

Subramanian, A., Tamayo, P., Mootha, V. K., Mukherjee, S., Ebert, B. L., Gillette, M. A., et al. (2005). Gene set enrichment analysis: a knowledge-based approach for interpreting genome-wide expression profiles. *Proc. Natl. Acad. Sci. U.S.A.* 102, 15545–15550. doi: 10.1073/pnas.0506580102

Swaminathan, M., Stafford-Smith, M., Chertow, G. M., Warnock, D. G., Paragamian, V., Brenner, R. M., et al. (2018). Allogeneic mesenchymal stem cells for treatment of AKI after cardiac surgery. *J. Am. Soc. Nephrol.* 29, 260–267. doi: 10.1681/asn.2016101150

Togel, F. E., and Westenfelder, C. (2012). Kidney protection and regeneration following acute injury: progress through stem cell therapy. *Am. J. Kidney Dis.* 60, 1012–1022. doi: 10.1053/j.ajkd.2012.08.034

Van Koppen, A., Joles, J. A., Bongartz, L. G., Van Den Brandt, J., Reichardt, H. M., Goldschmeding, R., et al. (2012). Healthy bone marrow cells reduce progression of kidney failure better than CKD bone marrow cells in rats with established chronic kidney disease. *Cell Transpl.* 21, 2299–2312. doi: 10.3727/096368912x636795

Vandenbussche, C., Van Der Hauwaert, C., Dewaeles, E., Franczak, J., Hennino, M. F., Gnemmi, V., et al. (2018). Tacrolimus-induced nephrotoxicity in mice is associated with microRNA deregulation. *Arch. Toxicol.* 92, 1539–1550. doi: 10.1007/s00204-018-2158-3

Wang, Y., Wang, Y. P., Zheng, G., Lee, V. W., Ouyang, L., Chang, D. H., et al. (2007). Ex vivo programmed macrophages ameliorate experimental chronic inflammatory renal disease. *Kidney Int.* 72, 290–299. doi: 10.1038/sj.ki.5002275

Yu, G., Wang, L. G., Han, Y., and He, Q. Y. (2012). clusterProfiler: an R package for comparing biological themes among gene clusters. *OMICS* 16, 284–287. doi: 10.1089/omi.2011.0118

Yun, C. W., and Lee, S. H. (2019). Potential and therapeutic efficacy of cell-based therapy using mesenchymal stem cells for acute/chronic kidney disease. *Int. J. Mol. Sci.* 20:1619. doi: 10.3390/ijms20071619

Zhang, N., Schroppel, B., Lal, G., Jakubzick, C., Mao, X., Chen, D., et al. (2009). Regulatory T cells sequentially migrate from inflamed tissues to draining lymph nodes to suppress the alloimmune response. *Immunity* 30, 458–469. doi: 10.1016/j.immuni.2008.12.022

Zhu, X. Y., Urbieta-Caceres, V., Krier, J. D., Textor, S. C., Lerman, A., and Lerman, L. O. (2013). Mesenchymal stem cells and endothelial progenitor cells decrease renal injury in experimental swine renal artery stenosis through different mechanisms. *Stem Cells* 31, 117–125. doi: 10.1002/stem.1263

Conflict of Interest: The authors declare that the research was conducted in the absence of any commercial or financial relationships that could be construed as a potential conflict of interest.

frontiers in Physiology

ORIGINAL RESEARCH
published: 19 June 2020
doi: 10.3389/fphys.2020.00599

Oxymatrine Inhibits Twist-Mediated Renal Tubulointerstitial Fibrosis by Upregulating Id2 Expression

Ying Xiao[1,2†], Can Peng[1,2†], Yawen Xiao[1,2], Dan Liang[1,2], Zhiping Yuan[4], Zhiyang Li[1,2], Mingjun Shi[1,2], Yuanyuan Wang[1,2], Fan Zhang[1,2] and Bing Guo[1,2,3]*

[1] Department of Pathophysiology, Guizhou Medical University, Guiyang, China, [2] Guizhou Provincial Key Laboratory of Pathogenesis & Drug Research on Common Chronic Diseases, Guizhou Medical University, Guiyang, China, [3] State Key Laboratory of Functions and Applications of Medicinal Plants, Guizhou Medical University, Guiyang, China, [4] School Hospital, Guizhou Medical University, Guiyang, China

The final pathway for the development of diabetic nephropathy (DN) into chronic renal failure in DN is glomerulosclerosis and tubulointerstitial fibrosis. Renal tubular lesions can occur in the early stage of DN renal injury. Cumulative evidence shows that oxymatrine (OMT) has a variety of biological and pharmacological properties. In recent years, more attention has been paid on the preventive and therapeutic influence of OMT on organ fibrosis. In this experiment, db/db mice were intraperitoneally injected with OMT 120 mg/kg for 8 weeks, and NRK-52E cultured with 30 mmol/L glucose and 0.1 mg/mL OMT for 48-hour. We investigated the relationship between Id2 and Twist in NRK-52E cells and the effect of OMT on the expression of E-cadherin, α-SMA, Fibronectin, and Collagen-IV by Western blot, Real-time PCR, Immunofluorescence, cell transfection, Co-Immunoprecipitation, and Luciferase assays. OMT increased the expression of Id2 but decreased that of Twist under high glucose condition *in vitro* and *in vivo*. The promoted recovery of Id2 facilitated its binding to Twist and affected E-cadherin activity inhibiting EMT and the excessive proliferation and abnormal deposition of ECM. In brief, OMT promotes Id2 to reverse EMT and exert anti-fibrotic effect in diabetic renal tubular epithelial cells by binding Id2 to Twist and affecting its transcriptional activation of downstream target genes. Or findings provide a new experimental basis for delaying the progress and for treatment of diabetic renal fibrosis.

Keywords: oxymatrine, diabetes mellitus, renal tubulointerstitial fibrosis, inhibitor of differentiation 2, Twist

OPEN ACCESS

Edited by:
Natalia Lopez-Andres, NavarraBiomed, Spain

Reviewed by:
Raúl Rodrigues Díez, Fundación para la Investigación Biomédica del Hospital Universitarios La Paz (FIBHULP), Spain
Xiao-ming Meng, Anhui Medical University, China

****Correspondence:***
Bing Guo
guobingbs@126.com

† These authors have contributed equally to this work

Specialty section:
This article was submitted to Renal and Epithelial Physiology, a section of the journal Frontiers in Physiology

Received: *17 February 2020*
Accepted: *14 May 2020*
Published: *19 June 2020*

Citation:
Xiao Y, Peng C, Xiao Y, Liang D, Yuan Z, Li Z, Shi M, Wang Y, Zhang F and Guo B (2020) Oxymatrine Inhibits Twist-Mediated Renal Tubulointerstitial Fibrosis by Upregulating Id2 Expression. Front. Physiol. 11:599. doi: 10.3389/fphys.2020.00599

INTRODUCTION

With the increase in the incidence of diabetes mellitus (DM) each year, diabetic nephropathy (DN), also known as diabetic kidney disease (DKD), has become one of its most serious complications. It is also one of the main causes of death in patients with DM. DN is also one of the main causes of end-stage renal disease globally and one of the main reasons for the decline of quality of life and increased mortality in patients with DM (Hakim and Pflueger, 2010). Therefore, it is of great clinical significance to clarify the occurrence and development mechanism of DN as soon as possible to provide an effective target for the prevention and treatment of DN and drug therapy of DN.

The main pathological features of DN are loss of normal nephron, proliferation of a large number of fibroblasts and myofibroblasts, excessive production and accumulation of extracellular matrix, thickening of the glomerular and tubular basement membrane, and renal tubulointerstitial fibrosis (Conserva et al., 2019; Li X. et al., 2019). Renal tubulointerstitial fibrosis is the most important renal interstitial lesion, which is almost the most common pathway and main pathological basis for the progression of various renal diseases to end-stage renal failure (Zhang et al., 2019). The process of renal tubulointerstitial fibrosis is epithelial–mesenchymal transition (EMT), which results in the loss of epithelioid properties and the acquisition of mesenchymal properties. The decreased expression of E-cadherin and increased the expression of α-SMA, accompanied by excessive proliferation and abnormal deposition of in extracellular matrix (ECM). The expression of Collagen-IV and Fibronectin was upregulated. Therefore, inhibiting or reversing the occurrence of EMT is of great significance in delaying chronic kidney diseases such as DN.

Oxymatrine (OMT) has many pharmacological effects, such as immune regulation, anti-arrhythmia, anti-inflammation, anti-tumor, anti-fibrosis (Ding et al., 2019; Halim et al., 2019; Jung et al., 2019; Wang et al., 2019b; Zhou et al., 2019; Lan et al., 2020). It has beneficial influence on myocardial fibrosis, hepatic fibrosis, pulmonary fibrosis and renal fibrosis in rats (Chen et al., 2008; Shen et al., 2011; Liu et al., 2012; Fu et al., 2016; Wang et al., 2016; Ozturk et al., 2017; Xu et al., 2017; Zhao et al., 2018). Our previous study showed that after OMT intervention of NRK-52E cells cultured with high glucose, the protein and mRNA levels of α-SMA and fibronectin decreased, while the protein and mRNA of E-cadherin increased, suggesting that OMT can inhibit the occurrence of EMT and improve the degree of renal fibrosis (Liu et al., 2016). Wang interfered with renal interstitial fibrosis induced by unilateral ureteral obstruction (UUO) in mice, which confirmed that OMT could significantly reduce the protein expression of Collagen-I and Fibronectin and prevent renal injury and renal interstitial fibrosis (Wang et al., 2016). However, the specific mechanism of OMT against renal tubulointerstitial fibrosis is yet to be elucidated.

The regulatory factors of fibrosis in a normal body are balanced with the anti-fibrotic ones. However, in the process of EMT progression, many fibrogenic regulators play a major role, and the expression of some anti-fibrotic regulators is reduced, such as inhibitors of differentiation (Yu et al., 2016; Cantelli et al., 2017; Higgins et al., 2017; Wang et al., 2018, Wang et al., 2019a; Zhao and Liu, 2020). Inhibitor of differentiation 2 (Id2), also known as Inhibitor of DNA binding, belongs to the helix-ring-helix family, which negatively regulates the activity of basic HLH (bHLH) transcription factors (Benezra et al., 1990; Zhou et al., 2018; Xiao et al., 2019; Jeyarajah et al., 2020; Xu et al., 2020). The binding region of bHLH regulates the expression of genes by binding to DNA in the form of dimers or heterodimers. However, Id2 protein lacks the basic region that binds to DNA and needs to bind to alkaline HLH to form a heterodimer, which then inhibits the regulation of alkaline HLH on gene and exerts negative effects on gene regulation (Norton, 2000; Roschger et al., 2018). Previous studies on diabetic rats established that the expression of Id2 in renal tubular epithelial cells decreased gradually with the progression of diabetes. The expression of E-cadherin and α-SMA decreased significantly, accompanied by the deposition of renal interstitial ECM. It is suggested that the EMT process of renal tubular epithelial cells may be related to the decrease of Id2 expression. Twist is a transcription factor belonging to the bHLH family. This protein has a basic region that binds to E-box on DNA to form a dimer or heterodimer to regulate gene expression. It was initially thought to play a key role in embryonic development. Recent evidence reveals that it is an oncogene closely related to EMT and malignant tumor growth, invasion and metastasis, and apoptosis (Ansieau et al., 2008; Zhu et al., 2016; Kim et al., 2017; Zhao et al., 2017; Georgakopoulos-Soares et al., 2020; Sonongbua et al., 2020). Twist is one of the main genes regulating EMT, and the reduction or loss of E-cadherin is the most important landmark change in EMT. Twist can negatively regulate the expression of E-cadherin, and the deletion of E-cadherin induces the expression of Twist, thus forming a positive feedback to maintain the interstitial state and induce EMT (Sasaki et al., 2009; Zhu et al., 2016; Wu et al., 2019). The Twist-related studies are focused mainly on tumors, but the regulatory mechanism of Twist in organ fibrosis, especially in DN, is not clear (Qin et al., 2012). Yang et al. (2015) established that Id2 can bind to Twist and block the expression of Collagen-I mediated by TGF-β in pulmonary fibrosis. Then, in the high-glucose stimulation of renal tubular epithelial cells, through which mechanism Twist and Id2 participate in the process of EMT still needs to be explored.

In this study, the protective effect of OMT on diabetic renal fibrosis and the putative mechanism underlying diabetic renal tubulointerstitial fibrosis were investigated *in vitro* and *in vivo*. We also assessed whether OMT can inhibit Twist-mediated tubulointerstitial fibrosis by upregulating the expression of Id2. Thus, the present study is of great clinical significance for the rational use of matrine resources and provides new experimental evidence for the treatment of DN, as well as, effective targets for the prevention and treatment of DN.

MATERIALS AND METHODS

Experimental Animals

A total of 20 healthy 6-week-old db/db mice, SPF grade, weighting (40 ± 5) g and 10 non-transgenic db/m mice with the same background at the same age, weighing (20 ± 2) g were provided by Nanjing University-Nanjing Biomedical Research Institute (batch number: T002407, strain: BSK-DB). The study followed the guidelines of the Code of Nursing and use of Animal Science of the National Health and Medical Research Council of China. At the same time, this study is based on the animal experiment ethics committee of Guizhou Medical University (No. 1800046) for the purpose of scientific care and use of animals. The db/db mice were randomly and equally divided into the diabetic group (DM group) and the oxymatrine treatment group (OMT group). Non-transgenic age-matched db/m mice comprised the control group (NC group). After 2 weeks of adaptive feeding, the mice in the OMT group were intraperitoneally injected with OMT 120 mg/kg · d for 8 weeks. 24-hour urine was collected before the mice were sacrificed,

and the eyeball was removed and blood was taken under ether anesthesia after 4-hour fasting. Also, the urine protein and fasting blood glucose were measured. Some kidney tissues were fixed with 4% paraformaldehyde at room temperature for paraffin sections, and the rest were stored at −80°C in the refrigerator for RNA and protein extractions.

Double Staining of Renal Histology and Immunofluorescence

The kidney tissue was fixed with 4% neutral formaldehyde, and then the kidney tissue block was dehydrated with ethanol gradient. After embedding in paraffin, it was fixed in a microtome for continuous sectioning (thickness is 3 μm). The cut tissue slices were unfolded and fixed on the glass sheet. HE, Masson, and PAS staining was performed following the instructions of the kit. The morphological and structural changes of the kidney tissue were observed under a light microscope. Paraffin sections were taken for tissue immunofluorescence staining. First, the paraffin sections were placed in an oven at 60°C for 2 h and dehydrated by gradient ethanol. Add 1.0 mol/L pH 6.0 citrate buffer solutions and place in microwave oven to repair antigen. Cellular immunofluorescence was directly fixed with 4% paraformaldehyde and followed by the same follow-up experiment as tissue staining, that is, 30 ml/L H_2O_2 deionized water, 5% bovine serum albumin was sealed at room temperature for 30 min. The first antibody was incubated (rabbit anti-Twist polyclonal antibody, rabbit anti-Id2 polyclonal antibody, mouse anti-Collagen-IV monoclonal antibody (Sigma, United States), rabbit anti-Fibronectin polyclonal antibody, rabbit anti-α-SMA polyclonal antibody (Santa Cruz Biotech, Santa Cruz, CA, United States). Mouse anti-E-cadherin monoclonal antibodies (CST, United States) were diluted at 1:80 overnight. The slices incubated with phosphate buffer solution (PBS) were used as negative control. They were subjected to rewarming at room temperature for 30 min, washing three times, for 5 min each time. The corresponding CY3 labeled sheep anti-mouse IgG (1:400) or FITC-labeled sheep anti-rabbit IgG fluorescent second antibody (1:200, Santa Cruz, United States) were incubated for 1 h. After washing PBS, the nucleus was stained with DAPI solution (Sigma, United States). Finally, the film was sealed with anti-fluorescence quenchant and observed and photographed under a fluorescence microscope (Olympus FV 1000, Olympus, Japan).

Cell Culture, Cell Administration and Cell Transfection

Rat renal tubular epithelial cell (NRK-52E) cell line was purchased from the Cell Bank of Chinese Academy of Sciences (Shanghai, China). NRK-52E was cultured in (DMEM, Gibco, United States) medium containing 10% fetal bovine serum (Hyclone, United States) at 37°C and 5% CO_2. The cells were randomly divided into three groups: normal glucose control group (NG group, glucose medium containing 5.5 mmol/L) and normal glucose group (NC+OMT group), It contains 5.5 mmol/L glucose and 0.1 mg/mL OMT (Nanjing Guangrun Biological products Co., Ltd., batch number: GR-134-171229), high-glucose group (HG group, containing 30 mmol/L glucose), high glucose oxymatrine treatment group (DM+OMT group, It contains 30 mmol/L glucose and 0.1 mg/mL OMT). The shRNA plasmid expressing Id2 gene was transfected into NRK-52E cells, and the pCMVPuro04-Id2 plasmid was designed in Yi le Biotech (Shanghai). The structure of the plasmid was as follows: Forward pGL-F: 5′-TAATACGACTCACTATAGG-3′, Reverse pGL-R:5′-GCCGGGCCTTTCTTTATG-3′. The construction sequence of siRNA with low Id2 gene (Jima, Shanghai) was as follows: Forward: 5′-GCAGCACGUCAUCGAUUAUTT-3′, Reverse:5′-AUAAUCGAUGACGUGCUGCTT-3′. An equivalent of 4×10^5 NRK-52E cells/well were inoculated into 6-well plate. At 80% confluency, the corresponding plasmids and siRNA were transfected with Lipofectamine 3000 reagent (Invitrogen, United States) for 6-hour in medium containing 1% FBS; and high glucose stimulation and drug intervention were carried out simultaneously. Other experiments were carried out after 48 h.

Western Blot

The renal cortex homogenate and cell culture samples were dissolved in RIPA lysis buffer (Beyotime, Jiangsu, China). After centrifugation, the supernatant was removed and the protein concentration was detected according to the BCA kit instructions. The protein was isolated by polyacrylamide gel electrophoresis (proteins between 40 and 280 kDa were separated by 8% gel, proteins between 10 and 40 kDa were separated by 15% gel) after boiling with an equal volume of 5× sample buffer, and the membrane was blocked with 50 g/L skim milk. After washing the membrane with TBST, we added mouse anti-β-actin antibody (1:4000), rabbit anti-Id2 (1:1000), rabbit anti-Twist antibody (1:1000), rabbit anti-α-SMA antibody (1:1000), rabbit anti-Fibronectin antibody (1:1000), mouse anti-collagen-IV antibody (1:1000), or mouse anti-E-cadherin antibody (1:1000), followed by overnight incubation at 4°C. Further, after washing, the corresponding horseradish peroxidase labeled goat anti-mouse IgG or horseradish peroxidase labeled goat anti-rabbit second antibody IgG (1:4000, PMK, China) were incubated at room temperature for 1-h. We employed enhanced chemiluminescence, Bio-Rad gel imaging system (Bio-Rad company) exposure, and Image Lab 5.1 software processing and analysis of images.

Real-Time PCR

Total RNA was extracted from renal tissues and cells by TRIzol reagent (Ambion). Then cDNA was synthesized by RevertAId^{TM} First Strand cDNA Synthesis Kit (Thermo, United States). Quantitative PCR was detected by 2 × SuperReal PreMix Plus (SYBR Green) (TIANGEN, Beijing, China) and iQ SYBR Green SuperMix (Bio-Rad). The primers of each gene were designed by DNA MAN software and synthesized by Generay Biotech Co., Ltd. (Shanghai, China). The gene expression was related to the expression level of β-actin, and the data were processed by $2^{-\Delta\Delta Ct}$ method.

Co-immunoprecipitation

Immunoprecipitation test was carried out according to the instructions of the kit using Dynabeads Protein G Immunoprecipitation Kit (10007D, Invitrogen, United States). First, the cell lysate was added, the cell supernatant was extracted, the magnetic beads were pretreated, the 5 μL rabbit anti-Id2

antibody was incubated at room temperature for 1 h, or the 5 μL mouse anti-Twist antibody was added. In IgG group, 5 μL normal rabbit IgG antibody or normal mouse IgG antibody (PMK, China) was added to form antibody-magnetic bead complex, and then incubated at room temperature for 1 h. The antigen in the supernatant was combined with the corresponding antibody magnetic bead complex to form an antigen-antibody-magnetic bead complex. Then, we performed 1000 rpm centrifugation for 2 min, added 20 μL of 5× sample buffer at 70°C for 10 min, and conducted Western blot.

Dual-Luciferase Reporter Assay

The ampicillin-resistant glycerol bacteria (Shanghai Leyi) containing Luciferase E-cadherin promoter sequence pGL3-rno-Cdh1 was constructed and the bacteria were amplified and the plasmid was extracted. The day before the transfection, NRK-52E cells with good logarithmic growth were digested by trypsin and inoculated with 20% to 24-well cell culture plate at 37°C for 5% CO_2. 24-hour after cell inoculation (50–60%), the transfection operation was carried out according to the instructions of the transfection reagent. Three multiple holes were set in each group. After 5 min, the two solutions were evenly mixed, followed by incubation for 20 min at room temperature. Then, the transfection complex of 50 μL was transferred into the 24-well plate covered with cells, and 500 μL was replenished after 6-hour. Next, 48-hour after the transfection, the cells were lysed, 12,000 rpm, centrifuged for 15 min, the supernatant was taken; each pore sample was of 100 μL. The Luciferase activity was detected by Dual-Luciferase Reporter Assay System (Promega, cat: E1960), and the ratio of Renilla Luciferase reading to Firefly Luciferase reading was measured. The structure of the constructed plasmid is as follows: Forward pGL-F:5′-CTAGCAAAATAGGCTGTCC-3′, Reverse pGL-R:5′-GCCGGGCCTTTCTTTATG-3′.

Statistical Analysis

SPSS 19.0 statistical software was used for data processing and statistical analysis. The experimental data were expressed by mean ± standard deviation (mean ± SD). First, the normality and homogeneity of variance were tested. After satisfying the homogeneity of normal distribution and variance, single factor analysis of variance was used for comparison between groups. There was significant difference between the two groups ($P < 0.05$).

RESULTS

The Effect of OMT on EMT and ECM in Mouse Kidney

General Changes and Biochemical Indicators of the Mice in Each Group

Compared with the NC group, blood glucose (BG), 24-hour urine protein (24 h UP), serum total cholesterol (TC) and blood triglyceride (TG) in the DM group were significantly increased and statistically significant. Compared with the DM group, the 24-hour urinary protein, serum total cholesterol and blood triglyceride in the OMT group were significantly lower than those in the control group. See **Table 1**.

Pathological Changes of Kidney Tissue in Each Group of Mice

The results of HE staining showed that in NC group, the outline of glomerulus was clear, the epithelial cells of renal tubules were neatly arranged, with intact basement membrane, and without inflammatory cell infiltration in the stroma. In DM group, most of renal tubular epithelial cells disintegrated with vacuolar degeneration, renal tubular lumen dilated obviously and a large number of inflammatory cells infiltrated in the renal interstitial area. After OMT treatment, the glomerular and tubular lesions were improved and the infiltration of inflammatory cells in the interstitium was reduced in the OMT group (**Figure 1A**). The results of PAS staining showed that the structure of glomeruli and renal tubules in NC group was clear, and there was a small amount of purplish red PAS positive staining substance, and there was no obvious abnormality. In the DM group, mesangial matrix slightly proliferated and PAS positive staining increased than those in NC group. Compared with DM group, PAS positive substance in OMT group decreased significantly (**Figure 1B**). The results of Masson staining showed that there was no collagen deposition in glomerular basement membrane and Mesangial area and no increase in renal tubulointerstitium in NC group. In DM group, a large number of collagen fibers were deposited in the interstitial area of glomeruli and tubules, that is, blue cord-like substances in the interstitial area of glomeruli and tubules, and the blue cord-like substances in the whole visual field in OMT group were significantly lower than those in DM group (**Figure 1C**).

OMT Inhibited the Process of EMT and the Deposition of ECM in Renal Tissue of Mice

The results of Western blot assay showed that compared with NC group, the expression of E-cadherin protein in DM group decreased significantly, while the expression of Twist, α-SMA, Collagen-IV and Fibronectin protein increased significantly. After the OMT treatment, the expression of E-cadherin protein significantly increased, whereas the expression of α-SMA, Collagen-IV, and Fibronectin protein significantly decreased (**Figures 2A,B**). The results of tissue immunofluorescence were consistent with those of Western blot assay (**Figures 2C–E**). We confirmed that OMT inhibited the process of EMT and the deposition of ECM in the mouse kidneys.

TABLE 1 | Biochemical indexes of mice in each group ($n = 6$, $\bar{x} \pm s$).

Specimen	BG/(mmol/L)	24 h UP/mg	TC/(mmol/L)	TG/(mmol/L)
NC	7.53 ± 0.38	7.61 ± 0.42	2.21 ± 0.39	1.33 ± 0.30
DM	38.36 ± 3.95**	36.34 ± 5.24**	4.15 ± 0.48*	2.59 ± 0.33*
OMT	32.43 ± 5.97	24.51 ± 9.02#	2.49 ± 0.76#	1.38 ± 0.13#

*$P < 0.05$, **$P < 0.01$ vs. NC group; #$P < 0.05$ vs. DM group.*

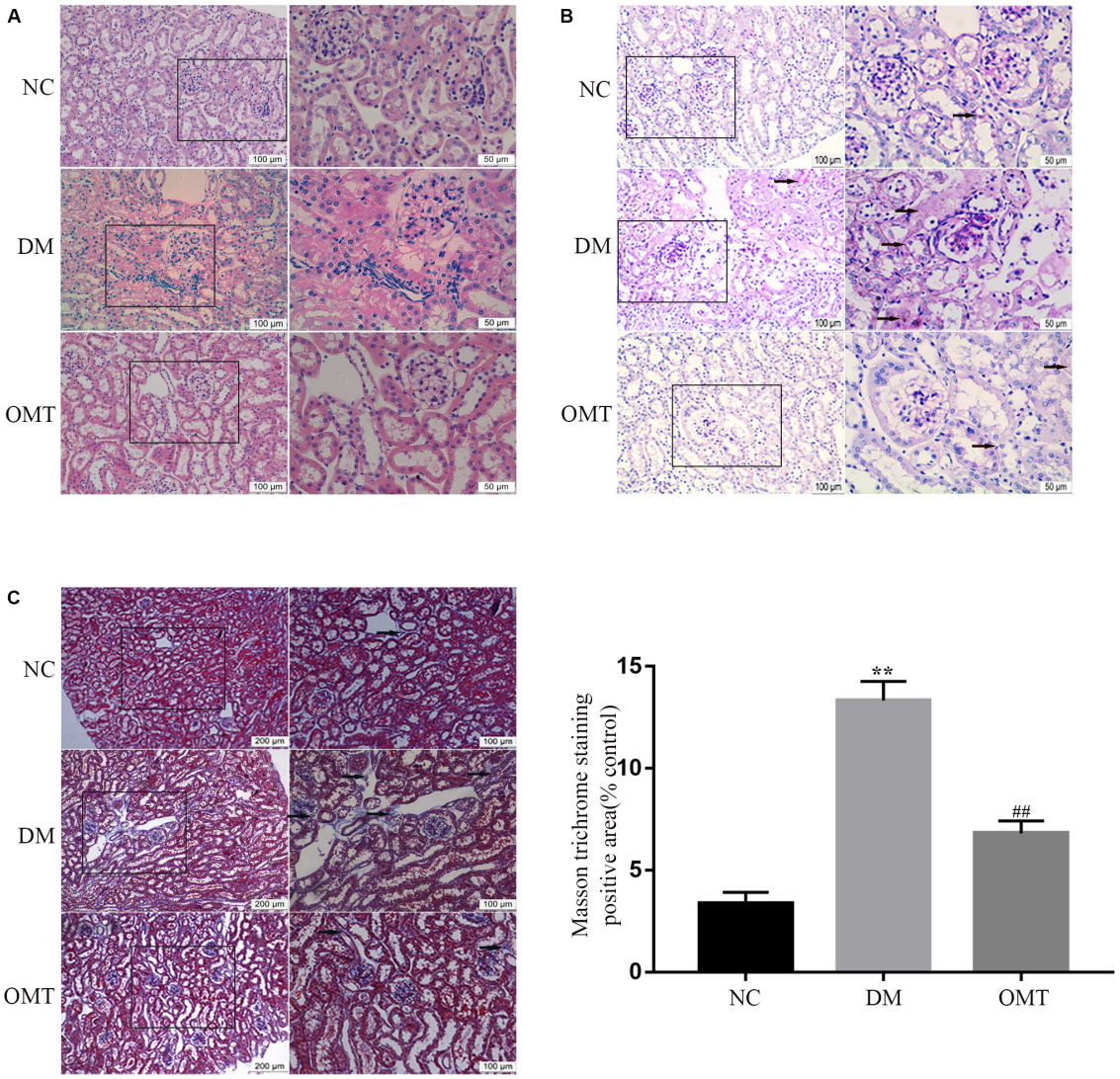

FIGURE 1 | Morphological changes of renal tissue in mice in NC, DM and OMT groups. **(A)** Renal tissues of the NC, DM and OMT groups were stained with hematoxylin on the scale of 100 and 50 mm; **(B)** PAS staining of kidney tissue in NC, DM, and OMT groups was 100 and 50 mm; **(C)** Masson staining of renal tissues in NC group, DM group and OMT group; the scales were 200 and 100 mm (**$P < 0.01$ vs. NC group; ##$P < 0.01$ vs. DM group).

By Promoting the Recovery of Id2 Expression in Mouse Renal Tissue, OMT Binds Id2 to Twist and Inhibits the Process of EMT and the Overproliferation and Abnormal Deposition of ECM

The results of Western blot and real-time PCR showed that the expression levels of Id2 protein and mRNA in the renal tissue of the DM group were significantly lower than those in the NC group, whereas the expression levels of Twist protein and mRNA were significantly lower. After OMT treatment, the expression levels of Id2 protein and mRNA were significantly increased, whereas the expression levels of Twist protein and mRNA were significantly decreased (**Figures 3A–D**). The results of tissue immunofluorescence were consistent with those of Western blot assay (**Figures 3E,F**).

OMT Inhibits EMT Processes and Deposition of ECM in High-Glucose-Cultured NRK-52E Cells

NRK-52E cells were cultured with normal or high glucose content, and added to the samples of the NG+OMT and HG+OMT groups. The results of Western blot and real-time PCR showed that the levels of E-cadherin protein and mRNA in HG group were significantly lower than those in NG group. However, the expressions of α-SMA, Collagen-IV, Fibronectin protein and mRNA were significantly increased. Compared to the HG group, the levels of E-cadherin protein and mRNA

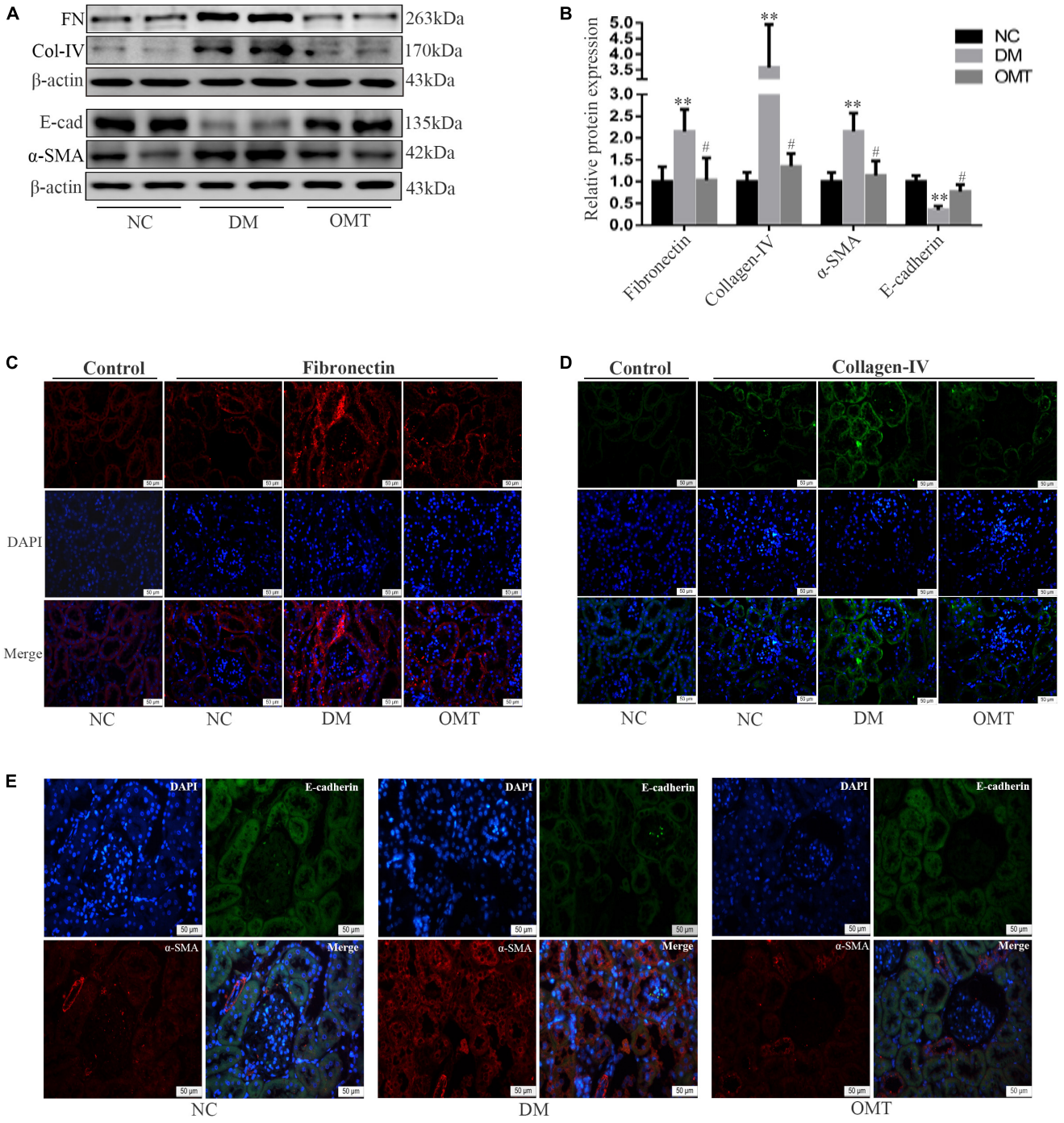

FIGURE 2 | Effects of OMT on the expression of Fibronectin, collagen-IV, E-cadherin, and α-SMA in the mouse kidneys. **(A,B)** Expressions of FN (Fibronectin), E-cad (E-cadherin), α-SMA and Col-IV (Collagen-IV) in the mouse renal cortex were detected by Western blot ($n = 6$. $^{**}P < 0.01$ vs. NC group; $n = 6$. $^{\#}P < 0.05$ vs. DM group. **(C–E)** Immunofluorescence staining showed the expression of Fibronectin, Collagen-IV, E-cadherin and α-SMA in mouse kidney (scale is 50 μm).

in HG+OMT group were significantly increased, while the expressions of α-SMA, Collagen-IV, Fibronectin protein and mRNA were significantly decreased (**Figures 4A–F**). The results of cellular immunofluorescence showed that the fluorescence brightness of α-SMA, Collagen- IV and Fibronectin in the HG group was significantly higher than that in the NG group, mainly in cytoplasm, but not in nucleus, and the fluorescence brightness of E-cadherin in HG group was considerably darker than that in

the NG group. The fluorescence brightness of α-SMA, Collagen-IV, and Fibronectin in the HG+OMT group was significantly lower than those in the HG group, whereas the fluorescence brightness of E-cadherin significantly increased (**Figures 4G–I**).

In NRK-52E Cells, OMT Can Inhibit the Process of EMT and the Overproliferation and Abnormal Deposition of ECM by Promoting the Recovery of Id2

In normal glucose or high-glucose-cultured NRK-52E cells, Western blot in the NG+overexpression Id2 group and HG+overexpression Id2 group showed that the level of E-cadherin protein in HG group was significantly lower than that in NG group. The expression of SMA, Collagen-IV, and Fibronectin proteins was significantly increased. Compared to the HG group, the level of E-cadherin protein in HG+overexpression Id2 group increased significantly, while the expression of α-SMA, Collagen-IV, and Fibronectin protein decreased significantly (**Figures 5A,B**). NRK-52E cells cultured with normal glucose and high glucose were applied to the NG+OMT and HG+OMT groups. Using Western blot and real-time PCR, we found that the levels of Id2 protein and mRNA in HG group were significantly lower than those in NG group, while the levels of Id2 protein and mRNA in the HG+OMT group were

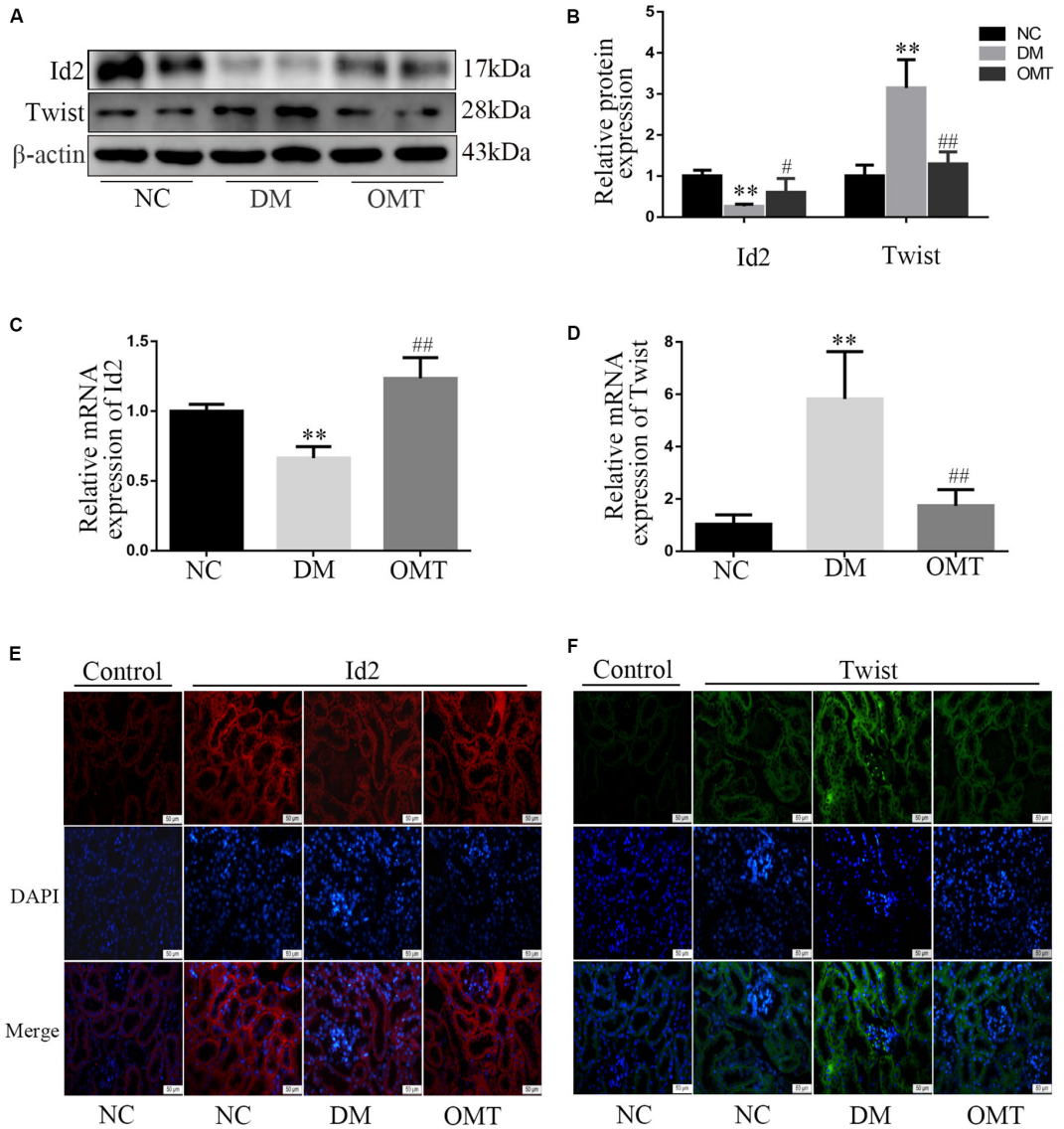

FIGURE 3 | Effect of OMT on the expression of Id2 and Twist in mouse kidney tissue. **(A,B)** Western blot was used to detect the expression of Id2 and Twist protein in mouse kidney tissues ($n = 6$. $^{**}P < 0.01$ vs. NC group; $^{\#}P < 0.05$ vs. DM group, $^{\#\#}P < 0.01$ vs. DM group; **(C,D)** Real-time PCR was used to detect the expression of Id2 and Twist mRNA in mouse kidney tissues ($n = 6$. $^{**}P < 0.01$ vs. NC group; $^{\#\#}P < 0.01$ vs. DM group; **(E,F)** Immunofluorescence staining showed the expression of Id2 and Twist in mouse kidney tissues (scale is 50 μm).

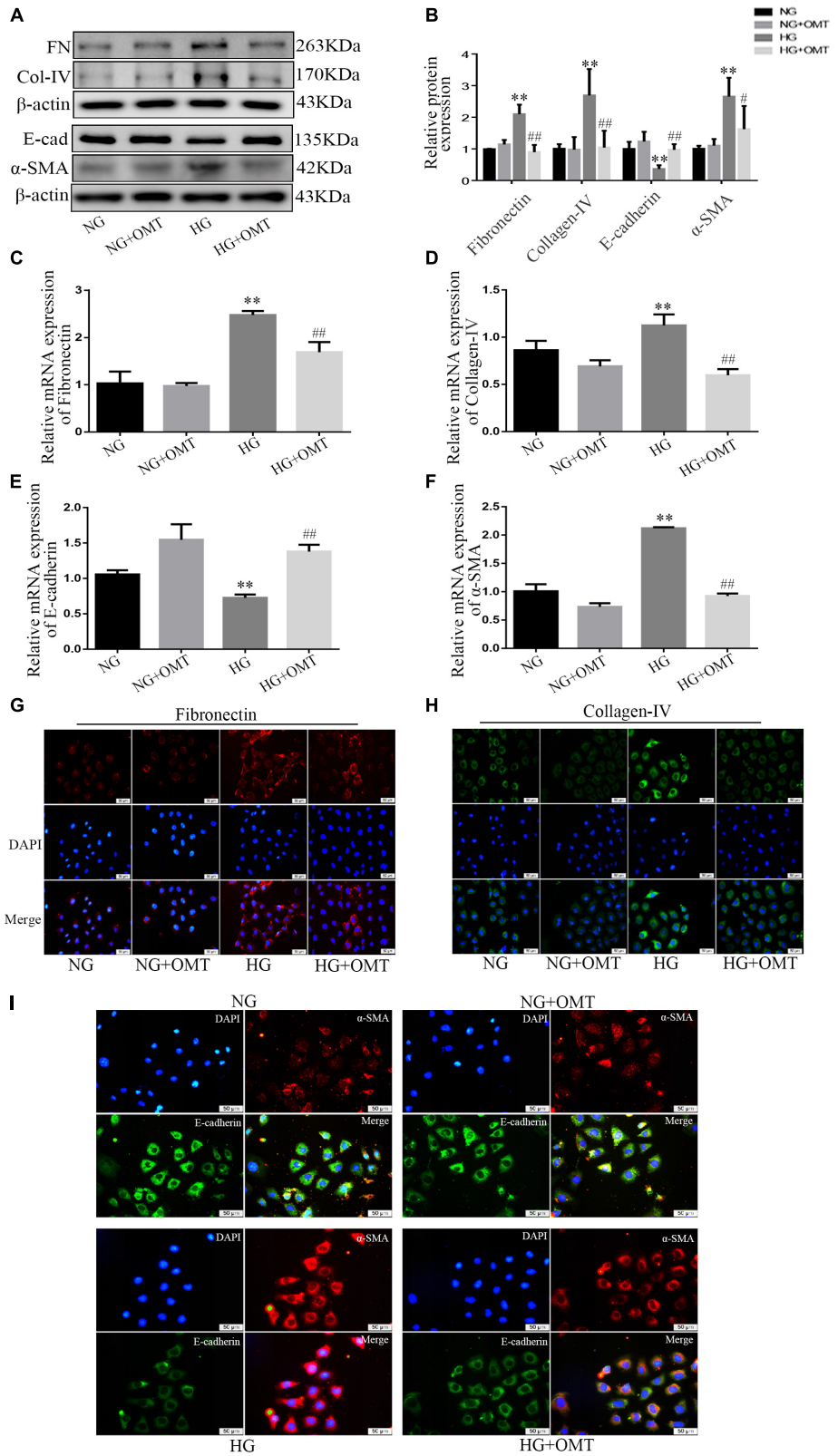

FIGURE 4 | Effects of OMT on the expression of Fibronectin, Collagen-IV, E-cadherin and α-SMA in NRK-52E cells. **(A–F)** Western blot and RT-PCR were used to detect the expression of FN (Fibronectin), E-cad (E-cadherin), α-SMA and Col-IV (Collagen-IV) in NRK-52E ($n = 3$. $^{**}P < 0.01$ vs. NG group; $^{\#}P < 0.05$, $^{\#\#}P < 0.01$ vs. HG group); **(G–I)** Immunofluorescence staining showed expression of Fibronectin, Collagen-IV, E-cadherin, and α-SMA in NRK-52E cells (scale bar is 50 μm).

significantly higher than those in the HG group (**Figures 5C,D**). The NRK-52E cells cultured with normal glucose and high glucose were treated with drugs and Id2 siRNA groups, that is, NG+OMT group, NG+OMT+Id2 siRNA group, HG+OMT group and HG+OMT+Id2 siRNA group. The results of Western blot showed that compared with NG group, the levels of Id2 and E-cadherin protein in HG group decreased significantly, while the expression of α-SMA, Collagen-IV and Fibronectin protein increased significantly. The level of E-cadherin protein in the HG+OMT group was significantly higher, whereas the expression of α-SMA, Collagen-IV, and Fibronectin protein was significantly lower in the Id2 group than in the HG groups. In the NG+OMT+Id2 siRNA and HG+OMT+Id2 siRNA groups, the levels of Id2 and E-cadherin proteins decreased significantly compared with the corresponding NG+OMT and HG+OMT groups, while that of α-SMA, Collagen-IV, and Fibronectin proteins increased significantly (**Figure 5E**).

In NRK-52E Cells, OMT Inhibits the Process of EMT and ECM Deposition by Promoting the Recovery of Id2 Expression and Affecting the Transcriptional Activation of Downstream Target Genes After Id2 Binding to Twist

NG+OMT and HG+OMT groups were set up in both normal glucose and high glucose culture NRK-52E cells. The results of the Western blot revealed that the level of Twist protein in HG group was significantly higher than that in NG group, and compared with HG group. The level of Twist protein in HG+OMT group was significantly decreased (**Figures 6A,B**). NRK-52E cells were cultured in normal sugar and high glucose, treated with OMT and transfected with Id2 siRNA, i.e., NG+OMT group, NG+OMT+Id2 siRNA group, HG+OMT group, and HG+OMT+Id2 siRNA group. The results of Western blot showed that compared to the NG group, the level of Id2 protein in the HG group was decreased significantly, while the expression of Twist protein was increased significantly. Compared to the HG group, the level of Id2 protein in the HG+OMT group was increased significantly, and that of the Twist protein was reduced significantly. Furthermore, Compared to the HG+OMT group, the Id2 protein level was decreased significantly in the HG+OMT+Id2 siRNA group, while the expression of Twist protein was only slightly increased (**Figure 6C**). Immunoprecipitation assay revealed that Twist protein was a component of the complex precipitated by Id2 antibody in the NG+OMT group of NG group or in the HG+OMT group of HG group. Also, the Id2 protein was detected in the complex precipitated by Twist antibody, thereby indicating an interaction between Id2 and Twist proteins (**Figures 6D,E**). Then, the Luciferase assay showed that the activity of the E-cadherin promoter Luciferase was significantly reduced in the HG group as compared to the NG group. Compared to the HG group, OMT intervention promoted the recovery of the Luciferase activity of the E-cadherin promoter, while the Luciferase activity of E-cadherin promoter after transfection of Id2 siRNA was significantly lower than that of OMT intervention group stimulated by high glucose. In addition, it was confirmed that OMT inhibited the process of EMT and the deposition of ECM by promoting the restoration of Id2, which was formed by binding Id2 to Twist to form a heterodimer, thereby affecting the regulation of downstream genes by Twist (**Figure 6F**).

DISCUSSION

In recent years, the incidence of diabetes has been steadily increasing, seriously affecting human physical and mental health. Type 2 diabetes is most prevalent. Currently, the research and development of drugs for treatment of type 2 diabetes has intensified considerably spot (Santulli, 2019). In this study, we carried out both *in vivo* and *in vitro* experiments. In our *in vivo* experiments, we selected an animal model of type 2 diabetes, db/db mice, a spontaneous type 2 diabetic mouse caused by a defect in the Leptin receptor gene on chromosome 4 discovered by the Jackson Laboratory in the United States in 1966. Bulimia and obesity appeared from the age of 4 weeks, and then showed obvious characteristics of hyperglycemia, hyperlipidemia and insulin resistance with the increase of age. The pathogenesis of hyperglycemia was very similar to that of patients with type 2 diabetes mellitus. It is also an ideal animal model for the experimental study of type 2 DN in the world (Lutz and Woods, 2012; Zar Kalai et al., 2014; Zhu et al., 2019).

Our previous study found that oxymatrine played an anti-fibrotic effect in renal tubular epithelial cells (Liu et al., 2016). This experiment was confirmed again *in vivo*, and it was found that after intraperitoneal injection of oxymatrine in db/db mice for 8 weeks, The state of the mice was improved, the biochemical indexes such as fasting blood glucose, serum cholesterol and blood triglyceride were improved, the levels of Fibronectin, Collagen-IV, α-SMA protein and mRNA were decreased, while the levels of E-cadherin were increased. It is confirmed that oxymatrine can improve the degree of renal fibrosis in diabetic mice, but the specific mechanism is not very clear. Earlier studies showed that the expression of Id2 protein is closely related to fibrosis in mouse proximal renal tubular cells. With the development of EMT, the expression of Id2 decreased significantly (Gervasi et al., 2012; Vigolo et al., 2019). Our results also found that compared with the wild-type mice, the expression of Id2 in renal tissue of db/db mice decreased significantly, and the level of Twist increased significantly. After treatment with oxymatrine, the expression of Id2 recovered and Twist decreased. Therefore, we speculated that Id2 and Twist were key regulatory factors of diabetic renal fibrosis EMT, and there may be a regulatory relationship between them. Nevertheless, it was still unclear what the exact relationship between Id2 and Twist in diabetic renal fibrosis was and whether oxymatrine exerted protective effects in diabetic nephropathy through both of them. To address these questions, we performed the present study.

Firstly, we stimulated the renal tubular epithelial cells of rats with high glucose and treated with oxymatrine to explore the

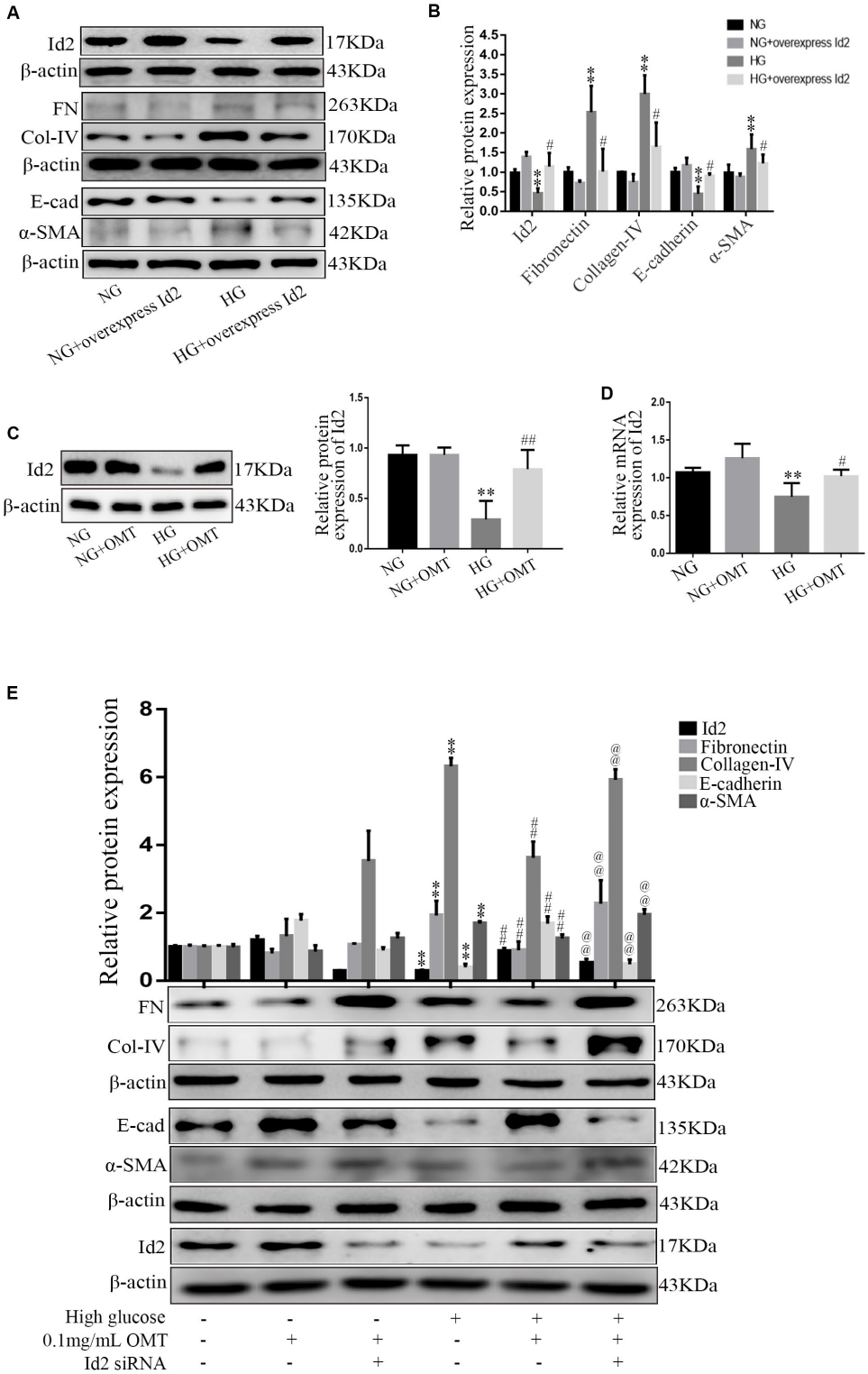

FIGURE 5 | Effects of Id2 on the expression of Fibronectin, Collagen-IV, E-cadherin, and α-SMA in NRK-52E cells were observed by Western blot and Real-time PCR. **(A,B)** Western blot was used to detect the changes of FN (Fibronectin), E-cad (E-cadherin), α-SMA, and Col-IV (Collagen-IV) after Id2 expression ($n = 3$, $^{**}P < 0.01$, vs. NG group; $^{\#}P < 0.05$ vs. HG group). **(C,D)** Western blot and RT-PCR were used to detect the changes of protein and mRNA levels of Id2 after OMT treatment ($n = 3$, $^{**}P < 0.01$ vs. NG group; $^{\#}P < 0.05$, $^{\#\#}P < 0.01$ vs. HG group); **(E)** The expression of Id2, Fibronectin, E-cadherin, α-SMA and Collagen-IV in NRK-52E was observed by Western blot and RT-PCR after OMT treatment and knock-down of Id2 after OMT treatment ($n = 3$, $^{**}P < 0.01$ vs. NG group; $^{\#\#}P < 0.01$ vs. HG group; $^{@@}P < 0.01$ vs. HG+OMT group).

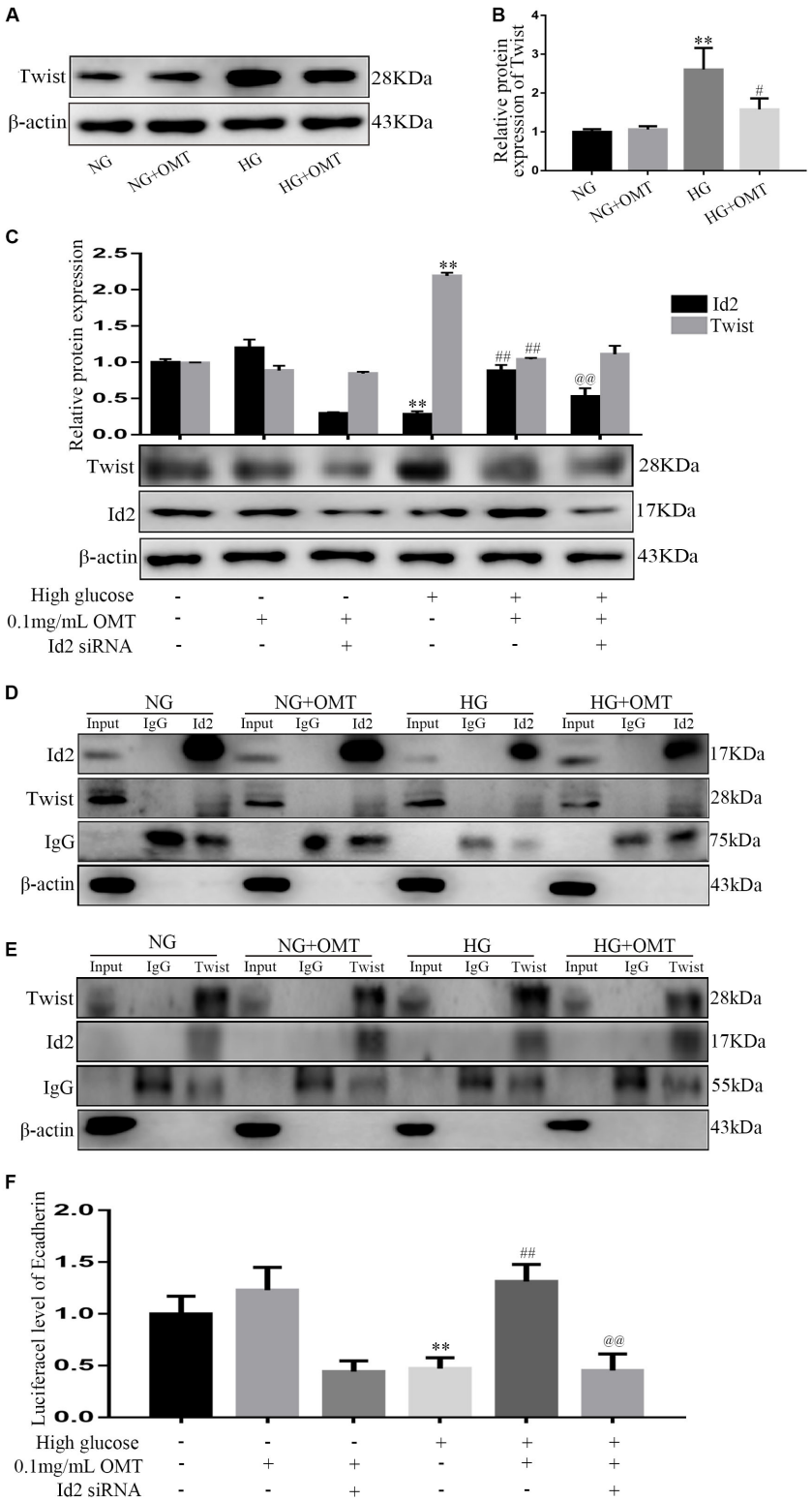

FIGURE 6 | Relationship between Id2 and Twist in NRK-52E cells, established by Western blot, Co-IP, and Luciferase assays. **(A,B)** Western blot was used to detect the changes of Twist protein level after administration of OMT ($n = 3$, $^{**}P < 0.01$ vs. NG group; $^{\#}P < 0.05$ vs. HG group); **(C)** The protein levels of Id2 and Twist were detected by Western blot after knocking down Id2 after OMT treatment. $^{**}P < 0.01$ vs. NG group; $^{\#\#}P < 0.01$ vs. HG group; $^{@@}P < 0.01$ vs. HG+OMT group; **(D,E)** Correlation between Id2 and Twist was detected by Co-IP. **(F)** The luciferase activity of the downstream target gene of Twist, namely the promoter of E-cadherin gene, was observed by Luciferase assay after treatment with OMT and treatment with OMT to knock-down Id2. $^{**}P < 0.01$ vs. NG group; $^{\#\#}P < 0.01$ vs. HG group; $^{@@}PP < 0.01$ vs. HG+OMT group.

effects of OMT on EMT and ECM. The results showed that the EMT process of NRK-52E cells cultured with high glucose was reversed and the secretion of ECM was decreased after treatment with oxymatrine, suggesting that OMT can reverse the process of EMT and reduce the deposition of ECM *in vitro* and *in vivo*. Second, through the transfection of Id2 plasmid, the process of EMT and the deposition of ECM were improved. Compared with the treatment group treated with OMT, no differences were found in the effect exerted. It is suggested that the anti-EMT and ECM effect of OMT may play a role by promoting the recovery of Id2 expression. Therefore, after the administration of OMT, we knocked down the Id2, and found that the anti-EMT and ECM deposition effect of OMT was significantly diminished, which confirmed that OMT could play the role of anti-diabetic renal fibrosis by promoting the recovery of Id2 expression. Finally, in the course of the experiment, we found that the expression of Twist was significantly lower after the OMT treatment and that Id2 was a transcription factor of the HLH family. Id2 protein lacked the basic region bound to DNA and needed to bind to bHLH to form a heterodimer. Twist is a member of the bHLH family (Yang et al., 2015; Li N. et al., 2019). Thus, we speculated that oxymatrine promoted the recovery of Id2, which inhibited Twist itself or affected the gene regulation of Twist, and play an anti-diabetic role in renal fibrosis. Therefore, by knocking down Id2, while giving OMT, we found that after knocking down Id2, Twist itself has not changed significantly, suggesting that OMT may affect the transcriptional activation of downstream target genes through the binding of Id2 and Twist to affect the EMT process. Hence, we conducted a Co-IP experiment on Id2 and Twist protein and established that no matter whether it was normal, high glucose or medication group, The Twist protein was found in the complex precipitated by the Id2 antibody. Also, the Id2 protein was detected in the complex precipitated by the Twist antibody, indicating a mutual binding between Id2 and Twist proteins. Then the Luciferase reporter gene experiment was carried out by constructing the downstream target gene of Twist, that is, the promoter of E-cadherin gene. It was found that the Luciferase activity of E-cadherin promoter was significantly lowered under high-glucose culture, and recovered after oxymatrine treatment. After the treatment with oxymatrine and knocking down Id2, the luciferase activity of E-cadherin promoter decreased significantly, which confirmed once again that Id2 did not affect the expression of Twist itself, but through the effect of binding to Twist.

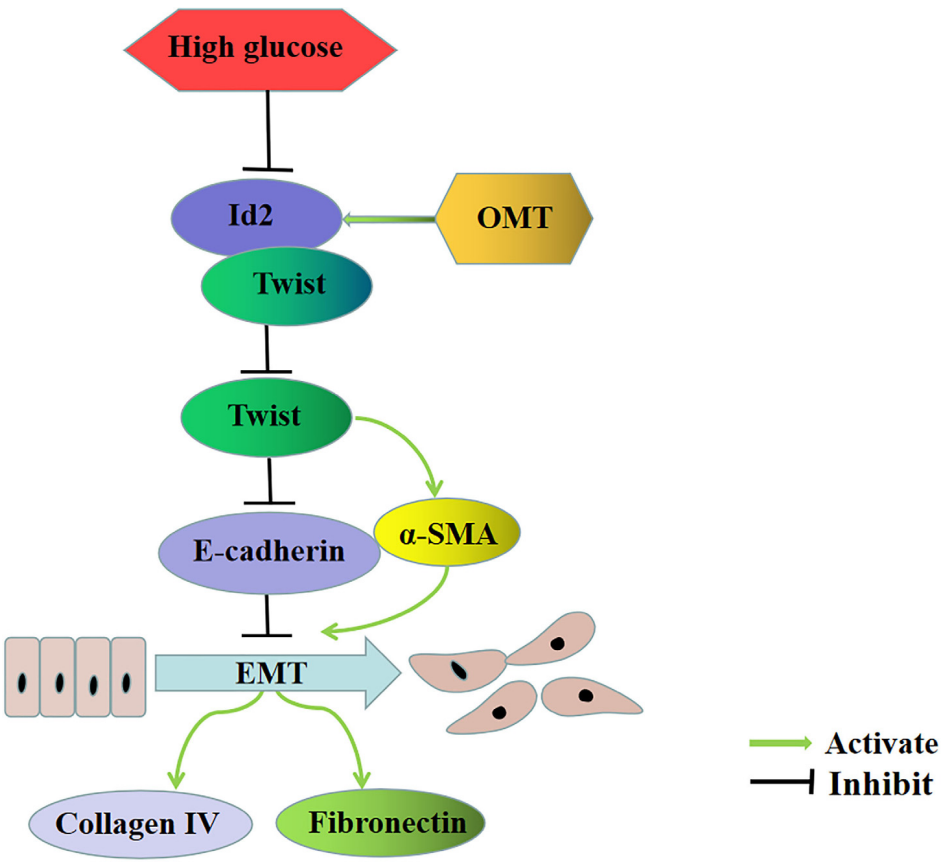

FIGURE 7 | Oxymatrine is involved in the main signal pathway of diabetic renal tubulointerstitial fibrosis. OMT can block the inhibitory effect of HG on Id2, promote the recovery of Id2, and further promote the binding of Id2 and Twist, thus affecting the regulation of downstream target genes E-cadherin and α-SMA by Twist, inhibiting the process of EMT, and downregulating the expression of ECM such as Collagen-IV and Fibronectin.

Thus affecting the expression of downstream target genes to play the role of EMT and ECM deposition, indicating that oxymatrine can promote the recovery of Id2 and further promote the binding of Id2 and Twist, thus inhibiting the regulation of downstream target genes by Twist and exerting anti-diabetic functions against renal fibrosis (**Figure 7**).

In this study, we investigated the protective mechanism of oxymatrine on renal tubular epithelial cell injury, induced by high glucose, and confirmed the interaction between Id2 and Twist. Our findings provide a new experimental basis for the rational utilization of *Sophora flavescens* resources, elucidating its target and increasing the function of "diabetic nephropathy," and brings new hope for delaying the progress and treatment of diabetic renal fibrosis.

DATA AVAILABILITY STATEMENT

The raw data supporting the conclusions of this article will be made available by the authors, without undue reservation, to any qualified researcher.

ETHICS STATEMENT

This study follows the guidelines of the National Animal Health Care and Use Guidelines of the National Health and Medical Research Council of China, and the protocol has been approved by the Guizhou Medical University the Animal Care Welfare Committee.

AUTHOR CONTRIBUTIONS

YiX and CP participated in the design and conducted the experiment, analyzed the results, and wrote the manuscript. YaX, DL, ZY, and ZL contributed to the conduction of the experiments and the maintenance of cell culture. MS, YW, and FZ reviewed the results and manuscript. BG designed and supervised the project and reviewed the results and manuscript.

FUNDING

This study was supported by the National Natural Science Foundation of China (grant no. 81860656), the Science and Technology Foundation of Guizhou Province [grant no. (2017) 1419], and the Science and Technology Bureau, Guiyang Municipal Government [grant no. (2017) 15-29].

ACKNOWLEDGMENTS

The authors thank the Cell Bank of Chinese Academy of Sciences (Shanghai, China) for providing the NRK-52E cell line.

REFERENCES

Ansieau, S., Bastid, J., Doreau, A., Morel, A. P., Bouchet, B. P., Thomas, C., et al. (2008). Induction of EMT by twist proteins as a collateral effect of tumor-promoting inactivation of premature senescence. *Cancer Cell* 14, 79–89. doi: 10.1016/j.ccr.2008.06.005

Benezra, R., Davis, R. L., Lockshon, D., Turner, D. L., and Weintraub, H. (1990). The protein Id: a negative regulator of helix-loop-helix DNA binding proteins. *Cell* 61, 49–59. doi: 10.1016/0092-8674(90)90214-y

Cantelli, G., Crosas-Molist, E., Georgouli, M., and Sanz-Moreno, V. (2017). TGFB-induced transcription in cancer. *Semin. Cancer Biol.* 42, 60–69. doi: 10.1016/j.semcancer.2016.08.009

Chen, X., Sun, R., Hu, J., Mo, Z., Yang, Z., Liao, D., et al. (2008). Attenuation of bleomycin-induced lung fibrosis by oxymatrine is associated with regulation of fibroblast proliferation and collagen production in primary culture. *Basic Clin. Pharmacol. Toxicol.* 103, 278–286. doi: 10.1111/j.1742-7843.2008.00287.x

Conserva, F., Barozzino, M., Pesce, F., Divella, C., Oranger, A., Papale, M., et al. (2019). Urinary miRNA-27b-3p and miRNA-1228-3p correlate with the progression of kidney fibrosis in diabetic nephropathy. *Sci. Rep.* 9:11357. doi: 10.1038/s41598-019-47778-1

Ding, Y., Li, N., Sun, J., Zhang, L., Guo, J., Hao, X., et al. (2019). Oxymatrine inhibits bocavirus MVC replication, reduces viral gene expression and decreases apoptosis induced by viral infection. *Virol. Sin.* 34, 78–87. doi: 10.1007/s12250-019-00088-2

Fu, L., Xu, Y., Tu, L., Huang, H., Zhang, Y., Chen, Y., et al. (2016). Oxymatrine inhibits aldosterone-induced rat cardiac fibroblast proliferation and differentiation by attenuating smad-2,-3 and-4 expression: an in vitro study. *BMC Complement. Altern. Med.* 16:241. doi: 10.1186/s12906-016-1231-9

Georgakopoulos-Soares, I., Chartoumpekis, D. V., Kyriazopoulou, V., and Zaravinos, A. (2020). EMT factors and metabolic pathways in cancer. *Front. Oncol.* 10:499. doi: 10.3389/fonc.2020.00499

Gervasi, M., Bianchi-Smiraglia, A., Cummings, M., Zheng, Q., Wang, D., Liu, S., et al. (2012). JunB contributes to Id2 repression and the epithelial-mesenchymal transition in response to transforming growth factor-β. *J. Cell Biol.* 196, 589–603. doi: 10.1083/jcb.201109045

Hakim, F. A., and Pflueger, A. (2010). Role of oxidative stress in diabetic kidney disease. *Med. Sci. Monit.* 16, RA37–RA48.

Halim, C. E., Xinjing, S. L., Fan, L., Bailey Vitarbo, J., Arfuso, F., Tan, C. H., et al. (2019). Anti-cancer effects of oxymatrine are mediated through multiple molecular mechanism(s) in tumor models. *Pharmacol. Res.* 147:104327. doi: 10.1016/j.phrs.2019.104327

Higgins, D. F., Ewart, L. M., Masterson, E., Tennant, S., Grebnev, G., Prunotto, M., et al. (2017). BMP7-induced-Pten inhibits Akt and prevents renal fibrosis. *Biochim. Biophys. Acta Mol. Basis Dis.* 1863, 3095–3104. doi: 10.1016/j.bbadis.2017.09.011

Jeyarajah, M. J., Jaju Bhattad, G., Hillier, D. M., and Renaud, S. J. (2020). The Transcription factor OVOL2 represses ID2 and drives differentiation of trophoblast stem cells and placental development in mice. *Cells* 9:E840. doi: 10.3390/cells9040840

Jung, Y. Y., Shanmugam, M. K., Narula, A. S., Kim, C., Lee, J. H., Namjoshi, O. A., et al. (2019). Oxymatrine attenuates tumor growth and deactivates STAT5 signaling in a lung cancer xenograft model. *Cancers* 11:49. doi: 10.3390/cancers11010049

Kim, S., Twigg, S., Scanlon, V. A., Chandra, A., Hansen, T. J., Alsubait, A., et al. (2017). Localized TWIST1 and TWIST2 basic domain substitutions cause four distinct human diseases that can be modeled in *Caenorhabditis elegans*. *Hum. Mol. Genet.* 26, 2118–2132. doi: 10.1093/hmg/ddx107

Lan, X., Zhao, J., Zhang, Y., Chen, Y., Liu, Y., and Xu, F. (2020). Oxymatrine exerts organ- and tissue-protective effects by regulating inflammation, oxidative stress, apoptosis, and fibrosis: from bench to bedside. *Pharmacol. Res.* 151:104541. doi: 10.1016/j.phrs.2019.104541

Li, X., Zhang, T., Geng, J., Wu, Z., Xu, L., Liu, J., et al. (2019). Advanced oxidation protein products promote lipotoxicity and tubulointerstitial fibrosis

via CD36/β-catenin pathway in diabetic nephropathy. *Antioxid. Redox Signal.* 31, 521–538. doi: 10.1089/ars.2018.7634

Li, N., Yang, L., Sun, Y., and Wu, X. (2019). MicroRNA-16 inhibits migration and invasion via regulation of the Wnt/β-catenin signaling pathway in ovarian cancer. *Oncol. Lett.* 17, 2631–2638. doi: 10.3892/ol.2019.9923

Liu, L., Lu, W., Ma, Z., and Li, Z. (2012). Oxymatrine attenuates bleomycin-induced pulmonary fibrosis in mice via the inhibition of inducible nitric oxide synthase expression and the TGF-β/Smad signaling pathway. *Int. J. Mol. Med.* 29, 815–822. doi: 10.3892/ijmm.2012.923

Liu, L., Wang, Y., Yan, R., Li, S., Shi, M., Xiao, Y., et al. (2016). Oxymatrine inhibits renal tubular EMT induced by high glucose via upregulation of snon and inhibition of TGF-??1/Smad signaling pathway. *PLoS One* 11:e0151986. doi: 10.1371/journal.pone.0151986

Lutz, T. A., and Woods, S. C. (2012). Overview of animal models of obesity. *Curr. Protoc. Pharmacol. Chapter* 5:Unit5.61. doi: 10.1002/0471141755.ph0561s58

Norton, J. D. (2000). ID helix-loop-helix proteins in cell growth, differentiation and tumorigenesis. *J. Cell. Sci.* 113(Pt 22), 3897–3905.

Ozturk, H., Cetinkaya, A., Yilmaz, F., and Ozturk, H. (2017). Protective effect of oxymatrine against renal ischemia/reperfusion injury in rats. *Bratisl. Lek. Listy* 118, 217–222. doi: 10.4149/BLL_2017_043

Qin, Q., Xu, Y., He, T., Qin, C., and Xu, J. (2012). Normal and disease-related biological functions of Twist1 and underlying molecular mechanisms. *Cell Res.* 22, 90–106. doi: 10.1038/cr.2011.144

Roschger, C., Verwanger, T., Krammer, B., and Cabrele, C. (2018). Reduction of cancer cell viability by synergistic combination of photodynamic treatment with the inhibition of the Id protein family. *J. Photochem. Photobiol. B Biol.* 178, 521–529. doi: 10.1016/j.jphotobiol.2017.11.038

Santulli, G. (2019). In type 2 diabetes, intensive glucose control for 5.6 years did not differ from usual care for major CV events at 14 years. *Ann. Intern. Med.* 171:JC31. doi: 10.7326/ACPJ201909170-031

Sasaki, K., Natsugoe, S., Ishigami, S., Matsumoto, M., Okumura, H., Setoyama, T., et al. (2009). Significance of Twist expression and its association with E-cadherin in esophageal squamous cell carcinoma. *J. Exp. Clin. Cancer Res.* 28:158. doi: 10.1186/1756-9966-28-158

Shen, X. C., Yang, Y. P., Xiao, T. T., Peng, J., and Liu, X. D. (2011). Protective effect of oxymatrine on myocardial fibrosis induced by acute myocardial infarction in rats involved in TGF-β1-Smads signal pathway. *J. Asian Nat. Prod. Res.* 13, 215–224. doi: 10.1080/10286020.2010.550883

Sonongbua, J., Siritungyong, S., Thongchot, S., Kamolhan, T., Utispan, K., Thuwajit, P., et al. (2020). Periostin induces epithelial-to-mesenchymal transition via the integrin α5β1/TWIST-2 axis in cholangiocarcinoma. *Oncol. Rep.* 43, 1147–1158. doi: 10.3892/or.2020.7485

Vigolo, E., Markó, L., Hinze, C., Müller, D. N., Schmidt-Ullrich, R., and Schmidt-Ott, K. M. (2019). Canonical BMP signaling in tubular cells mediates recovery after acute kidney injury. *Kidney Int.* 95, 108–122. doi: 10.1016/j.kint.2018.08.028

Wang, H. W., Shi, L., Xu, Y. P., Qin, X. Y., and Wang, Q. Z. (2016). Oxymatrine inhibits renal fibrosis of obstructive nephropathy by downregulating the TGF-β1-Smad3 pathway. *Ren. Fail.* 38, 945–951. doi: 10.3109/0886022X.2016.1164185

Wang, Y., Liu, L., Peng, W., Liu, H., Liang, L., Zhang, X., et al. (2019a). Ski-related novel protein suppresses the development of diabetic nephropathy by modulating transforming growth factor-β signaling and microRNA-21 expression. *J. Cell. Physiol.* 234, 17925–17936. doi: 10.1002/jcp.28425

Wang, Y., Shou, Z., Fan, H., Xu, M., Chen, Q., Tang, Q., et al. (2019b). Protective effects of oxymatrine against DSS-induced acute intestinal inflammation in mice via blocking the RhoA/ROCK signaling pathway. *Biosci. Rep.* 39:BSR20182297. doi: 10.1042/BSR20182297

Wang, Z., Fei, S., Suo, C., Han, Z., Tao, J., Xu, Z., et al. (2018). Antifibrotic effects of hepatocyte growth factor on endothelial-to-mesenchymal transition via transforming growth factor-beta1 (TGF-β1)/Smad and Akt/mTOR/P70S6K signaling pathways. *Ann. Transplant.* 23, 1–10. doi: 10.12659/aot.906700

Wu, Z., Xue, S., Zheng, B., Ye, R., Xu, G., Zhang, S., et al. (2019). Expression and significance of c-kit and epithelial-mesenchymal transition (EMT) molecules in thymic epithelial tumors (TETs). *J. Thorac. Dis.* 11, 4602–4612. doi: 10.21037/jtd.2019.10.56

Xiao, Y., Jiang, X., Peng, C., Zhang, Y., Xiao, Y., Liang, D., et al. (2019). BMP-7/Smads-induced inhibitor of differentiation 2 (Id2) upregulation and Id2/Twist interaction was involved in attenuating diabetic renal tubulointerstitial fibrosis. *Int. J. Biochem. Cell Biol.* 116:105613. doi: 10.1016/j.biocel.2019.105613

Xu, S., Wang, Y., Li, Y., Zhang, L., Wang, C., and Wu, X. (2020). Comprehensive analysis of inhibitor of differentiation/DNA-binding gene family in lung cancer using bioinformatics methods. *Biosci. Rep.* 40:BSR2019307. doi: 10.1042/BSR20193075

Xu, Y., Xiao, H., Luo, H., Chen, Y., Zhang, Y., Tao, L., et al. (2017). Inhibitory effects of oxymatrine on TGF-β1-induced proliferation and abnormal differentiation in rat cardiac fibroblasts via the p38MAPK and ERK1/2 signaling pathways. *Mol. Med. Rep.* 16, 5354–5362. doi: 10.3892/mmr.2017.7277

Yang, J., Velikoff, M., Agarwal, M., Disayabutr, S., Wolters, P. J., and Kim, K. K. (2015). Overexpression of inhibitor of DNA-binding 2 attenuates pulmonary fibrosis through regulation of c-Abl and Twist. *Am. J. Pathol.* 185, 1001–1011. doi: 10.1016/j.ajpath.2014.12.008

Yu, Z., Zai-Chun, X., Wun-Lun, H., and Yun-Yun, Z. (2016). BMP-7 attenuates TGF-β1-induced fibronectin secretion and apoptosis of NRK-52E cells by the suppression of miRNA-21. *Oncol. Res.* 23, 147–154. doi: 10.3727/096504016X14519157902645

Zar Kalai, F., Han, J., Ksouri, R., Abdelly, C., and Isoda, H. (2014). Oral administration of nitraria retusa ethanolic extract enhances hepatic lipid metabolism in db/db mice model 'BKS.C*g-Dock7*(m)+/+ Lepr(db/)J' through the modulation of lipogenesis-lipolysis balance. *Food Chem. Toxicol.* 72, 247–256. doi: 10.1016/j.fct.2014.07.029

Zhang, X., Lu, H., Xie, S., Wu, C., Guo, Y., Xiao, Y., et al. (2019). Resveratrol suppresses the myofibroblastic phenotype and fibrosis formation in kidneys via proliferation-related signalling pathways. *Br. J. Pharmacol.* 176, 4745–4759. doi: 10.1111/bph.14842

Zhao, L., Xu, Y., Tao, L., Yang, Y., Shen, X., Li, L., et al. (2018). Oxymatrine inhibits transforming growth factor β1 (TGF-β1)-Induced cardiac fibroblast-to-myofibroblast transformation (FMT) by Mediating the notch signaling pathway in vitro. *Med. Sci. Monit.* 24, 6280–6288. doi: 10.12659/MSM.910142

Zhao, Y. X., and Liu, J. (2020). Inhibitor of differentiation 1 (ID1) facilitates the efficacy of sorafenib in non-small cell lung cancer cells through suppressing epithelial to mesenchymal transition. *Med. Sci. Monit.* 26:e922148. doi: 10.12659/MSM.922148

Zhao, Z., Rahman, M. A., Chen, Z. G., and Shin, D. M. (2017). Multiple biological functions of Twist1 in various cancers. *Oncotarget* 8, 20380–20393. doi: 10.18632/oncotarget.14608

Zhou, W., Wu, Y., Pan, M., Liu, D., and Liu, B. (2019). Proliferation and migration of lung cancer could be inhibited by oxymatrine through the regulation for miR-520/VEGF. *Am. J. Chin. Med.* 47, 865–878. doi: 10.1142/S0192415X19500459

Zhou, X. L., Zeng, Ye, Y. H., Sun, S. M., Lu, X. F., Liang, W. Q., et al. (2018). Prognostic values of the inhibitor of DNA-binding family members in breast cancer. *Oncol. Rep.* 40, 1897–1906. doi: 10.3892/or.2018.6589

Zhu, Q. Q., Ma, C., Wang, Q., Song, Y., and Lv, T. (2016). The role of TWIST1 in epithelial-mesenchymal transition and cancers. *Tumour. Biol.* 37, 185–197. doi: 10.1007/s13277-015-4450-7

Zhu, Y., Li, Z. L., Ding, A., Yang, H., Zhu, W. P., Cui, T. X., et al. (2019). Olmesartan medoxomil, an angiotensin II-receptor blocker, ameliorates renal injury In db/db mice. *Drug Des. Dev. l Ther.* 13, 3657–3667. doi: 10.2147/DDDT.S217826

Conflict of Interest: The authors declare that the research was conducted in the absence of any commercial or financial relationships that could be construed as a potential conflict of interest.

frontiers in Medicine

ORIGINAL RESEARCH
published: 10 July 2020
doi: 10.3389/fmed.2020.00409

Characteristics of Renal Function in Patients Diagnosed With COVID-19: An Observational Study

Xu-wei Hong[1†], Ze-pai Chi[1†], Guo-yuan Liu[1†], Hong Huang[1], Shun-qi Guo[2], Jing-ru Fan[2], Xian-wei Lin[3], Liao-zhun Qu[4], Rui-lie Chen[5], Ling-jie Wu[5], Liang-yu Wang[6], Qi-chuan Zhang[7], Su-wu Wu[8], Ze-qun Pan[9], Hao Lin[9], Yu-hua Zhou[10] and Yong-hai Zhang[1]*

[1] Department of Urology, Shantou Central Hospital, Shantou, China, [2] Department of Emergency, Shantou Central Hospital, Shantou, China, [3] Department of Laboratory Medicine, Shantou Central Hospital, Shantou, China, [4] Department of Nephrology, Shantou Central Hospital, Shantou, China, [5] Department of Infectious Diseases, Shantou Central Hospital, Shantou, China, [6] Department of Ultrasonic Medicine, Shantou Central Hospital, Shantou, China, [7] Department of Respiratory Medicine, Shantou Central Hospital, Shantou, China, [8] Department of Intensive Care Unit, Shantou Central Hospital, Shantou, China, [9] Medical Department, Shantou Central Hospital, Shantou, China, [10] Nursing Department, Shantou Central Hospital, Shantou, China

OPEN ACCESS

Edited by:
Natalia Lopez-Andres, NavarraBiomed, Spain

Reviewed by:
Michael Hutchens, Oregon Health and Science University, United States
Minnie M. Sarwal, University of California, San Francisco, United States

***Correspondence:**
Yong-hai Zhang
zhang_yonghai@126.com

[†]These authors have contributed equally to this work and share first authorship

Specialty section:
This article was submitted to Nephrology, a section of the journal Frontiers in Medicine

Received: *13 March 2020*
Accepted: *29 June 2020*
Published: *10 July 2020*

Citation:
Hong X, Chi Z, Liu G, Huang H, Guo S, Fan J, Lin X, Qu L, Chen R, Wu L, Wang L, Zhang Q, Wu S, Pan Z, Lin H, Zhou Y and Zhang Y (2020) Characteristics of Renal Function in Patients Diagnosed With COVID-19: An Observational Study. Front. Med. 7:409. doi: 10.3389/fmed.2020.00409

Objective: The aim of the study was to analyze the characteristics of renal function in patients diagnosed with COVID-19.

Methods: In this retrospective, single-center study, we included all confirmed cases of COVID-19 in a tertiary hospital in Guangdong, China from January 20, 2020 to March 20, 2020. Blood and urine laboratory findings related to renal function were summarized, and the estimated glomerular filtration rate (eGFR) and endogenous creatinine clearance (Ccr) were also calculated to assess the renal function.

Results: A total of 12 admitted hospital patients were diagnosed with COVID-19, included 3 severe cases, and 9 common cases. Serum creatinine (Scr) was not abnormally elevated in all of the patients, and blood urea nitrogen (BUN) was abnormally elevated in only 25.0% of the patients. However, compared with the recovery period, the patient's Scr and BUN increased significantly in peak of disease (p-scr = 0.002 & p-bun < 0.001). By observing the fluctuations in Scr and BUN from admission to recovery, it was found that the peak of Scr and BUN appeared within the first 14 day of the course of the disease. Urinary microprotein detection indicated that the abnormally elevated rates of urine microalbumin (UMA), α1-microglobulin (A1M), urine immunoglobulin-G (IGU), and urine transferring (TRU) standardized by urinary creatinine in peak of disease were 41.7, 41.7, 50.0, and 16.7%, respectively. The abnormal rates of the calculated eGFR and Ccr were 66.7 and 41.7%.

Conclusion: Scr and BUN were generally increased during the course of COVID-19. Detection of urinary microproteins and application of multiple indicators assessment could be helpful for discovering abnormal renal function in patients with COVID-19. However, the evidence is limited due to the small sample size and observational nature. Additional studies, especially large prospective cohort studies, are required to confirm these findings.

Keywords: 2019-nCoV, COVID-19, renal function, urinary microprotein, multiple indicators

INTRODUCTION

Since December 2019, unexplained clustered pneumonia cases have started to appear in Wuhan, Hubei Province, China. It is identified as a pneumonia caused by a novel coronavirus infection (1, 2). The World Health Organization (WHO) named the coronavirus 2019-nCoV, which was the third coronavirus that infects humans from wild hosts across germlines after severe acute respiratory syndrome coronavirus (SARS-CoV) and Middle East respiratory syndrome coronavirus (MERS-CoV) and can cause severe pneumonia. It is also the seventh species of pathogenic human respiratory coronaviruses (3, 4). On February 11, 2020, the WHO named the novel coronavirus-infected disease2019 novel coronavirus disease shorted for COVID-19. With the spread of the epidemic, other cases in China and abroad have also occurred (5). The spread of disease has caused huge lives and economic losses to the world.

The 2019-nCoV human infection cases combine the characteristics of the previous 6 coronaviruses, which can cause mild cases, easily lose vigilance, and can also cause severe cases, with a high mortality rate (6). Multiple organ failure is the main cause of death of COVID-19. The latest research reports that the incidence of COVID-19 with organ dysfunction is about 33%, of which the acute renal injury is about 3∼7% (7, 8). Impaired renal function can lead to obstruction of excretion of metabolites and toxins in the body, which will adversely affect the maintenance of the electrolyte and acid-base balance of the human body. In addition, when renal function is severely damaged, uremia will occur, and endanger life. Early detection of evidence of renal injury and timely effective interventions are of great significance for reducing complications and improving prognosis.

This study intends to use a number of laboratory test indexes, including serum creatinine, blood urea nitrogen, urine creatinine, urine microprotein, and eGFR et al. to comprehensively assess renal function and make a deep characterization of renal function in patients diagnosed with COVID-19.

MATERIALS AND METHODS

Patients

From January 20, 2020 to March 20, 2020, 12 patients with pneumonia of unknown cause were admitted to a tertiary hospital in Guangdong, China. Nasopharyngeal swab samples of all patients were tested positive for 2019-nCoV virus nucleic acid and confirmed to be infected with 2019-nCoV by Guangdong Province CDC (Center for Disease Control and Prevention). The disease diagnostic criteria and case classification were refer to the guidelines for diagnosis and treatment of COVID-19 (Trial Version 7) issued by China National Health Commission (9).

Data Collection

A standardized case collection form was designed to collect case data. It mainly included the following information: (1) General information: gender, age, weight. (2) Medical history: fever, chills, sore throat, cough, headache, fatigue, myalgia, diarrhea, and other symptoms, hypertension, diabetes, chronic lung, heart, kidney, liver disease history, and history of malignant tumor. (3) Laboratory data: blood routine, electrolytes, liver and kidney function, myocardial enzymes, heart failure indicators, coagulation function, infection indexes, etc. Urine routine, urine creatinine, urinary microprotein detection, etc.

Evaluation of Renal Function

Serum creatinine (Scr), blood urea nitrogen (BUN), urine protein (PRO), urine occult blood urine (BLD), 24-h urine creatinine (UCr), 24-h urine K (UK), 24-h urine Na (UNa), microalbumin (UMA), α1-microglobulin (A1M), urine immunoglobulin G (IGU), and urine transferrin (TRU) were detected. The estimated glomerular filtration rate (eGFR) and endogenous creatinine clearance (Ccr) were calculated.

Among them, the eGFR was calculated according to the simplified MDRD

formula modified by the Chinese.

$$\mathrm{eGFR(ml/(min^{*}1.73m^{2})} = 186\times \mathrm{Scr(mg/dl)}^{-}1.154\times \mathrm{Age(year-old)}^{-}0.203(\mathrm{female}\times 0.742).$$

(the Counahan-Barrat method was applied when the patient is younger than 14- year-old)

The Ccr was calculated according to Cockcroft's formula.

$$\mathrm{Ccr} = [140-\mathrm{Age(year-old)}]\times \mathrm{weight(kg)}\div[72\times \mathrm{Scr(mg/dl)}](\mathrm{female}\times 0.85).$$

Statistical Methods

The paired-samples *T*-test was used to compare the differences of Scr and BUN between patients in the course of disease and in the period of recovery. It was considered statistically significant when the *P*-value was < 0.05. All statistical analyses were processed using SPSS 25.0 statistical software.

RESULTS

Clinical Characteristics of the COVID-19 Patients

Of the 12 patients with COVID-19, 3 (25.0%) and 9 (75.0%) were categorized into severe and common group, respectively. The severe patients required oxygen to support, the average oxygen saturation (SpO2) of the severe patients was 86.7% (81–92%). The common group included 7 (58.3%) mild cases and 2 (16.7%) non-pneumonia cases. There were 7 (58.3%) male and 5 (41.7%) female patients. The oldest patient was 69 years old and the youngest was 12 years old, with an average age of 41.3 ± 18.2 years old. Among the patients, only one patient (case 9) had never been to Wuhan City and became ill after contacting a person diagnosed with COVID-19 after going on a trip. The remaining 11 patients all came from Wuhan city within 14 days. Clinical symptoms of 12 patients included fever, sore throat, cough, headache, fatigue, myalgia, and some patients had no obvious clinical symptoms. Three patients had pre-existing diseases,

including diabetes, hypertension, and chronic emphysema, as shown in **Table S1**.

Laboratory Characteristics of the COVID-19 Patients

Laboratory testing items included blood routine, electrolyte, metabolism, heart, liver, kidney function indicators, coagulation function, and infection indicators. As shown in **Table S2**, the common abnormal indicators (abnormal rate ≥ 50%) included: increased neutrophil ratio (50%), increased monocyte ratio (75%), hypokalemia (50%), hyponatremia (50%), hypoproteinemia (75%), and increased C-reactive protein (83.3%).

Characteristics of Renal Function of the COVID-19 Patients

As shown in **Table 1**, Scr was not abnormally elevated in all of the patients, and BUN was abnormally elevated in only 25.0% of the patients. However, compared with the recovery period, which was defined as the virus nucleic

TABLE 1 | Renal function indicators of the COVID-19 patients in peak of disease.

Renal function indexes	Normal range	Case 1	Case 2	Case 3	Case 4	Case 5	Case 6	Case 7	Case 8	Case 9	Case 10	Case 11	Case 12	Abnormal rate (%)
Blood detection														
Scr, umol/L	40∼133	63.8	75.3	119.5	106.6	91.3	111.2	105.5	50.8	53.8	89.1	93.1	56.9	0
BUN, mmol/L	2.5∼7.14	7.54	5.55	4.59	5.88	8.37	10.54	7.07	4.91	4.80	4.25	4.69	3.22	25.0
eGFR, ml/(min*1.73 m2)	≥90	85.9	75.7	66.8	87.7	75.9	62.6	67.7	112	105.4	91.8	84.2	110.3	66.7
Ccr, ml/min	≥80	78.3	70.9	83.6	100.6	71.3	63.1	78.4	104.7	93.4	82.2	104.1	143.0	41.7
Urine detection														
PRO	–	–	–	1+	–	2+	2+	1+	–	1+	–	–	–	41.7
BLD	–	–	1+	–	–	–	–	–	–	–	–	–	–	8.3
24H UCr, umol/24 h	7,000–17,600	9,126	9,666	12,428	NA	9,760	15,369	11,478	NA	11,436	NA	11,077	7,084	0
24H UK, mmol/24 h	25–100	156	85	56	NA	125	168	224	NA	27	NA	25	36	44.4
24H UNa, mmol/24 h	130–260	206	311	145	NA	320	360	282	NA	363	NA	111	104	55.6
Urinary micro-protein detection														
UMA/Ucr, mg/g	<30	11.3	9.5	35.2	7.07	58	60.5	42.9	10.1	32.5	6.4	22.2	5.8	41.7
A1M/Ucr, mg/g	<20	12.4	54.8	10.6	4.7	133.4	123.2	107.7	10.5	29.4	18.2	16.7	16.2	41.7
IGU/Ucr, mg/g	<12.6	8.8	14.3	5.6	5.7	20.7	64.6	43.9	9.6	34.0	7.7	14.2	9.4	50.0
TRU/Ucr, mg/g	<3.2	3.0	9.5	2.8	2.1	3.5	4.1	9.1	2.8	3.0	2.5	2.8	3.0	33.3

Scr, serum creatinine; BUN, blood urea nitrogen; eGFR, estimated glomerular filtration rate; Ccr, endogenous creatinine clearance; PRO, urine protein; BLD, urine occult blood; Ucr, urine creatinine; UK, urine K; UNa, urine Na; UMA, urine microalbumin; A1M, α1-microglobulin; IGU, urine immunoglobulin G; TRU, urine transferrin; NA, no accepted.

TABLE 2 | Comparison of Scr and BUN between peak of disease and recovery period.

		Scr (umol/L)			BUN (mmol/L)		
	Cases	Peak of disease	Recovery period	*P*	Peak of disease	Recovery period	*P*
Total	12	84.74 ± 24.05	66.14 ± 19.36	0.002	5.95 ± 2.07	3.77 ± 0.72	<0.001
Case classification							
Severe	3	102.67 ± 10.25	61.13 ± 9.94	0.008	8.66 ± 1.75	4.56 ± 0.56	0.028
Common	9	78.77 ± 24.66	67.81 ± 21.87	0.002	5.04 ± 1.20	3.51 ± 0.57	0.002
Gender							
Male	7	102.33 ± 11.43	77.56 ± 16.54	0.011	6.48 ± 2.32	4.08 ± 0.76	0.011
Female	5	60.12 ± 9.76	50.16 ± 8.56	0.001	5.20 ± 1.56	3.33 ± 0.39	0.035
Age							
≥50	4	92.95 ± 21.16	58.40 ± 9.79	0.019	8.38 ± 1.54	4.34 ± 0.63	0.004
<50	8	80.64 ± 25.67	70.01 ± 22.28	0.006	4.74 ± 0.81	3.49 ± 0.61	0.001

Scr, Serum creatinine; BUN, Blood urea nitrogen.

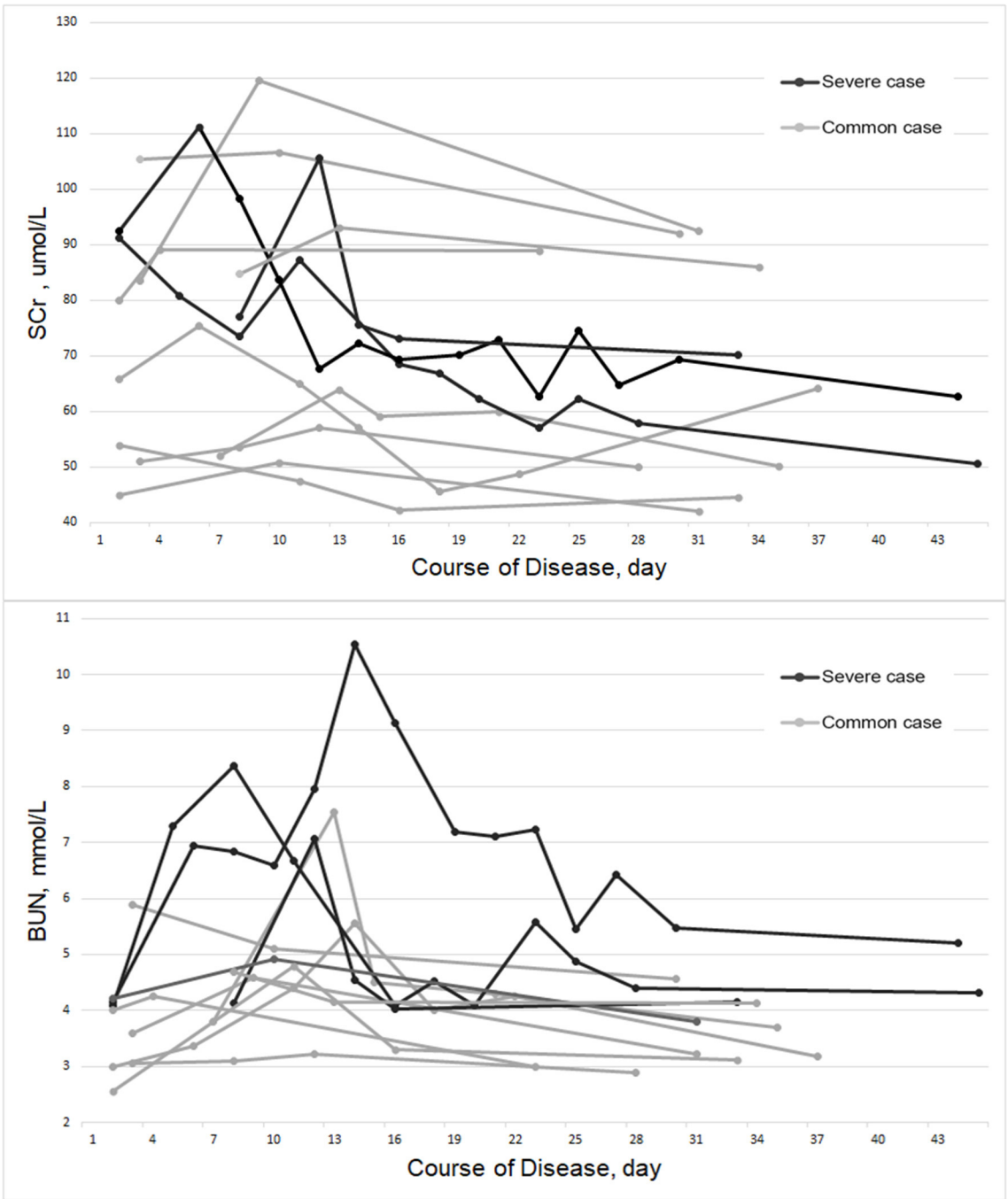

FIGURE 1 | Fluctuations in Scr and BUN of the COVID-19 patients from admission to recovery.

acid test of 2019-nCoV turned negative and at least 2 weeks after discharge, the patient's Scr and BUN increased significantly in peak of disease (p-scr = 0.002 & p-bun < 0.001). By conducting subgroup analyses, stratified by case classification (severe vs. common case), gender (male vs. female) and age (≥50 and <50 years old), the results were found to be consistent with the primary findings (**Table 2**). By observing the fluctuations in Scr and BUN from admission to recovery, we found that the peak values appeared within the first 14 days of the course of the disease, as shown in **Figure 1**.

Urinary microprotein detection showed that the abnormally elevated rates of urine microalbumin (UMA), α1-microglobulin (A1M), urine immunoglobulin-G (IGU), and urine transferring (TRU) standardized by urinary creatinine in peak of disease were 41.7, 41.7, 50.0, and 16.7%, respectively. The

abnormal rates of calculated eGFR and Ccr were 66.7 and 41.7% (**Table 1**).

DISCUSSION

Although diffuse alveolar damage and acute respiratory failure are the main features of COVID-19, the involvement of other organs also need to be considered. Early data suggests that acute kidney impairment is more common in COVID-19 patients than in patients with other coronavirus syndromes, and that kidney impairment associates with mortality (10). However, very little is known about renal involvement in COVID-19 patients. The present study intends to summarize the renal laboratory findings and make a deep characterization of renal function in COVID-19.

In this study, we report the renal laboratory findings in 12 sequential COVID-19 patients. The abnormally elevated rates of Scr and BUN are quite low. However, compared with the recovery period, the patient's Scr and BUN increased significantly in peak of disease. The abnormal rates of the calculated eGFR and Ccr are also higher in peak of disease. Scr and BUN are commonly used indicators for the detection of renal function. However, the sensitivities of both of them are poor. Usually, abnormalities occur only when renal function is significantly damaged. By calculating eGFR and CCr, which relies on age, gender, weight, and Scr, it can better reflect the early renal function impairment. The microproteins in urine are potential early biomarkers associated with renal impairment, most of them are closely related to glomerular filtration function and renal reabsorption function. Urinary microprotein detection in the included 12 COVID-19 patients find that the abnormally elevated rates of UMA, A1M, IGU, and TRU standardized by urinary creatinine in peak of disease are higher. The study also find that hypokalemia and hyponatremia are common in patients with COVID-19. By conducting 24-h urine electrolyte testing, it is found that patients with hypokalemia and hyponatremia also have excessive potassium and urinary sodium excretion, which suggest that these patients may have renal tubular reabsorption dysfunction.

Previously, an ongoing case study reported 59 patients infected by 2019-nCoV, including 28 severe cases and 3 death. In that study, 63% of the patients exhibited proteinuria, and 19 and 27% of the patients had an elevated level of Scr and BUN, respectively. Computed tomography (CT) scans revealed abnormal renal imaging in all patients. The results suggest that renal impairment is common in COVID-19, which may contribute to multiorgan failure and death eventually (11). Zhou et al. (12) reported the identification and characterization of 2019-nCoV. Through full-length genome sequences analysis, they found that the whole genome of 2019-nCoV shared 79.5% sequence identify to SARS-CoV. The pairwise protein sequence analysis of seven conserved non-structural proteins showed that this virus belongs to the species of severe acute respirator syndrome-related coronaviruses (SARSr-CoV). In addition, they also confirmed that 2019-nCov used the same cell entry receptor, Angiotensin converting enzyme II (ACE2), as SARS-CoV. The high degree of similarity in gene sequence and cellular mechanism of 2019-nCoV and SARS-CoV suggests that the risk factors of mortality could also be similar (12). Zou et al. (13) analyzed the single-cell RNA sequencing datasets to explore the expression of ACE2 in the main physiological systems of the human body, including the respiratory, cardiovascular, digestive and urinary system. The study showed that heart, esophagus, kidney, bladder, and ileum have similar or higher ACE2 expression than in alveoli. In the analysis of specific cell types, the expression of ACE2 in renal proximal tubule cells was about four times higher than that of type II alveolar cells (AT2) (13). The results suggest that the kidney may be one of the primary targets of attack for the 2019-nCov.

Strengths and Limitations

This is an initial study on renal function associated with COVID-19. It is important to show the clinical evidence of infection of 2019-nCoV which is not simply pneumonia. In this study, we summarize the renal laboratory findings in 12 sequential COVID-19 patients, addressing a critical question with data which is not available from other sources. This summary of data is important to share with the scientific community. However, the present study has some limitations that must be taken into account when considering its contribution. First and most significantly is the small sample size of this study. COVID-19 is a newly emerging epidemic. The cases found in this city are all imported cases. After strict prevention and control, there are fewer confirmed cases in this city. Therefore, the number of cases included in this research is also small. Secondly, considering COVID-19 is a completely new disease, and we do not yet fully know the characteristics of its cases, the type of research used in this study is designed as a descriptive study, which initially explores the basic characteristics of the disease and does not set the control group. Thirdly, in this study, we have evaluated some potential early biomarkers of kidney injury, such as UMA, IGU, and TRU. However, there are still some important biomarkers that have not been detected, like urinary Kim-1, MCP-1, and NGAL. As a retrospective study, we cannot retest these indicators. For the same reason, we are unable to retest the urine samples of patients to see if the 2019-nCoV could be detected. If there are new cases, we will try to tested the urine 2019-nCoV, and we hope our study can inspire more researchers to carry out relevant studies.

CONCLUSIONS

This study found that Scr and BUN were generally increased during the course of COVID-19. Detection of urinary microproteins and application of multiple indicators assessment could be helpful for discovering abnormal renal function in patients with COVID-19. However, the evidence is limited due to the small sample size and observational nature. Additional studies, especially large prospective cohort studies, are required to confirm these findings.

DATA AVAILABILITY STATEMENT

All datasets generated for this study are included in the article/**Supplementary Material**.

ETHICS STATEMENT

The studies involving human participants were reviewed and approved by the institutional research ethics committee of Shantou Central Hospital. Written informed consent to participate in this study was provided by the participants.

AUTHOR CONTRIBUTIONS

YZha obtained funding. XH and LQ designed the study. HH, JF, XL, LWu, and YZho collected the data. ZC and GL were involved in data verification and analyzed the data. SG, RC, QZ, SW, LWa, ZP, and HL are responsible for the diagnosis and treatment of patients. XH drafted the manuscript. YZha and LQ contributed to the interpretation of the results and critical revision of the manuscript for important intellectual content and approved the final version of the manuscript. All authors have read and approved the final manuscript.

FUNDING

This work was supported by the Special Project of New Coronavirus Pneumonia Prevention and Treatment funded by the Science and Technology Agency of Shantou City, No. (2020)16-6.

ACKNOWLEDGMENTS

We greatly appreciate all the people, particularly the clinicians, nurses, and scientists who are heroically battling to eradicate this disaster for days and nights. We also thank all patients involved in this study.

SUPPLEMENTARY MATERIAL

The Supplementary Material for this article can be found online at: https://www.frontiersin.org/articles/10.3389/fmed.2020.00409/full#supplementary-material

REFERENCES

1. Wang C, Horby PW, Hayden FG, Gao GF. A novel coronavirus outbreak of global health concern. *Lancet*. (2020) 395:470–3. doi: 10.1016/S0140-6736(20)30185-9
2. Zhu N, Zhang D, Wang W, Li X, Yang B, Song J, et al. A novel coronavirus from patients with pneumonia in China, 2019. *N Engl J Med*. (2020) 382:727–33. doi: 10.1056/NEJMoa2001017
3. Munster VJ, Koopmans M, van Doremalen N, van Riel D, de Wit E. A novel coronavirus emerging in china - key questions for impact assessment. *N Engl J Med*. (2020) 382:692–4. doi: 10.1056/NEJMp2000929
4. Perlman S. Another decade, another coronavirus. *N Engl J Med*. (2020) 382:760–2. doi: 10.1056/NEJMe2001126
5. Heymann DL, Shindo N. COVID-19: what is next for public health? *Lancet*. (2020) 395:542–5. doi: 10.1016/S0140-6736(20)30374-3
6. Wang LH. Characteristics and countermeasures of 2019-nCoV infection. *Chin J Exp Clin Infect Dis*. (2020) 14:1–5. doi: 10.3877/cma.j.issn.1674-1358.2020.01.001
7. Huang C, Wang Y, Li X, Ren L, Zhao J, Hu Y, et al. Clinical features of patients infected with 2019 novel coronavirus in Wuhan, China. *Lancet*. (2020) 395:497–506. doi: 10.1016/S0140-6736(20)30183-5
8. Chen N, Zhou M, Dong X, Qu J, Gong F, Han Y, et al. Epidemiological and clinical characteristics of 99 cases of 2019 novel coronavirus pneumonia in Wuhan, China: a descriptive study. *Lancet*. (2020) 395:507–13. doi: 10.1016/S0140-6736(20)30211-7
9. Commission CNH. Guidelines for diagnosis and treatment of COVID-19 (Trial Version 7). *J Cardiovasc Pulm Dis*. (2020) 46:1–7. doi: 10.13885/j.issn.1000-2812.2020.02.001
10. Cheng Y, Luo R, Wang K, Zhang M, Wang Z, Dong L, et al. Kidney disease is associated with in-hospital death of patients with COVID-19. *Kidney Int*. (2020) 97:829–38. doi: 10.1016/j.kint.2020.03.005
11. Li Z, Wu M, Yao J, Guo J, Liao X, Song S, et al. Caution on kidney dysfunctions of COVID-19 patients. *SSRN*. (2020) 20:3–19. doi: 10.2139/ssrn.3559601
12. Zhou P, Yang XL, Wang XG, Hu B, Zhang L, Zhang W, et al. A pneumonia outbreak associated with a new coronavirus of probable bat origin. *Nature*. (2020) 579:270–3. doi: 10.1038/s41586-020-2012-7
13. Zou X, Chen K, Zou J, Han P, Hao J, Han Z. The single-cell RNA-seq data analysis on the receptor ACE2 expression reveals the potential risk of different human organs vulnerable to Wuhan 2019-nCoV infection. *Front Med*. (2020) 14:185–92. doi: 10.1007/s11684-020-0754-0

Conflict of Interest: The authors declare that the research was conducted in the absence of any commercial or financial relationships that could be construed as a potential conflict of interest.

frontiers in Physiology

REVIEW
published: 14 July 2020
doi: 10.3389/fphys.2020.00735

An Overview of the Role of Calcium/Calmodulin-Dependent Protein Kinase in Cardiorenal Syndrome

Carolina Victoria Cruz Junho[1], Wellington Caio-Silva[1†], Mayra Trentin-Sonoda[2†] and Marcela Sorelli Carneiro-Ramos[1]*

[1] Center of Natural and Human Sciences (CCNH), Universidade Federal do ABC, Santo André, Brazil, [2] Division of Nephrology, Department of Medicine, Kidney Research Centre, Ottawa Hospital Research Institute, University of Ottawa, Ottawa, ON, Canada

OPEN ACCESS

Edited by:
Jonatan Barrera-Chimal, Universidad Nacional Autónoma de México, Mexico

Reviewed by:
Przemyslaw Radwanski, The Ohio State University, United States
Prasanth Puthanveetil, Midwestern University, United States

***Correspondence:**
Marcela Sorelli Carneiro-Ramos
marcela.ramos@ufabc.edu.br;
msorelli@gmail.com

[†] These authors have contributed equally to this work

Specialty section:
This article was submitted to Renal and Epithelial Physiology, a section of the journal Frontiers in Physiology

Received: 16 March 2020
Accepted: 08 June 2020
Published: 14 July 2020

Citation:
Junho CVC, Caio-Silva W, Trentin-Sonoda M and Carneiro-Ramos MS (2020) An Overview of the Role of Calcium/Calmodulin-Dependent Protein Kinase in Cardiorenal Syndrome. Front. Physiol. 11:735. doi: 10.3389/fphys.2020.00735

Calcium/calmodulin-dependent protein kinases (CaMKs) are key regulators of calcium signaling in health and disease. CaMKII is the most abundant isoform in the heart; although classically described as a regulator of excitation–contraction coupling, recent studies show that it can also mediate inflammation in cardiovascular diseases (CVDs). Among CVDs, cardiorenal syndrome (CRS) represents a pressing issue to be addressed, considering the growing incidence of kidney diseases worldwide. In this review, we aimed to discuss the role of CaMK as an inflammatory mediator in heart and kidney interaction by conducting an extensive literature review using the database PubMed. Here, we summarize the role and regulating mechanisms of CaMKII present in several quality studies, providing a better understanding for future investigations of CamKII in CVDs. Surprisingly, despite the obvious importance of CaMKII in the heart, very little is known about CaMKII in CRS. In conclusion, more studies are necessary to further understand the role of CaMKII in CRS.

Keywords: CaMKII, cardiorenal syndrome, inflammation, immune system, cardiovascular diseases

GENERAL CONSIDERATIONS

Calmodulin (CaM) is a low-molecular-weight protein highly conserved in the eukaryotes (Clapham, 2007). CaM was discovered in 1970 as a calcium (Ca^{2+}) regulator in the brain, responsible for the nucleotide phosphodiesterase. It was first mentioned as a Ca^{2+}-dependent regulator (Kakiuchi and Yamazaki, 1970). Since the origin of eukaryotes, the amino acids that compound CaM have not changed at all (Friedberg and Rhoads, 2001). It plays a fundamental role in every cell by amplification of the Ca^{2+} signal (Clapham, 2007). Ca^{2+} is a versatile messenger molecule implied in many basic processes, such as contraction, potentiation, cell proliferation and apoptosis, and others (Carafoli and Krebs, 2016). To maintain a homeostasis of Ca^{2+} in the intracellular environment, it has many mechanisms and signaling paths that help to establish a gradient of this ion, holding at approximately 2 mM (Clapham, 2007). One of them is the CaM that triggers conformational changes in response to Ca^{2+} oscillations (Carafoli and Krebs, 2016). In other words, when Ca^{2+} binds to CaM, it induces a structural modification, forming a Ca^{2+}/CaM complex (Clapham, 2007).

There is a vast quantity of proteins that can bind to Ca^{2+}/CaM via an α-helical region. This region is composed of approximately 20 amino acids, positively charged and containing hydrophobic residues (Islam, 2020). To amplify the signal generated by Ca^{2+}, this complex activates or deactivates phosphorylation pathways, targeting a protein kinase dependent on Ca^{2+}/CaM (CaMK) (Clapham, 2007). In other words, the binding of Ca^{2+}/CaM and phosphorylate serine/threonine residues of target proteins are the main trigger of CaMKs activation, initiating signaling activation of the substrates (Takemoto-Kimura et al., 2017).

The Ca^{2+}/CaM-stimulated protein kinases are divided based their substrate specificity. They can be restricted to a small number of substrates (Islam, 2020) while the multifunctional kinases have wide specificity and regulate multiple functions in the same and different cell types (Skelding et al., 2011). Restricted CaMK have three main families: phosphorylase kinase (PhK), elongation factor 2 kinase (eEF2K), and myosin light chain kinase (MLCK) (Skelding and Rostas, 2012). These families do not share common domains or structures, making them more specific to certain stimuli and pathways. On the other hand, the multifunctional kinases control many cell functions in different cell types, which makes them a powerful controller of other kinases. Regulation of Ca^{2+} dynamics is the most basal method to control the function of a kinase, mainly intracellular concentration of Ca^{2+} (Skelding and Rostas, 2012). The main multifunctional families of kinases proteins are CaMKI, CaMKIV, CaMKK, and CaMKII (Hudmon and Schulman, 2002).

The CaMKI family constitutes four elements, each of them encoding a different gene: CAMK1 (CaMKIα), PNCK (CaMKIβ/Pnck), CAMK1G (CaMKIγ/CLICK3), and CAMK1D (CaMKIδ/CKLiK), which are found in higher quantity in mice brains (Picciotto et al., 1995). CaMKI function is observed in many cellular activities, including synapsis in terminal nerves, motility, axon growth, synthesis of aldosterone, and the cell cycle (Condon et al., 2002; Skelding et al., 2011). It is known that CaMKI translocates to the nucleus mediated by CRM1 complex after an influx of intracellular Ca^{2+} induced by potassium depolarization or glutamate (Sakagami et al., 2005). CaMKIV only encodes one gene, CAMK4, coding the monomerics isofroms: α and β (Skelding and Rostas, 2020). CaMKIV is observed in the regulation of cyclic AMP, plasticity, fear memory, inflammatory sensibility, and control of the cell cycle (Skelding and Rostas, 2020). The CaMKIV can translocate between the cytoplasm and nucleus. For that action, it involves some catalytic activity as catalytically inactive CaMKIV remains in the cytoplasm (Lemrow et al., 2004).

Ca^{2+}/CaM-stimulated protein kinase kinase (CaMKK), CAMKK1 and CAMKK2, produce CaMKKα and CaMKKβ, respectively. They are responsible for many functions (Skelding and Rostas, 2020). Studies show this kinase's function, suggesting that CaMKK translocates to the nucleus under stimulation, and the inhibition of translocation directly implies the deactivation of monocytic cells (Guest et al., 2008). CaMKI, CaMKIV, and CaMKK share the same signaling pathway. It is called the Ca^{2+}/CaM-dependent kinase cascade (Tokumitsu and Soderling, 1996). This pathway is mainly related to several cellular processes, including glucose homeostasis, hematopoietic stem cell maintenance, cell proliferation, apoptosis, and normal immune cell function (Skelding and Rostas, 2012). Last but not least, among the CaMKs, we have the CaMKII. Its function is further explained in the next section. Together with this, the present study aims to focus on CaMKII relevance and how it is implied specifically during cardiorenal syndrome (CRS).

THE CALCIUM-CALMODULIN-CAMKII SIGNALING AXIS HAS A CRUCIAL ROLE IN CARDIAC FUNCTION

Among the CaMKs, the most abundant in the heart is CaMKII (Luczak and Anderson, 2014). CaMKII is a serine-threonine kinase, and it was first identified in the central nervous system, where it represents only 2% of the total protein. It was later discovered that this enzyme is present in many tissues, including the pancreas, where it has an important role in the secretion of insulin, and in heart tissue, where it is responsible for Ca^{2+} homeostasis (Yamauchi, 2005).

The functional CaMKII enzyme structure is formed by 12 subunits (dodecameric); each monomer has an N-terminal catalytic domain and a C-terminal domain with a regulatory domain in the middle as shown in **Figure 1**. The catalytic domain is blocked by the regulatory domain in an autoinhibitory way, keeping the enzyme inactive (**Figure 1**). CaMKII becomes active when the Ca^{2+}/CaM complex binds to the binding site of the regulatory domain of CaM. This provokes a successive autophosphorylation of Thr287 monomers, causing conformational changes that expose the catalytic domain and enable the kinase activity at all (Beckendorf et al., 2018). As proposed by Beckendorf et al. (2018), the Thr287 autophosphorylation causes what they denominate "CaM trapping," increasing the CaM binding affinity to 1000-fold, maintaining the CaMKII activity even under low Ca^{2+} conditions (Beckendorf et al., 2018). Besides the activation via Ca^{2+}/CaM that is dependent on several Ca^{2+} factors, such as the total Ca^{2+} available in a dose-dependent manner and its spark frequency, amplitude, and duration, the CaMKII can be activated via post-translational modifications as, for example, by reactive oxygen species (ROS) (Beckendorf et al., 2018).

CaMKII is observed in eukaryotes in four distinct isoforms (α, β, γ, δ). They encode four distinct genes (Luczak and Anderson, 2014). CaMKIIα and β are expressed mainly in the neural system while the CaMKIIδ and γ isoforms are predominantly expressed in cardiac tissue (Backs et al., 2009). This kinase modulates numerous biological processes, such as the Ca^{2+} homoeostasis, excitement of membrane, cell cycle, cytoskeletal organization, and gene expression (Yamauchi, 2005; Backs et al., 2009).

As the contraction is a Ca^{2+}-dependent process, it is indisputable that CaMKII performs an important role in the heart. It regulates Ca^{2+}-handling proteins by facilitating the L-type Ca^{2+} channel (LTCC) phosphorylation (Bers and Morotti, 2014); promotes phosphorylation of phospholamban (PLN) at site T17, promoting its dissociation from SERCA2a and, thus increasing SERCA2a activity; and phosphorylates ryanodine

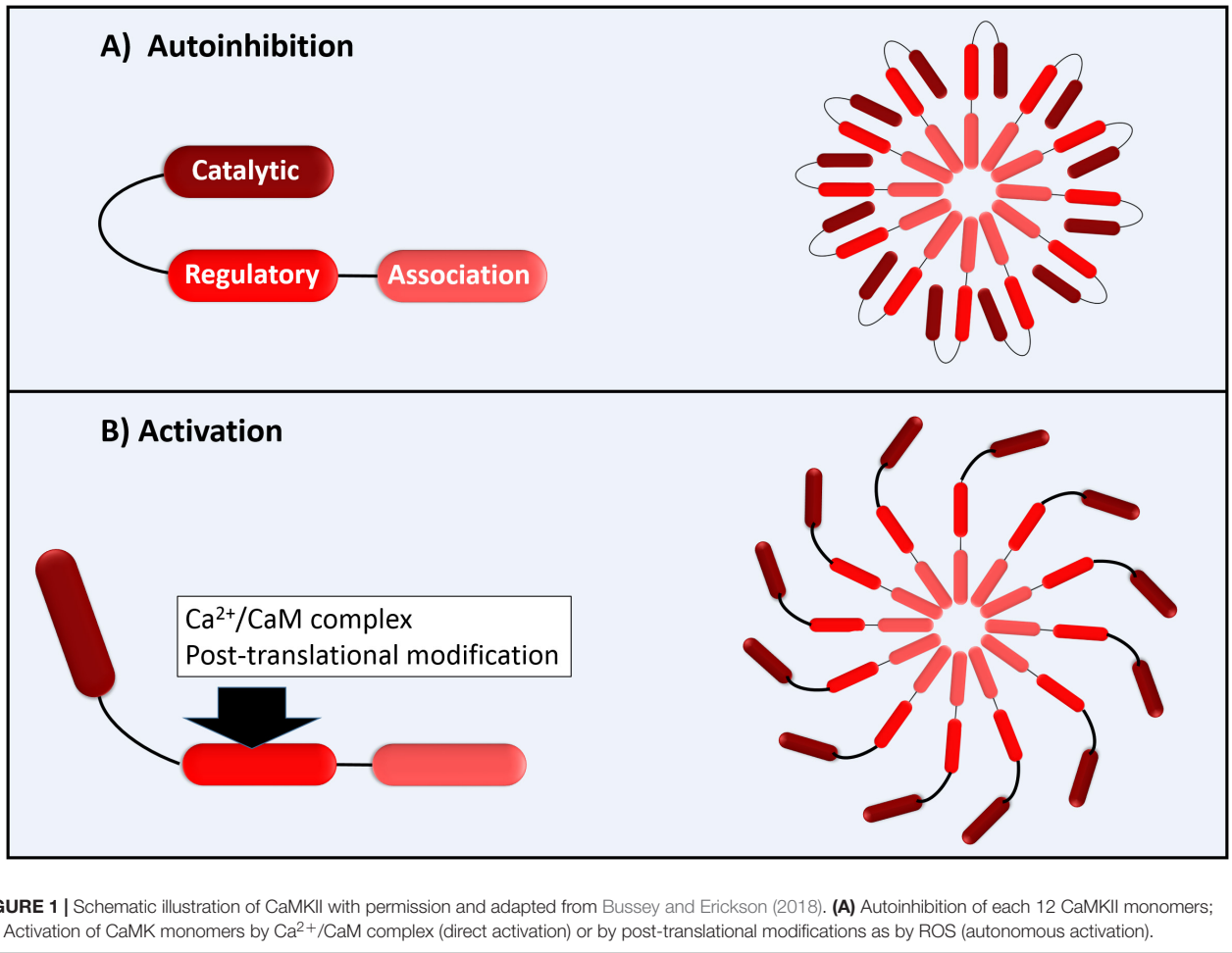

FIGURE 1 | Schematic illustration of CaMKII with permission and adapted from Bussey and Erickson (2018). **(A)** Autoinhibition of each 12 CaMKII monomers; **(B)** Activation of CaMK monomers by Ca^{2+}/CaM complex (direct activation) or by post-translational modifications as by ROS (autonomous activation).

(RYR) at site S2814, consequently improving its opening probability (Mattiazzi and Kranias, 2014). Hyperphosphorylation caused by CaMKII of this site leads to an increase of spontaneous elementary Ca^{2+}-release events from the sarcoplasmic reticulum especially during diastole (Mustroph et al., 2017). In pathological situations, increased diastolic Ca^{2+} in cytosol can activate the electrogenic NCX, which can cause delayed afterdepolarizations. The last ones can trigger atrial and ventricular arrhythmias (Mustroph et al., 2017). In other words, CaMKII is a pro-arrhythmogenic protein in the heart. Besides arrhythmias, CaMKII is strongly increased during myocardial injury (Ren et al., 2003), atrial fibrillation (Liu et al., 2019), cardiac hypertrophy (Kamada et al., 2019), ischemia/reperfusion injury (Rajtik et al., 2016), and heart failure (HF) (Beckendorf et al., 2018). Its inhibition has been constantly suggested as treatment for these pathologies (Rokita and Anderson, 2012; Cipolletta et al., 2015).

There are studies using transgenic (TG) overexpression of CaMKIIδ, to evaluate its effect during pathogenesis. TG mice developed severe HF and susceptibility to induced ventricular arrhythmias via programmed electrical stimulation (Maier and Bers, 2007). The cardiomyocytes isolated from TG mice presented increased diastolic Ca^{2+} leak together with prolonged action potential and increased incidence of early afterdepolarization (a peculiarity of CaMK-induced increased late I_{Na}) (Wagner et al., 2006).

In summary, TG mice led to a worsening of the arrhythmogenic profile of the mice in addition to increasing their risk of life. On the other hand, the silencing of CaMKII brings hope for the treatment of chronic or acute heart diseases, presenting itself as a potential clinical therapist against these pathologies.

THE ROLE OF CAMKII IN CARDIORENAL SYNDROME

The kidneys and the heart share an important role in the biochemical maintenance of homeostatic function of extracellular fluid. In general, while the heart is responsible for providing nutrients and oxygen-rich fluids to the body through blood flow, the kidney is responsible for providing electrolytes, acid-base homeostasis, vitamin D activation, and erythropoietin synthesis (Ronco and Di Lullo, 2014). Understanding how the kidney and heart relate has been a challenge since the Middle Ages, when Aetius of Amida initially attempted to

explain fluid overlay by attributing it to kidney hardening (Diamandopoulos, 1999).

Fast-forwarding to contemporary times, several studies approach this topic with more precision. Nowadays, it is well established that an adverse imbalance in hemodynamics caused by impaired kidney function can directly impact the heart (Anavekar et al., 2004). The pathological crosstalk between both organs is called cardiorenal syndrome (CRS), in which cardiac and renal dysfunction overlap; a disorder in one organ leads to acute or chronic dysfunction of the other organ (Ronco, 2011; Ronco and Di Lullo, 2014).

CRS is divided into two major groups, the cardiorenal and nephron-cardiac, dependent on the origin of the primary pathology, both of which can be acute or chronic (Ronco and Di Lullo, 2014). Type 1 and 2 CRS are considered cardiorenal and are characterized by a loss of cardiac function leading to renal injury (Damman et al., 2007). CRS type 1, known as acute, is described by acute cardiac injury leading a renal one through hemodynamic mechanisms (Di Lullo et al., 2017). The presence of acute decompensated HF leads to decreased renal function due to low renal arterial flow and decrease of the glomerular filtration rate. Once hemodynamic parameters are restored, renal and cardiac homeostasis is also restored (Hanada et al., 2012). Type 2 CRS rises as a consequence of chronic abnormalities in cardiac function that cause renal injury or dysfunction. Examples of such abnormalities are conditions including atrial fibrillation, congenital heart disease, pericarditis constrictions, and chronic cardiac ischemia. Determining whether the CRS is a type 1 or 2 represents a challenge for clinicians since the majority of diagnostics are made when both organs are already injured.

The other two types of CRS (3 and 4) are described as nephron-cardiac syndromes, where the renal injury leads to cardiac dysfunction (Damman et al., 2007). Type 3 CRS is defined as acute nephron-cardiac syndrome, occurring when acute renal failure leads to the development of acute cardiac injury. It is intimately related to events triggering increased inflammatory processes, such as oxidative stress and secretion of neurohormones (Di Lullo et al., 2017). Type 4 CRS is studied as chronic nephron-cardiac disease, initiated by chronic kidney disease (CKD), leading to cardiovascular disease. Approximately 70–80% of patients with end-stage renal disease present type 4 CRS, presenting cardiac complications, such as infarct and long-term arrhythmias (Di Lullo et al., 2017).

Finally, CRS type 5 is a systemic disorder that reaches both organs simultaneously. Many factors have been suggested to contribute to these conditions, for instance, sepsis, infections, drugs, toxins, and diabetes. It is important to note that acute type 5 CRS can overlap a chronic injury (Ronco and Di Lullo, 2014). CRS type 5 results in cardiac and renal dysfunction coming from a larger and systematic situation. Hence, differently from other types of CRS, type 5 is relatively easier to identify the starting point of the CRS.

The study of CRS is of great relevance for clinical treatment, considering that cardiovascular diseases represent the main cause of death in the United States for at least the last 15 years, according to the Centers for Disease Control and Prevention (CDC)[1]. In addition, incidence of CVDs have been increasing alongside incidence of CKDs worldwide (Thomas et al., 2017), showing the importance of studies regarding CRS type 4, for example. Besides, CKDs significantly affects the regulation of cardiac Ca^{2+} by mechanisms not yet clarified (Ke et al., 2020).

CaMKII has already been described as a cause of many heart dysfunctions, such as arrhythmia, hypertrophy, and infarction (Yoo et al., 2018; Rusciano et al., 2019), and has been demonstrated to play a critical role in CRS types 1 and 2. The CaMKII inhibitor (CaMK2n) has been shown to protect cardiac dysfunction and ameliorate injuries observed in metabolic syndrome (Prasad et al., 2015). However, Alfazema and collaborators showed, recently, in a translational study, that deletion of CaMK2n1, diminishes CaMKII activity in the kidney and heart without affecting adipose tissue (Alfazema et al., 2019). Yet there are few studies involving both organs in a systemic profile.

It is known that elements, such as the immune system, can mediate the communication between them. In an inflammatory process as observed during CKD and chronic heart failure (CHF), cytokines are released by circulating and tissue-resident inflammatory cells (monocytes mainly) and play an important role in the progression of these diseases (Yogasundaram et al., 2019). Since Ca^{2+} has been associated with several events of the inflammatory response, including the activation of T cells and awakening memory (Boubali et al., 2012). The CaMKII ability to act as an intracellular sensor of Ca^{2+} makes it a crucial regulator in the inflammatory process (Rusciano et al., 2019). On the other hand, the Ca^{2+}-independent form of CaMKIIγ also modulates cell death and T cell memory formation (Bui et al., 2000). Studies have already shown that CaMKII is capable of modulating NF-κB, IL-10, IL-2, and IL-4 production (Rusciano et al., 2019).

In CRS, the tissue injury is strongly followed by inflammation. Many inflammatory cytokines are enhanced in experimental models of renal ischemia (TNF-a, IL-1, and IL-6) and also markers, including the factor nuclear kappa B (NF-kB), which is very important for cell signaling during inflammatory processes (Trentin-Sonoda et al., 2015). Given that, some studies present the participation of inflammation as a cause of CKD progression in CHF patients (House et al., 2019; Marsico et al., 2019). During cardiac ischemia, myocytes release inflammatory cytokines (Colombo et al., 2012), and they can reach renal tissue, inducing local inflammation, apoptosis, or oxidative stress (Ronco and Di Lullo, 2014).

Colombo et al. (2012) suggest that inflammation during CRS is controlled by positive feedback mechanisms. Inflammation initiates vascular dysfunction, reducing the myocardial contractility and increasing myocardial cell death, linking CRS to apoptosis (Virzì et al., 2015b). Inflammation also causes progressive renal dysfunction and fibrosis, which continues to injure the organ, maintaining the cycle. Additionally, inflammation leads to the release of renin, activating the renin-angiotensin-aldosterone system (RAAS), which activates

[1]Centers for Disease Control and Prevention. National Center for Health Statistics. "Leading Causes of Death: Deaths: Leading Causes for 2017, table 1. Available at: http://www.cdc.gov/nchs/fastats/leading-causes-of-death.htm [Accessed March 14, 2020].

the sympathetic nervous system (SNS) by increasing serum norepinephrine concentrations and is the cause of ROS release from the inflammatory cells (Bongartz et al., 2005).

A previous study suggests that the toll-like receptor (TLR) pathway is linked with the activation of CaMKII in a model of myocardial infarction (Singh et al., 2012). Recently, Wu and collaborators demonstrated that miR-148a attenuates ischemia/reperfusion injury in liver, once CaMKIIα represses the TLR4 signaling pathway in vivo and in vitro, decreasing the production of pro-inflammatory factors (Zheng et al., 2018). Moreover, activation of CaMKII in macrophages is initiated by a significant trigger elevation of intracellular Ca^{2+}. This progresses to the activation of myeloid differentiation factor 88 (MyD88)-dependent and Toll/interleukin-1 receptor domain, prompting proinflammatory factors. Ca^{2+}/CaMKII is fundamental for macrophage response once it requires the complete activation of the TLR pathway (Liu X. et al., 2008).

As mentioned above and summarized by Rusciano et al. (2019) there is evidence that suggests the important role of CaMKII in many cardiac pathologies involving inflammation due its ability to enhance pro-inflammatory signaling and its responsiveness to inflammation by dysregulating the Ca^{2+} balance. In the kidneys, CaMKIIβ expression is associated to aldosterone-induced fibrosis (Park et al., 2018; Zhang et al., 2018) and also shows that the increase in mitochondrial fragmentation observed in hyperglycemia stress-mediated renal damage is due to the JNK-CaMKII-Fis1 pathway (Zhang et al., 2018).

CamKII Inhibition Displays Cardioprotection

As discussed above, silencing CaMKII has great therapeutic value. There are many blockers and inhibitors used nowadays in research. The most known are KN-93 and AC3-I.

The first inhibitor described was KN-62 in 1990 (Tokumitsu et al., 1990). One year later, in 1991, Sumi M and collaborators described a new and more selective inhibitor called KN-93 (Sumi et al., 1991). They act by blocking the enveloping of Ca^{2+}/CaM around the CaM-binding segment and automatically freeing this segment from the catalytic domain (Pellicena and Schulman, 2014). In other words, it is a CaM-competitive CaMKII inhibitor. It was already discovered that KN-93 can directly block the potassium current I_{Kr} and potassium voltaged channels, preventing arrhythmic properties of CamKII (Mustroph et al., 2017). An important item to bring up is that KN-62/93 binds to the holoenzyme and directly steps in the interaction of Ca^{2+}/CaM but does not directly bind to CaM (Sumi et al., 1991). Besides belonging to a family of CaM antagonists, KN-93 cannot avoid the activity of autophosphorylation of CaMKII (Wong et al., 2019).

Some studies have proven the efficiency of KN-93 in heart pathologies in several animal models. Under in vitro and in vivo stimulations with isoproterenol, arrhythmias have been abolished after using NK-93 (Sag et al., 2011). It also prevents arrhythmias after models of acidosis, DOX-induced, NO-donor SNAP (Mustroph et al., 2017). On some models, the KN-93 does not seem to prevent but to slow the arrhythmia (as longer cycle length) without marked alterations in baseline ECG characteristics (Hoeker et al., 2016). KN-93 also reduces diastolic cytosolic [Ca^{2+}] after induced HF (Sag et al., 2011). It is also an attenuator of Ca^{2+}-leak in a diabetes model of GlcNAcase inhibition (Erickson et al., 2013) and myocardial hypertrophy. Another study shows the high capacity to inhibit the binding of CaM with $Na_V1.5$, increasing the calcium release from RYR2 in cardiomyocytes independent from CamKII (Johnson et al., 2019). This suggests that KN-93 has interactions with the CaM-Ca^{2+} binding; however, to inhibit CaMKII specifically, more affinized compound is necessary.

Experiments using TG RYR-mutant mice (S2814D mutant) are naturally more susceptible to atrial fibrillation, and because of this, it is used as a well-established model. Atrial fibrillation, phospholamban phosphorylation, and diastolic Ca^{2+}-leak are reduced after prior injection of KN-93 in these TG mice (Voigt et al., 2012). Cardiomyocytes isolated from TG CaMKIIδc knockout mice completely recover the contraction ability after acidosis injury (Mustroph et al., 2017).

There is also a highly specific inhibitor of CaMKII called autocamtide-3-derived inhibitory peptide (AC3-I). It is the most used one in studies that require the blocking of CaMKII, and it is resistant even to proteolysis. As mentioned, AC3-I is derived from autocamtide-3. The last one is a substrate for CaMKII and acts mainly in the Thr-9 phosphorylation site substituted with Ala (Maier and Bers, 2007). As the research regarding CaMKII increases, its therapeutic use implicated in pharmaceuticals has been studied more. Several studies, using these inhibitors mentioned above, impart a cardio protection.

As mentioned, the AC3-I blocker, is a highly specific inhibitor of CaMKII. This is the main reason it is used more in the studies concerning the participation of CaMKII in many cell functions. It can inhibit CAMKII more selectively than CaMKIV (more and a hundredfold). Studies using this blocker also imply cardio protection: preventing hypertrophy, reducing ventricular arrhythmias, improving mechanical function, reducing RyR2 lacking, and decreasing mortality of diabetic mice (Sag et al., 2011).

Some studies have proven the efficiency of AC3-I in pathologies in some animal models. As cited with KN-93, the AC3-I also reduces atrial fibrillation in TG RYR knockout mice (Chelu et al., 2009) and seems to protect the heart from the same atrial fibrillation in Ang II models *in vivo* and *in vitro* (Purohit et al., 2013). There is a study from our group using interference RNA (RNAi) to block the expression of CaMKIIδ. It demonstrates that CaMKIIδ is fundamental for cardiomyocyte hypertrophy; once blocking the expression, the LPS-induced hypertrophy is reverted (Cruz Junho et al., 2019).

There are several models of heart problems leading to CaMKII. CRS, already cited, seems to be one of them. Both kidneys and heart share many mechanisms of homeostasis, and any injury to one can lead to one in the other. It is known that CaMKII is increased in many models of heart injury, and some models of CRS can cause arrhythmias and AP chances as well as contraction irregularities (Navarro-García et al., 2018; Alarcon et al., 2019). CaMKII could be crucial to the progression of CRS, more specifically related to the progression from acute HF to

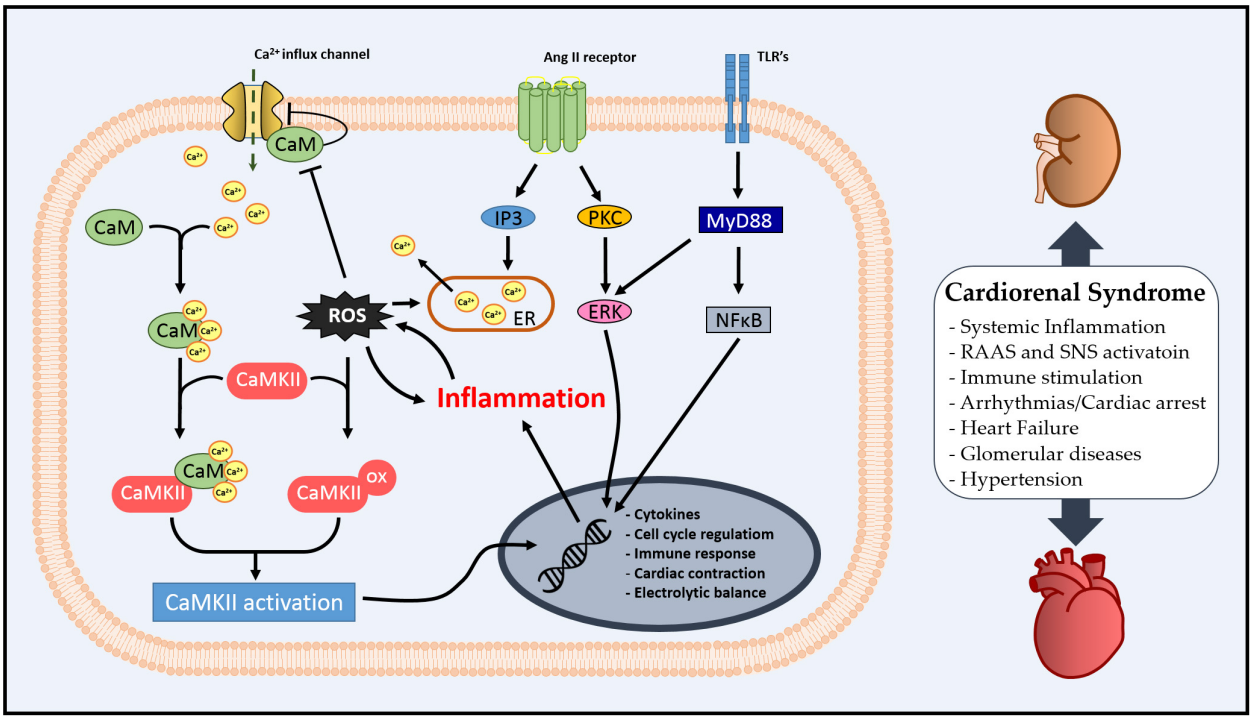

FIGURE 2 | Schematic illustration of cellular Ca^{2+}/calmodulin-dependent (CaMK) II involvement in cardiorenal syndrome (CRS).

chronic (types 1 and 2). In this scenario, the inhibition of CaMKII would be cardioprotective.

OXIDATIVE STRESS AND EPIGENETICS FACTORS AS CAMKII REGULATORS

The close relation between inflammation and oxidative stress in pathophysiological processes also makes the balance between oxidant and antioxidant forces and, therefore, oxidative stress, one of the most important mechanisms as has been demonstrated in heart and kidney injury studies (Li et al., 2017; Oliveira et al., 2017; Liu and Liu, 2018; Songbo et al., 2019).

Even though physiological levels of oxidative species are necessary for cellular function, the oxidative stress caused by the overproduction of these molecules in both organs leads to a series of structural abnormalities via immune system activation and fibrotic promotion (Virzì et al., 2015a). Some of these pathologies include left ventricle hypertrophy, atherosclerosis, endothelial dysfunction, and fibrosis in the heart while in the kidney ROS promotes interstitial fibrosis and increased inflammation (Kumar et al., 2019). A study involving patients with CRS type 3 shows that they have an increased level of inflammatory and oxidative stress factors, including IL-6, myeloperoxidase, nitric oxide (NO), copper/zinc superoxide dismutase (SOD), and endogenous peroxidase (Virzì et al., 2015a). Oxidative stress triggers an inflammatory response, and this response induces more oxidative stress. This stress may be maintaining the previously mentioned cycle of damage. While Ca^{2+} is associated with inflammation, studies have shown a connection between oxidative stress and CaMKII activation (Erickson et al., 2008). Erickson et al. (2008) also demonstrate a dynamic mechanism for CaMKII activation, which occurs via oxidation of the methionine residue site on the CaMKII regulatory domain; this oxidation-dependent CaMKII activation is important to Ang II and apoptosis since CaMKII remains active after ROS oxidation even in the absence of the Ca^{2+}/CaM complex. Some proteins maintain a redox sensor that regulates the cell response to oxidative stress (Kim et al., 2014). CaM is one of these proteins, and this oxidation leads to a regulatory cascade response with specific targets, including CaMKII (Snijder et al., 2011), plasma membrane Ca^{2+} (Anbanandam et al., 2005), and nitric oxide synthase (NOS) (Montgomery et al., 2003). As mentioned above, one of the mechano-chemotransductions that ROS induces Ca^{2+} release by CaMKII involves NOS (Jian et al., 2014). The endothelial dysfunction caused by oxidative stress leads to uncoupling of endothelial NOS (eNOS), leading to the production of more ROS (Münzel et al., 2017). In pathological conditions, such as inflammation, the vasculature expresses the inducible form of NOS (iNOS) (Münzel et al., 2017). This isoform of NOS produces an excessive amount of NO that mediates impaired vasoconstriction, which may be further worsened by the decreased of eNOS activity (Jian et al., 2014). The continuous exposure of NO induced by pro-inflammatory mediators inhibits endothelium-dependent relaxation by impairing the via CaMKII-dependent activation of eNOS (Kassler et al., 1997). In addition, studies have shown the role of NOS in the kidney, demonstrating that, when NOS

activity is compromised, there are a series of renal dysfunctions that reduce glomerular perfusion and filtration, which may lead to a progressive scenario of hypertension and kidney injuries (Carlstrom and Montenegro, 2019).

Oxidative stress in CaMKII by methionine-oxidized CaMKII was also observed in patients with atrial fibrillation (Purohit et al., 2013; Yoo et al., 2018), which also demonstrates that oxidative stress can act in part through increased constitutive activity of CaMKII, creating a highly vulnerable substrate within the HF that promotes atrial fibrillation beyond fibrosis. On the other hand, Kong et al. (2018) shows that the oxidative stress in mitochondria can be reduced after the inhibition of CaMKII, alleviating the myocardial ischemia-reperfusion injury. In addition to the redox balance, other factors indirectly contribute to cardiac and renal alterations. Many approaches have been studied in order to set a start point for the CRS. One of them is epigenetics factors.

Epigenetics is the area of biology that studies changes in the functioning of a gene that is not caused by alterations in the DNA sequence and that perpetuate in the meiotic or mitotic cell divisions (Wu and Morris, 2001). Epigenetic modifications are highly coordinated processes of change that are not restricted to a specific phase of life. These characteristics are fundamental to diseases acquired throughout life. Epigenetic changes are divided into DNA methylation, histone modification, and noncoding RNA expression (Liu L. et al., 2008).

Studies have been developed to innovate the way to prevent CRS. Slowly, epigenetics is gaining space, and traditional mechanisms (such as RAAS and inflammation) are being replaced by other patterns of findings and prevention. Imaging the scale of modifications and mutations in a syndrome such as CRS, numerous cell lines may be altered and reprogrammed, in both heart and kidney. Studies have pointed out the role of epigenetics in the development of CRS (Gaikwad et al., 2010). In types 3 and 4, for example, renal failure increases cardiac histone H3 epigenetics, evidencing the crosstalk between renal failure and the transcription of cardiomyopathy-related genes (Gaikwad et al., 2010). It is important to mention that epigenetics in CRS itself are little studied when compared to the traditional mechanisms even though it is very promising. The focus of studies is linked to inflammation and oxidative stress, which we know to be the consequences of CRS. Abnormal defects in DNA methylation, histone modifications, and microRNA (miR) participate in renal injury (Beckerman et al., 2014); however, none of them are related to post-progression of HF. During HF independent of renal injury, we can note the expression of transcription factors, angiogenic factors, and natriuretic factors, often used as biomarkers of this condition. Epigenetic modifications regulate them. Pathological hypertrophy and compromised contractility are described to increase DNA methylation levels. Inhibition of DNA methylation has already been suggested as treatment for CHF (Yang et al., 2015); however, it should be carefully studied once the DNA methylation is comprehended.

Ca^{2+} signaling is involved in epigenetic regulation, and the study of its signaling can contribute to the development of new therapeutic strategies (Awad et al., 2015; Puri, 2020). CaMKIIδ has been already described as fundamental for cardiac hypertrophy development (Cruz Junho et al., 2019). This mechanism occurs after CaMKIIδ selectively phosphorylates HDAC4. During cardiac hypertrophy, there is an activation of fetal cardiac genes, an important mechanism regulated by CaMKIIδ-mediated H3 chromatin regulation. With the recent development of epigenetic studies, the use of ChIP-seq to evaluate H3 phosphorylation and binding of CaMKIIδ across the genome enables a profound knowledge of the genome-wide functional effect of H3 alteration by CaMKIIδ (Awad et al., 2015). This connection can lead to CRS types 1 and 2 and can be strongly linked to the diagnosis of heart dysfunction. In addition, it is extremely important to highlight the role of micro RNA (miR). miR is a short and noncoding RNA that interacts with the 3-untranslated region (UTR) of mRNAs blocking gene expression, degrading mRNAs and regulating protein expression (Winter et al., 2009; Krol et al., 2010; Qi et al., 2019; Yang et al., 2019).

To identify signaling pathways, there is a serviceable tool called gene set analysis (GSA). It uses statistical analysis to predefine gene sets involved in a specific cellular process. Thus, GSA is especially useful to infer functions of different miRNAs. For example, miR-185 has a key role during cardiac hypertrophy. This miRNA targets pro-hypertrophic genes, such as RhoA, Cdc42, and Stim1 in the heart. Given that, miR-185 is also a potent therapeutic target for cardiac diseases (Brown et al., 2006; Carè et al., 2007; Liu et al., 2011; Zhang et al., 2015). In addition, Kim et al. (2015) show that miR-185 not only acts as the genes mentioned, but also targeting genes involved in Ca^{2+}-associated pathological hypertrophy, including CamKII. It is worth mentioning the role of miR-1, once alterations in its expression or inhibition have been discovered in many cardiac pathologies (Yang et al., 2007; Lu et al., 2009).

Recently, Zhang et al. proposed a possible mechanism by which *Lycium barbarum* polysaccharides (LBP) restore cardiac contractility induced by miR-1 overexpression. The authors show that LBPs prevent the reduction of CaM and cardiac myosin light chain kinase and their corresponding downstream proteins, including CaMKII due to miR-1 overexpression (Zhang et al., 2018).

Regarding inflammatory processes, miR-625-5p has been illustrated to inhibit inflammatory response in human bronchial epithelial cells and is downregulated in heart diseases once miR-625-5p is able to inhibit STAT3 and reduce the expression of CaMKII. Moreover, miR-625-5p attenuated Ang II-induced cardiac hypertrophy through CaMKII/STAT3 (Qian et al., 2019).

In relation to kidney disease, Park et al. (2018) shows that miR-34c-5p and CaMKII are involved in aldosterone-induced fibrosis in the kidneys. In addition, recent studies have focused on MiR regulation and exosomes, specialized nanosized membranous vesicles, in different experimental models. These membrane-bound vesicles (30–100 nm) are released from different cell types and deliver bioactive molecules, including microRNAs (miRs). Recently, literature demonstrated the regulation of oxidative stress in cardiac stem cells through the miR-214/CaMKII pathway after using exosomes derived from miR-214-enriched bone marrow-derived mesenchymal cells (Wang et al., 2018).

In addition to miRs, the role of long noncoding RNAs (lncRNAs) is well known. lncRNAs are transcribed RNA

molecules >200 nucleotides in length without known protein-coding function, regulating gene expression at epigenetic, transcriptional, and post-transcriptional levels (Mercer et al., 2009). Previous studies report that lncRNAs play critical roles in the modulation of heart development and cardiovascular diseases (Wang et al., 2014, 2015; Zhang et al., 2016, 2017). For example, Shao et al. (2017) demonstrated that the expression of long noncoding RNAs TINCR was downregulated in the heart after a transverse aortic constriction (TAC) model (Shao et al., 2017). More recently, the same group showed that TINCR could epigenetically inhibit the transcription of CaMKII inhibiting cardiac hypertrophy induced by angiotensin II (Shao et al., 2017).

The evidence in the literature suggests that CaMKII is a key molecule for understanding the physiology and physiopathology of cardiovascular diseases as well as a prominent target for new strategies of treatment.

CONCLUSION

In this review, we aimed to stimulate a discussion on the role of CaM as an inflammatory mediator in the systemic profile of CRS via regulation of CaMKII. The literature suggests that the Ca^{2+}/CaM complex might be an important modulator of inflammation and oxidative stress via CaMKII in the kidney–heart interaction (summarized in **Figure 2**), and CaMKII regulation by pre- or post-translational mechanisms is essential for cardiac or renal homeostasis. Additionally, we have observed that CaM/CaMKII has been extensively studied in cardiovascular diseases; however, there is still the necessity of exploring how CaM could integrate Ca^{2+} signal in different scenarios, such as CRS.

AUTHOR CONTRIBUTIONS

CJ and MC-R proposed the idea and writing. All authors contributed to the article and approved the submitted version.

FUNDING

This work was supported by FAPESP: São Paulo Research Foundation, Brazil, Grants: 2008/10175-4, 2015/19105-7, 2014/16908-4, and 2018/3089-6.

REFERENCES

Alarcon, M. M. L., Trentin-Sonoda, M., Panico, K., Schleier, Y., Duque, T., Moreno-Loaiza, O., et al. (2019). Cardiac arrhythmias after renal I/R depend on IL-1β. *J. Mol. Cell. Cardiol.* 131, 101–111. doi: 10.1016/j.yjmcc.2019.04.025

Alfazema, N., Barrier, M., De Procé, S. M., Menzies, R. I., Carter, R., Stewart, K., et al. (2019). Camk2n1 is a negative regulator of blood pressure, left ventricular mass, insulin sensitivity, and promotes adiposity. *Hypertension* 74, 687–696. doi: 10.1161/HYPERTENSIONAHA.118.12409

Anavekar, N. S., McMurray, J. J. V., Velazquez, E. J., Solomon, S. D., Kober, L., Rouleau, J. L., et al. (2004). Relation between renal dysfunction and cardiovascular outcomes after myocardial infarction. *N. Engl. J. Med.* 351, 1285–1295. doi: 10.1056/NEJMoa041365

Anbanandam, A., Bieber Urbauer, R. J., Bartlett, R. K., Smallwood, H. S., Squier, T. C., and Urbauer, J. L. (2005). Mediating molecular recognition by methionine oxidation: conformational switching by oxidation of methionine in the carboxyl-terminal domain of calmodulin. *Biochemistry* 44, 9486–9496. doi: 10.1021/bi0504963

Awad, S., Al-Haffar, K. M. A., Marashly, Q., Quijada, P., Kunhi, M., Al-Yacoub, N., et al. (2015). Control of histone H3 phosphorylation by CaMKII. in response to haemodynamic cardiac stress. *J. Pathol.* 235, 606–618. doi: 10.1002/path.4489

Backs, J., Backs, T., Neef, S., Kreusser, M. M., Lehmann, L. H., Patrick, D. M., et al. (2009). The δ isoform of CaM kinase II is required for pathological cardiac hypertrophy and remodeling after pressure overload. *Proc. Natl. Acad. Sci. U.S.A.* 106, 2342–2347. doi: 10.1073/pnas.0813013106

Beckendorf, J., van den Hoogenhof, M. M. G., and Backs, J. (2018). Physiological and unappreciated roles of CaMKII in the heart. *Basic Res. Cardiol.* 113, 1–12. doi: 10.1007/s00395-018-0688-8

Beckerman, P., Ko, Y. A., and Susztak, K. (2014). Epigenetics: a new way to look at kidney diseases. *Nephrol. Dial. Transplant.* 29, 1821–1827. doi: 10.1093/ndt/gfu026

Bers, D. M., and Morotti, S. (2014). Ca2+ current facilitation is CaMKII-dependent and has arrhythmogenic consequences. *Front. Pharmacol.* 5:144. doi: 10.3389/fphar.2014.00144

Bongartz, L. G., Cramer, M. J., Doevendans, P. A., Bram, B. A., and Joles, J. A. (2005). The severe cardiorenal syndrome: 'Guyton revisited. *Eur. Heart J.* 25, 11–17. doi: 10.1093/eurheartj/ehi020

Boubali, S., Liopeta, K., Virgilio, L., Thyphronitis, G., Mavrothalassitis, G., Dimitracopoulos, G., et al. (2012). Calcium/calmodulin-dependent protein kinase II regulates IL-10 production by human T lymphocytes: a distinct target in the calcium dependent pathway. *Mol. Immunol.* 52, 51–60. doi: 10.1016/j.molimm.2012.04.008

Brown, J. H., Del Re, D. P., and Sussman, M. A. (2006). The Rac and Rho Hall of Fame. *Circ. Res.* 98, 730–742. doi: 10.1161/01.RES.0000216039.75913.9e

Bui, J. D., Calbo, S., Hayden-Martinez, K., Kane, L. P., Gardner, P., and Hedrick, S. M. (2000). A role for CaMKII in T cell memory. *Cell* 100, 457–467. doi: 10.1016/S0092-8674(00)80681-9

Bussey, C. T., and Erickson, J. R. (2018). Physiology and pathology of cardiac CaMKII. *Curr. Opin. Physiol.* 1, 52–58. doi: 10.1016/j.cophys.2017.07.003

Carafoli, E., and Krebs, J. (2016). Why calcium? How calcium became the best communicator. *J. Biol. Chem.* 291, 20849–20857. doi: 10.1074/jbc.R116.735894

Carè, A., Catalucci, D., Felicetti, F., Bonci, D., Addario, A., Gallo, P., et al. (2007). MicroRNA-133 controls cardiac hypertrophy. *Nat. Med.* 13, 613–618. doi: 10.1038/nm1582

Carlstrom, M., and Montenegro, M. F. (2019). Therapeutic value of stimulating the nitrate-nitrite-nitric oxide pathway to attenuate oxidative stress and restore nitric oxide bioavailability in cardiorenal disease. *J. Intern. Med.* 285, 2–18. doi: 10.1111/joim.12818

Chelu, M. G., Sarma, S., Sood, S., Wang, S., Van Oort, R. J., Skapura, D. G., et al. (2009). Calmodulin kinase II-mediated sarcoplasmic reticulum Ca2+ leak promotes atrial fibrillation in mice. *J. Clin. Invest.* 119, 1940–1951. doi: 10.1172/jci37059

Cipolletta, E., Rusciano, M. R., Maione, A. S., Santulli, G., Sorriento, D., Del Giudice, C., et al. (2015). Targeting the CaMKII/ERK interaction in the heart prevents cardiac hypertrophy. *PLoS One* 10:e0130477. doi: 10.1371/journal.pone.0130477

Clapham, D. E. (2007). Calcium signaling. *Cell* 131, 1047–1058. doi: 10.1016/j.cell.2007.11.028

Colombo, P. C., Ganda, A., Lin, J., Onat, D., Harxhi, A., Iyasere, J. E., et al. (2012). Inflammatory activation: cardiac, renal, and cardio-renal interactions in patients with the cardiorenal syndrome. *Heart Fail. Rev.* 17, 177–190. doi: 10.1007/s10741-011-9261-3

Condon, J. C., Pezzi, V., Drummond, B. M., Yin, S., and Rainey, W. E. (2002). Calmodulin-dependent kinase I regulates adrenal cell expression of aldosterone synthase. *Endocrinology* 143, 3651–3657. doi: 10.1210/en.2001-211359

Cruz Junho, C. V., Trentin-Sonoda, M., Alvim, J. M., Gaisler-Silva, F., and Carneiro-Ramos, M. S. (2019). Ca2+/calmodulin-dependent kinase ii delta b is essential for cardiomyocyte hypertrophy and complement gene expression

after LPS and HSP60 stimulation in vitro. *Braz. J. Med. Biol. Res.* 52:e8732. doi: 10.1590/1414-431x20198732

Damman, K., Navis, G., Voors, A. A., Asselbergs, F. W., Smilde, T. D. J., Cleland, J. G. F., et al. (2007). Worsening renal function and prognosis in heart failure: systematic review and meta-analysis. *J. Card. Fail.* 13, 599–608. doi: 10.1016/j.cardfail.2007.04.008

Di Lullo, L., Bellasi, A., Barbera, V., Russo, D., Russo, L., Di Iorio, B., et al. (2017). Pathophysiology of the cardio-renal syndromes types 1–5: An uptodate. *Indian Heart J.* 69, 255–265. doi: 10.1016/j.ihj.2017.01.005

Diamandopoulos, A. (1999). Plenary lecture. Twelve centuries of nephrological writings in The Graeco-Roman world of the Eastern Mediterranean (from Hippocrates to Aetius Amidanus). *Nephrol. Dial. Transplant.* 14, 2–9. doi: 10.1093/ndt/14.suppl_2.2

Erickson, J. R., Ling, M., Joiner, A., Guan, X., Kutschke, W., Yang, J., et al. (2008). A dynamic pathway for calcium-independent activation of CaMKII by methionine oxidation. *Cell* 133, 462–474. doi: 10.1016/j.cell.2008.02.048

Erickson, J. R., Pereira, L., Wang, L., Han, G., Ferguson, A., Dao, K., et al. (2013). Diabetic hyperglycaemia activates CaMKII and arrhythmias by O-linked glycosylation. *Nature* 502, 372–376. doi: 10.1038/nature12537

Friedberg, F., and Rhoads, A. R. (2001). Evolutionary aspects of calmodulin. *IUBMB Life* 51, 215–221. doi: 10.1080/152165401753311753

Gaikwad, A. B., Sayyed, S. G., Lichtnekert, J., Tikoo, K., and Anders, H. J. (2010). Renal failure increases cardiac histone H3 acetylation, dimethylation, and phosphorylation and the induction of cardiomyopathy-related genes in type 2 diabetes. *Am. J. Pathol.* 176, 1079–1083. doi: 10.2353/ajpath.2010.090528

Guest, C. B., Deszo, E. L., Hartman, M. E., York, J. M., Kelley, K. W., and Freund, G. G. (2008). Ca2+/Calmodulin-dependent kinase kinase α is expressed by monocytic cells and regulates the activation profile. *PLoS One* 3:e1606. doi: 10.1371/journal.pone.0001606

Hanada, S., Takewa, Y., Mizuno, T., Tsukiya, T., Taenaka, Y., and Tatsumi, E. (2012). Effect of the technique for assisting renal blood circulation on ischemic kidney in acute cardiorenal syndrome. *J. Artif. Organs* 15, 140–145. doi: 10.1007/s10047-011-0613-5

Hoeker, G. S., Hanafy, M. A., Oster, R. A., Bers, D. M., and Pogwizd, S. M. (2016). Reduced arrhythmia inducibility with calcium/ calmodulin-dependent protein kinase II inhibition in heart failure rabbits. *J. Cardiovasc. Pharmacol.* 67, 260–265. doi: 10.1097/FJC.0000000000000343

House, A. A., Wanner, C., Sarnak, M. J. I, Piña, L., McIntyre, C. W., Komenda, P., et al. (2019). Heart failure in chronic kidney disease: conclusions from a kidney disease: improving Global Outcomes (KDIGO) Controversies Conference. *Kidney Int.* 95, 1304–1317. doi: 10.1016/j.kint.2019.02.022

Hudmon, A., and Schulman, H. (2002). Structure-function of the multifunctional Ca2+/calmodulin-dependent protein kinase II. *Biochem. J.* 364, 593–611. doi: 10.1042/BJ20020228

Islam, M. S. (2020). Calcium signaling: from basic to bedside. *Adv. Exp. Med. Biol.* 1131, 1–6. doi: 10.1007/978-3-030-12457-1_1

Jian, Z., Han, H., Zhang, T., Puglisi, J., Izu, L. T., Shaw, J. A., et al. (2014). Mechanochemotransduction during cardiomyocyte contraction is mediated by localized nitric oxide signaling. *Sci. Signal* 7:ra27. doi: 10.1126/scisignal.2005046

Johnson, C. N., Pattanayek, R., Potet, F., Rebbeck, R. T., Blackwell, D. J., Nikolaienko, R., et al. (2019). The CaMKII inhibitor KN93-calmodulin interaction and implications for calmodulin tuning of NaV1.5 and RyR2 function. *Cell Calcium* 82:102063. doi: 10.1016/j.ceca.2019.102063

Kakiuchi, S., and Yamazaki, R. (1970). Calcium dependent phosphodiesterase activity and its activating factor (PAF) from brain. Studies on cyclic 3',5'-nucleotide phosphodiesterase (III). *Biochem. Biophys. Res. Commun.* 41, 1104–1110. doi: 10.1016/0006-291X(70)90199-3

Kamada, R., Yokoshiki, H., Mitsuyama, H., Watanabe, M., Mizukami, K., Tenma, T., et al. (2019). Arrhythmogenic β-adrenergic signaling in cardiac hypertrophy: the role of small-conductance calcium-activated potassium channels via activation of CaMKII. *Eur. J. Pharmacol.* 844, 110–117. doi: 10.1016/j.ejphar.2018.12.011

Kassler, P., Bauersachs, J., Busse, R., and Schini-Kerth, V. B. (1997). Inhibition of inducible nitric oxide synthase restores endothelium- dependent relaxations in proinflammatory mediator-induced blood vessels. *Arterioscler. Thromb. Vasc. Biol.* 17, 1746–1755. doi: 10.1161/01.ATV.17.9.1746

Ke, H. Y., Chin, L. H., Tsai, C. S., Lin, F. Z., Chen, Y. H., Chang, Y. L., et al. (2020). Cardiac calcium dysregulation in mice with chronic kidney disease. *J. Cell. Mol. Med.* 24, 3669–3677. doi: 10.1111/jcmm.15066

Kim, G., Weiss, S. J., and Levine, R. L. (2014). Methionine oxidation and reduction in proteins. *Biochim. Biophys. Acta* 1840, 901–905. doi: 10.1016/j.bbagen.2013.04.038

Kim, J. O., Song, D. W., Kwon, E. J., Hong, S.-E., Song, H. K., Min, C. K., et al. (2015). miR-185 Plays an Anti-hypertrophic role in the heart via multiple targets in the calcium-signaling pathways. *PLoS One* 10:e0122509. doi: 10.1371/journal.pone.0122509

Kong, L. H., Chen, Y. L., Sun, N., Wei, M., Zhu, J. X., and Su, X. L. (2018). Inhibition of CaMKII alleviates myocardial ischemia? Reperfusion injury by reducing mitochondrial oxidative stress in isolated perfused rat heart. *Nan Fang Yi Ke Da Xue Xue Bao* 38, 181–186. doi: 10.3969/J.ISSN.1673-4254.2018.02.10

Krol, J., Loedige, I., and Filipowicz, W. (2010). The widespread regulation of microRNA biogenesis, function and decay. *Nat. Rev. Genet.* 11, 597–610. doi: 10.1038/nrg2843

Kumar, U., Wettersten, N., and Garimella, P. S. (2019). Cardiorenal syndrome: pathophysiology. *Cardiol. Clin.* 37, 251–265. doi: 10.1016/j.ccl.2019.04.001

Lemrow, S. M., Anderson, K. A., Joseph, J. D., Ribar, T. J., Noeldner, P. K., and Means, A. R. (2004). Catalytic activity is required for calcium/calmodulin-dependent protein kinase IV to enter the nucleus. *J. Biol. Chem.* 279, 11664–11671. doi: 10.1074/jbc.M312613200

Li, M. S., Adesina, S. E., Ellis, C. L., Gooch, J. L., Hoover, R. S., and Williams, C. R. (2017). NADPH oxidase-2 mediates zinc deficiency-induced oxidative stress and kidney damage. *Am. J. Physiol. Physiol.* 312, C47–C55. doi: 10.1152/ajpcell.00208.2016

Liu, H. J., and Liu, B. (2018). Inhibition of MicroRNA-23 contributes to the isoflurane-mediated cardioprotection against oxidative stress. *Cardiovasc. Toxicol.* 18, 450–458. doi: 10.1007/s12012-018-9455-1

Liu, L., Li, Y., and Tollefsbol, T. O. (2008). Gene-environment interactions and epigenetic basis of human diseases. *Curr. Issues Mol. Biol.* 10, 25–36.

Liu, M., Lang, N., Chen, X., Tang, Q., Liu, S., Huang, J., et al. (2011). MiR-185 targets RhoA and Cdc42 expression and inhibits the proliferation potential of human colorectal cells. *Cancer Lett.* 301, 151–160. doi: 10.1016/j.canlet.2010.11.009

Liu, X., Yao, M., Li, N., Wang, C., Zheng, Y., and Cao, X. (2008). CaMKII promotes TLR-triggered proinflammatory cytokine and type I interferon production by directly binding and activating TAK1 and IRF3 in macrophages. *Blood* 112, 4961–4970. doi: 10.1182/blood-2008-03-144022

Liu, Z., Finet, J. E., Wolfram, J. A., Anderson, M. E., Ai, X., and Donahue, J. K. (2019). Calcium/calmodulin-dependent protein kinase II causes atrial structural remodeling associated with atrial fibrillation and heart failure. *Hear. Rhythm* 16, 1080–1088. doi: 10.1016/j.hrthm.2019.01.013

Lu, Y., Zhang, Y., Shan, H., Pan, Z., Li, X., and Li, B. (2009). MicroRNA-1 downregulation by propranolol in a rat model of myocardial infarction: a new mechanism for ischaemic cardioprotection. *Cardiovasc. Res.* 84, 434–441. doi: 10.1093/cvr/cvp232

Luczak, E. D., and Anderson, M. E. (2014). CaMKII oxidative activation and the pathogenesis of cardiac disease. *J. Mol. Cell. Cardiol.* 73, 112–116. doi: 10.1016/j.yjmcc.2014.02.004

Maier, L. S., and Bers, D. M. (2007). Role of Ca2+/calmodulin-dependent protein kinase (CaMK) in excitation-contraction coupling in the heart. *Cardiovasc. Res.* 73, 631–640. doi: 10.1016/j.cardiores.2006.11.005

Marsico, F., Paolillo, S., Gargiulo, P., Parisi, V., Nappi, C., Assante, R., et al. (2019). Renal function and cardiac adrenergic impairment in patients affected by heart failure. *J. Nucl. Cardiol.* doi: 10.1007/s12350-019-01975-7 [Epub ahead of print].

Mattiazzi, A., and Kranias, E. G. (2014). The role of CaMKII regulation of phospholamban activity in heart disease. *Front. Pharmacol.* 5:5. doi: 10.3389/fphar.2014.00005

Mercer, T. R., Dinger, M. E., and Mattick, J. S. (2009). Long non-coding RNAs: insights into functions. *Nat. Rev. Genet.* 10, 155–159. doi: 10.1038/nrg2521

Montgomery, H. J., Bartlett, R., Perdicakis, B., Jervis, E., Squier, T. C., and Guillemette, J. G. (2003). Activation of constitutive nitric oxide synthases by oxidized calmodulin mutants. *Biochemistry* 42, 7759–7768. doi: 10.1021/bi027097h

Münzel, T., Camici, G. G., Maack, C., Bonetti, N. R., Fuster, V., and Kovacic, J. C. (2017). Impact of oxidative stress on the heart and vasculature: part 2 of a 3-part series. *J. Am. Coll. Cardiol.* 70, 212–229. doi: 10.1016/j.jacc.2017.05.035

Mustroph, J., Neef, S., and Maier, L. S. (2017). CaMKII as a target for arrhythmia suppression. *Pharmacol. Ther.* 176, 22–31. doi: 10.1016/j.pharmthera.2016.10.006

Navarro-García, J. A., Fernández-Velasco, M., Delgado, C., Delgado, J. F., Kuro-o, M., Ruilope, L. M., et al. (2018). PTH, vitamin D, and the FGF-23–klotho axis and heart: going beyond the confines of nephrology. *Eur. J. Clin. Invest.* 48:e12902. doi: 10.1111/eci.12902

Oliveira, R. C., Brito, M. V., Ribeiro, R. F., Oliveira, L. O., Monteiro, A. M., Brandão, F. M., et al. (2017). Influence of remote ischemic conditioning and tramadol hydrochloride on oxidative stress in kidney ischemia/reperfusion injury in rats. *Acta Cir. Bras.* 32, 229–235. doi: 10.1590/S0102-865020170030000007

Park, E.-J., Jung, H. J., Choi, H.-J., Cho, J.-I., Park, H.-J., and Kwon, T.-H. (2018). miR-34c-5p and CaMKII are involved in aldosterone-induced fibrosis in kidney collecting duct cells. *Am. J. Physiol. Physiol.* 314, F329–F342. doi: 10.1152/ajprenal.00358.2017

Pellicena, P., and Schulman, H. (2014). CaMKII inhibitors: from research tools to therapeutic agents. *Front. Pharmacol.* 5:21. doi: 10.3389/fphar.2014.00021

Picciotto, M. R., Zoli, M., Bertuzzi, G., and Nairn, A. C. (1995). Immunochemical localization of calcium/calmodulin-dependent protein kinase I. *Synapse* 20, 75–84. doi: 10.1002/syn.890200111

Prasad, A. M., Morgan, D. A., Nuno, D. W., Ketsawatsomkron, P., Bair, T. B., Venema, A. N., et al. (2015). Calcium/Calmodulin−dependent kinase II inhibition in smooth muscle reduces angiotensin II–induced hypertension by controlling aortic remodeling and baroreceptor function. *J. Am. Heart Assoc.* 4:e001949. doi: 10.1161/JAHA.115.001949

Puri, B. K. (2020). Calcium signaling and gene expression. *Adv. Exp. Med. Biol.* 1131, 537–545. doi: 10.1007/978-3-030-12457-1_22

Purohit, A., Rokita, A. G., Guan, X., Chen, B., Koval, O. M., Voigt, N., et al. (2013). Oxidized Ca2+/Calmodulin-dependent protein kinase II triggers atrial fibrillation. *Circulation* 128, 1748–1757. doi: 10.1161/CIRCULATIONAHA.113.003313

Qi, H., Ren, J., Mingyao, E., Zhang, Q., Cao, Y., Ba, L., et al. (2019). MiR-103 inhibiting cardiac hypertrophy through inactivation of myocardial cell autophagy via targeting TRPV3 channel in rat hearts. *J. Cell. Mol. Med.* 23, 1926–1939. doi: 10.1111/jcmm.14095

Qian, F. H., Deng, X., Zhuang, Q. X., Wei, B., and Zheng, D. D. (2019). MiR-625-5p suppresses inflammatory responses by targeting AKT2 in human bronchial epithelial cells. *Mol. Med. Rep.* 19, 1951–1957. doi: 10.3892/mmr.2019.9817

Rajtik, T., Carnicka, S., Szobi, A., Giricz, Z., O-Uchi, J., Hassova, V., et al. (2016). Oxidative activation of CaMKIIδ in acute myocardial ischemia/reperfusion injury: a role of angiotensin AT1 receptor-NOX2 signaling axis. *Eur. J. Pharmacol.* 771, 114–122. doi: 10.1016/j.ejphar.2015.12.024

Ren, G., Dewald, O., and Frangogiannis, N. (2003). Inflammatory mechanisms in myocardial infarction. *Curr. Drug Target Inflamm. Allergy* 2, 242–256. doi: 10.2174/1568010033484098

Rokita, A. G., and Anderson, M. E. (2012). New therapeutic targets in cardiology: arrhythmias and Ca2+/calmodulin- dependent kinase II (CaMKII). *Circulation* 126, 2125–2139. doi: 10.1161/CIRCULATIONAHA.112.124990

Ronco, C. (2011). The cardiorenal syndrome: basis and common ground for a multidisciplinary patient-oriented therapy. *Cardiorenal Med.* 1, 3–4. doi: 10.1159/000323352

Ronco, C., and Di Lullo, L. (2014). Cardiorenal syndrome. *Heart Fail. Clin.* 10, 251–280. doi: 10.1016/j.hfc.2013.12.003

Rusciano, M. R., Sommariva, E., Douin-Echinard, V., Ciccarelli, M., Poggio, P., and Maione, A. S. (2019). CaMKII activity in the inflammatory response of cardiac diseases. *Int. J. Mol. Sci.* 20:4374. doi: 10.3390/ijms20184374

Sag, C. M., Köhler, A. C., Anderson, M. E., Backs, J., and Maier, L. S. (2011). CaMKII-dependent SR Ca leak contributes to doxorubicin-induced impaired Ca handling in isolated cardiac myocytes. *J. Mol. Cell. Cardiol.* 51, 749–759. doi: 10.1016/j.yjmcc.2011.07.016

Sakagami, H., Kamata, A., Nishimura, H., Kasahara, J., Owada, Y., Takeuchi, Y., et al. (2005). Prominent expression and activity-dependent nuclear translocation of Ca $^{2+}$ /calmodulin-dependent protein kinase Iδ in hippocampal neurons. *Eur. J. Neurosci.* 22, 2697–2707. doi: 10.1111/j.1460-9568.2005.04463.x

Shao, M., Chen, G., Lv, F., Liu, Y., Tian, H., Tao, R., et al. (2017). LncRNA TINCR attenuates cardiac hypertrophy by epigenetically silencing CaMKII. *Oncotarget* 8, 47565–47573. doi: 10.18632/oncotarget.17735

Singh, M. V., Swaminathan, P. D., Luczak, E. D., Kutschke, W., Weiss, R. M., and Anderson, M. E. (2012). MyD88 mediated inflammatory signaling leads to CaMKII oxidation, cardiac hypertrophy and death after myocardial infarction. *J. Mol. Cell. Cardiol.* 52, 1135–1144. doi: 10.1016/j.yjmcc.2012.01.021

Skelding, K. A., and Rostas, J. A. P. (2012). The role of molecular regulation and targeting in regulating calcium/calmodulin stimulated protein kinases. *Adv. Exp. Med. Biol.* 740, 703–730. doi: 10.1007/978-94-007-2888-2_31

Skelding, K. A., and Rostas, J. A. P. (2020). Regulation of multifunctional calcium/calmodulin stimulated protein kinases by molecular targeting. *Adv. Exp. Med. Biol.* 1131, 649–679. doi: 10.1007/978-3-030-12457-1_26

Skelding, K. A., Rostas, J. A. P., and Verrills, N. M. (2011). Controlling the cell cycle: the role of calcium/calmodulin-stimulated protein kinases I and II. *Cell Cycle* 10, 631–639. doi: 10.4161/cc.10.4.14798

Snijder, J., Rose, R. J., Raijmakers, R., and Heck, A. J. R. (2011). Site-specific methionine oxidation in calmodulin affects structural integrity and interaction with Ca2+/calmodulin-dependent protein kinase II. *J. Struct. Biol.* 174, 187–195. doi: 10.1016/j.jsb.2010.12.002

Songbo, M., Lang, H., Xinyong, C., Bin, X., Ping, Z., and Liang, S. (2019). Oxidative stress injury in doxorubicin-induced cardiotoxicity. *Toxicol. Lett.* 307, 41–48. doi: 10.1016/j.toxlet.2019.02.013

Sumi, M., Kiuchi, K., Ishikawa, T., Ishii, A., Hagiwara, M., Nagatsu, T., et al. (1991). The newly synthesized selective Ca2+ calmodulin dependent protein kinase II inhibitor KN-93 reduces dopamine contents in PC12h cells. *Biochem. Biophys. Res. Commun.* 181, 968–975. doi: 10.1016/0006-291X(91)92031-E

Takemoto-Kimura, S., Suzuki, K., Horigane, S. I., Kamijo, S., Inoue, M., Sakamoto, M., et al. (2017). Calmodulin kinases: essential regulators in health and disease. *J. Neurochem.* 141, 808–818. doi: 10.1111/jnc.14020

Thomas, B., Matsushita, K., Abate, K. H., Al-Aly, Z., Ärnlöv, J., Asayama, K., et al. (2017). Global cardiovascular and renal outcomes of reduced GFR. *J. Am. Soc. Nephrol.* 28, 2167–2179. doi: 10.1681/ASN.2016050562

Tokumitsu, H., and Soderling, T. R. (1996). Requirements for calcium and calmodulin in the calmodulin kinase activation cascade. *J. Biol. Chem.* 271, 5617–5622. doi: 10.1074/jbc.271.10.5617

Tokumitsu, H. H., Chijiwa, T., Hagiwara, M., Mizutani, A., Terasawa, M., and Hidaka, H. (1990). KN-62, 1-[N,O-bis(5-isoquinolinesulfonyl)-N-methyl-L-tyrosyl]-4-phenylpiperazi ne, a specific inhibitor of Ca2+/calmodulin-dependent protein kinase II. *J. Biol. Chem.* 65:4315.

Trentin-Sonoda, M., da Silva, R. C., Kmit, F. V., Abrahão, M. V., Monnerat Cahli, G., Brasil, G. V., et al. (2015). Knockout of toll-like receptors 2 and 4 prevents renal ischemia-reperfusion-induced cardiac hypertrophy in mice. *PLoS One* 10:e0139350. doi: 10.1371/journal.pone.0139350

Virzì, G. M., Clementi, A., De Cal, M., Brocca, A., Day, S., Pastori, S., et al. (2015a). Oxidative stress: dual pathway induction in cardiorenal syndrome type 1 pathogenesis. *Oxid. Med. Cell. Longev.* 2015:391790. doi: 10.1155/2015/391790

Virzì, G. M., De Cal, M., Day, S., Brocca, A., Cruz, D. N., Castellani, C., et al. (2015b). Pro-apoptotic effects of plasma from patients with cardiorenal syndrome on human tubular cells. *Am. J. Nephrol.* 41, 474–484. doi: 10.1159/000438459

Voigt, N., Li, N., Wang, Q., Wang, W., Trafford, A. W., Abu-Taha, I., et al. (2012). Enhanced sarcoplasmic reticulum Ca 2+ Leak and increased Na +-Ca 2+ exchanger function underlie delayed afterdepolarizations in patients with chronic atrial fibrillation. *Circulation* 125, 2059–2070. doi: 10.1161/CIRCULATIONAHA.111.067306

Wagner, S., Dybkova, N., Rasenack, E. C. L., Jacobshagen, C., Fabritz, L., Kirchhof, P., et al. (2006). Ca2+/calmodulin-dependent protein kinase II regulates cardiac Na+ channels. *J. Clin. Invest.* 116, 3127–3138. doi: 10.1172/JCI26620

Wang, K., Liu, C. Y., Zhou, L. Y., Wang, J. X., Wang, M., Zhao, B., et al. (2015). APF lncRNA regulates autophagy and myocardial infarction by targeting miR-188-3p. *Nat. Commun.* 6:6779. doi: 10.1038/ncomms7779

Wang, K., Liu, F., Zhou, L. Y., Long, B., Yuan, S. M., Wang, Y., et al. (2014). The long noncoding RNA CHRF regulates cardiac hypertrophy by targeting miR-489. *Circ. Res.* 114, 1377–1388. doi: 10.1161/CIRCRESAHA.114.302476

Wang, Y., Zhao, R., Liu, D., Deng, W., Xu, G., Liu, W., et al. (2018). Exosomes derived from miR-214-enriched bone marrow-derived mesenchymal stem cells regulate oxidative damage in cardiac stem cells by targeting CaMKII. *Oxid. Med. Cell. Longev* 2018:4971261. doi: 10.1155/2018/4971261

Winter, J., Jung, S., Keller, S., Gregory, R. I., and Diederichs, S. (2009). Many roads to maturity: MicroRNA biogenesis pathways and their regulation. *Nat. Cell Biol.* 11, 228–234. doi: 10.1038/ncb0309-228

Wong, M. H., Samal, A. B., Lee, M., Vlach, J., Novikov, N., Niedziela-Majka, A., et al. (2019). The KN-93 molecule inhibits Calcium/Calmodulin-dependent protein kinase II (CaMKII) activity by binding to Ca2+/CaM. *J. Mol. Biol.* 431, 1440–1459. doi: 10.1016/j.jmb.2019.02.001

Wu, C. T., and Morris, J. R. (2001). Genes, genetics, and epigenetics: a correspondence. *Science* 293, 1103–1105. doi: 10.1126/science.293.5532.1103

Yamauchi, T. (2005). Neuronal Ca2+/Calmodulin-dependent protein kinase II—discovery, progress in a quarter of a century, and perspective: implication for learning and memory. *Biol. Pharm. Bull.* 28, 1342–1354. doi: 10.1248/bpb.28.1342

Yang, B., Lin, H., Xiao, J., Lu, Y., Luo, X., Li, B., et al. (2007). The muscle-specific microRNA miR-1 regulates cardiac arrhythmogenic potential by targeting GJA1 and KCNJ2. *Nat. Med.* 13, 486–491. doi: 10.1038/nm1569

Yang, J., Xu, W. W., and Hu, S. J. (2015). Heart failure: advanced development in genetics and epigenetics. *BioMed Res. Int.* 2015:352734. doi: 10.1155/2015/352734

Yang, T., Liu, T., Cao, C., and Xu, S. (2019). miR-200a-5p augments cardiomyocyte hypertrophy induced by glucose metabolism disorder via the regulation of selenoproteins. *J. Cell. Physiol.* 234, 4095–4103. doi: 10.1002/jcp.27206

Yogasundaram, H., Chappell, M. C., Braam, B., and Oudit, G. Y. (2019). Cardiorenal syndrome and heart failure—challenges and opportunities. *Can. J. Cardiol.* 35, 1208–1219. doi: 10.1016/j.cjca.2019.04.002

Yoo, S., Aistrup, G., Shiferaw, Y., Ng, J., Mohler, P. J., Hund, T. J., et al. (2018). Oxidative stress creates a unique, CaMKII-mediated substrate for atrial fibrillation in heart failure. *JCI Insight* 3:e120728. doi: 10.1172/jci.insight.120728

Zhang, M., Gu, H., Chen, J., and Zhou, X. (2016). Involvement of long noncoding RNA MALAT1 in the pathogenesis of diabetic cardiomyopathy. *Int. J. Cardiol.* 202, 753–755. doi: 10.1016/j.ijcard.2015.10.019

Zhang, R., Xu, Y., Niu, H., Tao, T., Ban, T., Zheng, L., et al. (2018). Lycium barbarum polysaccharides restore adverse structural remodelling and cardiac contractile dysfunction induced by overexpression of microRNA-1. *J. Cell. Mol. Med.* 22, 4830–4839. doi: 10.1111/jcmm.13740

Zhang, Y., Feng, J., Wang, Q., Zhao, S., Yang, S., Tian, L., et al. (2018). Hyperglycaemia stress-induced renal injury is caused by extensive mitochondrial fragmentation, attenuated MKP1 signalling, and activated JNK-CaMKII-Fis1 biological axis. *Cell. Physiol. Biochem* 51, 1778–1798. doi: 10.1159/000495681

Zhang, Y., Zhang, M., Xu, W., Chen, J., and Zhou, X. (2017). The long non-coding RNA H19 promotes cardiomyocyte apoptosis in dilated cardiomyopathy. *Oncotarget* 8, 28588–28594. doi: 10.18632/oncotarget.15544

Zhang, Z., Liu, X., Feng, B., Liu, N., Wu, Q., Han, Y., et al. (2015). STIM1, a direct target of microRNA-185, promotes tumor metastasis and is associated with poor prognosis in colorectal cancer. *Oncogene* 34, 4808–4820. doi: 10.1038/onc.2014.404

Zheng, D., Li, Z., Wei, X., Liu, R., Shen, A., He, D., et al. (2018). Role of miR-148a in mitigating hepatic ischemia-reperfusion injury by repressing the TLR4 signaling pathway via targeting CaMKIIα in vivo and in vitro. *Cell. Physiol. Biochem.* 49, 2060–2072. doi: 10.1159/000493716

Conflict of Interest: The authors declare that the research was conducted in the absence of any commercial or financial relationships that could be construed as a potential conflict of interest.

frontiers in Medicine

ORIGINAL RESEARCH
published: 11 September 2020
doi: 10.3389/fmed.2020.00512

Prevalence and Description of Hyponatremia in a Swiss Tertiary Care Hospital: An Observational Retrospective Study

Henri Lu[1]*, *Peter Vollenweider*[2], *Sébastien Kissling*[3] and *Pedro Marques-Vidal*[2]

[1] Department of Cardiology, Lausanne University Hospital and University of Lausanne, Lausanne, Switzerland, [2] Department of Internal Medicine, Lausanne University Hospital and University of Lausanne, Lausanne, Switzerland, [3] Service of Nephrology, Department of Internal Medicine, Lausanne University Hospital and University of Lausanne, Lausanne, Switzerland

Background: Hyponatremia (serum sodium concentration <135 mEq/L) is the most common electrolyte abnormality among hospitalized patients. Our aim was to study the epidemiology of hyponatremia in hospitalized patients, as well as the short-term mortality rates, the length of stay (LOS), and associated hospital costs.

Methods: This retrospective cohort study included 6,539 hospitalizations in the internal medicine ward of a Swiss tertiary-care teaching hospital between January 1, 2012, and December 31, 2018 (42.7% women, mean age 69 years). Using serum sodium concentration, we identified hospitalizations with hyponatremia and calculated the prevalence of overall hyponatremia, admission hyponatremia (AH), hospital-acquired hyponatremia (HAH), and persistent hyponatremia (PH) at discharge. We also studied the impact of hyponatremia on 30-day readmissions, in-hospital and 30-day mortality, and hospital LOS and costs, using multivariable logistic regression and Cox proportional hazards models, with normal natremia as reference.

Results: Prevalence of overall hyponatremia was 32.5% [95% confidence interval (CI), 31.3–33.6%], while prevalence of PH among hospitalizations with AH and HAH was 33.7% (31.7–35.8%). After multivariable adjustment, hyponatremia was associated with increased hospital costs (CHF 19,025 ± 485 vs. 14,962 ± 341, $p < 0.001$) and LOS (13.4 ± 0.2 vs. 10.7 ± 0.2 days, $p < 0.001$). Increased severity of hyponatremia was associated with higher hospital costs and LOS (p for trend <0.001). There was a trend toward more frequent 30-day readmissions associated with hyponatremia [adjusted odds ratio (OR), 1.15 (1.01–1.31), $p = 0.032$], mainly with PH: adjusted OR = 1.41 (1.17–1.71), $p < 0.001$. No association was found between severity of hyponatremia and readmissions. Hyponatremia was associated with an increase of in-hospital [adjusted OR = 1.94 (1.49–2.53), $p < 0.001$] and 30-day mortality: adjusted OR = 1.80 (1.44–2.24), $p < 0.001$. Increased severity of hyponatremia was associated with higher in-hospital and 30-day mortality (p for trend < 0.001).

OPEN ACCESS

Edited by:
Natalia Lopez-Andres, NavarraBiomed, Spain

Reviewed by:
Karl Martin Wissing, University Hospital Brussels, Belgium
Swastika Sur, University of California, San Francisco, United States

***Correspondence:**
Henri Lu
henri.lu@chuv.ch

Specialty section:
This article was submitted to Nephrology, a section of the journal Frontiers in Medicine

Received: *09 May 2020*
Accepted: *23 July 2020*
Published: *11 September 2020*

Citation:
Lu H, Vollenweider P, Kissling S and Marques-Vidal P (2020) Prevalence and Description of Hyponatremia in a Swiss Tertiary Care Hospital: An Observational Retrospective Study. Front. Med. 7:512. doi: 10.3389/fmed.2020.00512

Conclusions: Hyponatremia is highly prevalent among hospitalized patients and associated with an increase of LOS, early hospital readmission, in-hospital and 30-day mortality, and hospital costs. PH was associated with a substantial increase of the risk of early hospital readmission and 30-day mortality.

Keywords: hyponatremia, epidemiology, mortality, hospital costs, risk factors

BACKGROUND

Hyponatremia, usually defined as a serum sodium concentration <135 mEq/L, is the most prevalent electrolyte abnormality in hospitalized patients (1). The reported frequency of hyponatremia varies according to the health-care setting, the clinical circumstances, and the definition of hyponatremia used but can affect up to 30% of patients in some series (1–3). In a hospital setting, conditions that are associated with hyponatremia include the syndrome of inappropriate antidiuretic hormone secretion (SIADH) (4), congestive heart failure, cirrhosis, chronic kidney disease, and use of specific medications, such as thiazide diuretics (5, 6). Age is strongly associated with hyponatremia, with a relative risk ranging from 1.54 for patients aged between 41 and 50, to 5.8 for patients aged ≥81 (7). Given the increasing age of patients hospitalized in internal medicine wards in Western countries (8), the prevalence of hyponatremia is expected to increase. Hyponatremia is also associated with higher mortality: in a large multicentric study, Zilberberg and colleagues found a 55% increase in the risk of death in patients admitted with hyponatremia compared with patients with normal natremia (9). Hyponatremia is also associated with increased morbidity such as falls and fractures (5), cognitive impairment and impaired quality of life (10), increased length of stay (LOS) (11), hospitalization costs, and use of medical resources (12).

Among hospitalized patients, hyponatremia can be either present on admission or acquired during hospital stay. Up to two thirds of hyponatremia cases may be hospital-acquired (2). In Singapore, Hawkins and colleagues analyzed a large database of over 120,000 patients and showed that the prevalence of hyponatremia among hospitalized patients was 42%, with 28% at admission and 14% hospital-acquired (7). Hoorn and colleagues reported that the occurrence of severe hyponatremia during hospital stay was associated with inadequate management and treatment-related factors such as thiazide diuretics, drugs stimulating the secretion of antidiuretic hormone, hypotonic intravenous fluids, and surgery (13).

Treatment of hyponatremia remains suboptimal despite recommendations regarding its diagnosis and management. In a US hospital, Donzé and colleagues reported that 42% of 4,195 patients with diagnoses of heart failure and hyponatremia on admission still had hyponatremia at discharge (14). In this particular setting, PH was associated with an increased rate of readmission and 30-day mortality [odds ratio (OR) 1.45, 95% confidence interval (CI): 1.27–1.67].

Apart from the previous study, few have examined the consequences of persistent hyponatremia (PH) at discharge (regardless of its etiology), namely, the risk of early hospital readmission. Furthermore, few data on hyponatremia among hospitalized patients exist in Switzerland. Hence, we performed an observational, monocentric, retrospective study to investigate the epidemiology of hyponatremia (including the incidence of hospital-acquired and PH at discharge) among hospitalized patients.

MATERIALS AND METHODS

Study Design and Patient Population

The study was designed as a retrospective cohort study and conducted in the internal medicine service of Lausanne University hospital (*Centre hospitalier universitaire vaudois* or CHUV), a large tertiary referral center and teaching hospital in Lausanne, Switzerland. This internal medicine service has 140 beds and receives over 4,000 admissions per year.

All patients aged ≥18 who stayed ≥24 h in the internal medicine wards from January 1, 2012, to December 31, 2018, were screened. For patients to be included, two conditions were necessary: (1) to have signed the general consent for research (*Consentement général pour la recherche* or CGR) form and (2) to be transferred from the emergency department or the intensive care unit (ICU). The CGR is required by the Swiss legislation on research involving humans (*Loi relative à la recherche sur l'être humain*) to use patients' clinical and biological data for research purposes. It complies with the ethical principles mentioned in the Oviedo Convention, the Declaration of Helsinki, and the Declaration of Taipei. The second inclusion criterion was added because we did not have authorization from the local Ethics Committee to include patients from other departments (e.g., surgery departments). Moreover, in our institution, the emergency department and the ICU account for the majority of patients hospitalized in the internal medicine ward. Our study was approved by the Cantonal Ethics Committee on research involving humans (CER-VD, decision dated September 3, 2019).

Patients were excluded if (1) no serum sodium concentration value was available in the first 24 h following admission; (2) they were transferred from departments or wards other than the emergency department or the ICU of the CHUV; or (3) they were transferred to another ward, department, or hospital (other than a rehabilitation unit) before the end of acute care.

The following data were retrieved from patients' electronic medical records: age; gender; main diagnosis on discharge; number of comorbidities; natremia on admission, during hospitalization, and at discharge; LOS; status at discharge

(alive/dead); and any 30-day readmission in any department of the CHUV. Vital status at 30 days after discharge was retrieved from the Swiss Federal Statistical Office data.

Hospitalization costs were extracted from the CHUV financial database. The diagnosis-related group (DRG) system was also used to evaluate hospitalization costs. The DRG system has been in use in Switzerland since 2012. It classifies hospitalizations into three categories on the basis of their LOS: "inlier" (LOS is similar to nationwide average LOS for a given DRG), "highlier" (LOS is longer than nationwide average LOS), and "lowlier" (LOS is shorter than nationwide average LOS). Given the small percentage of "lowliers" (<4%), they were included in the "inlier" group.

The main diagnoses were identified by extracting the International Classification of Diseases, 10th revision (ICD-10), codes in discharge letters, and were categorized into the following groups: infectious diseases, cancers, pulmonary diseases, cardiac diseases, liver diseases, neurological diseases, endocrine disorders, psychiatric disorders, and others (**Supplementary Table 1**). Kidney diseases represented <0.5% of main diagnoses and were included in the "other diagnoses" category.

All data were extracted and anonymized by the Data Science & Research (DS&R) group, which is the only entity authorized to extract data from the CHUV databases. After extraction, the source database provided by the DS&R group was converted into a statistical-friendly format. All modifications and analyses were performed via programming, a new database was created, and no changes were being made to the original database. All files were stored in a secured server within the research folder of the internal medicine ward. Access to this folder was limited to the principal investigator and the persons in charge of the analyses.

Endpoints

The main endpoint was the prevalence of overall hyponatremia, admission hyponatremia (AH), hospital-acquired hyponatremia (HAH), and PH.

Hyponatremia was defined as a serum sodium concentration <135 mEq/L and further categorized into mild (130–135 mEq/L), moderate (125–129 mEq/L), and severe (<125 mEq/L) (6). Hyponatremia at admission was defined by hyponatremia evidenced during the first 24 h of hospitalization. HAH was defined as hyponatremia diagnosed after the first 24 h of hospitalization, with natremia within normal range (135–145 mEq/L) on admission. Overall hyponatremia was defined as AH or HAH. Lastly, PH was defined as hyponatremia evidenced at admission or after the first 24 h of hospitalization, and on the last available blood test before discharge.

Secondary objectives included studying (1) the demographic and clinical characteristics (age, gender, and main diagnosis during hospitalization) associated with hyponatremia, with normal natremia as reference; (2) the impact of hyponatremia on hospital LOS and costs, 30-day readmissions, in-hospital all-cause mortality, and all-cause 30-day mortality, using normal natremia as reference.

Covariates

To account for potential confounders when comparing hospital LOS and costs, readmissions, and all-cause mortality rates between patients with and without hyponatremia, the following covariates were selected on the basis of previous reports (14–16): age group (four categories: <60, 60–69, 70–79, and >80 years old), gender, main diagnosis group (eight categories, as mentioned above), and the number of comorbidities.

Statistical Analyses

Statistical analyses were conducted using Stata version 16.0 for Windows® (Stata Corp, College Station, TX, USA). As some patients were hospitalized several times, the unit of analysis was the total number of hospitalizations (and not the total number of patients), unless specified otherwise. Results were expressed as number and (percentage) for categorical variables and as average ± standard deviation (SD) or as median [interquartile range (IQR)] for continuous variables. Between-group bivariate comparisons were performed using chi-square for categorical variables and Student's *t*-test, analysis of variance (ANOVA), or Kruskal–Wallis test for continuous variables. As LOS and costs showed a right-skewed distribution, a multivariable analysis was performed on log-transformed values. Multivariable analyses were conducted using multilevel mixed-effects linear regression for continuous variables and multilevel mixed-effects logistic regression for categorical variables to take into account multiple hospitalizations for the same patient, or plain ANOVA and logistic regression when single individual data were used. Results were expressed as multivariable-adjusted mean ± standard error for continuous variables and as multivariable-adjusted OR and (95% CI) for categorical variables. For mortality analyses, only the last hospitalization of each patient was considered. Mortality was assessed using Cox regression, and results were expressed as hazard ratios (HRs) and (95% CI) (17). Multivariable analyses were performed adjusting for age (four categories), gender, main cause for hospitalization (eight categories), and number of associated comorbidities. *Post-hoc* trend analyses were performed using the contrast p. command of Stata.

Due to the number of tests performed and as suggested by others (18), a conservative value of 0.005 was used to define statistical significance.

RESULTS

From January 1, 2012, to December 31, 2018, a total of 18,241 hospitalizations in the internal medicine wards of the CHUV, with available sodium values in the first 24 h after admission, were recorded. A total of 4,307 patients, representing 7,133 hospitalizations (35% of total hospitalizations), had signed the CGR and were eligible for inclusion. A total of 594 hospitalizations were excluded because of missing data or exclusion criteria, with 6,539 hospitalizations included in the analyses. The characteristics of the included and excluded hospitalizations are summarized in **Supplementary Table 2**: included patients were significantly older and had significantly shorter LOS.

Prevalence and Determinants of Hyponatremia

The trends and prevalence of overall, AH, HAH, and PH are summarized in **Table 1**. Prevalence of AH was 24.7% (95% CI, 23.7–25.8%), and prevalence of HAH among participants devoid of AH was 10.3% (95% CI, 9.4–11.1%). Interestingly, nearly one third of patients had PH at discharge (33.7%). Most cases of hyponatremia were mild (69.1%), with 20.2% moderate and 10.7% severe.

The demographic and clinical characteristics of hospitalizations with and without hyponatremia are shown in **Table 2**. Hospitalizations with severe hyponatremia had a lower frequency of women and a lower frequency of subjects aged <60. Furthermore, the main diagnoses on discharge groups were significantly different according to the severity of hyponatremia, with a higher proportion of endocrine disorders associated with severe hyponatremia.

The demographic and clinical characteristics of hospitalizations with and without PH are reported in **Supplementary Table 3**. Hospitalizations with PH tended to have a higher frequency of women and different main diagnosis groups, while no differences were found for age groups.

Supplementary Table 4 shows the number of sodium measurements and the natremia values, according to categories of sodium levels. The number of measurements increased with the severity of hyponatremia. Increases in natremia across hospital stay were stronger among the most severe categories. No differences were observed for PH as expressed by the median rises of natremia from admission to discharge.

Hyponatremia, Length of Stay, Hospital Costs, and Readmissions

The associations between natremia levels and hospital costs and DRG categories are summarized in **Table 3**. Admissions with hyponatremia incurred higher costs and were more frequently DRG highliers than admissions with normal natremia, and this difference persisted after a multivariate analysis. The severity of hyponatremia was positively associated with an increase in hospital costs and in the likelihood of being DRG highlier. Non-PH was associated with an increase in hospital costs and the likelihood of being DRG highlier, while PH was not.

The associations between natremia levels and LOS and 30-day readmissions are summarized in **Table 4**. Admissions with hyponatremia had a longer LOS and a 15% higher likelihood of readmission. LOS increased with the severity of hyponatremia, but no association was found between severity of hyponatremia and readmission. Non-PH had a longer LOS while PH presented a higher likelihood of readmission.

Hyponatremia and Mortality

The associations between hyponatremia and in-hospital or 30-day mortality are summarized in **Table 5**. Overall hyponatremia was associated with an almost doubling of in-hospital mortality, and the association increased with the severity of the condition. Similar findings were obtained for 30-day mortality. Non-PH and PH were associated an increase of in-hospital and 30-day mortality, the increase being stronger for PH.

DISCUSSION

The main results of our study are (1) hyponatremia was very common in hospitalized patients, one patient out of four having AH, one patient out of 10 developing HAH, and, among patients with AH or HAH, one out of three (33.7%) having PH; (2) hyponatremia was associated with increased readmissions, LOS, hospital costs, in-hospital, and 30-day mortality.

Prevalence and Determinants of Hyponatremia

The overall prevalence of hyponatremia in our study was close to 33%, a value almost 10-fold higher than reported in a previous retrospective study conducted in three hospitals in Basel, Switzerland (368/10,500 admissions or 3.5%) (19). A possible explanation is that the authors used diagnostic codes in discharge letters to identify hyponatremia; this might have led to

TABLE 1 | Annual trends in the prevalence of hyponatremia: Lausanne University Hospital, 2012–2018.

	2012	2013	2014	2015	2016	2017	2018	All
All hospitalizations	376	885	963	1,014	982	1,052	1,267	6,539
Hyponatremia, all								
Overall	78 (20.7)	273 (30.9)	309 (32.1)	278 (27.4)	365 (37.2)	358 (34)	462 (36.5)	2,123 (32.5)
Admission	58 (15.4)	205 (23.2)	218 (22.6)	197 (19.4)	277 (28.3)	289 (27.6)	371 (29.3)	1,615 (24.7)
Hospital-acquired[a]	20 (6.3)	68 (10.0)	91 (12.2)	81 (9.9)	87 (12.4)	69 (9.1)	89 (10.0)	505 (10.3)
Persistent[b]	16 (20.5)	85 (31.1)	111 (35.9)	72 (25.9)	133 (36.4)	129 (36.0)	170 (36.8)	716 (33.7)
Severity of hyponatremia								
Mild (130–135 mEq/L)	52 (66.7)	173 (63.4)	214 (69.3)	192 (69.1)	258 (70.7)	242 (67.6)	336 (72.7)	1,467 (69.1)
Moderate (125–129 mEq/L)	16 (20.5)	66 (24.2)	64 (20.7)	56 (20.1)	70 (19.2)	74 (20.7)	82 (17.8)	428 (20.2)
Severe (<125 mEq/L)	10 (12.8)	34 (12.5)	31 (10.0)	30 (10.8)	37 (10.1)	42 (11.7)	44 (9.5)	228 (10.7)

Results are expressed as number of hospitalizations (percentage).

[a] *Among hospitalizations without hyponatremia at admission.*

[b] *Among hospitalizations with hyponatremia at admission or hospital-acquired hyponatremia.*

TABLE 2 | Demographic and clinical characteristics of hospitalizations according to categories of sodium levels.

	All	Normal	Mild	Moderate	Severe	*p* value
N	6,539	4,416	1,467	428	228	
Women (%)	2,794 (42.7)	1,925 (43.6)	564 (38.5)	187 (43.7)	118 (51.8)	<0.001
Age groups (%)						<0.001
<60	1,561 (23.9)	1,036 (23.5)	378 (25.8)	104 (24.3)	43 (18.9)	
60–69	1,340 (20.5)	817 (18.5)	343 (23.4)	120 (28.0)	60 (26.3)	
70–79	1,597 (24.4)	1,095 (24.8)	352 (24.0)	93 (21.7)	57 (25.0)	
≥80	2,041 (31.2)	1,468 (33.2)	394 (26.9)	111 (25.9)	68 (29.8)	
Main diagnosis on discharge (%)						<0.001
Pulmonary disease	1,669 (25.5)	1,228 (27.8)	333 (22.7)	79 (18.5)	29 (12.7)	
Heart disease	1,121 (17.1)	826 (18.7)	195 (13.3)	56 (13.1)	44 (19.3)	
Cancer	537 (8.2)	342 (7.7)	138 (9.4)	43 (10.1)	14 (6.1)	
Neurological disease	326 (5.0)	234 (5.3)	57 (3.9)	22 (5.1)	13 (5.7)	
Liver disease	211 (3.2)	86 (2.0)	89 (6.1)	22 (5.1)	14 (6.1)	
Endocrine disorders	139 (2.1)	42 (1.0)	46 (3.1)	19 (4.4)	32 (14.0)	
Psychiatric disorders	85 (1.3)	57 (1.3)	18 (1.2)	7 (1.6)	3 (1.3)	
Other diseases	2,451 (37.5)	1,601 (36.3)	591 (40.3)	180 (42.1)	79 (34.7)	

Hyponatremia values include acquired-hyponatremia and hospital-acquired hyponatremia: Lausanne University Hospital, 2012–2018.
Results are expressed as number of hospitalizations (percentage). Between-group comparisons performed using chi-square test.

TABLE 3 | Bivariate and multivariable analysis of the association between natremia levels and hospital costs or diagnosis-related group (DRG) categories: Lausanne University Hospital, 2012–2018.

	Hospital costs (CHF)				Diagnosis-related group categories				
	Bivariate		Multivariable		Bivariate			Multivariable	
	Median [IQR]	*p* value	Mean ± SE	*p* value[§]	Inlier	Highlier	*p* value	OR (95% CI)	*p* value[§]
Natremia levels		<0.001		<0.001			<0.001		
Normal	10,299 [7,029–16,025]		14,962 ± 341		3,851 (69.6)	565 (56.3)		1 (reference)	
Decreased	13,142 [8,644–22,586]		19,025 ± 485		1,684 (30.4)	439 (43.7)		1.66 (1.41–1.95)	<0.001
Natremia levels		<0.001		<0.001			<0.001		
Normal	10,299 [7,029–16,025]		14,920 ± 340		3,851 (69.6)	565 (56.3)		1 (reference)	
Mild (130–135 mEq/L)	12,610 [8,470–21,318]		17,516 ± 567		1,194 (21.6)	273 (27.2)		1.49 (1.24–1.78)	<0.001
Moderate (125–129 mEq/L)	14,577 [9,789–26,675]		22,210 ± 1,030		317 (5.7)	111 (11.1)		2.19 (1.66–2.88)	<0.001
Severe (<125 mEq/L)	14,628 [9,232–27,542]		23,395 ± 1,422		173 (3.1)	55 (5.5)		1.95 (1.34–2.82)	<0.001
p value for trend			< 0.001					< 0.001	
Persistent hyponatremia		<0.001		0.001			<0.001		
Normal	10,299 [7,029–16,025]		14,966 ± 341		3,851 (69.6)	565 (56.3)		1 (reference)	
Non-persistent	13,725 [9,073–24,295]		20,188 ± 582		1,084 (19.6)	323 (32.2)		1.90 (1.58–2.27)	<0.001
Persistent	12,305 [7,932–18,851]		16,695 ± 807		600 (10.8)	116 (11.6)		1.23 (0.96–1.57)	0.109
p value for trend[‡]			0.001					0.109	

CHF, Swiss Francs; CI, confidence interval; IQR, interquartile range; OR, odds ratio; SE, standard error; Inlier, length of stay is similar to nationwide average for a given DRG; highlier, length of stay is longer than nationwide average.
[‡] *Multivariable model.*
[§] *Based on log-transformed data.*
Results are expressed as median [interquartile range] or multivariable-adjusted mean ± standard error for continuous variables and as number of hospitalizations (percentage) or multivariable-adjusted odds ratio (95% confidence interval) for categorical variables. Between-group bivariate analysis performed using Kruskal–Wallis test for continuous variables and chi-square for categorical variables. Multivariable analysis conducted using multilevel mixed-effects linear regression for continuous variables and multilevel mixed-effects logistic regression for categorical variables. Multivariable analyses were performed adjusting for age (four categories), gender, main cause for hospitalization (eight categories), and number of associated comorbidities.

TABLE 4 | Bivariate and multivariable analysis of the association between natremia levels and lengths of stay or 30-day unplanned readmissions: Lausanne University Hospital, 2012–2018.

	Length of stay (days)				Readmissions				
	Bivariate		Multivariable		Bivariate			Multivariable	
	Median [IQR]	*p* value	Mean ± SE	*p* value[§]	No	Yes	*p* value	OR (95% CI)	*p* value
Natremia levels		<0.001		<0.001			<0.001		
Normal	8 [5–13]		10.7 ± 0.2		2,946 (69.4)	1,470 (64.1)		1 (reference)	
Decreased	10 [7–17]		13.4 ± 0.2		1,301 (30.6)	822 (35.9)		1.15 (1.01–1.31)	0.031
Natremia levels		<0.001		<0.001			<0.001		
Normal	8 [5–13]		10.6 ± 0.2		2,946 (69.4)	1,470 (64.1)		1 (reference)	
Mild (130–135 mEq/L)	10 [7–16]		12.6 ± 0.3		910 (21.4)	557 (24.3)		1.14 (0.98–1.31)	0.080
Moderate (125–129 mEq/L)	12 [8–20]		15.2 ± 0.5		253 (6.0)	175 (7.6)		1.22 (0.96–1.54)	0.106
Severe (<125 mEq/L)	12 [8–21]		16.1 ± 0.7		138 (3.3)	90 (3.9)		1.14 (0.82–1.56)	0.438
p value for trend			< 0.001					0.381	
Persistent hyponatremia		<0.001		0.003			<0.001		
Normal	8 [5–13]		10.7 ± 0.2		2,946 (69.4)	1,470 (64.1)		1 (reference)	
Non-persistent	11 [7–19]		14.2 ± 0.3		890 (21)	517 (22.6)		1.04 (0.89–1.20)	0.644
Persistent	10 [6–15]		11.9 ± 0.4		411 (9.7)	305 (13.3)		1.41 (1.17–1.71)	<0.001
p value for trend[‡]			0.003					<0.001	

CI, confidence interval; IQR, interquartile range; OR, odds ratio; SE, standard error.

[‡]*Multivariable model.*

[§]*Based on log-transformed data.*

Results are expressed as median [interquartile range] or multivariable-adjusted mean ± standard error for continuous variables and as number of hospitalizations (percentage) or multivariable-adjusted odds ratio (95% confidence interval) for categorical variables. Between-group bivariate analysis performed using Kruskal–Wallis test for continuous variables and chi-square for categorical variables. Multivariable analysis conducted using multilevel mixed-effects linear regression for continuous variables and multilevel mixed-effects logistic regression for categorical variables. Multivariable analyses were performed adjusting for age (four categories), gender, main cause for hospitalization (eight categories), and number of associated comorbidities.

an underestimation, as hyponatremia is usually underreported in hospital codifications (20). Conversely, our estimation is in the same range as previous reports: Hawkins using data from over 120,000 patients in a Singaporean hospital, found a prevalence of hyponatremia of ∼42% (7); Hoorn et al. using data from 2,900 patients in a Dutch hospital, reported an incidence of hospital-associated hyponatremia of ∼30% (13). Hence, our results suggest that hyponatremia (all types) is a common condition among patients hospitalized in internal medicine.

A striking finding was the relatively high rate of HAH and PH. In a previous single-center study including 53,236 hospitalizations, Wald et al. found an even higher incidence of HAH (38.2%) (15), which may be partly explained by the use of different cutoff values: hyponatremia was defined as serum sodium concentration <138 mEq/L. Concerning PH, Donzé et al. found an incidence of 41.9% among 4,295 patients hospitalized with a diagnosis of congestive heart failure (14), while Greenberg and colleagues, in a large multicentric American and European prospective study, reported that as many as 78% of patients, initially hospitalized with hypervolemic or euvolemic hyponatremia, still had PH at discharge (21). The mechanisms underlying HAH and PH are probably different, as HAH may be the marker of a transient event during hospitalization while PH is possibly the marker of a chronic disease. The high prevalence of HAH may be due to several factors such as a lack of medical awareness, inaccurate diagnostic, and volume status assessment (21, 22), and lack of a hospital warning system (13), while PH may be partly due to variable effectiveness of available treatments (6) or the fact that hyponatremia is frequently considered as the consequence of an underlying disorder (which diverts attention from hyponatremia itself).

Hyponatremia, Lengths of Stay, Hospital Costs, and Readmissions

Hyponatremia was associated with increased LOS and hospitalization costs, a finding in agreement with the literature (1, 9, 15). In a large meta-analysis including almost 4,000,000 patients from the United States and Europe, Corona et al. reported that hyponatremia was associated with an increase of LOS (+3.30 days, 95% CI, 2.90–3.71) and of hospital costs up to $3,000 compared with normonatremia (23). Our study extended these data by adding there was a "dose–response" relationship between LOS or hospitalization costs, and the severity of hyponatremia. In a Swiss setting, Althaus and Krapf found a median average LOS of 9 days, which was slightly lower to ours (19). However, the study was not limited to internal medicine wards and may have included patients with fewer comorbidities.

The severity of the hyponatremia was not significantly associated with the risk of early readmission. However, hyponatremia overall was associated with an increased risk of early hospital readmission, as was PH, but not non-PH. Accordingly, the last in-hospital sodium level is part of the HOSPITAL score, which has been developed to predict 30-day

TABLE 5 | Bivariate and multivariable analysis of the association between natremia levels and in-hospital or 30-day mortality: Lausanne University Hospital, 2012–2018.

	In-hospital mortality					30-day mortality				
	Bivariate			Multivariable		Bivariate			Multivariable	
	Alive	Dead	*p* value	HR (95% CI)	*p* value	Alive	Dead	*p* value	HR (95% CI)	*p* value
Natremia levels			<0.001							
Normal	2,560 (68.2)	138 (50.2)		1 (reference)		2,473 (68.5)	225 (53.2)	<0.001	1 (reference)	
Decreased	1,196 (31.8)	137 (49.8)		1.82 (1.43–2.33)	<0.001	1,135 (31.5)	198 (46.8)		1.68 (1.37–2.04)	<0.001
Natremia levels			<0.001							
Normal	2,560 (68.2)	138 (50.2)		1 (reference)		2,473 (68.5)	225 (53.2)	<0.001	1 (reference)	
Mild (130–135 mEq/L)	825 (22)	78 (28.4)		1.48 (1.12–1.97)	0.007	792 (22.0)	111 (26.2)		1.34 (1.06–1.69)	0.013
Moderate (125–129 mEq/L)	230 (6.1)	38 (13.8)		2.54 (1.75–3.67)	<0.001	209 (5.8)	59 (14.0)		2.52 (1.88–3.39)	<0.001
Severe (<125 mEq/L)	141 (3.8)	21 (7.6)		3.00 (1.88–4.79)	<0.001	134 (3.7)	28 (6.6)		2.47 (1.65–3.69)	<0.001
p value for trend				<0.001					<0.001	
Persistent hyponatremia			<0.001							
Normal	2,560 (68.2)	138 (50.2)		1 (reference)		2,473 (68.5)	225 (53.2)		1 (reference)	
Non-persistent	797 (21.2)	77 (28.0)		1.57 (1.18–2.09)	0.002	767 (21.3)	107 (25.3)		1.39 (1.09–1.76)	0.007
Persistent	399 (10.6)	60 (21.8)		2.29 (1.68–3.12)	<0.001	368 (10.2)	91 (21.5)		2.20 (1.72–2.83)	<0.001
p value for trend‡				<0.001					<0.001	

HR, hazard ratio; CI, confidence interval.

‡Multivariable model.

Results are expressed as number (column percentage) for bivariate comparisons and as multivariable-adjusted odds ratio and (95% confidence interval) for multivariable comparisons. Between-group comparisons performed using chi-square (bivariate) and Cox regression (multivariable). Multivariable analyses were performed adjusting for age (four categories), gender, main cause for hospitalization (eight categories), and number of associated comorbidities.

potentially avoidable hospital readmissions (24). Importantly, the risk of early hospital readmission was mainly found for PH, as opposed to normalized natremia on discharge. This again highlights the fact that PH should not be overlooked before discharging patients.

Hyponatremia and Mortality

Our in-hospital and 30-day mortality rates were in the same range as previous reports: Wald et al. reported AH and HAH (with hyponatremia defined as serum sodium concentration <138 mEq/L) to be associated with an increase of in-hospital mortality [respectively adjusted OR of 1.52 (95% CI, 1.36–1.69) and adjusted OR of 1.66 (95% CI, 1.39–1.98)] (15), while Holland-Bill et al. in a large Danish study including 41,803 hospitalized patients, found hyponatremia to be associated with an increased 30-day mortality risk [adjusted relative risk, 1.5 (95% CI, 1.4–1.5)] (25). In our study, in-hospital mortality was significantly increased, even in cases of mild hyponatremia, while PH was associated with a substantial increase of 30-day mortality. Compared with AH, HAH was associated with a 66% increase in the adjusted odds of in-hospital mortality. Whether hyponatremia by itself contributes to mortality or reflects the severity of the underlying diseases remains unclear. We also observed a "dose–response" relationship between in-hospital or 30-day mortality risk, and hyponatremia severity, in contrast with what was previously published (25).

Implications for Clinical Practice

Whether hyponatremia should solely be considered as a simple consequence of another disease or as a main issue in itself remains to this day debatable (26). Further studies are needed to establish if rapid diagnosis, close clinical, and biological monitoring, and adequate management of hyponatremia could reduce short-term mortality risk, LOS and associated costs, and early readmission and improve quality of life. Accurate clinical volume status (22) and the use of specific and complete testing [for example, urine and plasma osmolality, as well as urine sodium at a minimum for a proper diagnosis of SIADH (6)] are paramount. Moreover, outpatient follow-up should not be overlooked, as close follow-up visits may help to prevent relapse and development of chronic hyponatremia (19).

Strengths and Limitations

This study has several strengths. Firstly, it is based on a cohort of patients with a wide array of comorbid conditions, from an acute care setting, who had complete available follow-up data, *via* hospital and government registries. The size of the cohort allowed us to explore multiple outcomes related to hyponatremia while adjusting for variable potential confounders. We were able to investigate less studied outcomes, such as the proportion of PH and the risk of early readmission, in addition to studying common endpoints usually described in hyponatremia (prevalence, risk of mortality, and LOS). Secondly, contrary to several previous studies, which used diagnostic codes in discharge letters to identify patients with hyponatremia, we were able to directly use plasma sodium levels in our analyses. Using diagnostic codes, only, may lead to an underestimation, as hyponatremia is usually underreported in hospital codifications (20).

This study has several limitations. Firstly, the study was conducted in a single center in a high-volume Swiss tertiary hospital and may not be applicable to other settings. Still, the

characteristics of the patients are similar to those found in general internal medicine wards. Secondly, almost two thirds of patients eligible were excluded because they did not sign the CGR. This might have created a selection bias, as younger people tend to provide consent more frequently (27); still, the direction and magnitude of the bias are hard to estimate. Thirdly, our epidemiological study was limited in the identification of important clinical and biological determinants of hyponatremia (volume status, plasma and urine electrolytes, and osmolality), which are critical to understand its diagnostic, therapeutic, and prognosis significations. Also, a causal relation between hyponatremia and the main diagnosis and/or underlying medical conditions cannot be concluded. Finally, we did not assess medical therapy on admission and during hospital stay. Indeed, medical therapy on admission is not systematically documented in the software used in our institution. Moreover, when medical therapy on admission is documented, it may not be reliable. Since therapy on admission was unavailable, we chose not to include therapy received during hospital stay either, because analyzing the association between hospital treatment only and all categories of hyponatremia (AH, HAH, and PH) would be challenging. Therefore, we were unable to analyze if some of the cases of hyponatremia were iatrogenic or if inadequate management was partly responsible for PH. Knowing the causative diagnosis and the determinant factors for PH as well as knowing the reasons for readmission and 30-day mortality would be critical to improve our understanding and the treatment of these patients.

CONCLUSIONS

Hyponatremia remains highly prevalent among hospitalized patients and associated with an increase of early hospital readmission, in-hospital and 30-day mortality, LOS, and hospital costs. PH was associated with a substantial increase of the risk of early hospital readmission and 30-day mortality.

DATA AVAILABILITY STATEMENT

Due to lack of consent for posting, individual data cannot be made publicly available to other investigators as it would not comply with the Swiss legislation [Federal Act on Research involving Human Beings (Human Research Act, HRA), of 30 September 2011 (Status as of 1 January 2020)]. For more details: www.admin.ch/opc/en/classified-compilation/20061313/index.html. Requests to access the datasets should be directed to henri.lu@chuv.ch.

ETHICS STATEMENT

The protocol of this study was reviewed and approved by the Cantonal Ethics Committee on research involving humans (CER-VD, decision dated September 3rd, 2019). The participants provided their written informed consent to participate in this study. Written informed consent was obtained from the individuals for the publication of any potentially identifiable images or data included in this article.

AUTHOR CONTRIBUTIONS

HL designed the study, interpreted the data, and wrote most of the manuscript. PM-V analyzed the data and wrote part of the manuscript. PV and SK revised the manuscript for important intellectual content. All authors read and approved the final manuscript.

SUPPLEMENTARY MATERIAL

The Supplementary Material for this article can be found online at: https://www.frontiersin.org/articles/10.3389/fmed.2020.00512/full#supplementary-material

REFERENCES

1. Upadhyay A, Jaber BL, Madias NE. Epidemiology of hyponatremia. *Semin Nephrol.* (2009) 29:227–38. doi: 10.1016/j.semnephrol.2009.03.004
2. Upadhyay A, Jaber BL, Madias NE. Incidence and prevalence of hyponatremia. *Am J Med.* (2006) 119:S30–5. doi: 10.1016/j.amjmed.2006.05.005
3. Mannesse CK, Vondeling AM, van Marum RJ, van Solinge WW, Egberts TCG, Jansen PAF. Prevalence of hyponatremia on geriatric wards compared to other settings over four decades: a systematic review. *Ageing Res Rev.* (2013) 12:165–73. doi: 10.1016/j.arr.2012.04.006
4. Shapiro DS, Sonnenblick M, Galperin I, Melkonyan L, Munter G. Severe hyponatraemia in elderly hospitalized patients: prevalence, aetiology and outcome. *Intern Med J.* (2010) 40:574–80. doi: 10.1111/j.1445-5994.2010.02217.x
5. Rittenhouse KJ, To T, Rogers A, Wu D, Horst M, Edavettal M, et al. Hyponatremia as a fall predictor in a geriatric trauma population. *Injury.* (2015) 46:119–23. doi: 10.1016/j.injury.2014.06.013
6. Spasovski G, Vanholder R, Allolio B, Annane D, Ball S, Bichet D, et al. Clinical practice guideline on diagnosis and treatment of hyponatraemia. *Eur J Endocrinol.* (2014) 170:G1–47. doi: 10.1530/EJE-13-1020
7. Hawkins RC. Age and gender as risk factors for hyponatremia and hypernatremia. *Clin Chim Acta.* (2003) 337:169–72. doi: 10.1016/j.cccn.2003.08.001
8. Larson EB. General internal medicine at the crossroads of prosperity and despair: caring for patients with chronic diseases in an aging society. *Ann Intern Med.* (2001) 134:997–1000. doi: 10.7326/0003-4819-134-10-200105150-00013
9. Zilberberg MD, Exuzides A, Spalding J, Foreman A, Graves Jones A, Colby C, et al. Epidemiology, clinical and economic outcomes of admission hyponatremia among hospitalized patients. *Curr Med Res Opin.* (2008) 24:1601–8. doi: 10.1185/03007990802081675
10. Robertson GL. Syndrome of inappropriate antidiuresis. *N Engl J Med.* (1989) 321:538–9. doi: 10.1056/NEJM198908243210810
11. Gill G, Huda B, Boyd A, SkagenK, Wile D, Watson I, et al. Characteristics and mortality of severe hyponatraemia— a hospital–based study. *Clin Endocrinol.* (2006) 65:246–9. doi: 10.1111/j.1365-2265.2006.02583.x
12. Boscoe A, Paramore C, Verbalis JG. Cost of illness of hyponatremia in the United States. *Cost Eff Resour Alloc.* (2006) 4:10. doi: 10.1186/1478-7547-4-10
13. Hoorn EJ, Lindemans J, Zietse R. Development of severe hyponatraemia in hospitalized patients: treatment–related risk factors and inadequate management. *Nephrol Dial Transplant.* (2006) 21:70–6. doi: 10.1093/ndt/gfi082

14. Donzé JD, Beeler PE, Bates DW. Impact of hyponatremia correction on the risk for 30–day readmission and death in patients with congestive heart failure. *Am J Med.* (2016) 129:836–42. doi: 10.1016/j.amjmed.2016.02.036
15. Wald R, Jaber BL, Price LL, Upadhyay A, Madias NE. Impact of hospital–associated hyponatremia on selected outcomes. *Arch Intern Med.* (2010) 170:294. doi: 10.1001/archinternmed.2009.513
16. Kuwabara K, Imanaka Y, Matsuda S, Fushimi K, Hashimoto H, Ishikawa KB, et al. The association of the number of comorbidities and complications with length of stay, hospital mortality and LOS high outlier, based on administrative data. *Environ Health Prev Med.* (2008) 13:130–7. doi: 10.1007/s12199-007-0022-9
17. Green MS, Symons MJ. A comparison of the logistic risk function and the proportional hazards model in prospective epidemiologic studies. *J Chronic Dis*. (1983) 36:715–23. doi: 10.1016/0021-9681(83)90165-0
18. Ioannidis JPA. Publishing research with P–values: prescribe more stringent statistical significance or proscribe statistical significance? *Eur Heart J.* (2019) 40:2553–4. doi: 10.1093/eurheartj/ehz555
19. Althaus AE, Krapf R. Quality and cost considerations in hyponatraemic patients needing hospitalisation. *Swiss Med Wkly.* (2018) 148:w14662. doi: 10.4414/smw.2018.14662
20. Marco J, Barba R, Matía P, Plaza S, Méndez M, Canora J, et al. Low prevalence of hyponatremia codification in departments of internal medicine and its prognostic implications. *Curr Med Res Opin.* (2013) 29:1757–62. doi: 10.1185/03007995.2013.836079
21. Greenberg A, Verbalis JG, Amin AN, Burst VR, Chiodo III JA, Chiong JR, et al. Current treatment practice and outcomes. Report of the hyponatremia registry. *Kidney Int.* (2015) 88:167–77. doi: 10.1038/ki.2015.4
22. Hoorn EJ, Zietse R. Diagnosis and treatment of hyponatremia: compilation of the guidelines. *J Am Soc Nephrol.* (2017) 28:1340–9. doi: 10.1681/ASN.2016101139
23. Corona G, Giuliani C, Parenti G, Colombo GL, Sforza A, Maggi M, et al. The economic burden of hyponatremia: systematic review and meta–analysis. *Am J Med.* (2016) 129:823–35. doi: 10.1016/j.amjmed.2016.03.007
24. Donzé JD, Williams MV, Robinson EJ, Zimlichman E, Aujesky D, Vasilevskis EE, et al. International validity of the HOSPITAL score to predict 30–day potentially avoidable hospital readmissions. *JAMA Intern Med.* (2016) 176:496. doi: 10.1001/jamainternmed.2015.8462
25. Holland–Bill L, Christiansen CF, Heide–Jørgensen U, Ulrichsen SP, Ring T, Jørgensen JOL, et al. Hyponatremia and mortality risk: a Danish cohort study of 279 508 acutely hospitalized patients. *Eur J Endocrinol.* (2015) 173:71–81. doi: 10.1530/EJE-15-0111
26. Mohan S, Gu S, Parikh A, Radhakrishnan J. Prevalence of hyponatremia and association with mortality: results from NHANES. *Am J Med.* (2013) 126:1127–1137.e1. doi: 10.1016/j.amjmed.2013.07.021
27. Bochud M, Currat C, Chapatte L, Roth C, Mooser V. High participation rate among 25 721 patients with broad age range in a hospital–based research project involving whole–genome sequencing – the Lausanne Institutional Biobank. *Swiss Med Wkly.* (2017) 147:w14528. doi: 10.4414/smw.2017.14528

Conflict of Interest: The authors declare that the research was conducted in the absence of any commercial or financial relationships that could be construed as a potential conflict of interest.

frontiers in Physiology

REVIEW
published: 15 September 2020
doi: 10.3389/fphys.2020.572355

Cardiovascular Functional Changes in Chronic Kidney Disease: Integrative Physiology, Pathophysiology and Applications of Cardiopulmonary Exercise Testing

Kenneth Lim[1], Gordon McGregor[2,3], Andrew R. Coggan[4], Gregory D. Lewis[5] and Sharon M. Moe[1]*

[1] Division of Nephrology, Indiana University School of Medicine, Indianapolis, IN, United States, [2] Coventry University Hospital, Coventry and Warwickshire NHS Trust, Coventry, United Kingdom, [3] Warwick Clinical Trials Unit, Warwick Medical School, University of Warwick, Coventry, United Kingdom, [4] Department of Kinesiology, Indiana University – Purdue University, Indianapolis, IN, United States, [5] Division of Cardiology, The Massachusetts General Hospital and Harvard Medical School, Boston, MA, United States

OPEN ACCESS

Edited by:
Natalia Lopez-Andres, NavarraBiomed, Spain

Reviewed by:
Panagiotis I. Georgianos, University General Hospital of Thessaloniki AHEPA, Greece
Rajesh Mohandas, University of Florida, United States

***Correspondence:**
Kenneth Lim
kjlim@iu.edu

Specialty section:
This article was submitted to Renal and Epithelial Physiology, a section of the journal Frontiers in Physiology

Received: *13 June 2020*
Accepted: *21 August 2020*
Published: *15 September 2020*

Citation:
Lim K, McGregor G, Coggan AR, Lewis GD and Moe SM (2020) Cardiovascular Functional Changes in Chronic Kidney Disease: Integrative Physiology, Pathophysiology and Applications of Cardiopulmonary Exercise Testing. Front. Physiol. 11:572355. doi: 10.3389/fphys.2020.572355

The development of cardiovascular disease during renal impairment involves striking multi-tiered, multi-dimensional complex alterations encompassing the entire oxygen transport system. Complex interactions between target organ systems involving alterations of the heart, vascular, musculoskeletal and respiratory systems occur in Chronic Kidney Disease (CKD) and collectively contribute to impairment of cardiovascular function. These systemic changes have challenged our diagnostic and therapeutic efforts, particularly given that imaging cardiac structure at rest, rather than ascertainment under the stress of exercise, may not accurately reflect the risk of premature death in CKD. The multi-systemic nature of cardiovascular disease in CKD patients provides strong rationale for an integrated approach to the assessment of cardiovascular alterations in this population. State-of-the-art cardiopulmonary exercise testing (CPET) is a powerful, dynamic technology that enables the global assessment of cardiovascular functional alterations and reflects the integrative exercise response and complex machinery that form the oxygen transport system. CPET provides a wealth of data from a single assessment with mechanistic, physiological and prognostic utility. It is an underutilized technology in the care of patients with kidney disease with the potential to help advance the field of cardio-nephrology. This article reviews the integrative physiology and pathophysiology of cardio-renal impairment, critical new insights derived from CPET technology, and contemporary evidence for potential applications of CPET technology in patients with kidney disease.

Keywords: cardiopulmonary exercise testing (CPET), cardiovascular functional capacity, VO_2Peak, chronic kidney disease (CKD), end-stage kidney disease (ESKD), dialysis

INTRODUCTION

Cardiovascular disease is a modern-day global epidemic (Kwan and Benjamin, 2015). Over the past century, our world has witnessed a striking epidemiologic transition in the predominant cause of death, from communicable diseases and nutritional deficiencies to non-communicable diseases (Nascimento et al., 2014). At the forefront of non-communicable conditions are diseases of the cardiovascular system. A number of models that include health behaviors, population aging, and increasing rates of urbanization and globalization that increase the burden of cardiovascular risk factors, partially account for this epidemiologic transition in cardiovascular disease (CVD) (Yusuf et al., 2001). Other well-established risk factors for CVD include hyperlipidemia, hypertension, smoking and diabetes. However, in recent years, Chronic Kidney Disease (CKD) has emerged as a risk factor of considerable importance (Sarnak et al., 2003). In fact, CVD is now well-recognized to be the leading cause of death in CKD patients. Individuals with only mild decrements in glomerular filtration rate (GFR) to $<$60 ml/min/1.73 m^2 have already a two-fold increased risk of cardiovascular mortality and this risk increases up to 20-fold by the time a patient needs renal replacement therapy, or end-stage kidney disease (ESKD) (Gansevoort et al., 2013). The pattern of overt CVD in CKD patients differs substantially from the general population. Occlusive coronary artery disease (CAD) accounts for only a minority of cardiovascular deaths in advanced CKD, with the majority being attributed to sudden cardiac death (SCD) and congestive heart failure, in contrast to the general population [Wilson et al., 2001; Wayhs et al., 2002; US Renal Data System (USRDS), 2013].

As members of the scientific and health care community, we are challenged with an ethical and moral obligation to help reduce premature mortality from CVD in our growing CKD population. However, the challenge of helping to improve patient outcomes in this population is compounded by the highly complex processes involved in CVD development as kidney failure ensues. As renal function declines, the development of CVD involves both traditional and non-traditional risk factors such as uremia, pro-inflammatory cytokines, volume overload, mineral disorders, electrolyte disturbances, anemia, sympathetic nerve activation, renin-angiotensin-aldosterone (RAAS) activation and vitamin D deficiency. Additionally, emerging risk factors such as elevated fibroblast growth factor (FGF)-23, low Klotho levels, post-translational protein modifications, and gut derived uremic toxins have now been tightly linked with CVD development in CKD (Rhee and Gerszten, 2012; Kahn et al., 2013; Verbrugge et al., 2015) (**Figure 1**). Central to these processes are complex interactions between multiple target organ systems that include the renal, musculoskeletal, pulmonary, gastrointestinal, vascular, and cardiovascular systems. Interactions between these organ systems underlie critical homeostatic processes such as endocrine loops that tightly regulate mineral metabolism and other organ cross-talk. Their collective failure originates from kidney dysfunction and contributes to overall cardiovascular impairment (Ting et al., 2015; Lim et al., 2020). These organ system interactions, therefore, provide strong rationale for an integrated physiologic approach to assessing cardiovascular changes in CKD.

The striking multi-tiered, multi-dimensional complexities of CVD development in CKD have challenged our diagnostic and therapeutic efforts. For example, imaging of single organs such as the heart by echocardiography or MRI does not adequately reflect the complex systemic processes that lead to cardiovascular impairment in CKD and is therefore insufficiently sensitive to accurately reflect cardiovascular health in this population. Despite huge scientific, economic and financial investment, many of our cardio-renal outcome trials in nephrology have yielded neutral results and have not demonstrated a treatment benefit (Lim et al., 2018). This may be secondary to multiple reasons such as patient heterogeneity, complexity of cardio-renal pathophysiology, competing risks and importantly, limitations of resting cardiac geometric endpoints for tracking disease improvement or decline in the CKD population. As a result, clinicians are left with potentially equivocal recommendations and patients are left without evidence-based guidance to manage their condition. This state of the union therefore demands alternative or novel approaches to investigative, diagnostic and therapeutic efforts to help combat the burden of cardiovascular disease in CKD.

The emergence of state-of-the-art Cardiopulmonary Exercise Testing (CPET) technology and its application to cardiovascular disease research in nephrology is one such alternative approach gaining significant traction. While only a handful of studies have applied CPET technology to study patients with CKD, these studies have already revealed significant mechanistic and physiological insights, and have provided evidence to support the potential use of CPET-derived indices in a variety of applications in nephrology. This article considers integrative physiological and pathophysiological insights into cardiovascular impairment in CKD derived from CPET technology, and appraises contemporary evidence for the potential application of CPET to help advance the field of cardio-nephrology.

INTEGRATIVE PHYSIOLOGY AND THE FICK PRINCIPLE

The Fick Principle and the Fick Equation

As CKD progresses, the integrated metabolic machinery required for the cardiovascular system to function and enable optimal exercise performance is impaired. At the level of the heart and vasculature, kidney failure leads to a uremic phenotype that recapitulates many features of cardiovascular aging, including myocyte hypertrophy, reduced myocardial capillarization and non-vascularized myocardial interstitial fibrosis and calcification as well as vascular calcification, arteriosclerosis and arterial stiffening of systemic vasculature (Aoki et al., 2005; Edwards et al., 2014). The molecular, ultrastructural and geometric changes of the heart and vasculature collectively lead to reduced cardiac efficiency and hence increased myocardial energy expenditure and oxygen consumption. Unfortunately, cardiac

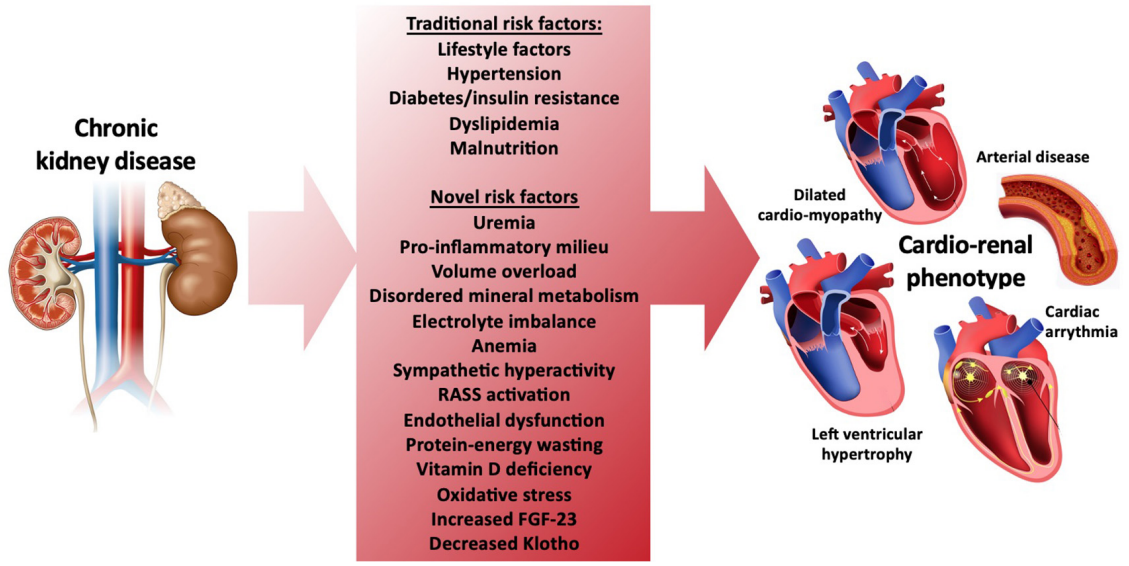

FIGURE 1 | Traditional and novel risk factors for development of cardiovascular disease and the cardio-renal phenotype in CKD.

remodeling occurs early in the course of CKD leading to left ventricular (LV) diastolic then systolic dysfunction and sudden cardiac death (Edwards et al., 2014; Rutherford and Mark, 2017).

Critically, CKD results in the failure of multiple organ systems beyond alterations to the heart and vasculature (**Figure 2**) (Walsh, 1997; Wasserman, 1997; Moorthi and Avin, 2017; Lim et al., 2018): The musculoskeletal system is subject to impairment as CKD progresses resulting in biomechanical failure. This involves muscle wasting (sarcopenia) and alterations in bone mineral metabolism occur leading to widespread consequences, including increased risk of bone mineral disorders (BMD), falls and frailty, hospitalizations, and poorer quality of life (Moorthi and Avin, 2017). Significant interactions between the kidneys and the lungs are also well-known. For example, pulmonary-renal syndromes due to small-vessel vasculitis can cause significant renal impairment, including rapidly progressive glomerulonephritis (RPGN) and pulmonary hemorrhage. Diabetes can cause diabetic nephropathy as well as impaired lung function, involving decreased lung diffusion capacity and increased risk for pulmonary hypertension (Sorino et al., 2019). Additionally, the development of restrictive lung disease has been associated with progressive CKD (Mukai et al., 2018). Underlying these systemic target organ changes are widespread ultrastructural and molecular alterations that contribute to subclinical disease early in the course of CKD and may not be readily detected with conventional resting imaging studies (Ting et al., 2015; Kim et al., 2018; McGregor et al., 2018).

These diverse systemic alterations contribute to the impairment of the cardiovascular system to fulfill its primary function, that is, to be an effective oxygen transport system (Dunn et al., 2016). The role of the many individual components of the cardiovascular system to function effectively in oxygen transport is defined by the Fick Principle. This principle was first described by the German physiologist, Adolf Fick in 1870 and for over 150 years has remained one of the most solid fundamental principles of human cardiovascular physiology (Albouaini et al., 2007). The Fick principle (mathematically expressed by the Fick equation) states that oxygen uptake (VO_2) equals cardiac output multiplied by the arterial minus venous oxygen content, as illustrated in **Figure 2**.

The resting oxygen uptake of a healthy individual in a sitting position approximately equals 3.5 $ml/min^{-1}/kg^{-1}$ or one metabolic equivalent (MET). However, it has now become clear that resting cardiac and pulmonary function testing cannot reliably predict exercise performance and functional capacity, and that overall health status is more strongly associated with exercise tolerance than with resting measurements (Albouaini et al., 2007). This understanding, together with the principle that the fundamental role of the cardiovascular system is to function as an effective oxygen transport system, provides the rationale for the assessment of oxygen uptake (VO_2) at maximal or peak exercise (VO_2Peak) as a robust, objective and reproducible index of cardiovascular functional capacity. While the definition of VO_2Max and VO_2Peak are different and will be discussed in further detail below, for the purposes of this article we will use the term VO_2Peak (unless where VO_2Max has been explicitly referred too in an original article). VO_2Peak reflects the maximal ability of an individual to take in, transport and use oxygen and defines the individual's functional aerobic capacity (Mezzani, 2017).

Applying the Fick Principle to Patients With CKD

Understanding the Fick equation is of critical importance in order to appreciate how progressive CKD alters cardiovascular function in this population, and thus the utility of functional

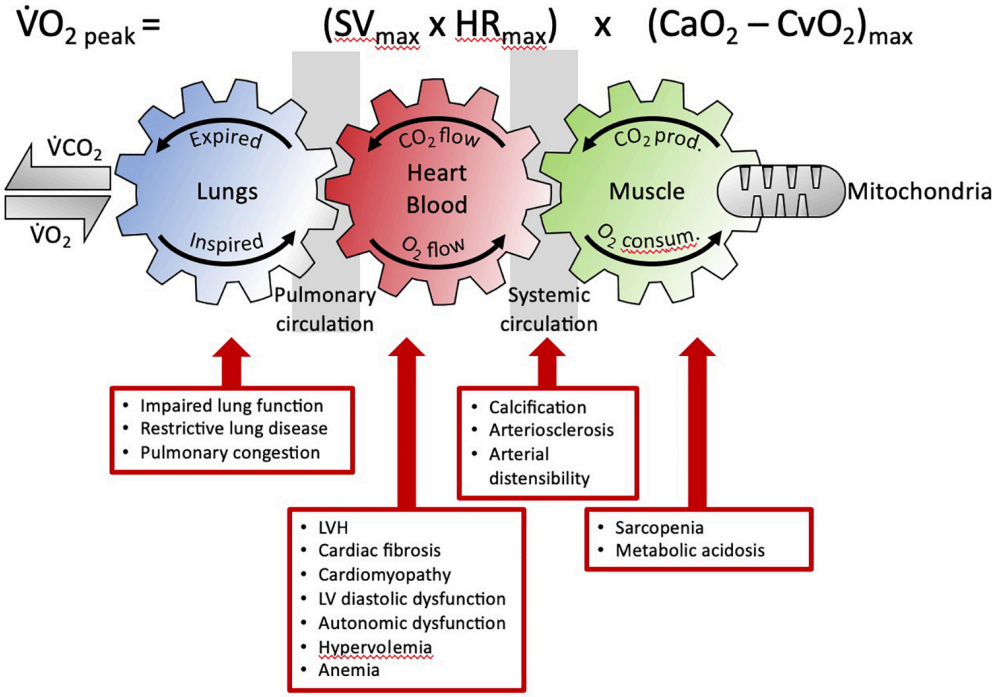

FIGURE 2 | The Fick equation and the coupling of external and cellular respiration. The three interlinked gears represent the functional interdependence between the lungs, circulation and muscle. This facilitates O_2 transport from the lungs to the mitochondria and, in reverse, CO_2 from the muscle to the lungs (adapted from Wasserman, 1997). The detrimental multisystemic effects of kidney disease on this integrated physiological process are indicated. $\dot{V}O_2$, oxygen uptake; $\dot{V}CO_2$, carbon dioxide output; prod, production; consum, consumption; SV, stroke volume; HR, heart rate; CaO_2, arterial O_2 content; CaO_2, venous O_2 content; LVH, left ventricular hypertrophy.

testing. Lessons learned from the Fick equation, as applied to the complex systemic changes that occur with declining kidney function, demand that we look beyond cardiac or vascular changes alone, toward an integrative viewpoint when assessing overall cardiovascular health status in CKD patients rather than static single-organ measures. For example, left ventricular hypertrophy (LVH) is highly prevalent in the dialysis population and is associated with high rates of all-cause and cardiovascular mortality (Silberberg et al., 1989; Foley et al., 1995; London, 2002). However, not all incident dialysis patients have LVH; in fact, approximately 20% do not. Furthermore, a small proportion of dialysis patients experience some regression, and daily dialysis compared to thrice weekly can prevent worsened LVH (Group et al., 2010). Still, dialysis patients who do not have LVH or exhibit regression continue to have elevated risk of cardiovascular mortality (Charytan, 2014). Similarly, kidney transplantation is associated with improved cardiovascular survival (Meier-Kriesche et al., 2004); however, serial cardiac magnetic resonance (CMR) imaging which provides accurate and reproducible assessment of cardiac dimensions, has failed to identify significant regression in LV mass after transplantation (Patel et al., 2008). Taken together, these clinical observations therefore suggest that measures of LV geometry may not accurately reflect the risk of premature cardiovascular death in advanced CKD.

Importantly, an alteration of any of the four variables in the Fick equation that determines VO_2 peak can occur in CKD. As an example, in advanced CKD patients, a reduction in maximal heart rate or a blunted chronotropic response occurs, leading to reduced cardiac output (Ting et al., 2015). These maladaptive processes coupled with widespread arterial calcification and stiffening that contribute to increased afterload, lead to further reductions in cardiac output (Ferro et al., 2012). Impairment of the musculoskeletal system from sarcopenia with muscle mitochondrial dysfunction and progressive anemia are common complications of advanced CKD, can also have profound effects on maximal arterial minus mixed venous oxygen content (Cao_2 – Cvo_2max) (Lim et al., 2020). All pathophysiological states that impair oxygen transport from air to mitochondria, and oxygen use during exercise can contribute to cardiovascular dysfunction and reduced cardiovascular functional capacity. This makes the assessment of VO_2Peak and other cardiovascular functional variables particularly powerful measures for assessing cardiovascular health. Reduction in VO_2Peak has been observed not only in several different organ or systemic conditions (such as chronic heart failure and chronic obstructive pulmonary disease), or conditions that affect the musculoskeletal system (such as mitochondrial myopathies and amyotrophic lateral sclerosis) and are too numerous to completely list here, but have also been described in bed-rest and deconditioning (Mezzani, 2017).

CARDIOPULMONARY EXERCISE TESTING (CPET)

Cardiopulmonary exercise testing is a powerful, dynamic technology that incorporates ventilatory gas exchange measurements during graded exercise. CPET assesses gas exchange measures of O_2uptake (VO_2), carbon dioxide output (VCO_2) and minute ventilation (V_E) and some CPET systems, can provide breath-by-breath analysis of these variables. These measures are used to derive various other gas exchange patterns and can provide organ-specific information on the dysregulated responses to exercise. In the general heart failure population, CPET-derived indices have been recognized as robust markers for the assessment of cardiovascular disease compared to conventional resting imaging for several reasons. Firstly, the coupling of morphological cardiac alterations to cardiovascular performance is largely unknown; secondly, resting cardiopulmonary imaging tests cannot reliably predict functional performance; and thirdly, there is increasing appreciation that overall health status correlates better with exercise tolerance (American Thoracic Society and American College of Chest Physicians, 2003). Here, we will provide a brief discussion of major CPET variables and a summary of commonly derived CPET data is provided in **Table 1**.

Oxygen Uptake and Peak Oxygen Uptake

Maximum oxygen uptake (VO_2Max) is defined as the highest rate of oxygen uptake during intense, maximal exercise whereby no further increases in work rate can cause additional rises in VO_2 (i.e., plateau) (Bassett and Howley, 2000). Peak VO_2 (VO_2Peak) is directly reflective of VO_2Max and is defined as the highest value of VO_2 obtained upon an incremental or other high-intensity exercise test that brings the individual to the limit of tolerance (Whipp and Ward, 1990). VO_2Peak considers the integrative exercise response involving the degree of ventricular function (pumping capacity), oxygen transport in blood (O_2 carrying capacity), pulmonary and vascular function (O_2 delivery), skeletal muscle metabolic capacity (O_2 utilization), and as well as ultrastructural and molecular changes of organ systems involved, and their interactions (Malhotra et al., 2016). During incremental exercise testing, it is defined as the highest volume of VO_2 averaged over a period of time 20- to 30- s period achieved at presumed maximal effort (**Figure 3**). The period of which VO_2Peak is measured isn't standardized, but generally range between a 20- to 30- s period to a minute depending on investigator preference. VO_2Peak is quantified in liters or milliliters of oxygen per minute or in milliliters per kilogram of body weight per minute. It is a parameter that describes the maximal amount of energy obtainable by aerobic metabolism per unit time (aerobic power) at peak or incremental exercise (Mezzani, 2017). It is therefore powerfully reflective of cardiovascular functional capacity by taking into consideration maximal exercise tolerance.

On average, VO_2Peak declines by 10% per decade after the age of 30 and this has been attributed to decreasing maximal heart rate, stroke volume, blood flow to skeletal muscle and skeletal muscle aerobic potential (Betik and Hepple, 2008). Due to higher hemoglobin levels, greater muscle mass and stroke volume, VO_2Peak is approximately 10–20% greater in men than in women of comparable age (Astrand, 1960). Because VO_2Peak is influenced by age, gender, and muscle mass, it is therefore appropriate to interpret VO_2Peak normalized to age, gender and weight-based normative values (Grassi et al., 2009).

Submaximal Oxygen Uptake Measurements

Although VO_2Peak has been the most commonly used variable for assessing cardiovascular functional capacity, gas exchange indices obtainable during submaximal exercise have emerged and may rival or even exceed the prognostic utility of VO_2Peak in various settings (Malhotra et al., 2016). Incremental exercise can be divided into two phases, firstly an initial phase that lasts until 50–60% of VO_2Peak during which expired ventilation (VE) increasing linearly with VO_2 and VCO_2. This is followed by a second phase during which VE increases disproportionately relative to first VO_2 and then VCO_2 (Albouaini et al., 2007). This transition point was initially termed the anaerobic threshold (AT), because in healthy subjects it tends to coincide with the exercise intensity at which the rates of glycolysis and especially glycogenolysis accelerate rapidly, leading to accumulation of pyruvate and hence lactate in muscle and blood (i.e., the lactate threshold). It has long been known, however, the muscle is only truly anaerobic at intensities $>$ 100% of VO_2max. Furthermore, numerous studies have demonstrated that it is possible to dissociate changes in VE from changes in lactate (Poole and Gaesser, 1985; McLellan and Gass, 1989). For example, the muscles of patients with McArdle's disease lack the ability to produce lactate due to the absence of glycogen phosphorylase activity. Such individuals therefore do not exhibit a lactate threshold, but their VE increases non-linearly with exercise intensity similar to that of a normal person (Hagberg et al., 1990). Similarly, high or low muscle glycogen levels, high or low pedaling rates, different types of exercise training, etc., have all been shown to dissociate changes in VE from changes in lactate (Hughes et al., 1982). The "breakpoint" in VE with increasing exercise intensity is therefore more appropriately described as simply a ventilatory threshold (VT), and can be estimated non-invasively using various quantitative methods, such as the V-slope method. In the V-slope method, VT is defined as the VO_2 at which the rate of increase in VCO_2 relative to VO_2 increases in the absence of hyperventilation (Beaver et al., 1986). Although estimation of VT can be replaced by direct blood sampling to determine the lactate threshold (LT), this is rarely performed in a clinical setting.

Submaximal CPET indices such as VT are attractive due to the relative ease with which they are ascertained during low-level exercise, their independence from volitional effort, and their relevance to an individual's ability to perform activities of daily living. Ascertainment of submaximal VO_2 parameters becomes particularly relevant in patients with heart failure who fail to fulfill the criteria for maximum volitional effort, and this is discussed in more detail below. For example, the

TABLE 1 | Summary of CPET variables and description.

Abbreviation	Parameter	Units	Description
WR	Work rate	Watts (W)	Work per unit time (where work represents the movement resulting from force being exerted against a mass, e.g., cycle ergometry).
RPE	Rating of perceived exertion		Self-reported subjective measure of the sensations of exertion being experienced by the participant.
t	Endurance time	s	Total exercise time (excluding warm-up).
HR	Heat rate	min^{-1}	Number of heart beats (cardiac cycles) per minute.
HRR	Heart rate reserve	min^{-1}	Difference between the predicted maximal heart rate and actual peak heart rate achieved.
SBP	Systolic blood pressure	mmHg	
DBP	Diastolic blood pressure	mmHg	
RPP	Rate pressure product	–	Product of HR and SBP. Indirect measure of myocardial work.
FEV_1	Forced expiratory volume in one second	l	Volume of air expelled from the lungs during first second of forced expiration (measured at rest).
FVC	Forced vital capacity	l	Maximal volume of air expelled from the lungs after maximal inspiration (measured at rest).
BF	Breathing frequency	min^{-1}	Number of breaths (ventilatory cycles) per minute.
V_T	Tidal volume	l	Volume of air inhaled or exhaled in a single breath.
$\dot{V}_E$	Minute ventilation	$l.min^{-1}$	Volume of air inhaled or exhaled per minute.
MVV	Maximum voluntary ventilation	$l.min^{-1}$	Maximal ventilatory ability measured by repeated maximal inspiration and expiration over a given time period, e.g., 10 s).
BR	Breathing reserve	%	Difference between resting MVV and maximal V_E during exercise. Represents remaining capacity to increase ventilation at maximal exercise.
$\dot{V}O_2$	Oxygen uptake	$ml.min^{-1}$ $ml.kg^{-1}{\cdot}min^{-1}$	Volume of O_2 uptake per minute measured in expired air.
$\dot{V}O_2$ max	Oxygen uptake at maximal exercise	$ml.min^{-1}$ $ml.kg^{-1}{\cdot}min^{-1}$	Highest O_2 uptake achievable during incremental exercise.
$\dot{V}O_2$ peak	Oxygen uptake at peak exercise	$ml.min^{-1}$ $ml.kg^{-1}{\cdot}min^{-1}$	Highest O_2 uptake achievable during incremental exercise in the context of any physiological limitation (often used synonymously with $\dot{V}O_{2max}$).
$\dot{V}O_2$ % pred	Oxygen uptake as a percentage of predicted	%	Highest O_2 uptake achieved during incremental exercise relative to predicted value (values of 80–120% predicted are considered normal).
$\dot{V}CO_2$	Carbon dioxide output	$ml.min^{-1}$	Volume of CO_2 exhaled per minute measured in expired air.
RER	Respiratory exchange ratio	–	Ratio of CO_2 output to O_2 uptake measured in expired gas.
VAT	Ventilatory anaerobic threshold	$ml.kg^{-1}{\cdot}min^{-1}$	O_2 uptake at the ventilatory anaerobic threshold.
VAT % pred. $\dot{V}O_{2peak}$	Ventilatory anaerobic threshold as a percentage of predicted $\dot{V}O_2$ peak	%	Oxygen uptake at the ventilatory anaerobic threshold relative to predicted $\dot{V}O_{2peak}$. Values below 40% are generally considered indicative of pathology.
$P_{ET}O_2$	End tidal partial pressure of O_2	mmHg	Partial pressure (tension) of O_2 in exhaled gas at the end of expiration
$P_{ET}CO_2$	End tidal partial pressure of CO_2	mmHg	Partial pressure (tension) of CO_2 in exhaled gas at the end of expiration
O_2 pulse	Oxygen pulse	ml	Amount of O_2 extracted by tissue per heart beat (i.e., stroke volume) Measure of overall cardiovascular efficiency.
OUES	Oxygen uptake efficiency slope	–	Regression-derived variable representing the relationship between log-transformed V_E and $\dot{V}O_2$. Measure of overall cardio-pulmonary function.
$\Delta\dot{V}O_2/\Delta WR$ slope	Oxygen uptake/work slope	–	Increase in O_2 uptake in relation to a simultaneous increase in work rate. Lower values indicate inability to augment $\dot{V}O_2$ in response to increase in WR.
$\dot{V}E/\dot{V}O_2$	Ventilatory equivalent for O_2	–	Volume of O_2 uptake per unit of ventilation.
$\dot{V}E/\dot{V}CO_2$	Ventilatory equivalent for CO_2	–	Volume of CO_2 output per unit of ventilation.
$\dot{V}E/\dot{V}CO_2$ slope	Slope of the ventilatory response	–	The slope of the response of the ventilatory equivalent for CO_2. Measure of ventilatory efficiency (ventilation/perfusion matching).
Sao2	Oxyhemoglobin saturation	%	Oxyhemoglobin saturation measured by pulse oximetery

ability to exercise beyond the VT can help distinguish impaired cardiovascular functional capacity from non-cardiac (pulmonary or musculoskeletal) causes of exercise limitation (Albouaini et al., 2007). However, this is not universally true as patients with mitral stenosis for example, often stop exercising before they reach VT, while patients with chronic obstructive pulmonary disease (COPD) commonly pass the VT.

Respiratory Exchange Ratio

The respiratory exchange ratio or RER is the ratio between VCO_2 and VO_2. During steady-state exercise below VT, RER provides an indication of substrate selection (i.e., fat vs. carbohydrate). Above VT, however, progressive increases in VE result in the liberation of "excess" CO_2 from bicarbonate stores. This helps to buffer the protons being produced as a result of high rates

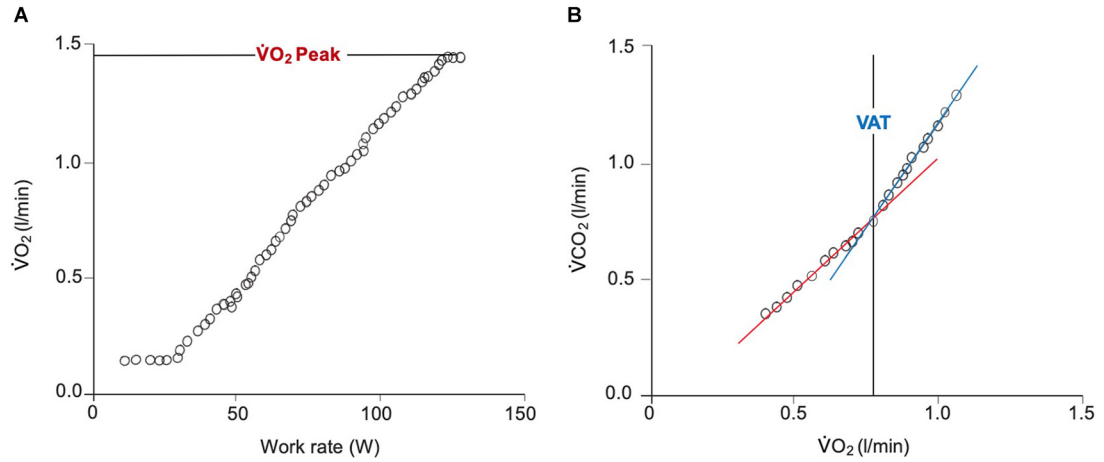

FIGURE 3 | Breath-by-breath gas exchange measurements during a ramp protocol CPET. **(A)** Demonstrates the linear increase in $\dot{V}O_2$ in response to a linear increase in work rate. Achievement of $\dot{V}O_2$Peak is confirmed by the plateau in $\dot{V}O_2$ beginning at approximately 125 W. **(B)** Displays the derivation of the VAT using the 'V-slope' method. The point at which the lower (blue) and upper (red) slopes intersect indicates the VAT. $\dot{V}O_2$, oxygen uptake; $\dot{V}CO_2$, carbon dioxide output; VAT, ventilatory anaerobic threshold.

of glycolysis/glycogenolysis, but invalidates the use of RER as a measure of substrate oxidation. Nonetheless, RER still provides an objective descriptor of subject motivation. An RER greater than approximately 1.0 implies that an individual has attained a maximal volitional effort, whereas an RER less than this value suggests that they have not. Measurement of RER during CPET testing and is therefore of crucial significance to assist in the attainment of reliable and clinically meaningful VO_2Peak values (Mezzani, 2017).

Oxygen Pulse

Oxygen pulse is the ratio between VO_2 and heart rate, and reflects the amount of oxygen consumed per heartbeat. It is a measure for stroke volume and peripheral oxygen extraction during exercise, and can be calculated as stroke volume multiplied by $C(a\text{-}v)O_2$ (Mezzani, 2017). Flattening or downward displacement of oxygen pulse kinetics during incremental exercise has been shown to be reflective of peripheral vascular perfusion or extraction or central cardiogenic performance limitations (Mezzani, 2017). Under certain conditions, the morphological analysis of its curve can aid in the diagnosis of ventricular dysfunction and exercise-induced myocardial ischemia (Herdy et al., 2016).

CARDIOVASCULAR FUNCTIONAL CHANGES IN CKD

End-Stage Kidney Disease (ESKD)

In a matched cohort study, Ting et al. (2015) examined cardiovascular functional capacity changes in a study that recruited 80 dialysis patients and 80 hypertensive controls. The authors reported that dialysis patients had a reduction in VO_2Peak (18 ± 4.1 ml/min^{-1}/kg^{-1}) compared to controls (24.5 ± 7.1 ml/min^{-1}/kg^{-1}, $p < 0.001$) (Ting et al., 2015). The study also found that LV ejection fraction was significantly lower in dialysis patients compared to hypertensive controls, however, this was not predictive of VO_2Peak. Further analysis revealed that LV filling pressure and pulse wave velocity were independent predictors of reduced VO_2Peak in dialysis patients. Conversely, LV mass index and LV end-diastolic volume were predictive of VO_2Peak in the hypertensive control group. These results suggest important mechanistic differences leading to reduced cardiovascular function in advanced CKD as opposed to those in hypertensive cardiovascular disease alone. The finding that LV ejection was not predictive of VO_2Peak is not surprising, given that the majority of CKD patients with heart failure have diastolic rather than systolic dysfunction (Loutradis et al., 2018). It is possible that increased LV diastolic stiffness may in part contribute to impaired cardiovascular functional capacity as CKD progresses; further studies are required to elucidate this. Although myocardial growth and remodeling may be a dynamic, adaptive process that occurs early in the course of CKD, it is likely that sustained cardiac afterloads due to volume overload in ESKD is a major contributor to progressive cardiac remodeling. Additionally, in the study by Ting et al. (2015) dialysis patients exhibited chronotropic incompetence with a reduced maximal heart rate. Taken together, these results suggest that maladaptive LV changes and blunted chronotropic responses are involved in impairment of cardiovascular function in dialysis patients.

The CAPER (Cardiopulmonary Exercise Testing in Renal Failure and After Kidney Transplantation) study by Lim et al. (2020) was the first study to assess cardiovascular functional changes using CPET before and after kidney transplantation. CAPER was a prospective, non-randomized, single-center, 3-arm controlled cohort study that recruited a total of 253 patients: 81 stage 5 CKD patients who underwent kidney transplantation, 85 non-transplanted waitlisted stage 5 CKD patients, and 87 hypertensive controls. All patients underwent CPET and echocardiography assessment at baseline and were followed longitudinally for up to 1 year. In the

non-transplanted CKD stage 5 group, who were waitlisted but did not undergo transplantation after 1 year follow-up, CPET was sensitive enough to detect a decline in cardiovascular functional capacity (as assessed by VO_2Peak) (18.9 ± 4.7 to 17.7 ± 4.1 mL.min^{-1}.kg^{-1}, $p < 0.001$). These results become even more revealing considering that the study found that LV mass index did not change ($p = 0.20$). This highlights the limitations of using LV mass or hypertrophy as a surrogate endpoint for tracking disease progression in advanced CKD patients, and that other processes beyond LV geometric indices are likely involved in driving overall cardiovascular functional decline in this population.

CAPER found that LV ejection fraction declined after 1 year ($p = 0.003$). Among the variables that were correlated with VO_2Peak changes from baseline to 12 months in the non-transplanted dialysis group, were LV mass index, LV ejection fraction, and maximal heart rate as well as hemoglobin level (anemia). It is currently unknown how cardiovascular functional capacity alters with increasing dialysis vintage (length of time on dialysis) beyond 1 year and this data will be critical to help inform cardiovascular risk. Additionally, it is unknown how processes such as myocardial remodeling through fibrosis, myocardial arteriole calcification, capillary rarefaction, myocardial stunning and complex circulating factors such as FGF23, Klotho and metabolites modulate VO_2Peak decline in dialysis. We postulate that these factors may contribute to reduced cardiac compliance and ventricular contractility, loss of arterial elasticity, as well as end-organ damage of the lungs and skeletal muscle system. Further studies are needed to evaluate this.

Data from the CAPER study highlight the complex organ system interactions that are involved in regulating cardiovascular function in advanced CKD patients and provide evidence of the contribution of multiple target organs that collectively regulate the oxygen transport system (**Figure 2**). Given that CKD severity is associated with restrictive lung disease (Mukai et al., 2018) and that the lungs are an integral part of the oxygen transport system, it is worrying that few studies have comprehensively assessed pulmonary function changes with advancing CKD, and no studies have examined its relative contribution to impaired cardiovascular functional capacity in CKD. Studies that couple CPET with advanced imaging techniques such as Magnetic Resonance Imaging will help to better elucidate background lung, cardiac and arterial changes that occur and their contribution to impaired cardiovascular functional capacity in this population.

Additionally, given that sarcopenia is a feature of advanced CKD, we are in need of further studies to evaluate the relationship between direct measures of skeletal muscle contractile function and segmental lean muscle mass with changes in cardiovascular functional capacity. Of note, exercise intolerance is an important comorbidity in patients with advanced CKD and is associated with arterial stiffening and endothelial dysfunction (Downey et al., 2017). Emerging data has suggested that reduced cardiovascular functional capacity may be improved with exercise training. In a pilot randomized clinical trial, McGregor et al. (2018) demonstrated parallel improvements in isometric quadriceps strength and exercise cardiovascular functional capacity without significant changes in resting echocardiographic cardiac morphologies, following 10-weeks of exercise training among dialysis patients in a randomized, assessor-blinded, controlled study.

CPET has raised many other questions, for example, how cardiovascular functional capacity changes during short and long interdialytic periods, and how the effects of conventional thrice weekly hemodialysis versus intensive hemodialysis and peritoneal dialysis may alter cardiovascular functional capacity. Further studies are needed.

Kidney Transplant Recipients

In the CAPER study, Lim et al. (2020) reported significantly improved cardiovascular functional capacity as assessed by VO_2Peak in the kidney transplant group 1 year after transplantation (20.7 ± 5.8 to 22.5 ± 6.3 mL.min^{-1}.kg^{-1}, $p < 0.001$). However, cardiovascular functional capacity was not restored to the level observed in the control group without CKD, and this was consistent with the incomplete normalization of kidney function with transplantation (mean eGFR 59.1 ± 18.4 mL.min^{-1}.1.73 m^{-2}, to the level of CKD stage 3). These findings become all the more meaningful considering that LVMI did not change after kidney transplantation, despite a significant improvement in VO_2Peak and when contrasted with the inverse direction of change in non-transplanted dialysis patients. Despite unaltered LVMI, the study reported an improvement in LVEF in the transplanted group at 12 months. These latter findings are consistent with a recent study using volume-independent cardiac magnetic imaging that failed to show significant change in LVMI and LVEF after transplantation (Patel et al., 2008).

Among the variables that were correlated with transplanted-associated VO_2Peak improvement at 1 year in the CAPER study were cardiac variables (improved LV ejection fraction, maximum heart rate) as well as corrected calcium level (Lim et al., 2020). This latter finding of an association between calcium and change in VO_2Peak is intriguing given that disordered bone mineral metabolism is a cardinal feature of the failing kidney, and that calcium is centrally involved in regulating cardiac myocyte contractility and relaxation (Hohendanner et al., 2013) and may play a role in regulating myocardial function in uremia. The study did not find a change in plasma corrected calcium levels after kidney transplantation and further studies are needed to explore this. Additionally, improvement in VO_2Peak at 1 year after transplantation in the CAPER study was also associated with improvements in uremia and fluid overload that were already notable at 2 months after transplantation. These results suggest that reversal of cardiovascular molecular and ultrastructural changes takes at least several months before an improvement in cardiovascular function can be detected in kidney transplant recipients. The pattern of cardiovascular functional changes beyond 1 year after kidney transplantation is unknown and further studies are warranted to evaluate this.

Chronic Kidney Disease (CKD)

Few studies have assessed cardiovascular functional capacity in pre-dialytic CKD patients. In a study by Nelson et al. (2016) the authors analyzed CPET data from 933 pre-operative patients and found that 93/933 (9.97%) had CKD stage 3 (Nelson et al.,

2016). The authors reported that patients with CKD stage 3 had a significantly lower VO_2Peak (mean difference 6%, 95% CI 1-11%, $p = 0.02$), lower peak heart rate (mean difference 9 bpm, 95% CI 3–14%, $p = 0.03$) and impaired heart rate recovery (mean difference 4 bpm, 95% CI 1–7, $p < 0.001$) compared to patients with a GFR > 60. These findings are suggestive of subclinical cardiovascular disease that can be objectively assessed in pre-dialytic CKD patients. Given that microvascular dysfunction has been shown to be involved in cardiovascular disease in CKD and subclinical disease (Bajaj et al., 2020), further studies are needed to determine whether CPET indices could be used as a surrogate for assessing microvascular dysfunction in CKD. To date, it is unknown how cardiovascular functional capacity alters in the early stages of CKD or its natural history across the spectrum of CKD severity. Additionally, further prospective studies are desperately needed to link changes in VO_2Peak with cardiovascular outcomes in the CKD population. A summary of observational studies and clinical trials that have utilized CPET-derived endpoints in kidney patients is provided in **Table 2**.

POTENTIAL APPLICATIONS OF CPET TECHNOLOGY IN NEPHROLOGY

CPET is currently widely used for risk stratification, clinical evaluation and other applications in several medical specialities outside of nephrology. The possibility of adopting global indices such as VO_2Peak in the field of nephrology has been made more feasible due to technological advances in state-of-the-art CPET and the prognostic value of submaximal indices. Here, we will review several of its existing applications and discuss its potential role in kidney patients.

Comprehensive Endpoints for Cardio-Renal Trials

Given the limitations of current endpoints such as the LV geometric indices discussed above for assessing cardiovascular alterations in CKD, the potential to use comprehensive endpoints such as VO_2Peak for cardio-renal outcome trials represents an incredibly attractive alternative. There remains strong experimental and observational evidence that adaptations of cardiovascular structure and function can occur bidirectionally, that is, that adverse cardiovascular remodeling can regress with the potential for recovery in kidney patients (Melchor et al., 2002; Wali et al., 2005). Because significant improvement in cardiovascular outcomes has been reported after kidney transplantation (Pilmore et al., 2010), these data suggest that cardiovascular change in CKD is a modifiable process that can potentially be controlled or halted. Moreover, these data call for sensitive endpoints that can accurately track disease progression or improvement. Considering the complex systemic and widespread ultrastructural and molecular alterations that occur in CKD, a comprehensive or aggregate endpoint such as VO_2Peak, that considers the complexity of cardiovascular and systemic alterations, may therefore be a particularly appropriate index for assessing cardiovascular improvement or decline in the setting of shifting GFR.

The development of LV hypertrophy, and systolic and diastolic dysfunction are well-recognized predictors of worse cardiovascular outcomes in CKD patients (Charytan, 2014). However, as previously noted above, imaging cardiac structure at rest rather than under the stress of exercise, may be insufficiently sensitive to detect impairment of the cardiovascular system due to renal dysfunction, and may not reliably predict functional performance (Ting et al., 2015). Imaging modalities such as dobutamine stress echocardiography (DSE) have been used in CKD patients. However, DSE has a reduced sensitivity of 80% for detecting inducible ischemia in advanced CKD patients (Parnham et al., 2014). This has been suggested to be secondary to blunted chronotropic responses in CKD; LVH with small intracavitary volume that can obscure detection of wall motion abnormalities at stress, and microvascular CAD that can be difficult to appreciate. Additionally, DSE does not consider other organ system interactions that may affect cardiovascular functional capacity in advancing CKD. Furthermore, there is significant intrinsic value in improving cardiovascular exercise capacity in patients (Malhotra et al., 2016). A low VO_2Peak defines functional aerobic impairment or exercise intolerance, while an improvement in cardiovascular exercise capacity is sensitively reflected by an increased VO_2Peak (Albouaini et al., 2007). A summary comparing risk stratification methods, and their advantages and disadvantages in CKD is provided in **Table 3** (Hakeem et al., 2014; Parnham et al., 2014).

From a regulatory standpoint, a significant advantage of CPET-derived endpoints is that they have already been used extensively in clinical trials in the general heart failure population (Malhotra et al., 2016). Importantly, the US Food and Drug Administration (FDA) has evaluated and approved new drugs and devices that have utilized CPET-derived endpoints in clinical trials (Malhotra et al., 2016).

Cardiovascular Risk Stratification and Prognostic Utility

One of the main manifestations of heart failure is exercise intolerance and this varies with severity of disease. Decreased exercise capacity is associated with higher New York Heart Association (NYHA) functional class, worse symptoms, poor quality of life and decreased patient survival. Exercise capacity is reduced even in mild heart failure and is reflective of an inability of cardiac output to increase adequately with mild exertion (Reddy et al., 1988). VO_2Peak has been shown to be strongly correlated with maximal cardiac output (Mitchell et al., 1958; Ekblom and Hermansen, 1968). In heart failure, the inability of cardiac output to appropriately increase may result in insufficient perfusion of exercising muscles and premature muscle fatigue (Harrington et al., 1997). Because the NYHA classification of functional impairment in heart failure can be inaccurate due to its subjective nature, objective assessment of cardiovascular functional capacity by CPET offers a significant advantage. Additionally, measures of cardiovascular functional

TABLE 2 | Summary of clinical studies involving kidney patients that have utilized cardiopulmonary exercise testing (CPET) technology.

References	Year	Population	Summary
Observational studies			
Weaver et al.	2008	Pediatric patients: stage 2–4 CKD (n = 46), renal transplant recipients (n = 33), maintenance HD patients (n = 12) and age-matched healthy controls (n = 33)	VO_2max is decreased in children with CKD stages 3 to 4, those on hemodialysis and transplant recipients. Lower VO_2max can be predicted by the presence of diastolic dysfunction, even if systolic function is normal.
Ting et al.	2013	N = 70 living donor kidney recipients.	Reduced AT predicts critical care unit admission in patients undergoing kidney transplantation.
De Souza Faria et al.	2013	N = 9 healthy adults, n = 29 pre-dialytic CKD stages 3, 4, and 5.	VO_2Peak as well as submaximal exercise tolerance was impaired in pre-dialytic CKD patients.
Fassbinder et al.	2014	N = 54 patients with CKD, 27 stage 1 and 27 stage 2.	No statistically significant difference between stage 1 and 2 patients in VO_2Peak.
Ting et al.	2014	N = 240 patients waitlisted for kidney transplantation, and followed for $\leq$ 5 years.	Patients with AT $<$ 40% of predicted VO_2Peak had significantly reduced 5-year cumulative survival rate compared to those with $\geq$ 40%. Among the patients with AT $<$ 40%, those who underwent kidney transplantation had significantly better survival compared with non-transplanted patients.
Ting et al.	2015	N = 80 patients with CKD (61 were dialysis dependent) and 80 patients with essential hypertension.	VO_2Peak was significantly lower in patients in CKD patients compared to hypertensive controls. Maladaptive LV changes and blunted chronotropic responses were mechanistically involved in reduced cardiovascular functional reserve.
Van Craenenbroeck et al.	2016	N = 63 CKD stages 1–5 and n = 18 healthy controls.	Impaired VO_2Peak in mild CKD (stages 1–3A) and correlated with eGFR. Pulse wave velocity was one of the strongest independent determinants of VO_2Peak.
Nelson et al.	2016	N = 993 pre-operative patients, that included n = 93 CKD stage 3 patients.	Patients with CKD stage 3 had reduced VO_2Peak.
Rogan et al.	2017	143 CKD stage 5 or 5d patients and 83 hypertensive controls.	CKD patients had reduced VO_2Peak, and this was a significant independent predictor of the physical component score (PCS) of the SF-36.
Kirkman et al.	2018	N = 31 stage 3–4 CKD and 21 matched healthy controls.	VO_2Peak, AT, maximum heart rate and 1-min heart rate recovery was reduced in CKD stage 3 patients compared to healthy controls. CKD patients had ventilation perfusion mismatching.
Clinical trials			
Mustata et al.	2010	CKD patients, n = 10 randomized to 12 months of exercise and n = 10 to standard of care.	Long-term exercise training improves VO_2Peak, augmentation index and health-related quality of life in patients with predialysis CKD.
McGregor et al.	2018	N = 46 hemodialysis patients randomized to 10 weeks intra-dialytic cycling, intra-dialytic low-frequency electrical muscle stimulation (LF-EMS) or non-exercise control	Ten weeks of intra-dialytic LF-EMS or cycling improved VO_2Peak and muscular strength.

HD, hemodialysis; AT, anaerobic threshold.

capacity obtained under incremental exercise load reflect overall circulatory health and the ability to respond to physiological and pathological cardio-circulatory stresses (Melchor et al., 2002; Ting et al., 2014). Measures of resting central hemodynamics do not correlate well with functional impairment. For these reasons, CPET has become an integral tool for accurately risk stratifying congestive heart failure patients for timely heart transplantation worldwide (Mancini et al., 1991). The identification of heart failure patients at high risk is crucial to guide their management. In addition to providing robust markers for cardiovascular functional capacity and exercise intolerance, CPET permits assessment of the organ system limiting gas exchange. This technology therefore has significant advantages over 6 min walk tests (6MWT) for evaluating exercise limitations.

Indices of cardiovascular functional capacity have been independently associated with survival in multiple settings. Mancini et al. (1991) in a landmark study involving 114 ambulatory patients with heart failure and reduced ejection fraction in the general population, established VO_2Peak $\leq$ 14 mL.min^{-1}.kg^{-1} as a criterion for which 1 year survival was significantly lower than that achieved through transplantation. Individuals with a VO_2Peak $>$ 14 mL.min^{-1}.kg^{-1} had a 6% 1 year mortality and this suggests that heart transplantation can be safely deferred in this subgroup of symptomatic heart failure patients. VO_2Peak potently risk stratifies heart failure patients (with reduced ejection fraction and preserved ejection fraction) into Weber classes A, B, C, and D corresponding to VO_2Peak $>$ 20, 16–20, 10–16, $<$10 mL.min^{-1}.kg^{-1} which associate with 3 years transplant and mechanical circulatory support-free survival of 97, 93, 83, and 64% respectively (Ritt et al., 2015). Importantly, in heart failure patients with reduced ejection fraction on beta-blockers, VO_2Peak retains its prognostic significance (O'Neill et al., 2005), and is an important predictor of mortality in heart failure with preserved ejection fraction (Haykowsky et al., 2011; Dhakal et al., 2015). This latter finding is particularly relevant to the renal population given that there is a disproportionate increase in heart failure with preserved ejection compared with reduced ejection fraction in CKD patients (Loutradis et al., 2018).

TABLE 3 | Cardiovascular risk stratification methods in CKD.

	Advantages	Disadvantages
Serum biomarker assessment, e.g., Troponin T	Easy to obtain; can sensitively detect myocardial necrosis; FDA approved in patients with ESKD	Lack of specificity, elevated in more than one-third of patients with ESKD, may require extended evaluation
Exercise stress EKG	Widely used methodology for ruling in and ruling out CAD with sensitivity ranging between 71 to 97% and specificity between 64 to 90%.	Requires some functional mobility; does not provide measure of cardiovascular functional capacity; patients with abnormal baseline EKG may limit standard testing
Resting echocardiography	Widely available, easy to obtain, low cost; allows assessment of LV geometry and ejection fraction	Inaccuracies with echo interpretation; significant volume shifts occur in dialysis patients; most CKD patients have diastolic failure (thereby limiting usefulness of ejection fraction); LV geometric indices do not sensitivity track disease progression in CKD
Exercise stress echocardiography	Allows imaging of extent of regional wall motion responses to stress; has better accuracy for detecting significant coronary stenosis ranging from 80 to 90% compared to exercise EKG	Requires some functional mobility; does not provide measure of cardiovascular functional capacity; technique can be challenging
Dobutamine stress echocardiography (DSE)	Well-validated and multiple studies have shown incremental prognostic utility over clinical data for demonstrating resting and stress-induced regional WMA	Increased LV mass or concentric remodeling limits sensitivity for subtle WMA
Cardiac Magnetic Resonance Imaging (CMR)	Can detect scar pattern and burden, presence of subendocardial scar by delayed enhancement on CMR has been associated with CAD risk factors, depressed LV ejection fraction and severe CAD on angiography	Little data available on prognostic value of myocardial scar pattern and burden using this technique in CKD population; risk of gadolinium-induced nephrogenic systemic fibrosis
Myocardial perfusion single-photon emission computed tomography (MPS)	Well validated prognostic tool in CKD; high prevalence of perfusion defects in ESKD patients	Presence of LVH can compromise sensitivity, due to partial volume effect; can have false negative results in multi-vessel disease due to balanced ischemia
Coronary artery calcium score (CACS)	Coronary calcification is highly prevalent in CKD; offers incremental predictive value to clinical risk factors	Does not sensitively track overall cardiovascular disease progression or improvement
Cardiopulmonary Exercise Testing (CPET)*	Comprehensive, takes into account alterations within the entire oxygen transport chain in CKD; sub-maximal derived indices can be obtained with relative ease and does not require maximal volitional effort; can be coupled with imaging or invasive techniques that can provide incremental prognostic data	Selects for patients that have some functional mobility; standardization of CPET testing is not yet uniform across different CPET labs

**All risk stratification methods above except for CPET do not reflect overall functional ability and are reflective of only single-organ changes. CAD, Coronary artery disease; LV, left ventricular; WMA, wall motion abnormality.*

In addition to heart failure, VO_2Peak has also been shown to be a predictor of survival in chronic lung disease (Nixon et al., 1992; Gitt et al., 2002; Oga et al., 2003; Arena and Sietsema, 2011) and perioperative risk with major surgery (Older et al., 1999; Wilson et al., 2010; Ting et al., 2013).

CPET-derived indices of cardiovascular functional capacity have recently been shown to be robust predictors of cardiovascular morbidity and premature death among patients with advanced CKD, independent of LV measures (Ting et al., 2013, 2014). In a landmark study by Ting et al. (2014) the authors recruited 240 advanced CKD patients who underwent CPET and were followed for $\leq$5 years. The authors reported that patients with a VT $<$ 40% of predicted peak VO_2 had a significantly reduced 5 years cumulative survival rate compared with those that had VT $\geq$ 40% ($P < 0.001$). Significantly, among the patients who had VT $<$ 40%, those that underwent kidney transplantation had a significantly better survival compared with the non-transplanted patients. Among the patients with VT $\geq$ 40%, survival did not differ significantly between those who were transplanted and those who were not. These results suggest that assessment of VT using CPET can provide a high level of discrimination to risk stratify patients for timely kidney transplantation, and that those with a VT $<$ 40% may benefit from early transplantation. These findings are critical given the growing body of evidence that single surrogate markers from the most established clinicopathologic factors, such as age and LV mass index, have limited prognostic value for cardiovascular outcomes in CKD.

Physiological Insights

A significant strength of CPET is that the technology provides a wealth of data from a single assessment, including hemodynamics, ventilatory efficiency, stability and O_2 uptake patterns and mechanical or musculoskeletal parameters. In the general heart failure population, a number of indices have been associated with important measures of cardiovascular physiology such as circulatory power (an index of cardiac systolic function), VE/VCO_2 (an index of ventilatory efficiency and pulmonary vascular resistance) and mean response time (MRT, an index of right ventricular-pulmonary vascular function during exercise) that can be easily attainable using CPET non-invasively (Malhotra et al., 2016; Mezzani, 2017). CPET assessment, particularly when coupled with hemodynamic, advanced imaging or invasive measures can shed critical insight into the pathophysiology and determinants of cardiovascular alterations, elucidate changes in specific

Fick components and provide in-depth insight on the organ limiting gas exchange.

CPET that is coupled with invasive hemodynamic assessment, for example using radial or pulmonary arterial catheters enables highly detailed patient phenotyping. This permits accurate assessment of blood pressure and oxyhemoglobin measurement, as well as simultaneous measurement of VO_2 and arterial, as well as mixed venous blood gasses during linear ramp exercise. These data will allow Fick cardiac output derivation and evaluation of the component variables of the Fick equation. Patients with identical VO_2Peak values with a diagnosis of heart failure, may have significantly different levels of impairment in the reserve capacity of each Fick variable (Malhotra et al., 2016). No studies to date have comprehensively assessed CKD patients using invasive CPET, or evaluated how the various Fick variables alter as CKD progresses. By elucidating the mechanisms of cardiovascular dysfunction during progressive CKD, new therapeutic targets for improving cardiovascular outcomes in CKD patients may be identified.

CONCLUSION AND FUTURE DIRECTIONS

The significant public health need for better diagnostic and therapeutic approaches to help improve cardiovascular outcomes in CKD requires the implementation of effective, holistic and forward-thinking strategies in our research efforts. Given the multi-systemic nature of CVD development in CKD, an integrative approach at all levels to study mechanisms of disease, to track disease progression or improvement, for risk stratification, and for implementation of appropriate clinical trial endpoints maybe warranted. CPET provides a global test of cardiovascular functional capacity that reflects the entire oxygen transport system and may provide a potential solution for an integrative approach to assessing the cardiovascular system in CKD. The technology provides a wealth of data per single assessment with mechanistic, physiological and prognostic utility. Because a significant advantage of CPET is the ability to couple the technology with other investigative modalities such as invasive CPET and advanced imaging techniques, this can provide comprehensive phenotyping and characterization of multisystem changes that determine overall cardiovascular functional capacity with a wide array of applications. While CPET is a powerful technology, there are also important limitations to the technology that warrants a brief discussion. Firstly, CPET assessment does select for patients who retain some functional ability and therefore, patients who are unable to complete a cycle or treadmill test would be inherently excluded from assessment; Secondly, like all types of exercise testing, patients are required to present to a CPET lab and tests must be conducted by a trained exercise physiologist or clinician. Development of CPET technology has now enabled measurement of ventilatory parameters using handheld devices that can be used in an office-based setting, making the technology increasingly more accessible.

Although CPET is a tool that is now widely available and supported by sound scientific evidence in several clinical fields, only a handful of studies have utilized CPET to study kidney patients. Despite this, CPET has already provided a wealth of hypothesis-generating data and has opened up many other exciting questions in the cardio-renal field. The potential to capitalize on next-generation CPET technology to help move the cardio-renal field forward has provided strong rationale for the urgent need for further CPET-related research in nephrology. Here in the Division of Nephrology at Indiana University School of Medicine, we have developed the first nephrology-based CPET laboratory in the United States dedicated to studying kidney patients. These efforts are in parallel with increasing interest among nephrologists worldwide in exercise impairment and musculoskeletal disorders in CKD patients. CPET technology has the potential to drive actionable strategies in our collective efforts to help reduce the burden of CVD in CKD. Strong efforts to recognize these promising advances and to place them as a primary research agenda in cardio-nephrology are needed.

AUTHOR CONTRIBUTIONS

KL wrote the manuscript. GM generated all the figures. AC, GL, and SM provided the intellectual guidance and edited the manuscript. All the authors read and approved the manuscript.

FUNDING

KL was supported through an NIH 5K23DK115683 grant.

REFERENCES

Albouaini, K., Egred, M., Alahmar, A., and Wright, D. J. (2007). Cardiopulmonary exercise testing and its application. *Heart* 93, 1285–1292.

American Thoracic Society, and American College of Chest Physicians (2003). ATS/ACCP statement on cardiopulmonary exercise testing. *Am. J. Respir. Crit. Care Med.* 167, 211–277. doi: 10.1164/rccm.167.2.211

Aoki, J., Ikari, Y., Nakajima, H., Mori, M., Sugimoto, T., Hatori, M., et al. (2005). Clinical and pathologic characteristics of dilated cardiomyopathy in hemodialysis patients. *Kidney Int.* 67, 333–340. doi: 10.1111/j.1523-1755.2005.00086.x

Arena, R., and Sietsema, K. E. (2011). Cardiopulmonary exercise testing in the clinical evaluation of patients with heart and lung disease. *Circulation* 123, 668–680. doi: 10.1161/circulationaha.109.914788

Astrand, I. (1960). Aerobic work capacity in men and women with special reference to age. *Acta Physiol. Scand. Suppl.* 49, 1–92.

Bajaj, N. S., Singh, A., Zhou, W., Gupta, A., Fujikura, K., Byrne, C., et al. (2020). Coronary microvascular dysfunction, left ventricular remodeling, and clinical outcomes in patients with chronic kidney impairment. *Circulation* 141, 21–33. doi: 10.1161/circulationaha.119.043916

Bassett, D. R. Jr., and Howley, E. T. (2000). Limiting factors for maximum oxygen uptake and determinants of endurance performance. *Med. Sci. Sports Exerc.* 32, 70–84. doi: 10.1097/00005768-200001000-00012

Beaver, W. L., Wasserman, K., and Whipp, B. J. (1986). A new method for detecting anaerobic threshold by gas exchange.

J. Appl. Physiol. 60, 2020–2027. doi: 10.1152/jappl.1986.60.6.2020

Betik, A. C., and Hepple, R. T. (2008). Determinants of VO2 max decline with aging: an integrated perspective. *Appl. Physiol. Nutr. Metab.* 33, 130–140. doi: 10.1139/h07-174

Charytan, D. (2014). Is left ventricular hypertrophy a modifiable risk factor in end-stage renal disease. *Curr. Opin. Nephrol. Hypertens.* 23, 578–585. doi: 10.1097/mnh.0000000000000067

Dhakal, B. P., Malhotra, R., Murphy, R. M., Pappagianopoulos, P. P., Baggish, A. L., Weiner, R. B., et al. (2015). Mechanisms of exercise intolerance in heart failure with preserved ejection fraction: the role of abnormal peripheral oxygen extraction. *Circ. Heart Fail.* 8, 286–294. doi: 10.1161/circheartfailure.114.001825

Downey, R. M., Liao, P., Millson, E. C., Quyyumi, A. A., Sher, S., and Park, J. (2017). Endothelial dysfunction correlates with exaggerated exercise pressor response during whole body maximal exercise in chronic kidney disease. *Am. J. Physiol. Renal Physiol.* 312, F917–F924.

Dunn, J.-O., Mythen, M., and Grocott, M. (2016). Physiology of oxygen transport. *BJA Educ.* 16, 341–348.

Edwards, N. C., Moody, W. E., Chue, C. D., Ferro, C. J., Townend, J. N., and Steeds, R. P. (2014). Defining the natural history of uremic cardiomyopathy in chronic kidney disease: the role of cardiovascular magnetic resonance. *JACC Cardiovasc. Imaging* 7, 703–714. doi: 10.1016/j.jcmg.2013.09.025

Ekblom, B., and Hermansen, L. (1968). Cardiac output in athletes. *J. Appl. Physiol.* 25, 619–625. doi: 10.1152/jappl.1968.25.5.619

Ferro, C. J., Steeds, R. P., and Townend, J. N. (2012). Hypertension, arterial haemodynamics and left ventricular disease: historical observations. *QJM* 105, 709–716. doi: 10.1093/qjmed/hcs059

Foley, R. N., Parfrey, P. S., Harnett, J. D., Kent, G. M., Martin, C. J., Murray, D. C., et al. (1995). Clinical and echocardiographic disease in patients starting end-stage renal disease therapy. *Kidney Int.* 47, 186–192. doi: 10.1038/ki.1995.22

Gansevoort, R. T., Correa-Rotter, R., Hemmelgarn, B. R., Jafar, T. H., Heerspink, H. J., Mann, J. F., et al. (2013). Chronic kidney disease and cardiovascular risk: epidemiology, mechanisms, and prevention. *Lancet* 382, 339–352.

Gitt, A. K., Wasserman, K., Kilkowski, C., Kleemann, T., Kilkowski, A., Bangert, M., et al. (2002). Exercise anaerobic threshold and ventilatory efficiency identify heart failure patients for high risk of early death. *Circulation* 106, 3079–3084. doi: 10.1161/01.cir.0000041428.99427.06

Grassi, B., Porcelli, S., Marzorati, M., Lanfranconi, F., Vago, P., Marconi, C., et al. (2009). Metabolic myopathies: functional evaluation by analysis of oxygen uptake kinetics. *Med. Sci. Sports Exerc.* 41, 2120–2127. doi: 10.1249/mss.0b013e3181aae96b

Group, F. H. N. T., Chertow, G. M., Levin, N. W., Beck, G. J., Depner, T. A., Eggers, P. W., et al. (2010). In-center hemodialysis six times per week versus three times per week. *N. Engl. J. Med.* 363, 2287–2300. doi: 10.1056/nejmoa1001593

Hagberg, J. M., King, D. S., Rogers, M. A., Montain, S. J., Jilka, S. M., Kohrt, W. M., et al. (1990). Exercise and recovery ventilatory and VO2 responses of patients with McArdle's disease. *J. Appl. Physiol.* 68, 1393–1398. doi: 10.1152/jappl.1990.68.4.1393

Hakeem, A., Bhatti, S., and Chang, S. M. (2014). Screening and risk stratification of coronary artery disease in end-stage renal disease. *JACC Cardiovasc. Imaging* 7, 715–728. doi: 10.1016/j.jcmg.2013.12.015

Harrington, D., Anker, S. D., Chua, T. P., Webb-Peploe, K. M., Ponikowski, P. P., Poole-Wilson, P. A., et al. (1997). Skeletal muscle function and its relation to exercise tolerance in chronic heart failure. *J. Am. Coll. Cardiol.* 30, 1758–1764. doi: 10.1016/s0735-1097(97)00381-1

Haykowsky, M. J., Brubaker, P. H., John, J. M., Stewart, K. P., Morgan, T. M., and Kitzman, D. W. (2011). Determinants of exercise intolerance in elderly heart failure patients with preserved ejection fraction. *J. Am. Coll. Cardiol.* 58, 265–274.

Herdy, A. H., Ritt, L. E., Stein, R., Araujo, C. G., Milani, M., Meneghelo, R. S., et al. (2016). Cardiopulmonary exercise test: background, applicability and interpretation. *Arq. Bras. Cardiol.* 107, 467–481.

Hohendanner, F., Ljubojevic, S., Macquaide, N., Sacherer, M., Sedej, S., Biesmans, L., et al. (2013). Intracellular dyssynchrony of diastolic cytosolic [Ca2+] decay in ventricular cardiomyocytes in cardiac remodeling and human heart failure. *Circ. Res.* 113, 527–538. doi: 10.1161/circresaha.113.300895

Hughes, E. F., Turner, S. C., and Brooks, G. A. (1982). Effects of glycogen depletion and pedaling speed on "anaerobic threshold". *J. Appl. Physiol. Respir. Environ. Exerc. Physiol.* 52, 1598–1607. doi: 10.1152/jappl.1982.52.6.1598

Kahn, M. R., Robbins, M. J., Kim, M. C., and Fuster, V. (2013). Management of cardiovascular disease in patients with kidney disease. *Nat. Rev. Cardiol.* 10, 261–273.

Kim, S. K., Bae, J. C., Baek, J. H., Hur, K. Y., Lee, M. K., and Kim, J. H. (2018). Is decreased lung function associated with chronic kidney disease? A retrospective cohort study in Korea. *BMJ Open* 8:e018928. doi: 10.1136/bmjopen-2017-018928

Kwan, G. F., and Benjamin, E. J. (2015). Global health and cardiovascular disease. *Circulation.* 132:1217.

Lim, K., Hamano, T., and Thadhani, R. (2018). Vitamin D and calcimimetics in cardiovascular disease. *Semin. Nephrol.* 38, 251–266. doi: 10.1016/j.semnephrol.2018.02.005

Lim, K., Ting, S. M. S., Hamborg, T., McGregor, G., Oxborough, D., Tomkins, C., et al. (2020). Cardiovascular functional reserve before and after kidney transplant. *JAMA Cardiol.* 5, 420–429. doi: 10.1001/jamacardio.2019.5738

London, G. M. (2002). Left ventricular alterations and end-stage renal disease. *Nephrol. Dial. Transplant.* 17(Suppl. 1), 29–36. doi: 10.1093/ndt/17.suppl_1.29

Loutradis, C., Sarafidis, P. A., Papadopoulos, C. E., Papagianni, A., and Zoccali, C. (2018). The ebb and flow of echocardiographic cardiac function parameters in relationship to hemodialysis treatment in patients with ESRD. *J. Am. Soc. Nephrol.* 29, 1372–1381. doi: 10.1681/asn.2017101102

Malhotra, R., Bakken, K., D'Elia, E., and Lewis, G. D. (2016). Cardiopulmonary exercise testing in heart failure. *JACC Heart Fail.* 4, 607–616. doi: 10.1016/j.jchf.2016.03.022

Mancini, D. M., Eisen, H., Kussmaul, W., Mull, R., Edmunds, L. H. Jr., and Wilson, J. R. (1991). Value of peak exercise oxygen consumption for optimal timing of cardiac transplantation in ambulatory patients with heart failure. *Circulation* 83, 778–786. doi: 10.1161/01.cir.83.3.778

McGregor, G., Ennis, S., Powell, R., Hamborg, T., Raymond, N. T., Owen, W., et al. (2018). Feasibility and effects of intra-dialytic low-frequency electrical muscle stimulation and cycle training: a pilot randomized controlled trial. *PLoS One* 13:e0200354. doi: 10.1371/journal.pone.0200354

McLellan, T. M., and Gass, G. C. (1989). The relationship between the ventilation and lactate thresholds following normal, low and high carbohydrate diets. *Eur. J. Appl. Physiol. Occup. Physiol.* 58, 568–576. doi: 10.1007/bf00418501

Meier-Kriesche, H. U., Schold, J. D., Srinivas, T. R., Reed, A., and Kaplan, B. (2004). Kidney transplantation halts cardiovascular disease progression in patients with end-stage renal disease. *Am. J. Transplant.* 4, 1662–1668. doi: 10.1111/j.1600-6143.2004.00573.x

Melchor, J. L., Espinoza, R., and Gracida, C. (2002). Kidney transplantation in patients with ventricular ejection fraction less than 50 percent: features and posttransplant outcome. *Transplant. Proc.* 34, 2539–2540. doi: 10.1016/s0041-1345(02)03478-4

Mezzani, A. (2017). Cardiopulmonary exercise testing: basics of methodology and measurements. *Ann. Am. Thorac. Soc.* 14, S3–S11.

Mitchell, J. H., Sproule, B. J., and Chapman, C. B. (1958). The physiological meaning of the maximal oxygen intake test. *J. Clin. Invest.* 37, 538–547. doi: 10.1172/jci103636

Moorthi, R. N., and Avin, K. G. (2017). Clinical relevance of sarcopenia in chronic kidney disease. *Curr. Opin. Nephrol. Hypertens.* 26, 219–228. doi: 10.1097/mnh.0000000000000318

Mukai, H., Ming, P., Lindholm, B., Heimburger, O., Barany, P., Stenvinkel, P., et al. (2018). Lung dysfunction and mortality in patients with chronic kidney disease. *Kidney Blood Press Res.* 43, 522–535. doi: 10.1159/000488699

Nascimento, B. R., Brant, L. C., Moraes, D. N., and Ribeiro, A. L. (2014). Global health and cardiovascular disease. *Heart* 100, 1743–1749.

Nelson, A., Otto, J., Whittle, J., Stephens, R. C., Martin, D. S., Prowle, J. R., et al. (2016). Subclinical cardiopulmonary dysfunction in stage 3 chronic kidney disease. *Open Heart* 3:e000370. doi: 10.1136/openhrt-2015-000370

Nixon, P. A., Orenstein, D. M., Kelsey, S. F., and Doershuk, C. F. (1992). The prognostic value of exercise testing in patients with cystic fibrosis. *N. Engl. J. Med.* 327, 1785–1788.

Oga, T., Nishimura, K., Tsukino, M., Sato, S., and Hajiro, T. (2003). Analysis of the factors related to mortality in chronic obstructive pulmonary disease: role of

exercise capacity and health status. *Am. J. Respir. Crit. Care Med.* 167, 544–549. doi: 10.1164/rccm.200206-583oc

Older, P., Hall, A., and Hader, R. (1999). Cardiopulmonary exercise testing as a screening test for perioperative management of major surgery in the elderly. *Chest* 116, 355–362. doi: 10.1378/chest.116.2.355

O'Neill, J. O., Young, J. B., Pothier, C. E., and Lauer, M. S. (2005). Peak oxygen consumption as a predictor of death in patients with heart failure receiving beta-blockers. *Circulation* 111, 2313–2318. doi: 10.1161/01.cir.0000164270.72123.18

Parnham, S. F., Gleadle, J. M., De Pasquale, C. G., and Selvanayagam, J. B. (2014). Myocardial ischemia assessment in chronic kidney disease: challenges and pitfalls. *Front. Cardiovasc. Med.* 1:13. doi: 10.3389/fcvm.2014.00013

Patel, R. K., Mark, P. B., Johnston, N., McGregor, E., Dargie, H. J., and Jardine, A. G. (2008). Renal transplantation is not associated with regression of left ventricular hypertrophy: a magnetic resonance study. *Clin. J. Am. Soc. Nephrol.* 3, 1807–1811. doi: 10.2215/cjn.01400308

Pilmore, H., Dent, H., Chang, S., McDonald, S. P., and Chadban, S. J. (2010). Reduction in cardiovascular death after kidney transplantation. *Transplantation* 89, 851–857. doi: 10.1097/tp.0b013e3181caeead

Poole, D. C., and Gaesser, G. A. (1985). Response of ventilatory and lactate thresholds to continuous and interval training. *J. Appl. Physiol.* 58, 1115–1121. doi: 10.1152/jappl.1985.58.4.1115

Reddy, H. K., Weber, K. T., Janicki, J. S., and McElroy, P. A. (1988). Hemodynamic, ventilatory and metabolic effects of light isometric exercise in patients with chronic heart failure. *J. Am. Coll. Cardiol.* 12, 353–358. doi: 10.1016/0735-1097(88)90405-6

Rhee, E. P., and Gerszten, R. E. (2012). Metabolomics and cardiovascular biomarker discovery. *Clin. Chem.* 58, 139–147. doi: 10.1373/clinchem.2011.169573

Ritt, L. E., Myers, J., Stein, R., Arena, R., Guazzi, M., Chase, P., et al. (2015). Additive prognostic value of a cardiopulmonary exercise test score in patients with heart failure and intermediate risk. *Int. J. Cardiol.* 178, 262–264. doi: 10.1016/j.ijcard.2014.10.025

Rutherford, E., and Mark, P. B. (2017). What happens to the heart in chronic kidney disease? *J. R. Coll. Physicians Edinb.* 47, 76–82. doi: 10.4997/jrcpe.2017.117

Sarnak, M. J., Levey, A. S., Schoolwerth, A. C., Coresh, J., Culleton, B., Hamm, L. L., et al. (2003). Kidney disease as a risk factor for development of cardiovascular disease: a statement from the American heart association councils on kidney in cardiovascular disease, high blood pressure research, clinical cardiology, and epidemiology and prevention. *Circulation* 108, 2154–2169. doi: 10.1161/01.cir.0000095676.90936.80

Silberberg, J. S., Barre, P. E., Prichard, S. S., and Sniderman, A. D. (1989). Impact of left ventricular hypertrophy on survival in end-stage renal disease. *Kidney Int.* 36, 286–290. doi: 10.1038/ki.1989.192

Sorino, C., Scichilone, N., Pedone, C., Negri, S., Visca, D., and Spanevello, A. (2019). When kidneys and lungs suffer together. *J. Nephrol.* 32, 699–707. doi: 10.1007/s40620-018-00563-1

Ting, S. M., Hamborg, T., McGregor, G., Oxborough, D., Lim, K., Koganti, S., et al. (2015). Reduced cardiovascular reserve in chronic kidney failure: a matched cohort study. *Am. J. Kidney Dis.* 66, 274–284. doi: 10.1053/j.ajkd.2015.02.335

Ting, S. M., Iqbal, H., Hamborg, T., Imray, C. H., Hewins, S., Banerjee, P., et al. (2013). Reduced functional measure of cardiovascular reserve predicts admission to critical care unit following kidney transplantation. *PLoS One* 8:e64335. doi: 10.1371/journal.pone.0064335

Ting, S. M., Iqbal, H., Kanji, H., Hamborg, T., Aldridge, N., Krishnan, N., et al. (2014). Functional cardiovascular reserve predicts survival pre-kidney and post-kidney transplantation. *J. Am. Soc. Nephrol.* 25, 187–195. doi: 10.1681/asn.2013040348

US Renal Data System (USRDS) (2013). *(Annual) Data Report: Atlas of Chronic Kidney Disease and End-Stage renal Disease in the United States*. Bethesda, MD: National Institute of Health.

Verbrugge, F. H., Tang, W. H., and Hazen, S. L. (2015). Protein carbamylation and cardiovascular disease. *Kidney Int.* 88, 474–478. doi: 10.1038/ki.2015.166

Wali, R. K., Wang, G. S., Gottlieb, S. S., Bellumkonda, L., Hansalia, R., Ramos, E., et al. (2005). Effect of kidney transplantation on left ventricular systolic dysfunction and congestive heart failure in patients with end-stage renal disease. *J. Am. Coll. Cardiol.* 45, 1051–1060. doi: 10.1016/j.jacc.2004.11.061

Walsh, R. A. (1997). Microtubules and pressure-overload hypertrophy. *Circ. Res.* 80, 295–296. doi: 10.1161/01.res.80.2.295

Wasserman, K. (1997). Diagnosing cardiovascular and lung pathophysiology from exercise gas exchange. *Chest* 112, 1091–1101. doi: 10.1378/chest.112.4.1091

Wayhs, R., Zelinger, A., and Raggi, P. (2002). High coronary artery calcium scores pose an extremely elevated risk for hard events. *J. Am. Coll. Cardiol.* 39, 225–230. doi: 10.1016/s0735-1097(01)01737-5

Whipp, B. J., and Ward, S. A. (1990). Physiological determinants of pulmonary gas exchange kinetics during exercise. *Med. Sci. Sports Exerc.* 22, 62–71.

Wilson, P. W., Kauppila, L. I., O'Donnell, C. J., Kiel, D. P., Hannan, M., Polak, J. M., et al. (2001). Abdominal aortic calcific deposits are an important predictor of vascular morbidity and mortality. *Circulation* 103, 1529–1534. doi: 10.1161/01.cir.103.11.1529

Wilson, R. J., Davies, S., Yates, D., Redman, J., and Stone, M. (2010). Impaired functional capacity is associated with all-cause mortality after major elective intra-abdominal surgery. *Br. J. Anaesth.* 105, 297–303. doi: 10.1093/bja/aeq128

Yusuf, S., Reddy, S., Ounpuu, S., and Anand, S. (2001). Global burden of cardiovascular diseases: part I: general considerations, the epidemiologic transition, risk factors, and impact of urbanization. *Circulation* 104, 2746–2753. doi: 10.1161/hc4601.099487

Conflict of Interest: The authors declare that the research was conducted in the absence of any commercial or financial relationships that could be construed as a potential conflict of interest.

frontiers in Medicine

ORIGINAL RESEARCH
published: 30 September 2020
doi: 10.3389/fmed.2020.588967

Peripheral Arterial Stiffness Increases the Risk of Progression of Renal Disease in Type 2 Diabetic Patients

Tae Hoon Lim[1†], Seung Min Chung[2†], Dong Sung Lee[1], Se Ra Choi[1], Jun Sung Moon[2], Ji Sung Yoon[2], Kyu Chang Won[2] and Hyoung Woo Lee[2]*

[1] College of Medicine, Yeungnam University, Daegu, South Korea, [2] Division of Endocrinology and Metabolism, Department of Internal Medicine, Yeungnam University Medical Center, Daegu, South Korea

Aims: Our aim was to investigate the effects of peripheral arterial stiffness on the risk of progression of renal disease in patients with type 2 diabetes (T2D).

Methods: This was a single center, retrospective cohort study. Brachial-ankle pulse wave velocity (baPWV) tests were performed on T2D patients in 2015. Increased arterial stiffness was defined as baPWV of ≥ 1800 cm/s. We applied criteria for progression of renal disease according to EMPA-REG OUTCOME trial.

Results: In total, 186 patients were enrolled in the final study. The mean age was 59.1 years and male:female ratio was 1.73:1. Thirteen (7%) patients progressed to renal disease during the average follow-up time of 35.3 months. In particular, the risk of progression to macroalbuminuria was significantly higher in the baPWV ≥ 1800 cm/s group (HR 6.216, $p = 0.020$). Individuals with a baPWV of ≥ 1800 cm/s (when comparisons were adjusted for age, sex, blood pressure, diabetes duration, eGFR, and use of renin-angiotensin system inhibitors) had a significantly higher risk of the progression of renal disease (HR = 8.480, $p = 0.014$).

Conclusion: These results suggest that peripheral arterial stiffness (baPWV ≥ 1800 cm/s) may be a risk factor for the progression of renal disease in T2D patients.

Keywords: arterial stiffness, diabetes mellitus, diabetic nephropathy, pulse wave velocity, renal function decline

OPEN ACCESS

Edited by:
Jonatan Barrera-Chimal, National Autonomous University of Mexico, Mexico

Reviewed by:
Audrey Adji, Victor Chang Cardiac Research Institute, Australia
Gergo A. Molnar, University of Pécs, Hungary

***Correspondence:**
Jun Sung Moon
mjs7912@yu.ac.kr

† These authors have contributed equally to this work

Specialty section:
This article was submitted to Nephrology, a section of the journal Frontiers in Medicine

Received: *30 July 2020*
Accepted: *24 August 2020*
Published: *30 September 2020*

Citation:
Lim TH, Chung SM, Lee DS, Choi SR, Moon JS, Yoon JS, Won KC and Lee HW (2020) Peripheral Arterial Stiffness Increases the Risk of Progression of Renal Disease in Type 2 Diabetic Patients. Front. Med. 7:588967. doi: 10.3389/fmed.2020.588967

INTRODUCTION

Type 2 diabetes mellitus (T2D), along with hypertension, is one of the leading chronic diseases in Korea (1). In addition to the increasing prevalence of diabetes, diabetic complications such as cardiovascular disease, retinopathy, neuropathy, and nephropathy have significant negative effects on quality of life among T2D patients.

Aside from the microvascular complications that affect T2D patients, diabetic kidney disease (DKD) is the most common cause of end-stage renal disease (ESRD) resulting in the increased morbidity and mortality of diabetic patients. According to the Korean Society of Nephrology, for the past 20 years diabetes has been identified as the leading cause of ESRD requiring renal replacement treatment, accounting for 48.8% of cases (2). ESRD causes a heavy socioeconomic and health burden (3), so it is important to closely monitor T2D

patients and try to preserve renal function, as the progression of renal disease is often irreversible (4). Recent guidelines strongly recommend the annual screening of renal function, which can be determined by measuring urinary albumin, blood creatinine, and glomerular filtration rate from the time of diagnosis (4, 5). Previous clinical trials have shown that close monitoring and controlling of glucose levels and blood pressure can aid in delaying the progression of DKD, but some clinical needs remain a challenge.

Arterial stiffness is often a consequence of the physiological aging process or atherosclerosis, and it has been also described as a biomarker of hypertension (6), subclinical (7) or overt cardiovascular disease, stroke (8), and mortality (9) in the general population. Arterial stiffness is best characterized by measuring the pulse wave velocity (PWV), which is a commonly used biomarker (10–13). Previous studies have found that PWV can predict CKD progression and mortality (14, 15). Additionally, the level of PWV is significantly higher in people with diabetes compared to those without (16, 17). However, few studies have explored the possible causal relationship between PWV and the progression of diabetic kidney disease in patients with T2D.

To address this research gap, we investigated the relationship between arterial stiffness and renal dysfunction in T2D patients, as well as whether brachial-ankle pulse wave velocity (baPWV) can be used clinically as a predictor of the progression of renal disease.

SUBJECTS, MATERIALS AND METHODS

Study Population

This was a retrospective cohort study, in which data were collected from the electronic medical records of T2D patients who underwent baPWV testing in 2015 and were subsequently assessed for the progression of renal disease from 2016–2019 at Yeungnam University Hospital. In total, 391 patients initially qualified for this study. Patients were excluded for any of the following reasons: not aged 21–79 years ($n = 7$); missing initial estimated glomerular filtration rate data (eGFR; $n = 51$); chronic kidney disease stage <3b (eGFR $\leq$ 45 ml/min/1.73 m^2); treated with renal replacement therapy at baseline ($n = 9$); presence of peripheral arterial stenosis confirmed by an ankle brachial index (ABI) of < 0.9 ($n = 5$) (18, 19); or follow-up of renal function was not possible ($n = 133$). In total, 186 patients were finally determined to be eligible. The study protocol was developed in accordance with the tenets of the Declaration of Helsinki and reviewed and approved by the institutional review board of the Yeungnam University Hospital (IRB no. 2020-05-020).

Anthropometrics and Laboratory Measurements

Body mass index (BMI) was calculated as weight divided by height squared (kg/m^2). Data on diabetes duration, comorbidities (hypertension, stroke, and coronary artery disease), and use of renin-angiotensin system (RAS) inhibitors were collected. All laboratory tests were performed in the central laboratory of the Yeungnam University Hospital. Venous blood sampling was taken from the antecubital vein after an overnight fast. The levels of serum glucose, glycated hemoglobin (HbA1c), total protein, albumin, aspartate aminotransferase (AST), alanine aminotransferase (ALT), total cholesterol, triglyceride, high-density lipoprotein (HDL) cholesterol, low-density lipoprotein (LDL) cholesterol, blood urea nitrogen (BUN), and creatinine were measured. The levels of urine creatinine and albumin were also measured.

TABLE 1 | Baseline characteristics according to the presence of peripheral arterial stiffness (baPWV $\geq$ 1800 cm/s).

	baPWV <1800 cm/s ($n = 142$)	baPWV ≥1800 cm/s ($n = 44$)	*p* value
Age (yrs)	57.4 ± 10.2	64.3 ± 9.5	**<0.001**
Male, *n* (%)	95 (66.9%)	23 (52.3%)	0.078
Diabetes duration (yrs)	8.1 ± 7.3	12.2 ± 8.5	**0.002**
BMI (kg/m²)	24.8 ± 5.0	24.1 ± 3.2	0.258
Hypertension *n* (%)	76 (71.0%)	31 (70.5%)	0.091
Stroke *n* (%)	10 (7.0%)	2 (4.5%)	0.556
Coronary artery disease *n* (%)	5 (3.5%)	3 (7.0%)	0.329
RAS inhibitors, *n* (%)	65 (45.8%)	27 (61.4%)	0.071
Systolic BP (mmHg)	125.8 ± 15.4	145.3 ± 19.1	**<0.001**
Diastolic BP (mmHg)	77.0 ± 10.2	83.7 ± 10.8	**<0.001**
baPWV (cm/s)	1490.1 ± 194.0	2118.6 ± 308.2	**<0.001**
ABI	1.15 ± 0.08	1.17 ± 0.09	**0.020**
HbA1c (%)	8.3 ± 2.3	8.6 ± 1.7	0.230
Total protein (g/dl)	7.3 ± 0.7	7.4 ± 0.5	0.781
Albumin (g/dl)	4.7 ± 0.6	4.7 ± 0.4	0.835
AST (unit/L)	28.7 ± 17.5	28.0 ± 10.1	0.899
ALT (unit/L)	31.6 ± 21.9	28.2 ± 15.4	0.300
Total cholesterol (mg/dl)	186.1 ± 59.9	188.1 ± 50.7	0.634
Triglyceride (mg/dl)	194.4 ± 181.9	175.2 ± 110.6	0.520
HDL cholesterol (mg/dl)	51.1 ± 15.5	50.6 ± 13.3	0.822
LDL cholesterol (mg/dl)	98.6 ± 48.5	101.3 ± 42.4	0.510
Creatinine (mg/dl)	1.01 ± 0.20	1.02 ± 0.22	0.603
eGFR (ml/min/1.73 m^2)	80.8 ± 16.4	72.6 ± 14.3	**0.005**
uACR (mg/g)	55.7 ± 163.1	92.2 ± 172.6	0.172

BMI, body mass index; RAS, renin-angiotensin system; BP, blood pressure; baPWV, brachial-ankle pulse wave velocity; ABI, ankle brachial index; AST, aspartate aminotransferase; ALT, alanine aminotransferase; HDL, high-density lipoprotein; LDL, low-density lipoprotein; eGFR, estimated glomerular filtration rate; uACR, urinary albumin:creatinine ratio. The bold values mean statistically significant data.

TABLE 2 | Correlation between baPWV and multiple variables at baseline.

	baPWV	
	r	*P*-value
Age	0.405	<0.001
Diabetes duration	0.213	0.004
Systolic blood pressure	0.645	<0.001
eGFR	−0.193	0.011

Measurement and Definition of Arterial Stiffness

The blood pressure (BP), baPWV, and ABI were measured using a non-invasive vascular screening device (BP-203RPEIII, OMRON

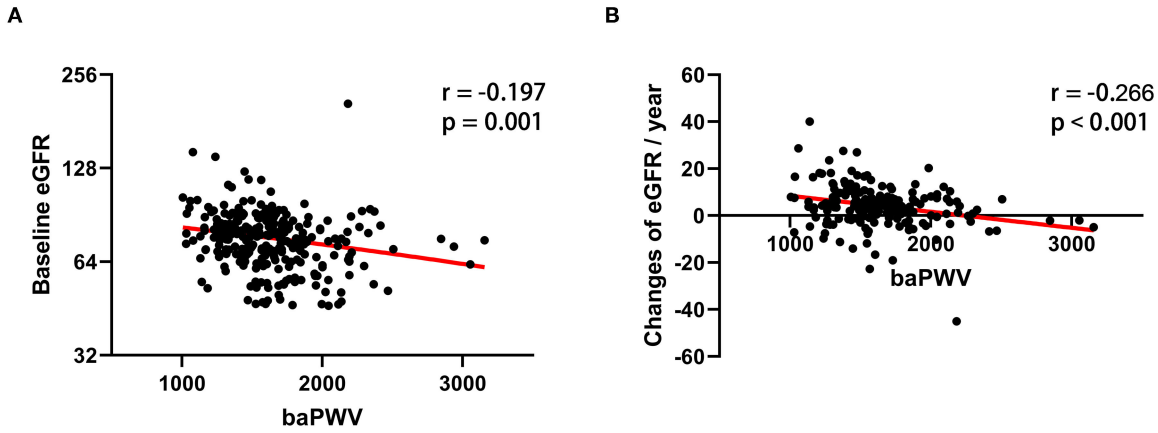

FIGURE 1 | Scatter plot of the relationship between baPWV and **(A)** baseline eGFR and **(B)** annual changes in eGFR. The red line represents the regression line.

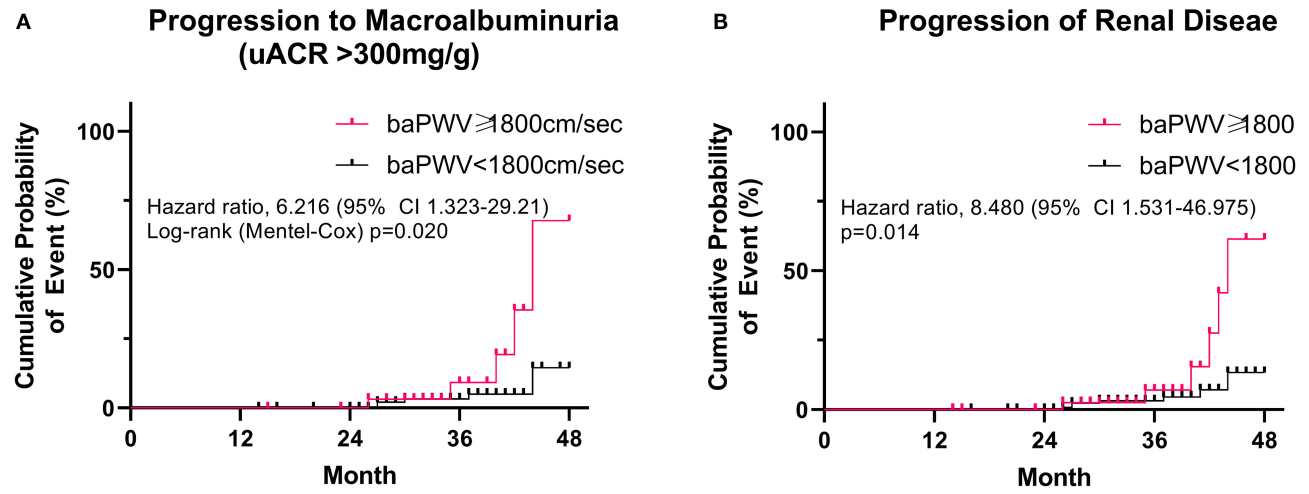

FIGURE 2 | Risk of peripheral arterial stiffness (baPWV ≥ 1800 cm/s) on **(A)** progression to macroalbuminuria (uACR > 300 mg) and **(B)** progression of renal disease. A log-rank (Mantel-Cox) survival analysis was used.

healthcare, Japan), which was operated by a trained examiner who placed pneumatic cuffs on each ankle and each upper arm of patients in the supine position. The validity of baPWV compared to aortic PWV using invasive catheter manometer was reported to be favorable ($r = 0.87$, $p < 0.01$) (20). We defined a person with a baPWV of ≥ 1800 cm/s as having a higher level of arterial stiffness, in accordance with the Japanese Circulation Society. A baPWV of ≥ 1800 cm/s is regarded as the threshold for a high-risk category (18) and is known to increase the risk for cardiovascular and heart failure-related events (7, 21).

Measurement and Definition of the Progression of Renal Disease

Estimated glomerular filtration rate (eGFR) was calculated using the chronic kidney disease epidemiology collaboration equation (CKD-EPI). Urinary albumin:creatinine ratio (uACR) was calculated. In accordance with the EMPA-REG OUTCOME trial, any of the following criteria were used to describe progression of renal disease (22): progression to macroalbuminuria (uACR > 300 mg); doubling of serum creatinine level accompanied by an eGFR of ≤ 45 ml/min/1.73 m^2; treatment with renal replacement therapy; or death from renal disease.

Statistical Analysis

Numerical data are expressed as the mean ± standard deviation (SD), and categorical data are expressed as numbers and percentages. The independent *t*-test was used to compare the groups with continuous variables. The chi-square test was used to compare categorical variables. A Cox proportional hazards regression was used to evaluate the risk of progression of renal disease. IBM Statistical Package for Social Sciences for Windows, version 21.0 (SPSS Inc. Chicago, IL) software was used for statistical analyses. Graphs were produced using GraphPad Prism 8.0 software (GraphPad Software Inc., San Diego, CA, USA). A value of $p < 0.05$ was considered statistically significant.

RESULTS

Comparison of Baseline Characteristics Between High and Low Pulse Wave Velocity

The mean age of patients was 59.1 ± 10.5 years (range 22–79) and the male:female ratio was 1.73:1. The mean duration of diabetes was 9 ± 7.8 years (range 0–39). The prevalence of comorbid hypertension, stroke, and coronary artery disease in the patient cohort was 57.5, 6.5, and 4.3%, respectively. 23.7% of enrolled patients ($n = 44$) had a baPWV of ≥ 1800 cm/s.

Table 1 lists baseline characteristics according to baPWV (≥ 1800 cm/s vs. < 1800 cm/s). Individuals with a baPWV of ≥ 1800 cm/s were significantly older ($p < 0.001$), had longer duration of diabetes ($p = 0.002$), higher systolic and diastolic blood pressure ($p < 0.01$), and higher ABI ($p = 0.02$) compared to patients with a baPWV of < 1800 cm/s. Factors including sex, BMI, comorbid hypertension, stroke or coronary artery disease, and use of RAS inhibitor medication did not differ significantly between the two groups. Baseline HbA1c, albumin, liver and lipid profiles also did not differ significantly between the two groups. In the baPWV of ≥ 1800 cm/s group, eGFR was significantly lower (72.6 vs. 80.8 ml/min/1.73 m^2, $p = 0.005$) and uACR was higher but without statistical significance (92.2 vs. 55.7 mg/g, $p = 0.172$). **Table 2** lists correlations between baPWV and age, diabetes duration, systolic blood pressure, and eGFR at baseline. Age, diabetes duration, and systolic blood pressure were positively correlated with baPWV ($r = 0.405$, 0.213, and 0.645, respectively; all $p < 0.01$), whereas baPWV was negatively correlated with eGFR ($r = -0.193$, $p = 0.011$; **Figure 1A**).

TABLE 3 | Characteristics according to progressors and non-progressors regarding albuminuria.

	Non-progressors ($n = 176$)	Progressors ($n = 10$)	*p* value
Age (yrs)	58.9 ± 10.5	61.5 ± 10.6	0.401
Male, *n* (%)	110 (62.5%)	8 (80.0%)	0.330
Diabetes duration (yrs)	8.8 ± 7.9	12.8 ± 5.5	0.051
RAS inhibitors, *n* (%)	84 (47.7%)	8 (80.0%)	0.056
Systolic BP (mmHg)	130.4 ± 18.6	131.2 ± 11.4	0.623
Diastolic BP (mmHg)	78.7 ± 10.8	75.1 ± 9.1	0.425
baPWV (cm/s)	1627.8 ± 348.5	1831.2 ± 334.8	**0.041**
ABI	1.16 ± 0.08	1.17 ± 0.11	0.913
HbA1c (%)	8.3 ± 2.1	9.0 ± 2.2	0.199
eGFR (ml/min/1.73m^2)	75.9 ± 18.3	77.7 ± 12.4	0.465

Mann-Whitney U test, Fisher's exact test was used. The bold values mean statistically significant data.

Comparison of the Risk for the Progression of Renal Disease Between High and Low Pulse Wave Velocity

The mean follow-up period was 35.3 ± 7.25 months (range 14–48). During the follow-up period, 13 patients developed renal disease (13.6% of the baPWV of ≥ 1800 cm/s group and 4.9% of the baPWV of < 1800 cm/s group). Specifically, 10 patients progressed to macroalbuminuria and 3 patients exhibited doubling of serum creatinine levels accompanied by an eGFR of ≤ 45 ml/min/1.73 m^2. No patients were treated with renal replacement therapy or died from renal disease. The annual changes in eGFR were significantly negatively correlated with baPWV ($r = -0.226$, $p < 0.001$; **Figure 1B**), meaning that the higher the baPWV, the greater the annual decrement of eGFR. Individuals with a baPWV of ≥ 1800 cm/s had a significantly higher risk for progression to macroalbuminuria (HR 6.216, 95% CI 1.323–29.21, $p = 0.020$; **Figure 2A**), whereas no significant risk was observed for the doubling of serum creatinine level accompanied by an eGFR of ≤ 45 ml/min/1.73 m^2 (HR 2.762, 95% CI 0.146–52.07, $p = 0.497$). The additional analysis of comparing the progressors and non-progressors regarding macroalbuminuria group are presented in **Table 3**. Compared to the non-progressor group, baseline baPWV was significantly higher in the progressor group (1627.8 vs. 1831.2 cm/s, $p = 0.041$). And although not statistically significant, the duration of diabetes was longer (8.8 vs. 12.8 years, $p = 0.051$) and the rate of taking RAS inhibitors were higher (47.7 vs. 80.0%, $p = 0.056$) in the progressor group. **Table 4** lists the risk of arterial stiffness for

TABLE 4 | Risk of peripheral arterial stiffness (baPWV ≥ 1800 cm/s) on the progression of renal disease.

	Non-adjusted model			Adjusted model*		
	HR	95% CI	*p*-value	HR	95% CI	*p*-value
Age	1.008	[0.954-1.064]	1.008	0.965	[0.898-1.037]	0.330
Male	3.078	[0.681-13.913]	0.144	5.009	[0.838-29.952]	0.077
Systolic BP	0.986	[0.953-1.021]	0.443	0.993	[0.923-1.068]	0.847
Diastolic BP	0.962	[0.909-1.019]	0.180	0.926	[0.823-1.041]	0.197
Diabetes duration	1.038	[0.983-1.095]	0.185	1.017	[0.945-1.094]	0.653
Baseline eGFR	0.977	[0.959-0.995]	**0.015**	1.003	[0.986-1.020]	0.741
RAS inhibitor medication	2.598	[0.789-8.559]	0.116	2.097	[0.576-7.631]	0.261
baPWV ≥1800 cm/s	3.271	[1.096-9.769]	**0.034**	8.480	[1.531-46.975]	**0.014**

Any one of the following criteria was used to describe the progression of renal disease: progression to macroalbuminuria, doubling of serum creatinine levels accompanied by an estimated glomerular filtration rate (eGFR) of ≤ 45 ml/min/1.73 m^2, treatment with renal replacement therapy, or death from renal disease.

**Adjusted for age, sex, systolic BP, diastolic BP, diabetes duration, baseline eGFR, use of RAS inhibitors, and baPWV. The bold values mean statistically significant data.*

progression of renal disease based on a Cox-regression analysis. Age, sex, systolic BP, diastolic BP, diabetes duration, eGFR, use of RAS inhibitors, and baPWV were considered as covariates. In non-adjusted regression analysis, the lower baseline eGFR, and baPWV of $\geq$ 1800 cm/s increased the risk of progression of renal disease. After adjustments, individuals with a baPWV of $\geq$ 1800 cm/s had an increased risk for progression of renal disease compared to those with a baPWV of $<$ 1800 cm/s (HR 8.480, 95% CI 1.531-46.975, $p = 0.014$; **Figure 2B**).

DISCUSSION

After following patients for an average duration of 35 months, we found that T2D patients with a baPWV $\geq$ 1800 cm/s are at 8.5-fold greater risk of progression of renal disease, regardless of classical risk factors. This finding suggests that peripheral arterial stiffness represented by a high baPWV may accelerate the progression of CKD in patients with type 2 diabetes.

Many previous studies have suggested that arterial (or aortic) stiffness is closely related with the risk of mortality and specifically cardiovascular disease, not only in the general population but also in patients with underlying comorbidities such as hypertension and diabetes (6, 8–10). The CRIC study (Chronic Renal Insufficiency Cohort) revealed that high aortic stiffness increases the risk of chronic kidney disease progression and all-cause death in patients with impaired kidney function (23). Other studies have demonstrated that arterial stiffness is increased in patients with T2D (24) and that PWV can be used as a predictor for cardiovascular events and all-cause mortality (17). Arterial stiffness may cause left ventricular hypertrophy and dysfunction due to higher pressure pulse pulsation (19). A plausible explanation for the impact of arterial stiffness on the progression of renal disease is that arterial stiffness increases hemodynamic shear stress, which may result in endothelial dysfunction and microvascular ischemia, ultimately causing kidney injury (25, 26).

High PWV has been shown to be associated with diabetic retinopathy (27), neuropathy (28, 29), and nephropathy. A Rotterdam study of 3,666 subjects from the general population included an 11-year follow-up and revealed that carotid-femoral pulse wave velocity (cfPWV) was associated with a rapid reduction in eGFR and CKD progression (14). Another 9-year follow-up of 211 T2D patients in the UK revealed that cfPWV was associated with a decrease in eGFR among patients under 60 years of age (30). A study in Singapore involving 1012 T2D patients of differing Asian ethnicities and an average follow-up period of 3.1 years revealed that cfPWV was an independent predictor for albuminuria progression (31). These results indicate that cfPWV can be a predictor of DKD progression in T2D. Nevertheless, a study involving 913 subjects from the general Korean population and an average follow-up period of 3.2 years found that neither cfPWV nor baPWV are related to renal dysfunction and that the significance of baPWV in T2D patients is likely invalid due to the relatively small proportion of T2D patients (32). The most important aspect of the present study is that baPWV was associated with a decrease in renal function when Korean patients with T2D were followed-up for an average of 3 years. Additionally, the present study used the validated cut-off value for baPWV and demonstrated that this association exists, despite applying very strict criteria for the progression of renal disease.

A study of 461 Japanese T2D patients, with an average of 5.9 years follow-up, investigated the risks of arterial stiffness on progression of renal disease in T2D. It found that patients with a cfPWV of $\geq$ 910 cm/s were at increased risk of albuminuria (transition from normo- to micro-albuminuria or from micro- to macro-albuminuria; HR = 1.23), and a linear regression analysis revealed a negative correlation between cfPWV and annual change in eGFR (33). Our study produced similar results: patients with a baPWV of $\geq$ 1800 cm/s were at increased risk of progression of renal disease; specifically, progression to macroalbuminuria and the annual change of eGFR were negatively correlated with baPWV. In addition to cfPWV, baPWV would be a useful screening tool for predicting progression of renal disease in T2D patients, due to the ease and convenience of measurements.

This study had a limitation that it enrolled a relatively small number of patients and used the single measurement of baPWV. However, to our knowledge, this is the first study to identify the risk of peripheral arterial stiffness on the progression of renal disease with the capability of distinguishing a causal relationship.

In conclusion, baPWV representing peripheral arterial stiffness can be used as a predictor of the progression of renal disease in T2D patients.

DATA AVAILABILITY STATEMENT

The raw data supporting the conclusions of this article will be made available by the authors, without undue reservation.

ETHICS STATEMENT

The studies involving human participants were reviewed and approved by Institutional review board of the Yeungnam University Hospital. The patients/participants provided their written informed consent to participate in this study.

AUTHOR CONTRIBUTIONS

SMC and JSM: conceptualization and study design. THL, DSL, and SRC: data collection. THL, SMC, DSL, and SRC: data analysis and interpretation. THL, SMC, and JSM: writing. JSY, KCW, and HWL: review and editing. All authors contributed to the article and approved the submitted version.

FUNDING

The present study was supported by a National Research Foundation of Korea grant funded by the Korean government (grant no. NRF-2020R1A2C4002626, NRF-2019M3E5D1A02068104). The funders had no role in study design, data collection and analysis, decision to publish or preparation of the manuscript.

REFERENCES

1. Won JC, Lee JH, Kim JH, Kang ES, Won KC, Kim DJ, et al. Diabetes fact sheet in Korea, 2016: an appraisal of current status. *Diabetes Metab J.* (2018) 42:415–24. doi: 10.4093/dmj.2018.0017
2. ESRD Registry Committee: Korean Society of Nephrology. *Current Renal Replacement Therapy in Korea*. (2019). Available online at: http://www.ksn.or.kr/rang_board/list.html?code=sinchart_eng
3. Kim SH, Jo MW, Go DS, Ryu DR, Park J. Economic burden of chronic kidney disease in Korea using national sample cohort. *J Nephrol.* (2017) 30:787–93. doi: 10.1007/s40620-017-0380-3
4. National Kidney F. KDOQI clinical practice guideline for diabetes and CKD: 2012 update. *Am J Kidney Dis.* (2012) 60:850–86. doi: 10.1053/j.ajkd.2012.07.005
5. American Diabetes Association. Microvascular Complications and Foot Care: Standards of Medical Care in Diabetes-2020. *Diabetes Care*. (2020). 43(Suppl 1):S135–51. doi: 10.2337/dc20-S011
6. Oh YS. Arterial stiffness and hypertension. *Clin Hypertens.* (2018) 24:17. doi: 10.1186/s40885-018-0102-8
7. Chung YK, Lee YJ, Kim KW, Cho RK, Chung SM, Moon JS, et al. Serum cystatin C is associated with subclinical atherosclerosis in patients with type 2 diabetes: A retrospective study. *Diab Vasc Dis Res.* (2018) 15:24–30. doi: 10.1177/1479164117738156
8. Mattace-Raso FU, van der Cammen TJ, Hofman A, van Popele NM, Bos ML, Schalekamp MA, et al. Arterial stiffness and risk of coronary heart disease and stroke: the Rotterdam Study. *Circulation.* (2006) 113:657–63. doi: 10.1161/CIRCULATIONAHA.105.555235
9. Cruickshank K, Riste L, Anderson SG, Wright JS, Dunn G, Gosling RG. Aortic pulse-wave velocity and its relationship to mortality in diabetes and glucose intolerance: an integrated index of vascular function? *Circulation.* (2002) 106:2085–90. doi: 10.1161/01.CIR.0000033824.02722.F7
10. Yamashina A, Tomiyama H, Arai T, Hirose K, Koji Y, Hirayama Y, et al. Brachial-ankle pulse wave velocity as a marker of atherosclerotic vascular damage and cardiovascular risk. *Hypertens Res.* (2003) 26:615–22. doi: 10.1291/hypres.26.615
11. Covic A, Haydar AA, Bhamra-Ariza P, Gusbeth-Tatomir P, Goldsmith DJ. Aortic pulse wave velocity and arterial wave reflections predict the extent and severity of coronary artery disease in chronic kidney disease patients. *J Nephrol.* (2005) 18:388–96.
12. Munakata M, Sakuraba J, Tayama J, Furuta T, Yusa A, Nunokawa T, et al. Higher brachial-ankle pulse wave velocity is associated with more advanced carotid atherosclerosis in end-stage renal disease. *Hypertens Res.* (2005) 28:9–14. doi: 10.1291/hypres.28.9
13. Avolio A. Arterial stiffness. *Pulse (Basel).* (2013) 1:14–28. doi: 10.1159/000348620
14. Sedaghat S, Mattace-Raso FU, Hoorn EJ, Uitterlinden AG, Hofman A, Ikram MA, et al. Arterial Stiffness And Decline In Kidney Function. *Clin J Am Soc Nephrol.* (2015) 10:2190–7. doi: 10.2215/CJN.03000315
15. van Varik BJ, Vossen LM, Rennenberg RJ, Stoffers HE, Kessels AG, de Leeuw PW, et al. Arterial stiffness and decline of renal function in a primary care population. *Hypertens Res.* (2017) 40:73–8. doi: 10.1038/hr.2016.113
16. Taniwaki H, Kawagishi T, Emoto M, Shoji T, Kanda H, Maekawa K, et al. Correlation between the intima-media thickness of the carotid artery and aortic pulse-wave velocity in patients with type 2 diabetes. Vessel wall properties in type 2 diabetes. *Diabetes Care.* (1999) 22:1851–7. doi: 10.2337/diacare.22.11.1851
17. Cardoso CR, Ferreira MT, Leite NC, Salles GF. Prognostic impact of aortic stiffness in high-risk type 2 diabetic patients: the Rio deJaneiro Type 2 Diabetes Cohort Study. *Diabetes Care.* (2013) 36:3772–8. doi: 10.2337/dc13-0506
18. Munakata M. Brachial-ankle pulse wave velocity in the measurement of arterial stiffness: recent evidence and clinical applications. *Curr Hypertens Rev.* (2014) 10:49–57. doi: 10.2174/15734021100114111160957
19. Kim HL, Kim SH. Pulse wave velocity in atherosclerosis. *Front Cardiovasc Med.* (2019) 6:41. doi: 10.3389/fcvm.2019.00041
20. Yamashina A, Tomiyama H, Takeda K, Tsuda H, Arai T, Hirose K, et al. Validity, reproducibility, and clinical significance of noninvasive brachial-ankle pulse wave velocity measurement. *Hypertens Res.* (2002) 25:359–64. doi: 10.1291/hypres.25.359
21. Takae M, Yamamoto E, Tokitsu T, Oike F, Nishihara T, Fujisue K, et al. Clinical significance of brachial-ankle pulse wave velocity in patients with heart failure with reduced left ventricular ejection fraction. *Am J Hypertens.* (2019) 32:657–67. doi: 10.1093/ajh/hpz048
22. Wanner C, Inzucchi SE, Lachin JM, Fitchett D, von Eynatten M, Mattheus M, et al. Empagliflozin and progression of kidney disease in type 2 diabetes. *N Engl J Med.* (2016) 375:323–34. doi: 10.1056/NEJMoa1515920
23. Townsend RR, Anderson AH, Chirinos JA, Feldman HI, Grunwald JE, Nessel L, et al. Association of pulse wave velocity with chronic kidney disease progression and mortality: findings from the CRIC Study (Chronic Renal Insufficiency Cohort). *Hypertension.* (2018) 71:1101–7. doi: 10.1161/HYPERTENSIONAHA.117.10648
24. Schram MT, Henry RM, van Dijk RA, Kostense PJ, Dekker JM, Nijpels G, et al. Increased central artery stiffness in impaired glucose metabolism and type 2 diabetes: the Hoorn Study. *Hypertension.* (2004) 43:176–81. doi: 10.1161/01.HYP.0000111829.46090.92
25. Chung SM, Oh JH, Moon JS, Kim YK, Yoon JS, Won KC, et al. Critical shear stress is associated with diabetic kidney disease in patients with type 2 diabetes. *Sci Rep.* (2018) 8:908. doi: 10.1038/s41598-018-25252-8
26. Safar ME, London GM, Plante GE. Arterial stiffness and kidney function. *Hypertension.* (2004) 43:163–8. doi: 10.1161/01.HYP.0000114571.75762.b0
27. Yun YW, Shin MH, Lee YH, Rhee JA, Choi JS. Arterial stiffness is associated with diabetic retinopathy in Korean type 2 diabetic patients. *J Prev Med Public Health.* (2011) 44:260–6. doi: 10.3961/jpmph.2011.44.6.260
28. Ha BK, Kim BG, Kim DH, Lee SI, Jung SM, Park JY, et al. Relationships between brachial-ankle pulse wave velocity and peripheral neuropathy in type 2 diabetes. *Diabetes Metab J.* (2012) 36:443–51. doi: 10.4093/dmj.2012.36.6.443
29. Wu N, Cai X, Ye K, Li Y, He M, Zhao W, et al. Association between Brachial-Ankle pulse wave velocity and cardiac autonomic neuropathy in type 2 diabetes. *Diabetol Metab Syndr.* (2014) 6:82. doi: 10.1186/1758-5996-6-82
30. Fountoulakis N, Thakrar C, Patel K, Viberti G, Gnudi L, Karalliedde J. Increased arterial stiffness is an independent predictor of renal function decline in patients with type 2 diabetes mellitus younger than 60 years. *J Am Heart Assoc.* (2017) 6:4. doi: 10.1161/JAHA.116.004934
31. Zhang X, Low S, Sum CF, Tavintharan S, Yeoh LY, Liu J, et al. Arterial stiffness is an independent predictor for albuminuria progression among Asians with type 2 diabetes-A prospective cohort study. *J Diabetes Complications.* (2017) 31:933–8. doi: 10.1016/j.jdiacomp.2017.02.004
32. Kim CS, Kim HY, Kang YU, Choi JS, Bae EH, Ma SK, et al. Association of pulse wave velocity and pulse pressure with decline in kidney function. *J Clin Hypertens (Greenwich).* (2014) 16:372–7. doi: 10.1111/jch.12302
33. Bouchi R, Babazono T, Mugishima M, Yoshida N, Nyumura I, Toya K, et al. Arterial stiffness is associated with incident albuminuria and decreased glomerular filtration rate in type 2 diabetic patients. *Diabetes Care.* (2011) 34:2570–5. doi: 10.2337/dc11-1020

Conflict of Interest: The authors declare that the research was conducted in the absence of any commercial or financial relationships that could be construed as a potential conflict of interest.

frontiers in Medicine

ORIGINAL RESEARCH
published: 20 October 2020
doi: 10.3389/fmed.2020.579021

Combining Pulse Wave Velocity With Galectin-3 to Predict Mortality and Cerebrovascular and Cardiovascular Events in Hemodialysis Patients

Qi Zhang[1,2†], *Kanhua Yin*[3†], *Mingli Zhu*[1], *Xinghui Lin*[1], *Yan Fang*[1], *Jiayue Lu*[1], *Zhenyuan Li*[1] *and Zhaohui Ni*[1*]

[1] Department of Nephrology, Renji Hospital, School of Medicine, Shanghai Jiaotong University, Shanghai, China, [2] Division of Nephrology, Shanghai Ninth People's Hospital, School of Medicine, Shanghai Jiaotong University, Shanghai, China, [3] Harvard T.H. Chan School of Public Health, Harvard University, Boston, MA, United States

OPEN ACCESS

Edited by:
Natalia Lopez-Andres,
NavarraBiomed, Spain

Reviewed by:
Jia Rao,
Fudan University, China
Hoon Young Choi,
Yonsei University, South Korea

***Correspondence:**
Zhaohui Ni
profnizh@126.com

[†]These authors have contributed equally to this work

Specialty section:
This article was submitted to Nephrology, a section of the journal Frontiers in Medicine

Received: 01 July 2020
Accepted: 14 September 2020
Published: 20 October 2020

Citation:
Zhang Q, Yin K, Zhu M, Lin X, Fang Y, Lu J, Li Z and Ni Z (2020) Combining Pulse Wave Velocity With Galectin-3 to Predict Mortality and Cerebrovascular and Cardiovascular Events in Hemodialysis Patients. Front. Med. 7:579021. doi: 10.3389/fmed.2020.579021

Background: Cerebrovascular and cardiovascular diseases contribute substantially to the mortality of end-stage renal disease patients. We sought to combine pulse wave velocity (PWV) with galectin-3 to predict the mortality and cerebrovascular and cardiovascular events in hemodialysis patients.

Methods and Results: End-stage renal disease patients who underwent stable hemodialysis were screened for inclusion. Patients with preexisting cardiovascular and cerebrovascular diseases were excluded. The primary endpoint was a composite of all-cause mortality and major adverse cerebrovascular and cardiovascular events. Receiver operating characteristic curve analysis was used to determine the optimal cutoffs to dichotomize PWV and galectin-3. The study population was then stratified into four groups based on these cutoffs. Both univariable and multivariable Cox regression analyses were performed to estimate the hazard ratio and 95% confidence interval (CI) for clinical factors. Model performance was compared among models with or without PWV and galectin-3. A total of 284 patients were enrolled. During a median follow-up of 31 months, 57 patients (20.1%) reached the primary endpoint. The optimal cutoffs for PWV and galectin-3 were 7.9 m/s and 30.5 ng/ml, respectively. In the multivariable regression analysis, the high PWV–high galectin-3 group was associated with a 3-fold increased risk of all-cause mortality and major adverse cerebrovascular and cardiovascular events (hazard ratio = 3.19, 95% CI: 1.05–9.66, $p = 0.04$) compared with the low PWV–low galectin-3 group. The combination of PWV and galectin-3 was associated with improved model discrimination, calibration, and reclassification.

Conclusions: The combination of PWV and galectin-3 can be used to predict mortality and cerebral and cardiovascular complications in hemodialysis patients.

Keywords: Galectin-3, pulse wave velocity (PWV), cerebrovascular and cardiovascular events, mortality, hemodialysis (HD)

INTRODUCTION

Chronic kidney disease (CKD) is a significant clinical and public health problem with a prevalence of up to 15%. The incidence of cerebrovascular and cardiovascular diseases in CKD patients is two times that in those without CKD, and patients with end-stage renal disease (ESRD) are associated with an even higher risk (1). Despite the advances in treatment, cerebrovascular and cardiovascular complications contribute substantially to the mortality of dialysis patients, accounting for 54% of all deaths (2). Early detection of these potentially fatal complications can allow targeted interventions and eventually lead to improved survival and quality of life.

Several non-invasive tests have been developed to predict cerebrovascular or cardiovascular events among hemodialysis patients. Pulse wave velocity (PWV), recommended by the 2018 European Society of Hypertension/European Society of Cardiology hypertension management guidelines as a gold standard for measuring the stiffness of large arteries (3), has been shown to predict mortality and non-fatal cardiovascular events in dialysis patients (4). However, recent studies have revealed that the predictive power of PWV is inferior to that of simple clinical risk scores in ESRD patients (5) and compromised elderly patients (6).

Galectin-3, a member of the β-galactoside-binding lectin family, has emerged as a new prognostic biomarker for a series of cardiovascular diseases, such as congestive heart failure and coronary artery disease (7). It is a 29–35-kDa protein secreted by activated macrophages and other inflammatory cells and plays an essential role in cell adhesion, activation, growth, and differentiation (8). Many research teams, including us, have demonstrated the associations between galectin-3 and multiple cardiovascular complications and survival outcomes in CKD and ESRD patients (9, 10).

Both PWV and galactin-3 measurements are non-invasive tests and can be performed in the dialysis clinic. However, no data have been reported on the predictive power of combining these two assays. In this work, we aimed to combine PWV with galectin-3 measurement to predict the mortality and cerebrovascular and cardiovascular events in hemodialysis patients.

METHODS

Study Population

ESRD patients who underwent stable hemodialysis at Renji Hospital, Shanghai Jiaotong University, Shanghai, China, between June 2014 and January 2015 were prospectively enrolled. Stable hemodialysis was defined as receiving hemodialysis for three sessions a week, lasting 4 to 5 h each session, for at least 3 months. Patients with the following conditions were excluded: congestive heart failure (New York Heart Association class III or IV or left ventricular ejection fraction $< 40\%$), moderate or severe aortic valve stenosis, atrial fibrillation, second- or third-degree atrioventricular block, use of a pacemaker, recent myocardial infarction (MI) ($\leq$3 months), recent stroke ($\leq$3 months), recent transient ischemic attack ($\leq$3 months), pulseless extremity, malignancy, acute infectious diseases ($\leq$3 months), and those who refused to participate in this study.

All enrolled patients signed an informed consent form, and the Ethics Committee of Renji Hospital, Shanghai Jiaotong University, approved this study. This study was performed following the ethical standards in the 1964 Declaration of Helsinki and its later amendments.

Measurement of Galectin-3, Pulse Wave Velocity, and Blood Pressure

The methods of measuring serum galectin-3, PWV, and blood pressure were described in our previous work (9). In short, we collected patients' blood samples before their midweek dialysis session and measured the serum galectin-3 concentration with an enzyme-linked immunosorbent assay (Human Galectin-3 Quantikine ELISA Kit; R&D Systems Inc., Minneapolis, MN, USA). The baseline laboratory data were collected, including albumin, calcium, phosphorus, creatinine, total triglyceride, total lipoprotein, high-density lipoprotein, low-density lipoprotein, B-type brain natriuretic peptide, and C-reactive protein (CRP). The single-pool Kt/V for urea was used to estimate the dialysis adequacy.

Both the PWV and blood pressure were assessed at the same time as galectin-3. PWV was calculated as the ratio of the distance that the pulse wave traveled (in meters) to the pulse transit time (in seconds) and was assessed using a portable device (Sphygmocor XCEL; AtCor Medical, New South Wales, Australia). The blood pressure was recorded as the average of three consecutive brachial blood pressure readings.

Primary Endpoint and Definitions of Comorbidities

The primary endpoint of this study was a composite of all-cause mortality and major adverse cerebrovascular and cardiovascular events (MACCE), including acute MI, new-onset heart failure, ischemic stroke, and cerebral hemorrhage. The diagnosis of acute MI required both ECG changes and the elevation of cardiac biomarkers. Heart failure was diagnosed clinically according to typical dyspnea symptoms, pulmonary edema on chest X-ray, and the requirement of additional hemodialysis. Stroke and cerebral hemorrhage were diagnosed by neurologists and confirmed by either magnetic resonance imaging or computed tomography. All enrolled patients were followed until the primary endpoint or July 31, 2017, whichever occurred earlier.

In this study, hypertension was defined as predialysis blood pressure $\geq$ 140/90 mmHg (11). Diabetes was defined as a fasting plasma glucose level $\geq$ 7.0 mmol/L, 2-h plasma glucose or random glucose level of $\geq$11.1 mmol/L with symptoms of hyperglycemia, or an A1C value $\geq$ 6.5% (12). Prior coronary artery disease was defined as patients with documented significant coronary artery stenosis (>70%) or a history of MI, percutaneous coronary intervention, or coronary artery bypass grafting surgery.

Risk Stratification, Model Building, Performance Evaluation, and Statistical Analysis

Receiver operating characteristic (ROC) curve analysis was conducted, and the areas under the ROC curve (AUCs) for PWV and galectin-3 were calculated. The optimal cutoffs of PWV and galectin-3 for the classification of the composite endpoint were obtained based on the Youden index's maximization. Based on the ROC-optimal cutoffs for PWV and galectin-3, we further stratified the entire study population into four groups: group 1: low PWV–low galectin-3; group 2: low PWV–high galectin-3; group 3: high PWV–low galectin-3; and group 4: high PWV–high galectin-3. The cumulative incidences of the primary endpoint for these four groups were estimated using the Kaplan–Meier method and compared using the log-rank test.

Univariable Cox proportional-hazards regression was performed to estimate the hazard ratio (HR) and 95% confidence intervals (CIs) of clinical factors, and PWV and galectin-3 were included as continuous and categorical variables (cutoffs derived from the ROC curve analysis were used) separately. A multivariable Cox proportional-hazards model was built with factors associated with the primary outcomes with a two-sided $p < 0.1$ in the univariable analysis combined with other well-known predictive factors. The overall goodness of fit and the proportional-hazards assumption of the Cox regression were assessed based on the Cox–Snell residuals.

We then evaluated the performance of four multivariable Cox models that included different variables and determined whether adding PWV and galectin-3 values would increase the model performance. The model performance was assessed based on discrimination (C statistics), calibration (Hosmer–Lemeshow statistic), and reclassification (net reclassification improvement and integrated discrimination improvement).

The continuous variables were tested for normal distribution by the Kolmogorov–Smirnov test and presented as means ± standard deviations or medians with interquartile ranges as appropriate. Categorical variables were presented as the number and percentage and compared using the chi-square test. For all statistical tests, a $p < 0.05$ was considered significant. All statistical analyses were performed with IBM SPSS 21.0 software (SPSS Inc., Chicago, IL) or the R language statistical software version 4.0.2 (The R Foundation for Statistical Computing, Vienna, Austria).

RESULTS

Study Cohort and Baseline Characteristics

From June 2014 to January 2015, a total of 332 hemodialysis patients were screened for inclusion. Twenty-one patients were excluded because they met one or more of the exclusion criteria. The other 27 patients were excluded because they refused to participate in the follow-up, resulting in a total of 284 patients eventually included in this analysis (**Figure 1**).

The median age in this 284-patient cohort was 61 years, and males comprised 58.1% of the cohort. All patients had undergone stable hemodialysis for an average of 90 months. The mean serum concentration of galectin-3 was 29.68 ± 9.95 ng/ml, and the median PWV was 8.7 m/s (interquartile range: 7.65, 10.61). The baseline demographic characteristics, hemodialysis data, and serum parameters of the entire population are summarized in the first column of **Table 1**.

Receiver Operating Characteristic Curve Analysis and Risk Stratification

In the ROC curve analysis (**Supplementary Figure 1**), the optimal cutoff point for galectin-3 was 30.5 ng/ml (AUC = 0.61, $p = 0.01$), and the cutoff for PWV was 7.9 m/s (AUC = 0.60, $p = 0.02$).

Based on the ROC-optimal cutoffs for PWV and galectin-3, we divided the study patients into four groups: group 1: low PWV–low galectin-3; group 2: low PWV–high galectin-3; group 3: high PWV–low galectin-3; and group 4: high PWV–high galectin-3. The baseline characteristics of these four groups are presented in the second to fifth columns of **Table 1**. The differences in age, history of hypertension and diabetes, several hemodialysis-related variables, and the low-density lipoprotein level were statistically significant between the four groups.

Follow-Up and the Primary Endpoint

The median follow-up duration was 31 months. A total of 57 patients (20.1%) reached the composite endpoint of all-cause mortality and MACCE. Twenty-four (57.1%) of the deaths were caused by cerebrovascular or cardiovascular diseases (2 MIs, 3 heart failure cases, 5 sudden cardiac deaths, 10 cerebral hemorrhages, and 4 ischemic strokes), and seven (16.7%) were attributable to infection.

Univariable and Multivariable Cox Regression Analysis

In the univariable Cox regression analysis (**Supplementary Figure 2**), both PWV and galectin-3 were associated with increased risk of the composite endpoint (HR for PWV = 1.11, 95% CI: 1.01–1.22, $p = 0.033$; HR for galectin-3 = 1.03, 95% CI: 1.01–1.06, $p = 0.014$). In addition, age, hypertension, and phosphorus levels were also significant predictors for the composite endpoint. Using group 1 (low PWV–low galectin-3) as the reference group, we found that only group 4 (high PWV–high galectin-3) was associated with a significantly increased risk of the composite endpoint (HR = 4.74, 95% CI = 1.67–13.47, $p = 0.003$). The increased risks in the other two groups were not statistically significant. The Kaplan–Meier curves of these four groups are plotted in **Figure 2**. Similarly, compared with group 1, group 4 had significantly worse outcomes (i.e., increased risk of composite endpoints, log-rank $p = 0.001$).

In the multivariable Cox regression analysis adjusted for age, mean arterial pressure, albumin, CRP, and phosphorus (**Table 2**), we observed that only group 4 (high PWV–high galectin-3) was associated with a significantly increased risk of the composite endpoint (HR = 3.19, 95% CI = 1.05–9.66, $p = 0.04$).

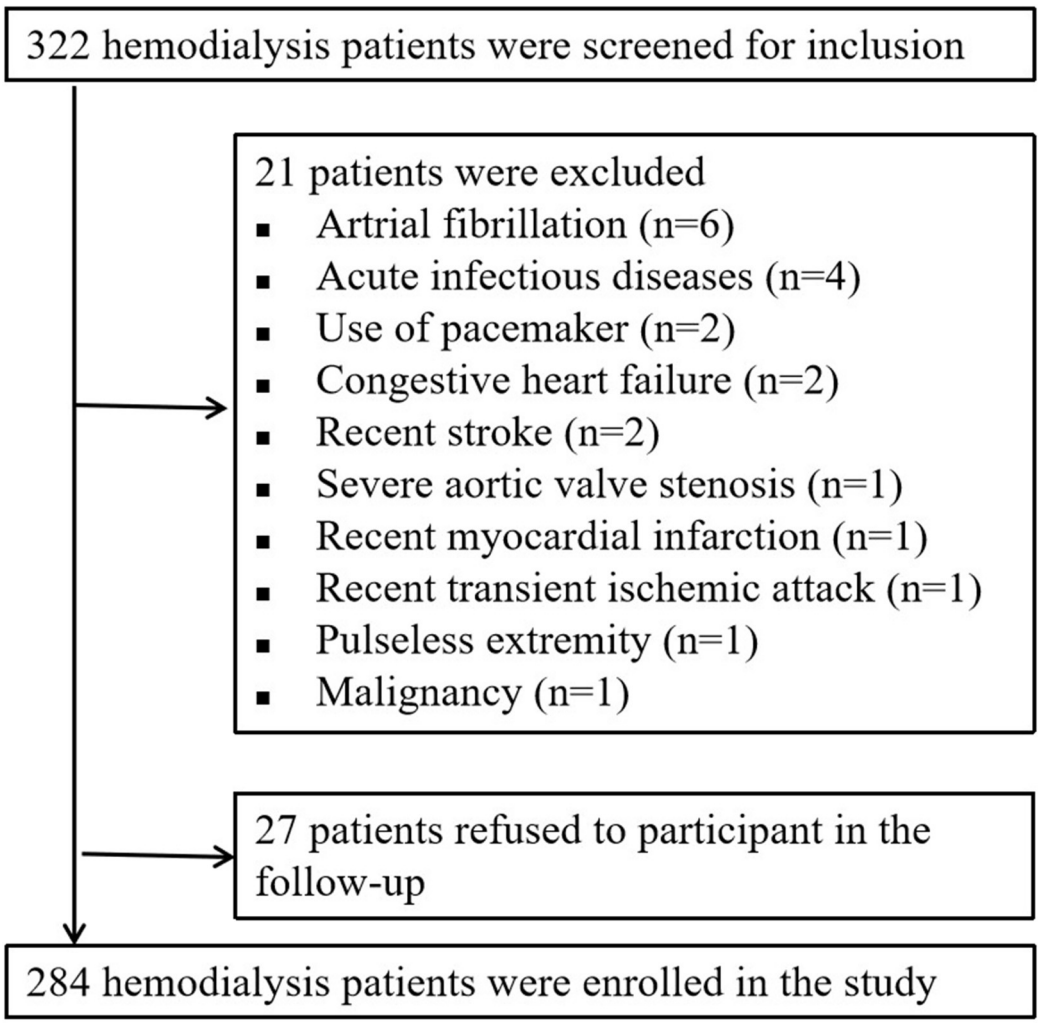

FIGURE 1 | Flow chart of patient enrollment and exclusion.

Model Performance Comparison

We built four multivariable Cox regression models and compared their model performances. Model 1 only included age, mean arterial pressure, albumin, CRP, and phosphorus; model 2 included all variables in model 1 plus PWV; model 3 included all variables in model 1 plus galectin-3; model 4 included all variables in model 1 plus both PWV and galectin-3. Among these four models, model 4 had the best performance in terms of discrimination, calibration, and reclassification (**Table 3**).

DISCUSSION

Our study innovatively combined PWV with galectin-3 to predict mortality and MACCE in hemodialysis patients. We successfully identified the appropriate cutoffs to dichotomize both measures separately. We demonstrated that patients with high PWV and high galactin-3 levels are associated with a 3-fold increased risk of mortality and MACCE. Our study provides a foundation for incorporating these two measures into the cerebral and cardiovascular risk assessment for hemodialysis patients.

Arterial stiffness is associated with primary coronary events, fatal stroke, and all-cause and cardiovascular mortality in patients with hypertension (13–15), and its prognostic value for mortality has also been confirmed in type 2 diabetes and glucose intolerance patients (16). The association between arterial stiffness and the composite endpoint of MACCE in patients with ST-elevation MI has also been established (17).

PWV is considered the gold standard for measuring arterial stiffness (3, 18). However, it remains controversial whether PWV can predict cardiovascular events in dialysis patients. Blacher et al. first demonstrated that PWV was associated with both all-cause mortality and cardiovascular mortality in ESRD patients. In their multivariable model, each PWV increase of 1 m/s was associated with a 1.39-fold increased risk of all-cause death (19). In the CORD study, Verbeke et al. also confirmed that central arterial stiffness is an independent predictor of mortality and

TABLE 1 | Baseline characteristics.

Characteristics	Overall ($n = 284$)	Group 1[a] ($n = 56$)	Group 2 ($n = 34$)	Group 3 ($n = 98$)	Group 4 ($n = 96$)	*P*
Age, years	61 (51.25, 68)	54 (38.25, 62)	58.5 (47, 65.25)	64 (58.75, 71.25)	63 (55.25, 70)	<0.001
Male, n (%)	165 (58.1)	33 (58.93)	19 (55.89)	53 (54.08)	60 (62.5)	0.683
BMI, kg/m^2	21.81 ± 3.33	21.37 ± 3.35	22.93 ± 3.54	21.63 ± 3.17	21.84 ± 3.36	0.164
Hemodialysis data						
Dry weight, kg	59.84 ± 11.33	58.28 ± 10.59	63.59 ± 12.55	59.13 ± 11.52	60.13 ± 10.96	0.155
Dialysis duration, months	90 (56, 155)	99 (59, 181)	91 (47.25, 138.25)	82 (48.75, 145.5)	92.5 (62, 158.25)	0.129
Brachial SBP, mmHg	150.46 ± 25.64	136.96 ± 22.55	130.71 ± 20.19	158.76 ± 22.13	156.87 ± 25.75	<0.001
Brachial DBP, mmHg	82.91 ± 13.64	82.14 ± 15.81	78.06 ± 12.50	84.25 ± 12.83	83.70 ± 13.26	0.125
PP, mmHg	46.5 (36.25, 59)	38.5 (30.25, 49.5)	37 (30.75, 41.25)	50 (44, 67)	53.5 (39, 65.75)	<0.001
MAP, mmHg	105.38 ± 16.57	100.59 ± 18.07	95.59 ± 15.38	109.10 ± 14.62	107.84 ± 16.14	<0.001
spKt/V for urea	1.60 (1.41, 1.91)	1.55 (1.41, 2.00)	1.52 (1.33, 1.80)	1.67 (1.44, 1.89)	1.61 (1.43, 1.93)	0.414
Comorbidities						
Hypertension, n (%)	238 (83.80)	40 (71.43)	28 (82.35)	90 (91.84)	80 (83.33)	0.011
Diabetes, n (%)	36 (12.68)	0 (0)	3 (8.82)	12 (12.24)	21 (21.88)	0.001
Prior CAD, n (%)	19 (6.69)	3 (5.36)	0 (0)	8 (8.16)	8 (8.33)	0.340
Stroke history, n (%)	19 (6.69)	1 (1.79)	6 (17.65)	6 (6.12)	6 (6.25)	0.032
Current medication						
Antihypertensives, n (%)	204 (71.83)	35 (62.5)	22 (64.71)	79 (80.61)	68 (70.83)	0.070
Phosphate binders, n (%)	223 (78.52)	44 (78.57)	32 (94.12)	77 (78.57)	70 (72.92)	0.082
Statins, n (%)	46 (16.2)	8 (14.29)	5 (14.71)	14 (14.29)	19 (19.79)	0.709
Lab result						
Total triglyceride, mmol/L	1.46 (1.07, 2.29)	1.43 (0.93, 1.86)	1.91 (1.26, 3.01)	1.58 (1.16, 2.37)	1.37 (1.02, 2.06)	0.051
Total lipoprotein, mmol/L	3.95 (3.34, 4, 59)	3.97 (3.54, 4.41)	4.13 (3.56, 4.46)	3.97 (3.28, 4.90)	3.81 (3.30, 4.53)	0.519
HDL, mmol/L	1.06 ± 0.31	1.11 ± 0.29	1.10 ± 0.38	1.06 ± 0.30	1.01 ± 0.30	0.252
LDL, mmol/L	2.23 ± 0.77	2.16 ± 0.62	2.33 ± 0.73	2.40 ± 0.79	2.05 ± 0.81	0.011
BNP, pg/ml	251.5 (131, 484.75)	276 (103, 553)	210 (121.75, 382.75)	247.5 (150.5, 462.75)	274 (141, 498.5)	0.736
Albumin, g/L	39.33 ± 3.32	39.97 ± 3.42	39.53 ± 3.31	38.74 ± 3.43	39.50 ± 3.08	0.141
CRP, mg/L	2.2 (0.96, 6.15)	1.52 (0.89, 4.11)	1.80 (0.70, 5.89)	2.17 (0.95, 6.57)	3.42 (1.17, 7.37)	0.064
Calcium, mmol/L	2.35 ± 0.26	2.32 ± 0.24	2.37 ± 0.22	2.33 ± 0.29	2.39 ± 0.23	0.335
Phosphorus, mmol/L	1.81 ± 0.51	1.93 ± 0.56	1.84 ± 0.53	1.78 ± 0.44	1.74 ± 0.54	0.170
Creatinine, μmol/L	1,034.35 ± 235.75	1,049.94 ± 238.68	1,116.14 ± 229.72	1,006.05 ± 231.48	1,025.20 ± 236.96	0.117
PWV, m/s	8.70 (7.65, 10.61)	7.11 (6.50, 7.59)	7.15 (6.46, 7.67)	9.72 (8.84, 10.97)	9.69 (8.63, 11.63)	<0.001
Galectin-3, ng/ml	29.68 ± 9.95	21.56 ± 6.03	36.22 ± 3.68	22.90 ± 5.93	39.02 ± 6.61	<0.001

BMI, body mass index; BNP, B-type brain natriuretic peptide; CAD, coronary artery disease; CRP, C-reactive protein; DBP, diastolic blood pressure; HDL, high-density lipoprotein; LDL, low-density lipoprotein; MAP, mean arterial pressure; PP, pulse pressure; PWV, pulse wave velocity; SBP, systolic blood pressure; spKt/V, single-pool Kt/V.
[a]*Group 1: low PWV–low galectin-3; group 2: low PWV–high galectin-3; group 3: high PWV–low galectin-3; and group 4: high PWV–high galectin-3 values.*

non-fatal cardiovascular events in dialysis patients (4). However, a more recent study showed that the prognostic power of PWV is inferior to that of simple clinical risk scores, and the risk discrimination and reclassification in patients with ESRD was only modestly improved (5). In a head-to-head comparison, the impact of PWV was insignificant when the ankle-brachial BP index was included as a covariate in the multivariable analysis (20). Additionally, the prognostic value of PWV was found to be compromised in elderly patients (6) and dialysis patients with moderate to severe aortic calcification (4).

As a member of the β-galactoside-binding lectin family, galectin-3 can amplify inflammatory and fibrotic processes (21). It has been well-established that a high concentration of galectin-3 is independently associated with all-cause and cardiovascular mortality and an increased risk of heart failure in the general population (22). Galectin-3 has also been shown to be an excellent predictor of mortality in heart failure patients (23). Furthermore, one experimental study demonstrated that inhibition of galectin-3 reduces atherosclerosis in apolipoprotein E-deficient mice (24), suggesting that galectin-3 plays a critical role in the development of atherosclerosis. The association between galectin-3 and atherosclerosis has also been verified by studies in MI patients and patients who received coronary angiography (7, 25).

However, the association between galectin-3 and cardiovascular diseases in CKD patients is unclear. The prognostic power of galectin-3 was found to be compromised by adding renal function into the models (26). Additionally, Zamora et al. found that renal function significantly influenced the prognostic value of galectin-3 in heart failure patients (27). In contrast, in the LURIC study, which was based on a group of patients with impaired renal function, the galectin-3

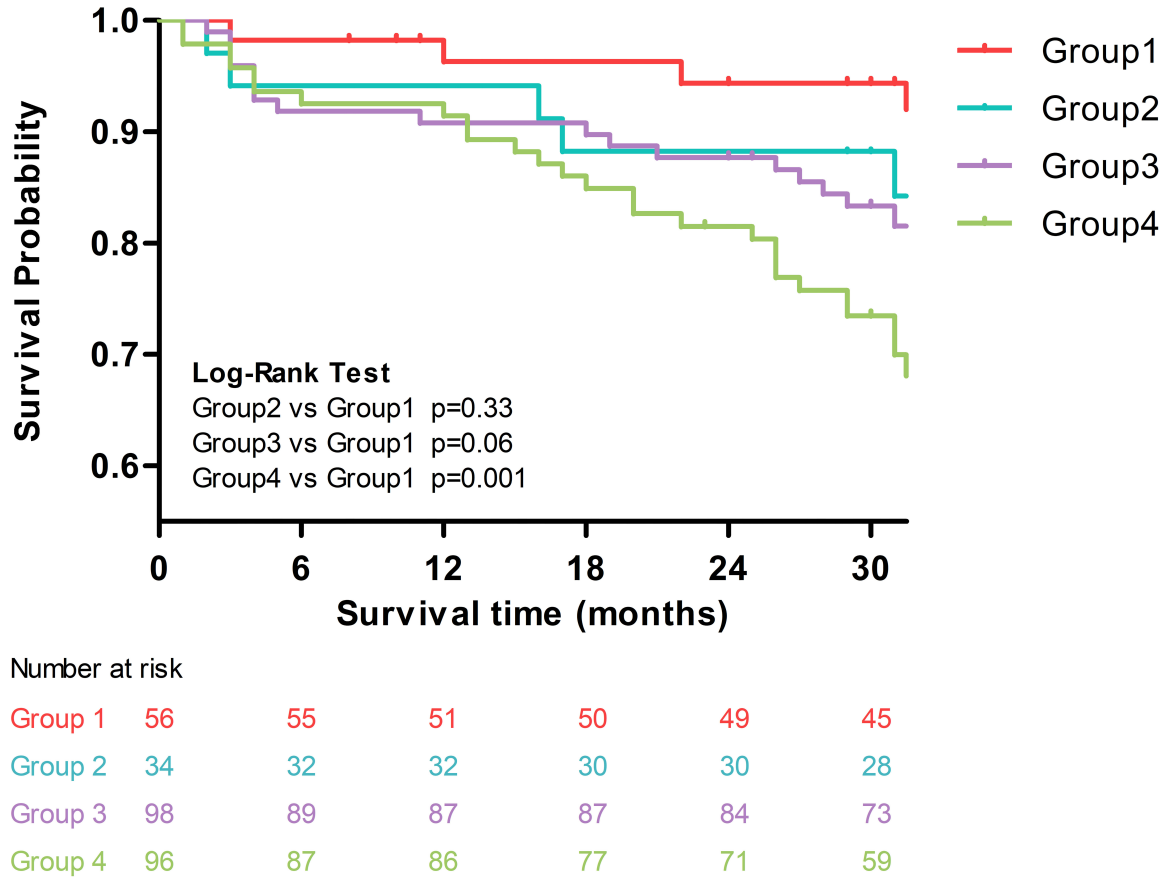

FIGURE 2 | Kaplan–Meier curves of the four groups: group 1: low PWV–low galectin-3; group 2: low PWV–high galectin-3; group 3: high PWV–low galectin-3; and group 4: high PWV–high galectin-3.

TABLE 2 | Multivariable Cox regression model for the composite endpoint.

Variables	HR	95% CI	*p*-value
Age, years	1.04	1.01–1.07	0.011
MAP, mmHg	0.99	0.97–1.01	0.164
Albumin, g/L	0.99	0.90–1.09	0.858
CRP, mg/L	1.01	0.99–1.04	0.245
Phosphorus, mmol/L	0.79	0.43–1.46	0.446
PWV and Galectin-3 groups[a]			
Group 1	1 (reference)		
Group 2	1.37	0.34–5.48	0.660
Group 3	1.94	0.62–6.12	0.258
Group 4	3.19	1.05–9.66	0.040

CI, confidence interval; CRP, C-reactive protein; HR, hazard ratio; MAP, mean arterial pressure; PWV, pulse wave velocity.

[a]*Group 1: low PWV–low galectin-3; group 2: low PWV–high galectin-3; group 3: high PWV–low galectin-3; and group 4: high PWV–high galectin-3 values.*

concentration was significantly associated with all-cause and cardiovascular mortality (10). Consistent with the LURIC study, Obakata et al. found that galectin-3 had independent and incremental prognostic value for all-cause death and a composite of all-cause mortality and MACCE in chronic hemodialysis patients (28).

Although the evidence is conflicting, PWV and galectin-3 are still considered new predictors of cardiovascular diseases. Combining these two indicators may be a reasonable and promising approach for predicting cerebral and cardiovascular risks. Our study showed that appropriate risk stratification could help identify the patients at the highest risk, who will also be candidates for aggressive intervention. There is compelling evidence that combining multiple biomarkers is beneficial for therapy and may improve early risk stratification. In a model in which the risk factors were adjusted, the highest risks of death due to all-causes and cardiovascular death in patients with heart failure were observed when both B-type brain natriuretic peptide and galectin-3 were elevated (29). It is also worth noting that in our study, the model performance comparison showed that adding PWV and galectin-3 can improve model discrimination, calibration, and reclassification.

This study has several limitations. First, it was a single-center observational study that cannot define the cause–effect relationship. Second, all enrolled patients in the current study were Chinese, and the results may not be generalizable

TABLE 3 | Model performance comparison.

	Model 1[a]	Model 2	Model 3	Model 4
Discrimination				
C statistics (95% CI)	0.364 (0.196, 0.601)	0.421 (0.242, 0.523)	0.526 (0.341, 0.622)	0.625 (0.59, 0.66)
Calibration				
H-L	$X^2 = 12.623$, $p = 0.5947$	$X^2 = 9.156$, $p = 0.609$	$X^2 = 7.263$, $p = 0.764$	$X^2 = 4.539$, $p = 0.806$
Reclassification				
IDI, 95%CI	Reference	0.005 (−0.012, 0.051)	0.006 (−0.009, 0.058)	0.090 (0.049, 0.133)
NRI, 95%CI	Reference	0.102 (−0.167, 0.521)	0.201 (−0.148, 0.407)	0.457 (0.323, 0.573)

CI, confidence interval; H-L, Hosmer–Lemeshow statistic; NRI, net reclassification improvement; IDI, integrated discrimination improvement.
[a] Model 1 included the following variables: age, mean arterial pressure, albumin, C-reactive protein, and phosphorus; Model 2 = Model 1 + pulse wave velocity; Model 3 = Model 1 + galectin-3; Model 4 = Model 1 + pulse wave velocity + galectin-3.

to other populations. Third, we did not perform serial measurements of galectin-3 during the follow-up, making it impossible to conduct a longitudinal analysis. Fourth, the sample size in the current study was still limited, and only midterm follow-up results were available. Further studies with a larger sample size and longer follow-up time are warranted.

DATA AVAILABILITY STATEMENT

The raw data supporting the conclusions of this article will be made available by the authors, without undue reservation.

ETHICS STATEMENT

The studies involving human participants were reviewed and approved by The Ethics Committee of Renji Hospital, Shanghai Jiaotong University. The patients/participants provided their written informed consent to participate in this study. Written informed consent was obtained from the individual(s) for the publication of any potentially identifiable images or data included in this article.

AUTHOR CONTRIBUTIONS

QZ and ZN conceived and designed the study. QZ performed the experiments. QZ, MZ, XL, YF, JL, and ZL collected the clinical data. QZ and KY analyzed the data and wrote the paper. ZN reviewed and edited the manuscript. All authors read and approved the manuscript.

FUNDING

This study was partly funded by the National Natural Science Foundation of China (81770666), National Health and Family Planning Commission of China (201740037), Clinical Research Center, Shanghai Jiao Tong University, School of Medicine (DLY201805), and the Science and Technology Innovation Fund of Shanghai Ninth People's Hospital (CK2019010).

SUPPLEMENTARY MATERIAL

The Supplementary Material for this article can be found online at: https://www.frontiersin.org/articles/10.3389/fmed.2020.579021/full#supplementary-material

REFERENCES

1. United States renal data system 2018 annual data report. *Volume 2: End-Stage Renal Disease. Chapter 8: Cardiovascular Disease in Patients With ESRD*. Available online at: https://www.Usrds.Org/2018/view/default.Aspx (accessed June 15, 2020).
2. United States renal data system 2018 annual data report. *Volume 2: End-Stage Renal Disease. Chapter 5: Mortality*. Available from: https://www.Usrds.Org/2018/view/default.Aspx (accessed June 15, 2020).
3. Williams B, Mancia G, Spiering W, Agabiti Rosei E, Azizi M, Burnier M, et al. Practice guidelines for the management of arterial hypertension of the European society of hypertension and the European society of cardiology: ESH/ESC task force for the management of arterial hypertension. *J Hypertens*. (2018) 36:2284–309. doi: 10.1097/HJH.0000000000001961
4. Verbeke F, Van Biesen W, Honkanen E, Wikstrom B, Jensen PB, Krzesinski JM, et al. Prognostic value of aortic stiffness and calcification for cardiovascular events and mortality in dialysis patients: outcome of the calcification outcome in renal disease (CORD) study. *Clin J Am Soc Nephrol*. (2011) 6:153–9. doi: 10.2215/CJN.05120610
5. Tripepi G, Agharazii M, Pannier B, D'Arrigo G, Mallamaci F, Zoccali C, et al. Pulse wave velocity and prognosis in end-stage kidney disease. *Hypertension*. (2018) 71:1126–32. doi: 10.1161/HYPERTENSIONAHA.118.10930
6. Ferreira JP, Girerd N, Pannier B, Rossignol P, London GM. High pulse-wave velocity defines a very high cardiovascular risk cohort of dialysis patients under age 60. *Am J Nephrol*. (2017) 45:72–81. doi: 10.1159/000453338
7. Lisowska A, Knapp M, Tycinska A, Motybel E, Kaminski K, Swiecki P, et al. Predictive value of Galectin-3 for the occurrence of coronary artery disease and prognosis after myocardial infarction and its association with carotid IMT values in these patients: a mid-term prospective cohort study. *Atherosclerosis*. (2016) 246:309–17. doi: 10.1016/j.atherosclerosis.2016.01.022
8. Ochieng J, Furtak V, Lukyanov P. Extracellular functions of galectin-3. *Glycoconj J*. (2002) 19:527–35. doi: 10.1023/B:GLYC.0000014082.99675.2f
9. Zhang Q, Yin K, Zhu M, Lin X, Fang Y, Lu J, et al. Galectin-3 is associated with arterial stiffness among hemodialysis patients. *Biomark Med*. (2019) 13:437–43. doi: 10.2217/bmm-2018-0488
10. Drechsler C, Delgado G, Wanner C, Blouin K, Pilz S, Tomaschitz A, et al. Galectin-3, renal function, and clinical outcomes: results from the LURIC and 4D studies. *J Am Soc Nephrol*. (2015) 26:2213–21. doi: 10.1681/ASN.2014010093

11. Mancia G, Fagard R, Narkiewicz K, Redon J, Zanchetti A, Bohm M, et al. ESH/ESC guidelines for the management of arterial hypertension: the Task Force for the Management of Arterial Hypertension of the European Society of Hypertension (ESH) and of the European Society of Cardiology (ESC). *Eur Heart J.* (2013) 34:2159–219. doi: 10.1093/eurheartj/eht151
12. American Diabetes A. 2. Classification and Diagnosis of Diabetes: Standards of Medical Care in Diabetes-2020. *Diabetes Care.* (2020) 43(Suppl. 1):S14–31. doi: 10.2337/dc20-S002
13. Boutouyrie P, Tropeano AI, Asmar R, Gautier I, Benetos A, Lacolley P, et al. Aortic stiffness is an independent predictor of primary coronary events in hypertensive patients: a longitudinal study. *Hypertension.* (2002) 39:10–5. doi: 10.1161/hy0102.099031
14. Laurent S, Boutouyrie P, Asmar R, Gautier I, Laloux B, Guize L, et al. Aortic stiffness is an independent predictor of all-cause and cardiovascular mortality in hypertensive patients. *Hypertension.* (2001) 37:1236–41. doi: 10.1161/01.HYP.37.5.1236
15. Laurent S, Katsahian S, Fassot C, Tropeano AI, Gautier I, Laloux B, et al. Aortic stiffness is an independent predictor of fatal stroke in essential hypertension. *Stroke.* (2003) 34:1203–6. doi: 10.1161/01.STR.0000065428.03209.64
16. Cruickshank K, Riste L, Anderson SG, Wright JS, Dunn G, Gosling RG. Aortic pulse-wave velocity and its relationship to mortality in diabetes and glucose intolerance: an integrated index of vascular function? *Circulation.* (2002) 106:2085–90. doi: 10.1161/01.CIR.0000033824.02722.F7
17. Feistritzer HJ, Klug G, Reinstadler SJ, Reindl M, Niess L, Nalbach T, et al. Prognostic value of aortic stiffness in patients after ST-elevation myocardial infarction. *J Am Heart Assoc.* (2017) 6:e005590. doi: 10.1161/JAHA.117.005590
18. Willum-Hansen T, Staessen JA, Torp-Pedersen C, Rasmussen S, Thijs L, Ibsen H, et al. Prognostic value of aortic pulse wave velocity as index of arterial stiffness in the general population. *Circulation.* (2006) 113:664–70. doi: 10.1161/CIRCULATIONAHA.105.579342
19. Blacher J, Guerin AP, Pannier B, Marchais SJ, Safar ME, London GM. Impact of aortic stiffness on survival in end-stage renal disease. *Circulation.* (1999) 99:2434–9. doi: 10.1161/01.CIR.99.18.2434
20. Kitahara T, Ono K, Tsuchida A, Kawai H, Shinohara M, Ishii Y, et al. Impact of brachial-ankle pulse wave velocity and ankle-brachial blood pressure index on mortality in hemodialysis patients. *Am J Kidney Dis.* (2005) 46:688–96. doi: 10.1053/j.ajkd.2005.06.016
21. Li LC, Li J, Gao J. Functions of galectin-3 and its role in fibrotic diseases. *J Pharmacol Exp Ther.* (2014) 351:336–43. doi: 10.1124/jpet.114.218370
22. Ho JE, Liu C, Lyass A, Courchesne P, Pencina MJ, Vasan RS, et al. Galectin-3, a marker of cardiac fibrosis, predicts incident heart failure in the community. *J Am Coll Cardiol.* (2012) 60:1249–56. doi: 10.1016/j.jacc.2012.04.053
23. Imran TF, Shin HJ, Mathenge N, Wang F, Kim B, Joseph J, et al. Meta-Analysis of the usefulness of plasma galectin-3 to predict the risk of mortality in patients with heart failure and in the general population. *Am J Cardiol.* (2017) 119:57–64. doi: 10.1016/j.amjcard.2016.09.019
24. MacKinnon AC, Liu X, Hadoke PW, Miller MR, Newby DE, Sethi T. Inhibition of galectin-3 reduces atherosclerosis in apolipoprotein E-deficient mice. *Glycobiology.* (2013) 23:654–63. doi: 10.1093/glycob/cwt006
25. Maiolino G, Rossitto G, Pedon L, Cesari M, Frigo AC, Azzolini M, et al. Galectin-3 predicts long-term cardiovascular death in high-risk patients with coronary artery disease. *Arterioscler Thromb Vasc Biol.* (2015) 35:725–32. doi: 10.1161/ATVBAHA.114.304964
26. de Boer RA, Lok DJ, Jaarsma T, van der Meer P, Voors AA, Hillege HL, et al. Predictive value of plasma galectin-3 levels in heart failure with reduced and preserved ejection fraction. *Ann Med.* (2011) 43:60–8. doi: 10.3109/07853890.2010.538080
27. Zamora E, Lupon J, de Antonio M, Galan A, Domingo M, Urrutia A, et al. Renal function largely influences Galectin-3 prognostic value in heart failure. *Int J Cardiol.* (2014) 177:171–7. doi: 10.1016/j.ijcard.2014.09.011
28. Obokata M, Sunaga H, Ishida H, Ito K, Ogawa T, Ando Y, et al. Independent and incremental prognostic value of novel cardiac biomarkers in chronic hemodialysis patients. *Am Heart J.* (2016) 179:29–41. doi: 10.1016/j.ahj.2016.05.018
29. Zhang Y, Zhang R, An T, Huang Y, Guo X, Yin S, et al. The utility of galectin-3 for predicting cause-specific death in hospitalized patients with heart failure. *J Card Fail.* (2015) 21:51–9. doi: 10.1016/j.cardfail.2014.10.006

Conflict of Interest: The authors declare that the research was conducted in the absence of any commercial or financial relationships that could be construed as a potential conflict of interest.

frontiers in Medicine

ORIGINAL RESEARCH
published: 29 October 2020
doi: 10.3389/fmed.2020.568350

Older Age and High Serum Ferritin Levels Associated With the Risk of Chronic Cytopenia in Hemodialysis Patients

Yu-Ting Lee[1], *Wei-Yu Wang*[1], *Chin-Ho Kuo*[1,2], *Ming-Yang Lee*[1,2], *Yin-Che Lu*[1,2], *Chih-Yen Hsiao*[3,4], *Yueh-Han Hsu*[2,3†] *and Peir-Haur Hung*[3,5*†]

[1] *Division of Hematology and Oncology, Department of Medicine, Ditmanson Medical Foundation Chia-Yi Christian Hospital, Chiayi, Taiwan,* [2] *Min-Hwei Junior College of Health Care Management, Tainan, Taiwan,* [3] *Division of Nephrology, Department of Medicine, Ditmanson Medical Foundation Chia-Yi Christian Hospital, Chiayi, Taiwan,* [4] *Department of Hospital and Health Care Administration, Chia Nan University of Pharmacy and Science, Tainan, Taiwan,* [5] *Department of Applied Life Science and Health, Chia Nan University of Pharmacy and Science, Tainan, Taiwan*

OPEN ACCESS

Edited by:
Natalia Lopez-Andres, NavarraBiomed, Spain

Reviewed by:
Maria-Eleni Roumelioti, University of New Mexico, United States
Ashish K. Solanki, Medical University of South Carolina, United States

***Correspondence:**
Peir-Haur Hung
dtmedg3@yahoo.com.tw

† These authors have contributed equally to this work

Specialty section:
This article was submitted to Nephrology, a section of the journal Frontiers in Medicine

Received: *01 June 2020*
Accepted: *22 September 2020*
Published: *29 October 2020*

Citation:
Lee Y-T, Wang W-Y, Kuo C-H, Lee M-Y, Lu Y-C, Hsiao C-Y, Hsu Y-H and Hung P-H (2020) Older Age and High Serum Ferritin Levels Associated With the Risk of Chronic Cytopenia in Hemodialysis Patients. Front. Med. 7:568350. doi: 10.3389/fmed.2020.568350

Leukopenia or thrombocytopenia is sometimes observed in end-stage renal disease (ESRD) patients, but the association between chronic leukopenia or thrombocytopenia and hemodialysis (HD) is still unclear. We aimed to investigate the incidence of chronic leukopenia or thrombocytopenia in patients with ESRD who received HD and to determine the risk factors of this complication. We retrospectively analyzed ESRD patients treated with HD at Ditmanson Medical Foundation Chia-Yi Christian Hospital in 2018. The risk factors for the occurrence of chronic leukopenia and thrombocytopenia were analyzed by Cox regression models. Of the 473 patients in our study cohort, 46 (9.7%) patients had a hematologic abnormality, including 18 patients with chronic leukopenia, 18 with chronic thrombocytopenia, and 10 with pancytopenia. Multivariate analysis revealed that patient age ≥60 years at the initiation of dialysis was a significant predictor for both chronic leukopenia [adjusted hazard ratio (aHR), 2.71; 95% confidence interval (CI), 1.06-6.89] and chronic thrombocytopenia (aHR, 2.83; 95% CI, 1.08–7.35). Chronic liver disease (aHR, 3.31; 95% CI, 1.27–8.61) and serum ferritin levels >800 mg/dl (aHR, 3.29; 95% CI, 1.29–8.39) were risk factors for chronic thrombocytopenia. A trend showed that vitamin D from intravenous supplementation (aHR, 0.13; 95% CI, 0.01–1.16, $P = 0.066$) and serum phosphorous level (aHR, 0.73; 95% CI, 0.53–1.02, $P = 0.068$) may be associated with chronic thrombocytopenia. Our study demonstrated that hematological abnormality was a long-term complication of HD. These results reveal that older patients with HD and high serum ferritin levels are at an elevated risk for chronic cytopenia. Healthcare professionals should be aware of this risk when treating HD patients in order to improve their prognosis.

Keywords: end stage renal disease, leucopenia, thrombocytopenia, hemodialysis, risk factors

INTRODUCTION

Taiwan has one of the highest prevalence rates of end-stage renal disease (ESRD) in the world (1). In 2018, the incidence rate of dialysis was 493 patients per million people in the general population in Taiwan (2–4).

The life expectancy of ESRD patients has been greatly improved by multidisciplinary patient education and high-quality care (2, 5). Long-term complications affect patients' quality of life. Dialysis is associated with complications such as anemia, secondary hyperparathyroidism, and bone disorder (6). Anemia is a well-known hematological problem in chronic kidney disease. The use of erythropoiesis-stimulating agents increases hemoglobin concentrations and improves patient-perceived quality of life (7).

In contrast to anemia, other hematologic abnormalities are less explored (8–11). Leukopenia and thrombocytopenia are observed temporarily at the initiation of dialysis therapy and are usually associated with dialyzer membranes and activation of the complement system (9, 12, 13). The cause of cytopenia is complex. For example, platelet may be consumed between blood and artificial surfaces. Malnutrition, not uncommon in ESRD, may probably suppress hematopoiesis (14, 15). Chronic cytopenia and bone marrow fibrosis directed by secondary hyperparathyroidism have been reported (8, 10, 16–18); however, the prevalence of chronic leukopenia and thrombocytopenia is poorly understood. Therefore, we developed this retrospective study to identify the risk factors and incidence of chronic leukopenia and chronic thrombocytopenia in patients with ESRD.

MATERIALS AND METHODS

Study Population

Patients treated with hemodialysis (HD) at Ditmanson Medical Foundation Chia-Yi Christian Hospital from January 1, 2018, to December 31, 2018, were enrolled in this study. Patients with chronic leukopenia and thrombocytopenia before or on regular HD for <6 months were excluded in order to eliminate the impact of early mortality (19, 20). This retrospective study was conducted in concordance with institutional patient safety laws and the Declaration of Helsinki and was duly approved by the institutional review board of Ditmanson Medical Foundation Chia-Yi Christian Hospital (CYCH-IRB- 2019042).

Definition of Leukopenia and Thrombocytopenia

Participants' clinical information [including age, gender, body mass index (BMI), vitamin D from intravenous (IV) supplementation, and iron supplementation], comorbidities [including hepatitis C virus (HCV), hepatitis B virus (HBV), chronic liver disease, rheumatologic disease, diabetes mellitus (DM), cerebral vascular disease, hypertension, and cancer], laboratory data [complete blood count (CBC), white blood cell count (WBC), platelet (PLT) counts, C-reactive protein, phosphate, ferritin, albumin, uric acid, calcium × phosphate product (Ca × P product), and intact parathyroid hormone (iPTH) measurements], and duration of dialysis session were assessed for further analysis.

Patients' CBC was calculated by automated hematology analyzers. Leukopenia or thrombocytopenia is usually described as total WBC or PLT counts that are 2 standard deviations below the mean. Leukopenia was defined as WBC <4,000/μl, and thrombocytopenia was defined as PLT $<100 \times 10^3/\mu l$ in this study (21). Parathyroidectomy was indicated if patients had an iPTH level >800 pg/ml with failure to vitamin D therapy. iPTH level was determined using a chemiluminescence immunoassay (CLIA, Immulite 2000) (22). CBC was checked at least every 3 months. Ferritin, iPTH, and clearance of urea to the volume of distribution (Kt/V) were examined every 6 months. Single-pool Kt/V was determined using 2-point urea remodeling with the Daugirdas equation: single-pool $Kt/V = -\ln[(1-\text{urea reduction ratio}) - 0.008 \times \text{session length}] - [4 - 3.5 \times (1-\text{urea reduction ratio})] \times \text{ultrafiltration/postdialysis weight}$ (23). Chronic liver disease was defined as a persistent inflammatory condition of the liver in which biochemical and imaging abnormalities were present over a period of 6 months (24, 25). The following disorders were defined as rheumatic diseases: rheumatoid arthritis, systemic lupus erythematosus, Sjogren's syndrome, and spondyloarthropathies.

In our research, we determined that leukopenia or thrombocytopenia that continued for more than 6 months was defined as chronic leukopenia or thrombocytopenia. Patients who had leukopenia or thrombocytopenia at the initiation of ESRD but had normal CBC (WBC ≥4,000/μl or PLT $\geq 100 \times 10^3/\mu l$) within 6 months after HD were classified as having transient leukopenia or thrombocytopenia.

Statistical Analysis

The baseline characteristics of the enrolled patients in our study are displayed as the total number (n) and proportion (%). Pearson's chi-square test was used to compare categorical variables. Adjusted hazard ratios (aHRs) and 95% confidence intervals (CIs) were examined using the Cox proportional hazards model. Risk factors with $P < 0.1$ in the univariate model were selected for further evaluation in the multivariate analysis. The cumulative incidence of chronic leukopenia and thrombocytopenia was illustrated by means of the Kaplan–Meier method. Data management and statistical analysis were carried out using R software, version 3.5.2 (R Foundation for Statistical Computing, Vienna, Austria).

RESULTS

Clinical Characteristics of the Study Population

At the end of our study period, a total of 509 patients, including three with post kidney transplantation, with HD were identified at the Ditmanson Medical Foundation Chia-Yi Christian Hospital. Nineteen patients in our cohort were followed up for <6 months. Patients who had chronic leukopenia ($n = 1$), chronic thrombocytopenia ($n = 8$), or pancytopenia ($n = 8$) before dialysis therapy were excluded (**Figure 1**). Ultimately, 473 patients (55% male and 45% female) were enrolled in the final

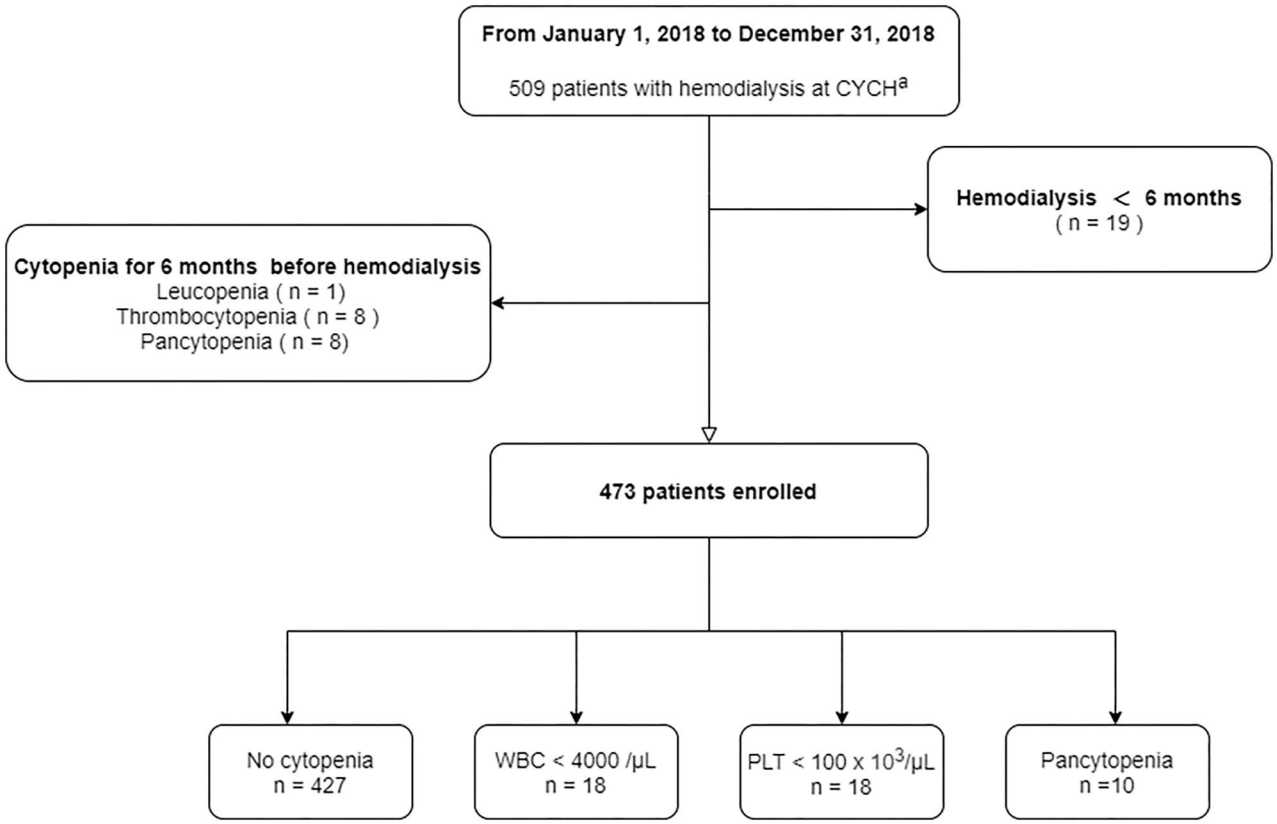

FIGURE 1 | Patient selection. [a]CYCH, Ditmanson Medical Foundation Chia-Yi Christian Hospital.

cohort. The median age of our patients at the end of follow-up was 64.6 years, with the interquartile range (IQR) from 57.0 to 72.4. Patients were followed up for a median of 5.7 years.

Transient Leukopenia and Transient Thrombocytopenia

In this study, we found 18 (3.8%) and 24 (5%) patients with transient leukopenia and transient thrombocytopenia, respectively. All of them had WBC ≥4,000/μl and PLT ≥100 × 10^3/μl within 6 months after HD. Nevertheless, we did not identify any risk factors or biomarkers to predict transient leukopenia and transient thrombocytopenia based on the univariate analysis (**Supplementary Table 1**).

At the end of follow-up, 46 (9.7%) patients had a hematologic abnormality, including 18 (3.8%) with chronic leukopenia, 18 (3.8%) with chronic thrombocytopenia, and 10 (2.1%) with pancytopenia. The incidence of chronic leukopenia and thrombocytopenia was 5.1 cases per 1,000 individuals. The median times to leukopenia and thrombocytopenia were 4.8 (IQR, 2.5–7.2) and 3.8 (IQR, 1.1–8.9) years. The cumulative incidence curve of leukopenia and thrombocytopenia in HD patients is displayed in **Figure 2**. The clinical characteristics of chronic leukopenia, chronic thrombocytopenia, and pancytopenia patients are summarized in **Table 1**. In this cohort, the PLT count and WBC count trends decreased with time (**Figure 3**).

Risk Factors for Chronic Leukopenia and Thrombocytopenia

In the univariate analysis, an age of ≥60 years at the initiation of HD, serum ferritin levels >1,000 ng/ml, and transient leukopenia were associated with chronic leukopenia. Age at the initiation of HD, HCV infection, liver parenchymal disease, serum ferritin levels >800 ng/ml, Kt/V < 1.2, vitamin D from IV supplementation, serum phosphorous level, parathyroidectomy, and transient thrombocytopenia were risk factors for chronic thrombocytopenia (**Table 2**). In the multivariate Cox analysis, age ≥60 years at the initiation of HD (aHR, 2.71; 95% CI, 1.06–6.89, $P = 0.036$) was an independent risk factor of chronic leukopenia. Conversely, an age ≥60 years at the initiation of HD (aHR, 2.83; 95% CI, 1.08–7.35, $P = 0.032$), liver parenchymal disease (aHR, 3.31; 95% CI, 1.27–8.61, $P = 0.013$), and serum ferritin levels >800 mg/dl (aHR, 3.29; 95% CI, 1.29–8.39, $P = 0.012$) were predictors for chronic thrombocytopenia (**Table 2**). Additionally, we found patients with vitamin D from IV supplementation (aHR, 0.13; 95% CI, 0.01–1.16, $P = 0.066$) and higher serum phosphorous level (aHR, 0.73; 95% CI, 0.53–1.02, $P = 0.068$) were prone to have a lower risk

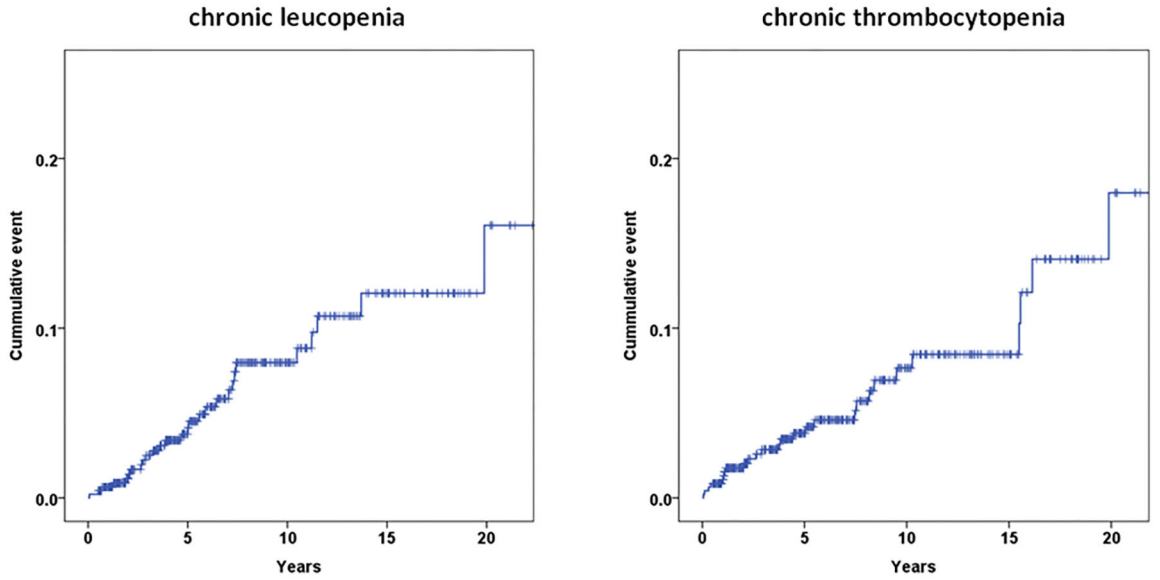

FIGURE 2 | Cumulative incidence of chronic leukopenia and chronic thrombocytopenia.

of chronic thrombocytopenia (**Table 2**). Finally, cancer type, strategy of cancer treatment, and HD access were not risk factors (**Supplementary Table 2**).

DISCUSSION

To the best of our knowledge, this is the first study to report that chronic leukopenia and thrombocytopenia are long-term complications of HD. We find that patient age above 60 years at the initiation of dialysis is a risk factor for both chronic leukopenia and thrombocytopenia. High serum ferritin levels and transient thrombocytopenia are risk factors for chronic thrombocytopenia. Furthermore, vitamin D from IV supplementation and serum phosphorous levels have been shown to be associated with chronic thrombocytopenia. Cancer type and cancer treatment were not associated with cytopenia. In spite of lacking direct evidence, we suppose that HD may play a role in chronic cytopenia.

Transient leukopenia during HD has been well-described and is usually associated with hypersensitivity reactions to dialyzer membranes and the activation of the complement cascade pathway, which leads to the pulmonary sequestration of neutrophils (12, 26, 27). Several studies have shown that the presence of leukemia during the initiation of HD can predict mortality (28, 29); however, the association between transient leukopenia and patients' outcome is unknown (30). In the present study, we identified 3.8% of patients had transient leukopenia. Additionally, HCV infection may relate to leukopenia and/or thrombocytopenia in HD patients. A retrospective study conducted by Ng et al. (31) reported that 11 out of 28 HD patients who were anti-HCV-positive had leukopenia, and the odds ratio (OR) was 6.22. Nevertheless, HCV infection was insignificant in our study. The possible reason contributing to this discrepancy is unknown.

Compared to healthy populations, reduced PLT counts in predialysis and HD patients have been observed (13, 32). The effect of dialysis on PLT count is multiple; for example, some patients start HD in critical condition and the development of thrombocytopenia is not uncommon (33). Some medications, such as antibiotics used in acute sepsis, are suspected to suppress bone marrow function (34, 35). Heparin, which is usually used for extracorporeal circuit anticoagulation, has the potential to induce thrombocytopenia (13, 36). Consumption of platelets may be attributed to either an intravascular graft or dialysis catheter, thrombotic microangiopathy caused by hypertensive crisis, or thrombotic thrombocytopenic purpura (37, 38). In addition, dialyzer membranes also initiate the complement cascade pathway, platelet adhesion, aggregation, and activation leading to thrombocytopenia (13, 39, 40). Ng et al. (31) also demonstrated that HCV infection was a risk factor (OR = 3.27) for thrombocytopenia in dialysis patients. In our research, we used a lower cutoff point for the PLT count ($<100 \times 10^3/\mu l$) to define thrombocytopenia, and the OR of HCV infection was 2.14 with a borderline significance.

Chronic leukopenia and thrombocytopenia are rarely described in dialysis patients. The present study discloses that hematologic abnormalities are long-term complications of dialysis. One possible etiology is secondary hyperparathyroidism and renal osteodystrophy, which are long-term complications of dialysis. Here, we found vitamin D from IV supplementation, a medical treatment for dialysis related to hyperparathyroidism, is a risk factor for chronic thrombocytopenia (41). Both primary and secondary hyperparathyroidism are known causes of secondary myelofibrosis (8, 10, 16, 17). Reversal of bone marrow fibrosis has been demonstrated after parathyroidectomy (42).

TABLE 1 | Characteristics of patients with hemodialysis ($n = 473$).

Characteristics	Total* $n = 473$	Leukopenia $n = 18$	Thrombocytopenia $n = 18$	Both $n = 10$	*P*-value
	n (%)	*n* (%)	*n* (%)	*n* (%)	
Median age, years (IQR) at last F/U	64.6 (57.1–72.5)	64.0 (54.0–71.8)	67.0 (59.9–79.1)	65.4 (58.9–78.1)	0.632
≥65	233 (49.2)	10 (55.6)	9 (50)	5 (50)	0.991
<65	240 (50.8)	8 (44.4)	9 (50)	5 (50)	
Median age, years (IQR) at HD	58.3 (48.2–67.1)	57.5 (42.2–63.0)	59.3 (46.2–71.9)	56.6 (44.8–70.6)	0.859
≥60	211 (44.6)	8 (44.4)	9 (50)	5 (50)	0.935
<60	262 (55.4)	10 (55.6)	9 (50)	5 (50)	
Duration of hemodialysis, years (IQR)	5.7 (3.0–10.3)	7.4 (5.4–12.0)	6.7 (4.0–11.7)	9.9 (6.0–15.4)	0.006
Time to event, years (IQR)	–	5.1 (2.7–7.4)	–	4.4 (2.2–5.6)	
Time to event, years (IQR)	–	–	3.7 (1.0–9.1)	6.2 (2.1–8.1)	
BMI (IQR)	22.4 (20.2–25.7)	21.4 (19.8–24.6)	24.2 (22.0–25.7)	19.6 (17.3–21.0)	0.046
Gender					
Female	213 (45)	10 (55.5)	6 (33.3)	5 (50)	0.609
Male	260 (55)	8 (44.5)	12 (66.7)	5 (50)	
Comorbidities					
Chronic hepatitis C	79 (17.1)	2 (11.1)	5 (27.7)	4 (40)	0.124
Chronic hepatitis B	60 (13)	2 (11.1)	2 (11.1)	2 (20)	0.877
Chronic liver disease	69 (14.5)	1 (5.8)	6 (33.3)	5 (50)	0.001
Rheumatologic disease	26 (5.5)	1 (5.8)	0	0	0.836
Diabetes mellitus	248 (52.5)	5 (29.4)	9 (50)	3 (30)	0.104
Cerebral vascular disease	65 (13.7)	1 (5.8)	2 (11.1)	1 (10)	0.924
Hypertension	432 (91.5)	16 (94.1)	15 (83.3)	8 (80)	0.196
Cancer	71 (15.0)	2 (11.1)	4 (22.2)	1 (10)	0.776
Urothelial carcinoma	28 (5.9)	1 (5.5)	2 (11.1)	0	0.597
Hepatocellular carcinoma	9 (1.9)	1 (5.5)	1 (5.5)	0	0.576
Breast cancer	8 (1.7)	0	0	0	1.000
Others	26 (5.4)	0	1 (5.5)	1 (10)	0.693
Cancer treatment					
Surgical resection	59 (12.4)	2 (11.1)	4 (22.2)	1 (10)	0.648
Chemotherapy	23 (5.4)	1 (5.5)	2 (11.1)	0	0.561
Radiotherapy	10 (2.1)	0	1 (5.5)	0	0.654
Parameter					
P (mg/dl, IQR)	5.1 (4.2–6.1)	5.2 (4.5–5.9)	4.6 (4.0–5.8)	4.4 (4.3–4.7)	0.311
Ferritin (ng/ml, IQR)	500 (342–652)	487 (239–585)	615 (426–912)	546 (499–829)	0.153
Albumin (g/dl, IQR)	3.9 (3.7–4.1)	4.0 (3.7–4.1)	3.9 (3.6–4.0)	3.8 (3.7–4.1)	0.523
Ca × P product	47.0 (37.7–56.5)	47.9 (41.4–55.6)	42.3 (31.2–53.0)	41.8 (40.4–42.7)	0.237
iPTH* (pg/ml, IQR)	317 (129–696)	455 (260–937)	400 (219–776)	451 (138–862)	0.446
Ca × P product >55	127 (28.2)	4 (22.2)	7 (38.8)	3 (30)	0.613
Parathyroidectomy	84 (18.5)	6 (33.3)	5 (29.4)	2 (20)	0.250
*iPTH <240 pg/ml	178 (56.1)	6 (54.5)	7 (70)	4 (80)	0.611
*iPTH <300 pg/ml	155 (48.8)	4 (36.3)	7 (70)	3 (60)	0.430
*iPTH <600 pg/ml	112 (35.3)	3 (17.6)	5 (38.4)	2 (42.8)	0.486
Ferritin >800 ng/ml	49 (11.9)	2 (11.7)	4 (16.6)	3 (33.3)	0.047
Kt/V >1.2	424 (90.2)	16 (88.9)	15 (83.3)	8 (80)	0.276
P >5 mg/dl	241 (52.8)	10 (55.5)	7 (41.1)	2 (22.2)	0.215
Uric acid >7 mg/dl	228 (55.3)	12 (70.5)	11 (73.3)	4 (44.4)	0.246
Vitamin D supplementation	63 (13.7)	3 (16.6)	1 (5.8)	0	0.553
Iron supplementation	163 (35.5)	7 (38.8)	7 (41.1)	3 (30)	0.919
Erythropoiesis-stimulating agents	435 (94.9)	18 (100)	17 (100)	9 (90)	0.594
Hemodialysis access					0.319
A-V fistula	279 (69.9)	14 (87.5)	12 (75)	6 (66.6)	
A-V graft	97 (24.3)	1 (6.2)	2 (12.5)	3 (33.3)	
Catheter	23 (5.7)	1 (6.2)	2 (12.5)	0	

IQR, interquartile range; F/U, follow-up; HD, hemodialysis; BMI, body mass index.
**Excluding patients with parathyroidectomy.*

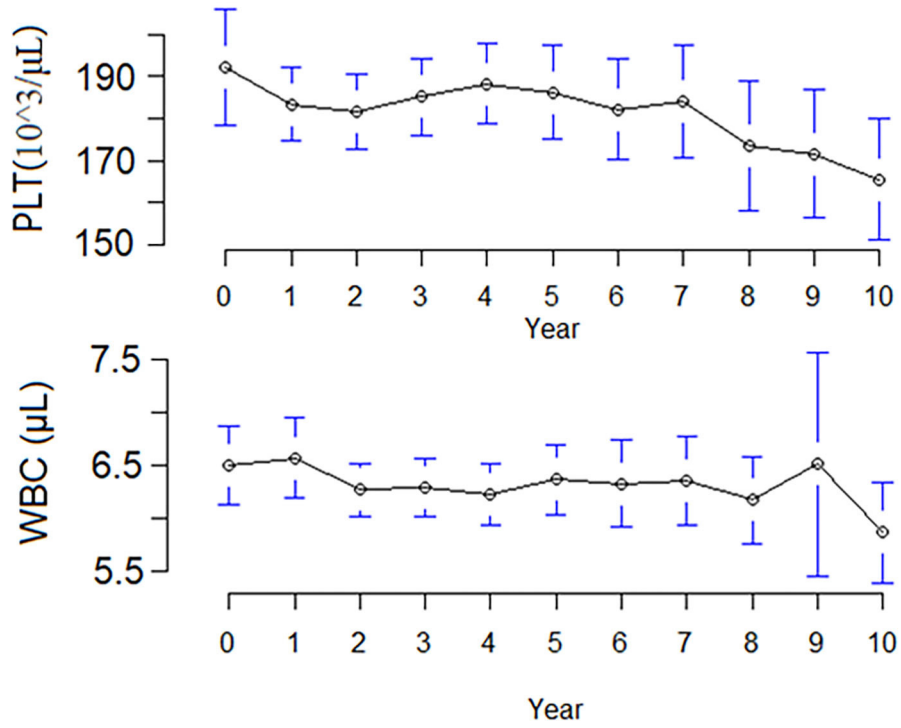

FIGURE 3 | The trend (mean) of patients' white blood cell and platelet counts after hemodialysis.

TABLE 2 | Risk factors for patients with chronic leukopenia and chronic thrombocytopenia.

	Chronic leukopenia		Chronic thrombocytopenia	
	HR (95% CI)[ab]	***P*-value**	**HR (95% CI)[ab]**	***P*-value**
Age ≥60 years (at HD)	2.71 (1.06–6.89)	0.036	2.83 (1.08–7.35)	0.032
Chronic liver disease	0.96 (1.03–3.39)	0.954	3.31 (1.27–8.61)	0.013
Ferritin >800 ng/ml	–	–	3.29 (1.29–8.39)	0.012
Ferritin >1,000 ng/ml	2.61 (0.72–9.45)	0.141	–	–
Transient thrombocytopenia at HD*	1.37 (0.37–5.01)	0.629	3.91 (1.70–8.97)	0.001
P mg/dl (continuous)			0.73 (0.53–1.02)	0.066
Vitamin D supplementation			0.13 (0.01–1.16)	0.068
HCV			0.76 (0.27–2.11)	0.606
Parathyroidectomy			0.56 (0.16–1.90)	0.357
Kt/V ≥ 1.2			0.62 (0.19–2.01)	0.431

HR, hazard ratio; CI, confidence interval; HD, hemodialysis; HCV, hepatitis C virus; BMI, body mass index.
[a] *Treatment was analyzed as a time-dependent covariate in the Cox regression model.*
[b] *Adjusted for gender, age at HD, BMI, parathyroidectomy, and chronic liver disease.*
[*] *PLT <100 × 10^3/μl at the beginning of HD. Return to normal range within 6 months.*

However, parathyroidectomy, a surgical intervention to control hyperparathyroidism, in our cohort was insignificant and may be ascribed to limited cases. Additionally, chronic inflammation in ESRD is another possible mechanism. It is well-known that aberrant inflammation signals impair hematopoietic stem cell self-renewal and the function of the bone marrow (43). Serum ferritin is a marker of chronic inflammation (44); we observed that high serum ferritin levels are associated with cytopenia. Ferritin levels are usually correlated with inflammatory activity (45). Recently, chronic innate immune signaling and ineffective hematopoiesis have been established (46). Basiorka et al. (47) reported that activation of the NLRP3 inflammasome contributed to hematopoietic stem cell death and led to myelodysplastic syndromes. Moreover, crystal deposition in bone marrow may be rare but has an adverse impact on hematopoiesis. For example, Sharma et al. (18) described bone marrow oxalate deposition in two patients with systemic oxalosis and ESRD. Ananthanarayanan and Kini (48) presented a case of

refractory thrombocytopenia receiving a bone marrow biopsy, and gout tophi were observed in the bone marrow.

This study had some limitations. First of all, we lacked bone marrow data and cytogenetic analysis to clarify the etiology of leukopenia or thrombocytopenia, such as myelodysplastic syndrome or acute leukemia. Potential confounding factors, such as exposure to cytotoxic agents or chemicals in the workplace and lifestyle variations, were not completely available for our cohort. Patients were possibly exposed to bacterial endotoxin during the HD sessions, but the endotoxin level was not recorded in our patients. Second, the laboratory data, including WBC, PLT, iPTH, ferritin, and electrolytes, were dynamic. For instance, patients with active sepsis may have had hyperferritinemia and thrombocytopenia. Potential confounding factors, such as exposure to cytotoxic agents and lifestyle variations, were not completely available for our cohort. Third, it is a small, single-center, retrospective cohort analysis of HD patients. Lastly, damage of hematopoietic stem cells is a continuous process (49), and it takes time for an abnormal hematological profile to develop. Generally, the adjusted 3- and 5-year survival rates were reported to be 70% and 50% in ESRD patients without kidney transplantation, respectively (2, 3). The median time to cytopenia in our patients was around 4 years, suggesting that mortality is an important competing factor. Thereafter, further prospective studies are needed to validate our findings.

In conclusion, our study indicates that hematological abnormality is a long-term complication of HD. Old age was a risk factor for chronic leukopenia. The risk of chronic thrombocytopenia included patients' age at the initiation of HD, serum ferritin levels >800 mg/dl, and transient thrombocytopenia. Finally, the role of cytopenia on uremic prognosis and the impact of uremic toxins on hematopoietic stem cells are worth investigating to find out the possible mechanism and to improve patients' quality of life.

DATA AVAILABILITY STATEMENT

The datasets generated during and/or analyzed during the current study are available from the corresponding author on reasonable request. Requests to access these datasets should be directed to dtmedg3@yahoo.com.tw.

ETHICS STATEMENT

This study was conducted in concordance with institutional patient safety laws and has been approved by the Institutional Review Board of Chiayi Christian Hospital (approval no. CYCH-IRB-2019042). This study was performed in accordance with the Declaration of Helsinki. Written informed consent for participation was not required for this study in accordance with the national legislation and the institutional requirements.

AUTHOR CONTRIBUTIONS

Y-TL and P-HH contributed to protocol/project development, contributed to data collection or management, and contributed to manuscript writing/editing. Y-TL contributed to data analysis. W-YW, C-HK, M-YL, Y-CL, Y-HH, and P-HH contributed to manuscript review. Y-HH and P-HH were the scientific advisers. All authors participated in the interpretation of the studies and analysis of the data and reviewed and approved the final version of the manuscript.

FUNDING

This study was funded by an unrestricted research grant from Ditmanson Medical Foundation Chia-Yi Christian Hospital (R109-009).

ACKNOWLEDGMENTS

The authors would like to acknowledge the support of Dr. Tsung-Hsien Chen for the preparation of this manuscript. We would like to thank Editage (www.editage.com) for English language editing.

SUPPLEMENTARY MATERIAL

The Supplementary Material for this article can be found online at: https://www.frontiersin.org/articles/10.3389/fmed.2020.568350/full#supplementary-material

REFERENCES

1. Kuo HW, Tsai SS, Tiao MM, Yang CY. Epidemiological features of CKD in Taiwan. *Am J Kidney Dis.* (2007) 49:46–55. doi: 10.1053/j.ajkd.2006.10.007
2. Hsu CC. *Annual Report on Kidney Disease in Taiwan 2018. National Health Research Institutes, Taiwan Society of Nephrology.* Taipei (2019). 1–313p.
3. Robinson BM, Akizawa T, Jager KJ, Kerr PG, Saran R, Pisoni RL. Factors affecting outcomes in patients reaching end-stage kidney disease worldwide: differences in access to renal replacement therapy, modality use, and haemodialysis practices. *Lancet.* (2016) 388:294–306. doi: 10.1016/S0140-6736(16)30448-2
4. Yen CC, Tsai CF, Luo YY, Yang HYI, Liu MY, Hung PH, et al. Factors affecting fistula failure in patients on chronic hemodialysis: a population-based case-control study. *BMC Nephrol.* (2018) 19:213. doi: 10.1186/s12882-018-1010-6
5. Wu MY, Wu MS. Taiwan renal care system: a learning health-care system. *Nephrology.* (2018) 23:112–5. doi: 10.1111/nep.13460
6. Himmelfarb J, Ikizler TA. Hemodialysis. *N Engl J Med.* (2010) 363:1833–45. doi: 10.1056/NEJMra0902710
7. Hung SC, Lin YP, Tarng DC. Erythropoiesis-stimulating agents in chronic kidney disease: what have we learned in 25 years? *J Formos Med Assoc.* (2014) 113:3–10. doi: 10.1016/j.jfma.2013.09.004
8. Lim DJ, Oh EJ, Park CW, Kwon HS, Hong EJ, Yoon KH, et al. Pancytopenia and secondary myelofibrosis could be induced

by primary hyperparathyroidism. *Int J lab Hematol.* (2007) 29:464–8. doi: 10.1111/j.1365-2257.2006.00877.x
9. Posadas MA, Hahn D, Schleuter W, Paparello J. Thrombocytopenia associated with dialysis treatments. *Hemodial Int.* (2011) 15:416–23. doi: 10.1111/j.1542-4758.2011.00561.x
10. Sharma SP, Siu K. Pancytopenia in secondary hyperparathyroidism due to end-stage renal disease. *Am J Med.* (2013) 126:e11–2. doi: 10.1016/j.amjmed.2013.06.028
11. Yeo JH, Islam A. Renal failure and progressive pancytopenia. *J R Coll Physicians Edinb.* (2018) 48:318–20. doi: 10.4997/JRCPE.2018.406
12. Hakim RM, Breillatt J, Lazarus JM, Port FK. Complement activation and hypersensitivity reactions to dialysis membranes. *N Engl J Med.* (1984) 311:878–82. doi: 10.1056/NEJM198410043111403
13. Daugirdas JT, Bernardo AA. Hemodialysis effect on platelet count and function and hemodialysis-associated thrombocytopenia. *Kidney Int.* (2012) 82:147–57. doi: 10.1038/ki.2012.130
14. Ikizler TA, Cano NJ, Franch H, Fouque D, Himmelfarb J, Kalantar-Zadeh K, et al. Prevention and treatment of protein energy wasting in chronic kidney disease patients: a consensus statement by the International Society of renal nutrition and metabolism. *Kidney Int.* (2013) 84:1096–107. doi: 10.1038/ki.2013.147
15. Nakajima K, Crisma AR, Silva GB, Rogero MM, Fock RA, Borelli P. Malnutrition suppresses cell cycle progression of hematopoietic progenitor cells in mice via cyclin D1 down-regulation. *Nutrition.* (2014) 30:82–9. doi: 10.1016/j.nut.2013.05.029
16. Rao DS, Shih MS, Mohini R. Effect of serum parathyroid hormone and bone marrow fibrosis on the response to erythropoietin in Uremia. *N Engl J Med.* (1993) 328:171–5. doi: 10.1056/NEJM199301213280304
17. Sethi SK, Bansal SB, Wadhwani N, Makasana M, Nandwani A, Kher V, et al. Myelofibrosis-induced erythropoietin-resistant anemia due to severe refractory hyperparathyroidism. *Kidney Int Rep.* (2018) 3:1010–4. doi: 10.1016/j.ekir.2018.04.003
18. Sharma S, Rao RN, Pani KC, Paul P. Bone marrow oxalosis: an unusual cause of cytopenia in end-stage renal disease; report of two cases. *Indian J Pathol Microbiol.* (2018) 61:268–70. doi: 10.4103/IJPM.IJPM_572_17
19. Foley RN, Chen SC, Solid CA, Gilbertson DT, Collins AJ. Early mortality in patients starting dialysis appears to go unregistered. *Kidney Int.* (2014) 86:392–8. doi: 10.1038/ki.2014.15
20. Sim JJ, Zhou H, Shi J, Shaw SF, Henry SL, Kovesdy CP, et al. Disparities in early mortality among chronic kidney disease patients who transition to peritoneal dialysis and hemodialysis with and without catheters. *Int Urol Nephrol.* (2018) 50:963–71. doi: 10.1007/s11255-018-1837-6
21. Wang MC, Huang CE, Lin MH, Yang YH, Lu CH, Chen PT, et al. Impacts of demographic and laboratory parameters on key hematological indices in an adult population of southern Taiwan: a cohort study. *PLoS ONE.* (2018) 13:e0201708. doi: 10.1371/journal.pone.0201708
22. Amal L, Bergmann P. Evaluation of a chemiluminescence immunoassay for the determination of intact parathyroid hormone using the ADVIA Centaur. *Clin Lab.* (2004) 50:695–702.
23. Daugirdas JT. Second generation logarithmic estimates of single-pool variable volume Kt/V: an analysis of error. *J Am Soc Nephrol.* (1993) 4:1205–13.
24. Chalasani N, Younossi Z, Lavine JE, Diehl AM, Brunt EM, Cusi K, et al. The diagnosis and management of non-alcoholic fatty liver disease: practice guideline by the American gastroenterological association, American association for the study of liver diseases, and American college of gastroenterology. *Gastroenterology.* (2012) 142:1592–609. doi: 10.1053/j.gastro.2012.04.001
25. Shiha G, Sarin SK, Ibrahim AE, Omata M, Kumar A, Lesmana LA, et al. Liver fibrosis: consensus recommendations of the Asian Pacific Association for the Study of the Liver (APASL). *Hepatol Int.* (2009) 3:323–33. doi: 10.1007/s12072-008-9114-x
26. Jacob AI, Gavellas G, Zarco R, Perez G, Bourgoignie JJ. Leukopenia, hypoxia, and complement function with different hemodialysis membranes. *Kidney Int.* (1980) 18:505–9. doi: 10.1038/ki.1980.164
27. Tabor B, Geissler B, Odell R, Schmidt B, Blumenstein M, Schindhelm K. Dialysis neutropenia: the role of the cytoskeleton. *Kidney Int.* (1998) 53:783–9. doi: 10.1046/j.1523-1755.1998.00813.x
28. Hsu CW, Lin JL, Lin-Tan DT, Yen TH, Chen KH. White blood cell count predicts all-cause, cardiovascular disease-cause and infection-cause one-year mortality of maintenance hemodialysis patients. *Ther Apher Dial.* (2010) 14:552–9. doi: 10.1111/j.1744-9987.2010.00849.x
29. Reddan DN, Klassen PS, Szczech LA, Coladonato JA, O'Shea S, Owen WF Jr, et al. White blood cells as a novel mortality predictor in haemodialysis patients. *Nephrol Dial Transplant.* (2003) 18:1167–73. doi: 10.1093/ndt/gfg066
30. Esteras R, Martin-Navarro J, Ledesma G, Fernández-Prado R, Carreño G, Cintra M, et al. Incidence of hypersensitivity reactions during hemodialysis. *Kidney Blood Press Res.* (2018) 43:1472–8. doi: 10.1159/000493662
31. Ng YY, Lin CC, Wu SC, Hwang SJ, Ho CH, Yang WC, et al. Leukopenia and thrombocytopenia in hemodialysis patients with hepatitis B or C virus infection and non-hemodialysis patients with hepatitis cirrhosis. *Clin Nephrol.* (2002) 57:289–95. doi: 10.5414/CNP57289
32. Gafter U, Bessler H, Malachi T, Zevin D, Djaldetti M, Levi J. Platelet count and thrombopoietic activity in patients with chronic renal failure. *Nephron.* (1987) 45:207–10. doi: 10.1159/000184118
33. Zarychanski R, Houston DS. Assessing thrombocytopenia in the intensive care unit: the past, present, and future. *Hematol Am Soc Hematol Educ Program.* (2017) 2017:660–6. doi: 10.1182/asheducation-2017.1.660
34. Naqvi TA, Ikhlaque N, Baumann MA. Thrombocytopenia due to hypotension unrelated to infection: shock marrow. *Int J Clin Pract.* (2005) 59:782–4. doi: 10.1111/j.1742-1241.2005.00418.x
35. Singer M, Deutschman CS, Seymour CW, Shankar-Hari M, Annane D, Bauer M, et al. The Third International consensus definitions for sepsis and septic shock (Sepsis-3). *JAMA.* (2016) 315:801–10. doi: 10.1001/jama.2016.0287
36. Syed S, Reilly RF. Heparin-induced thrombocytopenia: a renal perspective. *Nat Rev Nephrol.* (2009) 5:501–11. doi: 10.1038/nrneph.2009.125
37. Khanal N, Dahal S, Upadhyay S, Bhatt VR, Bierman PJ. Differentiating malignant hypertension-induced thrombotic microangiopathy from thrombotic thrombocytopenic purpura. *Ther Adv Hematol.* (2015) 6:97–102. doi: 10.1177/2040620715571076
38. van den Born BJ, van der Hoeven NV, Groot E, Lenting PJ, Meijers JC, Levi M, et al. Association between thrombotic microangiopathy and reduced ADAMTS13 activity in malignant hypertension. *Hypertension.* (2008) 51:862–6. doi: 10.1161/HYPERTENSIONAHA.107.103127
39. Post JB. Thrombocytopenia associated with use of a biocompatible hemodialysis membrane: a case report. *Am J Kidney Dis.* (2010) 55:e25–8. doi: 10.1053/j.ajkd.2009.10.059
40. Muir KB, Packer CD. Thrombocytopenia in the setting of hemodialysis using biocompatible membranes. *Case Rep Med.* (2012) 2012:358024. doi: 10.1155/2012/358024
41. Kidney Disease: Improving Global Outcomes (KDIGO) CKD-MBD Update Work Group. KDIGO 2017 clinical practice guideline update for the diagnosis, evaluation, prevention, and treatment of Chronic Kidney Disease-Mineral and Bone Disorder (CKD-MBD). *Kidney Int Suppl.* (2017) 7:1–59. doi: 10.1016/j.kisu.2017.04.001
42. Azevedo P, Cardoso PSR, Farah KP, de Melo FHC, Rezende SM. Complete reversal of bone marrow fibrosis after parathyroidectomy for secondary hyperparathyroidism. *Br J Haematol.* (2017) 178:500. doi: 10.1111/bjh.14774
43. Pietras EM. Inflammation: a key regulator of hematopoietic stem cell fate in health and disease. *Blood.* (2017) 130:1693–8. doi: 10.1182/blood-2017-06-780882
44. Kell DB, Pretorius E. Serum ferritin is an important inflammatory disease marker, as it is mainly a leakage product from damaged cells. *Metallomics.* (2014) 6:748–73. doi: 10.1039/C3MT00347G
45. Kernan KF, Carcillo JA. Hyperferritinemia and inflammation. *Int Immunol.* (2017) 29:401–9. doi: 10.1093/intimm/dxx031
46. Barreyro L, Chlon TM, Starczynowski DT. Chronic immune response dysregulation in MDS pathogenesis. *Blood.* (2018) 132:1553–60. doi: 10.1182/blood-2018-03-784116
47. Basiorka AA, McGraw KL, Eksioglu EA, Chen X, Johnson J, Zhang L, et al. The NLRP3 inflammasome functions as a driver of the myelodysplastic syndrome phenotype. *Blood.* (2016) 128:2960–75. doi: 10.1182/blood-2016-07-730556
48. Ananthanarayanan V, Kini AR. Bone marrow with gouty tophi. *Hum Pathol Case Rep.* (2017) 8:1. doi: 10.1016/j.ehpc.2016.12.001

49. Genovese G, Kahler AK, Handsaker RE, Lindberg J, Rose SA, Bakhoum SF, et al. Clonal hematopoiesis and blood-cancer risk inferred from blood DNA sequence. *N Engl J Med.* (2014) 371:2477–87. doi: 10.1056/NEJMoa1409405

Conflict of Interest: The authors declare that the research was conducted in the absence of any commercial or financial relationships that could be construed as a potential conflict of interest.

frontiers in Medicine

SYSTEMATIC REVIEW
published: 03 November 2020
doi: 10.3389/fmed.2020.588301

Chronic Kidney Diseases and Acute Kidney Injury in Patients With COVID-19: Evidence From a Meta-Analysis

Yangzhong Zhou[1†], Qidong Ren[2†], Gang Chen[1†], Qiao Jin[2], Quexuan Cui[1], Huiting Luo[1], Ke Zheng[1], Yan Qin[1] and Xuemei Li[1]*

[1] Department of Nephrology, Peking Union Medical College, Peking Union Medical College Hospital, Chinese Academy of Medical Sciences, Beijing, China, [2] School of Medicine, Tsinghua University, Beijing, China

Renal involvement has been implicated in coronavirus disease 2019 (COVID-19), but the related prevalence and prognosis were largely unknown. In this meta-analysis, we searched the literature from PubMed, Embase, through bioRxiv, and medRxiv until April 26, 2020. Studies reporting chronic kidney diseases (CKDs) and/or acute kidney injury (AKI) were included. Demographics, relevant data of disease severity, and patient's prognosis were extracted and aggregated. Twenty-one thousand one hundred sixty-four patients from 52 peer-reviewed studies were included. Thirty-seven studies (n = 16,922) reported CKD in COVID-19 patients at diagnosis, and the pooled prevalence was 3.52% (95% CI, 1.98–5.48%; I^2 = 93%). Subgroup analysis showed that CKD prevalence was higher in severe cases [odds ratio (OR), 3.42; 95% CI 2.05–5.61; I^2 = 0%] compared to those with non-severe disease and deceased cases (6.46, 3.40–12.29; I^2 = 1%) compared with survivors. Pooled prevalence of CKD was lower in Chinese patients (2.56%; 95% CI, 1.79–3.47%; I^2 = 80%) compared to those outside of China (6.32%; 95% CI, 0.9–16.12%; I^2 = 93%) (p = 0.08). The summary estimates for AKI prevalence was 11.46% (95% CI, 6.93–16.94%). Patients with AKI had a higher prevalence of developing into severe cases (OR, 6.97; 95% CI, 3.53–13.75; I^2 = 0%) and mortality risk (45.79, 36.88–56.85; I^2 = 17%). The prevalence estimates of CKD or AKI were not significantly different from preprint publications (p > 0.05). Our study indicates that renal condition, either in CKD or AKI, is associated with COVID-19 prognosis, and taking care of such patients needs further awareness and investigations.

Keywords: COVID-19, chronic kidney disease, acute kidney injury, severity, prognosis

OPEN ACCESS

Edited by:
Jonatan Barrera-Chimal, National Autonomous University of Mexico, Mexico

Reviewed by:
Matthew Michael James Edey, Hull University Teaching Hospitals NHS Trust, United Kingdom
Swastika Sur, University of California San Francisco, United States

****Correspondence:***
Xuemei Li
Prof.Lixm@outlook.com

[†]These authors have contributed equally to this work

Specialty section:
This article was submitted to Nephrology, a section of the journal Frontiers in Medicine

Received: *28 July 2020*
Accepted: *29 September 2020*
Published: *03 November 2020*

Citation:
Zhou Y, Ren Q, Chen G, Jin Q, Cui Q, Luo H, Zheng K, Qin Y and Li X (2020) Chronic Kidney Diseases and Acute Kidney Injury in Patients With COVID-19: Evidence From a Meta-Analysis. Front. Med. 7:588301. doi: 10.3389/fmed.2020.588301

INTRODUCTION

Since December 2019, the coronavirus disease 2019 (COVID-19) has rapidly developed into a global pandemic (1), with more than four million cases confirmed until the beginning of May 2020 (2). The variable clinical course of COVID-19 ranged from asymptomatic infection to severe cases, and 5–6% may need intensive care unit (ICU) admission (3–5).

The kidney is not a bystander during the disease course. Of the hospitalized patients, 43.9–75.4% had evidence of abnormal kidney function, and 5.1–10.5% of them presented acute kidney

injury (AKI) with an excess mortality rate (6, 7). Postmortem evaluations detected viral antigen in tubular epithelial cells and revealed severe acute tubular injury (8). Moreover, preexisting chronic kidney disease (CKD) could reasonably act as an ominous clinical predictor and associate with high mortality (6). Accumulating evidence has suggested that patients with chronic comorbidities were more likely to develop into severe cases (9). Data from multiple cohorts and meta-analyses have listed aging, hypertension, diabetes, and cardiovascular disease as adverse prognostic markers for COVID-19 patients (10, 11), which were also commonly seen in CKD (12, 13).

While AKI is often carefully monitored in such a complicated infectious disease (14), CKD, affecting over 10% of the general population, is often neglected (15). Data on the risk of patients with CKD are limited and highly variable, especially in a scenario of lung-dominated infectious disease (16). Still, it is difficult to picture the relationship between kidney diseases and the prognosis of COVID-19 infection in the surgent literature.

Therefore, we conducted a systematic review and meta-analysis of studies on the clinical characteristics of COVID-19 patients, irrespective of intervention or comparator. We focused on the prevalence of CKD and AKI, as well as their association with poor prognosis.

RESULTS

Search Results and Characteristics of Included Studies

The literature search yielded 9,405 articles and one additional record (6), of which 344 were reviewed in full text (**Figure 1**). Of these, 52 peer-reviewed articles (45 reported CKD, 15 reported AKI) and 36 preprint manuscripts met the inclusion criteria. Most studies identified by our search, but excluded from the final review, were not in proper study types, not relevant populations, or did not report CKD/AKI events, lacked AKI definitions, or were duplicates of cohorts already identified.

The characteristics of the included studies are summarized in **Supplementary Table 2**. All the included studies were cohort studies. Their sample sizes ranged from 5 to 5,700 participants, and follow-up durations were reported in 22 studies, ranging from 5 days to 1 month. Of all, 33 were conducted in a single center (5–7, 9, 17–45), while 19 studies were reporting data from multiple centers (4, 46–63). Of the 52 studies, 40 were from China; especially, 28 of them include data from the designated hospitals in Wuhan, and 12 were from other countries, including the US, Italy, France, Korea, and Singapore.

The median age of study participants ranged from 41 to 72 years, and 32.93–73.17% of them were male. Thirty-eight studies recruited consecutive patients in their centers, while the rest specified their participants as deceased, ICU patients, elderly, medical workers, or others.

Quality assessment of studies was performed according to the specific analysis they were applied separately, and the Newcastle–Ottawa Scale (NOS) scores of all the articles included were no <6.

Prevalence of Chronic Kidney Disease and Associations With Prognosis

A total of 16,922 COVID-19 patients from 37 studies were included in the meta-analysis for the prevalence of CKD (**Figure 2**). The pooled prevalence of CKD in these patients was 3.52% (95% CI, 1.98–5.48%), and the heterogeneity of the studies was significant ($I^2 = 93\%$, $p < 0.01$). Twenty-six studies were from China, and 11 were from other countries. Of the Chinese studies, 16 studies were reporting data from Wuhan in Hubei province. The pooled CKD prevalence was higher in the studies outside of China (6.56%; 95% CI, 2.82–11.71%) compared with those from China (2.66%; 95% CI, 1.22–4.65%), with a borderline level of statistical significance ($p = 0.08$). The heterogeneity was significant in either Chinese studies ($I^2 = 80\%$, $p < 0.01$) and the others ($I^2 = 93\%$, $p < 0.01$).

Eight studies, including 2,686 Chinese patients, were included in the meta-analysis of CKD prevalence in non-severe COVID-19 (**Figure 3**). The pooled prevalence was 1.02% (95% CI, 0.63–1.50%), with mild heterogeneity noted ($I^2 = 22\%$, $p = 0.25$). For severe COVID-19 cases, pooled CKD prevalence from 2,879 patients (18 studies) was 6.13% (95% CI, 2.81–10.64%). A meta-analysis from eight studies, reporting 1,310 severe and 2,686 non-severe cases, found that COVID-19 patients with CKD could have a higher risk of developing into severe cases (OR, 3.42; 95% CI, 2.05–5.61; heterogeneity $I^2 = 0\%$, $p = 0.43$).

Similarly, we calculated the pooled CKD prevalence in survived (1.17%; 95% CI, 0.02–4.00%) and deceased patients (6.36%; 95% CI, 2.34–12.17%) (**Figure 4**). The heterogeneities were both significant in these two analyses ($I^2 > 75\%$, $p < 0.01$). The mortality risk was increased in CKD patients (OR, 6.46; 95% CI, 3.40–12.29; heterogeneity $I^2 = 1\%$, $p = 0.40$), based on the analysis from 1,306 survived and 286 deceased patients (**Figure 4**).

Prevalence of Acute Kidney Injury and Associations With Prognosis

Thirteen studies have reported the prevalence in AKI in a total of 8,735 patients, with diagnostic criteria stated in the manuscripts (**Figure 5**). The summary estimates for AKI prevalence was 11.46% (95% CI, 6.93–16.94%), which was similar between Chinses studies and data from other countries. The pooled prevalences of AKI were 1.77% (95% CI, 0.00–6.88%) in non-severe patients, 18.53% (95% CI, 11.32–27.05%) in severe patients, 3.21 (95% CI, 1.27–5.99%) in survived patients, and 43.27% (95% CI, 30.53–56.48%) in deceased ones (**Figures 6, 7**). Significant heterogeneity for AKI prevalence was seen across studies, including those in the subgroup analyses ($I^2 > 75\%$, $p < 0.01$). The risk of deterioration was significantly higher in patients with AKI (OR, 6.97; 95% CI, 3.53–13.75; heterogeneity $I^2 = 0\%$, $p = 0.50$, **Figure 6**) and so was the mortality risk (OR, 45.79; 95% CI, 36.88–56.85; heterogeneity $I^2 = 17\%$, $p = 0.31$, **Figure 7**).

Preprint Studies and Other Comorbidities

We performed the same estimation based on publications in the preprint platforms (**Supplementary Figures 1**, **2**). The

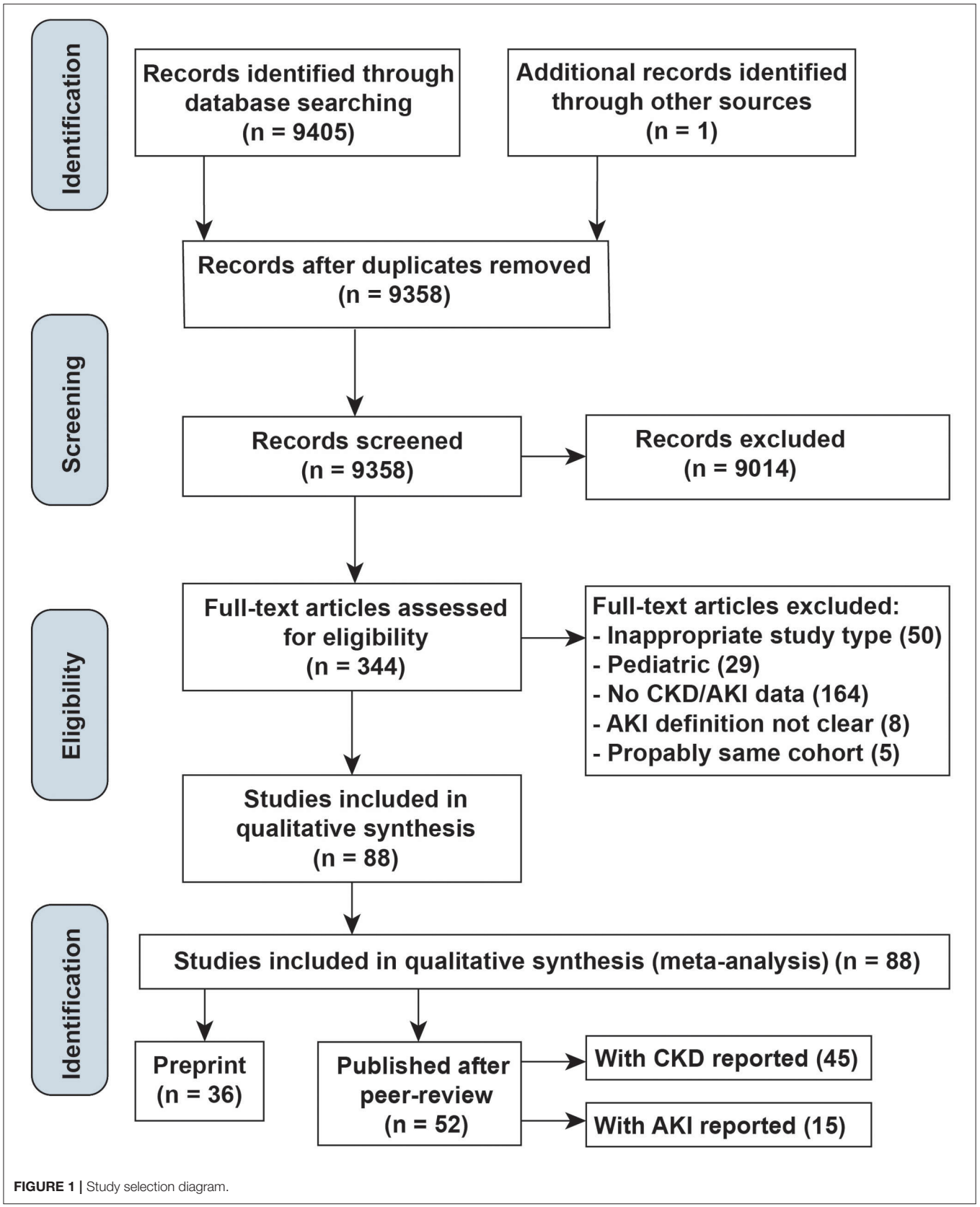

FIGURE 1 | Study selection diagram.

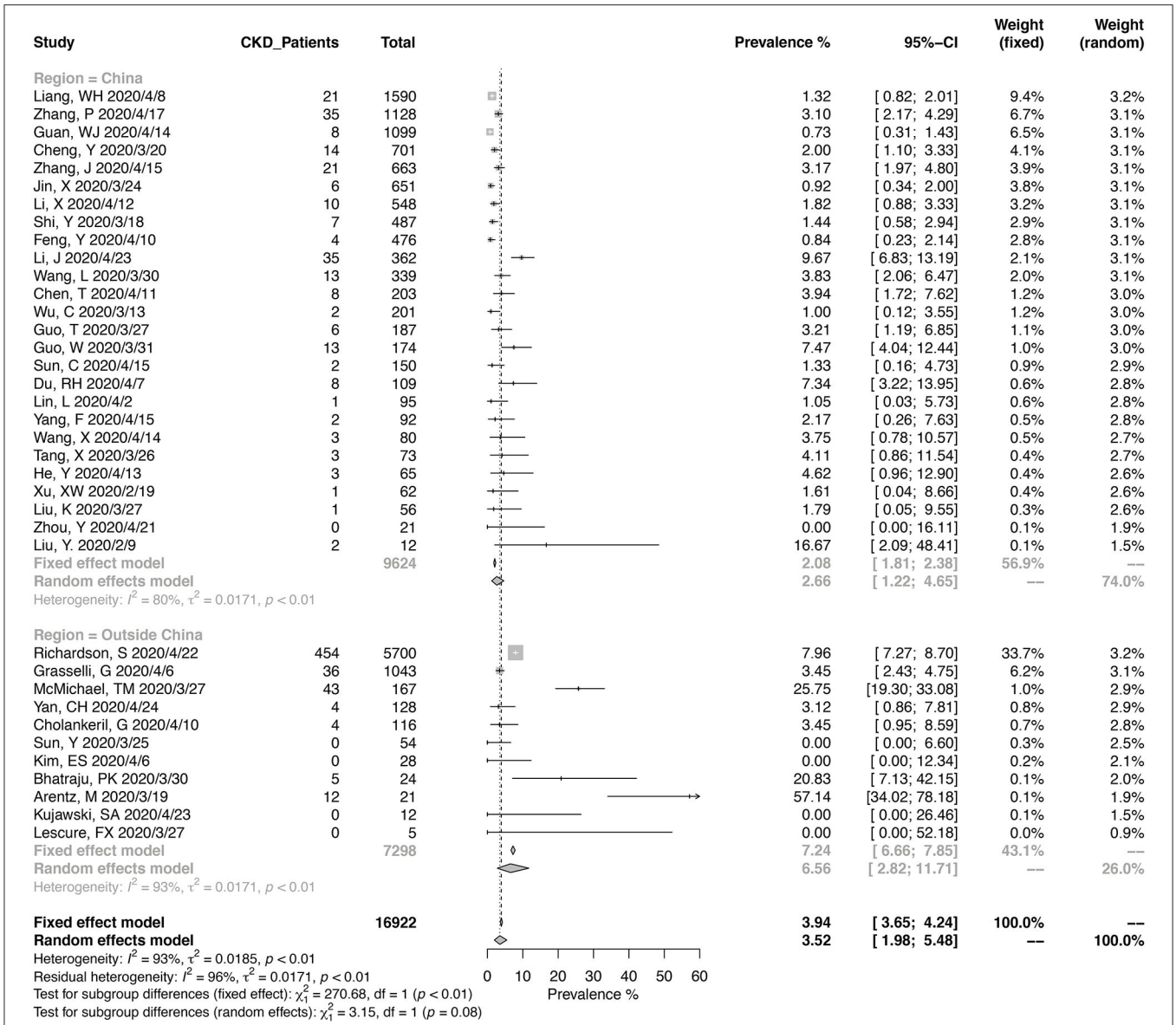

FIGURE 2 | Pooled prevalence of chronic kidney disease in coronavirus disease 2019 (COVID-19) patients.

pooled prevalences were 3.17% (95% CI, 2.15–4.39%) for CKD and 7.22% (95% CI, 2.95–13.19%) for AKI, and neither was significantly different compared to those from the peer-reviewed data ($p > 0.05$). The heterogeneity was significant for both ($I^2 > 75\%$, $p < 0.01$).

We estimated the prevalence of other comorbidities in the peer-reviewed publications (**Supplementary Figures 3–7**). The summary estimates for the prevalence of hypertension was 25.96% (95% CI, 21.15–31.08%), diabetes mellitus was 13.98% (95% CI, 11.04–17.20%), cardiovascular disease was 9.85% (95% CI, 6.66–13.59%), the cerebrovascular disease was 3.74% (95% CI, 2.09–5.85), and malignancy was 2.99% (95% CI, 2.18–3.92%). Significant heterogeneity was noted among all these studies ($I^2 > 75\%$, $p < 0.01$). The prevalences of hypertension, diabetes mellitus, and cardiovascular disease were significantly higher than that of CKD ($p < 0.05$).

Assessment for Publication Bias

The risk of publication bias was analyzed by the funnel plots and Eggers test, which suggested no significant publication bias (**Supplementary Figure 8**, all $p > 0.05$).

DISCUSSION

The global prevalence of CKD was estimated to be 9.1% recently (12), but a paucity of data was noted concerning the risk of these people in the COVID-19 pandemic. In this meta-analysis, we addressed the prevalence of kidney diseases in COVID-19

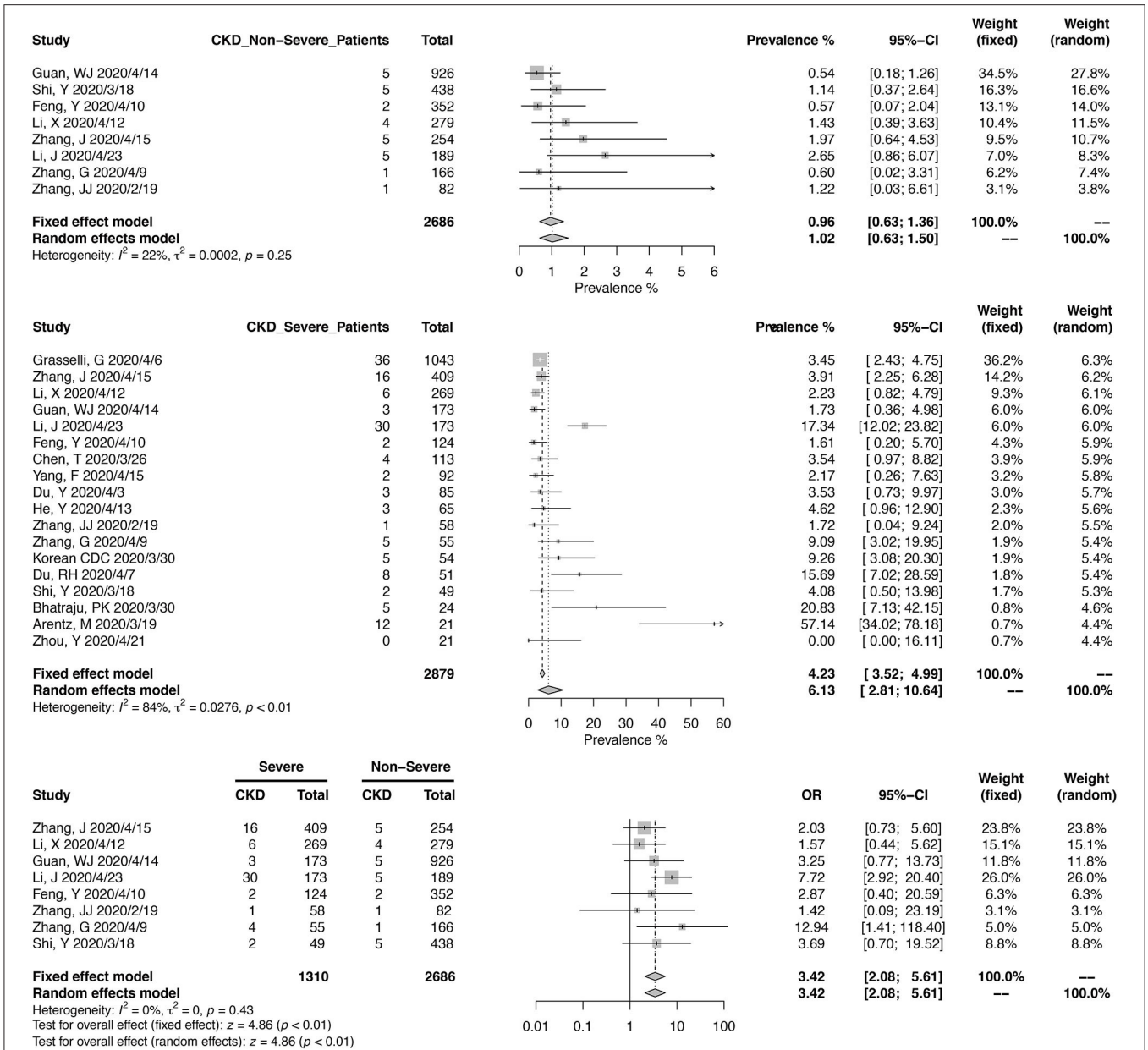

FIGURE 3 | Correlation between chronic kidney disease and disease severity in COVID-19 patients.

patients and their impacts on adverse disease courses based on the available reports. The presence of kidney diseases, in the forms of CKD and AKI, tended to develop into more severe cases and was associated with increased mortality. However, the presence of both CKD and AKI identified throughout the included cohorts seemed disproportionately scarce compared to data revealed in previous epidemiology studies (12).

Several reasons are urging us to emphasize the importance of CKD during the COVID-19 infection. First, CKD has not attracted enough awareness due to its inconspicuous course, especially in the early stage (13, 15, 64). Second, diabetes and hypertension are the leading causes of CKD in all developed countries and many developing countries, and the long-term or advanced CKD usually increases the risk of cardiovascular diseases (13, 65). To be noted, these conditions accompanying CKD are all risk factors that exacerbate the COVID-19 patients (10, 11). Third, glomerulonephritis is another relevant CKD entity, and patients falling into this category usually take immunosuppressive medicine (13). Some early reports suggested that patients with a compromised immune system, such as patients with advanced CKD or those undergoing immunosuppressives, hypothetically limited the cytokine strome in the COVID-19 infection and led to mild disease courses (66–70). This was not the case in our investigation. Either in terms

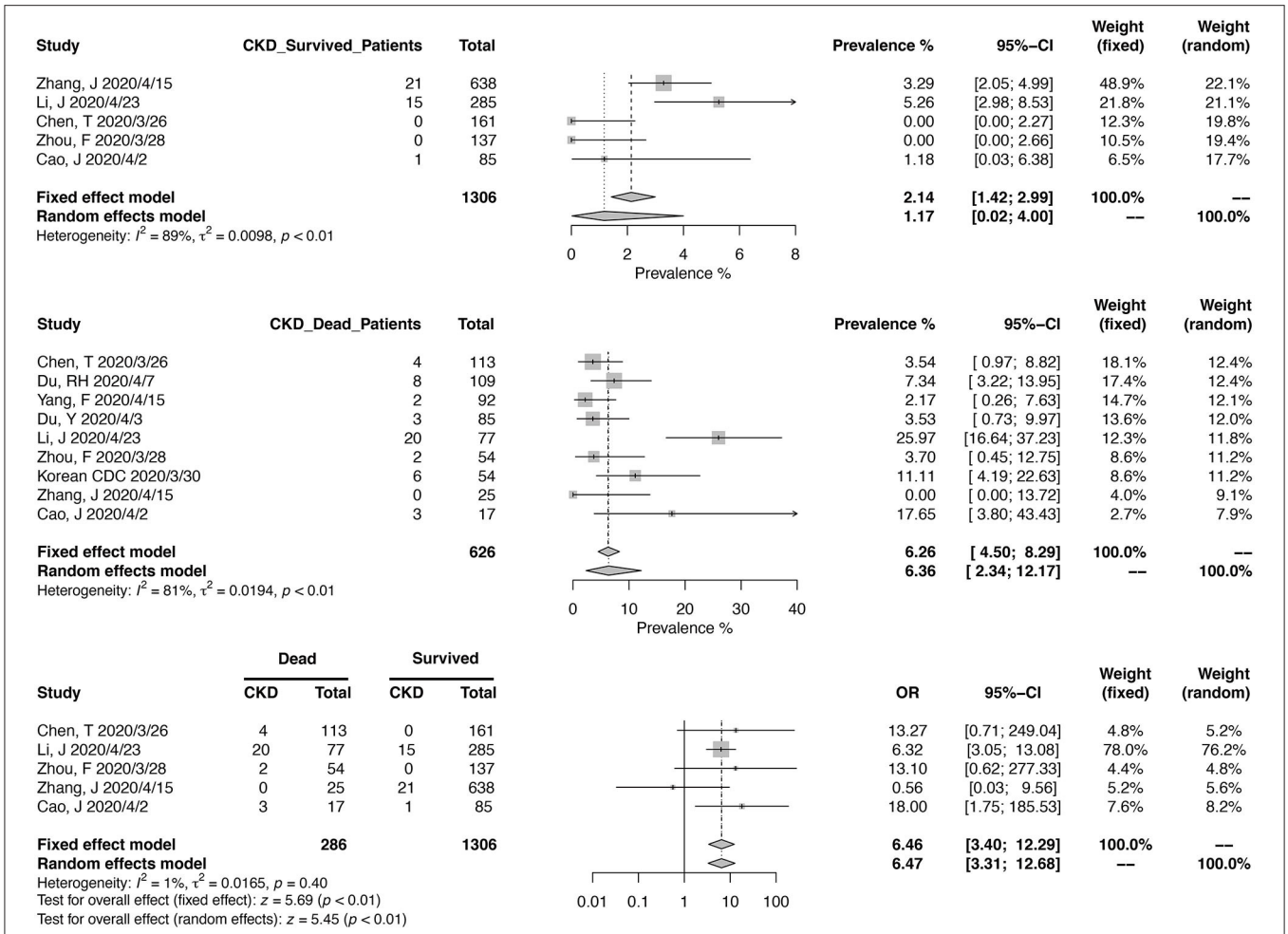

FIGURE 4 | Correlation between chronic kidney disease and mortality in COVID-19 patients.

of disease severity or mortality, we found that CKD unfavorably impacted the COVID-19 infection. Fourth, preexisting CKD is a significant risk factor for worsening of kidney function during a severe infection (71, 72). Once complicated by AKI, CKD itself was associated with a higher risk of mortality and less chance of kidney recovery (73).

Although far from detailed, the importance of AKI has been more profiled by several reports in COVID-19 patients (6, 7). More recently, several meta-analyses have proved the important prognostic values of AKI in severe COVID-19 patients (74–77). As a vital complication, the presence of AKI was associated with more adverse prognosis in the disease course. This was consistent with our findings in the current meta-analysis, which has signaled dissatisfied results associated with AKI. However, the prevalence of AKI ranged from 4 to 17% in these meta-analyses. The diagnosis criteria of AKI was not clarified in all meta-analysis, neither was the diagnosis of severe COVID-19 cases. We only included the studies referring to the Kidney Disease: Improving Global Outcomes (KDIGO) criteria of AKI diagnosis. The overlap of patients in the included studies was not addressed in these meta-analyses, which could promote bias. Moreover, the etiologies of AKI, another substantial issue (78), have not been thoroughly investigated in the current literature. Multiple factors may lead to AKI in the COVID-19 setting, such as the potential virus insulation in the kidney tissues (45), inflammatory factors (67), hemodynamic changes, volume depletion, and drug-induced damages. It is essential to respect the causes of different disease periods since they are the keys to improve kidney function and disease prognosis.

In reflection of our findings in this meta-analysis, we genuinely feel that our current prevention, control, and treatment measures for the COVID-19 have not yet been personalized. People with kidney disease have limited voice in this disease with lung-dominated involvement. As the pandemic persists, more precise prevention policies may be needed to guide patients with chronic kidney diseases, such as social distancing. Close monitoring of suspected symptoms for early recognition and interventions are important in the regular follow-ups of these patients. As in treating patients with severe COVID-19, the prevention and optimized management of AKI might help

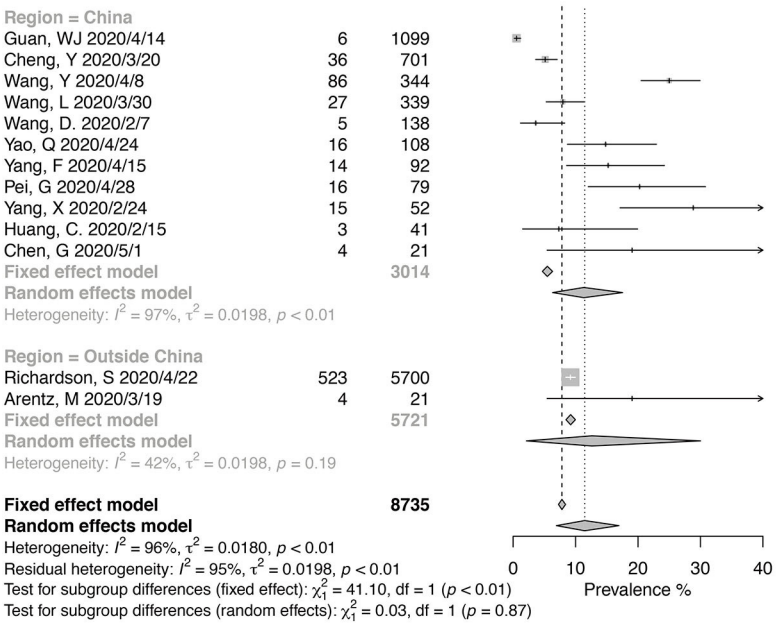

FIGURE 5 | Pooled prevalence of acute kidney injury in COVID-19 patients.

improve the prognosis, which is based on the notion that suspected intrinsic AKI accounted for the most frequent form of AKI (>80%) (6, 7). Risk factors and causes of AKI in COVID-19 are diverse and multifactorial, while severe hypoxia and hypercoagulability are the most important ones. It is necessary for intensive supporting and careful monitoring of patients with severe and critically ill pneumonia to ameliorate renal complications.

Therefore, there are some limitations to this study. First, this meta-analysis was mainly derived from retrospective cohort studies during a short period, which impaired the quality of data in several ways. A majority of studies were from China, and duplication reports of individual patients existed. We used NOS scores to evaluate the quality of included studies and matched the studies by the locations and recruitment time points to minimize the duplication in the pooled analysis. Second, the meta-analysis of prevalence was intrinsically heterogeneous, as shown in our results. Even though we performed the arcsine transformation, the heterogeneity was still significant for most of our prevalences. Third, the underreporting of CKD and AKI prevalence was a concern. Compared to hypertension and diabetes mellitus, the prevalence of CKD was disproportionally low. Meanwhile, the accurate diagnosis of AKI requires close monitoring of renal functions according to guidelines (78, 79), and defining the causes of AKI needs care differential diagnosis. Limited data were provided for further exploration. Fourth, it is difficult to profile specific confounding risk factors between renal insults and COVID-19 prognosis, based on the literature available until now. Although there is some inherited limitation in the meta-analysis, it signals some critical aspects of renal effects associated with the COVID-19 infection, providing clues for further well-designed researches.

With this meta-analysis of updated data, we found that CKD and AKI were all associated with worse prognosis of COVID-19. Patients with CKD should hence be advised to take extra precautions to minimize exposure to the virus. Physicians should also be engaged in close monitoring of COVID-19 patients with preexisting or new kidney involvements. Finally, the presence of CKD or AKI shall be regarded as essential factors in future risk stratification models for COVID-19.

METHODS

Search Strategy

A systematic review of the literature was performed according to the Preferred Reporting Items for Systemic Reviews and Meta-Analyses (PRISMA) statement. Publicly available publication list of COVID-19 living systematic review was retrieved up to April 26, 2020, containing studies on COVID-19 published on PubMed, Embase (via Ovid), bioRxiv, and medRxiv in a daily updated manner (80). We validated the list by manually searching relevant studies in the databases above (details in **Supplementary Table 1**). Additionally, we included studies that were available publicly but not on the list at the time of the search (6).

Study Selection

All studies were considered without limitations on language or publication status (peer-reviewed or preprint). Titles and abstracts were first reviewed by the investigators (YZ and QJ), and

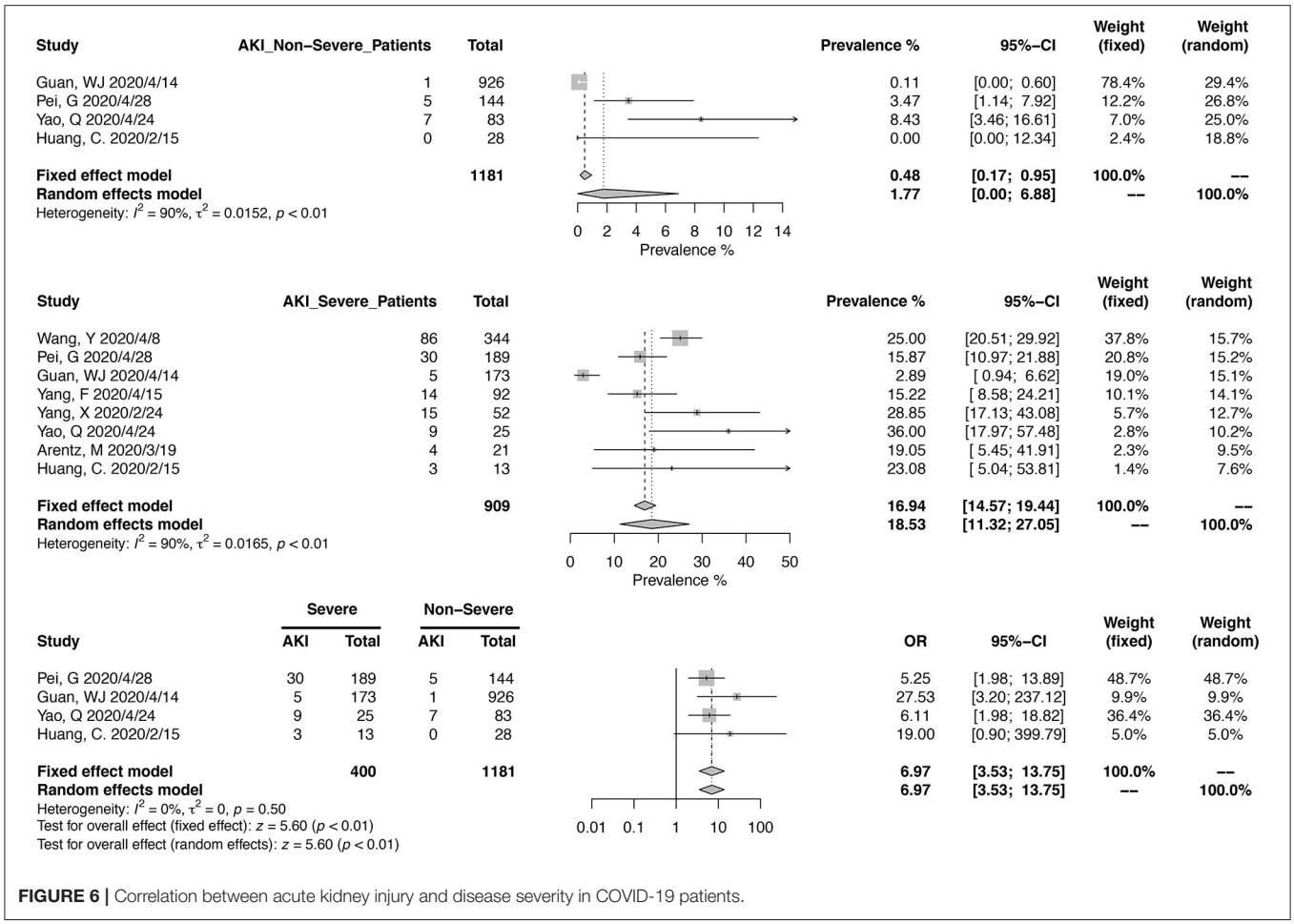

FIGURE 6 | Correlation between acute kidney injury and disease severity in COVID-19 patients.

potential COVID-19-related papers on clinical characteristics were retrieved. Duplicate studies and those reporting one patient were removed based on titles. Two investigators (QR and GC) independently determined the eligibility of studies, and dissonance was resolved through discussion with the third investigator (YZ). The inclusion criteria included the following: (1) study populations were adult COVID-19 patients with virologic proof and (2) study designs included case series, cohort studies, case–control studies, and randomized controlled trials. The exclusion criteria were the following: (1) review articles, meta-analyses, editorials or comments, and summaries; (2) studies that only report pediatric patients or one patient; (3) studies that did not report CKD and/or AKI data; and (4) studies that the diagnostic criteria of AKI were not defined.

Data Extraction and Quality Assessment

At least two independent reviewers (from YZ, QR, GC, HL, and QC) extracted the following information, including first authors, inclusion/exclusion criteria, patient's location and recruitment date, sample size, age, sex, disease severity, any morbidities (CKD, hypertension, diabetes mellitus, cardiovascular diseases, cerebrovascular diseases, or malignancies), presence of AKI, and death. Disease severity was defined according to the guideline from the American Thoracic Society and Infectious Disease Society (81), Chinese COVID-19 management guideline (82), need of ICU admission, or death. The diagnosis references of AKI were collected if available, including the 2012 KDIGO definition (78, 79) or others.

The NOS was used to evaluate the quality of enrolled studies in terms of patient selection, comparability, and results (83). Each study was scored according to the exposure (CKD or AKI) and endpoint (disease severity or prognosis) individually. The quality of the included studies was assessed independently by two independent reviewers (from YZ, QR, and GC). NOS scores of at least six were considered high-quality literature.

Data Synthesis and Statistical Analyses

To assess the prevalence of CKD or AKI and their relationship with COVID-19 disease courses, the meta-analysis was prespecified to be conducted for all the infected individuals and based on patient stratifications: (1) disease severities (mild or severe) and (2) clinical outcomes of COVID-19 (dead or survived). Studies from the same healthcare facilities were reviewed by three investigators (YZ, QR, and GC), and duplicate reports were carefully excluded.

Continuous variables were expressed as median [interquartile range (IQR)] or mean [±standard deviation (SD)]. The

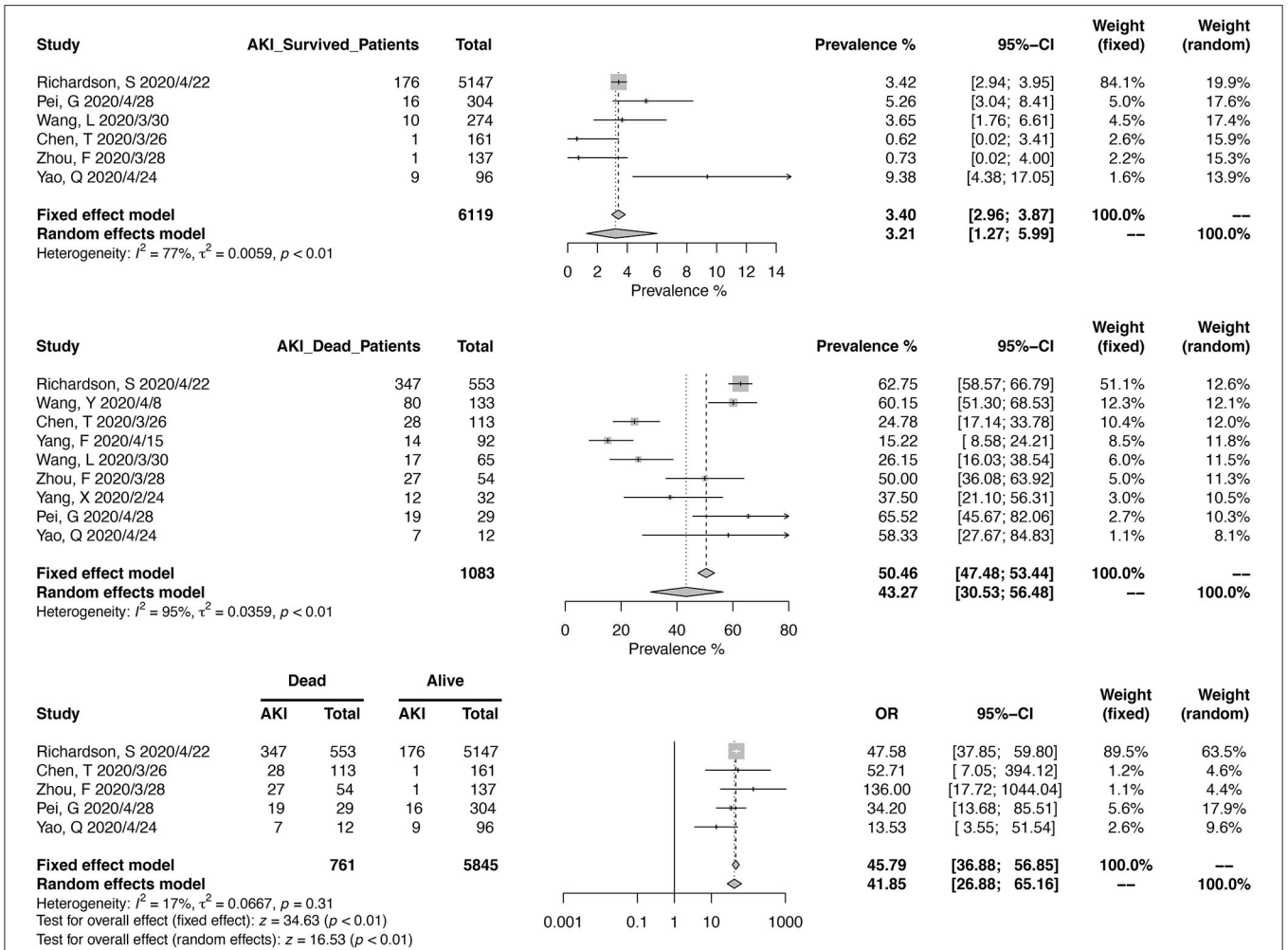

FIGURE 7 | Correlation between acute kidney injury and mortality in COVID-19 patients.

prevalence of CKD or AKI was expressed as proportion and 95% confidence interval (95% CI) using the random-effects model. Odds ratios (ORs) with 95% CI were calculated in evaluating the risk of severe diseases or death in patients with CKD or AKI separately. Heterogeneity among studies was detected with the Cochrane's Q-test, and a $p < 0.05$ was considered as significant heterogeneity. The I^2 statistic was performed to evaluate the contribution of heterogeneity in the overall study variation. τ^2 was calculated to estimate the between-study variance using the Paule–Mandel method, and the 95% CI was calculated using the Q-Profile method. Subgroup analysis was performed on the patients' locations (China or outside of China), disease severities (mild or severe), and prognosis (dead or survived). The Q test for heterogeneity was used to test the significance of the overall between-groups variance with the assumption of the shared common τ^2 across subgroups. All statistics were performed using the meta package (Version 4.11-0) in the R program (Version 3.6.3. R core team). We used arcsine transformation and inverse variance method to implement the calculation of the overall prevalence of CKD or AKI, and the confidence interval was calculated with the Clopper–Pearson method. All data shown in Forrest plots and results section was back transformed to the raw prevalences.

DATA AVAILABILITY STATEMENT

The raw data supporting the conclusions of this article will be made available by the authors, without undue reservation.

AUTHOR CONTRIBUTIONS

YZ, QR, and GC were responsible for study design, literature research, data extraction, data synthesis, and manuscript drafting. QJ, QC, and HL helped in data extraction. KZ and YQ helped in study design and manuscript revision. XL were responsible for study design, organizing, and manuscript revision. All authors contributed to the article and approved the submitted version.

FUNDING

This work was supported by the National Natural Sciences Foundation of China (Grant No. 81801632 to YZ).

SUPPLEMENTARY MATERIAL

The Supplementary Material for this article can be found online at: https://www.frontiersin.org/articles/10.3389/fmed.2020.588301/full#supplementary-material

REFERENCES

1. Organization WH. *WHO Director-General's Opening Remarks at the Media Briefing on COVID-19*. Geneva: WHO (2020).
2. JHU. *COVID-19 Dashboard by the Center for Systems Science and Engineering (CSSE) at Johns Hopkins University*. Baltimore, MD: JHU (2020).
3. Sun P, Qie S, Liu Z, Ren J, Li K, Xi J. Clinical characteristics of hospitalized patients with SARS-CoV-2 infection: a single arm meta-analysis. *J Med Virol.* (2020) 92:612–7. doi: 10.1002/jmv.25735
4. Guan WJ, Ni ZY, Hu Y, Liang WH, Ou CQ, He JX, et al. China medical treatment expert group for: clinical characteristics of coronavirus disease 2019 in China. *N Engl J Med.* (2020) 382:1708–20. doi: 10.1056/NEJMoa2002032
5. Yang X, Yu Y, Xu J, Shu H, Xia J, Liu H, et al. Clinical course and outcomes of critically ill patients with SARS-CoV-2 pneumonia in Wuhan, China: a single-centered, retrospective, observational study. *Lancet Respir Med.* (2020) 8:475–81. doi: 10.1016/S2213-2600(20)30079-5
6. Pei G, Zhang Z, Peng J, Liu L, Zhang C, Yu C, et al. Renal Involvement and Early Prognosis in Patients with COVID-19 Pneumonia. *J Am Soc Nephrol.* (2020) 31:1157–65. doi: 10.1681/ASN.2020030276
7. Cheng Y, Luo R, Wang K, Zhang M, Wang Z, Dong L, et al. Kidney disease is associated with in-hospital death of patients with COVID-19. *Kidney Int.* (2020) 97:829–38. doi: 10.1016/j.kint.2020.03.005
8. Su H, Yang M, Wan C, Yi LX, Tang F, Zhu HY, et al. Renal histopathological analysis of 26 postmortem findings of patients with COVID-19 in China. *Kidney Int.* (2020) 98:219–27. doi: 10.1016/j.kint.2020.04.003
9. Chen T, Wu D, Chen H, Yan W, Yang D, Chen G, et al. Clinical characteristics of 113 deceased patients with coronavirus disease 2019: retrospective study. *BMJ.* (2020) 368:m1091. doi: 10.1136/bmj.m1091
10. The Novel Coronavirus Pneumonia Emergency Response Epidemiology Team. The epidemiological characteristics of an outbreak of 2019 novel coronavirus diseases (COVID-19) — China, 2020. *China CDC Weekly.* (2020) 2:113–22. doi: 10.46234/ccdcw2020.032
11. Yang J, Zheng Y, Gou X, Pu K, Chen Z, Guo Q, et al. Prevalence of comorbidities and its effects in patients infected with SARS-CoV-2: a systematic review and meta-analysis. *Int J Infect Dis.* (2020) 94:91–95. doi: 10.1016/j.ijid.2020.03.017
12. GBDCKD Collaboration. Global, regional, and national burden of chronic kidney disease, 1990-2017: a systematic analysis for the global burden of disease study 2017. *Lancet.* (2020) 395:709–33. doi: 10.1016/S0140-6736(20)30045-3
13. Jha V, Garcia-Garcia G, Iseki K, Li Z, Naicker S, Plattner B, et al. Chronic kidney disease: global dimension and perspectives. *Lancet.* (2013) 382:260–72. doi: 10.1016/S0140-6736(13)60687-X
14. Hoste EAJ, Kellum JA, Selby NM, Zarbock A, Palevsky PM, Bagshaw SM, et al. Global epidemiology and outcomes of acute kidney injury. *Nat Rev Nephrol.* (2018) 14:607–25. doi: 10.1038/s41581-018-0052-0
15. Liu ZH. Nephrology in china. *Nat Rev Nephrol.* (2013) 9:523–8. doi: 10.1038/nrneph.2013.146
16. Wang B, Li R, Lu Z, Huang Y. Does comorbidity increase the risk of patients with COVID-19: evidence from meta-analysis. *Aging.* (2020) 12:6049–57. doi: 10.18632/aging.103000
17. Yao Q, Wang P, Wang X, Qie G, Meng M, Tong X, et al. A retrospective study of risk factors for severe acute respiratory syndrome coronavirus 2 infections in hospitalized adult patients. *Pol Arch Intern Med.* (2020) 130:390–9. doi: 10.20452/pamw.15312
18. Li J, Wang X, Chen J, Zhang H, Deng A. Association of renin-angiotensin system inhibitors with severity or risk of death in patients with hypertension hospitalized for coronavirus disease 2019 (COVID-19) infection in Wuhan, China. *JAMA Cardiol.* (2020) 5:825–30. doi: 10.1001/jamacardio.2020.1624
19. Zhou Y, Han T, Chen J, Hou C, Hua L, He S, et al. Clinical and autoimmune characteristics of severe and critical cases of COVID-19. *Clin Transl Sci.* (2020). doi: 10.1111/cts.12805. [Epub ahead of print].
20. Zhang G, Hu C, Luo L, Fang F, Chen Y, Li J, et al. Clinical features and short-term outcomes of 221 patients with COVID-19 in Wuhan, China. *J Clin Virol.* (2020) 127:104364. doi: 10.1016/j.jcv.2020.104364
21. Zhang J, Wang X, Jia X, Li J, Hu K, Chen G, et al. Risk factors for disease severity, unimprovement, and mortality in COVID-19 patients in Wuhan, China. *Clin Microbiol Infect.* (2020) 26:767–72. doi: 10.1016/j.cmi.2020.04.012
22. Wang X, Liu W, Zhao J, Lu Y, Wang X, Yu C, et al. Clinical characteristics of 80 hospitalized frontline medical workers infected with COVID-19 in Wuhan, China. *J Hosp Infect.* (2020) 105:399–403. doi: 10.1016/j.jhin.2020.04.019
23. Li X, Xu S, Yu M, Wang K, Tao Y, Zhou Y, et al. Risk factors for severity and mortality in adult COVID-19 inpatients in Wuhan. *J Allergy Clin Immunol.* (2020) 146:110–8. doi: 10.1016/j.jaci.2020.04.006
24. Yang F, Shi S, Zhu J, Shi J, Dai K, Chen X. Analysis of 92 deceased patients with COVID-19. *J Med Virol.* (2020). doi: 10.1002/jmv.25891. [Epub ahead of print].
25. Cholankeril G, Podboy A, Aivaliotis VI, Tarlow B, Pham EA, Spencer SP, et al. High prevalence of concurrent gastrointestinal manifestations in patients with severe acute respiratory syndrome coronavirus 2: early experience from California. *Gastroenterology.* (2020) 159:775–7. doi: 10.1053/j.gastro.2020.04.008
26. He Y, Li W, Wang Z, Chen H, Tian L, Liu D. Nosocomial infection among patients with COVID-19: a retrospective data analysis of 918 cases from a single center in Wuhan, China. *Infect Control Hosp Epidemiol.* (2020) 41:982–3. doi: 10.1017/ice.2020.126
27. Chen T, Dai Z, Mo P, Li X, Ma Z, Song S, et al. Clinical characteristics and outcomes of older patients with coronavirus disease 2019 (COVID-19) in Wuhan, China: a single-centered, retrospective study. *J Gerontol A Biol Sci Med Sci.* (2020) 75:1788–95. doi: 10.1093/gerona/glaa089
28. Wang Y, Lu X, Li Y, Chen H, Chen T, Su N, et al. Clinical course and outcomes of 344 intensive care patients with COVID-19. *Am J Respir Crit Care Med.* (2020) 201:1430–4. doi: 10.1164/rccm.202003-0736LE
29. Grasselli G, Zangrillo A, Zanella A, Antonelli M, Cabrini L, Castelli A, et al. Baseline characteristics and outcomes of 1591 patients infected with SARS-CoV-2 admitted to ICUs of the Lombardy Region, Italy. *JAMA.* (2020) 323:1574–81. doi: 10.1001/jama.2020.5394
30. Lin L, Jiang X, Zhang Z, Huang S, Zhang Z, Fang Z, et al. Gastrointestinal symptoms of 95 cases with SARS-CoV-2 infection. *Gut.* (2020) 69:997–1001. doi: 10.1136/gutjnl-2020-321013
31. Wang L, He W, Yu X, Hu D, Bao M, Liu H, et al. Coronavirus disease 2019 in elderly patients: characteristics and prognostic factors based on 4-week follow-up. *J Infect.* (2020) 80:639–45. doi: 10.1016/j.jinf.2020.03.019
32. Cao J, Tu WJ, Cheng W, Yu L, Liu YK, Hu X, et al. clinical features and short-term outcomes of 102 patients with coronavirus disease 2019 in Wuhan, China. *Clin Infect Dis.* (2020) 71:748–55. doi: 10.1093/cid/ciaa243
33. Guo W, Li M, Dong Y, Zhou H, Zhang Z, Tian C, et al. Diabetes is a risk factor for the progression and prognosis of COVID-19. *Diabetes Metab Res Rev.* (2020). doi: 10.1002/dmrr.3319. [Epub ahead of print].
34. Tang X, Du RH, Wang R, Cao TZ, Guan LL, Yang CQ, et al. Comparison of hospitalized patients with ARDS caused by COVID-19 and H1N1. *Chest.* (2020) 158:195–205. doi: 10.1016/j.chest.2020.03.032
35. McMichael TM, Currie DW, Clark S, Pogosjans S, Kay M, Schwartz NG, et al. Epidemiology of Covid-19 in a long-term

care facility in King County, Washington. *N Engl J Med.* (2020) 382:2005–11. doi: 10.1056/NEJMoa2005412
36. Guo T, Fan Y, Chen M, Wu X, Zhang L, He T, et al. Cardiovascular implications of fatal outcomes of patients with coronavirus disease 2019 (COVID-19). *JAMA Cardiol.* (2020) 5:811–8. doi: 10.1001/jamacardio.2020.1017
37. Chen G, Wu D, Guo W, Cao Y, Huang D, Wang H, et al. Clinical and immunological features of severe and moderate coronavirus disease 2019. *J Clin Invest.* (2020) 130:2620–9. doi: 10.1172/JCI137244
38. Arentz M, Yim E, Klaff L, Lokhandwala S, Riedo FX, Chong M, et al. Characteristics and outcomes of 21 critically ill patients with COVID-19 in Washington State. *JAMA.* (2020) 323:1612–4. doi: 10.1001/jama.2020.4326
39. Shi Y, Yu X, Zhao H, Wang H, Zhao R, Sheng J. Host susceptibility to severe COVID-19 and establishment of a host risk score: findings of 487 cases outside Wuhan. *Crit Care.* (2020) 24:108. doi: 10.1186/s13054-020-2833-7
40. Liu K, Chen Y, Lin R, Han K. Clinical features of COVID-19 in elderly patients: a comparison with young and middle-aged patients. *J Infect.* (2020) 80:e14–8. doi: 10.1016/j.jinf.2020.03.005
41. Wu C, Chen X, Cai Y, Xia J, Zhou X, Xu S, et al. Risk factors associated with acute respiratory distress syndrome and death in patients with coronavirus disease 2019 Pneumonia in Wuhan, China. *JAMA Intern Med.* (2020) 180:934–43. doi: 10.1001/jamainternmed.2020.0994
42. Zhang JJ, Dong X, Cao YY, Yuan YD, Yang YB, Yan YQ, et al. Clinical characteristics of 140 patients infected with SARS-CoV-2 in Wuhan, China. *Allergy.* (2020) 75:1730–41. doi: 10.1111/all.14238
43. Liu Y, Yang Y, Zhang C, Huang F, Wang F, Yuan J, et al. Clinical and biochemical indexes from 2019-nCoV infected patients linked to viral loads and lung injury. *Sci China Life Sci.* (2020) 63:364–74. doi: 10.1007/s11427-020-1643-8
44. Wang D, Hu B, Hu C, Zhu F, Liu X, Zhang J, et al. Clinical characteristics of 138 hospitalized patients with 2019 novel coronavirus-infected pneumonia in Wuhan, China. *JAMA.* (2020) 323:1061–9. doi: 10.1001/jama.2020.1585
45. Huang C, Wang Y, Li X, Ren L, Zhao J, Hu Y, et al. Clinical features of patients infected with 2019 novel coronavirus in Wuhan, China. *Lancet.* (2020) 395:497–506. doi: 10.1016/S0140-6736(20)30183-5
46. Xu XW, Wu XX, Jiang XG, Xu KJ, Ying LJ, Ma CL, et al. Clinical findings in a group of patients infected with the 2019 novel coronavirus (SARS-Cov-2) outside of Wuhan, China: retrospective case series. *BMJ.* (2020) 368:m606. doi: 10.1136/bmj.m606
47. Zhou F, Yu T, Du R, Fan G, Liu Y, Liu Z, et al. Clinical course and risk factors for mortality of adult inpatients with COVID-19 in Wuhan, China: a retrospective cohort study. *Lancet.* (2020) 395:1054–62. doi: 10.1016/S0140-6736(20)30566-3
48. Yan CH, Faraji F, Prajapati DP, Ostrander BT, DeConde AS. Self-reported olfactory loss associates with outpatient clinical course in COVID-19. *Int Forum Allergy Rhinol.* (2020) 10:821–31. doi: 10.1002/alr.22592
49. The COVID-19 Investigation Team. Clinical and virologic characteristics of the first 12 patients with coronavirus disease 2019 (COVID-19) in the United States. *Nat Med.* (2020) 26:861–8. doi: 10.1038/s41591-020-0877-5
50. Richardson S, Hirsch JS, Narasimhan M, Crawford JM, McGinn T, Davidson KW, et al. Presenting characteristics, comorbidities, and outcomes among 5700 patients hospitalized with COVID-19 in the New York City area. *JAMA.* (2020) 323:2052–9. doi: 10.1001/jama.2020.6775
51. Chen R, Liang W, Jiang M, Guan W, Zhan C, Wang T, et al. Medical treatment expert group for: risk factors of fatal outcome in hospitalized subjects with coronavirus disease 2019 from a nationwide analysis in China. *Chest.* (2020) 158:97–105. doi: 10.1016/j.chest.2020.04.010
52. Zhang P, Zhu L, Cai J, Lei F, Qin JJ, Xie J, et al. Association of inpatient use of angiotensin-converting enzyme inhibitors and angiotensin ii receptor blockers with mortality among patients with hypertension hospitalized with COVID-19. *Circ Res.* (2020) 126:1671–81. doi: 10.1161/CIRCRESAHA.120.317134
53. Sun C, Zhang XB, Dai Y, Xu XZ, Zhao J. Clinical analysis of 150 cases of 2019 novel coronavirus infection in Nanyang City, Henan province. *Zhonghua Jie He He Hu Xi Za Zhi.* (2020) 43:503–8. doi: 10.3760/cma.j.cn112147-20200224-00168
54. Feng Y, Ling Y, Bai T, Xie Y, Huang J, Li J, et al. COVID-19 with different severities: a multicenter study of clinical features. *Am J Respir Crit Care Med.* (2020) 201:1380–8. doi: 10.1164/rccm.202002-0445OC
55. Liang WH, Guan WJ, Li CC, Li YM, Liang HR, Zhao Y, et al. Clinical characteristics and outcomes of hospitalised patients with COVID-19 treated in hubei (epicentre) and outside hubei (non-epicentre): a nationwide analysis of China. *Eur Respir J.* (2020) 55:2000562. doi: 10.1183/13993003.00562-2020
56. Du RH, Liu LM, Yin W, Wang W, Guan LL, Yuan ML, et al. Hospitalization and critical care of 109 decedents with COVID-19 Pneumonia in Wuhan, China. *Ann Am Thorac Soc.* (2020) 17:839–46. doi: 10.1513/AnnalsATS.202003-225OC
57. Du Y, Tu L, Zhu P, Mu M, Wang R, Yang P, et al. Clinical features of 85 fatal cases of COVID-19 from Wuhan. A retrospective observational study. *Am J Respir Crit Care Med.* (2020) 201:1372–9. doi: 10.1164/rccm.202003-0543OC
58. Kim ES, Chin BS, Kang CK, Kim NJ, Kang YM, Choi JP, et al. Korea national committee for clinical management of: clinical course and outcomes of patients with severe acute respiratory syndrome coronavirus 2 infection: a preliminary report of the first 28 patients from the korean cohort study on COVID-19. *J Korean Med Sci.* (2020) 35:e142. doi: 10.3346/jkms.2020.35.e142
59. Korean Society of Infectious DC. Korea centers for disease and prevention: analysis on 54 mortality cases of coronavirus disease 2019 in the Republic of Korea from January 19 to March 10, 2020. *J Korean Med Sci.* (2020) 35:e132. doi: 10.3346/jkms.2020.35.e132
60. Bhatraju PK, Ghassemieh BJ, Nichols M, Kim R, Jerome KR, Nalla AK, et al. Covid-19 in critically ill patients in the Seattle Region - case series. *N Engl J Med.* (2020) 382:2012–2022. doi: 10.1056/NEJMoa2004500
61. Lescure FX, Bouadma L, Nguyen D, Parisey M, Wicky PH, Behillil S, et al. Clinical and virological data of the first cases of COVID-19 in Europe: a case series. *Lancet Infect Dis.* (2020) 20:697–706. doi: 10.1016/S1473-3099(20)30200-0
62. Jin X, Lian JS, Hu JH, Gao J, Zheng L, Zhang YM, et al. Epidemiological, clinical and virological characteristics of 74 cases of coronavirus-infected disease 2019 (COVID-19) with gastrointestinal symptoms. *Gut.* (2020) 69:1002–9. doi: 10.1136/gutjnl-2020-320926
63. Sun Y, Koh V, Marimuthu K, Ng OT, Young B, Vasoo S, et al. National centre for infectious diseases: epidemiological and clinical predictors of COVID-19. *Clin Infect Dis.* (2020) 71:786–792. doi: 10.1093/cid/ciaa322
64. Hasan M, Sutradhar I, Gupta RD, Sarker M. Prevalence of chronic kidney disease in South Asia: a systematic review. *BMC Nephrol.* (2018) 19:291. doi: 10.1186/s12882-018-1072-5
65. Mann JF, Gerstein HC, Pogue J, Bosch J, Yusuf S. Renal insufficiency as a predictor of cardiovascular outcomes and the impact of ramipril: the HOPE randomized trial. *Ann Intern Med.* (2001) 134:629–36. doi: 10.7326/0003-4819-134-8-200104170-00007
66. Wang R, Liao C, He H, Hu C, Wei Z, Hong Z, et al. COVID-19 in hemodialysis patients: a report of 5 cases. *Am J Kidney Dis.* (2020) 76:141–3. doi: 10.1053/j.ajkd.2020.03.009
67. Mehta P, McAuley DF, Brown M, Sanchez E, Tattersall RS, Manson JJ, et al. Hlh across speciality collaboration: COVID-19: consider cytokine storm syndromes and immunosuppression. *Lancet.* (2020) 395:1033–4. doi: 10.1016/S0140-6736(20)30628-0
68. Ke C, Wang Y, Zeng X, Yang CZ. Hu: 2019 Novel coronavirus disease (COVID-19) in hemodialysis patients: a report of two cases. *Clin Biochem.* (2020) 81:9–12. doi: 10.1016/j.clinbiochem.2020.04.008
69. Ritchie AI, Singanayagam A. Immunosuppression for hyperinflammation in COVID-19: a double-edged sword? *Lancet.* (2020) 395:1111. doi: 10.1016/S0140-6736(20)30691-7
70. Gandolfini I, Delsante M, Fiaccadori E, Zaza G, Manenti L, Degli Antoni A, et al. COVID-19 in kidney transplant recipients. *Am J Transplant.* 20:1941–43. doi: 10.1111/ajt.15891
71. He L, Wei Q, Liu J, Yi M, Liu Y, Liu H, et al. AKI on CKD: heightened injury, suppressed repair, and the underlying mechanisms. *Kidney Int.* (2017) 92:1071–83. doi: 10.1016/j.kint.2017.06.030
72. Findlay M, Donaldson K, Robertson S, Almond A, Flynn R, Isles C. Chronic kidney disease rather than illness severity predicts medium- to long-term mortality and renal outcome after acute kidney injury. *Nephrol Dial Transplant.* (2015) 30:594–8. doi: 10.1093/ndt/gfu185

73. Zhou Q, Zhao C, Xie D, Xu D, Bin J, Chen P, et al. Acute and acute-on-chronic kidney injury of patients with decompensated heart failure: impact on outcomes. *BMC Nephrol.* (2012) 13:51. doi: 10.1186/1471-2369-13-51
74. Shao M, Li X, Liu F, Tian T, Luo J, Yang Y. Acute kidney injury is associated with severe infection and fatality in patients with COVID-19: a systematic review and meta-analysis of 40 studies and 24,527 patients. *Pharmacol Res.* (2020) 161:105107. doi: 10.1016/j.phrs.2020.105107
75. Wu T, Zuo Z, Kang S, Jiang L, Luo X, Xia Z, et al. Multi-organ dysfunction in patients with COVID-19: a systematic review and meta-analysis. *Aging Dis.* (2020) 11:874–94. doi: 10.14336/AD.2020.0520
76. Yang X, Jin Y, Li R, Zhang Z, Sun R, Chen D. Prevalence and impact of acute renal impairment on COVID-19: a systematic review and meta-analysis. *Crit Care.* (2020) 24:356. doi: 10.1186/s13054-020-03065-4
77. Robbins-Juarez SY, Qian L, King KL, Stevens JS, Husain SA, Radhakrishnan J, et al. Outcomes for patients with COVID-19 and acute kidney injury: a systematic review and meta-analysis. *Kidney Int Rep.* (2020) 5:1149–60. doi: 10.1016/j.ekir.2020.06.013
78. KDIGO. KDIGO clinical practice guideline for acute kidney injury. *Kidney int.* (2012) 2:138. doi: 10.1038/kisup.2012.1
79. Khwaja. KDIGO clinical practice guidelines for acute kidney injury. *Nephron Clin Pract.* (2012) 120:c179–84. doi: 10.1159/000339789
80. Institute of Social and Preventive Medicine. *Living evidence on COVID-19.* Bern: ISPM (2020).
81. Metlay JP, Waterer GW, Long AC, Anzueto A, Brozek J, Crothers K, et al. Diagnosis and treatment of adults with community-acquired Pneumonia. An official clinical practice guideline of the American thoracic society and infectious diseases society of America. *Am J Respir Crit Care Med.* (2019) 200:e45–67. doi: 10.1164/rccm.201908-1581ST
82. National Health Commission of the People's Republic of China. *Diagnosis and Treatment Protocols of Pneumonia caused by a Novel Coronavirus.* Beijing: National Health Commission of the People's Republic of China (2020).
83. Stang A. Critical evaluation of the Newcastle-Ottawa scale for the assessment of the quality of nonrandomized studies in meta-analyses. *Eur J Epidemiol.* (2010) 25:603–5. doi: 10.1007/s10654-010-9491-z

Conflict of Interest: The authors declare that the research was conducted in the absence of any commercial or financial relationships that could be construed as a potential conflict of interest.

frontiers in Physiology

ORIGINAL RESEARCH
published: 10 November 2020
doi: 10.3389/fphys.2020.587204

Novel Potential Biomarker of Adult Cardiac Surgery-Associated Acute Kidney Injury

Zujun Chen[1†], Zhengliang Hu[1†], Yiqing Hu[1], Yixuan Sheng[2], Yuan Li[1] and Jiangping Song[1*]*

[1] State Key Laboratory of Cardiovascular Disease, Department of Cardiac Surgery, National Center for Cardiovascular Diseases, Fuwai Hospital, Chinese Academy of Medical Sciences and Peking Union Medical College, Beijing, China, [2] Department of Cardiovascular Surgery, Guangzhou First People's Hospital, School of Medicine, South China University of Technology, Guangzhou, China

Background: Acute kidney injury (AKI) occurs in about 30% of patients with cardiac surgery, but the pathogenesis of cardiac surgery-associated acute kidney injury (CSA-AKI) remains unclear and there are no predictive biomarkers or diagnostic criteria specific for CSA-AKI beyond the general clinical variables for AKI like serum creatinine (SCr).

Methods and Results: We measured the plasma levels of 48 cytokines within 24 h after cardiac surgery in a total of 306 adult patients including 204 with and 102 without AKI, and then evaluated the diagnostic efficacy of these cytokines for the development of CSA-AKI via ANOVA and Pearson correlation analysis. Among these 48 cytokines, 20 of them were significantly different in the AKI patients compared with the non-AKI patients. In particularly, 13 cytokines displayed tremendous changes with the $P < 1E^{-5}$. Moreover, 10 of the 48 cytokines in the plasma were significantly different among the patients with different stages of AKI. Specifically, 6 cytokines exhibited immense differences with the $P < 1E^{-5}$. Additionally, 7 of the 48 cytokines have the correlation coefficient of $r > 0.5$ with the postoperative changes of SCr after cardiac surgery.

Conclusion: Taken all the results together, IFN-γ and SCGF-β were the most relevant two cytokines that were not only remarkably changed in adult CSA-AKI patients during the first 24 h after cardiac surgery, but also significantly correlated with the postoperative changes of SCr after cardiac surgery. Therefore, IFN-γ and SCGF-β might be novel predictive plasma biomarker, as well as potential therapeutic targets specific for adult CSA-AKI.

Keywords: biomarker, acute kidney injury, cytokines, IFN-γ, SCGF-β

OPEN ACCESS

Edited by:
Natalia Lopez-Andres, NavarraBiomed, Spain

Reviewed by:
Anand R. Nair, Cedars Sinai Medical Center, United States
Hong Jiang, Zhejiang University, China

****Correspondence:***
Yuan Li
drleey@hotmail.com
Jiangping Song
fwsongjiangping@126.com

[†]These authors have contributed equally to this work

Specialty section:
This article was submitted to Renal and Epithelial Physiology, a section of the journal Frontiers in Physiology

Received: *25 July 2020*
Accepted: *13 October 2020*
Published: *10 November 2020*

Citation:
Chen Z, Hu Z, Hu Y, Sheng Y, Li Y and Song J (2020) Novel Potential Biomarker of Adult Cardiac Surgery-Associated Acute Kidney Injury. Front. Physiol. 11:587204. doi: 10.3389/fphys.2020.587204

INTRODUCTION

Acute renal injury (AKI), characterized by an abrupt loss of kidney function with sudden reduction of glomerular filtration rate (GFR) as well as dramatic retention of nitrogenous waste products, is a common clinical syndrome after cardiac surgery with an incidence of about 30%. The cardiac surgery-associated acute kidney injury (CSA-AKI) is associated with a series of postoperative

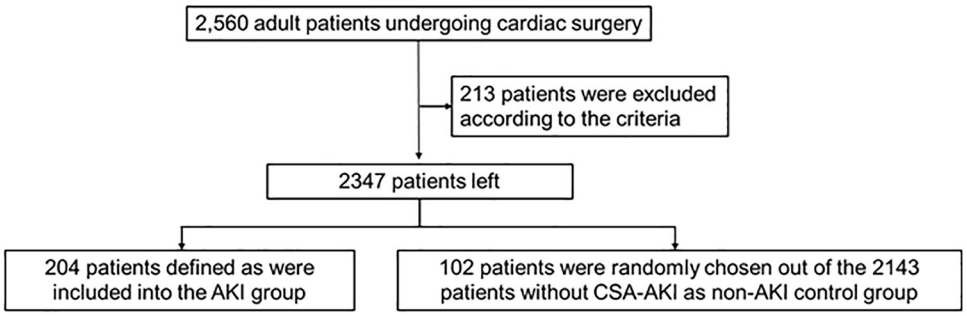

FIGURE 1 | Flowchart of patients selection.

adverse events, including prolonged intensive care, extended hospital stay, and increased patient mortality (Brinkman et al., 2015). According to the Kidney Disease Improving Global Outcomes (KDIGO), the diagnosis of AKI is generally based on a criteria of an increase in serum creatinine (SCr) by ≥0.3 mg/dl (26.5 μmol/L) within 48 h or an increase in SCr to 1.5 times of the baseline (Arsalan et al., 2018). Even though significant differences exist between CSA-AKI and other types of AKI in etiology, pathophysiology, symptoms and treatment, there is currently no available predictive biomarkers or diagnostic criteria specific for CSA-AKI beyond the general clinical variables for AKI, such as SCr and cystatin C.

A recent prospective cohort study assessed the correlation of a set of urinary and plasma biomarkers with the development of AKI in 408 children from 1 month old to 18 years old undergoing cardiac surgery. They found that among these biomarkers, plasma IL-8, a potent proinflammatory cytokine, exhibited the best discrimination for pediatric CSA-AKI (Greenberg et al., 2018). Several studies have also shown the association of some urinary or plasma biomarkers with the tubular damage or inflammatory response in adult CSA-AKI, but the prediction probability of these factors for the progression of AKI following cardiac surgery in adult patients have not been evaluated yet (Burke-Gaffney et al., 2014; Brinkman et al., 2015; Greenberg et al., 2015; de Fontnouvelle et al., 2017; Arsalan et al., 2018).

In the present study, we measured the plasma levels of 48 cytokines within 24 h after cardiac surgery in 204 adult AKI patients, as well as 102 non-AKI patients, and then evaluated the diagnostic efficacy of these cytokines for the development of CSA-AKI via ANOVA and Pearson correlation analysis.

MATERIALS AND METHODS

Study Design

This study was approved by the ethics committee of Fuwai hospital and all participants signed the informed consent. A total of 2,560 adult patients undergoing cardiac surgery at Fuwai hospital were registered during the enrollment period from 12/6/2017 to 11/27/2018, of which 213 patients were excluded according to the criteria including preoperative history of renal insufficiency, preoperative creatinine levels ≥2 times of the age-adjusted normal range, or ≥2 cardiac surgeries within a year. Among the remaining 2,347 patients, 204 patients were defined as CSA-AKI and all of them were included into the AKI group. Then, 102 patients were randomly chosen out of the 2,143 patients without CSA-AKI as non-AKI control group (**Figure 1**).

Peripheral blood sample was collected within the first 24 h after cardiac surgery and then centrifuged at 8,000 rpm for 5 min at 4°C to separate plasma. The baseline Src was measured within 72 h before surgery. All participants' demographic characteristics, medical histories, surgical procedures, as well as preoperative and postoperative clinical outcomes were recorded. The primary clinical outcomes were the occurrence and severity of AKI defined by the rise of SCr following cardiac surgery (non-AKI: < 1.5-fold; stage I AKI: 1.5–1.9-fold; stage II AKI: 2–2.9-fold; stage III AKI: ≥ 3-fold) (Mehta et al., 2007). The secondary clinical outcomes included the length of ICU and hospital stay, ventilator use, hemodialysis, renal replacement therapy, as well as hospitalization death.

Cytokine Array Measurement

The concentrations of a total of 48 cytokines including FGF basic, Eotaxin, G-CSF, GM-CSF, IFN-γ, IL-1β, IL-1Ra, IL-1α, IL-2Rα, IL-3, IL-12 (p40), IL-16, IL-2, IL-4, IL-5, IL-6, IL-7, IL-8, IL-9,GRO-α, HGF, IFN-α2, LIF, MCP-3, IL-10, IL-12 (p70), IL-13, IL-15, IL-17A, IP-10, MCP-1 (MCAF), MIG, β-NGF, SCF, SCGF-β, SDF-1α, MIP-1α, MIP-1β, PDGF-BB, RANTES, TNF-α, VEGF, CTACK, MIF, TRAIL, IL-18, M-CSF, and TNF-β in the plasma samples were measured with a Human Cytokine Screening Panel (12007283, Bio-Rad, United States) according to the manufacturer's instructions.

Statistical Analysis

Analysis of variance (ANOVA) was used to identify significantly changed cytokines between CSA-AKI and non-AKI groups. In order to exclude the possibility that variation in sex and age might influence the detection of significant cytokines, we

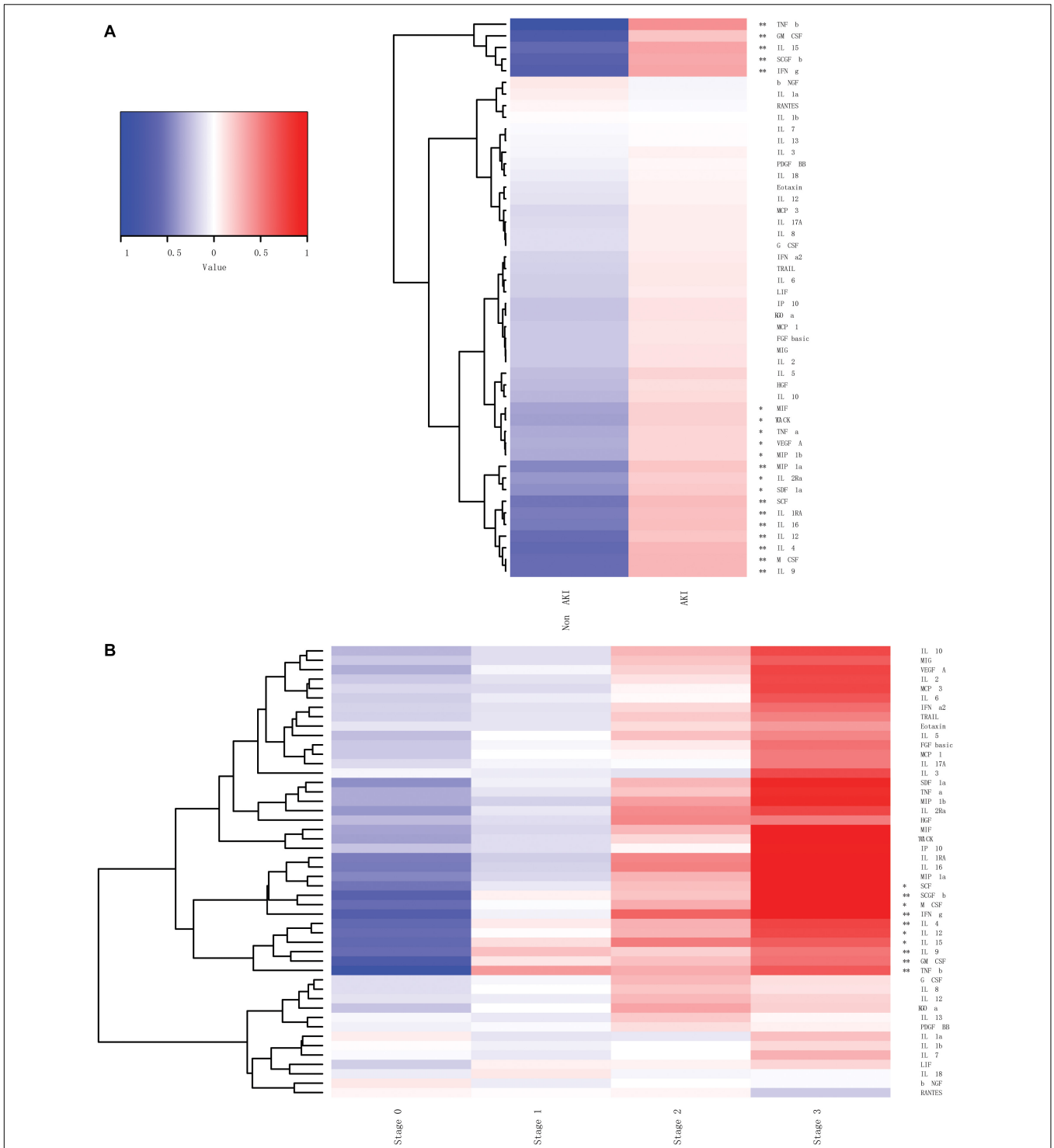

FIGURE 2 | The plasma concentrations of 48 cytokines within 24 h after cardiac surgery. **(A)** The plasma concentrations of 20 cytokines were significantly different between the AKI and non-AKI groups. **(B)** The plasma concentrations of these 48 cytokines between the groups with different AKI stages. $*p < 0.05$, $**p < 0.00001$.

included these two factors as covariates within our ANOVA model. Resulting *P*-values from ANOVA were corrected for multiple comparisons using the Bonferroni correction. A heatmap was plotted to display the concentration of these significantly changed cytokines in different groups. A Pearson correlation coefficient was calculated to evaluate the association between cytokine concentration and ΔSCr. We use regression analysis to calculate the prediction

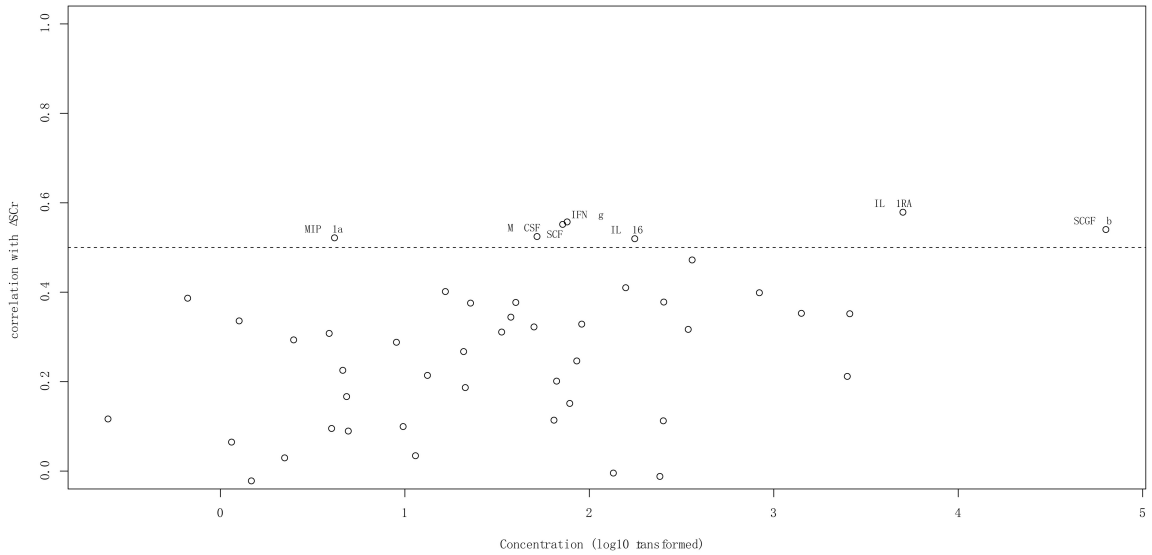

FIGURE 3 | The correlation coefficients of the plasma concentrations of these 48 cytokines with the postoperative ΔSCr.

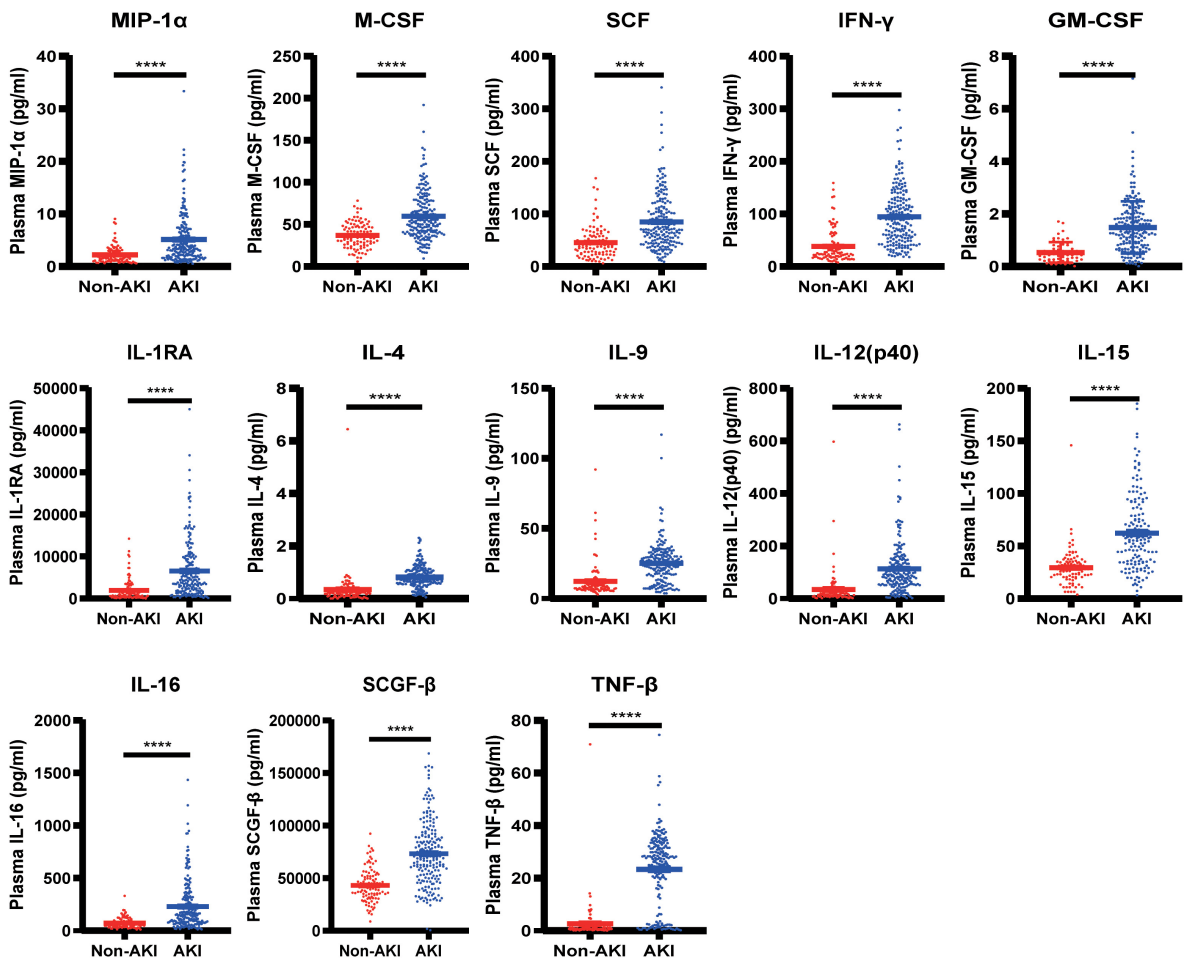

FIGURE 4 | The most significantly changed cytokines between the AKI and non-AKI groups. ****$p < 0.00001$.

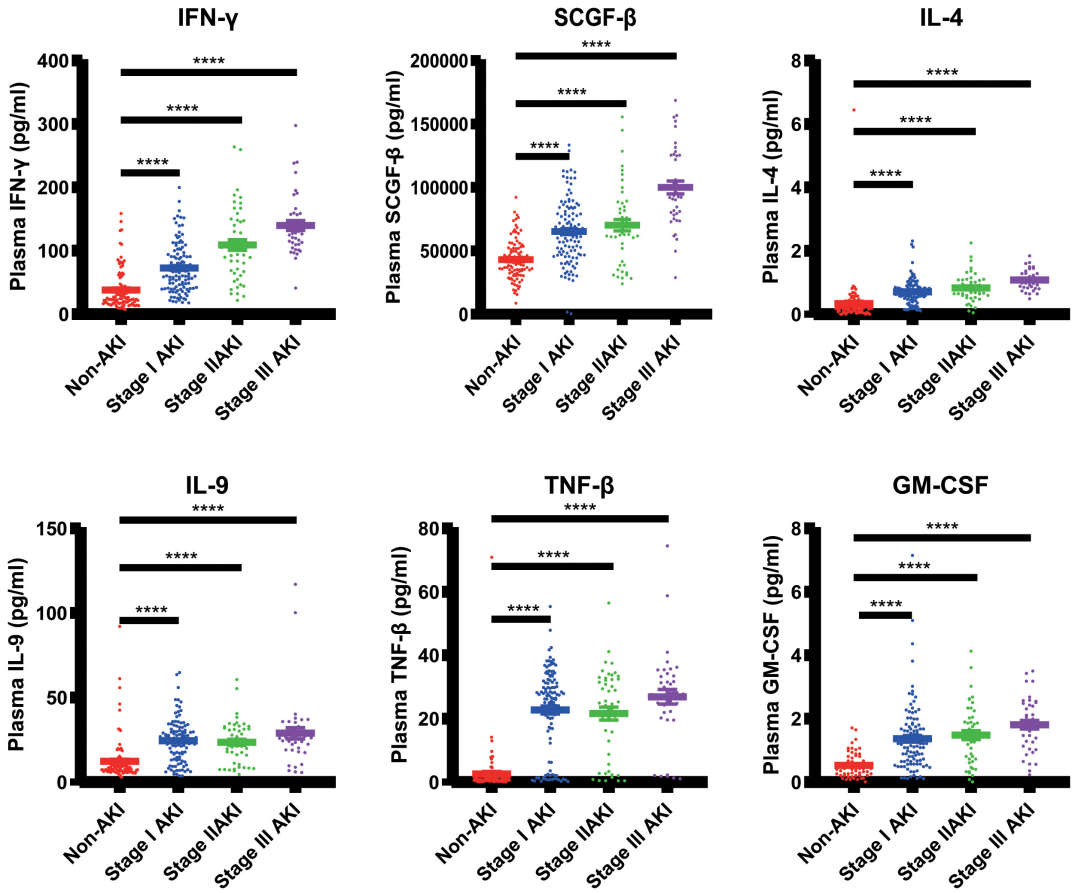

FIGURE 5 | The significantly different cytokines among the non-AKI, Stage I AKI, Stage II AKI, and Stage III AKI groups. ****$p < 0.00001$.

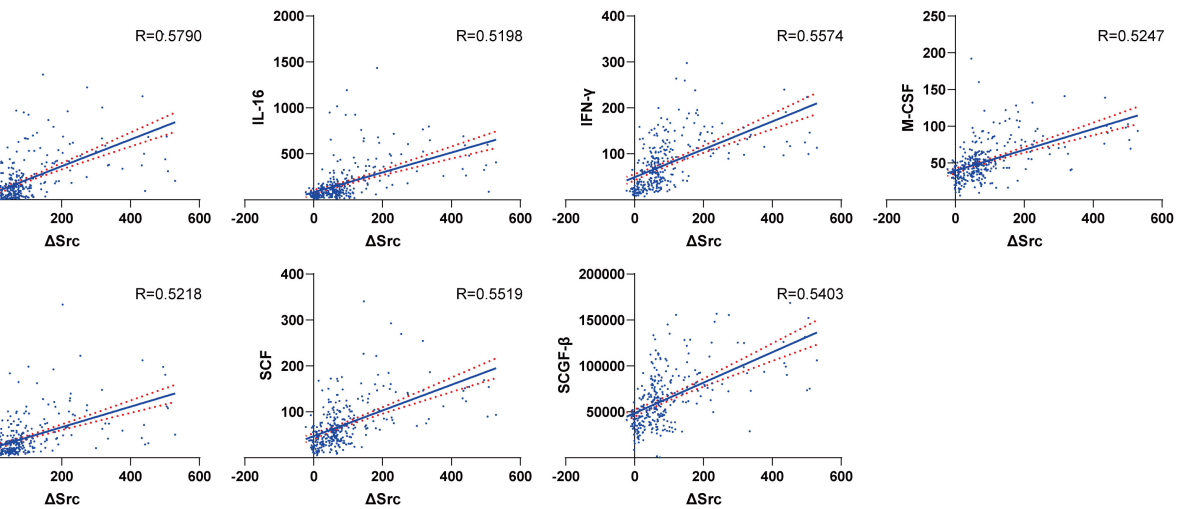

FIGURE 6 | The most significantly correlated plasma cytokines with the postoperative ΔSCr.

probability of factors combination, which was used to draw the ROC (receiver-operating characteristic curve) curve consequently to display the performance. Pearson correlation analysis was used to determine the relationship between the biomarkers and the clinical events. All statistical analysis was performed in R.

RESULTS

The Most Significantly Changed Plasma Cytokines in the CSA-AKI Patients

We measured the plasma concentrations of 48 cytokines within 24 h after cardiac surgery in 204 adult patients with CSAAKI and 102 patients without CSA-AKI (**Table 1**). We found that the plasma concentrations of 20 cytokines were significantly different between the AKI and non-AKI groups with the $P < 0.05$, in which 13 cytokines including TNF-β, IFN-γ, SCGF-β, IL-15, IL-9, IL-4, M-CSF, GM-CSF, SCF, IL-16, IL-12, IL-1RA, and MIP-1α, were the most significantly changed cytokines with the $P < 1E^{-5}$ (**Figures 2A**, **4**, **Supplementary Figure S1**, and **Supplementary Table S1**).

We also compared the plasma concentrations of These 48 cytokines between the non-AKI groups with different AKI stages (**Table 2**). We found that the plasma concentrations of 10 cytokines were significantly different among the non-AKI, Stage I AKI, Stage II AKI, and Stage III AKI groups, in which 6 cytokines including TNF-β, SCGF-β, IL-9, IFN-γ, GM-CSF, and IL-4, were the most significantly changed cytokines with the $P < 1E^{-5}$ (**Figures 2B**, **5**, **Supplementary Figure S2**, and **Supplementary Table S1**).

The Most Significantly Correlated Plasma Cytokines With the Postoperative Changes of Serum Creatinine in the CSA-AKI Patients

We assessed the correlation coefficients of the plasma concentrations of these 48 cytokines with the postoperative ΔSCr in all the 306 adult patients with cardiac surgery. We found that 7 out of these 48 cytokines, including IL-1RA, IFN-γ, SCF, SCGF-β, M-CSF, MIP-1α, and IL-16, were the most significantly correlated plasma cytokines with the postoperative ΔSCr, exhibiting the correlation coefficients $r > 0.5$ (**Figures 3**, **6**, **Supplementary Figure S3**, and **Supplementary Table S1**). We then performed multivariable logistic regression analysis for clinical factors to assess the prediction of CSA-AKI, and CPB time was independent predictor for AKI. So, we added each biomarker to the clinical factor to determine improvement in the predictive efficiency model. As **Table 3** shows, AUC increased when add each factor to CPB time. Especially TGF-β, the value of which could increase to 0.95.

TABLE 1 | Baseline characteristics of patients with non-AKI and AKI (*N* = 306).

Characteristics	Non-AKI (*n* = 102)	AKI (*N* = 204)	*P*
Male, n (%)	88 (86.27%)	149 (73.04%)	0.0090
Age (years)	58.91 ± 1.00	55.90 ± 0.88	0.0598
Height (cm)	169.80 ± 0.69	169.76 ± 0.59	0.6663
Weight (kg)	73.70 ± 1.10	75.07 ± 1.10	0.9759
Body weight index (BMI) (kg/m^2)	25.53 ± 0.32	25.97 ± 0.32	0.7360
Diabetes (n)	23 (22.55%)	27 (13.24%)	0.0485
Hyperlipidemia (n)	61 (59.80%)	103 (50.73%)	0.1459
Hypertension (n)	65 (63.73%)	135 (66.18%)	0.7031
Cardiopulmonary Bypass, n (%)	73 (71.57%)	170 (83.33%)	0.0239
Bypass time (minute)	112.05 ± 4.79	157.72 ± 6.52	<0.0001
Aortic cross clamp time (minute), (n)	81.12 ± 3.69	99.17 ± 3.89 (123)	0.0027
Preoperative Src (μmol/L)	88.78 ± 2.08	89.54 ± 1.35	0.4419
LVEF (%)	58.99 ± 0.74	60.57 ± 0.42	0.1880
NYHA			0.0059
I (%)	31 (30.39%)	86 (42.16%)	
II (%)	51 (50.00%)	61 (29.90%)	
III (%)	20 (19.61%)	55 (26.96%)	
IV (%)	0	2 (0.98%)	
ICU LOS (d)	3.43 ± 0.34	5.94 ± 0.40	<0.0001
Hospitalization	15.37 ± 0.80	19.46 ± 0.80	0.0013
Ventilator time (h)	19.83 ± 1.63	55.60 ± 5.51	<0.0001
Dialysis (n)	1	26	0.0002
In-hospital death or therapy failure (n)	1	15	0.0074

Data are expressed as either Mean ± SDE or as number and percentage. ICU LOS, Length of ICU stay; LVEF, left ventricular ejection fraction.

DISCUSSION

The present prospective cohort study evaluated the diagnostic efficacy of a total of 48 plasma cytokines within the first 24 h after cardiac surgery for the postoperative progression of AKI in 306 adult patients.

AKI occurs in up to 30% of patients who undergo cardiac surgery, but the pathogenesis of CSA-AKI remains unclear (Rosner and Okusa, 2006). Multiple factors, such as hemodynamics, inflammation and nephrotoxin, are thought to be involved and overlapped with each other resulting in renal injury, most likely the tubular necrosis, following an episode of cardiac surgery (Rosner and Okusa, 2006). To date, no pharmacologic interventions or clinical strategies have shown the conclusive efficacy to prevent CSA-AKI. Moreover, the diagnosis of CSA-AKI is still generally based on the criteria of postoperative ΔSCr (Rosner and Okusa, 2006; Thiele et al., 2015; O'Neal et al., 2016; Wang and Bellomo, 2017). Although SCr is considered as the best and golden standard biomarker indicating the changes of renal clearance function, it has been found to poorly correlate with the onset or the initiation of CSA-AKI when the cellular ATP depletion and oxidative injury triggers a proinflammatory response in the kidney while the GFR has not remarkably declined (Ho et al., 2012; Thiele et al., 2015; Bernardi et al., 2016; O'Neal et al., 2016). Therefore, to discover new biomarkers in the initiation phase of CSA-AKI is of great importance for both predictive diagnosis and potential therapeutics.

In a recent prospective cohort study of pediatric CSA-AKI, the urinary and plasma concentrations of a series of cytokines were measured during the early postoperative stage and their correlation coefficients with the progression of CSA-AKI were evaluated, in which the plasma level of IL-8, a

TABLE 2 | Baseline characteristics of patients with non-AKI and stage I, II, III AKI, respectively (*N* = 306).

Characteristics	Non-AKI (*n* = 102)	Stage I AKI (*N* = 115)	Stage II AKI (*N* = 49)	Stage III AKI (*N* = 40)	*P*
Male, n (%)	88 (86.27%)	95 (82.60%)	29 (59.18%)	25 (62.50%)	0.0001
Age (years)	58.91 ± 1.00	56.70 ± 1.15	56.88 ± 1.58	52.38 ± 2.23	0.0806
Height (cm)	169.80 ± 0.69	170.03 ± 0.73	168.04 ± 1.33	171.08 ± 1.40	0.5154
Weight (kg)	73.70 ± 1.10	75.21 ± 1.21	74.26 ± 2.92	75.67 ± 2.73	0.5456
Body weight index (BMI) (kg/m^2)	25.53 ± 0.32	25.96 ± 0.34	26.19 ± 0.87	25.73 ± 0.76	0.8522
Diabetes (n)	23 (22.55%)	20 (17.39%)	7 (14.29%)	0	0.0097
Hyperlipidemia (n)	61 (59.80%)	58 (50.43%)	29 (59.18%)	16 (40.00%)	0.1310
Hypertension (n)	65 (63.73%)	73 (63.49%)	36 (73.47%)	26 (65.00%)	0.6312
Cardiopulmonary Bypass, n (%)	73 (71.57%)	100 (84.03%)	41 (83.67%)	29 (72.50%)	0.0228
Bypass time (minute)	112.05 ± 4.79	144.95 ± 6.16[c]	165.96 ± 17.27[b]	187.48 ± 19.53[d]	<0.0001
Aortic cross clamp time (minute), (n)	81.12 ± 3.69	91.21 ± 4.23	103.04 ± 8.73	121.73 ± 11.61[b]	0.0023
Preoperative Src (μmol/L)	88.78 ± 2.08	95.44 ± 1.41[a]	86.26 ± 2.98	76.61 ± 3.40[a]	<0.0001
LVEF (%)	58.99 ± 0.74	60.42 ± 0.58	61.37 ± 0.87	60.05 ± 0.81	0.3781
NYHA					0.0158
I (%)	31 (30.39%)	43 (37.39%)	20 (40.82%)	23 (57.50%)	
II (%)	51 (50.00%)	35 (30.43%)	16 (32.65%)	10 (25.00%)	
III (%)	20 (19.61%)	35 (30.43%)	13 (26.53%)	7 (14.28%)	
IV (%)	0	2 (1.74%)	0	0	
ICU LOS (d)	3.43 ± 0.34	3.98 ± 0.28	6.39 ± 1.02[a]	11.00 ± 1.06[d]	<0.0001
Hospitalization	15.37 ± 0.80	17.06 ± 0.82	21.31 ± 1.98[a]	24.08 ± 2.13[c]	0.0001
Ventilator time (h)	19.83 ± 1.63	33.56 ± 3.57[b]	73.24 ± 17.12[d]	97.35 ± 12.95[d]	<0.0001
Dialysis (n)	1	2	6	18	<0.0001
In-hospital death or therapy failure (n)	1	3	6	6	0.0005

[a]*p<0.05;* [b]*p<0.01;*[c]*p<0.001;* [d]*p<0.0001. Data are expressed as either Mean ± SDE or as number and percentage. ICU LOS, Length of ICU stay; LVEF, left ventricular ejection fraction.*

TABLE 3 | The performance of a predictive model after add a factor to clinical model.

	AUC	95% CI
Clinical model	0.7271	(0.6521, 0.8021)
+GM-CSF	0.8063	(0.7419, 0.8708)
+INF-γ	0.8727	(0.8157, 0.9298)
+IL-1RA	0.8305	(0.7683, 0.8928)
+IL-4	0.9048	(0.8569, 0.9526)
+IL-8	0.8595	(0.8028, 0.9161)
+IL-9	0.8042	(0.7983, 0.8687)
+IL-12 (P70)	0.8300	(0.7626, 0.8973)
+IL-12 (P40)	0.9038	(0.8465, 0.9612)
+SCGF-β	0.8766	(0.8249, 0.9284)
+TGF-β	0.9470	(0.9156, 0.9784)

potent proinflammatory cytokine, was found to display the best discrimination for the AKI progression after pediatric cardiac surgery (Greenberg et al., 2018). However, neither the cytokines array profiles in the initiation phase after adult cardiac surgery nor their correlation with the development of CSA-AKI have been investigated before.

Therefore, in the present study, we measured the plasma concentrations of 48 cytokines within 24 h after cardiac surgery in a total of 306 adult patients including 204 with and 102 without CSA-AKI. Among the 48 cytokines in the plasma, 20 of them were significantly different in the CSA-AKI patients compared with the non-AKI subjects. In particularly, 13 out of these 20 cytokines including TNF-β, IFN-γ, SCGF-β, IL-15, IL-9, IL-4, M-CSF, GM-CSF, SCF, IL-16, IL-12, IL-1RA, and MIP-1α, displayed tremendous changes with the $P < 1E^{-5}$.

Moreover, we compared the levels of 48 cytokines between the patients with different stages of AKI. We found that 10 of the 48 cytokines in the plasma were significantly different among the subjects of non-AKI, Stage I AKI, Stage II AKI, and Stage III AKI. In particularly, 6 out of these 10 cytokines including TNF-β, SCGF-β, IL-9, IFN-γ, GM-CSF, and IL-4, exhibited immense differences with the $P < 1E^{-5}$.

To further evaluate the predictive efficacy of these 48 cytokines for the progression of CSA-AKI, we also assessed the correlation coefficients of the plasma concentration of each cytokine with the postoperative ΔSCr from baseline during hospitalization in all the 306 patients included. As shown in **Figure 3**, among the 48 cytokines, 7 cytokines including IL-1RA, IFN-γ, SCF, SCGF-β, M-CSF, MIP-1α, and IL-16, have the highest correlation coefficient with the $r > 0.5$.

Taken all the results together, we found that IFN-γ and SCGF-β were the most relevant two cytokines that have both the remarkable differences with $P < 1E^{-5}$ between AKI and non-AKI patients as well as among subjects with different AKI stages, and the highest correlation coefficients of $r > 0.5$ with the postoperative changes of SCr after cardiac surgery.

SCGF-β (stem cell growth factor β), a newly discovered hematopoietic growth factor exerting its activity at the early

stages of hematopoiesis, is rarely investigated in kidney, which indicates that the plasma SCGF-β might be a new biomarker not only for CSA-AKI but also for general AKI (Hiraoka et al., 1997; Mio et al., 1998; Ito et al., 2003). Additionally, IFN-γ (Interferon γ), a well-known pro-inflammatory factor produced mainly by activated T-cells and natural killer cells, has been extensively studied in AKI (Tau and Rothman, 1999; Schroder et al., 2004; Schoenborn and Wilson, 2007). Previous studies have reported that the plasma levels of IFN-γ during the early postoperative stage were either declined or not significantly changed in the kidney transplantation-associated AKI (Karczewski et al., 2009; Snoeijs et al., 2011; De Serres et al., 2012; Xu et al., 2013) and even the pediatric CSA-AKI (Greenberg et al., 2018), which suggests that plasma IFN-γ might be a novel potential biomarker selective for the CSA-AKI in adults.

In conclusion, the plasma levels of IFN-γ and SCGF-β are not only remarkably increased in adult CSA-AKI patients compared with non-AKI patients during the first 24 h after cardiac surgery, but also significantly correlated with the postoperative changes of SCr after cardiac surgery. Thus, IFN-γ and SCGF-β could be novel predictive plasma biomarker, as well as potential therapeutic targets specific for adult CSA-AKI.

There are several limitations to this study. For instance, described by numerous literatures, drugs treating heart failure such as diuretics, ACE inhibitors andAT1R blockers would impact inflammatory pathway. We lack data on drugs used by majority patients prior to cardiac surgery, which would thereafter lead to insufficient diagnostic efficacy of cytokines. Additionally, the circulating cytokines/chemokines are regulated on rapid timescales. Due to sampling difficulties, it is challenging to depict dynamic changes of those designated cytokines at fine resolution.

DATA AVAILABILITY STATEMENT

The raw data supporting the conclusions of this article will be made available by the authors, without undue reservation.

ETHICS STATEMENT

The studies involving human participants were reviewed and approved by the ethics committee of the Fuwai hospital. The patients/participants provided their written informed consent to participate in this study. Written informed consent was obtained from the individual(s) for the publication of any potentially identifiable images or data included in this article.

AUTHOR CONTRIBUTIONS

YL and JS designed the study. ZC and ZH carried out experiments. ZH analyzed the data and made the figures. ZC drafted the manuscript. All authors contributed to the article and approved the submitted version.

FUNDING

This study was supported by Shanghai Municipal Science and Technology Major Project (Grant No. 2017SHZDZX01), CAMS In- Novation Fund for Medical Sciences (CIFMS, 2016-I2M-1-015), the National Natural Science Foundation of China (81670376), and the PUMC Youth Fund and the Fundamental Research Funds for the Central Universities.

SUPPLEMENTARY MATERIAL

The Supplementary Material for this article can be found online at: https://www.frontiersin.org/articles/10.3389/fphys.2020.587204/full#supplementary-material

Supplementary Table S1 | Bonf_P-value between AKI and non-AKI.

Supplementary Table S2 | Bonf_P-value between different stage AKI and non-AKI.

Supplementary Table S3 | The correlation coefficients of the plasma concentrations of these 48 cytokines with the postoperative Δ SCr.

REFERENCES

Arsalan, M., Ungchusri, E., Farkas, R., Johnson, M., Kim, R. J., Filardo, G., et al. (2018). Novel renal biomarker evaluation for early detection of acute kidney injury after transcatheter aortic valve implantation. *Proc. Bayl. Univ. Med. Cent.* 31, 171–176. doi: 10.1080/08998280.2017.1416235

Bernardi, M. H., Schmidlin, D., Ristl, R., Heitzinger, C., Schiferer, A., Neugebauer, T., et al. (2016). Serum creatinine back-estimation in cardiac surgery patients: misclassification of AKI using existing formulae and a data-driven model. *Clin. J. Am. Soc. Nephrol.* 11, 395–404. doi: 10.2215/cjn.03560315

Brinkman, R., HayGlass, K. T., Mutch, W. A., and Funk, D. J. (2015). Acute kidney injury in patients undergoing open abdominal aortic aneurysm repair: a pilot observational trial. *J. Cardiothorac. Vasc. Anesth.* 29, 1212–1219. doi: 10.1053/j.jvca.2015.03.027

Burke-Gaffney, A., Svermova, T., Mumby, S., Finney, S. J., and Evans, T. W. (2014). Raised plasma Robo4 and cardiac surgery-associated acute kidney injury. *PLoS One* 9:e111459. doi: 10.1371/journal.pone.0111459

de Fontnouvelle, C. A., Greenberg, J. H., Thiessen-Philbrook, H. R., Zappitelli, M., Roth, J., Kerr, K. F., et al. (2017). Interleukin-8 and tumor necrosis factor predict acute kidney injury after pediatric cardiac surgery. *Ann. Thorac. Surg.* 104, 2072–2079. doi: 10.1016/j.athoracsur.2017.04.038

De Serres, S. A., Mfarrej, B. G., Grafals, M., Riella, L. V., Magee, C. N., Yeung, M. Y., et al. (2012). Derivation and validation of a cytokine-based assay to screen for acute rejection in renal transplant recipients. *Clin. J. Am. Soc. Nephrol.* 7, 1018–1025. doi: 10.2215/cjn.11051011

Greenberg, J. H., Whitlock, R., Zhang, W. R., Thiessen-Philbrook, H. R., Zappitelli, M., Devarajan, P., et al. (2015). Interleukin-6 and interleukin-10 as acute kidney injury biomarkers in pediatric cardiac surgery. *Pediatr. Nephrol.* 30, 1519–1527. doi: 10.1007/s00467-015-3088-4

Greenberg, J. H., Zappitelli, M., Jia, Y., Thiessen-Philbrook, H. R., de Fontnouvelle, C. A., Wilson, F. P., et al. (2018). Biomarkers of AKI progression after pediatric cardiac surgery. *J. Am. Soc. Nephrol.* 29, 1549–1556. doi: 10.1681/asn.2017090989

Hiraoka, A., Sugimura, A., Seki, T., Nagasawa, T., Ohta, N., Shimonishi, M., et al. (1997). Cloning, expression, and characterization of a cDNA encoding a novel

human growth factor for primitive hematopoietic progenitor cells. *Proc. Natl. Acad. Sci. U.S.A.* 94, 7577–7582. doi: 10.1073/pnas.94.14.7577

Ho, J., Reslerova, M., Gali, B., Nickerson, P. W., Rush, D. N., Sood, M. M., et al. (2012). Serum creatinine measurement immediately after cardiac surgery and prediction of acute kidney injury. *Am. J. Kidney Dis.* 59, 196–201. doi: 10.1053/j.ajkd.2011.08.023

Ito, C., Sato, H., Ando, K., Watanabe, S., Yoshiba, F., Kishi, K., et al. (2003). Serum stem cell growth factor for monitoring hematopoietic recovery following stem cell transplantation. *Bone Marrow Transpl.* 32, 391–398. doi: 10.1038/sj.bmt.1704152

Karczewski, M., Karczewski, J., Poniedzialek, B., Wiktorowicz, K., Smietanska, M., and Glyda, M. (2009). Distinct cytokine patterns in different states of kidney allograft function. *Transplant Proc.* 41, 4147–4149. doi: 10.1016/j.transproceed.2009.08.067

Mehta, R. L., Kellum, J. A., Shah, S. V., Molitoris, B. A., Ronco, C., Warnock, D. G., et al. (2007). Acute kidney injury Network: report of an initiative to improve outcomes in acute kidney injury. *Crit. Care* 11:R31.

Mio, H., Kagami, N., Yokokawa, S., Kawai, H., Nakagawa, S., Takeuchi, K., et al. (1998). Isolation and characterization of a cDNA for human mouse, and rat full-length stem cell growth factor, a new member of C-type lectin superfamily. *Biochem. Biophys. Res. Commun.* 249, 124–130. doi: 10.1006/bbrc.1998.9073

O'Neal, J. B., Shaw, A. D., and Billings, F. T. (2016). Acute kidney injury following cardiac surgery: current understanding and future directions. *Crit. Care* 20:187.

Rosner, M. H., and Okusa, M. D. (2006). Acute kidney injury associated with cardiac surgery. *Clin. J. Am. Soc. Nephrol.* 1, 19–32.

Schoenborn, J. R., and Wilson, C. B. (2007). Regulation of interferon-gamma during innate and adaptive immune responses. *Adv. Immunol.* 96, 41–101. doi: 10.1016/s0065-2776(07)96002-2

Schroder, K., Hertzog, P. J., Ravasi, T., and Hume, D. A. (2004). Interferon-gamma: an overview of signals, mechanisms and functions. *J. Leukoc. Biol.* 75, 163–189. doi: 10.1189/jlb.0603252

Snoeijs, M. G., van Bijnen, A., Swennen, E., Haenen, G. R., Roberts, L. J., Christiaans, M. H., et al. (2011). Tubular epithelial injury and inflammation after ischemia and reperfusion in human kidney transplantation. *Ann. Surg.* 253, 598–604. doi: 10.1097/sla.0b013e31820d9ae9

Tau, G., and Rothman, P. (1999). Biologic functions of the IFN-gamma receptors. *Allergy* 54, 1233–1251. doi: 10.1034/j.1398-9995.1999.00099.x

Thiele, R. H., Isbell, J. M., and Rosner, M. H. (2015). AKI associated with cardiac surgery. *Clin. J. Am. Soc. Nephrol.* 10, 500–514. doi: 10.2215/cjn.07830814

Wang, Y., and Bellomo, R. (2017). Cardiac surgery-associated acute kidney injury: risk factors, pathophysiology and treatment. *Nat. Rev. Nephrol.* 13, 697–711. doi: 10.1038/nrneph.2017.119

Xu, X., Huang, H., Cai, M., Qian, Y., Li, Z., Bai, H., et al. (2013). Combination of IL-1 receptor antagonist, IL-20 and CD40 ligand for the prediction of acute cellular renal allograft rejection. *J. Clin. Immunol.* 33, 280–287. doi: 10.1007/s10875-012-9777-x

Conflict of Interest: The authors declare that the research was conducted in the absence of any commercial or financial relationships that could be construed as a potential conflict of interest.

frontiers in Physiology

ORIGINAL RESEARCH
published: 12 November 2020
doi: 10.3389/fphys.2020.569881

Kidney Ischemia/Reperfusion Injury Induces Changes in the Drug Transporter Expression at the Blood–Brain Barrier *in vivo* and *in vitro*

Malgorzata Burek[1], Sandra Burmester[1], Ellaine Salvador[1], Kerstin Möller-Ehrlich[2], Reinhard Schneider[2], Norbert Roewer[1], Michiaki Nagai[3] and Carola Y. Förster[1]**

[1] Department of Anaesthesia and Critical Care, University of Würzburg, Würzburg, Germany, [2] Division of Nephrology, Department of Medicine I, University of Würzburg, Würzburg, Germany, [3] Department of Cardiology, Hiroshima City Asa Hospital, Hiroshima, Japan

OPEN ACCESS

Edited by:
Natalia Lopez-Andres, Navarrabiomed, Spain

Reviewed by:
Weidong Wang, Sun Yat-sen University, China
Yunwen Yang, Nanjing Children's Hospital, China

***Correspondence:**
Malgorzata Burek
Burek_M@ukw.de
Carola Y. Förster
Foerster_C@ukw.de

Specialty section:
This article was submitted to Renal and Epithelial Physiology, a section of the journal Frontiers in Physiology

Received: *05 June 2020*
Accepted: *20 October 2020*
Published: *12 November 2020*

Citation:
Burek M, Burmester S, Salvador E, Möller-Ehrlich K, Schneider R, Roewer N, Nagai M and Förster CY (2020) Kidney Ischemia/Reperfusion Injury Induces Changes in the Drug Transporter Expression at the Blood–Brain Barrier in vivo and in vitro. Front. Physiol. 11:569881. doi: 10.3389/fphys.2020.569881

Ischemia/reperfusion injury is a major cause of acute kidney injury (AKI). AKI is characterized by a sudden decrease in kidney function, systemic inflammation, oxidative stress, and dysregulation of the sodium, potassium, and water channels. While AKI leads to uremic encephalopathy, epidemiological studies have shown that AKI is associated with a subsequent risk for developing stroke and dementia. To get more insights into kidney–brain crosstalk, we have created an *in vitro* co-culture model based on human kidney cells of the proximal tubule (HK-2) and brain microvascular endothelial cells (BMEC). The HK-2 cell line was grown to confluence on 6-well plates and exposed to oxygen/glucose deprivation (OGD) for 4 h. Control HK-2 cells were grown under normal conditions. The BMEC cell line cerebED was grown to confluence on transwells with 0.4 μm pores. The transwell filters seeded and grown to confluence with cereEND were inserted into the plates with HK-2 cells with or without OGD treatment. In addition, cerebEND were left untreated or treated with uremic toxins, indole-3-acetic acid (IAA) and indoxyl sulfate (IS). The protein and mRNA expression of selected BBB-typical influx transporters, efflux transporters, cellular receptors, and tight junction proteins was measured in BMECs. To validate this *in vitro* model of kidney–brain interaction, we isolated brain capillaries from mice exposed to bilateral renal ischemia (30 min)/reperfusion injury (24 h) and measured mRNA and protein expression as described above. Both *in vitro* and *in vivo* systems showed similar changes in the expression of drug transporters, cellular receptors, and tight junction proteins. Efflux pumps, in particular Abcb1b, Abcc1, and Abcg2, have shown increased expression in our model. Thus, our *in vitro* co-culture system can be used to study the cellular mechanism of kidney and brain crosstalk in renal ischemia/reperfusion injury.

Keywords: kidney ischemia/reperfusion injury, brain pathology, blood–brain barrier, drug transporter, tight junctions

INTRODUCTION

Decreased kidney function in patients with chronic kidney disease (CKD) or acute kidney injury (AKI) often leads to neurological effects such as cognitive impairment, neuropathy and cerebrovascular disease (Tanaka and Okusa, 2020). Blood-borne toxins, normally eliminated by healthy kidneys, are thought to affect brain function through kidney-brain crosstalk (Lu et al., 2015). In general, in CKD or AKI, the accumulation of uremic toxins in the blood is mainly due to a decreased glomerular filtration rate (GFR). In ischemia/reperfusion injury, reduced GFR is usually due to decreased glomerular perfusion and tubular obstruction due to necrotic and shed tubular epithelial cells. This leads to the accumulation of uremic toxins in the body. Patients with CKD have an increased prevalence of microbleads in the brain, which is associated with an increased risk of stroke and a cognitive decline compared to healthy age-matched controls (Lau et al., 2020). The blood-brain barrier (BBB), an interface between blood and the brain, is the first line of contact with blood-borne toxins (Banks, 2016). Only the toxins, which are able to cross the BBB or modulate cellular processes at the BBB have an influence on neurons in the brain. The BBB is formed by BMECs, which interact with pericytes, astrocytes, microglia and neurons to form a cellular, transporter and metabolic barrier that protects the brain homeostasis (Keaney and Campbell, 2015). Endothelial cells of the BBB are tightly connected by tight and adherens junctions. Transmembrane proteins such as claudins, occludin, junctional adhesion molecules, and VE-cadherin are involved in establishing paracellular permeability (Haseloff et al., 2015). A low level of transendothelial endocytosis and a high expression of efflux transporters contribute to the barrier properties (Krizbai et al., 2016; Wilhelm et al., 2016). In addition, metabolizing enzymes such as cytochrome P450 family limit the amounts of toxins that approach the brain parenchyma (Dauchy et al., 2008). Systemic factors can influence the BMECs and lead to changes in BBB integrity (Lu et al., 2015). In a rat model of a chronic renal failure, a significant decrease of influx and efflux drug transporters on mRNA and protein level have been shown (Naud et al., 2012). Renal failure serum treatment of BMECs *in vitro*, showed similar effects on transporter expression. Interestingly, the brain permeability for drugs remained unchanged suggesting the sustained BBB integrity (Naud et al., 2012). Various uremic toxins are known. One example is indoxyl sulfate (IS), a metabolite of L-tryptophan from food. IS induces oxidative stress and contributes to cardiovascular disease by inhibiting the endothelial proliferation and wound healing (Yu et al., 2011). Organic anion transporters (OAT) at the BBB are involved in the brain uptake and efflux of IS (Ohtsuki et al., 2002). Elevated cerebral IS levels lead to negative effects on neurons (Iwata et al., 2007). Indole-3-acetic acid (IAA), a uremic toxin derived from tryptophan, is highly increased in renal failure and induces apoptosis (Edamatsu et al., 2014). Ischemia/reperfusion injury is a major cause of AKI. We analyze here brain microvessels isolated from mice exposed to bilateral renal ischemia (30 min)/reperfusion (24 h) injury and measured protein and mRNA expression of influx and efflux transporters, cellular receptors and tight junction proteins. We also created an *in vitro* co-culture model based on human proximal tubular kidney cells HK-2 and the BMEC cell line cerebEND. The addition of kidney injury toxins, IAA and IS should mimic serum toxin accumulation (Gondouin et al., 2013). We demonstrate the induction of selected efflux transporters in BMECs and altered tight junction protein expression using this *in vitro* model.

MATERIALS AND METHODS

Reagents

Indoxyl sulfate (IS) and Indole-3-acetic acid (IAA) were purchased from Sigma-Aldrich. A 50 mM stock solution of IAA was made in ethanol and used at a concentration of 1 mM. A 1 M stock solution of IS (potassium salt) was prepared in water and used in a concentration of 1 mM. Solvents alone (1 mM ethanol and 1mM potassium chloride) were used for the control treatment.

Mouse Brain Tissue and Isolation of Capillaries

Frozen mouse brain tissue from mice exposed to bilateral renal ischemia (30 min)/reperfusion (24 h) injury was provided by Dr. R. Schneider (Division of Nephrology, Department of Medicine I, University of Würzburg). The parameters that characterize the kidney function of sham and clamp-operated mice are shown in **Table 1**. Brain capillaries were isolated by mechanical separation and centrifugation with 25% bovine serum albumin (Dilling et al., 2017). After washing with phosphate buffered saline (PBS), the capillaries were used for protein and RNA isolation as described below.

Cell Culture

CerebEND cells were isolated and immortalized as previously described (Silwedel and Forster, 2006; Burek et al., 2012). The cells were grown in Dulbecco's Modified Eagle's Medium (DMEM) supplemented with 10% fetal calf serum (FCS) and 1% penicillin/streptomycin in 37°C and 5% CO_2 on plates coated with 0.5% gelatin. The immortalized human proximal tubule epithelial cells HK-2 (ATCC) were grown in DMEM supplemented with 10% FCS and 1% penicillin/streptomycin on plates coated with 0.5% gelatin. CerebEND cells were grown to confluence for 5 days, followed by differentiation in growth medium with 1% charcoal stripped FCS (without hormone and growth factors) for 24 h. For oxygen/glucose deprivation

TABLE 1 | Effects of bilateral renal ischemia (30 min)/reperfusion injury (24 h) (clamp) on kidney function in mice.

	Sham	Clamp
Weight (g)	24.6 ± 2.92	25.5 ± 1.69
Urine output volume in 30 min (ml)	0.203 ± 0.11	0.037 ± 0.05*
Inulin-clearance (ml/min/100 g)	1.338 ± 0.43	0.623 ± 0.12*

*Data are presented as mean ± SD, *p < 0.05 versus sham group.*

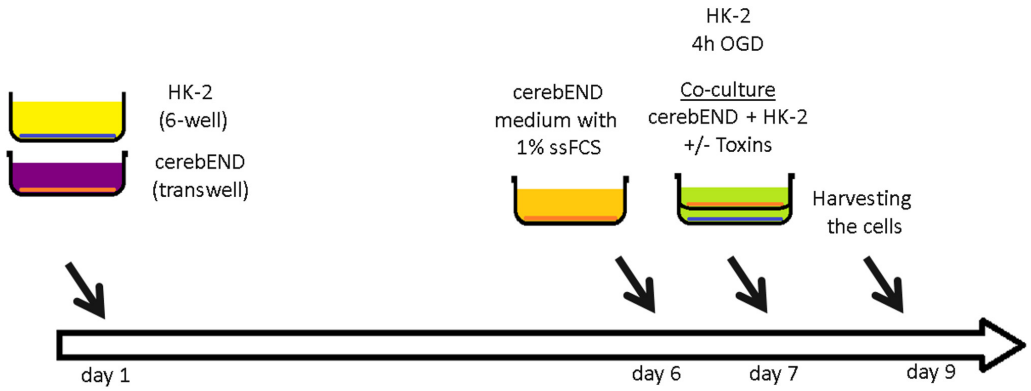

FIGURE 1 | Schematic representation of a co-culture model of proximal tubule kidney cells and brain microvascular endothelial cells. Human proximal tubule kidney cells (HK-2) were grown to confluence in a 6-well plate and treated with oxygen/glucose deprivation (OGD) for 4 h. Brain microvascular endothelial cells (BMEC, cerebEND) were grown to confluence in transwells. The transwells with confluent cerebEND were put together with HK-2 and additionally treated with kidney injury toxins indoxyl sulfate (IS) and indole-3-acetic acid (IAA). The cells were harvested 48 h later.

experiments, confluent HK-2 cells were grown in glucose-free DMEM with 1% FCS for 4 h in 1% O_2, 5% CO_2 with or without 1 mM IS and/or 1mM IAA. After 4 h OGD, glucose was added to the growth medium to a final concentration of 4g/l and HK-2 cells were used for co-culture with cerebEND cells. For co-culture, cerebEND cells were seeded in 6-well transwells (0.4 μm pores) and grown as described above (**Figure 1**). On day 6, the growth medium was replaced with the medium harvested from OGD-treated HK-2 cells supplemented with glucose with or without addition of 1 mM IS and/or 1 mM IAA. The cells were co-cultured for 48 h and then harvested for RNA and protein isolation as described below.

Real-Time PCR

RNA isolation and real-time PCR analysis were performed as described previously (Burek et al., 2014; Gerhartl et al., 2020). Briefly, total RNA was isolated using the Nucleospin-RNAII Kit (Macherey Nagel) according to the manufacturer's instructions. We used 1 μg of total RNA for reverse transcription with the High capacity cDNA synthase Kit (Thermo Fisher Scientific). Quantitative PCR was performed using commercially available Taqman® probes (Thermo Fisher Scientific). Calnexin (Canx) was used as endogenous control for the normalization and calculation of the relative expression by the comparative Ct method. Each sample was analyzed in triplicate. The measurements were carried out with the StepOnePlus Real-Time PCR System (Thermo Fisher Scientific).

Western Blot

Western blot was performed as previously described (Burek et al., 2010; Blecharz et al., 2014). Briefly, the cells were washed with ice-cold PBS and harvested on ice in 50 μl RIPA buffer (50 mM Tris, pH 8; 150 mM NaCl, 0.1% SDS, 0.5% sodium-deoxycholate, 1% NP40) supplemented with proteases and phosphatase inhibitor cocktail (Roche Applied Science). Protein content was quantified using the BCA protein Assay Kit (Thermo Fisher Scientific). Equal amounts of protein (20 μg) were subjected to SDS-PAGE electrophoresis. The proteins were transferred to a Hybond nitrocellulose membrane (Promega), which was blocked with 10% low-fat milk in PBS and incubated overnight at 4 °C with the respective primary antibody in blocking solution against Bcrp (1:1000 Abcam #Ab-24114), Cldn5 (1:200, Thermo Fisher Scientific, #34-1600), Glut-1 (1:200, Millipore #07-1401), Lrp1 (1:1000, Abcam #Ab92544), Mct1 (1:200 Santa Cruz Biotechnology #sc-14917), Mrp4 (1:1000, Enzo Life Science #ALX-801-039-C100), Ocln (1:200, Acris #AP26410PU-N), P-gp (1:200, Enzo Life Sciences #ALX-801-002), TFR (Transferrin Receptor, 1:500, Thermo Fisher Scientific #13-6800). β-actin was used as endogenous control (1: 20 000, Sigma-Aldrich #A3854). Horseradish peroxidase-labeled anti-mouse (Roche Applied Science), anti-rabbit (Cell Signaling Technology), anti-goat and anti-guinea pig (Santa Cruz Biotechnology) IgGs in a dilution of 1:3000 in blocking solution were used as secondary antibodies. The images were taken using an enhanced chemiluminescence detection reagents and FluorChem FC2 Multi-imager II (Alpha Innotech). Densitometric analysis was performed using the Image J software.

Statistical Analysis

The data are expressed as the mean ± standard deviation. To compare three or more groups, a one-way ANOVA followed by Dunnett's multiple comparisons test was performed using the GraphPad Prism 7.00 Software. P values less than 0.05 were considered significant.

RESULTS

Uremic Toxins and Co-culture With Stressed Kidney Cells Induce the Expression of Efflux Pumps in the BMEC Cell Line CerebEND

IS and IAA are uremic toxins that are upregulated in kidney ischemia/reperfusion injury. IS/IAA were selected for the

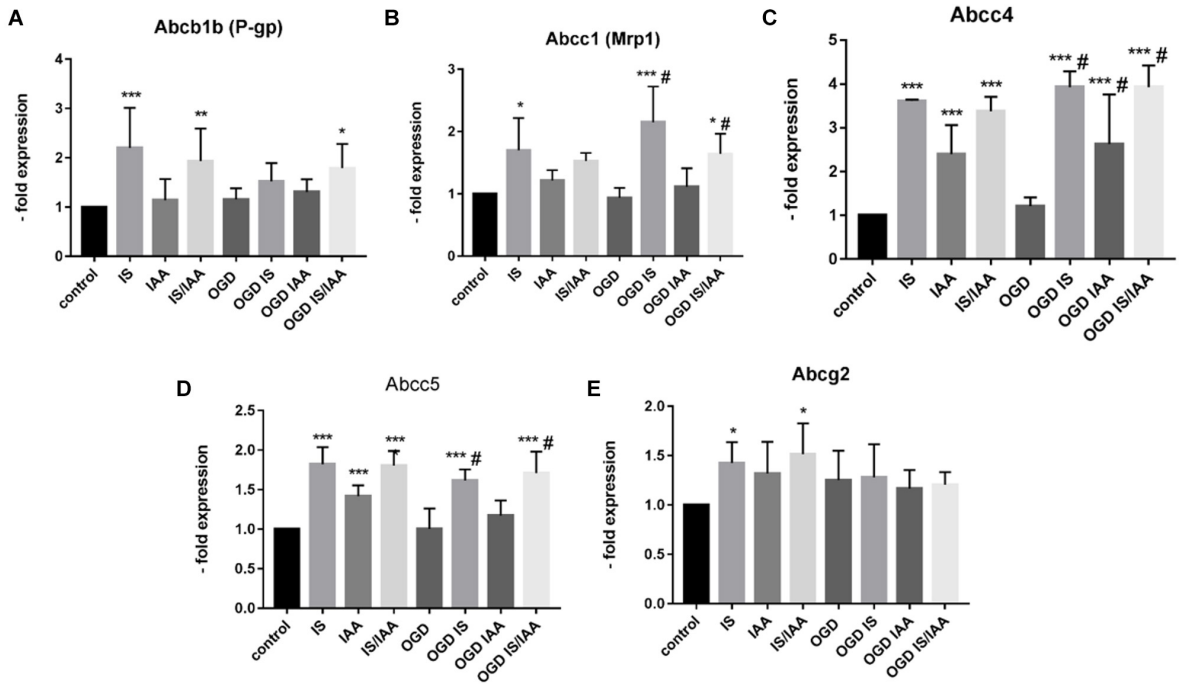

FIGURE 2 | Effects of ischemic HK-2 and uremic toxins on efflux pumps mRNA in brain microvascular endothelial cells. Mouse brain microvascular endothelial cells (BMEC) treated as described in **Figure 1** were lysed and used for RNA extraction. The expression of the efflux transporters Abcb1b (P-gp, Mdr1, ATP Binding Cassette Subfamily B Member1) **(A)**, Abcc1 (Mrp1, ATP Binding Cassette Subfamily C Member1) **(B)**, Abcc4 (Mrp4, ATP Binding Cassette Subfamily C Member 4) **(C)**, Abcc5 (Mrp5, ATP Binding Cassette Subfamily C Member 5) **(D)**, and Abcg2 (Bcrp, ATP Binding Cassette Subfamily G Member 2) **(E)** was measured by qPCR. The data are shown as an average of four independent experiments with standard deviations. A one-way ANOVA with Dunnett's or Sidak's multiple comparison test was used to compare each treatment to the normoxic cerebEND control without toxin treatment (*$p < 0.05$, **$p < 0.01$, ***$p < 0.001$) or to OGD treatment (#).

treatment of brain microvascular endothelial cells (BMEC) to mimic the uremic conditions in the cell culture medium (Yu et al., 2011; Edamatsu et al., 2014). Concentrations of 0.5 mM, 1 mM, 5 mM, and 10 mM of IS and IAA were examined for their toxic effects on BMEC during 24- and 48-h treatment (results not shown). IS and IAA at concentration of 0.5 mM and 1 mM had no toxic effect on BMEC, while higher concentrations were toxic. We selected the non-toxic 1mM concentration of IS and IAA for further experiments. These non-toxic concentrations also had no significant effects on mRNA and protein expression in BMEC (results not shown).

There may be an undefined mixture of toxins in the blood during kidney ischemia/reperfusion injury (Lu et al., 2015). In order to increase the number of kidney-derived factors in the cell culture medium, we co-cultured the human proximal tubule kidney cells HK-2 with BMEC as shown schematically in **Figure 1**. HK-2 cells were stressed by 4-h oxygen-glucose deprivation (OGD), as previously established (Kleinschnitz et al., 2011; Burek et al., 2019; Ittner et al., 2020) and were then cultured along with BMEC (Forster et al., 2005; Silwedel and Forster, 2006; Burek et al., 2012; Helms et al., 2016). OGD shows similar effects on kidney cells as AKI (Sauvant et al., 2009). HK-2 were incubated in glucose-free medium under 1% O_2. After 4 h, glucose was added to a final concentration of 4 g/ml. The HK-2-secreted factors during 4-h OGD period were preserved in medium. After that, the confluent BMEC seeded in transwells were placed to HK-2 wells and received a HK-2 conditioned medium. In addition, uremic toxins were added to selected transwells (**Figure 1**). A co-culture with HK-2 without OGD treatment was used as a control. BMEC were harvested 48 h later and were subjected to qPCR and Western blot. First, we analyzed the main efflux pumps that are expressed on the BBB. At the mRNA level, all efflux pumps examined were elevated due to treatment with uremic toxins and co-culture with either normoxic or OGD-treated HK-2 cells (**Figures 2A–E**). Interestingly, OGD-stressed HK-2 alone did not induced expression of efflux pumps in BMECs probably because of the recovery of the cells during the 48 h reoxygenation. The strongest effects were observed on Abcc4 and Abcc5 expression (**Figures 2C,D**) with 4- and 2-fold increased expression after IS, IAA or combination of both in either normoxic or OGD-treated HK-2 co-culture. The genes coding for proteins involved in the receptor-mediated transport at the BBB showed a moderate increase in the case of Ager and Insulin receptor (Insr) (**Figures 3A,B**). No significant changes in the Lrp1 and transferrin receptor (Tfrc) mRNA were found. We then examined the protein levels of Mrp4, Lrp1 and Tfr (**Figure 4**). Similarly to Abcc4 mRNA, the Mrp4 protein in BMEC treated with either IS or IS/IAA in co-culture with normoxic or OGD-treated HK-2 cells was significantly increased (**Figures 4A,B**). Lrp1 protein level was decreased due to OGD and increased in IS- and IAA-treated BMEC in co-culture with normoxic HK-2

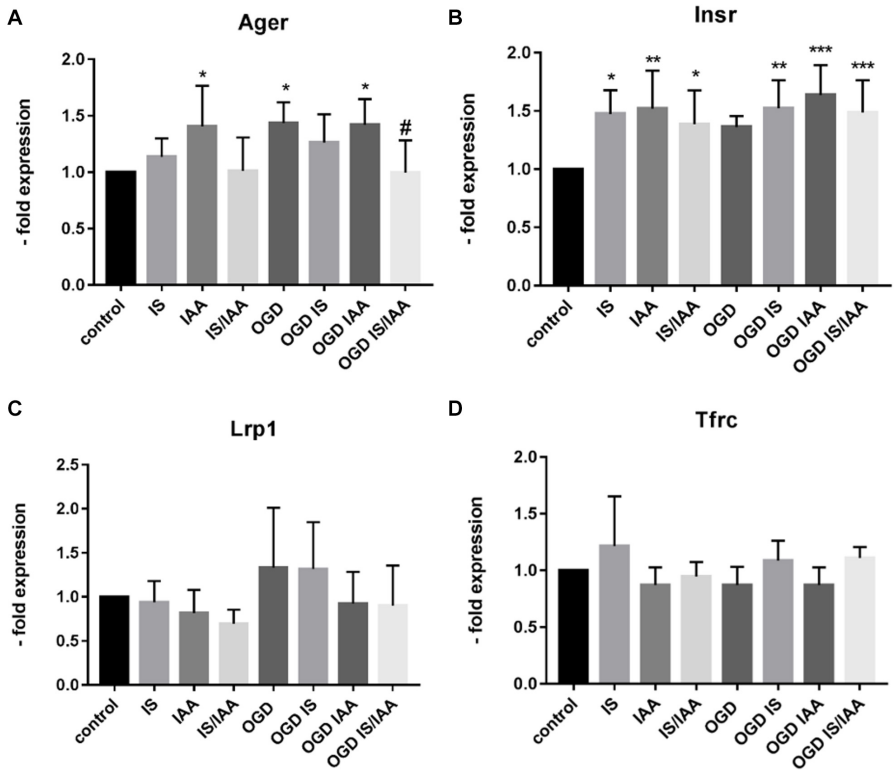

FIGURE 3 | Effects of ischemic HK-2 and uremic toxins on cellular receptor mRNA in brain microvascular endothelial cells. BMECs treated as described in **Figure 1** were lysed and used for RNA extraction. The expression of the cellular receptors Ager (Advanced Gylcosylation End-Product Specific Receptor) **(A)**, Insr (Insulin Receptor) **(B)**, Lrp1 (LDL Receptor Related Protein 1) **(C)**, and Tfrc (Transferrin Receptor) **(D)** was measured by qPCR. The data are shown as average of four independent experiments with standard deviations. One-way ANOVA with Dunnett's or Sidak's multiple comparison test was used to compare each treatment with the normoxic cerebEND control without toxin treatment (*$p < 0.05$, **$p < 0.01$, ***$p < 0.001$) or to OGD treatment (#).

(**Figure 4D**). Tfr protein level was not significantly changed under any condition (**Figure 4C**).

Uremic Toxins and Co-culture With OGD-Stressed Kidney Cells Have no Effects on the Expression of Solute Carrier Transporters

Solute carrier transporters (Slc) are strongly expressed at the BBB and are responsible for supplying the brain with nutrients such as glucose, amino acids or ions (Nalecz, 2017). We examined selected Slc genes, such as Slc2a1 (Glut1, glucose transporter), Slc5a1 (Sglt-1, Na + /Glucose Cotransporter), Slc7a1 (Cat1, Cationic Amino Acid Transporter), Slc7a5 (Lat1, Large Neutral Amino Acids Transporter) and Slc16a1 (Mct 1, Monocarboxylate Transporter) (**Figure 5**). Slc7a5 showed reduced expression after treatment with IS and IS/IAA in co-culture with normoxic HK-2 cells. The effects of IS on Slc5a1 were lower when combined with OGD, while OGD potentiated the effects of IS/IAA on Slc7a1. All other Slc mRNAs showed no changes under all experimental conditions. At the protein level, Mct1 (Slc16a1) was induced by IS treatment in co-culture with normoxic HK-2 (**Figure 6**).Under other conditions, the protein content was higher than in the control, but not statistically significant (**Figure 6**). Glut-1 (Slc2a1) protein levels were significantly increased in co-culture with OGD-treated HK2 cells with or without IS (**Figure 6**). We next examined the mRNA (**Figures 7A,B**) and protein expression (**Figures 7C–E**) of the tight junction proteins claudin-5 and occludin. The mRNA levels of Cldn5 were increased in all experimental arrangements compared to the control (**Figure 7A**), but these differences were not visible at the protein level (**Figures 7C,D**). Occludin expression was increased due to IS treatment, but remained unchanged at both mRNA and protein level (**Figures 7B–D**) under different conditions. Overall, claudin-5 and occludin showed increased mRNA and protein levels, without reaching the significance in most treatments.

To validate our *in vitro* results, we used isolated capillaries from frozen brains from mice that had undergone bilateral renal ischemia (30 minutes)/reperfusion (24 h) injury (Schneider R, unpublished) for mRNA and protein analysis (**Figures 8**, **9**). The capillaries of control mice (sham) and mice with renal ischemia/reperfusion injury (clamp) were examined for the expression of transporters, receptors and tight junction proteins. Among the efflux pumps, Abcb1b and Abcc1 were significantly increased in the clamp (**Figures 8A,B**). Abcg2 mRNA showed no changes (**Figure 8C**). The mRNA expression of solute carrier transporters Slc7a1, Slc9a1 and Slc20a2 was significantly increased in brain capillaries of uremic mice (**Figures 8G,I,K**).

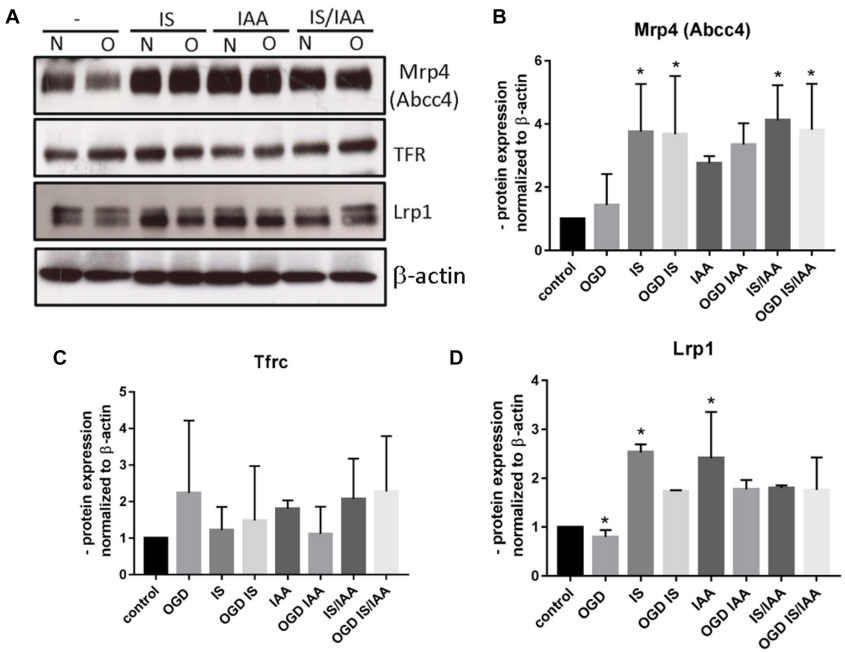

FIGURE 4 | Effects of ischemic HK-2 and uremic toxins on efflux pumps and cellular receptor protein level in brain microvascular endothelial cells. BMECs treated as described in **Figure 1** were lysed and used for protein extraction. The protein content of Mrp4 (Abcc4, ATP Binding Cassette Subfamily C Member 4), Tfrc (Transferrin Receptor), and Lrp1 (LDL Receptor Related Protein 1) was measured by Western blot **(A)**. The protein content was normalized to β-actin and to the untreated control. The densitometric analysis is shown as an average of four independent experiments with standard deviations **(B–D)**. One-way ANOVA with Dunnett's or Sidak's multiple comparison test was used to compare each treatment to the untreated control. *$p < 0.05$.

The mRNA of Slc7a5 and Slc16a1 remained unchanged (**Figures 8H,J**). Among the cellular receptors, the Ager and Lrp1 mRNAs were significantly increased in the clamp (**Figures 8D,L**) while no differences were seen in Insr and Trfc mRNA expression (**Figures 8F,N**). No changes in Cldn5 and Ocln mRNA expression were found (**Figures 8E,M**). We examined the protein expression of selected efflux and solute carrier transporters in capillaries of sham and clamp mice (**Figure 9**). Bcrp (Abcg2), P-gp (Abcb1) and Glut-1 (Slc2a1) (**Figures 9A–C,E**) were significantly increased at the protein level in brain capillaries of clamp mice. The Mrp4 (Abcc4) protein was not changed (**Figures 9A,D**).

In summary, we show that uremic conditions affect the BMEC *in vivo* and *in vitro* by altering the protein and mRNA expression of relevant efflux and influx transporters at the BBB.

DISCUSSION

Kidney failure not only leads to kidney damage, but can also have systemic effects on distant organs. Experiments with uremic mice showed cerebral inflammation (Liu et al., 2008) and in some cases cerebral edema (Kim et al., 2016). In this study, we used BMEC co-culture with kidney cells and treatment with the uremic toxins IS and IAA as *in vitro* model for kidney-brain crosstalk in the kidney ischemia/reperfusion injury model. We analyzed the effects of uremic toxins on BMEC and compared our results with the brain capillaries of mice exposed to renal ischemia/reperfusion injury. We selected the uremic toxins IS and IAA for treatment because they have previously been shown to affect endothelial cells (Gondouin et al., 2013). The limitation of our study is that we only used two selected uremic toxins. *In vivo*, multiple toxins accumulate in the blood during AKI due to the decreased GFR of dysfunctional kidneys. Most toxins are bound to albumin in the blood, so their total toxin concentration is unknown (Duranton et al., 2012). We selected a sub-toxic concentration of IA and IAA, which is much higher than that reported in patients (Vanholder et al., 2003). Co-culture with OGD-stressed kidney cells increased the amount of toxins and other kidney factors in the cell culture medium, but the effect of toxin accumulation over time could not be achieved *in vitro*. The neurological symptoms show only a low correlation with the uremic toxin concentrations in patients with kidney failure and mostly occur in the acute phase of AKI (Burn and Bates, 1998). The experimental times chosen for the experiments correspond to the acute phase of AKI. The *in vitro* and *in vivo* setting with isolated brain capillaries enables the molecular analysis of BMEC during AKI.

The level of tight junction proteins claudin-5 and occludin expression correlates with the tightness of the BBB (Balda et al., 1996; Forster et al., 2005; Burek et al., 2010; Kaiser et al., 2018). In our kidney-brain crosstalk *in vitro* model and in the brain capillaries of mice with kidney ischemia/reperfusion injury, we could not find any major differences in tight junction protein expression. Only claudin-5 was significantly increased on mRNA level in BMEC. These effects were not visible at the protein level during the selected experimental times.

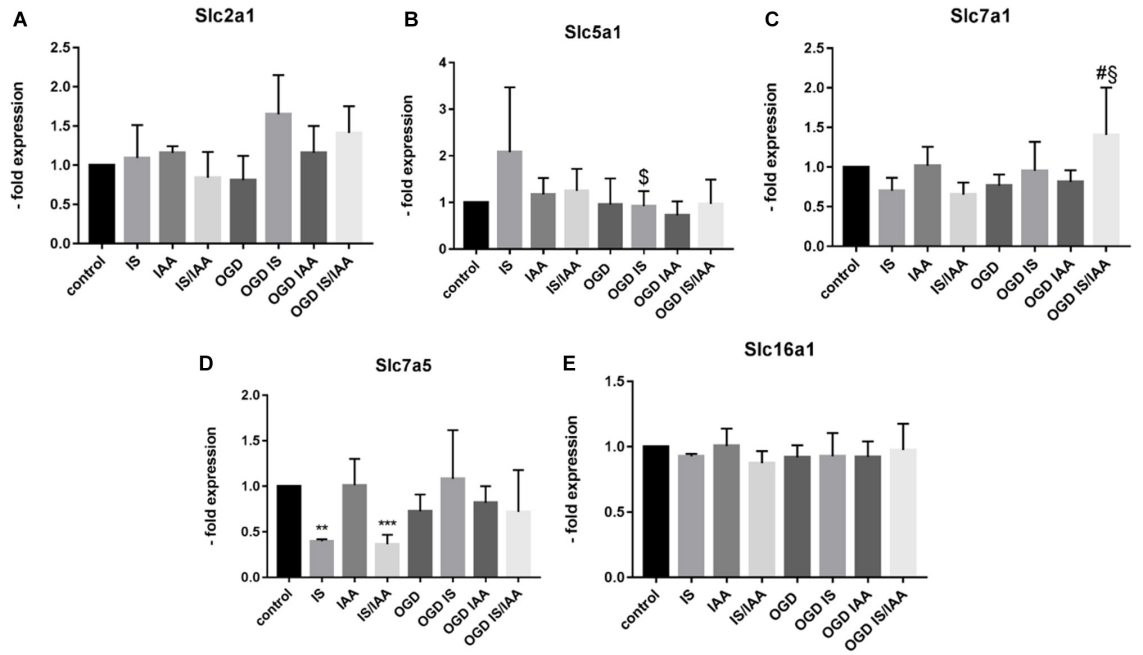

FIGURE 5 | Effects of ischemic HK-2 and uremic toxins on solute carrier transporter mRNA in brain microvascular endothelial cells. BMECs treated as described in **Figure 1** caption were lysed and used for RNA extraction. The expression of solute carrier transporter mRNA Slc2a1 (Glut-1, Solute Carrier Family 2 Member 1) **(A)**, Slc5a1 (Sglt1, Solute Carrier Family 5 Member 1) **(B)**, Slc7a1 (Cat1, Solute Carrier Family 7 Member 1) **(C)**, and Slc7a5 (Lat1, Solute Carrier Family 7 Member 5) **(D)**, and Slc16a1 (Mct1, Solute Carrier Family 16 Member 1) **(E)** was measured by qPCR. The data are shown as an average of four independent experiments with standard deviations. One-way ANOVA with Dunnett's or Sidak's multiple comparison test was used to compare each treatment to the untreated cerebEND control (**$p < 0.01$, ***$p < 0.001$) or to OGD treatment (#), $: statistically significant versus IS, §: statistically significant versus IS/IAA.

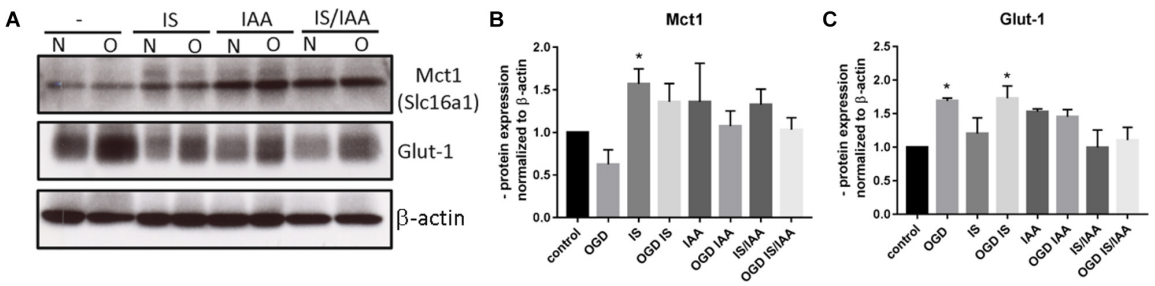

FIGURE 6 | Effects of ischemic HK-2 and uremic toxins on the protein level of solute carrier transporters in brain microvascular endothelial cells. BMECs treated as described in **Figure 1** were lysed and used for protein extraction. The protein content of Mct1 (Slc16a1, Solute Carrier Family 16 Member 1) and Glut-1 (Slc2a1, Solute Carrier Family 2 Member 1) was measured by Western blot **(A)**. The protein content was normalized to β-actin and the untreated control. The densitometric analysis is shown as an average of four independent experiments with standard deviations **(B,C)**. One-way ANOVA with Dunnett's multiple comparison test was used to compare each treatment to the control. *$p < 0.05$.

The glucose transporter showed an increased expression both in stressed cells and in mice capillaries. This indicates the brain endothelial cells are actively responding to toxins and ischemia/reperfusion injury factors and are trying to compensate for the changes in reduced metabolic activity (Burn and Bates, 1998) by increasing glucose transport and supporting the brain with nutrients. This increased Glut-1 expression is also in line with the hyperglycemia observed during AKI (Husi and Human, 2015). However, all other solute carrier transporter showed no significant changes *in vitro*. *In vivo*, an increased expression of solute carrier transporters was observed at the mRNA-level. Slc20a2 (sodium-dependent phosphate transporter), Slc9a1, and Slc7a1 showed a significantly increased mRNA-expression. Slc9a1 (Nhe1), a sodium-hydrogen antiporter 1, is involved in the volume and pH-regulation of vertebrate cells, and its increase may be one of the protective mechanisms of BMECs against uremic factors. Slc7a1 and Slc7a5 (Cat1, cationic amino acid transporter 1 and Lat1, large neutral amino acids transporter small subunit 1) were increased in the brain capillaries after kidney ischemia/reperfusion injury. Slc7a5 and Slc16a1 showed the same tendency. Slc16a1 (Mct1, monocarboxylate transporter 1) is the main regulator of the activation of the Hypoxia activated

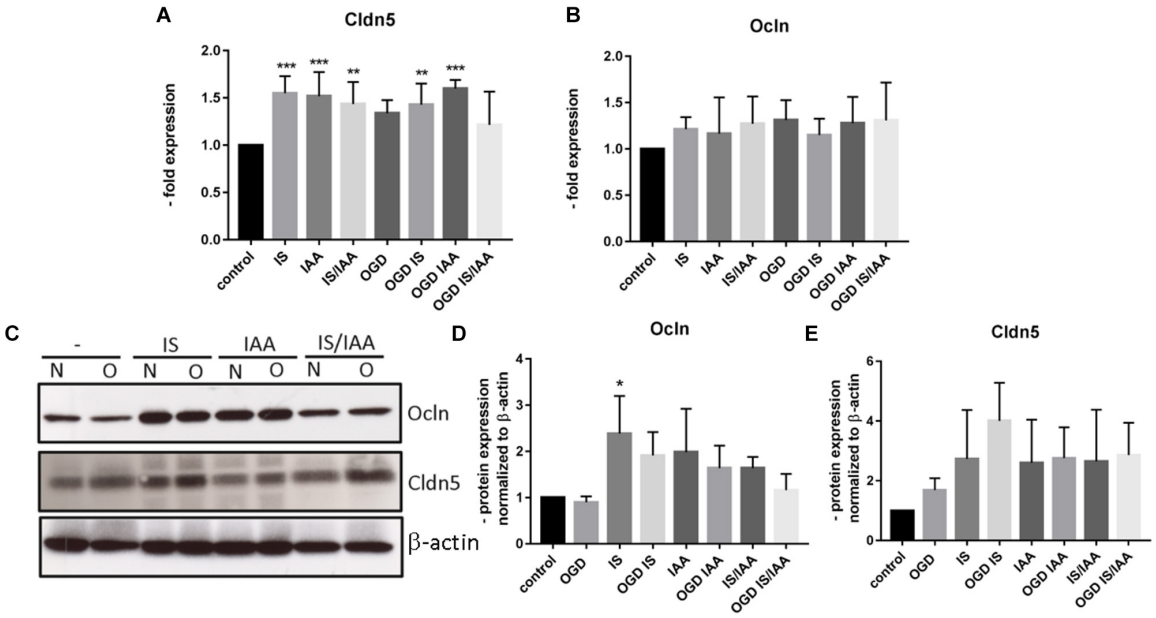

FIGURE 7 | Effects of ischemic HK-2 and uremic toxins on the mRNA and protein levels of tight junction proteins in brain microvascular endothelial cells. BMECs treated as described in **Figure 1** were lysed and used for RNA and protein extraction. Expression of tight junction protein Cldn5 (claudin-5) **(A)** and Ocln (occludin) **(B)** mRNA was measured by qPCR. The protein content was quantified by Western blot **(C–E)**. β-actin was used as an endogenous control. The data are shown as an average of four independent experiments with standard deviations. One-way ANOVA with Dunnett's multiple comparison test was used to compare each treatment to the control. $^{*}p < 0.05$, $^{**}p < 0.01$, $^{***}p < 0.001$.

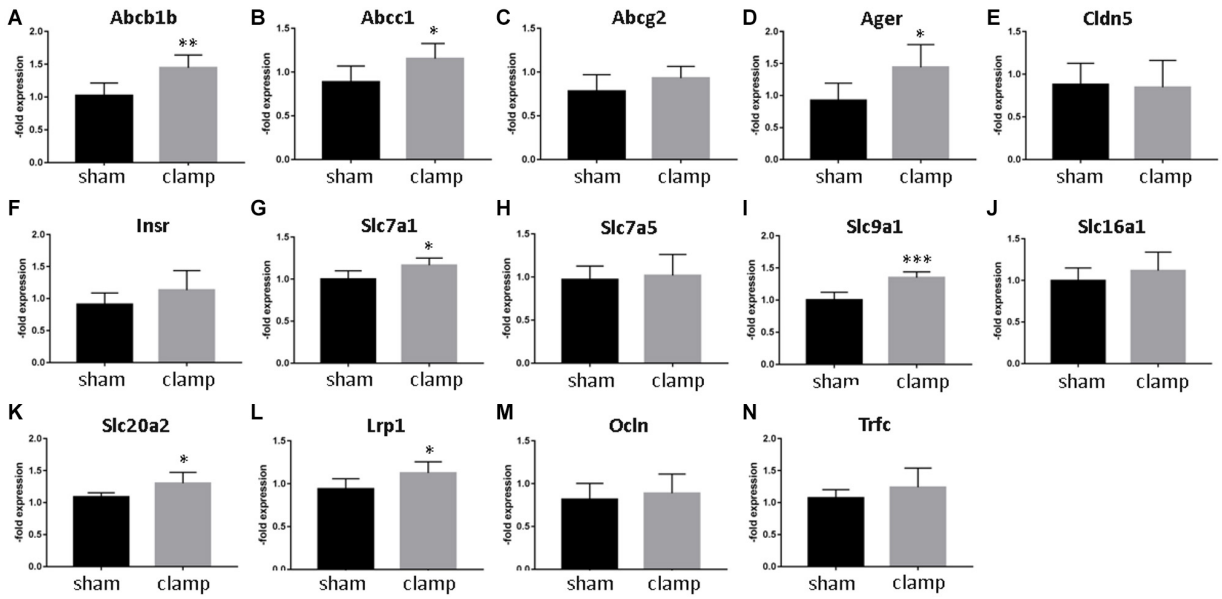

FIGURE 8 | Expression of selected transporters and tight junctions proteins in brain capillaries from mice exposed to bilateral renal ischemia/reperfusion injury on mRNA level. Brain capillaries were isolated from frozen brains of mice exposed to bilateral renal ischemia/reperfusion injury followed by RNA isolation and qPCR. Expression of Abcb1b (P-gp, Mdr1, ATP Binding Cassette Subfamily B Member1) **(A)**, Abcc1 (Mrp1, ATP Binding Cassette Subfamily C Member1) **(B)**, Abcg2 (Bcrp, ATP Binding Cassette Subfamily G Member 2) **(C)**, Ager (Advanced Gylcosylation End-Product Specific Receptor) **(D)**, Cldn5 (Claudin-5) **(E)**, Insr (Insulin Receptor) **(F)**, Slc7a1 (Cat1, Solute Carrier Family 7 Member 1) **(G)**, Slc7a5 (Lat1, Solute Carrier Family 7 Member 5) **(H)**, Slc9a1 (Nhe1, Solute Carrier Family 9 Member a1) **(I)** Slc16a1 (Mct1, Solute Carrier Family 16 Member 1) **(J)**, Slc20a2 (Pit2, Solute Carrier Family 20 Member 2) **(K)**, Lrp1 (LDL Receptor Related Protein 1) **(L)**, Ocln (Occludin) **(M)**, and Trfc (Transferrin Receptor) **(N)** was calculated by relative quantification method and is shown as average of $n = 3$ with standard deviations. $^{*}p < 0.05$, $^{**}p < 0.01$, $^{***}p < 0.001$.

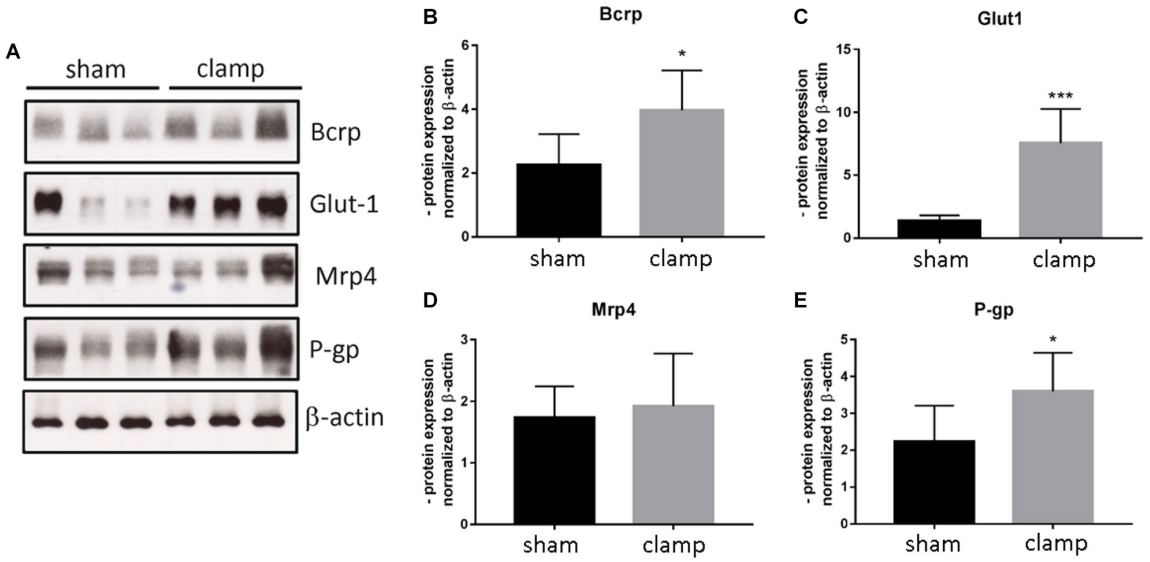

FIGURE 9 | Expression of selected transporters and tight junction proteins in brain capillaries of mice exposed to bilateral renal ischemia/reperfusion injury at the protein level. Brain capillaries were isolated from frozen brains of mice exposed to bilateral renal ischemia/reperfusion injury followed by protein extraction and Western blot **(A)**. The protein content of Bcrp (Abcg2, ATP Binding Cassette Subfamily G Member 2) **(B)**, Glut1 (Slc2a1, Solute Carrier Family 2 Member 1) **(C)**, Mrp4 (Abcc4, ATP Binding Cassette Subfamily C Member 4) **(D)**, and P-gp (Mdr1, Abcb1b ATP Binding Cassette Subfamily B Member1) **(E)** was normalized to β-actin and is shown as average of $n = 3$ with standard deviations. $^{*}p < 0.05$, $^{***}p < 0.001$.

factor (Hif-1) by lactate in endothelial cells (Sonveaux et al., 2012). Mct1 was also induced *in vitro* by treating BMECs with IS. At 48 h of *in vitro* treatment, most changes in expression were observed for the efflux pumps and not for solute carrier transporters. The cells try to pump out the toxins and the transport of only the most relevant nutrient glucose is increased. The reason for the low effects of co-culture with OGD-treated HK-2 cells on BMECs is the time chosen for sampling. The HK-2 cells were subjected to 4-h OGD and then reoxygenated for 48 h while co-cultured with BMECs with or without toxin treatment. The cells recovered and the demonstrated OGD effects on BMECs were low. However, the effects on a hypoxia/aglycemia marker Glut-1 were still visible at the protein level, which confirmed the correct experimental setting. The recovery during reoxygenation could also be observed in OGD-treated BMECs as published by us and others (Salvador et al., 2015; Tornabene et al., 2019).

We were able to show the effects of the two uremic toxins IS and IAA on BMECs. Our results further confirm the impact of IS and IAA on neurological symptoms of AKI (Iwata et al., 2007). IS has been shown to change drug delivery at the BBB (Ohtsuki et al., 2002). In our hands, IS and IAA also induced multiple changes in the gene and protein expression of drug transporters at the BBB. It will be interesting to use serum from AKI patients to treat the BMEC *in vitro*. The human BMEC would be the best choice for these studies.

Insr mRNA showed a significant increase in BMECs due to the treatment with IS and IAA under normoxic or OGD conditions. The same tendency was found for Insr in capillaries from mice with kidney ischemia/reperfusion injury. The increase in insulin signaling corresponds to the literature, in which it was shown, that inhibition of insulin signaling delays the onset of kidney failure (Ising et al., 2015).

The observed alterations at the BBB might play a role in the etiology of reported short- and long-term effects of AKI on brain function. Short-term effects are uremic encephalopathy while long-term effects are associated with a risk for developing stroke and dementia (Grams and Rabb, 2012; Guerra et al., 2012; Wu et al., 2014; Tsai et al., 2017). Studies with uremic mice showed that AKI leads to inflammation and functional changes in the brain (Liu et al., 2008). The authors of the study focused on the hippocampus, but effects on amygdala, insular and cingulate gyrus could be also possible as a background for the functional changes leading specifically to dementia. Moreover, an autonomic imbalance was suggested for the pathophysiology in CKD or AKI (Tanaka and Okusa, 2020), so that an impact of uremic toxin exposure on the autonomic areas of the brain could be associated with this relationship.

DATA AVAILABILITY STATEMENT

The original contributions presented in the study are included in the article/supplementary material, further inquiries can be directed to the corresponding authors.

ETHICS STATEMENT

All animal experiments were approved by the local animal care committee (Animal Care and Use Committee, Government of Lower Franconia, Wuerzburg, Germany).

AUTHOR CONTRIBUTIONS

MB, SB, ES, and MN performed and analyzed the experiments and drafted the manuscript. KM-E and RS provided frozen brains from uremic mice. MB, NR, RS, and CYF designed the study. All authors read and approved the final version of the manuscript.

ACKNOWLEDGMENTS

We thank Anja Neuhoff and Elisabeth Wilken for their excellent technical assistance. This publication was supported by the Open Access Publication Fund of the University of Wuerzburg.

REFERENCES

Balda, M. S., Whitney, J. A., Flores, C., Gonzalez, S., Cereijido, M., and Matter, K. (1996). Functional dissociation of paracellular permeability and transepithelial electrical resistance and disruption of the apical-basolateral intramembrane diffusion barrier by expression of a mutant tight junction membrane protein. *J. Cell Biol.* 134, 1031–1049. doi: 10.1083/jcb.134.4.1031

Banks, W. A. (2016). From blood-brain barrier to blood-brain interface: new opportunities for CNS drug delivery. *Nat. Rev. Drug Discov.* 15, 275–292. doi: 10.1038/nrd.2015.21

Blecharz, K. G., Burek, M., Bauersachs, J., Thum, T., Tsikas, D., Widder, J., et al. (2014). Inhibition of proteasome-mediated glucocorticoid receptor degradation restores nitric oxide bioavailability in myocardial endothelial cells in vitro. *Biol. Cell* 106, 219–235. doi: 10.1111/boc.201300083

Burek, M., Arias-Loza, P. A., Roewer, N., and Forster, C. Y. (2010). Claudin-5 as a novel estrogen target in vascular endothelium. *Arterioscler. Thromb. Vasc. Biol.* 30, 298–304. doi: 10.1161/atvbaha.109.197582

Burek, M., Haghikia, A., Gold, R., Roewer, N., Chan, A., and Förster, C. Y. (2014). Differential cytokine release from brain microvascular endothelial cells treated with dexamethasone and multiple sclerosis patient sera. *J. Steroids Hormonal Sci.* 5:128. doi: 10.4172/2157-7536.1000128

Burek, M., Konig, A., Lang, M., Fiedler, J., Oerter, S., Roewer, N., et al. (2019). Hypoxia-Induced MicroRNA-212/132 Alter Blood-Brain Barrier Integrity Through Inhibition of Tight Junction-Associated Proteins in Human and Mouse Brain Microvascular Endothelial Cells. *Transl. Stroke Res.* 10, 672–683. doi: 10.1007/s12975-018-0683-2

Burek, M., Salvador, E., and Forster, C. Y. (2012). Generation of an immortalized murine brain microvascular endothelial cell line as an in vitro blood brain barrier model. *J. Vis. Exp.* 66:e4022.

Burn, D. J., and Bates, D. (1998). Neurology and the kidney. *J. Neurol Neurosurg. Psychiatry* 65, 810–821. doi: 10.1136/jnnp.65.6.810

Dauchy, S., Dutheil, F., Weaver, R. J., Chassoux, F., Daumas-Duport, C., Couraud, P. O., et al. (2008). ABC transporters, cytochromes P450 and their main transcription factors: expression at the human blood-brain barrier. *J. Neurochem.* 107, 1518–1528. doi: 10.1111/j.1471-4159.2008.05720.x

Dilling, C., Roewer, N., Forster, C. Y., and Burek, M. (2017). Multiple protocadherins are expressed in brain microvascular endothelial cells and might play a role in tight junction protein regulation. *J. Cereb. Blood Flow Metab.* 37, 3391–3400. doi: 10.1177/0271678x16688706

Duranton, F., Cohen, G., De Smet, R., Rodriguez, M., Jankowski, J., Vanholder, R., et al. (2012). Normal and pathologic concentrations of uremic toxins. *J. Am. Soc. Nephrol.* 23, 1258–1270. doi: 10.1681/asn.2011121175

Edamatsu, T., Fujieda, A., Ezawa, A., and Itoh, Y. (2014). Classification of five uremic solutes according to their effects on renal tubular cells. *Int. J. Nephrol.* 2014:512178.

Forster, C., Silwedel, C., Golenhofen, N., Burek, M., Kietz, S., Mankertz, J., et al. (2005). Occludin as direct target for glucocorticoid-induced improvement of blood-brain barrier properties in a murine in vitro system. *J. Physiol.* 565, 475–486. doi: 10.1113/jphysiol.2005.084038

Gerhartl, A., Hahn, K., Neuhoff, A., Friedl, H. P., Forster, C. Y., Wunder, C., et al. (2020). Hydroxyethylstarch (130/0.4) tightens the blood-brain barrier in vitro. *Brain Res.* 1727:146560. doi: 10.1016/j.brainres.2019.146560

Gondouin, B., Cerini, C., Dou, L., Sallee, M., Duval-Sabatier, A., Pletinck, A., et al. (2013). Indolic uremic solutes increase tissue factor production in endothelial cells by the aryl hydrocarbon receptor pathway. *Kidney Int.* 84, 733–744. doi: 10.1038/ki.2013.133

Grams, M. E., and Rabb, H. (2012). The distant organ effects of acute kidney injury. *Kidney Int.* 81, 942–948. doi: 10.1038/ki.2011.241

Guerra, C., Linde-Zwirble, W. T., and Wunsch, H. (2012). Risk factors for dementia after critical illness in elderly Medicare beneficiaries. *Crit. Care* 16:R233.

Haseloff, R. F., Dithmer, S., Winkler, L., Wolburg, H., and Blasig, I. E. (2015). Transmembrane proteins of the tight junctions at the blood-brain barrier: structural and functional aspects. *Semin. Cell Dev. Biol.* 38, 16–25. doi: 10.1016/j.semcdb.2014.11.004

Helms, H. C., Abbott, N. J., Burek, M., Cecchelli, R., Couraud, P. O., Deli, M. A., et al. (2016). In vitro models of the blood-brain barrier: an overview of commonly used brain endothelial cell culture models and guidelines for their use. *J. Cereb. Blood Flow Metab.* 36, 862–890. doi: 10.1177/0271678x16630991

Husi, H., and Human, C. (2015). Molecular determinants of acute kidney injury. *J. Inj. Violence Res.* 7, 75–86.

Ising, C., Koehler, S., Brahler, S., Merkwirth, C., Hohne, M., Baris, O. R., et al. (2015). Inhibition of insulin/IGF-1 receptor signaling protects from mitochondria-mediated kidney failure. *EMBO Mol. Med.* 7, 275–287. doi: 10.15252/emmm.201404916

Ittner, C., Burek, M., Störk, S., Nagai, M., and Förster, C. Y. (2020). Increased catecholamine levels and inflammatory mediators alter barrier properties of brain microvascular endothelial cells in vitro. *Front. Cardiovasc. Med.* 7:73. doi: 10.3389/fcvm.2020.00073

Iwata, K., Watanabe, H., Morisaki, T., Matsuzaki, T., Ohmura, T., Hamada, A., et al. (2007). Involvement of indoxyl sulfate in renal and central nervous system toxicities during cisplatin-induced acute renal failure. *Pharm. Res.* 24, 662–671. doi: 10.1007/s11095-006-9183-2

Kaiser, M., Burek, M., Britz, S., Lankamp, F., Ketelhut, S., Kemper, B., et al. (2018). The influence of capsaicin on the integrity of microvascular endothelial cell monolayers. *Int. J. Mol. Sci.* 20:122. doi: 10.3390/ijms20010122

Keaney, J., and Campbell, M. (2015). The dynamic blood-brain barrier. *FEBS J.* 282, 4067–4079.

Kim, D. M., Lee, I. H., and Song, C. J. (2016). Uremic Encephalopathy: MR Imaging Findings and Clinical Correlation. *AJNR Am. J. Neuroradiol.* 37, 1604–1609. doi: 10.3174/ajnr.a4776

Kleinschnitz, C., Blecharz, K., Kahles, T., Schwarz, T., Kraft, P., Gobel, K., et al. (2011). Glucocorticoid insensitivity at the hypoxic blood-brain barrier can be reversed by inhibition of the proteasome. *Stroke* 42, 1081–1089. doi: 10.1161/strokeaha.110.592238

Krizbai, I. A., Nyul-Toth, A., Bauer, H. C., Farkas, A. E., Traweger, A., Hasko, J., et al. (2016). Pharmaceutical targeting of the brain. *Curr. Pharm. Des.* 22, 5442–5462.

Lau, W. L., Nunes, A. C. F., Vasilevko, V., Floriolli, D., Lertpanit, L., Savoj, J., et al. (2020). Chronic kidney disease increases cerebral microbleeds in mouse and man. *Transl. Stroke Res.* 11, 122–134. doi: 10.1007/s12975-019-00698-8

Liu, M., Liang, Y., Chigurupati, S., Lathia, J. D., Pletnikov, M., Sun, Z., et al. (2008). Acute kidney injury leads to inflammation and functional changes in the brain. *J. Am. Soc. Nephrol.* 19, 1360–1370. doi: 10.1681/asn.2007080901

Lu, R., Kiernan, M. C., Murray, A., Rosner, M. H., and Ronco, C. (2015). Kidney-brain crosstalk in the acute and chronic setting. *Nat. Rev. Nephrol.* 11, 707–719. doi: 10.1038/nrneph.2015.131

Nalecz, K. A. (2017). Solute carriers in the blood-brain barier: safety in abundance. *Neurochem. Res.* 42, 795–809. doi: 10.1007/s11064-016-2030-x

Naud, J., Laurin, L. P., Michaud, J., Beauchemin, S., Leblond, F. A., and Pichette, V. (2012). Effects of chronic renal failure on brain drug transporters in rats. *Drug Metab. Dispos.* 40, 39–46. doi: 10.1124/dmd.111.041145

Ohtsuki, S., Asaba, H., Takanaga, H., Deguchi, T., Hosoya, K., Otagiri, M., et al. (2002). Role of blood-brain barrier organic anion transporter 3 (OAT3) in the efflux of indoxyl sulfate, a uremic toxin: its involvement in neurotransmitter metabolite clearance from the brain. *J. Neurochem.* 83, 57–66. doi: 10.1046/j.1471-4159.2002.01108.x

Salvador, E., Burek, M., and Forster, C. Y. (2015). Stretch and/or oxygen glucose deprivation (OGD) in an in vitro traumatic brain injury (TBI) model induces calcium alteration and inflammatory cascade. *Front. Cell Neurosci.* 9:323. doi: 10.3389/fncel.2015.00323

Sauvant, C., Schneider, R., Holzinger, H., Renker, S., Wanner, C., and Gekle, M. (2009). Implementation of an in vitro model system for investigation of reperfusion damage after renal ischemia. *Cell Physiol. Biochem.* 24, 567–576. doi: 10.1159/000257513

Silwedel, C., and Forster, C. (2006). Differential susceptibility of cerebral and cerebellar murine brain microvascular endothelial cells to loss of barrier properties in response to inflammatory stimuli. *J. Neuroimmunol.* 179, 37–45. doi: 10.1016/j.jneuroim.2006.06.019

Sonveaux, P., Copetti, T., De Saedeleer, C. J., Vegran, F., Verrax, J., Kennedy, K. M., et al. (2012). Targeting the lactate transporter MCT1 in endothelial cells inhibits lactate-induced HIF-1 activation and tumor angiogenesis. *PLoS One* 7:e33418. doi: 10.1371/journal.pone.0033418

Tanaka, S., and Okusa, M. D. (2020). Crosstalk between the nervous system and the kidney. *Kidney Int.* 97, 466–476. doi: 10.1016/j.kint.2019.10.032

Tornabene, E., Helms, H. C. C., Pedersen, S. F., and Brodin, B. (2019). Effects of oxygen-glucose deprivation (OGD) on barrier properties and mRNA transcript levels of selected marker proteins in brain endothelial cells/astrocyte co-cultures. *PLoS One* 14:e0221103. doi: 10.1371/journal.pone.0221103

Tsai, H. H., Yen, R. F., Lin, C. L., and Kao, C. H. (2017). Increased risk of dementia in patients hospitalized with acute kidney injury: a nationwide population-based cohort study. *PLoS One* 12:e0171671. doi: 10.1371/journal.pone.0171671

Vanholder, R., De Smet, R., Glorieux, G., Argiles, A., Baurmeister, U., Brunet, P., et al. (2003). Review on uremic toxins: classification, concentration, and interindividual variability. *Kidney Int.* 63, 1934–1943. doi: 10.1046/j.1523-1755.2003.00924.x

Wilhelm, I., Nyul-Toth, A., Suciu, M., Hermenean, A., and Krizbai, I. A. (2016). Heterogeneity of the blood-brain barrier. *Tissue Barriers* 4, e1143544.

Wu, V. C., Wu, P. C., Wu, C. H., Huang, T. M., Chang, C. H., Tsai, P. R., et al. (2014). The impact of acute kidney injury on the long-term risk of stroke. *J. Am. Heart Assoc.* 3:e000933.

Yu, M., Kim, Y. J., and Kang, D. H. (2011). Indoxyl sulfate-induced endothelial dysfunction in patients with chronic kidney disease via an induction of oxidative stress. *Clin. J. Am. Soc. Nephrol.* 6, 30–39. doi: 10.2215/cjn.05340610

Conflict of Interest: The authors declare that the research was conducted in the absence of any commercial or financial relationships that could be construed as a potential conflict of interest.

frontiers in Physiology

ORIGINAL RESEARCH
published: 27 November 2020
doi: 10.3389/fphys.2020.583668

Astragalus mongholicus Bunge and Panax Notoginseng Formula (A&P) Combined With Bifidobacterium Contribute a Renoprotective Effect in Chronic Kidney Disease Through Inhibiting Macrophage Inflammatory Response in Kidney and Intestine

*Tan Rui-Zhi[1†], Diao Hui[1,2†], Li Jian-Chun[1], Zhong Xia[1], Wang Xiao-Jia[1], Wen Dan[1,2], Fan Jun-Ming[1,3] and Wang Li[1]**

[1] Research Center for Integrated Chinese and Western Medicine, Affiliated Traditional Medicine Hospital, Southwest Medical University, Luzhou, China, [2] Department of Nephrology, Affiliated Hospital of Southwest Medical University, Luzhou, China, [3] Department of Nephrology, Affiliated Hospital of Chengdu Medical College, Chengdu, China

There is increasing evidence that Chronic Kidney Disease (CKD) can cause intestinal dysfunction, which in turn aggravates the progression of kidney disease. Studies have shown that the immune response of macrophage plays an important role in promoting inflammation in kidney and intestine of CKD. *Astragalus mongholicus* Bunge and Panax notoginseng formula (A&P) is a widely used traditional medicine for the treatment of CKD in China, however, the underlying mechanism is largely unclear. In this study, we aimed to explore the role of A&P and Bifidobacterium combination treatment in regulation of inflammatory response of macrophage in kidney and intestine of CKD mouse, as well as the potential molecular mechanism. We established a CKD mouse model with 5/6 nephrectomy and a macrophage inflammatory cellular model with LPS and urotoxin *in vivo* and *in vitro*. The results showed that A&P combined with Bifidobacterium significantly reduced the expression and secretion of IL-1β, IL-6, TNFα, and MCP-1 in kidney and blood, as well as in inflammatory macrophage. Interestingly, A&P combined with Bifidobacterium strongly improved the intestinal flora and protected the intestinal barrier. Notably, the maintainer of macrophage polarization, Mincle, was activated in kidney and intestine of CKD mouse as well as in urotoxin stimulated macrophage, that was effectively inhibited by the treatment of A&P and Bifidobacterium combination. Overexpression of Mincle by genetic modification can abolish the inhibitory effects of A&P combined with Bifidobacterium on inflammation in urotoxin stimulated RAW264.7 cells. In summary, these findings demonstrated that A&P combined with Bifidobacterium can protect kidney against CKD by down-regulating macrophage inflammatory response in kidney and intestine via suppressing Mincle signaling, which provides a new insight in the treatment of CKD with traditional medicine.

Keywords: *Astragalus mongholicus* Bunge and Panax notoginseng formula, bifidobacterium, macrophage, CKD, Mincle

OPEN ACCESS

Edited by:
Jonatan Barrera-Chimal, National Autonomous University of Mexico, Mexico

Reviewed by:
Patrick Ming-Kuen Tang, The Chinese University of Hong Kong, China
Cristián A. Amador, Autonomous University of Chile, Chile

****Correspondence:***
Wang Li
wangli120@swmu.edu.cn

† These authors have contributed equally to this work

Specialty section:
This article was submitted to Renal and Epithelial Physiology, a section of the journal Frontiers in Physiology

Received: *16 July 2020*
Accepted: *03 November 2020*
Published: *27 November 2020*

Citation:
Rui-Zhi T, Hui D, Jian-Chun L, Xia Z, Xiao-Jia W, Dan W, Jun-Ming F and Li W (2020) Astragalus mongholicus Bunge and Panax Notoginseng Formula (A&P) Combined With Bifidobacterium Contribute a Renoprotective Effect in Chronic Kidney Disease Through Inhibiting Macrophage Inflammatory Response in Kidney and Intestine. Front. Physiol. 11:583668. doi: 10.3389/fphys.2020.583668

INTRODUCTION

Chronic Kidney Disease (CKD), which is defined as the presence of renal structural and/or functional abnormalities for at least 3 months, has been widely regarded as an important public health problem. Recent epidemiological surveys revealed high levels of prevalent incidence of CKD worldwide which varies from 5 to 13% among countries (De Nicola and Minutolo, 2016). Considering the great medical and social burden, it casts urgent importance to the prevention, diagnosis and treatment of this disease.

In the advanced stage of chronic kidney disease, metabolic waste cannot be excreted by the intestine and kidney, and is accumulated in the body in large amounts, which may further enter the intestinal wall through blood vessels. Meanwhile, increased urotoxin in blood after kidney injury also enter the intestine wall, which promotes fundamental changes of the living environment of intestinal epithelium and intestinal flora, leading to an increase of the number of pathogenic bacteria and a reduction of beneficial bacteria, which directly or indirectly promotes the entry of toxins into intestinal epithelial cells, causing severe damage to the structure and function of intestinal barrier. Therefore, the permeability of the intestinal epithelium is greatly increased, which in turn causes the intestinal toxins to invade into the blood and accelerates the progression of CKD (Vaziri et al., 2013; Vanholder and Glorieux, 2015; Sommer et al., 2017; Hugenholtz and de Vos, 2018). The intestinal mucosal immune system is one of the largest immunological compartments in human body, and any destruction of the microbiome may cause an imbalance of the body's immune system. Therefore, using modern medical methods to explore the mechanism of the intestinal microecological balance and the interaction between intestinal mucosal barrier function and CKD through animal model *in vivo* and cellular model *in vitro* are new directions worth exploring (Crespo-Salgado et al., 2016; Nallu et al., 2017).

Studies have shown that when an organ is injured, it starts an immune response and activates a variety of immune cells, including neutrophils, dendritic cells (DC), macrophages, natural killer cells (NK), T lymphocytes and regulatory T cells. Among them, macrophages are important innate immune cells with phagocytosis (Alikhan and Ricardo, 2013). Polarization of macrophages is divided according to their function (Murray and Wynn, 2011). Macrophages that secrete pro-inflammatory factors and exert pro-inflammatory functions are called M1 macrophages. On the contrary, macrophages that play a role in reducing inflammation and promoting tissue repair are called M2 macrophages (Barros et al., 2013; Peng et al., 2017; Soldano et al., 2018). Transition of the macrophage polarization is widespread in the occurrence and development of inflammatory diseases such as kidney disease, intestinal disease, obesity, and some cardiovascular disease (Bain and Mowat, 2014; De Schepper et al., 2018), in which the imbalance of macrophage polarization can reflect the inflammatory state of microenvironment of local tissues. Therefore, we believe that understanding the mechanism underlying polarization imbalance in intestinal macrophage is helpful for the treatment of CKD.

Mincle, macrophage-induced c-type lectin (Clec4e), is a transmembrane pattern recognition receptor involved in innate immunity and mainly expressed in innate immune cells, such as macrophages, dendritic cells, B cells and neutral Granulocytes (Patin et al., 2017; Lim and Lappas, 2019). Related studies have shown that Mincle is strictly regulated by TLR4/NF-κB signaling. Mincle plays a role in maintaining the M1 phenotype of pro-inflammatory macrophage in acute kidney disease (Hui et al., 2020). In the cisplatin-induced mouse AKI model, inhibition of Mincle on macrophage reduced the activity of M1 type macrophage in kidney, thereby improving kidney damage in mice (Inoue, 2017; Li et al., 2017; Wahi et al., 2019). Our previous research reported that isoliquiritigenin inhibited unilateral ureteral obstruction (UUO)-induced kidney damage by down-regulating the inflammation and fibrosis maintained by Mincle (Liao et al., 2020). However, the role of Mincle in chronic kidney disease and whether Mincle can be used as a therapeutic target for CKD are not clearly studied.

Astragalus mongholicus Bunge and Panax notoginseng formula is prescribed under the guidance of traditional Chinese medicine theory. It consists of Panax notoginseng, *Astragalus mongholicus* Bunge, Angelica sinensis, *Achyranthes bidentata* Blume, and *Ecklonia kurome* Okamura. Clinical studies have found that the combination of A&P and basic treatment can significantly improve the renal function and quality of life of patients with diabetic nephropathy and CKD (Hui et al., 2020; Wen et al., 2020). *Astragalus mongholicus* Bunge and Panax notoginseng are the main ingredients in this formula, which have high medicinal value. *Astragalus mongholicus* Bunge can improve metabolism, turnover of serum and liver proteins, immunity, cardiac function, as well as has the effects of lowering blood sugar, anti-tumor, anti-fatigue and antibacterial (Fu et al., 2014). Panax notoginseng is a widely used Chinese medicine, which can affect the central nervous system, circulatory system, digestive system, urinary system, reproductive system and immune system. It also has anti-aging, anti-tumor and anti-inflammatory effects (Wang et al., 2016). Previous study has found that in acute kidney injury, A&P can improve renal inflammation in mice by inhibiting the Mincle/NF-κB signaling pathway and M1 macrophage activity (Hui et al., 2020). Therefore, we try to reveal the effects and potential mechanism of A&P on CKD.

The probiotic Bifidobacterium is clinically used for diarrhea, constipation, indigestion and bloating caused by intestinal flora disorders, as well as adjuvant treatment of endotoxemia. Patients with intestinal dysfunction can take the preparation of Bifidobacteria to directly supplement the normal physiological bacteria of the human intestine, thereby adjusting the balance of intestinal microecology and rebuilding the integrity of intestinal barrier (Koppe et al., 2015; Jia et al., 2018; Tsai et al., 2019). From the point of immunology, bifidobacterium can improve the immune function of intestine (Cigarran Guldris et al., 2017), and promote the function of digestion and absorption of intestine. However, the use of Bifidobacteria alone in the treatment of CKD is controversial, whether the combination of Bifidobacteria and the traditional Chinese medicine formula A&P can enhance the improvement of chronic kidney disease remains to be studied.

In this present study, we used a novel 5/6 nephrectomy induced CKD mouse model *in vivo* and an inflammatory macrophage model *in vitro* to study the protective effects of A&P on kidney and intestine of CKD mice and explore whether A&P inhibited inflammation of kidney and intestine in CKD through regulating Mincle signaling, that may provides a new option for the treatment of CKD.

MATERIALS AND METHODS

Astragalus mongholicus Bunge and Panax Notoginseng Formula and Bifidobacterium

Astragalus mongholicus Bunge and Panax notoginseng formula is a traditional Chinese medicine formula used clinically to treat kidney diseases such as diabetic nephropathy, chronic kidney disease, and acute kidney disease (Wen et al., 2020). It consists of *Astragalus mongholicus* Bunge (3g), Panax notoginseng (1g), Angelica sinensis (3g), *Achyranthes bidentata* Blume (3g) and *Ecklonia kurome* Okamura (3g). The main component profile of A&P was analyzed by high performance liquid chromatography in our previous study (Hui et al., 2020). The formula was purchased from the affiliated traditional medicine hospital of Southwest Medical University, Luzhou City, Sichuan Province. The dosage for gavage is determined by referring to the conversion method of human and laboratory animals in "Pharmacological Experimental Methodology" edited by Professor Xu Shuyun. Mice daily dose = (human clinical daily dose × human defined body weight 70 kg × human and mouse body surface area conversion coefficient 0.0026) ÷ mouse defined body weight 20g. Therefore, the daily gavage dose of mice calculated by the formula is 1972 mg/kg/d. Bifidobacterium Lactobacillus triple live bacteria tablets (golden Bifidobacteria), its main components are Bifidobacterium, Lactobacillus bulgaricus and *Streptococcus thermophilus*. Bifidobacterium was purchased from Shenzhen Xinwanze Pharmaceutical Co., Ltd. The dose for gavage is also determined by referring to the conversion method of human and laboratory animals, and the daily gavage dose of Bifidobacterium in mice calculated by the formula is 303 mg/kg/d. Dissolve the powder of A&P and BB in distilled water, followed by intragastric administration of these drugs (200 μl) to mouse once a day. Mice in sham group were treated with gavage of equal volume of saline.

Preparation of Drug-Containing Serum

A&P (1972 mg/kg/d), Bifidobacterium (303 mg/kg/d), and their combination were administered to male C57BL/6 mice (8 weeks of age, 20–24g body weight) by gavage for seven consecutive days. On the 7th day, blood was taken from the heart 2 h after the gavage, and stored at 4°C overnight. The next day, the blood was centrifuged at 3000 rpm for 10 min at 4°C to extract serum and collect all serum for subsequent cellular experiments. In the cell experiment, we used the prepared medicated serum instead of ordinary fetal bovine serum (10%).

Simulate the Urotoxin Environment in RAW264.7 Cells

Add 200 ng/ml of Lipopolysaccharide (LPS) (L2630, Sigma-Aldrich, United States) to the complete medium of RAW264.7 cell to put the cells in an inflammatory stress state, then add indophenol sulfate (16926, Cayman, United States) 200 μM and *trans* aconitic acid (122750, Sigma, United States) 200 μM, respectively, to simulate the uremic environment.

5/6 Kidney Ligation Model (Nx5/6, CKD Model)

Male C57BL/6 mice (8 weeks of age and 22–25 g body weight) were classified into 5 groups: Sham, CKD, CKD + BB, CKD + A&P and CKD + BB + A&P group with 8 mice in each group. The CKD mouse model was constructed by directly ligating the upper and lower poles of left kidney after removal the right kidney 1 week later (Tan et al., 2019). Briefly, the right kidney was exposed and removed. One week later, the left kidney was exposed and the upper and lower poles were ligated with 3–0 non-absorbable suture. CKD mouse model can be obtained after six to 8 weeks of normal feeding after surgery. In this study, we determined that the model was successfully built at 7 weeks post-surgery, subsequently, the treatments were performed on these modeled mice for 4 weeks. Urine and feces of mice were collected by metabolic cage. All animal experiments were carried out according to the guidelines approved by the Animal Ethics Committee of Southwest Medical University.

CCK-8 Analysis

Cells were seeded in 96-well plates at a density of 3000 per well, with 6 replicate wells per group. After 24 h of starvation culture, cells were treated with a drug-containing medium for 24 h, then the medium was aspirated, 100 μl of 10% CCK-8 reagent was added to each well, and incubated in an incubator for 3 h. The absorbance value of each well was measured at 450 nm by BioTeK reader, and the cell survival rate was calculated according to the results.

Real-Time PCR

According to the instructions of the kit: Eastep qPCR Master Mix kit (LS2068, Promega, United States) is used to detect the mRNA expression levels of cells and kidneys; TRIzol Reagent (11596026, Invitrogen, United States) was used to extract total RNA from RAW264.7 cells and kidneys; RevertAid first-strand cDNA synthesis kit (K1622, Thermo Scientific, MA, United States) was used to reverse transcribe total RNA to cDNA; RT-PCR was performed with the Mastercycler ep Realplex2 real-time PCR system (LightCycle480II, Roche, United States). The relative expression of a given gene is calculated by the threshold cycle (CT) method. Primer sequences are listed in **Table 1**.

Enzyme-Linked Immunosorbent Assay

Collect CKD mouse serum and RAW264.7 cell culture supernatant. The concentration of IL-1β (Neobioscience, EMC001b), IL-6 (Neobioscience, EMC004), and TNF-α (Neobioscience, 500850) in serum and culture medium were

TABLE 1 | List of primers used for Real-time PCR.

Gene	Species	Forward sequence (5′-3′) Reverse sequence (5′-3′)
Mincle	mouse	F: ACCAAATCGCCTGCATCC
		R: CACTTGGGAGTTTTTGAAGCATC
IL-1β	mouse	F: TTCAGGCAGGCAGTATCACTC
		R: GAAGGTCCACGGGAAAGACAC
IL-6	mouse	F: CTGCAAGAGACTTCCATCCAG
		R: AGTGGTATAGACAGGTCTGTTGG
TNF-α	mouse	F: CATCTTCTCAAAATTCGAGTGACAA
		R: TGGGAGTAGACAAGGTACAACCC
iNOS	mouse	F: CAGCTGGGTCGTACAAAC
		R: CATTGGAAGTGAAGCGTTT
MCP-1	mouse	F: CTGAGTTGACTCCTACTGTGGA
		R: TCTTCCCAGGGTCGATAAAGT
GAPDH	mouse	F: ACAGCAACAGGGTGGTGGAC
		R: TTTGAGGGTGCAGCGAACTT

detected according to the instructions of the ELISA kit. The absorbance value of each well was measured at 450 nm by BioTeK reader.

Immunofluorescence Staining

After placing the frozen sections of the tissues at room temperature for 20 min, wash these sections for three times with PBS. Subsequently, block the samples with 10% goat serum for 30 min at 37°C, and then incubate the samples with rat anti-F4/80 primary antibody (Santa Cruz, 1:50, sc-52664) and mouse anti-Mincle primary antibody (Santa Cruz, 1:50, sc-390806) overnight at 4°C. The next day, wash these samples with PBS three times and conjugate with AlexaFluor488 conjugated anti-rabbit secondary antibody (CST, 1: 200, 4412S) and AlexaFluor647 conjugated anti-mouse secondary antibody (CST, 1: 200, 4410S) at room temperature for 1 h, followed by washing three times with PBS, then add diluted DAPI dropwise to stain the nuclei for 10 min in the dark. Finally, pictures were obtained with a confocal microscope (Nikon, Japan).

Western Blotting

The total protein was extracted from cell and tissues using RIPA lysis buffer containing protease inhibitors and phosphatase inhibitors. Proteins (25 μg of each sample) were separated on a 10% SDS-PAGE gel and transferred to a PVDF membrane by wet blotting. After blocking in 5% milk, the membranes were incubated with the antibodies against p-p65 (Rabbit anti-mouse, sc-136548, 1:1000, Santa Cruz), p65 (Mouse anti-mouse, #6956, 1:1000, CST), Mincle (Mouse anti-mouse, sc-390806, 1:500, Santa Cruz), iNOS (Rabbit anti-mouse, 13120S, 1:1000, CST), ZO-1 (Rabbit anti-mouse, 61–7300, 1:1000, Life technologies), Occludin (Mouse anti-mouse, 33–1500, 1:1000, Life technologies), Claudin-1 (Rabbit anti-mouse, 71–7800, 1:1000, Life technologies) and GAPDH (Mouse anti-mouse, AB2000, 1:5000, Abiways) and β-actin (Rabbit anti-mouse, 1:50000, abcam) at 4°C overnight. The next day, membranes were subsequently incubated with the secondary antibody of peroxidase-conjugated goat anti-mouse IgG (ZB-2305, 1:3000) and goat anti-rabbit IgG (ZB-2301, 1:3000) for 1 h at room temperature. The band was analyzed by the gel imaging system. Gray intensity of the band was calculated by ImageJ software.

Flow Cytometry Analysis

Fresh kidney tissue was digested with collagenase IV (RAW264.7 cells were digested with 0.25% trypsin-EDTA into cell suspension), then fixed at room temperature in 4% paraformaldehyde for 1 h. After washing with PBS for 2 times, cells were incubated with iNOS primary antibody (13120S, 1: 200, CST), CD206 primary antibody (ab64693, 1: 200, abcam, directly coupled antibody) and Mincle primary antibody (sc-390806, 1:50, Santa Cruz) at 4°C overnight. The next day, the cells were incubated with fluorescent secondary antibody for 1 h. After washing with PBS for 2 times, the cells were analyzed using a flow cytometer (FACSAria, BD Biosciences, United States), and the data were processed using FlowJo software (X 10.0.7).

Detection of Renal Function

The urine and the tail blood of the mice were collected to detect the serum creatinine (C011-1-1, Nanjing Jiancheng Bioengineering Institute), urea nitrogen (C013-2-1, Nanjing Jiancheng Bioengineering Institute) and urine protein (C035-1-1, Nanjing Jiancheng Bioengineering Institute) following the instructions of corresponding kits.

16s DNA Detection of Microorganisms

The feces from each group were collected and stored in a special feces storage reagent every week. All of the samples were sent to Shanghai Ouyi Biomedical Technology Co., Ltd., for 16s DNA detection.

Hematoxylin-Eosin Staining

The pre-treated tissue paraffin sections were stained in hematoxylin aqueous solution for 10 min, rinsed with running water for 5 min, then dehydrated in 100% alcohol, stained with Eosin (H&E, Beyotime, China) solution for 2–3 min, and finally transparent, and mounted. The tubulointerstitial injury index was graded as described previously (Radford et al., 1997). The degree of injury to the intestinal tissues was evaluated according to previous description (Chiu et al., 1970). Pictures were captured by the optical microscope (Eclipse 80i, Nikon, Japan).

Sirius Red Staining

The paraffin slices were stained with the Sirius red stain at 37°C for one and a half hour, rinsed with running water for 10 min, then stained with hematoxylin aqueous solution for 10 min, followed by rinsing with running water for 10 min, finally dehydrated, transparent, and mounted. Images were captured by the optical microscope (Eclipse 80i, Nikon, Japan).

Overexpression of Mincle by Plasmid Transfection

Extracting pcDNA3.1-Mincle and pcDNA3.1-vector plasmids from two Escherichia coli (purchased from GeneChem company)

by using plasmid extraction kit (NucleoBond Xtra MiDi EF, 740420.50). Then, the plasmid and DNA transfection reagent (ZETA life) were mixed with complete medium and added to RAW264.7 cells for 48 h.

Statistical Analysis

This study used SPSS22.0 and Prism 6 software for analysis. Data were presented as mean ± standard error. One-way analysis of variance (One-Way ANOVA) was used for multigroup comparison, followed by the Student-Newman-Keuls post-test. $P < 0.05$ was considered statistically significant.

RESULTS

A&P Combined With Bifidobacterium Treatment Improves Kidney Function and Pathology in CKD Mice

During the 7 weeks of modeling, compared with the sham group, the blood creatinine, urea nitrogen and urine protein in the 5/6 kidney ligation model group were all increased, and the body weight was reduced. In contrast, the blood creatinine, urea nitrogen and urine protein in A&P + Bifidobacterium treated mice were significantly decreased, and their body weight were increased. However, mice using Bifidobacteria alone did not exhibit significant improvement on renal function (**Figure 1A**). H&E and Sirius red stainings were employed to detect the protective effect of A&P on kidney of CKD model. The H&E staining results showed that compared with the sham group, the kidney in CKD model mice present glomerular atrophy and deformation, renal tubular expansion as well as necrosis and shedding of renal tubular epithelial cells. After treatment with A&P + Bifidobacteria, the expansion of renal tubules in CKD mice was significantly reduced, and the glomerular morphology was restored (**Figure 1B**). The result of Sirius red staining demonstrated that, compared with the sham group, the positive area of sirius red staining in kidney of CKD mice was increased, indicating severe renal fibrosis, accompanied by glomerular atrophy and renal tubular expansion. However, compared with CKD group, kidney in A&P and Bifidobacterium combination treatment group showed significantly reduction of fibrosis and other pathological damages (**Figure 1C**). The tubulointerstitial injury index was graded as described previously (**Figure 1D**). **Figure 1E** shows the morphology of each group of kidneys. These results suggested that A&P combined with bifidobacterium treatment can significantly improve the body weight and renal function in CKD mice.

A&P Combined With Bifidobacterium Treatment Improves Renal and Systemic Inflammation in CKD Mice

To investigate the effects of A&P + Bifidobacterium on inflammation in CKD mice, we performed Real-time PCR and ELISA to exam the expression and secretion of inflammatory cytokines. The PCR results showed that, compared with CKD group, A&P and Bifidobacterium combination significantly reduced mRNA expression of inflammatory indicators (IL-1β, IL-6, and TNF-α) in kidney of CKD mice (**Figure 2A**), whose inhibitory effect was better than using Bifidobacterium alone. Moreover, the ELISA results demonstrated that, compared with CKD group, A&P and Bifidobacterium combination strongly decreased secretion of inflammation indicators (IL-1β, IL-6, and TNF-α) in serum of CKD mice (**Figure 2B**). These results suggested that the combination of A&P and Bifidobacterium can effectively improve the renal and systemic inflammation in CKD mice.

A&P Combined With Bifidobacterium Treatment Restored the Intestinal Barrier of CKD Mice

Intestinal barrier is essential for maintaining intestinal function, we therefore detected the expression of indicators of intestinal barrier in intestines of each group. The H&E staining results showed that, compared with the CKD group, A&P and Bifidobacterium combination reduced the intestinal damage of the CKD mice (**Figure 3A**). Immunohistochemical staining results indicated that the ZO-1, Occludin-1 and claudin-1 proteins in intestine of Sham group were evenly distributed on the top of intestinal epithelial cells with a honeycomb or dot shape. However, these proteins were significantly reduced in intestine of CKD group. Compared with CKD group, the protein levels of ZO-1, Occludin-1 and claudin-1 in intestine of A&P and Bifidobacterium combination group were strongly recovered (**Figure 3B**). Intestinal damage was evaluated in each group according to Chiu's score (**Figure 3C**). The mean IOD of Claudin-1, Occludin-1 and ZO-1 IHC were illustrated in **Figure 3D**. The western blot results also proved the up-regulation of ZO-1, Occludin-1 and claudin-1 protein levels in A&P and Bifidobacterium combination group compared with the CKD model group (**Figure 3E**). These results suggested that A&P combined with Bifidobacterium had a protective effect on intestinal barrier of CKD mice.

A&P Combined With Bifidobacterium Treatment Has a Positive Effect on the Intestinal Flora of CKD Mice

To test whether A&P combined with Bifidobacterium improved the intestinal flora of CKD mice, we collected mouse feces and subjected to microbiological 16s DNA detection. Among them, alpha diversity is related to boxplot analysis. This method calculates the diversity index of the samples between each group and within the group on the basis of a uniform data depth, and draws a boxplot diagram of the diversity index of each group. Microbial 16s DNA test results showed that compared with CKD group, A&P combined with Bifidobacteria treatment recovered the intestinal flora to normal in CKD mice, which was better than using A&P or Bifidobacteria alone (**Figure 4**). These results showed that A&P combined with Bifidobacterium treatment has a positive effect on intestinal flora of CKD mice than treating with A&P or Bifidobacterium alone.

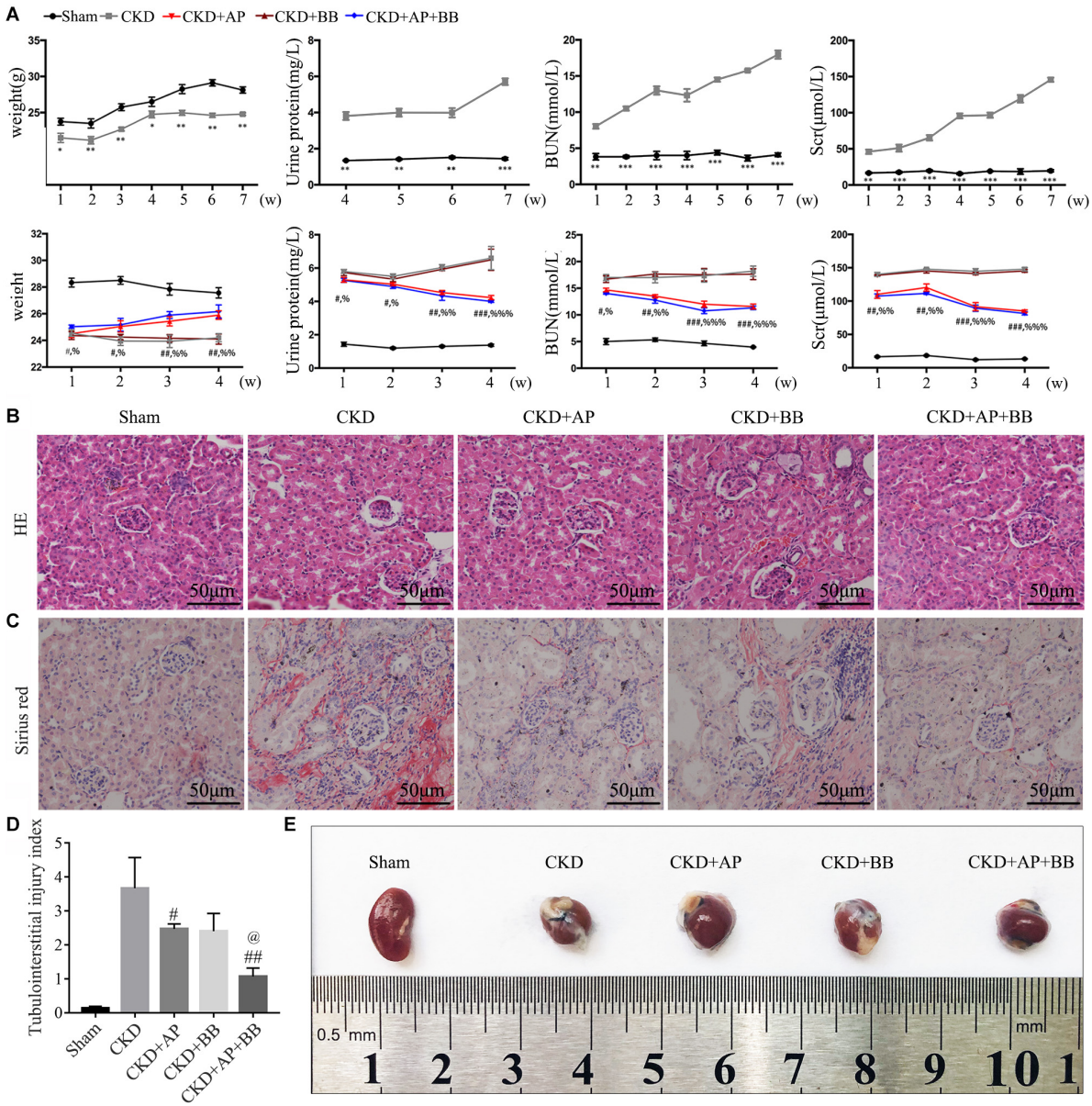

FIGURE 1 | A&P combined with Bifidobacterium treatment improves kidney function and pathology in CKD mice. **(A)** The first row of **Figure 1A** is the indexes of body weight, urine protein, serum creatinine and urea nitrogen of the sham group and model group during 7 weeks of CKD modeling. The second row is the indexes of body weight, urine protein, serum creatinine and urea nitrogen of each group during 4 weeks of drug treatment; **(B)** Pathological H&E staining of kidney tissue in each group; **(C)** The Sirius staining of kidney tissue in each group. **(D)** The tubulointerstitial injury index; **(E)** The kidneys from each group of mice; $^{*}P < 0.05$, $^{**}P < 0.01$, $^{***}P < 0.001$, vs. Sham group; $^{\#}P < 0.05$, $^{\#\#}P < 0.01$, $^{\#\#\#}P < 0.001$, vs. CKD group; $^{\%}P < 0.05$, $^{\%\%}P < 0.01$, $^{\%\%\%}P < 0.001$, vs. CKD group; $^{@}P < 0.05$, vs. CKD + AP group.

A&P Combined With Bifidobacterium Inhibited the Mincle/NF-κB Signaling Pathway and M1 Macrophage Activity in the Kidney of CKD Mice

To investigate the underlying mechanism of A&P and Bifidobacterium combination in protection of kidney in CKD, we detected the Mincle/NF-κB signaling pathway in the kidney of each group. The immunofluorescence results showed that the macrophage (marker F4/80: green spots) largely infiltrated in the CKD kidney, and Mincle (red spots) was also strongly increased in the CKD kidney. Interestingly, the green and red spots were largely merged together, which means that Mincle is mainly expressed on macrophage. Compared with CKD group, the macrophage infiltration in the kidney of A&P + Bifidobacterium treated mice was significantly reduced, and the expression of Mincle was also down-regulated (**Figure 5A**). Moreover, Real-time PCR results showed that A&P and Bifidobacterium

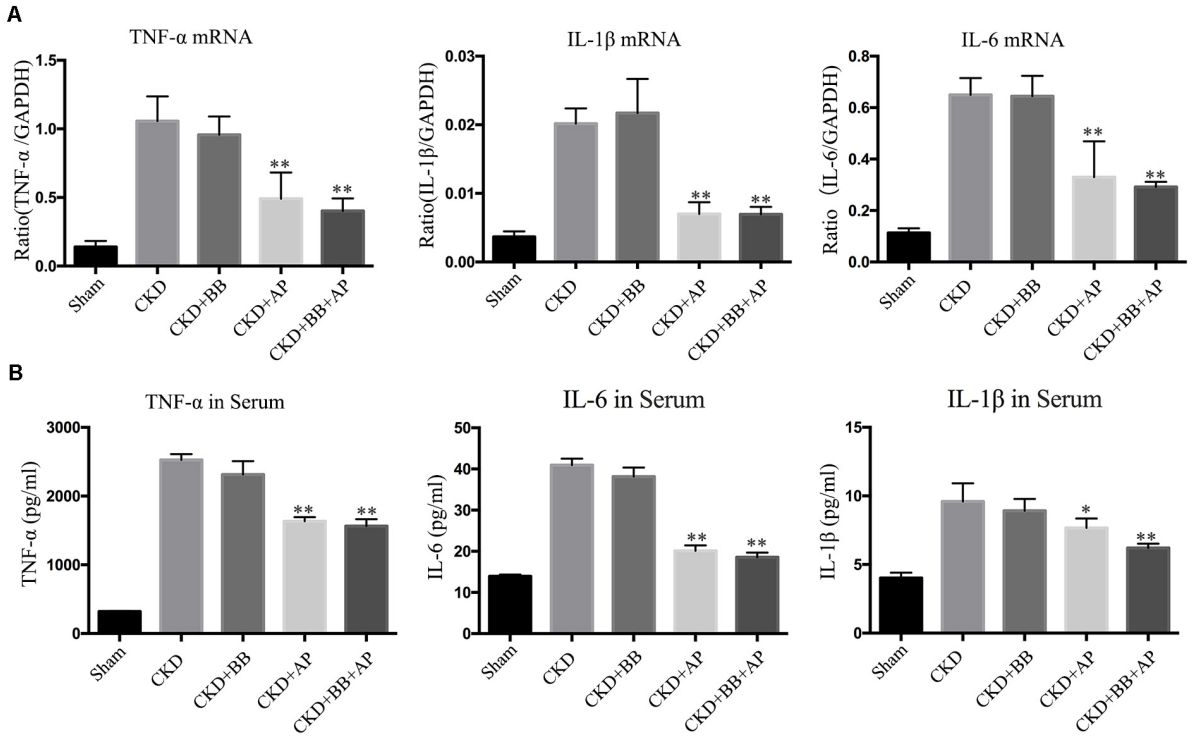

FIGURE 2 | A&P combined with bifidobacterium treatment improves renal and systemic inflammation in CKD mice. **(A)** Real-time PCR detected the mRNA expression of inflammatory indicators (IL-1β, IL-6, TNF-α) in kidney of each group; **(B)** ELISA detected the secretion of inflammatory factors in serum of each group. $^{*}P < 0.05$, $^{**}P < 0.01$, vs. CKD group.

combination effectively inhibited the mRNA expression of Mincle and iNOS (**Figure 5B**). Western blot results also demonstrated that the protein levels of Mincle and iNOS as well as the phosphorylated NF-κB were significantly reduced in A&P and Bifidobacterium treatment group, which was consistent with the results of immunofluorescence (**Figure 5C**), but levels of these protein in mice treated with Bifidobacterium alone did not changed significantly. Subsequently, the flow cytometry was employed to exam the changes of macrophage polarization in each group, and the results showed that the expression of Mincle and M1 macrophage markers (iNOS) in kidney of CKD mice were increased, while A&P combined with Bifidobacterium treatment significantly decreased Mincle and iNOS. On the other hand, the expression of M2 macrophage surface marker (CD206) in kidney of CKD mice was decreased, which was recovered by A&P and Bifidobacterium combination (**Figure 5D**). These above results suggested that A&P and Bifidobacterium combination can strongly inhibit the activity of M1 macrophages and increase the activity of M2 macrophages by suppressing the Mincle/NF-κB pathway.

A&P Combined With Bifidobacterium Inhibited the Mincle/NF-κB Signaling Pathway in the Intestine of CKD Mice

We further detected the Mincle/NF-κB signaling pathway in intestine of each group. The immunofluorescence results showed that the levels of F4/80 and Mincle were significantly increased in intestine of CKD mice, however, A&P and Bifidobacteria combination largely reduced macrophage infiltration and Mincle expression (**Figure 6A**). Western blot results showed that compared with the CKD group, the protein levels of Mincle, iNOS and phosphorylated NF-κB were significantly down-regulated in A&P and Bifidobacterium combined group, which is better than using A&P or Bifidobacterium alone (**Figure 6B**). These data suggested that A&P combined with Bifidobacterium can inhibit the Mincel/NF-κB signaling in intestine of CKD mice.

A&P and Bifidobacterium Containing Serum Inhibited Inflammation in RAW264.7 Cells Induced by LPS and Indophenol Sulfate Induced

To simulate the uremic environment, we used LPS and indophenol sulfate to stimulate the RAW264.7 macrophage. Morphological observation revealed that normal RAW264.7 cells were smooth and round, with high density and distinct particles. Compared with the LPS group or LPS + IS group, A&P and Bifidobacterium containing serum significantly reduced protrusions and pseudopods on cells, and the overall cell morphology was improved (**Figure 7A**). Real-time PCR results showed that, compared with the LPS or LPS + IS groups, A&P and Bifidobacterium containing serum

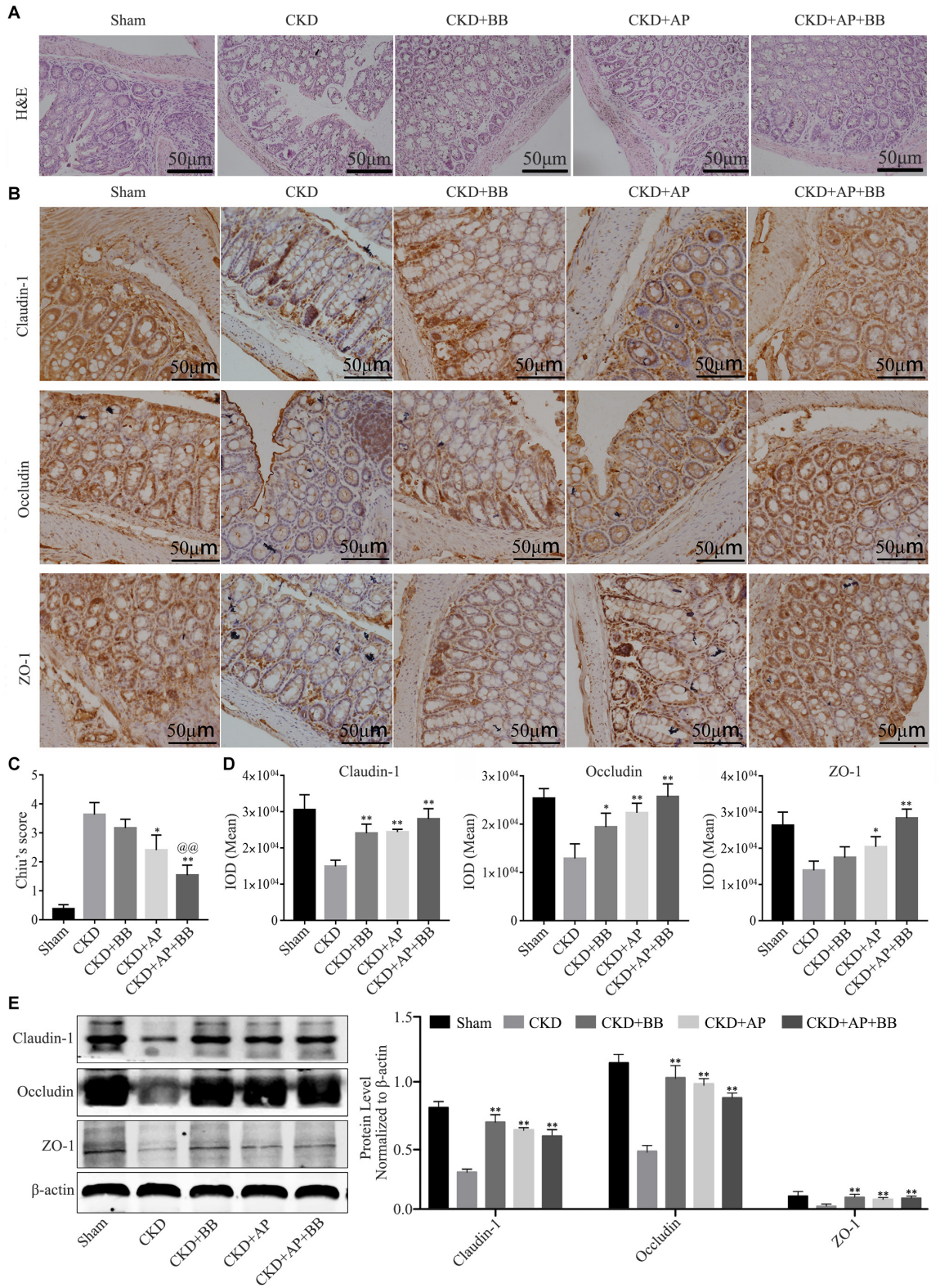

FIGURE 3 | A&P combined with Bifidobacterium treatment can restore the intestinal barrier of CKD mice. **(A)** H&E staining of intestine in each group (× 200); **(B)** Immunohistochemical staining of Claudin-1, Occludin and ZO-1 in intestines of each group (× 200); **(C)** Intestinal damage was evaluated in each group according to Chiu's score; **(D)** The mean IOD of Claudin-1, Occludin-1 and ZO-1 IHC in **(B)**; **(E)** Western blot detected the protein levels of Claudin-1, Occludin and ZO-1 in intestine of each group. $^{*}P < 0.05$, $^{**}P < 0.01$, vs. CKD group; $^{@@}P < 0.01$, vs. CKD + AP group.

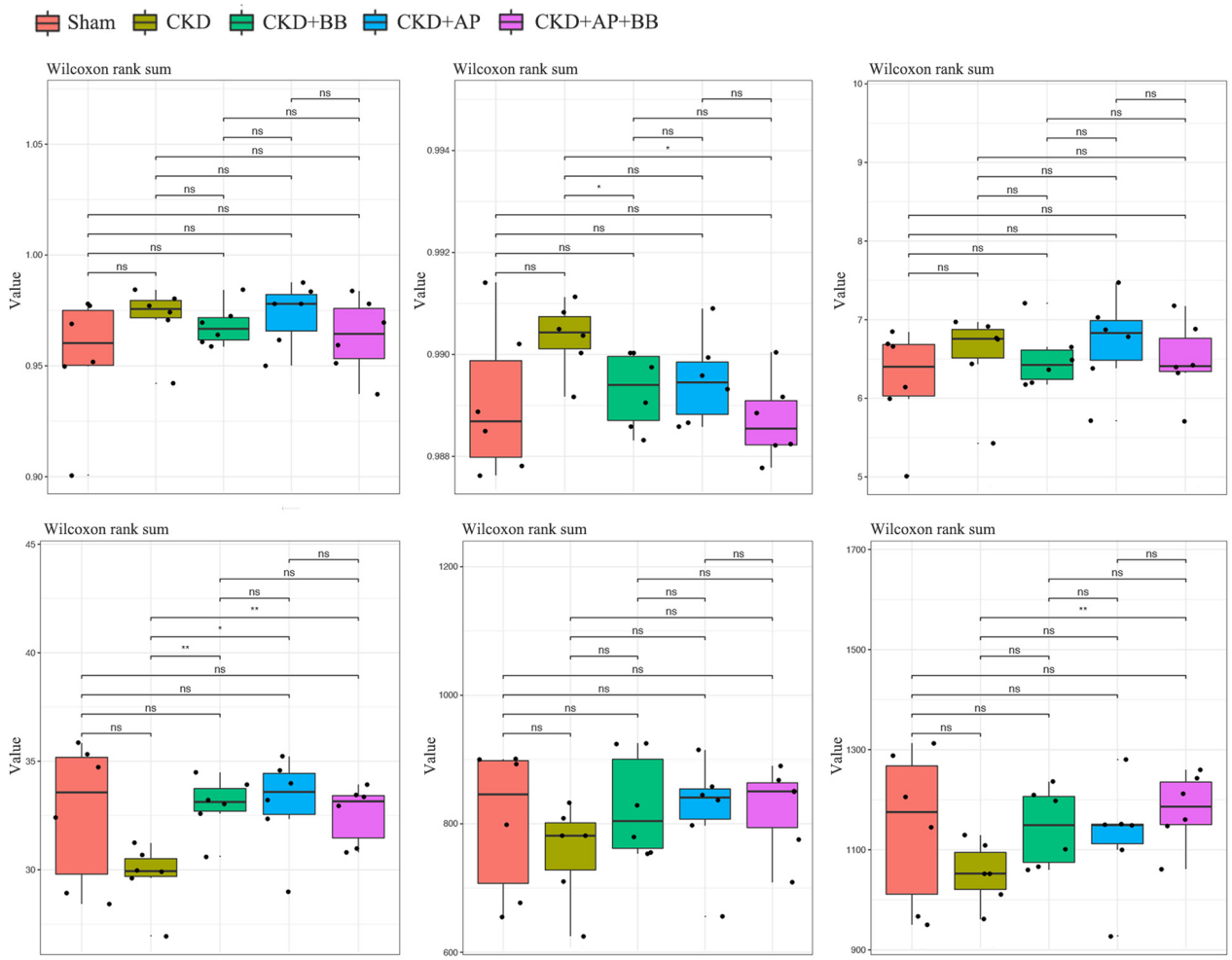

FIGURE 4 | A&P combined with Bifidobacterium treatment has a positive effect on the intestinal flora of CKD mice. 16s alpha diversity related boxplot analysis of mouse feces from each group. $^{*}P < 0.05$, $^{**}P < 0.01$.

largely decreased the mRNA expression of inflammatory indicators (IL-1β, IL-6, TNF-α, MCP-1), Mincle and iNOS, however, the cells treated with Bifidobacterium containing serum alone did not inhibited the mRNA expression of these indicators (**Figures 7B–G**). ELISA results demonstrated that, compared with the LPS group, administration of LPS plus different concentration of IS significantly up-regulated the secretion of inflammatory indicators (IL-1β, IL-6, TNF-α) in supernatant (**Figures 7H–J**), and the IS concentration of 200 μM was used in the subsequent experiments. Then, we found that, compared with the LPS + IS group, A&P and Bifidobacterium containing serum strongly reduced the secretion of inflammatory indicators, but the cells treated with Bifidobacterium containing serum alone did not inhibited the secretion of these indicators (**Figures 7K–M**). These results suggested that A&P and bifidobacterium containing serum can improve the macrophage morphology and inflammation under indophenol sulfate induced uremic environment.

A&P and Bifidobacterium Containing Serum Suppressed Inflammation in RAW264.7 Cells Induced by LPS and *Trans* Aconitic Acid Induced

We used another urotoxin (*trans* aconitic acid) to simulate uremic environment. We found that, compared with the LPS group or LPS + TA group, A&P and Bifidobacterium containing serum largely decreased protrusions and pseudopods on cells, and the overall cell morphology was improved (**Figure 8A**). Real-time PCR results demonstrated that, compared with the LPS or LPS + TA groups, A&P and Bifidobacterium containing serum significantly reduced the mRNA expression of inflammatory indicators, Mincle and iNOS, however, the cells treated with Bifidobacterium containing serum alone did not inhibited the mRNA expression of these indicators (**Figures 8B–G**). ELISA results determined the 200 μM concentration of TA was used in the subsequent experiments (**Figures 8H–J**). We then found that, compared with the

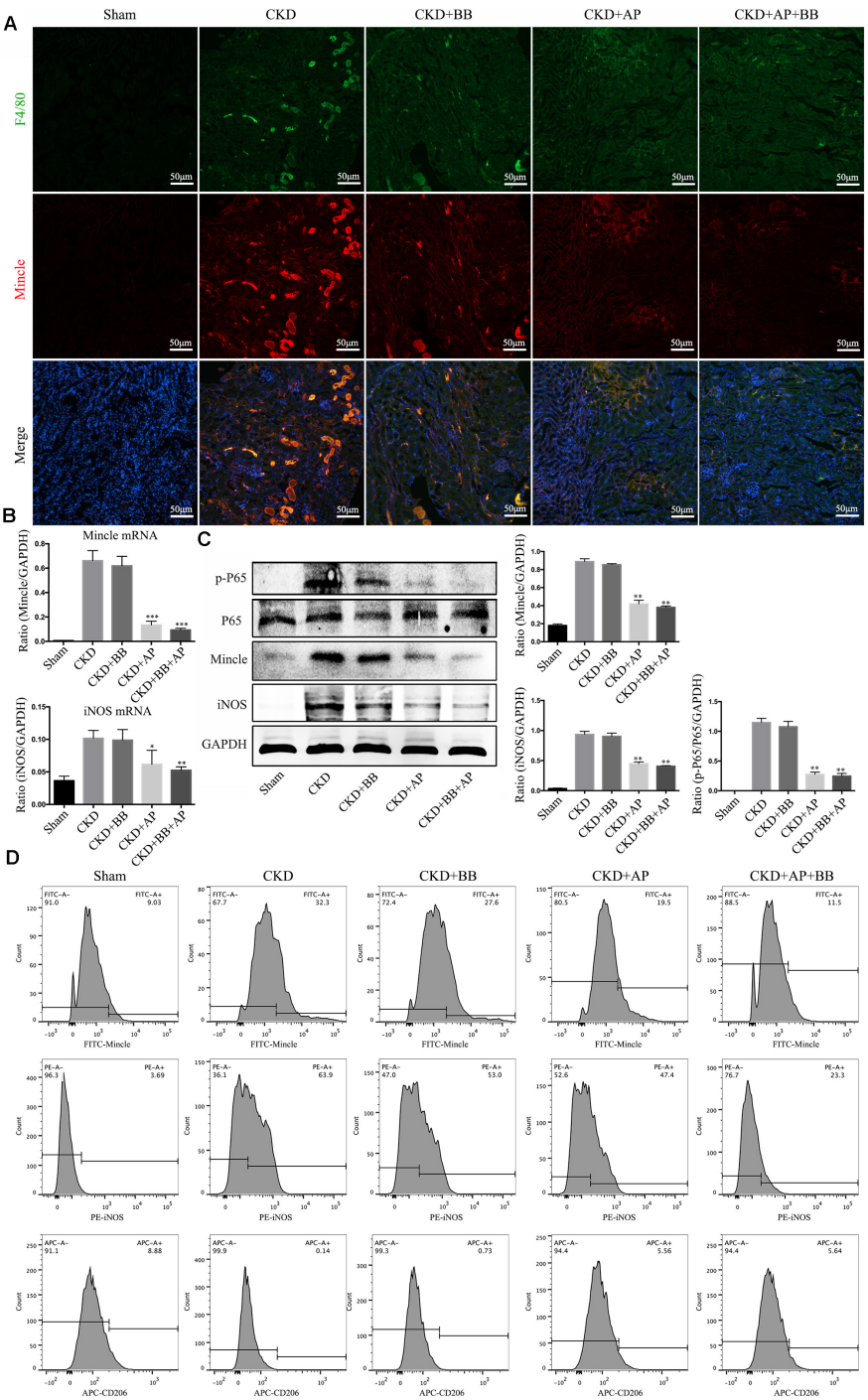

FIGURE 5 | A&P combined with Bifidobacterium inhibited the Mincle/NF-κB signaling pathway and M1 macrophage activity in kidney of CKD mice. **(A)** The immunofluorescence staining detected the expression and location of F4/80 (Green) and Mincle (Red) in kidney of each group (× 200); **(B)** The mRNA expression of Mincle and iNOS in kidney of each group detecting by Real-time PCR; **(C)** Western blot detected the protein levels of Mincle/iNOS/p-P65/p65 in kidney of each group; **(D)** Flow cytometry was performed to test the levels of Mincle/iNOS/CD206 in kidney of each group. $^{*}P < 0.05$, $^{**}P < 0.01$, $^{***}P < 0.001$, vs. CKD group.

LPS + TA group, A&P and Bifidobacterium containing serum strongly reduced the secretion of inflammatory indicators, but the cells treated with Bifidobacterium containing serum alone did not inhibited the secretion of these indicators (**Figures 8K–M**). These results also suggested that A&P and bifidobacterium containing serum can improve the macrophage morphology and inflammation under *trans* aconitic acid induced uremic environment.

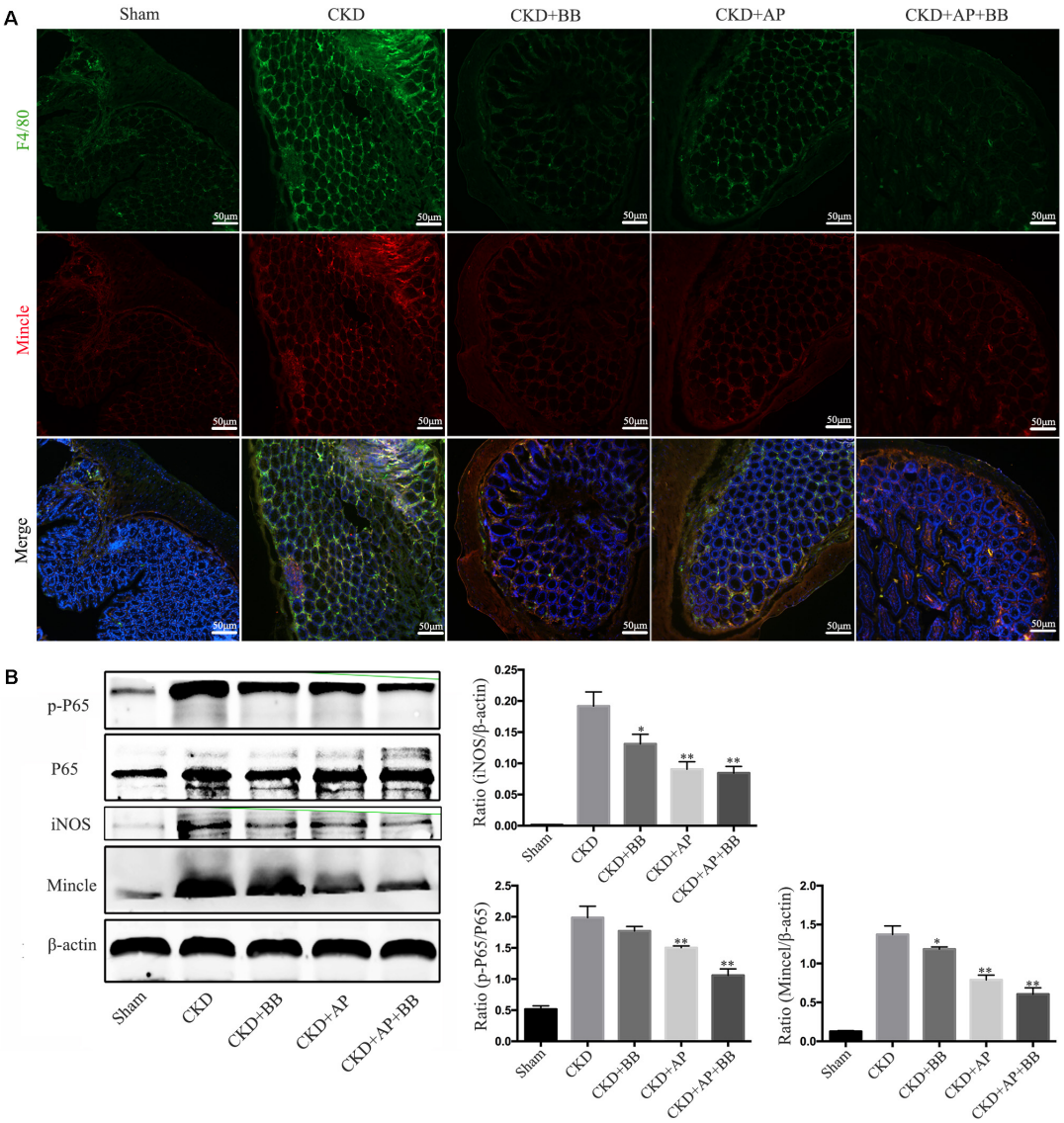

FIGURE 6 | A&P combined with Bifidobacterium inhibited the Mincle/NF-κB signaling pathway in the intestine of CKD mice. **(A)** The immunofluorescence staining detected the expression and location of F4/80 (Green) and Mincle (Red) in intestine of each group (× 200); **(B)** Western blot detected the protein levels of Mincle/iNOS/p-P65/p-65 in intestine of each group. *$P < 0.05$, **$P < 0.01$, vs. CKD group.

Overexpression of Mincle Abrogated A&P and Bifidobacterium Containing Serum Inhibited Inflammation in LPS + IS Stimulated RAW264.7 Cells

To further explore the relationship between Mincle and inflammatory response in macrophage, we overexpressed Mincle in A&P combined Bifidobacterium treatment group by plasmid transfection, and set up a positive control group (resveratrol (RV) 30 μM). Real-time PCR and ELISA results showed that after overexpression of Mincle in treatment group, the expression and secretion of inflammatory cytokines were significantly increased (**Figures 9A–H**). Western blot results demonstrated that the protein level of Mincle in the plasmid-transfected group (Mincle-OE) was strongly increased, which activated the Mincle/NF-κB signaling and M1 macrophage in A&P and Bifidobacterium containing serum treated inflammatory RAW264.7 cells (**Figure 9I**). These results suggested that the anti-inflammatory effect of A&P and Bifidobacterium in macrophage is dependent on the inhibition of the Mincle signaling pathway.

DISCUSSION

Current treatments for chronic kidney disease mainly include using drugs to control proteinuria, blood sugar, blood pressure, calcium and phosphorus metabolism and adjust diet. When CKD progresses to the uremic stage of late renal failure, dialysis or

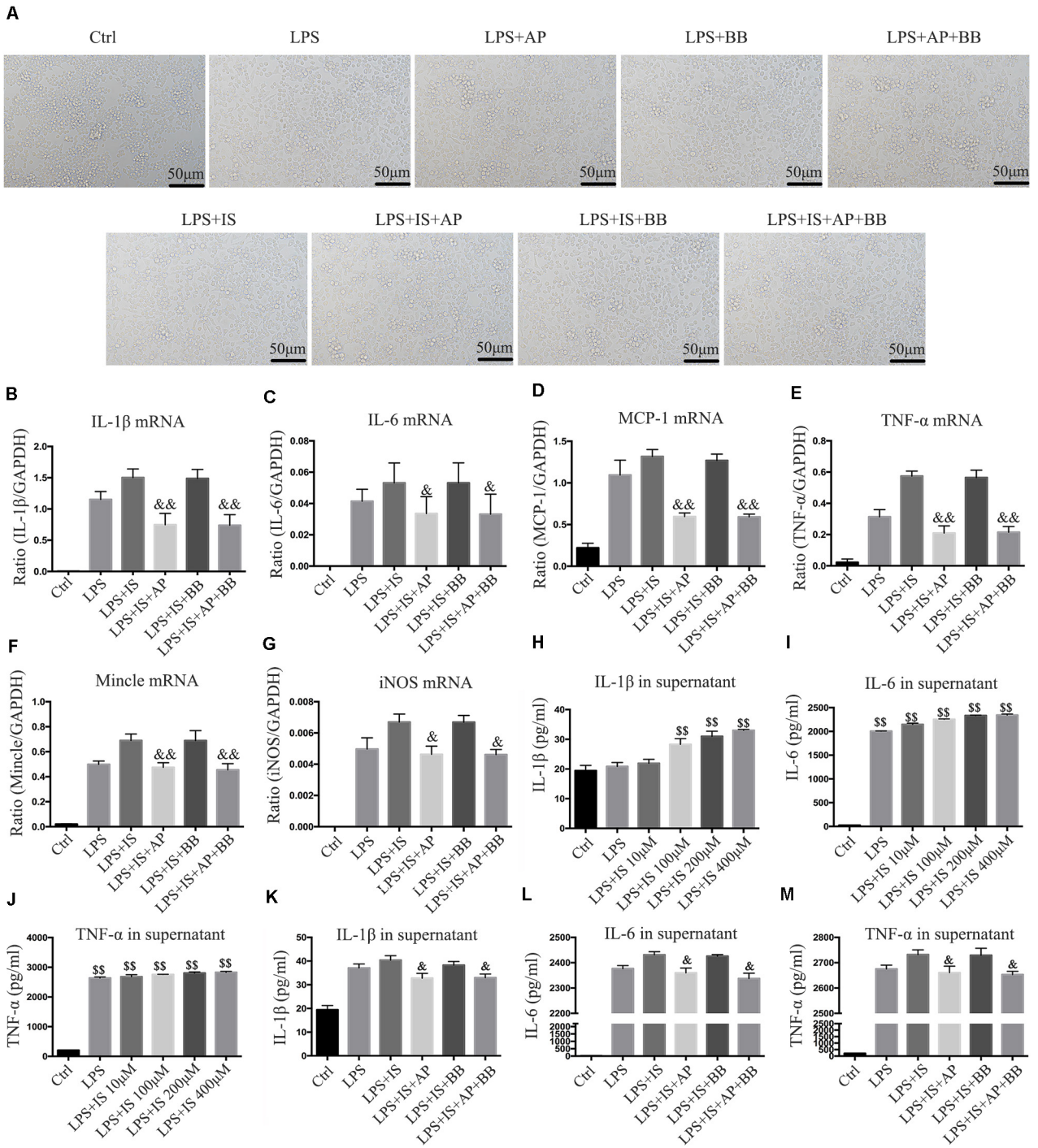

FIGURE 7 | A&P and Bifidobacterium containing serum inhibited LPS and indophenol sulfate induced inflammation in RAW264.7 cells. **(A)** The cell morphology of each group was observed under an microscope (×200); **(B–G)**. Real-time PCR was performed to detect the mRNA expression of inflammatory factors (IL-1β, IL-6, TNF-α, MCP-1), Mincle and iNOS in RAW264.7 cells after modeling with LPS and indophenol sulfate; **(H–M)**. ELISA was used to detect the secretion of inflammatory factors (IL-1β, IL-6, TNF-α) in supernatant of RAW264.7 cells after modeling with LPS and indophenol sulfate. $^{\&}P < 0.05$, $^{\&\&}P < 0.01$, vs. LPS + IS Group; $^{\$\$}P < 0.01$, vs. Ctrl Group.

kidney transplantation is the final choice. With the widespread clinical application of traditional Chinese medicine in the treatment of CKD (Zhong et al., 2013, 2015; Zhang et al., 2014), people have a new understanding of traditional Chinese medicine. Our team used the theory of "atrophic lung disease" from the traditional Chinese medicine book – "The Golden

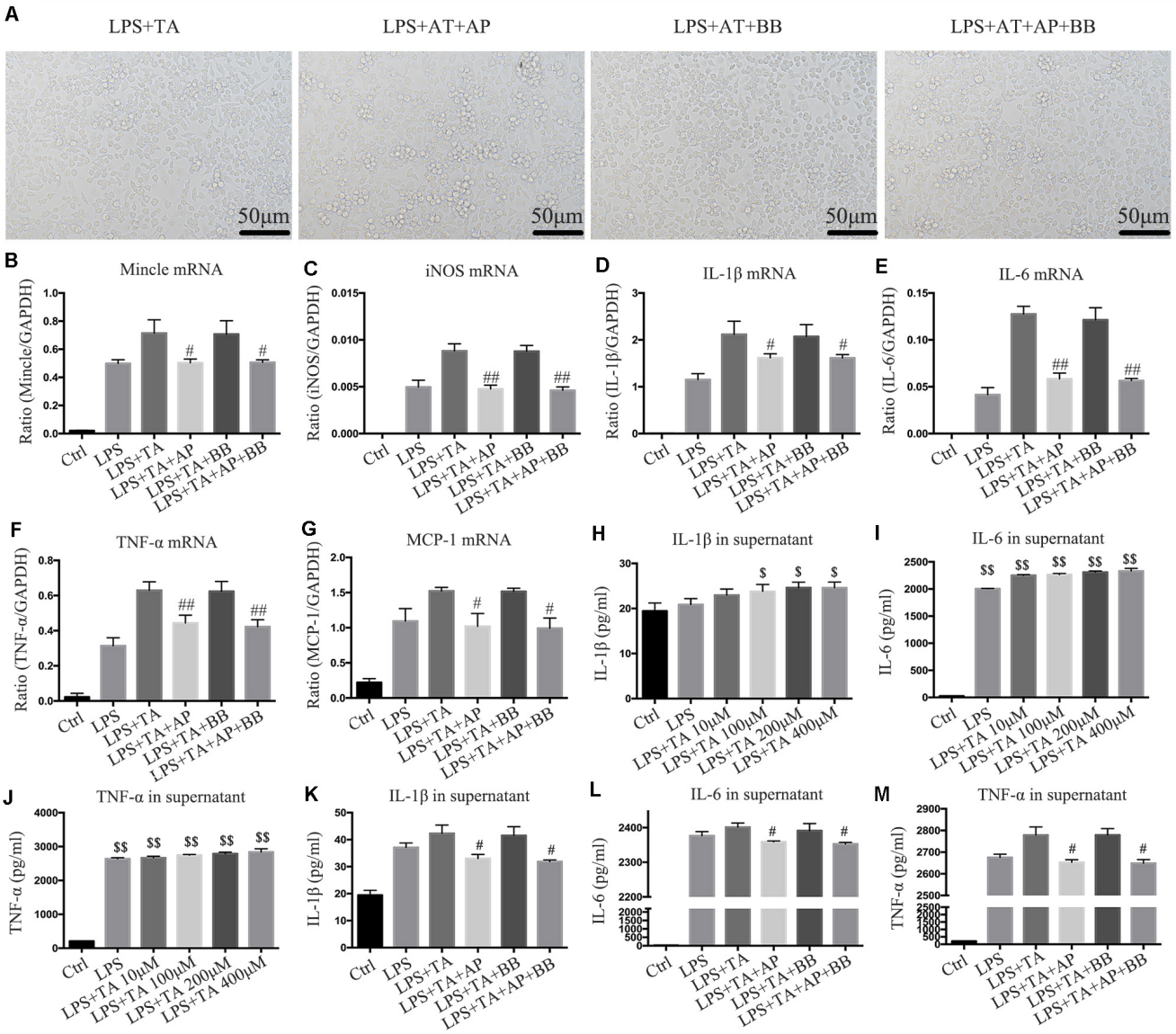

FIGURE 8 | A&P and Bifidobacterium containing serum suppressed LPS and *trans* aconitic acid induced inflammation in RAW264.7 cells. **(A)** The cell morphology of each group was observed under an microscope (×200); **(B–G)** Real-time PCR was performed to detect the mRNA expression of inflammatory factors (IL-1β, IL-6, TNF-α, MCP-1), Mincle and iNOS in RAW264.7 cells after modeling with LPS and *trans* aconitic acid; **(H–M)** ELISA was used to detect the secretion of inflammatory factors (IL-1β, IL-6, TNF-α) in supernatant of RAW264.7 cells after modeling with LPS and *trans* aconitic acid. $^{\#}P < 0.05$, $^{\#\#}P < 0.01$, vs. LPS + IS Group; $^{\$}P < 0.05$, $^{\$\$}P < 0.01$, vs. Ctrl Group.

Chamber" to propose the theory of "flaccidity caused by the disorder of the kidney" in CKD. Based on the above-mentioned traditional Chinese medicine theory, our team created the A&P formula, containing *Astragalus mongholicus* Bunge, Panax notoginseng, Angelica sinensis, *Achyranthes bidentata* Blume and *Ecklonia kurome* Okamura. Although A&P can effectively treat CKD in clinic in Chinese, its pharmacological mechanism for the treatment of CKD is not clear.

With the development of intestinal microbial medicine, Meijers et al. proposed the concept of "intestinal-kidney axis" in 2011 (Meijers and Evenepoel, 2011), which initially clarified the relationship between chronic kidney disease and intestinal microecology. Ritze et al. also proposed the concept of "intestinal-renal syndrome," revealing the vicious cycle between the occurrence and development of CKD and the increase of intestinal permeability (Ritz, 2011). Over the past few decades, clinical understanding of the structure and function of the gut microbiota has greatly enriched with the advancement of culture-related technologies (Hooper and Macpherson, 2010). The intestinal flora can maintain a very dynamic symbiosis of bacteria and interact with other systems of the human body to plays an important role in nutrition and energy

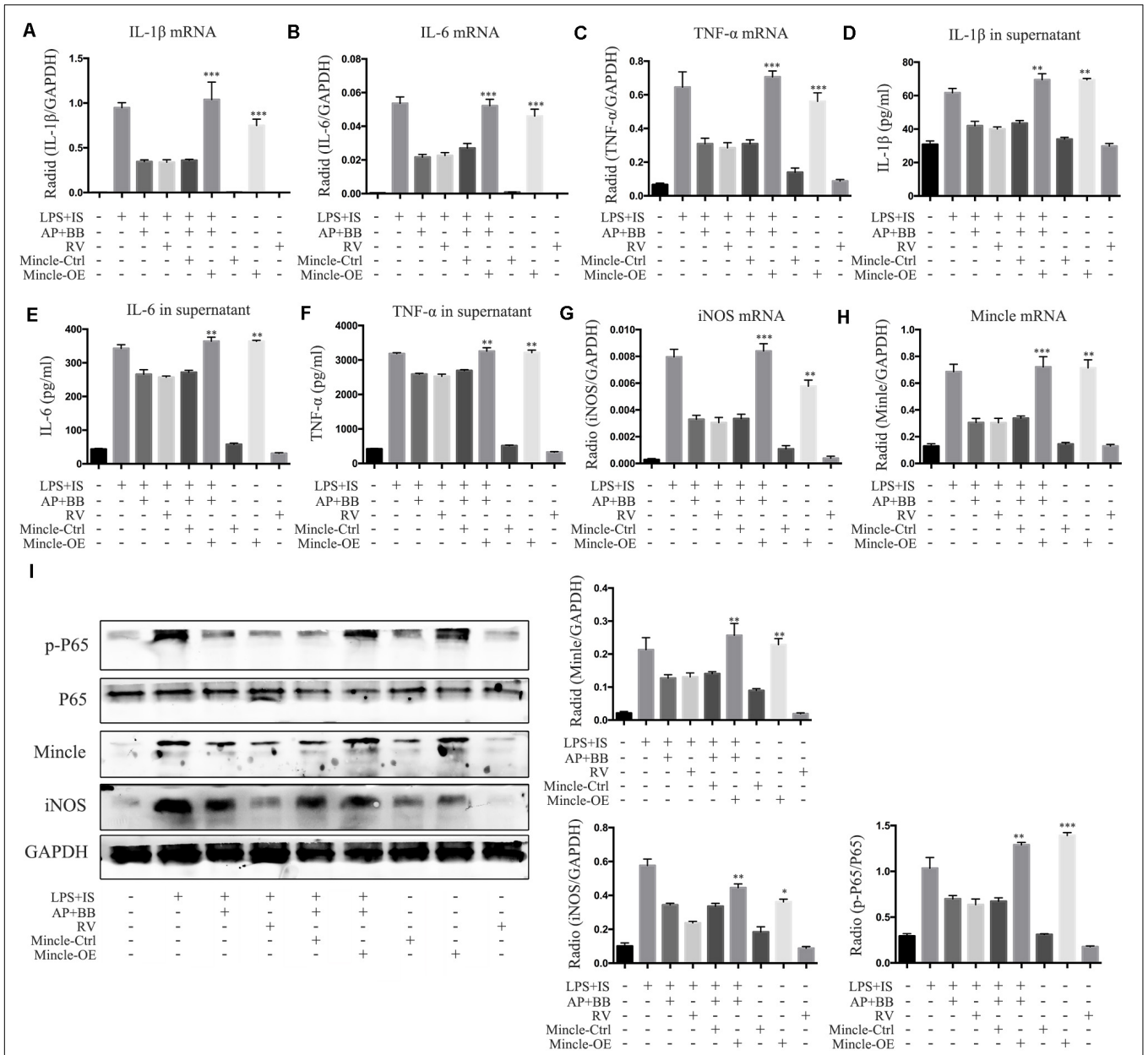

FIGURE 9 | Overexpression of Mincle recovered A&P and Bifidobacterium containing serum inhibited inflammation in LPS + IS stimulated RAW264.7 cells. **(A–C)** Real-time PCR was performed to detect the mRNA expression of inflammatory indicators (IL-1β, IL-6, TNF-α) in RAW264.7 cells after overexpression of Mincle; **(D–F)** ELISA was used to detect the secretion of inflammatory factors (IL-1β, IL-6, TNF-α) in supernatant of RAW264.7 cells after overexpression of Mincle; **(G,H)** The mRNA expression of iNOS and Mincle in RAW264.7 cells; **(I)** The protein levels of Mincle/iNOS/p-P65/p-65 in RAW264.7 cells after overexpression of Mincle. $^{*}P < 0.05$, $^{**}P < 0.01$, $^{***}P < 0.001$, vs. LPS + IS + A&P + BB Group.

metabolism, immune regulation and host defense (Round and Mazmanian, 2009; Morgan et al., 2012; Qin et al., 2012; Kamada et al., 2013; Ridaura et al., 2013). The harmful effects of intestinal flora in critical illness are multifaceted and can be divided into three areas: destruction of the microbial barrier, loss of colonization resistance and metabolic disorders (Ubeda et al., 2010; Andersen et al., 2017). Intestinal microflora dysregulation may lead to bacterial translocation by increasing intestinal permeability and inducing mucosal immune dysfunction (Anders et al., 2013). When the damage of bacteria's permeability to the intestinal mucosa increases to a certain degree, it activate the intestinal mononuclear macrophages and promote cells to release a large number of toxic cytokines and chemicals such as inflammatory factors and oxygen free radicals, which aggravate the damage to the protective barrier of the intestinal mucosa (Strzępa and Szczepanik, 2013). This repeated cycle leads to chronic inflammation of the system. The persistent chronic inflammation is one of the most

important independent factors that predict the poor prognosis of CKD patients.

Recently, the interaction between intestinal microflora and kidneys has received increasing attention. Dietary supplement of probiotics was widely used to improve intestinal microenvironment and reduced production of urotoxin (Wu et al., 2016; Tao et al., 2019). Probiotic is the ingredients of indigestible food that can beneficially affect the host by increasing the number of specific bacteria and changing the composition of the microbiome (Gibson and Roberfroid, 1995; Nakabayashi et al., 2011; Iwashita et al., 2018). It also has been reported that probiotic can improve the kidney function of humans and animals by improving the intestinal microenvironment (Ranganathan et al., 2010; Furuse et al., 2014; Yoshifuji et al., 2016), but using the probiotic alone to treat CKD is highly controversial, therefore, in this study we try to explore the effects of treatment with combination of probiotic and traditional Chinese medicine on CKD, and the underlying mechanism.

In this study, the data demonstrated that A&P combined with Bifidobacterium can significantly reduce the urine protein, serum creatinine and urea nitrogen, and increase the body weight in 5/6 nephrectomy induced CKD mice. In addition, we found that A&P combined with Bifidobacterium can also effectively improve the intestinal flora of CKD mice by using 16s DNA detection of microorganisms. It is worth noting that A&P combined with Bifidobacterium significantly inhibited the inflammation in kidney and intestine of CKD mice and also down-regulated the concentration of inflammatory factors in blood. All the above results showed that the treatment effects of A&P combined with Bifidobacteria on CKD is better than that of Bifidobacteria treatment alone. However, although the effects of combination of A&P and BB is not significantly different from A&P treatment alone on some indicators, the combination of A&P and BB is better than A&P treatment alone in the damage scores of the kidney and intestine, as well as the intestinal inflammation, it may be because of BB is a probiotic, which mainly improves the intestinal microecology. On the other hand, the effect of combination of A&P and BB on certain indicators is not statistically different compared with A&P alone, which may be related to the strong inhibitory effect of A&P, but in general, the combination of A&P and BB has a better effect on improving the kidney and intestinal damage induced by CKD. Taken together, these findings proved that A&P combined with Bifidobacterium can strongly improve renal function, reduce renal and intestinal inflammation as well as improve intestinal flora, suggesting that A&P combined with Bifidobacterium protects kidney in CKD may partially through regulating intestinal microenvironment.

Macrophages are important innate immune cells with phagocytic functions. In the past few decades, people have gradually discovered that macrophages have a high degree of diversity (Yonit et al., 2015; Wynn and Vannella, 2016). It plays a complex role in various physiological and pathological processes, such as tissue development and homeostasis, host defense, tissue damage and repair, and regulation of fibrosis. Recent studies have shown that macrophage plays an important role in the evolution of AKI to CKD (Black et al., 2018). But the research on the relationship between dynamic changes of macrophage and the development of CKD is not clear. Therefore, this study intends to study the changes in the polarization of macrophage during the development of renal and intestinal injury in CKD through *in vivo* and *in vitro* experiments (Honarpisheh et al., 2018; Komada et al., 2018). Mincle is a transmembrane recognition receptor on innate immune cells, which is expressed in macrophages and critical to maintain the M1 phenotype of macrophages and triggering M1 macrophage-mediated kidney inflammation (Lv et al., 2017). Our results confirmed that the combination of A&P and Bifidobacterium can reduce the activity of M1 macrophages and increase the activity of M2 macrophages by inhibiting Mincle in kidney of CKD. Studies have shown that drugs can block NF-κB signaling in intestinal epithelial cells and macrophages, and improve acute and chronic murine colitis model (Yonit et al., 2015; Lee et al., 2020). Our results also proved that A&P combined with Bifidobacterium can improve the intestinal inflammatory state by adjusting the polarization of macrophage. As we know, NF-κB is an important transcription factor that regulates the expression of pro-inflammatory cytokines, and Mincle is strictly regulated by the TLR4/NF-κB signaling (Zhao et al., 2014; Tan et al., 2020). The results of this study showed that combination of A&P and Bifidobacterium can significantly reduce the activation of NF-κB through targeted modulation of Mincle to improve the inflammation in kidney and intestine.

CONCLUSION

In summary, this study indicated that A&P combined with Bifidobacterium can significantly improve the renal function, down-regulate renal and intestinal inflammation, improve intestinal microenvironment in CKD, which may through inhibiting the Mincle/NF-κB signaling and suppressing inflammatory response in macrophage. This study provides a new insight in treatment of CKD with traditional Chinese medicine, and may optimize the application of A&P in clinical treatment of CKD.

DATA AVAILABILITY STATEMENT

The original contributions presented in the study are included in the article/supplementary material, further inquiries can be directed to the corresponding author.

ETHICS STATEMENT

The animal study was reviewed and approved by the Ethics Committee of Southwest Medical University.

AUTHOR CONTRIBUTIONS

WL, TR-Z, FJ-M, and DH conceived and designed the experiments. TR-Z, DH, LJ-C, WD,

and ZX performed the experiments. TR-Z, WX-J, and DH wrote the manuscript. All authors contributed to the article and approved the submitted version.

FUNDING

This work was supported by the Luzhou – Southwest Medical University Joint Project (2017LZXNYD-P01 and 2018LZXNYD-PT03), the Southwest Medical University–Affiliated Traditional Medicine Hospital Joint Project (2018XYLH-029), and the Luzhou Municipal – Southwest Medical University Joint Special Grant for the Introduction of High-level Talents (Lan Hui-Yao Team and Chen Chen Team), the Sichuan Provincial Health Committee project (16ZD034).

SUPPLEMENTARY MATERIAL

The Supplementary Material for this article can be found online at: https://www.frontiersin.org/articles/10.3389/fphys.2020.583668/full#supplementary-material

Supplementary Figure 1 | Cell viability test of indophenol sulfate and *trans* aconitic acid on RAW264.7 cells.

REFERENCES

Alikhan, M. A., and Ricardo, S. D. (2013). Mononuclear phagocyte system in kidney disease and repair. *Nephrology* 18, 81–91. doi: 10.1111/nep.12014

Anders, H.-J., Andersen, K., and Stecher, B. (2013). The intestinal microbiota, a leaky gut, and abnormal immunity in kidney disease. *Kidney Int.* 83, 1010–1016. doi: 10.1038/ki.2012.440

Andersen, K., Kesper, M. S., Marschner, J. A., Konrad, L., Ryu, M., Kumar, et al. (2017). Intestinal dysbiosis, barrier dysfunction, and bacterial translocation account for CKD-related systemic inflammation. *J. Am. Soc. Nephrol. JASN.* 28, 76–83. doi: 10.1681/ASN.2015111285

Bain, C. C., and Mowat, A. M. (2014). Macrophages in intestinal homeostasis and inflammation. *Immunol. Rev.* 260, 102–117. doi: 10.1111/imr.12192

Barros, M. H., Hauck, F., Dreyer, J. H., Kempkes, B., and Niedobitek, G. (2013). Macrophage polarisation: an immunohistochemical approach for identifying M1 and M2 macrophages. *PLoS One.* 8:e80908. doi: 10.1371/journal.pone.0080908

Black, L. M., Lever, J. M., Traylor, A. M., Chen, B., Yang, Z., Esman, S. K., et al. (2018). Divergent effects of AKI to CKD models on inflammation and fibrosis. *Am. J. Physiol. Renal Physiol.* 315, F1107–F1118. doi: 10.1152/ajprenal.00179.2018

Chiu, C. J., McArdle, A. H., Brown, R., Scott, H. J., and Gurd, F. N. (1970). Intestinal mucosal lesion in low-flow states. I. A morphological, hemodynamic, and metabolic reappraisal. *Arch. Surg.* 101, 478–483. doi: 10.1001/archsurg.1970.01340280030009

Cigarran Guldris, S., González Parra, E., and Cases Amenós, A. (2017). Gut microbiota in chronic kidney disease. *Nefrologia* 37, 9–19. doi: 10.1016/j.nefro.2016.05.008

Crespo-Salgado, J., Vehaskari, V. M., Stewart, T., Ferris, M., Zhang, Q., Wang, G., et al. (2016). Intestinal microbiota in pediatric patients with end stage renal disease: a midwest pediatric nephrology consortium study. *Microbiome* 4:50. doi: 10.1186/s40168-016-0195-9

De Nicola, L., and Minutolo, R. (2016). Worldwide growing epidemic of CKD: fact or fiction? *Kidney Int.* 90, 482–484. doi: 10.1016/j.kint.2016.05.001

De Schepper, S., Verheijden, S., Aguilera-Lizarraga, J., Viola, M. F., Boesmans, W., Stakenborg, N., et al. (2018). Self-Maintaining gut macrophages are essential for intestinal homeostasis. *Cell* 175, 400–415.e13. doi: 10.1016/j.cell.2018.07.048

Fu, J., Wang, Z., Huang, L., Zheng, S., Wang, D., Chen, S., et al. (2014). Review of the botanical characteristics, phytochemistry, and pharmacology of *Astragalus membranaceus* (Huangqi). *Phytotherapy Res. PTR.* 28, 1275–1283. doi: 10.1002/ptr.5188

Furuse, S. U., Ohse, T., Jo-Watanabe, A., Shigehisa, A., Kawakami, K., Matsuki, T., et al. (2014). Galacto-oligosaccharides attenuate renal injury with microbiota modification. *Physiol. Rep.* 2:e12029. doi: 10.14814/phy2.12029

Gibson, G. R., and Roberfroid, M. B. (1995). Dietary modulation of the human colonic microbiota: introducing the concept of prebiotics. *J. Nutrit.* 125, 1401–1412. doi: 10.1093/jn/125.6.1401

Honarpisheh, M., Foresto-Neto, O., Steiger, S., Kraft, F., Koehler, P., von Rauchhaupt, E., et al. (2018). Aristolochic acid I determine the phenotype and activation of macrophages in acute and chronic kidney disease. *Sci. Rep.* 8, 12169–12169. doi: 10.1038/s41598-018-30628-x

Hooper, L. V., and Macpherson, A. J. (2010). Immune adaptations that maintain homeostasis with the intestinal microbiota. *Nat. Rev. Immunol.* 10, 159–169. doi: 10.1038/nri2710

Hugenholtz, F., and de Vos, W. M. (2018). Mouse models for human intestinal microbiota research: a critical evaluation. *Cell. Mol. Life Sci. CMLS.* 75, 149–160. doi: 10.1007/s00018-017-2693-8

Hui, D., Rui-Zhi, T., Jian-Chun, L., Xia, Z., Dan, W., Jun-Ming, F., et al. (2020). Astragalus propinquus schischkin and panax notoginseng (A&P) compound relieved cisplatin-induced acute kidney injury through inhibiting the mincle maintained macrophage inflammation. *J. Ethnopharmacol.* 252:112637. doi: 10.1016/j.jep.2020.112637

Inoue, T. (2017). M1 macrophage triggered by Mincle leads to a deterioration of acute kidney injury. *Kidney Int.* 91, 526–529. doi: 10.1016/j.kint.2016.11.026

Iwashita, Y., Ohya, M., Yashiro, M., Sonou, T., Kawakami, K., Nakashima, Y., et al. (2018). Dietary changes involving bifidobacterium longum and other nutrients delays chronic kidney disease progression. *Am. J. Nephrol.* 47, 325–332. doi: 10.1159/000488947

Jia, L., Jia, Q., Yang, J., Jia, R., and Zhang, H. (2018). Efficacy of probiotics supplementation on chronic kidney disease: a systematic review and meta-analysis. *Kidney Blood Press Res.* 43, 1623–1635. doi: 10.1159/000494677

Kamada, N., Chen, G. Y., Inohara, N., and Núñez, G. (2013). Control of pathogens and pathobionts by the gut microbiota. *Nat. Immunol.* 14, 685–690. doi: 10.1038/ni.2608

Komada, T., Chung, H., Lau, A., Platnich, J. M., Beck, P. L., Benediktsson, H., et al. (2018). Macrophage uptake of necrotic cell DNA activates the AIM2 inflammasome to regulate a proinflammatory phenotype in CKD. *J. Am. Soc. Nephrol. JASN.* 29, 1165–1181. doi: 10.1681/ASN.2017080863

Koppe, L., Mafra, D., and Fouque, D. (2015). Probiotics and chronic kidney disease. *Kidney Int.* 88, 958–966. doi: 10.1038/ki.2015.255

Lee, J. W., Lee, S. M., Chun, J., Im, J. P., Seo, S. K., Ha, N., et al. (2020). Novel histone deacetylase 6 inhibitor CKD-506 inhibits NF-κB signaling in intestinal epithelial cells and macrophages and ameliorates acute and chronic murine colitis. *Inflamm. Bowel Dis.* 26, 852–862. doi: 10.1093/ibd/izz317

Li, L., Hou, X., Xu, R., Liu, C., and Tu, M. (2017). Research review on the pharmacological effects of astragaloside IV. *Fundam Clin. Pharmacol.* 31, 17–36. doi: 10.1111/fcp.12232

Liao, Y., Tan, R. Z., Li, J. C., Liu, T. T., Zhong, X., Yan, Y., et al. (2020). Isoliquiritigenin attenuates UUO-Induced renal inflammation and fibrosis by inhibiting mincle/Syk/NF-Kappa B signaling pathway. *Drug Des. Dev. Ther.* 14, 1455–1468. doi: 10.2147/DDDT.S243420

Lim, R., and Lappas, M. (2019). Expression and function of macrophage-inducible C-type lectin (Mincle) in inflammation driven parturition in fetal membranes and myometrium. *Clin. Exp. Immunol.* 197, 95–110. doi: 10.1111/cei.13281

Lv, L. L., Tang, P. M., Li, C. J., You, Y. K., Li, J., Huang, X. R., et al. (2017). The pattern recognition receptor, mincle, is essential for maintaining the M1 macrophage phenotype in acute renal inflammation. *Kidney Int.* 91, 587–602. doi: 10.1016/j.kint.2016.10.020

Meijers, B. K. I., and Evenepoel, P. (2011). The gut-kidney axis: indoxyl sulfate, p-cresyl sulfate and CKD progression. *Nephrol. Dial. Transplant.* 26, 759–761. doi: 10.1093/ndt/gfq818

Morgan, X. C., Tickle, T. L., Sokol, H., Gevers, D., Devaney, K. L., Ward, D. V., et al. (2012). Dysfunction of the intestinal microbiome in inflammatory bowel disease and treatment. *Genome Biol.* 13, R79–R79. doi: 10.1186/gb-2012-13-9-r79

Murray, P. J., and Wynn, T. A. (2011). Obstacles and opportunities for understanding macrophage polarization. *J. Leukocyte Biol.* 89, 557–563. doi: 10.1189/jlb.0710409

Nakabayashi, I., Nakamura, M., Kawakami, K., Ohta, T., Kato, I., Uchida, K., et al. (2011). Effects of synbiotic treatment on serum level of p-cresol in haemodialysis patients: a preliminary study. *Nephrol. Dial. Transplant.* 26, 1094–1098. doi: 10.1093/ndt/gfq624

Nallu, A., Sharma, S., Ramezani, A., Muralidharan, J., and Raj, D. (2017). Gut microbiome in chronic kidney disease: challenges and opportunities. *Trans. Res.* 179, 24–37. doi: 10.1016/j.trsl.2016.04.007

Patin, E. C., Orr, S. J., and Schaible, U. E. (2017). Macrophage inducible C-Type lectin as a multifunctional player in immunity. *Front. Immunol.* 8:861. doi: 10.3389/fimmu.2017.00861

Peng, H., Geil Nickell, C. R., Chen, K. Y., McClain, J. A., and Nixon, K. (2017). Increased expression of M1 and M2 phenotypic markers in isolated microglia after four-day binge alcohol exposure in male rats. *Alcohol* 62, 29–40. doi: 10.1016/j.alcohol.2017.02.175

Qin, J., Li, Y., Cai, Z., Li, S., Zhu, J., Zhang, F., et al. (2012). A metagenome-wide association study of gut microbiota in type 2 diabetes. *Nature* 490, 55–60. doi: 10.1038/nature11450

Radford, M. G. Jr., Donadio, J. V. Jr., Bergstralh, E. J., and Grande, J. P. (1997). Predicting renal outcome in IgA nephropathy. *J. Am. Soc. Nephrol.* 8, 199–207.

Ranganathan, N., Ranganathan, P., Friedman, E. A., Joseph, A., Delano, B., Goldfarb, D. S., et al. (2010). Pilot study of probiotic dietary supplementation for promoting healthy kidney function in patients with chronic kidney disease. *Adv. Therapy* 27, 634–647. doi: 10.1007/s12325-010-0059-9

Ridaura, V. K., Faith, J. J., Rey, F. E., Cheng, J., Duncan, A. E., Kau, A. L., et al. (2013). Gut microbiota from twins discordant for obesity modulate metabolism in mice. *Science (New York, N.Y.).* 341, 1241214–1241214. doi: 10.1126/science.1241214

Ritz, E. (2011). Intestinal-renal syndrome: mirage or reality? *Blood Purif.* 31, 70–76. doi: 10.1159/000321848

Round, J. L., and Mazmanian, S. K. (2009). The gut microbiota shapes intestinal immune responses during health and disease. *Nat. Rev. Immunol.* 9, 313–323. doi: 10.1038/nri2515

Soldano, S., Trombetta, A. C., Contini, P., Tomatis, V., Ruaro, B., Brizzolara, R., et al. (2018). Increase in circulating cells coexpressing M1 and M2 macrophage surface markers in patients with systemic sclerosis. *Ann. Rheum. Dis.* 77, 1842–1845. doi: 10.1136/annrheumdis-2018-213648

Sommer, F., Anderson, J. M., Bharti, R., Raes, J., and Rosenstiel, P. (2017). The resilience of the intestinal microbiota influences health and disease. *Nat. Rev. Microbiol.* 15, 630–638. doi: 10.1038/nrmicro.2017.58

Strzępa, A., and Szczepanik, M. (2013). Influence of natural gut flora on immune response. [Wpływ naturalnej flory jelitowej na odpowiedź immunologiczną]. *Postepy Higieny i Medycyny Doswiadczalnej (Online).* 67, 908–920. doi: 10.5604/17322693.1064563

Tan, R. Z., Wang, C., Deng, C., Zhong, X., Yan, Y., Luo, Y., et al. (2020). Quercetin protects against cisplatin-induced acute kidney injury by inhibiting Mincle/Syk/NF-κB signaling maintained macrophage inflammation. *Phytother Res.* 34, 139–152. doi: 10.1002/ptr.6507

Tan, R. Z., Zhong, X., Li, J. C., Zhang, Y. W., Yan, Y., Liao, Y., et al. (2019). An optimized 5/6 nephrectomy mouse model based on unilateral kidney ligation and its application in renal fibrosis research. *Ren. Fail.* 41, 555–566. doi: 10.1080/0886022X.2019.1627220

Tao, S., Sun, Q., Cai, L., Geng, Y., Hua, C., Ni, Y., et al. (2019). Caspase-1-dependent mechanism mediating the harmful impacts of the quorum-sensing molecule N-(3-oxo-dodecanoyl)-l-homoserine lactone on the intestinal cells. *J. Cell Physiol.* 234, 3621–3633. doi: 10.1002/jcp.27132

Tsai, Y. L., Lin, T. L., Chang, C. J., Wu, T. R., Lai, W. F., Lu, C. C., et al. (2019). Probiotics, prebiotics and amelioration of diseases. *J. Biomed. Sci.* 26:3. doi: 10.1186/s12929-018-0493-6

Ubeda, C., Taur, Y., Jenq, R. R., Equinda, M. J., Son, T., Samstein, M., et al. (2010). Vancomycin-resistant Enterococcus domination of intestinal microbiota is enabled by antibiotic treatment in mice and precedes bloodstream invasion in humans. *J. Clin. Invest.* 120, 4332–4341. doi: 10.1172/JCI43918

Vanholder, R., and Glorieux, G. (2015). The intestine and the kidneys: a bad marriage can be hazardous. *Clin. Kidney J.* 8, 168–179. doi: 10.1093/ckj/sfv004

Vaziri, N. D., Wong, J., Pahl, M., Piceno, Y. M., Yuan, J., DeSantis, T. Z., et al. (2013). Chronic kidney disease alters intestinal microbial flora. *Kidney Int.* 83, 308–315. doi: 10.1038/ki.2012.345

Wahi, K., Kodar, K., McConnell, M. J., Harper, J. L., Timmer, M. S. M., and Stocker, B. L. (2019). MSU crystals enhance TDB-mediated inflammatory macrophage IL-1beta secretion. *Inflammation* 42, 1129–1136. doi: 10.1007/s10753-019-00976-5

Wang, T., Guo, R., Zhou, G., Zhou, X., Kou, Z., Sui, F., et al. (2016). Traditional uses, botany, phytochemistry, pharmacology and toxicology of Panax notoginseng (Burk.) F.H. Chen: A review. *J. Ethnopharmacol.* 188, 234–258. doi: 10.1016/j.jep.2016.05.005

Wen, D., Tan, R. Z., Zhao, C. Y., Li, J. C., Zhong, X., Diao, H., et al. (2020). Astragalus mongholicus bunge and panax notoginseng (Burkill) F.H. Chen formula for renal injury in diabetic nephropathy-in vivo and in vitro evidence for autophagy regulation. *Front. Pharmacol.* 11:732. doi: 10.3389/fphar.2020.00732

Wu, Y., Zhu, C., Chen, Z., Chen, Z., Zhang, W., Ma, X., et al. (2016). Protective effects of Lactobacillus plantarum on epithelial barrier disruption caused by enterotoxigenic *Escherichia coli* in intestinal porcine epithelial cells. *Vet. Immunol. Immunopathol.* 172, 55–63. doi: 10.1016/j.vetimm.2016.03.005

Wynn, T. A., and Vannella, K. M. (2016). Macrophages in tissue repair. *Regenerat. Fibrosis. Immun.* 44, 450–462. doi: 10.1016/j.immuni.2016.02.015

Yonit, L., Arthur, M., Adeeb, R., and Miriam, M. (2015). Regulation of macrophage development and function in peripheral tissues. *Nat. Rev. Immunol.* 15:731. doi: 10.1038/nri3920

Yoshifuji, A., Wakino, S., Irie, J., Tajima, T., Hasegawa, K., Kanda, T., et al. (2016). Gut Lactobacillus protects against the progression of renal damage by modulating the gut environment in rats. *Nephrol. Dial. Transplant.* 31, 401–412. doi: 10.1093/ndt/gfv353

Zhang, H. W., Lin, Z. X., Tung, Y. S., Kwan, T. H., Mok, C. K., Leung, C., et al. (2014). Cordyceps sinensis (a traditional Chinese medicine) for treating chronic kidney disease. *Cochrane Database Syst Rev.* 18:Cd008353. doi: 10.1002/14651858.CD008353.pub2

Zhao, X. Q., Zhu, L. L., Chang, Q., Jiang, C., You, Y., Luo, T., et al. (2014). C-type lectin receptor dectin-3 mediates trehalose 6,6'-dimycolate (TDM)-induced Mincle expression through CARD9/Bcl10/MALT1-dependent nuclear factor (NF)-κB activation. *J. Biol. Chem.* 289, 30052–30062. doi: 10.1074/jbc.M114.588574

Zhong, Y., Deng, Y., Chen, Y., Chuang, P. Y., Cijiang, and He, J. (2013). Therapeutic use of traditional Chinese herbal medications for chronic kidney diseases. *Kidney Int.* 84, 1108–1118. doi: 10.1038/ki.2013.276

Zhong, Y., Menon, M. C., Deng, Y., Chen, Y., and He, J. C. (2015). Recent Advances in traditional Chinese medicine for kidney disease. *Am. J. Kidney Dis.* 66, 513–522. doi: 10.1053/j.ajkd.2015.04.013

Conflict of Interest: The authors declare that the research was conducted in the absence of any commercial or financial relationships that could be construed as a potential conflict of interest.

frontiers in Physiology

ORIGINAL RESEARCH
published: 17 December 2020
doi: 10.3389/fphys.2020.568812

The Prevalence and Independent Risk Factors of Significant Tricuspid Regurgitation Jets in Maintenance Hemodialysis Patients With ESRD

*Ying Zhang[1], Xiao-Han Ding[2], Fang Pang[1], Laiping Zhang[3,4], Yiqin Wang[1], Weili Wang[1], Rongsheng Rao[5] and Shi-Zhu Bian[3,4]**

[1] Department of Nephrology, The Key Laboratory for the Prevention and Treatment of Chronic Kidney Disease of Chongqing, Kidney Center of PLA, Xinqiao Hospital, Army Medical University (Third Military Medical University), Chongqing, China, [2] Department of Health Care and Geriatrics, The 940th Hospital of PLA Joint Logistics Support Force, Lanzhou, China, [3] Institute of Cardiovascular Diseases of PLA, Army Medical University (Third Military Medical University), Chongqing, China, [4] Department of Cardiology, Xinqiao Hospital, Chongqing, China, [5] Department of Ultrasound, Xinqiao Hospital, Army Medical University (Third Military Medical University), Chongqing, China

OPEN ACCESS

Edited by:
Jonatan Barrera-Chimal, National Autonomous University of Mexico, Mexico

Reviewed by:
Vladyslav Chubuchny, Gabriele Monasterio Tuscany Foundation (CNR), Italy
Fatih Gumus, Fatih University, Ankara, Turkey

***Correspondence:**
Shi-Zhu Bian
bianshizhu@163.com

Specialty section:
This article was submitted to Clinical and Translational Physiology, a section of the journal Frontiers in Physiology

Received: 02 June 2020
Accepted: 30 November 2020
Published: 17 December 2020

Citation:
Zhang Y, Ding X-H, Pang F, Zhang L, Wang Y, Wang W, Rao R and Bian S-Z (2020) The Prevalence and Independent Risk Factors of Significant Tricuspid Regurgitation Jets in Maintenance Hemodialysis Patients With ESRD. Front. Physiol. 11:568812. doi: 10.3389/fphys.2020.568812

Background and Aim: Tricuspid regurgitation (TR) is a frequent complication in various cardiovascular diseases. However, few studies have reported the prevalence of TR especially the moderate to severe or significant TR (ms-TR) maintenance dialysis patients. Thus, we aimed to identify the prevalence of ms-TR and its associated factors.

Methods: A total of 491 maintenance dialysis patients underwent echocardiographic examinations, while a subgroup ($n = 283$) also received routine blood tests, renal function examinations, and electrolyte analysis. We first compared the differences in abovementioned parameters among groups with various TR areas (TRAs). Finally, univariate and adjusted regression were also used to identify factors that were independently associated with ms-TR.

Results: The incidence of TR jets was 62.6%, which included a mildly increased TRA (47.8%), moderately increased TRA (10.4%), and severely increased TRA (3.5%). Most of the cardiac structures and functional parameters, such as the end-diastolic internal diameters of the left atrium (LA), left ventricle (LVDD), right atrium (RA), right ventricle (RV), left ventricular ejection fraction (LVEF), and fractional shortening (FS), were significantly associated with ms-TR. Among serum ions, only total CO_2 (TCO_2; $r = -0.141$, $p = 0.047$) was negatively correlated with TRA. After adjusted, only Na^+ [odds ratio (OR): 0.871 0.888, $p = 0.048$], RA (OR: 1.370, $p < 0.001$), and FS (OR: 0.887, $p < 0.001$) were independently associated with ms-TR.

Conclusion: Tricuspid regurgitation occurs in maintenance hemodialysis patients with ESRD. Na^+ FS and RA were independently associated with ms-TR, and these parameters may be potential risk factors/predictors for ms-TR.

Keywords: prevalence, tricuspid regurgitation, maintenance dialysis, end-stage renal disease, retrospective study

INTRODUCTION

End-stage renal disease (ESRD) has been demonstrated to be accompanied by various cardiovascular complications, which usually have poor outcomes (Kim and Parekh, 2015; Ramesh et al., 2016; Samanta et al., 2019). It has been reported that cardiovascular events, including heart failure, are the leading causes of death in ESRD patients (Kooman and van der Sande, 2019; Sugiura et al., 2019; Yogasundaram et al., 2019). The progressively deteriorating structure and function of the heart may be the consequence of renal failure (Cutshall et al., 2018; Unlu et al., 2018). On other hand, the insufficient perfusion of the kidney from the heart may aggravate renal dysfunction. Previous studies mainly focused on structural and functional cardiac changes in the left heart in ESRD patients and identified several biochemical markers, clinical factors, and hemodynamic predictors (Mahfouz et al., 2013; Minami et al., 2016; Lemor et al., 2018; Khan et al., 2019; Yogasundaram et al., 2019).

However, the structure and function of the right heart in ESRD patients, especially those who underwent dialysis treatment, have not been extensively studied. Tricuspid regurgitation (TR), which includes functional or mild TR, moderate TR and significant severe TR, is one of the most important functions of the right heart and is highly prevalent in various populations (Agricola et al., 2017; Al-Hijji et al., 2017; Sun and O'Gara, 2017). However, the prevalence and associated factors have not been identified in ESRD patients who received maintenance dialysis. TR may contribute to renal dysfunction in heart failure patients (Maeder et al., 2008).

Many previous studies have been studied the roles of tricuspid regurgitation in right heart failure in hemodialysis patients (Gumus and Saricaoglu, 2020). Part of the associated factors have also been found. However, interaction and relationship between TR especially ms-TR or significant TR and renal dysfunction attached less attentions. Furthermore, the prevalence of ms-TR in the special subgroup populations of dialysis patients has not been studied deeply (Cakici et al., 2020). Thus, we performed this retrospective study to identify the prevalence of ms-TR and potentially associated factors in a large sample size of a special population: ESRD patients who underwent maintenance dialysis.

Abbreviations: BAS, basophil ratio; BUN, blood urea nitrogen concentration; Ca^{2+}, serum calcium concentration; Cr, plasma creatinine; eGFR, estimated glomerular filtration rate; ESRD, end-stage renal disease; EO, eosinophil ratio; FS, fractional shortening; Hb, hemoglobin concentration; HCT, hematocrit; IVS, interventricular septum; K^{+}, serum potassium concentration; LA, left atrial end-diastolic internal diameter; LVDD, left ventricular end-diastolic internal diameter; LVEF, left ventricular ejection fraction; LVPW, left ventricular posterior wall; LYM, lymphocyte ratio; MCH, mean corpuscular hemoglobin; MCHC, mean corpuscular hemoglobin concentration; MCV, mean corpuscular volume; MONO, monocyte ratio; Na^{+}, sodium concentration; NEU, neutrophil ratio; ms-TR, moderate to severe TRA; P, phosphate concentration; PA, pulmonary arterial end-diastolic internal diameter; PLT, platelet; RA, right atrial end-diastolic internal diameter; RBC, red blood cell count; RDW, red blood cell distribution width; RV, right ventricular end-diastolic internal diameter; SV, stroke volume; TR, tricuspid regurgitation; TRA, TR area; TRV, TR velocity; WBC, white blood cell count; ΔP, mitral transmitral pressure gradient.

MATERIALS AND METHODS

Study Design and Populations

From March 2011 to June 2019, ESRD patients who received maintenance dialysis ($n = 491$) at the Nephrology of Chongqing and Kidney Center of PLA, Xinqiao Hospital, and Army Medical University (Third Military Medical University) were included in this retrospective study. These hemodialysis patients underwent echocardiographic examinations, while a subgroup ($n = 283$) of this population also received routine blood tests, renal function examinations, and electrolyte analysis, which are shown in **Figure 1**.

All of the ESRD patients were informed about the purpose and procedures of our study and provided written informed consent. Our present study complied with the Declaration of Helsinki.

In addition, the ethics committee of the Second Affiliated Clinic Hospital (Xinqiao Hospital) and Army Medical University (Third Military Medical University) approved the study.

Procedures of Echocardiographic Examinations

The echocardiographic examinations of each patient were carried out by a skilled echocardiographer, Dr. Rongsheng Rao, according to the American Society of Echocardiography recommendations (Mansour et al., 2010). Echocardiographic examinations were performed in a supine position after resting for 10 min after hemodialysis. Two-dimensional echocardiographically guided motion mode (M-mode) images were obtained from standardized views by using an ultrasonography system (CX50, Philips, United States) with an S5 probe.

Among the echocardiographic parameters, our trained physicians recorded the left atrial end-diastolic internal diameter (LA), left ventricular end-diastolic internal diameter (LVDD), right atrial end-diastolic internal diameter (RA), right ventricular end-diastolic internal diameter (RV), and pulmonary arterial end-diastolic internal diameter (PA).

Additionally, the mobility and size of the left ventricular posterior wall (LVPW), the mobility and the size of the interventricular septum (IVS), fractional shortening (FS) and left ventricular ejection fraction (LVEF) and stroke volume (SV) were also recorded. Finally, TR-related parameters, such as TR area (TRA), TR velocity (TRV), and TR pressure, were also measured and recorded.

Biomarker Determination

After admission to the hospital, we collected venous blood samples early in the morning after patients had fasted for more than 12 h before dialysis. The blood samples have also been obtained after dialysis in order to assess the effect of dialysis.

First, renal function, such as eGFR, plasma creatinine (Cr) and the blood urea nitrogen (BUN) concentration, was examined. Cr was also tested with Roche Diagnostics GmbH products (enzyme assay, Abbott, i2000, United States). BUN was also measured with ferene methods (Beckman AU5821, GA, United States).

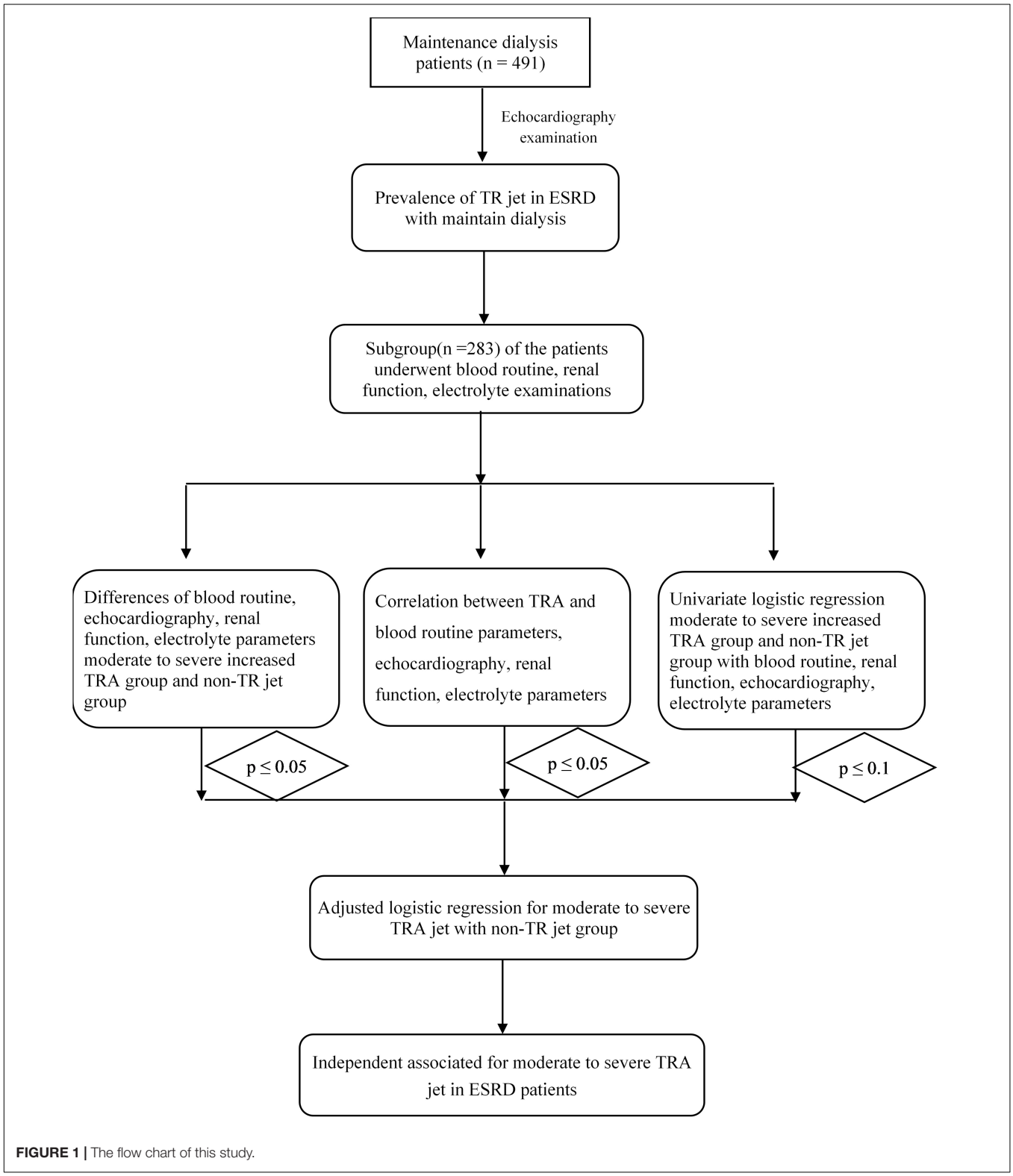

FIGURE 1 | The flow chart of this study.

Then, we performed routine blood examinations. An automated hematology chemistry analyzer was used to examine the hemoglobin concentration (Hb), red blood cell (RBC) count (RBC), hematocrit (HCT), mean corpuscular volume (MCV), mean corpuscular hemoglobin (MCH), mean corpuscular hemoglobin concentration (MCHC), and red blood cell distribution width (RDW) (type: AU400; Olympus Optical, Co., Tokyo, Japan). Furthermore, we also examined the white

blood cell (WBC) and platelet (PLT) counts. The lymphocyte ratio (LYM), basophil ratio (BAS), neutrophil ratio (NEU), eosinophil ratio (EO), and monocyte ratio (MONO) were also tested and recorded.

Finally, we also performed an electrolyte examination, which included the sodium concentration (Na^+, indirect ion selective electrode assay with EX-Z, JOKOH, Japan), serum calcium concentration (Ca^{2+}, tri-azo methods), and phosphate concentration (P, phosphomolybdate ultraviolet assay, Roche Diagnostics GmbH, United States). In addition, we also measured the serum potassium concentration (K^+, ferene methods, Beckman AU5821).

Variable Definitions

First, patients were divided into the non-TR group (without a TR jet), the mildly increased TRA group ($0 < \text{TRA} < 5\ \text{cm}^2$) and the moderately to severely increased TRA group (ms-TR, TRA $\geq 5\ \text{cm}^2$) which is also called significant TR (ms-TR in this study).

We calculated the estimated glomerular filtration rate (eGFR) by using the Chronic Kidney Disease Epidemiology Collaboration (CKD-EPI) formula: eGFR (ml/min/$1.73\,\text{m}^2$) $= 1.41 \times \min(\text{Cr/k},1)^{\alpha} \times \max(\text{Cr/},1)^{-1.209} \times 0.993^{age} \times 1.018$ [$k = 0.7$ (female) and 0.9 (male); $\alpha = -0.329$ (female) and -0.411 (male)].

Statistical Analysis

If a continuous variable was normally distributed, it is presented as the mean ± standard deviation (SD). We employed one-way ANOVA to compare differences among the non-TR, mildly increased TRA and moderately to severely increased TRA groups. Further analysis comparing two groups was performed using least significant difference (LSD) methods after one-way ANOVA.

If one variable was non-normally distributed, it is presented as the median (25–75%). Comparisons among the non-TR, mildly increased TRA and moderately to severely increased TRA groups of variables with non-normal distributions were performed by one-way ANOVA after being transformed to achieve normality.

We performed univariate logistic regression analyses with each variable to screen for factors associated with moderate to severe TR. Variables with a p value less than 0.1 in the univariate logistic regression were included in multivariate (adjusted) logistic regression analyses to identify factors that were independently associated with moderate to severe TR. Our statistical analyses were performed by using the statistical software SPSS 22.0 (CA, United States) for Mac.

RESULTS

Basic Information and the Prevalence of TR in the Study Populations

In our study, 491 ESRD patients were included. The mean age was 52.95 ± 14.21 years, and the mean body-mass index (BMI) was 21.89 ± 4.89 kg/m^2. The incidence of a TR jet was 62.6%, which included a mildly increased TRA (47.8%), a moderately increased TRA (10.4%), and a severely increased TRA (3.5%). Thus, the incidence of ms-TR was 13.9%. These results are shown in **Figure 2**.

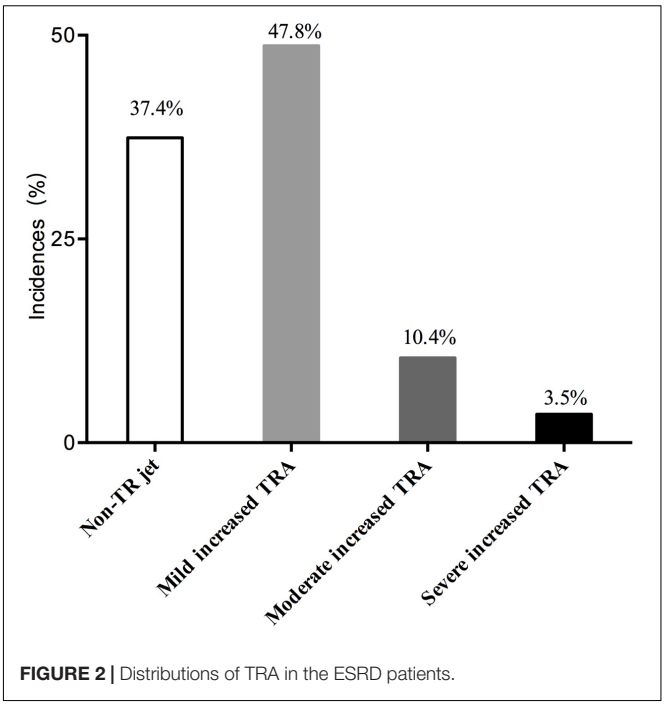

FIGURE 2 | Distributions of TRA in the ESRD patients.

Differences in Demographic, Echocardiographic, Routine Blood, Electrolyte and Renal Function Parameters Among Various TRA Groups

First, we did not find any differences in the demographic data (age and BMI, $p > 0.05$) among the non-TR, mildly increased TRA and ms-TR groups.

Second, in the echocardiographic parameters, both left heart and right heart structures and functions showed significant differences among these three groups. LA (43.93 ± 6.58 vs. 36.74 ± 4.75) and LVDD (54.11 ± 7.18 vs. 48.80 ± 5.25) were significantly higher in the ms-TR group than in the non-TR group (all p values < 0.001). These parameters were also significantly higher in the ms-TR group than in the mildly increased TRA group (all p values < 0.001). However, there were no differences in LA and LVDD between the mildly increased TRA and non-TR groups (all p values > 0.05). Though there were no differences in IVS and LVPW thickness among the three subpopulations, and their mobility was significantly different among the various TRA groups. ms-TR patients had worse IVS mobility [3.00 (6.00–6.00)] and a more dispersive LVPW mobility [10.00 (7.00–10.00)] than the other two groups (all p values < 0.001, **Table 1**). FS was also significantly lower in the ms-TR population [29.00 (18.75–33.25)] than in the non-TR [35.00 (32.00–37.00), $p < 0.001$] and mildly increased TRA [34.00 (32.00–37.00), $p < 0.001$] populations. The left heart functions, including LVEF, were significantly different among the three

TABLE 1 | Differences between of the hemodynamics, demographic data, renal function, electrolyte and routine blood examination parameters among various TRA groups.

	Overall	Non –TR patients	TRA increased groups		
Parameters	**(n = 491 Subgroup n_1 = 283)**	**(n = 84)**	**Mild increased TR (n = 153)**	**ms-TR group (n = 46)**	***p* value**
Demographic data					
Age (years)	52.54 ± 14.32	52.23 ± 12.50	53.22 ± 15.25	51.41 ± 14.19	0.719
BMI (kg/m^2)	22.45 ± 3.56	22.54 ± 3.17	22.56 ± 3.79	21.87 ± 3.92	0.503
Echocardiographic parameters					
LA (mm)	38.41 ± 5.77	36.74 ± 4.75	38.02 ± 4.86	43.93 ± 6.58**##	<0.001
LVDD (mm)	49.30 ± 6.29	48.80 ± 5.25	48.92 ± 5.93	54.11 ± 7.18**##	<0.001
RA (mm)	37.15 ± 5.11	35.52 ± 3.78	36.43 ± 4.03	44.41 ± 5.36**##	<0.001
RV (mm)	35.46 ± 5.56	34.40 ± 3.40	34.90 ± 3.51	40.98 ± 5.03**##	<0.001
PA (mm)	23.82 ± 2.70	23.65 ± 2.44	23.68 ± 2.49	25.14 ± 2.58**##	0.001
IVS (mm)	13.04 ± 8.57	12.65 ± 1.64	12.47 ± 1.57	12.22 ± 1.73	0.345
IVS mobility	6.00 (6.00–6.00)	6.00 (6.00–6.00)	6.00 (6.00–6.00)	3.00 (6.00–6.00) **##	<0.001
LVPW (mm)	11.00 (10.00–12.00)	11.00 (10.00–12.00)	11.80 (10.00–12.00)*	11.20 (10.00–12.00)	0.144
LVPW mobility	10.00 (10.00–10.00)	10.00 (10.00–10.00)	10.00 (10.00–10.00)	10.00 (7.00–10.00)**##	<0.001
FS (%)	34.00 (31.00–37.00)	35.00 (32.00–37.00)	34.00 (32.00–37.00)	29.00 (18.75–33.25)**##	<0.001
LVEF (%)	60.83 ± 9.44	62.55 ± 8.01	62.28 ± 7.78	50.28 ± 13.93**##	<0.001
SV (ml)	75.10 ± 20.22	74.57 ± 15.53	78.41 ± 21.86	75.20 ± 18.43**##	0.301
TRV (cm/s)	281.00 (243.00–336.00)	–	265.00 (240.00–311.50)	354.00 (322.00–384.25)	<0.001
ΔP (mmHg)	33.00 (22.00–46.00)	–	28.00 (23.00–38.25)	50.00 (40.50–59.00)	<0.001
Renal function (n = 283)					
eGFR [mL/(min·1.73 m^2)]	10.47 (5.62–13.00)	10.47 (5.88–12.04)	10.03 (5.88–13.00)	10.34 (5.28–13.50)	0.981
Cr (μmol/L)	815.50 (618.40–1016.90)	821.80 (618.92–1017.45)	814.40 (598.00–998.25)	817.35 (643.95–1126.22)	0.448
BUN (μmol/L)	21.75 ± 7.82	21.26 ± 7.64	21.77 ± 7.58	22.57 ± 8.98	0.659
Electrolyte parameters					
Mg^{2+} (mmol/L)	0.982 ± 0.158	0.983 ± 0.175	0.978 ± 0.153	0.991 ± 0.143	0.877
K^+ (mmol/L)	4.79 ± 0.787	4.78 ± 0.72	4.78 ± 0.79	4.83 ± 0.89	0.944
Ca^{2+} (mmol/L)	2.15 (2.03–2.28)	2.15 (2.05–2.280)	2.15 (2.02–2.28)	2.14 (1.97–2.36)	0.957
Na^+(mmol/L)	137.85 (136.40–139.80)	138.40 (136.50–140.00)	137.84 (136.35–140.0)	137.35 (136.07–139.20)	0.149
Cl^- (mmol/L)	102.45 (99.60–105.30)	102.45 (99.10–105.20)	102.45 (99.60–105.50)	102.45 (99.98–105.80)	0.882
TCO_2 (mmol/L)	20.66 (18.00–23.00)	21.05 (18.78–23.95)	20.50 (18.10–23.00)	19.90 (16.75–22.02)	0.075
P (mmol/L)	1.91 ± 0.64	1.96 ± 0.63	1.89 ± 0.62	1.91 ± 0.69	0.722
Dialysis time (days)	1230.00 (541.00–2549.00)	1214.00 (497.00–2101.25	1312.00 (539.00–2619.00)	1368.00 (555.750–2632.75)	0.183
Routine blood examination parameters					
RBC (10^{12}/L)	3.39 ± 0.72	3.37 ± 0.62	3.40 ± 0.73	3.39 ± 0.86	0.950
Hb (g/dl)	100.52 ± 19.42	99.98 ± 19.46	100.45 ± 19.07	101.74 ± 20.83	0.884
Hct (L/L)	31.85 ± 6.12	31.85 ± 6.07	31.70 ± 5.98	32.37 ± 6.78	0.809
MCV (fl)	95.14 ± 8.02	95.11 ± 8.11	94.75 ± 8.14	96.50 ± 7.46	0.431
MCH (pg)	30.03 ± 2.70	29.84 ± 2.57	30.03 ± 2.78	30.39 ± 2.65	0.547
MCHC (g/dl)	315.72 ± 12.98	313.92 ± 11.22	316.99 ± 13.97	314.79 ± 12.38	0.191
RDW-CV (%)	14.57 ± 1.65	14.65 ± 1.61	14.48 ± 1.71	14.69 ± 1.56	0.649
RDW-SD (%)	51.30 (47.00–55.40)	51.84 (47.00–55.78)	51.20 (46.75–54.15)	51.47 (48.70–56.60)	0.342
PLT (10^9/L)	167.00 (124.00–211.00)	171.756 (127.50–212.50)	165.00 (123.00–221.00)	150.00 (126.75–197.75)	0.258
WBC (10^9/L)	6.61 (5.22–8.18)	6.44 (5.24–8.09)	6.87 (5.22–8.40)	6.07 (5.10–6.98)	0.445
EO (%)	2.80 (1.60–4.70)	2.65 (1.50–4.35)	2.70 (1.50–4.85)	3.35 (1.88–5.00)	0.277
BASO (%)	0.500 (0.300–0.700)	0.500 (0.200–0.700)	0.500 (0.300–0.700)	0.500 (0.200–0.800)	0.763
MONO (%)	6.00 (4.60–7.50)	6.05 (4.48–6.98)	5.90 (4.55–7.60)	6.38 (4.80–7.62)	0.771
NEU (%)	71.43 ± 9.54	70.77 ± 9.82	72.16 ± 9.36	70.19 ± 9.59	0.352
LYMP (%)	17.78 ± 7.23	18.20 ± 6.87	17.16 ± 7.05	19.03 ± 8.37	0.249

p presents differences among various groups.
**: $p < 0.05$ compared with non-TR group; **: $p < 0.01$ compared with non-TR group; ##: $p < 0.01$ compared with mild increased TR group.*

groups. The ms-TR group was characterized by a lower LVEF (50.28 ± 13.93%) than the other two subgroups (62.55 ± 8.01 and 62.28 ± 7.78, $p < 0.001$). However, SV was similar in the three groups (all p values > 0.05). In addition, PA was also significantly higher in the ms-TR group than in the other groups (25.14 ± 2.58 vs. 23.65 ± 2.44 and 23.68 ± 2.49 mm, $p = 0.001$, **Table 1**).

In regard to renal function, none of the parameters (eGFR, Cr, and BUN) were significantly different among the three groups of patients (all p values were greater than 0.05, **Table 1**).

We further compared the differences in serum ions [Mg^{2+}, K^+, Ca^{2+}, Na^+, Cl^-, total CO_2 (TCO_2), and P]. However, none of these ions were significantly different among the non-TR, mildly increased TRA and ms-TR groups (**Table 1**).

Finally, we also investigated routine blood examinations. However, we did not find any differences among the three groups (**Table 1**).

Correlation Between TRA and Demographic, Echocardiographic, Routine Blood, Electrolyte and Renal Function Parameters

To identify associations between TRA and other parameters, we performed Spearman's correlation analysis. We found that LA ($r = 0.510$, $p < 0.001$), LVDD ($r = 0.389$, $p < 0.001$), RA ($r = 0.615$, $p < 0.001$), RV ($r = 0.586$, $p < 0.001$), and PA ($r = 0.322$, $p < 0.001$) were closely positively related to TRA. Meanwhile, the IVS mobility ($r = -0.338$, $p < 0.001$), LVPW mobility ($r = -0.344$, $p < 0.001$), LVEF ($r = -0.401$, $p < 0.001$), and FS ($r = -0.403$, $p < 0.001$) as well as TCO_2 ($r = -0.141$, $p = 0.047$) were negatively correlated with TRA. We did not find other associations between TRA and the rest of the parameters (**Table 2**).

Logistic Regressions for ms-TR With Demographic, Echocardiographic, Routine Blood, Electrolyte and Renal Function Parameters

In univariate regression analysis, demographic data (age and BMI) were not associated with ms-TR (all p values > 0.05) (**Table 3**).

Among the echocardiographic parameters, we identified several factors that were potentially associated with ms-TR. First, the diameter of the left and right heart as well as the PA, LA [odds ratio (OR): 1.281, 95% confidence interval (CI): 1.166–1.408, $p < 0.001$], LVDD (OR: 1.149, 95% CI: 1.076–1.227, $p < 0.001$), RA (OR: 1.437, 95% CI: 1.281–1.612, $p < 0.001$), RV (OR: 1.410, 95% CI: 1.251–1.589, $p < 0.001$), and PA (OR: 1.262, 95% CI: 1.083–1.471, $p = 0.003$) were associated with ms-TR (**Table 3**).

Furthermore, it was also found that IVS mobility (OR: 0.440, 95% CI: 0.295–0.655, $p < 0.001$), LVPW mobility (OR: 0.588, 95% CI: 0.449–0.770, $p < 0.001$), FS (OR: 0.853, 95% CI: 0.801–0.909, $p < 0.001$), and LVEF (OR: 0.905, 95% CI: 0.869–0.943, $p < 0.001$) may also have been associated with ms-TR (**Table 3**).

TABLE 2 | Relationship between TRA and other parameters.

	Relationship with TRA	
Parameters	***R***	***p* value**
Demographic data		
Age (years)	−0.064	0.371
BMI (kg/m^2)		
Echocardiographic parameters		
LA (mm)	0.510	<0.001
LVDD (mm)	0.389	<0.001
RA (mm)	0.615	<0.001
RV (mm)	0.586	<0.001
PA (mm)	0.322	<0.001
IVS (mm)	0.086	0.228
IVS mobility	−0.338	<0.001
LVPW (mm)	0.084	0.237
LVPW mobility	−0.344	<0.001
FS (%)	−0.403	<0.001
LVEF (%)	−0.401	<0.001
SV (ml)	0.095	0.184
Renal function		
eGFR [mL/(min·1.73 m^2)]	0.047	0.510
Cr (umol/L)	0.013	0.858
BUN (μmol/L)	0.056	0.433
Electrolyte parameters		
Mg^{2+} (mmol/L)	0.080	0.263
K^+ (mmol/L)	0.088	0.215
Ca^{2+} (mmol/L)	−0.039	0.583
Na^+(mmol/L)	−0.012	0.867
Cl^- (mmol/L)	0.109	0.127
TCO_2 (mmol/L)	−0.141	0.047
P (mmol/L)	0.067	0.345
Dialysis time (days)	−0.046	0.518
Blood routine examination parameters		
RBC (10^{12}/L)	0.033	0.641
Hb (g/dl)	0.062	0.381
Hct (L/L)	0.075	0.292
MCV (fl)	0.063	0.376
MCH (pg)	0.043	0.546
MCHC (g/dl)	−0.027	0.709
RDW-CV (%)	0.021	0.765
RDW-SD (%)	0.060	0.402
PLT (10^9/L)	−0.080	0.260
WBC (10^9/L)	−0.114	0.109
EO (%)	−0.054	0.449
BASO (%)	0.041	0.563
MONO (%)	0.058	0.418
NEU (%)	−0.023	0.750

However, none of the renal function parameters showed significant associations with ms-TR (Cr, BUN, and eGFR, **Table 3**).

Among the serum ions, we found that only Na^+ (OR: 0.864, 95% CI: 0.749–0.996, $p = 0.044$) and TCO_2 (OR: 0.890, 95%

TABLE 3 | Univariate logistic analysis for ms-TR jet.

Parameters	β	*p* value	OR	95CI%	
				Lower borderline	Upper borderline
Demographic data					
Age (years)	−0.005	0.734	0.995	0.968	1.023
BMI (kg/m^2)	−0.057	0.291	0.945	0.850	1.050
Echocardiographic parameters					
LA (mm)	0.248	<0.001	1.281	1.166	1.408
LVDD (mm)	0.139	<0.001	1.149	1.076	1.227
RA (mm)	0.362	<0.001	1.437	1.281	1.612
RV (mm)	0.343	<0.001	1.410	1.251	1.589
PA (mm)	0.233	0.003	1.262	1.083	1.471
IVS (mm)	−0.162	0.163	0.850	0.677	1.068
IVS mobility	−0.821	<0.001	0.440	0.295	0.655
LVPW (mm)	0.058	0.559	1.060	0.872	1.288
LVPW mobility	−0.531	<0.001	0.588	0.449	0.770
FS (%)	−0.159	<0.001	0.853	0.801	0.909
LVEF (%)	−0.100	<0.001	0.905	0.869	0.943
SV (ml)	0.002	0.835	1.002	0.981	1.024
Dialysis time (days)	0.001	0.203	1.000	1.000	1.001
Renal function					
eGFR [mL/(min·1.73 m^2)]	0.023	0.374	1.023	0.973	1.075
Cr (umol/L)	0.001	0.456	1.000	0.999	1.001
BUN (μmol/L)	0.020	0.380	1.020	0.976	1.066
Electrolyte parameters					
Mg^{2+} (mmol/L)	0.029	0.796	1.337	0.149	12.006
K^+ (mmol/L)	0.077	0.744	1.080	0.682	1.709
Ca^{2+} (mmol/L)	0.118	0.861	1.125	0.300	4.218
Na^+(mmol/L)	−0.146	0.044	0.864	0.749	0.996
Cl^- (mmol/L)	0.022	0.608	1.022	0.939	1.113
TCO_2 (mmol/L)	−0.116	0.017	0.890	0.809	0.980
P (mmol/L)	−0.105	0.711	0.901	0.517	1.568
Routine blood examination parameters					
RBC (10^{12}/L)	0.057	0.827	1.058	0.637	1.759
Hb (g/dl)	0.005	0.628	1.005	0.986	1.023
Hct (L/L)	0.013	0.655	1.013	0.957	1.073
MCV (fl)	0.023	0.339	1.023	0.976	1.072
MCH (pg)	0.084	0.255	1.088	0.941	1.258
MCHC (g/dl)	0.007	0.681	1.007	0.976	1.039
RDW-CV (%)	0.014	0.903	1.014	0.808	1.273
RDW-SD (%)	0.026	0.336	1.026	0.974	1.081
PLT (10^9/L)	−0.003	0.242	0.997	0.991	1.002
WBC (10^9/L)	−0.032	0.710	0.969	0.820	1.145
EO (%)	−0.006	0.742	0.994	0.958	1.031
BASO (%)	−0.025	0.544	0.976	0.901	1.057
MONO (%)	0.030	0.951	1.030	0.404	2.625
NEU (%)	0.015	0.542	1.015	0.967	1.066
RBC (10^{12}/L)	0.063	0.441	1.065	0.907	1.252

Primary screen for the independently associated factors.

TABLE 4 | Adjusted logistic regressions for ms-TR.

Parameters	β	*p* value	OR	95%CI	
				Lower borderline	Upper borderline
RA (mm)	0.3150	<0.001	1.370	1.234	1.520
FS (%)	−0.120	<0.001	0.887	0.822	0.957
Na^+ (mmol/L)	−0.137	0.048	0.871	0.760	0.999

Na^+, RA, and FS have been identified to be independently associated with ms-TR.

CI: 0.809–0.980, $p = 0.017$) were potentially related to ms-TR (**Table 3**).

Finally, in the routine blood examination, RBC- and WBC-related parameters showed no potential associations with ms-TR. In addition, the other parameters, such as the ratios of monocytes, lymphocytes, eosinophils, and basophilic granulocytes, were not associated with ms-TR (**Table 3**).

To identify factors that were independently associated with ms-TR, we performed an adjusted (multivariate) logistic regression. We found that only Na^+ (OR: 0.871 95% CI: 0.760–0.999, $p = 0.048$), RA (OR: 1.370, 95% CI: 1.234–1.520, $p < 0.001$), and FS (OR: 0.887, 95% CI: 0.822–0.957, $p < 0.001$) were independently associated with ms-TR (**Table 4**).

DISCUSSION

In our present study, we found that TR was prevalent (62.6%) in 491 ESRD patients who received maintenance dialysis treatment. Though TCO_2 and other renal functions were potentially associated with TR, adjusted regression showed that only Na^+, FS, and RA were independently associated with ms-TR; thus, further cohort studies are warranted to confirm their causality.

TR Was Prevalent in ESRD Patients Who Received Maintenance Dialysis Treatment

As discussed above, though TR is common in normal populations or populations with other cardiovascular diseases (Arsalan et al., 2017), TR was more prevalent and had a relatively higher incidence in a special subgroup, maintenance dialysis patients with ESRD (Walsh et al., 1998; Maeder et al., 2008; Al-Hijji et al., 2017; Del Forno et al., 2018; Dietz et al., 2019). Furthermore, we also found that ms-TR showed a higher incidence than other degrees of TRA. In particular, a few individuals had a TRA that was larger than 15 cm^2; these patients needed further examination or treatment by the cardiovascular disease department. In the past, few studies had investigated the roles of TR, as well as the function and structure of the left heart, in renal function in heart failure patients (Minami et al., 2016; Cutshall et al., 2018; Konigsbrugge and Ay, 2019). However, no papers have reported the prevalence of TR in a large population of maintenance dialysis patients with ESRD. Our study was the first to describe the prevalence and TRA degree in patients who received dialysis at our center. Our data revealed that a TR

jet occurred in maintenance dialysis patients with ESRD. Some patients had a TR jet with an extremely large area and may have needed cardiac surgery interventions. Thus, echocardiographic examinations are a highly valuable non-invasive method to evaluate the cardiovascular complications of ESRD, providing guidelines for the treatment of patients.

TR Was Not Closely Associated With Renal Function in ESRD Patients Undergoing Hemodialysis

It has been indicated that kidney dysfunction may contribute to cardiovascular complications (Yogasundaram et al., 2019). We investigated renal function in ESRD patients, but the eGFR, Cr and BUN were not significantly different among the various TRA groups and were not associated with TRA. Though few previous studies have indicated that renal dysfunction affects cardiac structure and function (Minami et al., 2016; Cutshall et al., 2018; Lemor et al., 2018), we did not find a potential association of eGFR, BUN and Cr with ms-TR. Thus, these parameters were not included in the final adjusted logistic regression. Though our present study did not find an association of renal functions with ms-TR, the causal relationship between renal function and TR jets may need further cohort studies or basic studies to be confirmed.

TR Was Significantly Associated With Serum Ions

Ions are known to play numerous key roles in signal transduction, protein synthesis, cell proliferation and differentiation. In ESRD patients, serum ion disturbances are the most common clinical manifestations. Thus, we also investigated the associations between serum ions (Mg^{2+}, Ca^{2+}, K^{+}, Cl^{-}, TCO_2, Na^{+}, and P) and TR jets. First, there were no significant differences in the abovementioned ions in the various TRA groups. Then, we found that TCO_2 was closely negatively correlated with TRA. In the past several decades, researchers have found that TCO_2 levels changed in uremia, indicating that renal dysfunction may alter TCO_2 levels, resulting in changes in respiration and oxygen usage. If this situation is persistent, it may cause hypoxia-induced cardiac injury or changes in cardiac structure and function. Through further univariate regression analysis, we found that TCO_2 and Na^{+} were potentially associated with an ms-TR jet. However, in the adjusted regression analysis, these factors were excluded by other variables and did not show independent associations with ms-TR.

TR Showed No Close Relationship With Routine Blood Parameters

Anemia, which is the consequence of the insufficient production of EPO and a higher demand for EPO, is another critical complication of ESRD and leads to insufficient Hb and RBC production (Santoro and Canova, 2005; van der Meer et al., 2008; Yokoro et al., 2017). It proposed that the anemia may contribute to TR jet. Thus, we investigated the association between RBC-related parameters and WBC-related parameters. However, we did not find any associations between RBC/WBC-related parameters and TR. This result may have been caused by the effect of anemia on cardiovascular diseases; this may involve a long-term process that requires cohort studies to identify their associations.

Na^{+}, FS, and RA May Contribute to the Development of ms-TR

Our present study found that Na^{+} FS and RA were independently associated with ms-TR. The structure and function of the left heart showed an association with ms-TR, which may have been caused by the interactions between the left and right heart. Furthermore, changes in the right heart may result in relative or absolute tricuspid insufficiency, which may aggravate changes in structure and function (enlargement and right heart failure) (Al-Hijji et al., 2017; Sun and O'Gara, 2017; Hahn, 2019).

We have identified that Na^{+} was independently associated with TR which was in concordant with the previous studies that Na^{+} was correlated to the cardiovascular diseases in ERSD dialysis patients. This may be caused by the roles of Na+ in the vascular systems. In according to the previous studies, cardiovascular diseases are the common complications in ESRD patients especially in the maintenance dialysis subset populations (Cakici et al., 2020; Gumus and Saricaoglu, 2020). The precise mechanisms of Na^{+} in TR have not been widely investigated.

Our present results were consistent with previous studies on various cardiovascular diseases that are induced by a TR jet (Lee et al., 2010; Al-Hijji et al., 2017; Kopic et al., 2017; Mangieri et al., 2017). However, the roles of FS in TR jets have not been reported before. We found that FS was significantly associated with ms-TR, which was a novel finding that revealed that left heart functions may affect the right heart (due to preloading or other hemodynamic changes), which is partly in according with the previous studies (Badano et al., 2019; Dietz et al., 2019; Prihadi et al., 2019). However, the precise cause and mechanisms were not confirmed; thus, further cohort studies and research to uncover the basic mechanisms are warranted.

Limitations

This was a retrospective study focusing on the prevalence of TR and its associated factors. However, there are several limitations that need to be improved in our future studies. First, our present study was a retrospective study that identified only the factors associated with ms-TR. The causality between clinical factors and ms-TR needs to be analyzed by further cohort studies. Another limitation is that we investigated only a few of the frequently used clinical parameters; however, there may be other valuable factors that should be examined. Finally, the parameters after dialysis were not included in this study, but these factors should be included in future research.

CONCLUSION

Tricuspid regurgitation is also prevalent in maintenance hemodialysis patients with ESRD. Na^{+}, FS, and RA were independently associated with ms-TR; these may be potential risk factors/predictors for ms-TR and warrant further cohort studies.

DATA AVAILABILITY STATEMENT

The raw data supporting the conclusions of this article will be made available by the authors, without undue reservation.

ETHICS STATEMENT

The studies involving human participants were reviewed and approved by the Second Affiliated Clinic Hospital (Xinqiao Hospital) and Army Medical University (Third Military Medical University). The patients/participants provided their written informed consent to participate in this study.

AUTHOR CONTRIBUTIONS

S-ZB and YZ designed the study, drafted the manuscript, and performed the statistical analysis. S-ZB and X-HD critically reviewed and revised the manuscript for important intellectual content. RR performed the echocardiographic examinations and LZ recorded the measurements of TR-related parameters. YZ and X-HD collected the demographic data and performed routine blood examinations. YW, FP, and LZ performed the laboratory measurements. YW and WW obtained the dialysis-related data. All authors contributed to the article and approved the submitted version.

FUNDING

This study was supported by the National Natural Science Foundation of China (grant no. 81901916), the Excellent Scientist Pool Program of Army Medical University ("Miaopu Program 2019R046"), and The Major Clinical Program of Xinqiao Hospital (2018JSLC0024).

ACKNOWLEDGMENTS

We would like to thank all the individuals who participated in this study for their support. Finally, S-ZB thank his wife Meng Zhou for her help and care during the preparation of this manuscript.

REFERENCES

Agricola, E., Marini, C., Stella, S., Monello, A., Fisicaro, A., Tufaro, V., et al. (2017). Effects of functional tricuspid regurgitation on renal function and long-term prognosis in patients with heart failure. *J. Cardiovasc. Med.* 18, 60–68. doi: 10.2459/jcm.0000000000000312

Al-Hijji, M., Fender, E. A., El Sabbagh, A., and Holmes, D. R. (2017). Current treatment strategies for tricuspid regurgitation. *Curr. Cardiol. Rep.* 19:106.

Arsalan, M., Walther, T., Smith, R. L. II, and Grayburn, P. A. (2017). Tricuspid regurgitation diagnosis and treatment. *Eur. Heart J.* 38, 634–638.

Badano, L. P., Hahn, R., Rodriguez-Zanella, H., Araiza Garaygordobil, D., Ochoa-Jimenez, R. C., and Muraru, D. (2019). Morphological assessment of the tricuspid apparatus and grading regurgitation severity in patients with functional tricuspid regurgitation: thinking outside the box. *JACC Cardiovasc. Imaging* 12, 652–664. doi: 10.1016/j.jcmg.2018.09.029

Cakici, E. K., Cakici, M., Gumus, F., Tan Kurklu, T. S., Yazilitas, F., Orun, U. A., et al. (2020). Effects of hemodialysis access type on right heart geometry in adolescents. *J. Vasc. Access.* 21, 658–664. doi: 10.1177/1129729819897454

Cutshall, B. T., Duhart, B. T. Jr., Saikumar, J., Samarin, M., Hutchison, L., and Hudson, J. Q. (2018). Assessing guideline-directed medication therapy for heart failure in end-stage renal disease. *Am. J. Med. Sci.* 355, 247–251. doi: 10.1016/j.amjms.2017.11.008

Del Forno, B., Lapenna, E., Dalrymple-Hay, M., Taramasso, M., Castiglioni, A., Alfieri, O., et al. (2018). Recent advances in managing tricuspid regurgitation. *F1000Res* 7:355. doi: 10.12688/f1000research.13328.1

Dietz, M. F., Prihadi, E. A., van der Bijl, P., Goedemans, L., Mertens, B. J. A., Gursoy, E., et al. (2019). Prognostic implications of right ventricular remodeling and function in patients with significant secondary tricuspid regurgitation. *Circulation* 140, 836–845. doi: 10.1161/circulationaha.119.039630

Gumus, F., and Saricaoglu, M. C. (2020). Assessment of right heart functions in the patients with arteriovenous fistula for hemodialysis access: right ventricular free wall strain and tricuspid regurgitation jet velocity as the predictors of right heart failure. *Vascular* 28, 96–103. doi: 10.1177/1708538119866616

Hahn, R. T. (2019). Assessment and procedural guidance with echocardiography for transcatheter tricuspid regurgitation devices. *Prog. Cardiovasc. Dis.* 62, 452–458. doi: 10.1016/j.pcad.2019.09.003

Khan, R. A., Khan, N. A., Bauer, S. R., Li, M., Duggal, A., Wang, X., et al. (2019). Association between volume of fluid resuscitation and intubation in high-risk patients with sepsis, heart failure, end-stage renal disease, and cirrhosis. *Chest* 3692:7.

Kim, E. D., and Parekh, R. S. (2015). Calcium and sudden cardiac death in end-stage renal disease. *Semin. Dial.* 28, 624–635. doi: 10.1111/sdi.12419

Konigsbrugge, O., and Ay, C. (2019). Atrial fibrillation in patients with end-stage renal disease on hemodialysis: magnitude of the problem and new approach to oral anticoagulation. *Res. Pract. Thromb. Haemost.* 3, 578–588. doi: 10.1002/rth2.12250

Kooman, J. P., and van der Sande, F. M. (2019). Body fluids in end-stage renal disease: statics and dynamics. *Blood Purif.* 47, 223–229. doi: 10.1159/000494583

Kopic, S., Stephensen, S. S., Heiberg, E., Arheden, H., Bonhoeffer, P., Ersboll, M., et al. (2017). Isolated pulmonary regurgitation causes decreased right ventricular longitudinal function and compensatory increased septal pumping in a porcine model. *Acta Physiol.* 221, 163–173. doi: 10.1111/apha.12904

Lee, J. W., Song, J. M., Park, J. P., Lee, J. W., Kang, D. H., and Song, J. K. (2010). Long-term prognosis of isolated significant tricuspid regurgitation. *Circ. J.* 74, 375–380. doi: 10.1253/circj.cj-09-0679

Lemor, A., Hernandez, G. A., Lee, S., Patel, N., Blumer, V., Badiye, A., et al. (2018). Impact of end stage renal disease on in-hospital outcomes of patients with systolic and diastolic heart failure (insights from the Nationwide Inpatient Sample 2010 to 2014). *Int. J. Cardiol.* 266, 174–179. doi: 10.1016/j.ijcard.2018.02.117

Maeder, M. T., Holst, D. P., and Kaye, D. M. (2008). Tricuspid regurgitation contributes to renal dysfunction in patients with heart failure. *J. Card. Fail.* 14, 824–830. doi: 10.1016/j.cardfail.2008.07.236

Mahfouz, R. A., Elawady, W., Hossein, E., and Yosri, A. (2013). Impact of atrioventricular compliance on clinical outcome of patients undergoing successful percutaneous balloon mitral valvuloplasty. *Echocardiography* 30, 1187–1193. doi: 10.1111/echo.12256

Mangieri, A., Montalto, C., Pagnesi, M., Jabbour, R. J., Rodes-Cabau, J., Moat, N., et al. (2017). Mechanism and implications of the tricuspid regurgitation: from the pathophysiology to the current and future therapeutic options. *Circ. Cardiovasc. Interv.* 10:12.

Mansour, I. N., Lang, R. M., Aburuwaida, W. M., Bhave, N. M., and Ward, R. P. (2010). Evaluation of the clinical application of the ACCF/ASE appropriateness criteria for stress echocardiography. *J. Am. Soc. Echocardiogr.* 23, 1199–1204. doi: 10.1016/j.echo.2010.07.008

Minami, Y., Kajimoto, K., Sato, N., Hagiwara, N., Takano, T., and Attend study investigators. (2016). End-stage renal disease patients on chronic maintenance hemodialysis in a hospitalized acute heart failure cohort: prevalence, clinical characteristics, therapeutic options, and mortality. *Int. J. Cardiol.* 224, 267–270. doi: 10.1016/j.ijcard.2016.09.038

Prihadi, E. A., Delgado, V., Leon, M. B., Enriquez-Sarano, M., Topilsky, Y., and Bax, J. J. (2019). Morphologic types of tricuspid regurgitation: characteristics and prognostic implications. *JACC Cardiovasc. Imaging* 12, 491–499. doi: 10.1016/j.jcmg.2018.09.027

Ramesh, S., Zalucky, A., Hemmelgarn, B. R., Roberts, D. J., Ahmed, S. B., Wilton, S. B., et al. (2016). Incidence of sudden cardiac death in adults with end-stage renal disease: a systematic review and meta-analysis. *BMC Nephrol.* 17:78. doi: 10.1186/s12882-016-0293-8

Samanta, R., Chan, C., and Chauhan, V. S. (2019). Arrhythmias and sudden cardiac death in end stage renal disease: epidemiology, risk factors, and management. *Can. J. Cardiol.* 35, 1228–1240. doi: 10.1016/j.cjca.2019.05.005

Santoro, A., and Canova, C. (2005). Anemia and erythropoietin treatment in chronic kidney diseases. *Minerva Urol. Nefrol.* 57, 23–31.

Sugiura, E., Dohi, K., Tanimura, M., Kumagai, N., Ishikawa, E., and Ito, M. (2019). Successful peritoneal dialysis for the treatment of inotrope-dependent end-stage heart failure. *Int. Heart J.* 60, 1211–1218. doi: 10.1536/ihj.18-550

Sun, Y. P., and O'Gara, P. T. (2017). Epidemiology, anatomy, pathophysiology and clinical evaluation of functional tricuspid regurgitation. *Minerva Cardioangiol.* 65, 469–479.

Unlu, S., Sahinarslan, A., Gokalp, G., Seckin, O., Arinsoy, S. T., Boyaci, N. B., et al. (2018). The impact of volume overload on right heart function in end-stage renal disease patients on hemodialysis. *Echocardiography* 35, 314–321. doi: 10.1111/echo.13768

van der Meer, P., Lipsic, E., van Gilst, W. H., and van Veldhuisen, D. J. (2008). Anemia and erythropoietin in heart failure. *Heart Fail. Monit.* 6, 28–33.

Walsh, J. T., Glennon, P., and Schofield, P. M. (1998). Tricuspid regurgitation following central line insertion in a patient undergoing haemodialysis. *Postgrad. Med. J.* 74, 631–632. doi: 10.1136/pgmj.74.876.631

Yogasundaram, H., Chappell, M. C., Braam, B., and Oudit, G. Y. (2019). Cardiorenal syndrome and heart failure-challenges and opportunities. *Can. J. Cardiol.* 35, 1208–1219. doi: 10.1016/j.cjca.2019.04.002

Yokoro, M., Nakayama, Y., Yamagishi, S. I., Ando, R., Sugiyama, M., Ito, S., et al. (2017). Asymmetric dimethylarginine contributes to the impaired response to erythropoietin in CKD-Anemia. *J. Am. Soc. Nephrol.* 28, 2670–2680. doi: 10.1681/asn.2016111184

Conflict of Interest: The authors declare that the research was conducted in the absence of any commercial or financial relationships that could be construed as a potential conflict of interest.

frontiers in Medicine

SYSTEMATIC REVIEW
published: 16 April 2021
doi: 10.3389/fmed.2021.592602

Uremic Toxins in Organ Crosstalk

Jerome Lowenstein[1]* *and Sanjay K. Nigam*[2]

[1] Department of Nephrology, New York University School of Medicine, New York, NY, United States, [2] Departments of Pediatrics and Medicine (Nephrology), San Diego School of Medicine, University of California, San Diego, La Jolla, CA, United States

Many putative uremic toxins—like indoxyl sulfate, p-cresol sulfate, kynurenic acid, uric acid, and CMPF—are organic anions. Both inter-organ and inter-organismal communication are involved. For example, the gut microbiome is the main source of indole, which, after modification by liver drug metabolizing enzymes (DMEs), becomes indoxyl sulfate. Various organic anion transporters (organic anion transporters, OATs; organic anion-transporting polypeptides, OATPs; multidrug resistance-associated proteins, MRPs, and other ABC transporters like ABCG2)—often termed "drug transporters"—mediate movement of uremic toxins through cells and organs. In the kidney proximal tubule, critical roles for OAT1 and OAT3 in regulating levels of protein-bound uremic toxins have been established using knock-out mice. OATs are important in maintaining residual tubular function in chronic kidney disease (CKD); as CKD progresses, intestinal transporters like ABCG2, which extrude urate and other organic anions into the gut lumen, seem to help restore homeostasis. Uremic toxins like indoxyl sulfate also regulate signaling and metabolism, potentially affecting gene expression in extra-renal tissues as well as the kidney. Focusing on the history and evolving story of indoxyl sulfate, we discuss how uremic toxins appear to be part of an extensive "remote sensing and signaling" network—involving so-called drug transporters and drug metabolizing enzymes which modulate metabolism and signaling. This systems biology view of uremic toxins is leading to a new appreciation of uremia as partly due to disordered remote sensing and signaling mechanisms–resulting from, and causing, aberrant inter-organ (e.g., gut-liver- kidney-CNS) and inter-organismal (e.g., gut microbiome-host) communication.

Keywords: indoxyl sulfate, aryl hydrocarbon receptor, organ crosstalk, uremia, OAT knockout

OPEN ACCESS

Edited by:
Frederic Jaisser, Institut National de la Santé et de la Recherche Médicale (INSERM), France

Reviewed by:
Gautam Bhave, Vanderbilt University, United States
Leslie Stuart Gewin, Vanderbilt University, United States

***Correspondence:**
Jerome Lowenstein
jerome.lowenstein@nyulangone.org

Specialty section:
This article was submitted to Nephrology, a section of the journal Frontiers in Medicine

Received: *07 August 2020*
Accepted: *18 March 2021*
Published: *16 April 2021*

Citation:
Lowenstein J and Nigam SK (2021) Uremic Toxins in Organ Crosstalk. Front. Med. 8:592602. doi: 10.3389/fmed.2021.592602

INTRODUCTION

There is a new appreciation of the role of the kidney in organ cross-talk and inter- organismal communication (e.g., gut microbiome-host) mediated by small organic molecules. Many of these molecules are organic anions transported by renal (e.g., OAT1) and non-renal transporters (OATP1B1) and altered by Phase 1 and Phase 2 drug metabolizing enzymes (DMEs); many of these molecules also have well-described roles in metabolism, signaling, and modulation of redox state (1). Among these are so-called protein-bound uremic toxins (e.g., indoxyl sulfate, kynurenate, CMPF, phenyl sulfate, p-cresol sulfate, uric acid), which accumulate in chronic kidney disease (CKD) as tubular secretion declines. One of the most fascinating aspects of current research in the field is the multifaceted nature of these uremic toxins and their roles in "remote sensing and signaling" between organs and organisms. Here, we detail a few examples from a systems biology perspective with an emphasis on how they illustrate aspects of the Remote Sensing and Signaling Theory.

Before discussing the role of uremic toxins in organ crosstalk, it is worth outlining several key concepts of the Remote Sensing and Signaling Theory (RSST) relevant to CKD. The RSST is a general systems biology theory of how transporters and enzymes help optimize remote communication by small organic molecules between organs (e.g., gut-liver-kidney-brain) and organisms [e.g., gut microbes-host; (1)].

At least 500 transporters, enzymes, and regulatory proteins (e.g., nuclear receptors and other transcription factors) participate in this remote sensing and signaling (RSS) system. Many of the proteins in the RSS system have a broad substrate specificity and are well-known in the pharmaceutical field for their involvement in the absorption, distribution, metabolism and excretion (ADME) of drugs such as NSAIDs, statins, antibiotics and antivirals. Thus, certain SLC and ABC transporters and enzymes in the RSS system are often referred to as drug transporters and drug metabolizing enzymes (DMEs).

However, while well-known for their pharmaceutical roles, homologs of many of the genes encoding these proteins are found in mice, fish, flies, and other organisms. This strongly suggests an important role for these proteins in the physiology of very diverse organisms. Furthermore, it is now clear from *in vitro* and *in vivo* studies in model organisms as well as human genome wide association studies (GWAS) that the proteins of the RSS system interact with a wide range of metabolites, signaling molecules, antioxidants, nutrients, and gut microbe products. These small molecules participate in key physiological and biochemical pathways, including those involving bile acids, the citric acid cycle, fatty acid oxidation, cellular redox state, and a wide variety of signaling events.

It is through the movement, modification, and action of these small organic molecules between organs and body fluids—as well as between organisms—that remote sensing and signaling is believed to occur. Thus, the transporters, enzymes, and regulatory proteins of the RSS system—a network of over 500 proteins differentially expressed across tissue and cell type—help maintain homeostasis and also help restore homeostasis in the context of injury to the kidney and other organs. Among the small molecules regulated by the RSS system are many protein-bound uremic solutes and uremic toxins accumulating in CKD that are taken up by the proximal tubule. One of the best-studied of these uremic toxins is indoxyl sulfate.

THE MANY FACES OF INDOXYL SULFATE

Although indoxyl sulfate has only become broadly known to nephrologists in recent decades as a small, protein-bound, likely uremic toxin, in fact, indoxyl sulfate—and the related *indigo* and *indican*—have a long and rich history. Indoxyl sulfate is a small organic molecule—an organic anion—that is considered to be one of the most important protein-bound uremic toxins originating in the gut. Early in the twentieth century the indigo-related molecule, indoxyl sulfate, was recognized as a solute capable of binding to plasma albumin (2). It was observed that plasma concentrations of indoxyl sulfate were increased in patients with reduced renal function, as judged by elevated serum creatinine concentration, and in a 5/6 nephrectomy rat model, administration of indoxyl sulfate in the diet or by gavage resulted in tubular and glomerular damage and hastened the development of uremia (3). Studies such as these led to the designation of indoxyl sulfate as a *uremic toxin* rather than a protein-bound uremic solute.

It is interesting to briefly contemplate the parallels, real, and analogical, between the binding of indoxyl sulfate to plasma proteins and the use of indigo—one of the most valued dyes from antiquity, a tight-binding dye applied to fabrics. This tight binding of indican or indoxyl sulfate to plasma proteins was of considerable interest to pharmacologists and physiologists (2). Pharmacologists have long recognized that many drugs (and colored dyes used as biological probes) are protein bound, and that binding is an important determinant of active (unbound) drug concentrations and drug removal. It was recognized that there was competition among solutes for binding to albumin, and some solutes bound more tightly than others. Indoxyl sulfate was shown to be 95% protein-bound in normal plasma and to compete, *in vitro*, for binding with other colored dyes for binding in uremic plasma (2).

Protein-binding is physiologically important because binding limits removal of solutes by glomerular filtration. Protein-bound solutes such as indoxyl sulfate, an organic anion, are transported from peritubular capillaries into the renal tubule largely by two major organic anion transporters (OATs) on the basolateral surface of proximal renal tubular cells (4). In progressive renal disease, indoxyl sulfate concentration in plasma increases as nephron (tubular) mass declines. Lacking transporters, removal by dialysis is limited by the low concentration of free (diffusible) solute. Although it was recognized that protein-binding would impede removal by glomerular filtration or removal across a dialysis membrane, the possible role of indoxyl sulfate as a uremic toxin initially received little attention. In early experiences with the membrane dialyzer, it was recognized that small molecules were removed much more readily than indoxyl sulfate. However, the long-term consequences of the limited removal of indoxyl sulfate and other protein-bound uremic solutes and uremic toxins were not evident in the early days in which hemodialysis was limited to one or two treatments (5).

Interest in the importance of "protein-bound uremic solutes" was stimulated when it became clear that patients with end-stage renal disease (ESRD) exhibited a high propensity to cardiac death during the first 3 years of hemodialysis (6). Most of the deaths were attributed to heart failure, cardiac arrhythmias, or "sudden death." Variation in hemodialysis techniques and dialysis membranes aimed at more efficient removal of urea and creatinine–taken as surrogates for other dialyzable uremic toxins—did not have a significant effect on this excess mortality (7). Although this was generally attributed to coincident risk factors (hypertension, diabetes, hyperlipidemia, and cigarette smoking) in the ESRD population,

a high incidence of cardiovascular disease was reported in dialysis patients with few conventional risk factors for cardiovascular disease (8).

During the period dating from 1960 through the early 2000's when chronic renal failure was treated by thrice-weekly hemodialysis, only modest attention was given to the nature of the toxins removed by hemodialysis (9). After almost 50 years, during which the population of patients receiving hemodialysis in the US swelled, nephrologists finally turned their attention to the protein-bound solutes retained in patients receiving standard hemodialysis. In 2003, the EUTox group, based on a thorough analysis of the literature, identified and categorized more than 100 solutes that were reported to be increased in concentration in the serum of patients with impaired renal function. Direct measurements largely confirmed this identification of uremic solutes (10). In the context of a growing interest in trying to improve dialysis outcomes, as well as attempting to understand the pathobiology of uremia in molecular terms, attention began to focus on small solutes rendered poorly-dialyzable by virtue of protein binding. The possibility that some of the group of poorly-dialyzed protein-bound solutes that accumulated in the blood of patients with advanced renal disease were responsible for the excess morbidity and mortality was implied but not established. Accordingly, the group of solutes identified by the EUTox group were termed either *uremic toxins* or *uremic retention solutes.*

Indoxyl sulfate is currently among the most widely discussed of uremic toxins and among the best studied in mechanistic terms. Indoxyl sulfate is but one of many on the list. Others include p-cresol sulfate, kynurenine, TMAO (trimethylamine oxide), polyamines, and CMPF (3-carboxy-4-methyl-5-propyl-2-furanpropanoic acid). Although some are organic cations (e.g., TMAO), a large number are, like indoxyl sulfate, small organic anions. In recent years, several lines of evidence have led to the view that indoxyl sulfate and some other uremic solutes function as *signaling molecules* as well as potential toxins. An effect of uremic plasma on gene expression was demonstrated in normal human renal tubular cells (11). In human renal tubular cells incubated for 24 h with control and pre- and post-dialysis uremic plasma, the expression of more than 2,000 genes was increased or decreased. These changes, in roughly 500 genes, were reversed when cells were incubated in post-dialysis plasma (**Figure 1A**) consistent with the fact that many retention solutes, such as urea and creatinine, are freely dialyzable.

However, more than 1,500 genes remained dysregulated when cells were incubated with post-dialysis plasma (**Figure 1B**), consistent with the conclusion that the stimulus for gene expression was probably protein-bound and therefore not readily dialyzable. Further, it was observed that spiking control plasma with indoxyl sulfate to a concentration typical of that observed in patients with ESRD, simulated roughly 80% of the dysregulation observed with uremic plasma (**Figures 1C–E**). The effects of indoxyl sulfate on gene expression with uremic plasma or control plasma spiked with indoxyl sulfate were blocked by probenecid, an inhibitor of organic anion transport. These findings suggested strongly that indoxyl sulfate activates a transcriptional program dependent upon one or more organic anion transporters.

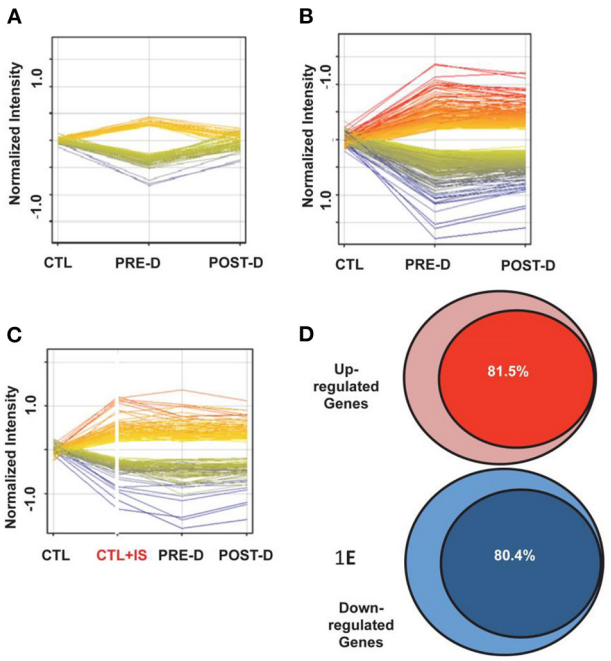

FIGURE 1 | Gene expression in reporter renal tubular cells. **(A)** Gene expression changes that returned to baseline post-dialysis. Each individual line represents the average value in the 10 uremic subjects for each gene that was dysregulated. The expression of 282 genes was upregulated (displayed as yellow to red lines) and the expression of 255 genes was downregulated (displayed as green to blue lines) in the pre-dialysis samples as compared to normal controls. Post-dialysis these values returned to baseline. **(B)** Gene expression that remained dysregulated after dialysis treatment. The expression of 843 genes was upregulated and the expression of 532 genes were downregulated. **(C)** Genes expressed following incubation in normal plasma spiked with indoxyl sulfate compared with their expression levels in cells treated with pre-dialysis and post-dialysis plasma. The expression of 908 genes was upregulated and the expression of 571 genes were downregulated. **(D)** 81.5% of upregulated genes that were not normalized by dialysis were mimicked by addition of indoxyl sulfate to normal plasma. **(E)** 80.4% of downregulated genes that were not normalized by dialysis were mimicked by addition of indoxyl sulfate to normal plasma.

UREMIC TOXINS AND THE RENAL ORGANIC ANION TRANSPORTERS, OAT1 AND OAT3

In addition to recent interest in signaling mechanisms involving indoxyl sulfate, there is renewed interest in the transport of uremic toxins like indoxyl sulfate by organic anion transporters (OATs) and other transporters in the proximal tubule in chronic kidney disease (CKD). Renal transport not only regulates the elimination of uremic toxins but also plays an important role in setting the systemic and proximal tubule cell levels of these small organic molecules. In a sense, this renewed attention on proximal tubule handling of solutes has led to the "rediscovery" of renal

tubule microperfusion studies performed in the 1970's (12, 13). Grantham observed that isolated rabbit renal proximal tubules could *secrete* fluid. It was argued that secretion of fluid must have been preceded by the transport of some solute into the tubular lumen that created an osmotic driving force. Grantham observed that addition of p-aminohippurate, which is now known to be taken up by OATs in the proximal tubule, to the bathing medium stimulated fluid transport. Further, it was observed that plasma from ESRD patients, added to the bathing medium, caused fluid *secretion* in perfused rabbit renal tubules, which in retrospect, suggests that some molecule(s) in uremic serum acted as a "signal" to induce tubular secretion of fluid. Much of the "signal" was most likely the osmotic effect of solute transported into the tubular lumen. But with a growing appreciation of the importance of these small organic molecules in signaling, it is possible that specific signaling mechanisms within the tubular cells also help explain the phenomenon. Nevertheless, these older studies suggested that, despite poor glomerular filtration, or possibly because of it, the OATs in the proximal tubule contribute to the elimination of indoxyl sulfate and other uremic solutes. As Grantham wrote, "under conditions of markedly reduced or complete cessation of glomerular filtration, mammalian proximal tubules could secrete fluid and hippurate and similar substances… elimination of some of the potentially toxic products normally excreted by the kidneys… would serve a useful survival function" (13). In this regard, it is interesting to note reports that proximal renal tubular secretion of indoxyl sulfate is increased in animals manifesting reduced overall renal function. Recent studies reported that increasing the production and serum concentration of indoxyl sulfate by protein-feeding resulted in the upregulation of OAT gene expression in isolated renal tubular cells and epithelial cells isolated from human urine (14). This might account for the observation that renal tubular secretion of indoxyl sulfate is increased in patients manifesting "residual renal function" (15, 16). Importantly, these patients have been observed to have a better quality of life, and longer survival independent of the intensity of hemodialysis or peritoneal dialysis (17).

These findings have focused on the role of OATs in the renal tubule handling of indoxyl sulfate. OATs appear to be the main *in vivo* transporters of indoxyl sulfate and other protein-bound uremic toxins (18, 19). This has been shown by metabolomics studies in OAT knockout mice (4, 20). It is important to note, however, that OAT1 and OAT3 knockout mice, while lacking the main route for elimination of indoxyl sulfate and many other "toxins," have normal life expectancy, despite many fold increase in some uremic toxins. In light of this, it is worth noting that they also have high levels of potentially beneficial metabolites, including those with antioxidant activity, which may be protective.

Furthermore, these uremic toxins have likely been elevated since birth and are known to affect tissue remodeling, which could conceivably be adaptive. Although indoxyl sulfate is one of the most altered uremic toxins in the OAT knockout mice, many other uremic toxins—mostly gut microbe-derived—are also elevated in the plasma of these knockout mice (4, 20). These other uremic solutes/uremic toxins include many indole derivatives, kynurenine, CMPF, p-cresol sulfate, phenyl sulfate, p-cresol sulfate, TMAO, urate, and other molecules that accumulate in uremic serum (21, 22). That OAT1 (originally called NKT for Novel Kidney Transporter) and/or OAT3 directly interact with many of these molecules has (with the possible exception of TMAO), been confirmed using *in vitro* cell- based transport assays. Thus, this *in vitro* data supports the *in vivo* genetic evidence (4) that OATs are part of a gut microbe-gut-liver-kidney axis (23).

Indoxyl sulfate is known to be derived from the breakdown of tryptophan to indole by gut bacteria that express tryptophanase (24, 25). The product, indole, passes into the hepatic portal system, where it undergoes hydroxylation (by cytochrome p450) and sulfation (by a sulfotransferase) before it enters the hepatic vein and the general circulation as indoxyl sulfate. In the kidney, indoxyl sulfate is transported across the basolateral membrane of proximal tubule by OAT 1 and 3; on the apical membrane it is likely eliminated via MRPs (ABCC family) and other transporters (26). Thus, multiple "drug" metabolizing enzymes work together with multiple transporters to produce indoxyl sulfate and allow it to enter the proximal tubule cell whereupon it is eliminated. Again, we emphasize the roles of these transporters and DMEs in mediating inter-organismal (e.g., gut microbes-human) and inter-organ (e.g., gut-liver-kidney) "remote" communication affecting the plasma and tissue levels of indoxyl sulfate (**Figure 2**).

INDOXYL SULFATE SIGNALING AND THE REMOTE SENSING AND SIGNALING THEORY

Homer Smith, a student of the evolution of the kidney (27), asked why so much fluid is filtered to yield a relatively small quantity of urine. The question seems to point to some kind of paradox with the appearance of a futile process. Smith answered by pointing out that glomerular filtration evolved when life moved into fresh water and the capacity to excrete fluid became a priority. A question of a similar sort might be asked.

"Are indoxyl sulfate and other uremic toxins made by a series of biochemical reactions only to be excreted?" The answer to this question, while far from fully resolved, is turning out to be quite interesting. Indoxyl sulfate and several other gut-derived protein- bound solutes are highly bound (>90%) in plasma. Renal excretion is facilitated by OATs on the basolateral (blood side) of proximal tubular cells that shift the equilibrium toward free solute that is readily transported into the tubular lumen. In this way, renal tubular secretion serves to remove suspect uremic toxins. A recent study (14) demonstrated, in intact mice and isolated human urinary epithelial cells, that increasing the plasma concentration of indoxyl sulfate by feeding protein resulted in a substantial increase in OAT1 synthesis and indoxyl sulfate excretion. When renal mass is reduced by renal disease, indoxyl sulfate concentration in plasma increases and enhanced transport of indoxyl sulfate into the proximal tubule by OAT1 and possibly OAT3 provides an important means for removing this potentially toxic solute. But this description of the role of OATs in the elimination of indoxyl sulfate and other anions might not have

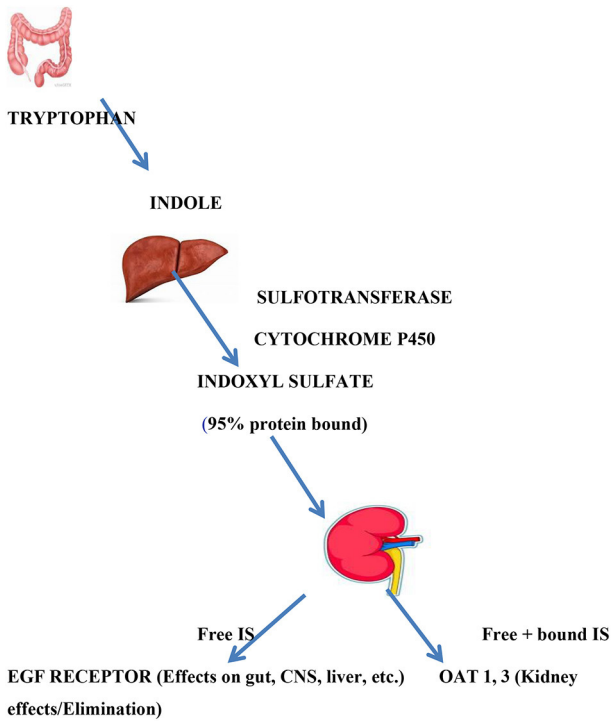

FIGURE 2 | Indoxyl sulfate production and actions. Indoxyl sulfate is the product of gut bacterial tryptophanase and hepatic hydroxylation and sulfation. It is 95% albumin bound. Renal excretion, which serves to remove bound and free IS, is mediated by OAT 1 and OAT 3 in proximal renal tubule where signaling events and elimination occur. Free (unbound) IS can act as a signaling molecule on distant tissues bearing EGF receptors.

satisfied Homer Smith. He might have asked whether it was reasonable to believe that indoxyl sulfate was synthesized only to be secreted by the kidney.

This hypothetical question provides glimpses into a whole new line of systems level thinking that challenges current thinking about uremic toxins. The capacity of indoxyl sulfate to affect a wide range of targets follows in large part from evidence that it can be transported across the plasma membrane and interact with aryl hydrocarbon receptors (AHR) in the cytoplasm (28). The complex is stabilized by binding heat-shock proteins of the HSP90 family and passes through a pore into the nucleus where it releases the heat-shock proteins and combines with the Aryl Receptor Nuclear Translocator (ARNT). This binds to the Xenobiotic Response Element (XRE) and activates transcription of a wide range of gene products. Though generally termed a "*xenobiotic* response element (XRE)"—implying that it functions to inactivate *foreign* molecules–it has become increasingly apparent that binding of the AHR-ARNT to the "xenobiotic response element" also mediates responses to *endogenous* stimuli presented through binding to the aryl hydrocarbon receptor. Indeed, it seems likely that the XRE, which was originally perhaps best known for mediating the response to *exogenous* 2,3,7,8-tetrachlorodibenzo-*p*-dioxin (TCDD) exposure, has responded to small *endogenous* solutes long before "modern society" produced TCDD as a side product in organic synthesis and burning of organic materials. The ARNT complex leads to the expression of "drug" metabolizing enzymes (DMEs), SLC transporters, and ABC transporters. Other nuclear receptors, such as PXR (pregnane X receptor) and HNF4a (hepatocyte nuclear factor 4 alpha) (29) also regulate the expression of drug transporters and drug metabolizing enzymes in the kidney proximal tubule, liver, intestine, and many other organs.

A number of studies have now identified AHR as an important target of indoxyl sulfate. Indoxyl sulfate, bound to AHR, can activate a great number of genes, including cytochrome P450 enzymes, as well as genes involved macrophage-dependent inflammation (30). Today, the aryl hydrocarbon receptor (AHR) is probably better characterized as a ligand-activated transcription factor that functions in the integration of environmental, dietary, microbial and metabolic cues by regulating transcriptional programs. The nature of this regulation appears to be ligand-dependent, cell-type-specific, and context-specific. Along these lines, it is worth considering the cells of the proximal tubule in this way—as well as specific metabolites and signaling molecules transported into the proximal tubule cells that might affect the activation of AHR and/or other nuclear receptors.

Recent data indicates that free (unbound) indoxyl sulfate (and other aryl hydrocarbons) can bind to the EGF receptor of cells lacking OATs and induce a signaling cascade that results in ARNT translocation and initiation of gene transcription (31). This proximal tubule signaling role of indoxyl sulfate is consistent with the Remote Sensing and Signaling Theory as applied to the context of CKD. The Remote Sensing and Signaling Theory describes how a large network of genes—differentially expressed in the gut, liver, kidney as well as other organs and traditionally viewed as central to the absorption, distribution, metabolism, and elimination (ADME) of drugs—regulates inter-organ and inter-organismal communication mediated by small organic molecules of "high informational content." Among these small organic molecules with high informational content are included rate-limiting metabolites (e.g., carnitine, TCA intermediates), signaling molecules (e.g., short chain fatty acids, prostaglandins), and antioxidants (e.g., uric acid, ergothionine). To this list of molecules with high informational content one can now add certain uremic solutes and uremic toxins.

So, the answer to the hypothetical question Homer Smith might have posed is that, while the renal clearance by OATs and other transporters serves to prevent excessive buildup of uremic toxins, unbound uremic solutes may be important signaling molecules, metabolites, and antioxidants acting upon remote organs (e.g., brain) or remote organisms (e.g., gut microbes, nursing infant; **Figure 2**).

ALTERED REMOTE SENSING AND SIGNALING IN CKD

It is generally held that chronic kidney disease (CKD) and uremia are complex syndromes involving altered inter-organ and inter-organismal remote communication affecting metabolism,

signaling, and redox potential—among many other biochemical and cellular processes. In the past decade, indoxyl sulfate has been the uremic toxin at or near the center of research in this field, and the mechanism of its action as a signaling molecule in the proximal tubule is even more complex than we have described— involving not only OAT1 and AHR, but also EGF receptor, oxidative state, and a microRNA (31). Furthermore, it is increasingly believed that, like indoxyl sulfate, many other uremic toxins act as both signaling molecules and are also the cause of many of the deleterious manifestations of uremia (**Figure 3**).

Indoxyl sulfate is a good example of the importance of small molecule inter-organ and inter-organismal (e.g., gut microbes-host) communication in the body in that, as described above, *in vivo* it follows the gut microbe-gut-liver-kidney axis and requires the participation of "hepatic drug metabolizing enzymes" (Phase 1 for hydroxylation and Phase 2 for sulfation) and drug "transporters" like the renal OATs (30). In other words, indoxyl sulfate is one of perhaps thousands of signaling molecules and metabolites regulated by the Remote Sensing and Signaling System described above. The network (and subnetworks) of ADME genes regulating this system's effort at optimizing small molecule levels in various tissues and body fluid compartments consists of multi- specific "drug" transporters, "drug" metabolizing enzymes, transcription factors,—and other transporters (oligospecific, monospecific), enzymes, and regulatory proteins. A preliminary Remote Sensing and Signaling Network has recently been built for the gut-liver-kidney axis (32). Many of the molecules that are optimized—such as metabolites and signaling molecules—are themselves ligands for receptors central to endogenous physiology (e.g., G-protein coupled receptors, nuclear receptors). This transporter- and DME-based Remote Sensing and Signaling System is also intimately connected to more classical homeostatic systems (e.g., neuroendocrine, autonomic), and like them, appears critical for helping the organism restore homeostasis after perturbation, whether acute or chronic (e.g., increased indoxyl sulfate concentration in chronic kidney disease).

Although the Remote Sensing and Signaling Theory was originally formulated over a decade ago to synthesize a growing amount of data related to the biological role of "drug" transporters that did not conform to the view that their primary role was in drug absorption, distribution, metabolism, and excretion (ADME), the applicability of the RSST to CKD and uremia has become increasingly apparent (33–36). A small sampling important of results are: (1) the fact that gene expression data has revealed changes in "drug" transporters and "drug" metabolizing enzymes in non-renal organs (e.g., intestine, liver) that appear to compensate for the inability of the injured kidney to transport small molecules like urate and indoxyl sulfate, (2) the realization that many protein-bound uremic toxins such as indoxyl sulfate are among the best substrates of "drug" transporters like the OATs, (3) an appreciation of the importance of inter- organismal communication between the gut-microbes and the host, the former being the ultimate source of many of the best-known uremic toxins.

With the intense recent attention given to the mechanisms by which uremic toxins and solutes affect cell and organ function, there is a rapidly growing appreciation of CKD and uremia as a multi-organ disorder involving altered metabolism and signaling mediated by small organic molecules—implying the involvement of specific metabolic and signaling pathways definable at the cellular and molecular levels–as well as a renewed appreciation of the importance of residual renal function which in large part represents the activity of proximal tubule transporters of protein-bound molecules (e.g., OAT1).

Given the emphasis in the Remote Sensing and Signaling Theory on the role of multi-specific transporters and enzymes, as well as their regulators (e.g., nuclear receptors) in remote inter-organ and inter-organismal small molecule communication (including gut microbe-host), the theory serves as a basis for understanding disordered small molecule communication in disease settings like CKD and uremia (35). In this context, it is worth mentioning that, in the setting of progressive renal disease, the predominantly intestinal multi-specific ABC transporter ABCG2 (BCRP) appears to play an important role in helping to restore human uric acid homeostasis by extruding it, and possibly other uremic toxins, into the intestinal lumen (36). This has been interpreted as an example of remote sensing and signaling in humans. Potential mechanisms include effects of uric acid or uremic toxins like indoxyl sulfate on ABCG2 expression or function in intestinal epithelial cells (37, 38).

The growing understanding of the mechanistic basis of indoxyl sulfate action serves as a good example of the need to think beyond toxins and examine effects upon specific signaling and metabolic pathways. While nephrologists have been conditioned to think in terms of uremic "toxins," this traditional view is challenged by a number of observations. First, most uremic toxins and uremic solutes are present in the body in the absence of kidney dysfunction. In addition to the OATs, there are transporters of these small molecules in many non-renal tissues. Crucially, some of these solutes, such as kynurenine and polyamines, are known to participate in major biological pathways independent of kidney disease. One possibility, consistent with a growing amount of biochemical and molecular data, is that so-called uremic toxins, while harmful when in excess in the setting of kidney failure, might have other important "non-toxic" roles in normal biology, including metabolism, signaling, regulating redox state, and gut microbiome population dynamics. For example, there is evidence that indoxyl sulfate, at physiologic plasma concentrations, acts as a superoxide radical scavenger (39). Indoxyl sulfate can also cross the blood–brain barrier, where it may limit CNS inflammation in astrocytes and microglia (40). In mice, the oral administration of indole prevented the expression of key proteins in the NF-KB pathway and downstream inflammatory proinflammatory gene expression that followed the infusion of lipopolysaccharide (33). Importantly, several studies have described alterations in the composition of the microbiome in patients with advanced renal disease or ESRD. It now seems likely this "gut dysbiosis" reflects dietary alterations and an effect of uremic solutes on the composition of the gut microbiome (41).

If we consider uremia as a disturbance of remote sensing and signaling, we might say that CKD alters the normal functioning of a highly-regulated transporter and "drug"

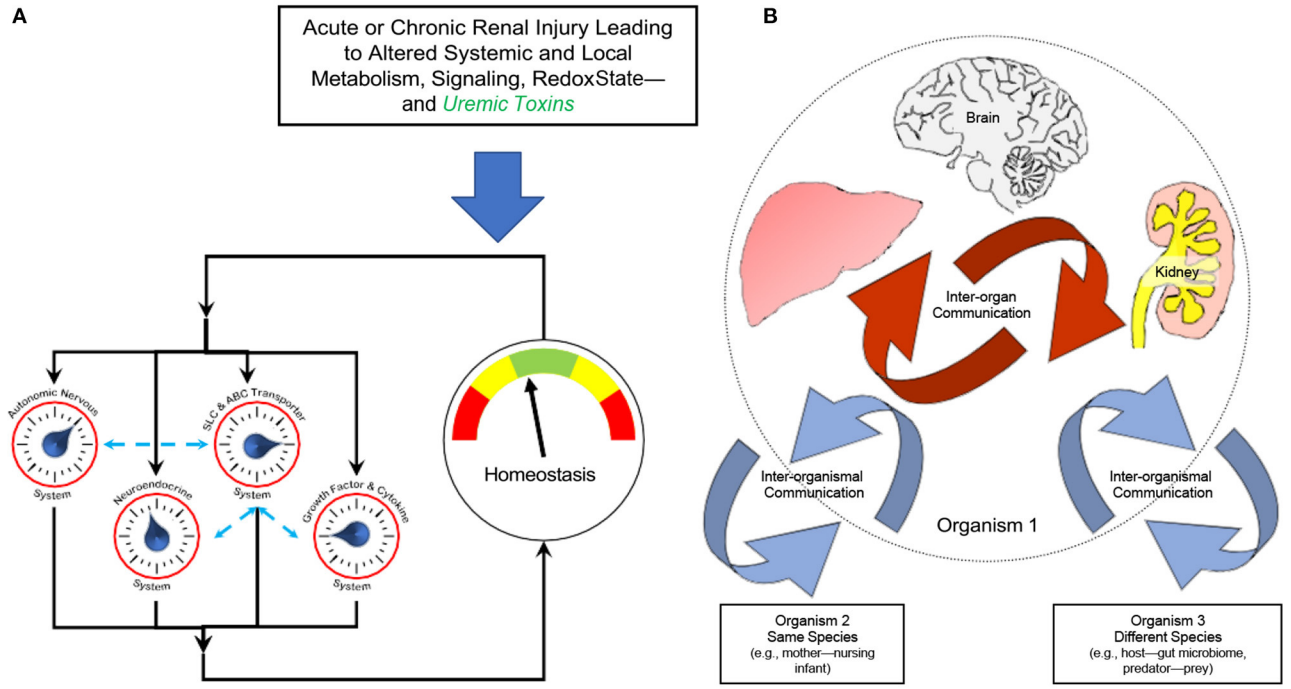

FIGURE 3 | Altered remote sensing and signaling in the context of kidney disease and uremic toxins. The Remote Sensing and Signaling Theory describes how proteins often considered to be primarily involved in the absorption, distribution, metabolism, and excretion (ADME) of small molecule drugs—including multispecific "drug" transporters like renal OAT1 and Phase 2 "drug" metabolizing enzymes like liver sulfotransferases—actually form a network mediating endogenous small molecule remote communication between organs and organisms. These small molecules have "high informational content" in that, like indoxyl sulfate, they are central to metabolism, signaling, and regulation of oxidative state. The expression of genes in the multiorgan (e.g., gut-liver-kidney) remote sensing and signaling network is regulated by, among other factors, nuclear receptors such as AHR, HNF4a, and FXR. A number of multi-specific transporters and enzymes work together with those of more limited (oligo- and mono-) specificity to potentially handle tens of thousands of endogenous and exogenous molecules in health and disease (e.g., CKD). **(A)** In acute or chronic organ injury, this complex adaptive system has the ability to reset until endogenous small molecule homeostasis is partially or completely restored. The Remote Sensing and Signaling System works in concert with other homeostatic systems (e.g., neuroendocrine system). **(B)** Inter-organismal communication can be between organisms of the same species (e.g., mother-nursing infant) or different species (e.g., gut microbes-host). Based on (1, 32, 34, 44).

metabolizing enzyme network involved in sensing and signaling to maintain homeostasis of small organic molecules that have "high informational content" with respect to remote inter-organ and inter-organismal communication. The body's attempt to restore homeostasis in the face of the perturbations caused by uremic syndrome and ongoing progression of kidney disease then depends upon the homeostasis-promoting properties of several interacting systems: the remote sensing and signaling system, the neuroendocrine system, the growth factor-cytokine system, and the autonomic nervous systems.

WHAT ORCHESTRATES THE SYSTEM?

If indoxyl sulfate is a key small molecule in a larger "remote sensing and signaling system" involved in inter-organ crosstalk within the body and inter-organismal communication mediated by transporters and "drug" metabolizing enzymes, it seems tempting to ask, what is the central conductor? For uremic toxins and uremic solutes derived from gut microbes, a plausible candidate for this role might be the gut microbiome–with its vast number of enzymes and signaling pathways. The small molecules produced by gut microbes, while perhaps of greatest current interest from the viewpoint of inter-organismal communication and kidney disease, do not, however, include the multitudes of endogenous metabolites and signaling molecules generated largely independent of the gut microbes and handled by "drug" transporters, "drug" metabolizing enzymes, and related proteins (42).

The Remote Sensing and Signaling Theory is a general theory that attempts to explain how multi-specific, oligo-specific, and monospecific transporters and enzymes work together, along with regulatory proteins (e.g., nuclear receptors, kinases) to achieve optimal levels of hundreds if not thousands of small molecules in different body tissues (e.g., CNS, kidney, liver, placenta) and body fluids [e.g., blood, CSF, urine, bile, amniotic fluid; (43–45)]. In such a multi-scale complex adaptive system, it is hard to posit a single orchestrator, for this is likely an emergent property of many interacting transporters, enzymes, nuclear receptors, metabolites, and signaling molecules—in many interacting organs and organisms.

While the systems pathophysiology of CKD is a new field, we conclude by again reminding the reader that the history of molecules related to indoxyl sulfate is very old. In the thirteenth

century, Marco Polo described many caravans traveling from the Middle East and India that contained cloths dyed with the precious indigo. An important feature of indigo or indican was tight binding of the dye to cloth, and even in recent times, indigo serves as the dye that gives jeans their distinctive color. Once more we note that many such organic dyes played an important role in furthering our early understanding of pathology and physiology, including that involving protein-bound uremic solutes.

Here we have provided a glimpse of the physiological and pathophysiological history of a close relative of a highly valued dye employed to dye fabrics 6,000 years ago—from a solute found to accumulate in the serum of patients with renal disease, to a protein-bound uremic toxin, to a ligand of the renal "drug" transporters OAT1 and OAT3, to one of many signaling molecules participating in a "remote sensing and signaling system" that can now be conceptualized as a network of hundreds of proteins.

Viewing indoxyl sulfate and other uremic toxins through the multiscale systems biology perspective of the Remote Sensing and Signaling Theory suggests, as discussed elsewhere (33), a wide range of therapeutic possibilities to moderate the toxic effects of small protein-bound, gut-derived uremic toxins and uremic solutes. There is much more to come.

DATA AVAILABILITY STATEMENT

The original contributions presented in the study are included in the article/supplementary material, further inquiries can be directed to the corresponding author/s.

AUTHOR CONTRIBUTIONS

JL and SN contributed equally in the authorship of this submission. Both authors contributed to the article and approved the submitted version.

FUNDING

This work was partly supported by a grant from the National Institutes of Health (NIH) to SN by the National Institute of Diabetes, Digestive and Kidney Disease (NIDDK) R01DK109392.

REFERENCES

1. Ahn SY, Nigam SK. Toward a systems level understanding of organic anion and other drug transporters: a remote sensing and signaling hypothesis. *Mol. Pharmacol.* (2009) 76:481–90. doi: 10.1124/mol.109.056564
2. Bowmer CJ, Lindup WE. Decreased drug binding in uraemia: effect of indoxyl sulphate and other endogenous substances on the binding of drugs and dyes to human albumin. *Biochem Pharmacol.* (1982) 31:319–23. doi: 10.1016/0006-2952(82)90177-0
3. Niwa T. Role of organic anion transporters in the tubular transport of indoxyl sulfate and the induction of its nephrotoxicity. *J Am Soc Nephrol.* (2002) 13:1711–20. doi: 10.1097/01.ASN.0000022017.96399.B2
4. Wu W, Bush KT, Nigam SJ. Key role for the anion transporters. OAT1 and OAT 3 in the *in vivo* handling of uremic toxins and solutes. *Sci Rep.* (2017) 7:4939. doi: 10.1038/s41598-017-04949-2
5. Kolff W. The artificial kidney: a dialyser with a great area. *Acta Med Scand.* (1944) 117:121–34. doi: 10.1111/j.0954-6820.1944.tb03951.x
6. USRDS. *Annual Data Report* (2017).
7. Eknoyan G, Beck JG, Cheung AK, Daugirdas JT, Greene T, Kusek JW, et al. Effect of dialysis dose and membrane flux in maintenance hemodialysis. *NEJM.* (2002) 347:2010–9. doi: 10.1056/NEJMoa021583
8. Lindner, A, Charra, B, Sherrard, DJ, Scribner BH. Accelerated atherosclerosis in prolonged maintenance hemodialysis. *NEJM.* (1974) 290:697–701. doi: 10.1056/NEJM197403282901301
9. Meyer TW, Hostetter TH. Uremia. *NEJM.* (2007) 357:316–25. doi: 10.1056/NEJMra071313
10. Vanholder R, Desmet R, Glorieux G, Argiles A, Baurmeister U, Brunet P, et al. Review on uremic toxins: classification, concentration, and interindividual variability. *Kidney Int.* (2003) 63:1934–43. doi: 10.1046/j.1523-1755.2003.00924.x
11. Jhawar S, Singh P, Torres D, Ramirez-Valle F, Kassem H, Banerjee T, et al. Functional genomic analysis identifies indoxyl sulfate as a major, poorly dialyzable uremic toxin in end stage renal disease *PLoS ONE.* (2015) 1:e0118703 doi: 10.1371/journal.pone.0118703
12. Grantham, JJ, Tucker DR, Whittier FC. Fluid secretion in isolated proximal straight t renal tubules: effect of human uremic serum. *J Clin Invest.* (1973) 52:2441–50. doi: 10.1172/JCI107435
13. Grantham JJ, Wallace DP. Return of the secretory kidney. *Am J Physiol.* (2002) 282 F1–9. doi: 10.1152/ajprenal.2002.282.1.F1
14. Jansen J, Jansen K, Neven E, Poesen R, Othman A, van Mil A, Sluijter J, et al. Remote sensing and signaling in kidney proximal tubules stimulates gut microbiome-derived organic anion secretion. *Proc Natl Acad Sci USA.* (2019) 116:16105–10. doi: 10.1073/pnas.1821809116
15. Martinez AW, Recht NS, Hostetter TH, Meyer TW. Removal of P-cresol sulfate by hemodialysis. *JASN.* (2005) 16:3430–6. doi: 10.1681/ASN.2005030310
16. Lowenstein J, Grantham JJ. Residual renal function: a paradigm shift. *Kidney Int.* (2017) 91:561–5. doi: 10.1016/j.kint.2016.09.052
17. Temorshuizen F, Korevaar JC, Dekker FW, van Manen JG, Boeschoten EW, Krediet RT, et al. The relative importance of residual renal function compared with peritoneal clearance for patient survival and quality of life: an analysis of the Netherlands Cooperative Study on the Adequacy of Dialysis (NECOSAD)-2. *JASN.* (2004) 15:1061–70. doi: 10.1016/s0272-6386(03)00362-7
18. Lopez-Nieto CE, You G, Bush KT, Barros EJ, Beier DR, Nigam SK. Molecular cloning and characterization of NKT, a gene product related to the organic cation transporter family that is almost exclusively expressed in the kidney. *J Biol Chem.* (1997) 272:6471–8. doi: 10.1074/jbc.272.10.6471
19. Eraly SA, Vallon V, Rieg T, Gangoiti JA, Wikoff WR, Siuzdak G, et al. Multiple anion transporters contribute to net renal excretion of uric acid. *Physiol Genomics.* (2008) 33:180–92. doi: 10.1152/physiolgenomics.00207.2007
20. Eraly SA, Vallon V, Vaughn DA, Gangoiti JA, Richter K, Nagle M, et al. Decreased renal organic anion secretion and plasma accumulation of endogenous organic anions in OAT1 knock-out mice. *J Biol Chem.* (2006) 281:5072–83. doi: 10.1074/jbc.M508050200
21. Nigam SK, Wu W, Bush KT, Hoenig MP, Blantz RC, Bhatnagar V. Handling of drugs, metabolites, and uremic toxins by kidney proximal tubule transporters. *CJASN.* (2015) 10:239–49. doi: 10.2215/CJN.02440314
22. Wikoff WR, Nagle MA, Kouznetsova SM, Nigam SK. Untargeted metabolomics identifies enterobiome metabolites and putative uremic toxins as substrates of organic anion transporter 1 (Oat1). *J Prot Res.* (2011) 10:2842–51. doi: 10.1021/pr200093w
23. Bush, KT, Wu W, Lun C, Nigam SK. The drug transporter OAT3 and endogenous metabolite communication via the gut-liver-kidney axis. *J Biol Chem.* (2017) 292:15789–803. doi: 10.1074/jbc.M117.796516
24. Poesen R, Mutsaers HA, Windey K, van den Broek PH, Verweij V, Augustijns P, et al. The influence of dietary protein intake on mammalian tryptophan and phenolic metabolites. *PLoS ONE.* (2015) 10:e0140820. doi: 10.1371/journal.pone.0140820

25. Nazzal L, Roberts J, Singh P, Jhawar S, Matalon A, Gao Z, et al. Microbiome perturbation by oral vancomycin reduces plasma concentration of two gut-derived uremic solutes, indoxyl sulfate and p-cresyl sulfate, in end-stage renal disease. *Nephrol Dial Transplant.* (2017) 32:1809–17. doi: 10.1093/ndt/gfx029
26. Rosenthal SB, Bush KT, Nigam SK. A network of SLC and ABC transporter and DME genes involved in remote sensing and signaling in the gut-liver-kidney axis. *Sci Rep.* (2019) 9:11879. doi: 10.1038/s41598-019-47798-x
27. Smith H. *From Fish to Philosopher: The Story of Our Internal Environment.* Boston, MA: Little Brown & Co. (1953).
28. Schroeder JC, Dinatale BC, Murray IA, Flaveny CA, Liu Q, Laurenzana EM, et al. The uremic toxin 3- indoxyl sulfate is a potent endogenous agonist for the human aryl hydrocarbon receptor. *Biochemistry*. (2010) 49:393–400. doi: 10.1021/bi901786x
29. Martovetsky G, Tee JB, Nigam SK. Hepatocyte nuclear factors 4α and 1α regulate kidney developmental expression of drug-metabolizing enzymes and drug transporters. *Mol Pharmacol.* (2013) 84:808–23. doi: 10.1124/mol.113.088229
30. Sherr DH. Another important biological function for the aryl hydrocarbon receptor. *Arterioscler Thromb Vasc Biol.* (2011) 31:1247–8. doi: 10.1161/ATVBAHA.111.227553
31. Chiao-Yin S, Young GH, Hsieh YT, Chen YH, Wu MS, Wu VC, et al. Protein-bound uremic toxins induce tissue remodeling by targeting the EGF receptor. *JASN*. (2015) 26:281–90. doi: 10.1681/ASN.2014010021
32. Wu W, Dynanmote, AV, Nigam SK. Remote communication through solute carriers and ATP binding cassette drug transporter pathways. *Mol Pharmacol.* (2011) 79:795–805. doi: 10.1124/mol.110.070607
33. Rothhammer V, Quintana FJ. The aryl hydrocarbon receptor: an environmental sensor integrating immune responses in health and disease. *Nat Rev Immunol.* (2019) 19:185. doi: 10.1038/s41577-019-0125-8
34. Nigam SK, Bush KT. Uraemic syndrome of chronic kidney disease: altered remote sensing and signaling. *Nature Rev Nephrol.* (2019) 15:301–16. doi: 10.1038/s41581-019-0111-1
35. Bush KT, Singh P, Nigam SK. Gut-derived uremic toxin handling *in vivo* requires OAT-mediated tubular secretion in chronic kidney disease. *JCI Insight.* (2020) 5:e133817. doi: 10.1172/jci.insight.133817
36. Bhatnagar V, Richard EL, Wu W, Nievergelt CM, Lipkowitz MS, Jeff J, et al. Analysis of ABCG2 and other urate transporters in uric acid homeostasis in chronic kidney disease: potential role of remote sensing and signaling. *Clin Kidney J.* (2016) 9:444–53. doi: 10.1093/ckj/sfw010
37. Lu Y, Nakanishi T, Hosomi A, Komori H, Tamai I. *In-vitro* evidence of enhanced breast cancer resistance protein-mediated intestinal urate secretion by uremic toxins in Caco-2 cells. *J Pharm Pharmacol.* (2015) 67:170–7. doi: 10.1111/jphp.12328
38. Chen M, Lu X, Lu C, Shen N, Jiang Y, Chen M, et al. Soluble uric acid increases PDZK1 and ABCG2 expression in human intestinal cell lines via the TLR4-NLRP3 inflammasome and PI3K/Akt signaling pathway. *Arthritis Res Ther*. (2018) 20:20. doi: 10.1186/s13075-018-1512-4
39. Miyamoto Y, Iwao Y, Tasaki Y, Sato K, Ishima Y, Watanabe H, et al. The uremic solute indoxyl sulfate acts as an antioxidant against superoxide anion radicals under normal-physiological conditions *FEBS Lett.* (2010) 584:2816–20. doi: 10.1016/j.febslet.2010.04.046
40. Rothhammer V, Mascanfroni ID, Bunse L, Takenaka MC, Kenison JE, Mayo L, et al. Type I interferons and microbial metabolites of tryptophan modulate astrocyte activity and central nervous system inflammation via the aryl hydrocarbon receptor. *Nat Med.* (2016) 22:586–59. doi: 10.1038/nm.4106
41. Ramezani A, Raj DS. The gut microbiome, kidney disease, and targeted interventions. *JASN*. (2014) 25:657–70. doi: 10.1681/ASN.2013080905
42. Nigam AK, Li J, Lall K, Shi D, Bush KT, Bhatnagar V, et al. Unique metabolite preferences of drug transporters OAT1 and OAT3 analyzed by machine learning. *J Biol Chem.* (2020) 296:1829–42. doi: 10.1074/jbc.RA119.010729
43. Nigam SK, Bush KT, Bhatnagar V, Poloyac SM, Momper JD. Systems biology of drug metabolizing enzymes and transporters: relevance to quantitative systems pharmacology. *Clin Pharmacol Ther.* (2020) 108:40–53. doi: 10.1002/cpt.1818
44. Nigam SK. What do drug transporters really do? *Nat Rev Drug Disc.* (2015) 1:29–44. doi: 10.1038/nrd4461
45. Torres AM, Dnyanmote A, Granados JC, Nigam SK. Renal and non-renal response of ABC and SLC transporters in chronic kidney disease. *Expert Opin Drug Metab Toxicol*. (2021). doi: 10.1080/17425255.2021.1899159

Conflict of Interest: The authors declare that the research was conducted in the absence of any commercial or financial relationships that could be construed as a potential conflict of interest.

Advantages of publishing in Frontiers

OPEN ACCESS
Articles are free to read for greatest visibility and readership

FAST PUBLICATION
Around 90 days from submission to decision

HIGH QUALITY PEER-REVIEW
Rigorous, collaborative, and constructive peer-review

TRANSPARENT PEER-REVIEW
Editors and reviewers acknowledged by name on published articles

Frontiers
Avenue du Tribunal-Fédéral 34
1005 Lausanne | Switzerland

Visit us: www.frontiersin.org
Contact us: frontiersin.org/about/contact

REPRODUCIBILITY OF RESEARCH
Support open data and methods to enhance research reproducibility

DIGITAL PUBLISHING
Articles designed for optimal readership across devices

FOLLOW US
@frontiersin

IMPACT METRICS
Advanced article metrics track visibility across digital media

EXTENSIVE PROMOTION
Marketing and promotion of impactful research

LOOP RESEARCH NETWORK
Our network increases your article's readership